

Université de Montréal

# **Copper and Nickel Catalysis for Alkynylation Reactions**

par

Jeffrey Santandrea

Département de chimie

Faculté des arts et des sciences

Thèse présentée à la Faculté des études supérieures et postdoctorales  
en vue de l'obtention du grade de  
*Philosophiæ Doctor* (Ph.D.) en chimie

Avril 2018

© Jeffrey Santandrea, 2018

## Résumé

Les alcynes sont reconnus comme étant des groupements fonctionnels polyvalents pouvant participer à de multiples transformations chimiques. Conséquemment, le développement de nouvelles méthodologies efficaces et chimiosélectives pour permettre la formation d'alcynes internes substitués par des atomes de carbone ou par des hétéroatomes est intéressant. La thèse suivante décrit ainsi le développement de nouveaux systèmes catalytiques à base de cuivre et de nickel pour effectuer des réactions d'alcynylation.

Les travaux présentés au Chapitre 3 décrivent le premier couplage croisé de type Sonogashira catalysé par le cuivre menant à la formation de macrocycles à partir de précurseurs linéaires non-biaisés conformationnellement. Le couplage croisé macrocyclique de type Sonogashira a exploité un système catalytique  $\text{CuCl}/\text{phen}/\text{Cs}_2\text{CO}_3$  pour générer 17 macrocycles de différentes tailles de cycle (10 à 25 chaînons) et différents groupements fonctionnels avec des rendements compris entre 38 et 83 %. De plus, la méthode a été réalisée à une concentration relativement élevée (24 mM) sans recourir à des techniques d'addition lente. Les conditions réactionnelles optimisées ont aussi été appliquées à la synthèse du (*S*)-zéaralane, un produit biologiquement actif.

Les travaux présentés au Chapitre 6 décrivent la première synthèse de thioalcynes arylés par le biais de la catalyse photorédox et de la catalyse au nickel. Le couplage  $\text{C}(\text{sp})\text{-S}$  a été réalisé entre des thiols et des bromoalcynes aromatiques en utilisant un système catalytique  $4\text{CzIPN}/\text{NiCl}_2\cdot\text{glyme}/\text{pyridine}$  sous irradiation de la lumière visible à température ambiante. Ainsi, des thioalcynes dérivés de plusieurs thiols et d'alcynes aromatiques électroniquement et stériquement variés ont été obtenus avec de bons rendements (50-96 %) en utilisant un photoréacteur impliquant lumière visible en flux continu. La méthodologie a également été appliquée à la synthèse d'un macrocycle, un exemple rare de macrocyclisation photochimique en flux continu. La procédure photochimique bi-catalytique représente aussi le premier exemple de macrocyclisation exploitant la double catalyse photorédox/nickel.

Les travaux présentés au Chapitre 7 décrivent la première méthode générale pour accéder à toutes les classes de thioalcynes, y compris les thioalcynes comportant des substituants aryle,

alkyle, silyle et des hétéroatomes, par le biais de la catalyse au cuivre. Le système catalytique  $\text{Cu}(\text{MeCN})_4\text{PF}_6/\text{dtbbpy}/2,6\text{-lutidine}$  a donné accès à des thioalcynes avec des rendements élevés en dix minutes, tout en étant hautement reproductible, même à grande échelle. De plus, la méthodologie a efficacement mené à la synthèse d'un alcyne di(thio-substitué), un exemple rare d'alcyne orné de deux hétéroatomes comme substituants.

**Mots-clés :** catalyse au cuivre, catalyse au nickel, catalyse photorédox, macrocyclisation, réaction de Sonogashira, thioalcynes, chimie en flux continu

## Abstract

Alkynes are recognized as versatile building blocks for chemical synthesis as they can participate in an array of transformations. Consequently, expanding the toolbox of efficient and chemoselective methodologies to access internal carbon- and heteroatom-substituted alkynes is of interest. The following thesis describes the development of new copper- and nickel-based catalytic systems to perform alkynylation reactions.

The research presented in Chapter 3 describes the first report of a copper-catalyzed Sonogashira-type cross-coupling toward the formation of macrocycles from conformationally unbiased linear precursors. The macrocyclic Sonogashira-type cross-coupling exploited a CuCl/phen/Cs<sub>2</sub>CO<sub>3</sub> catalytic system to generate 17 macrocycles with various ring sizes (10- to 25-membered rings) and functional groups in yields ranging between 38-83 %. Also, the method could be performed at relatively high concentrations (24 mM) without the need for slow addition techniques. The optimized reaction conditions were additionally applied toward the synthesis of a biologically active natural product, (*S*)-zearalane.

The research presented in Chapter 6 describes the first report of a photoredox/nickel dual-catalytic synthesis of aryl- and heteroaryl-substituted alkynyl sulfides. The C(sp)-S bond-forming coupling was achieved between thiols and aromatic bromoalkynes using a 4CzIPN/NiCl<sub>2</sub>•glyme/pyridine catalytic system under visible-light irradiation at room temperature. Alkynyl sulfides bearing a wide range of electronically and sterically diverse aromatic alkynes and thiols were obtained in good to excellent yields (50-96 %) using an in-house designed visible-light photoreactor in continuous flow. The methodology was also applied toward the synthesis of a macrocycle, a rare example of a photochemical macrocyclization performed in continuous flow. The photochemical dual-catalytic procedure represented the first example of a macrocyclization exploiting photoredox/nickel dual-catalysis.

The research presented in Chapter 7 describes the first general method to access all classes of alkynyl sulfides through copper catalysis, including aryl-, alkyl-, silyl-, and heteroatom-substituted alkynyl sulfides. The Cu(MeCN)<sub>4</sub>PF<sub>6</sub>/dtbbpy/2,6-lutidine catalyst system gave access to alkynyl sulfides in high yields under ten minutes, and was highly reproducible even on large scale. Furthermore, the methodology efficiently led to a bis(thio-

substituted)alkyne, a rare example of an alkyne functional group adorned with two heteroatom substituents.

**Keywords** : copper catalysis, nickel catalysis, photoredox catalysis, macrocyclization, Sonogashira reaction, alkynyl sulfides, continuous flow chemistry

# Table of Contents

Résumé.....	i
Abstract.....	iii
Table of Contents.....	v
List of Tables .....	ix
List of Figures .....	x
List of Schemes.....	xii
List of Abbreviations .....	xv
Acknowledgments.....	xxii
1. Introduction to Macrocycles .....	1
1.1 Importance and Applications of Macrocycles .....	1
1.1.1 Medicinal Chemistry .....	2
1.1.2 Aroma Chemistry .....	4
1.1.3 Supramolecular Chemistry .....	5
1.2 Synthetic Challenges in Macrocyclization Reactions.....	7
1.2.1 Kinetic Aspects.....	7
1.2.2 Reactive Conformation.....	10
1.3 Employing Catalysis for Macrocycle Synthesis .....	12
1.3.1 Ring-Closing Metathesis .....	12
1.3.2 Copper-Catalyzed Azide-Alkyne Cycloaddition.....	14
1.4 Conclusions.....	15
1.5 Bibliography .....	16
2. Introduction to the Sonogashira Reaction .....	19
2.1 Discovery and Evolution of C(sp <sup>2</sup> )-C(sp) Couplings .....	19
2.2 Applications Toward Macrocyclization.....	23
2.2.1 Synthesis of Macrocyclic Natural Products.....	23
2.2.2 Synthesis of Macrocyclic Nonnatural Products.....	25
2.3 Development of a Palladium-Free Variant .....	27
2.3.1 Iron-Catalyzed Sonogashira-Type Coupling .....	27

2.3.2 Copper-Catalyzed Sonogashira-Type Coupling .....	28
2.4 Conclusions.....	31
2.5 Research Goals .....	31
2.6 Bibliography .....	32
3. Cu(I)-Catalyzed Macrocyclic Sonogashira-Type Cross-Coupling .....	35
3.1 Abstract.....	36
3.2 Introduction.....	36
3.3 Results and Discussion .....	37
3.4 Conclusions.....	44
3.5 Bibliography .....	45
4. Introduction to Photochemistry.....	47
4.1 Principles of Photochemistry .....	47
4.2 Photocatalysis .....	49
4.2.1 Photoredox Catalysis .....	49
4.2.2 Photoredox/Nickel Dual Catalysis.....	53
4.3 Applications Toward Macrocyclization.....	58
4.3.1 UV-Mediated Thiol-Ene Reaction.....	59
4.3.2 Photoredox-Mediated Decarboxylation/Cyclization .....	60
4.4 Continuous Flow Chemistry .....	60
4.4.1 Description of Parameters and Equipment .....	61
4.4.2 Merging Continuous Flow Chemistry and Photochemistry .....	62
4.5 Conclusions.....	65
4.6 Bibliography .....	66
5. Introduction to Alkynyl Sulfides.....	70
5.1 Heteroatom-Substituted Alkynes .....	70
5.2 Approaches Toward Synthesis of Alkynyl Sulfides .....	71
5.2.1 Dehydrohalogenation.....	72
5.2.2 Sulfur Umpolung .....	73
5.2.3 Alkyne Umpolung .....	75
5.2.4 Nucleophilic Thioalkynylation .....	79
5.2.5 Electrophilic Thioalkynylation .....	80
5.3 Synthetic Applications of Alkynyl Sulfides .....	81

5.3.1 Nucleophilic Additions.....	82
5.3.2 Cycloadditions .....	85
5.3.3 Annulations.....	87
5.4 Conclusions.....	88
5.5 Research Goals .....	88
5.6 Bibliography .....	89
6. Photochemical Dual-Catalytic Synthesis of Alkynyl Sulfides.....	92
6.1 Abstract.....	93
6.2 Introduction.....	93
6.3 Results and Discussion .....	95
6.4 Conclusions.....	101
6.5 Bibliography .....	103
7. Cu(I)-Catalyzed Synthesis of Alkynyl Sulfides.....	105
7.1 Expanding the Scope of Reactivity.....	105
7.1.1 Initial Breakthrough: From Nickel to Copper .....	107
7.1.2 Copper-Catalyzed C-S Couplings.....	110
7.1.3 Preliminary Screening of Reaction Parameters with Model Aromatic Alkynyl Bromide....	112
7.2 Screening of Reaction Parameters for Coupling with Model Alkyl Alkynyl Bromide .....	115
7.2.1 Effect of Concentration .....	115
7.2.2 Effect of Reagent Stoichiometry .....	116
7.2.3 Effect of Base .....	118
7.2.4 Effect of Solvent.....	119
7.2.5 Fine-Tuning of Reagent Stoichiometry .....	120
7.3 Preliminary Substrate Scope.....	122
7.3.1 Aryl-Substituted Alkynyl Bromide Coupling Partners.....	122
7.3.2 Silyl-Substituted Alkynyl Bromide Coupling Partners .....	123
7.3.3 Alkyl-Substituted Alkynyl Bromide Coupling Partners.....	124
7.3.4 Heteroatom-Substituted Alkynyl Bromide Coupling Partners .....	125
7.3.5 Thiol Coupling Partners.....	126
7.4 Plausible Mechanisms for Cu-Catalyzed C-S Cross-Couplings.....	127
7.4.1 C(sp <sup>2</sup> )-S Bonds: Ullmann-Type Arylations.....	128
7.4.2 C(sp)-S Bonds.....	129
7.5 Conclusions.....	131



7.7 Bibliography .....	132
8. Conclusions and Perspectives .....	134
8.1 Cu-Catalyzed Macrocyclic Sonogashira-Type Cross-Coupling .....	134
8.1.1 Summary.....	134
8.1.2 Future Work.....	134
8.2 Photoredox/Ni Dual-Catalyzed Synthesis of Alkynyl Sulfides .....	135
8.2.1 Summary.....	135
8.2.2 Future Work.....	136
8.3 Cu-Catalyzed Synthesis of Alkynyl Sulfides.....	136
8.3.1 Summary.....	136
8.3.2 Future Work.....	137
8.4 Bibliography .....	139
9. Supporting Information of Chapter 3 .....	140
9.1 General.....	140
9.2 Synthesis of Macrocyclization Precursors .....	142
9.3 Synthesis of Macrocycles .....	152
9.4 Synthesis of ( <i>S</i> )-Zearalane .....	160
9.5 NMR Data for all New Compounds .....	166
10. Supporting Information of Chapter 6.....	201
10.1 General.....	201
10.2 Optimization/Scale-Up and Mechanism .....	203
10.3 Synthesis of Precursors.....	206
10.4 Synthesis of Alkynyl Sulfides.....	219
10.5 Post-Functionalization Reactions .....	233
10.6 Synthesis of Macrocycle.....	237
10.7 NMR Data for all New Compounds .....	241
11. Supporting Information of Chapter 7.....	284
11.1 General.....	284
11.2 Synthesis of Precursors.....	286
11.3 Synthesis of Alkynyl Sulfides.....	291
11.4 NMR Data for all New Compounds .....	298

## List of Tables

<b>Table 3.1</b>	Optimization of a Cu(I)-catalyzed macrocyclic Sonogashira-type cross-coupling .	38
<b>Table 3.2</b>	Scope of the Cu(I)-catalyzed macrocyclic Sonogashira-type cross-coupling.....	39
<b>Table 6.1</b>	Control reactions for photoredox/Ni dual-catalyzed C-S coupling.....	95
<b>Table 7.1</b>	Screening of diamine ligands .....	106
<b>Table 7.2</b>	Initial Cu-catalyzed coupling of an aryl bromoalkyne and control experiments ...	108
<b>Table 7.3</b>	Initial Cu-catalyzed coupling of an alkyl bromoalkyne and control experiments .	109
<b>Table 7.4</b>	Ligand screening toward formation of alkynyl sulfide <b>7.6</b> .....	113
<b>Table 7.5</b>	Atmosphere screening toward formation of alkynyl sulfide <b>7.6</b> .....	114
<b>Table 7.6</b>	Concentration screening toward formation of alkynyl sulfide <b>7.3</b> .....	116
<b>Table 7.7</b>	Stoichiometry screening toward formation of alkynyl sulfide <b>7.3</b> .....	117
<b>Table 7.8</b>	Base screening toward formation of alkynyl sulfide <b>7.3</b> .....	119
<b>Table 7.9</b>	Solvent screening toward formation of alkynyl sulfide <b>7.3</b> .....	120
<b>Table 7.10</b>	Fine-tuning of conditions toward formation of alkynyl sulfide <b>7.3</b> .....	121
<b>Table 9.1</b>	Optimization of a macrocyclic Pd-catalyzed Sonogashira cross-coupling .....	159
<b>Table 10.1</b>	Control & optimization experiments.....	203
<b>Table 10.2</b>	Scale screening.....	204

# List of Figures

<b>Figure 1.1</b> Macrocycles at the intersection of small molecules and larger biomolecules.....	1
<b>Figure 1.2</b> Structures of erythromycin A (1.1) and epothilone B (1.2).....	2
<b>Figure 1.3</b> Structures of tyrocidine (1.3) and gramicidin S (1.4).....	3
<b>Figure 1.4</b> Structure of BILN 2061 (1.5) .....	4
<b>Figure 1.5</b> Structures of musk ketone 1.6 and polycyclic musk 1.7 .....	5
<b>Figure 1.6</b> Structures of muscone (1.8), exaltolide (1.9) and isoambrettolide (1.10) .....	5
<b>Figure 1.7</b> Structures of 18-crown-6 (1.11) and [2.2.2]cryptand (1.12) .....	6
<b>Figure 1.8</b> Example of a [2]catenane .....	6
<b>Figure 1.9</b> Example of a shape-persistent macrocyclic framework (1.14) .....	7
<b>Figure 1.10</b> Reaction rates of intramolecular (a) and intermolecular (b) processes .....	8
<b>Figure 1.11</b> Rate of lactone formation as function of ring size.....	8
<b>Figure 2.1</b> Original proposed mechanism for the Sonogashira coupling.....	22
<b>Figure 2.2</b> Modified proposed mechanism of the Sonogashira coupling .....	22
<b>Figure 2.3</b> Miura's proposed mechanism for copper-catalyzed alkynylation reaction.....	29
<b>Figure 2.4</b> Bolm's proposed mechanism for copper-catalyzed alkynylation reaction.....	31
<b>Figure 3.1</b> Macrocyclic Sonogashira cross-coupling processes.....	37
<b>Figure 4.1</b> Electromagnetic spectrum .....	48
<b>Figure 4.2</b> Generalized Jablonski diagram of photocatalysts. $k_f$ , $k_{ic}$ , $k_{isc}$ , and $k_p$ are the rate constants for fluorescence, internal conversion, intersystem crossing, and phosphorescence, respectively and $\lambda_{em}$ is the maximum emission wavelength of the photocatalyst. Reprinted with permission from ref 8. Copyright 2012 American Chemical Society. ....	49
<b>Figure 4.3</b> Common metal-based and organic-based photoredox catalysts.....	52
<b>Figure 4.4</b> Oxidative and reductive quenching cycles of $^*\text{Ru}(\text{bpy})_3^{2+}$ .....	53
<b>Figure 4.5</b> Molander's proposed mechanism for photoredox/Ni-catalyzed cross-coupling ....	56
<b>Figure 4.6</b> Proposed mechanism for photochemical dual-catalytic C-S cross-coupling .....	58
<b>Figure 4.7</b> General schematic diagram of high-temperature/high-pressure continuous flow conditions.....	62
<b>Figure 4.8</b> Continuous flow UV photoreactor developed by Booker-Milburn. Reprinted with permission from ref 47. Copyright 2005 American Chemical Society. ....	64

<b>Figure 4.9</b> Continuous flow visible light photoreactors developed by: a) Seeberger; b) Gagné; c) Stephenson and Jamison. Reprinted with permission from ref 54. Copyright 2012 The Royal Society of Chemistry. Reprinted with permission from ref 55 & 56. Copyright 2012 John Wiley and Sons .....	65
<b>Figure 5.1</b> Common heteroatom-substituted alkynes .....	70
<b>Figure 5.2</b> Predictable regioselectivity from ynamines .....	71
<b>Figure 5.3</b> Synthetic disconnections toward alkynyl sulfides.....	71
<b>Figure 6.1</b> Selected examples of carbon-sulfur bond forming reactions between thiols and alkynes .....	94
<b>Figure 6.2</b> Mechanistic proposals for the synthesis of alkynyl sulfides. ....	101
<b>Figure 7.1</b> Observed electrochromism during formation of alkynyl sulfides .....	122
<b>Figure 7.2</b> Possible mechanistic pathways for copper-catalyzed Ullmann-type reactions ....	128
<b>Figure 7.3</b> General model system for copper-catalyzed C-S arylation studies .....	128
<b>Figure 7.4</b> Equilibriums of possible copper species in solution .....	129
<b>Figure 7.5</b> Proposed mechanism for copper-catalyzed S-alkynylation.....	131
<b>Figure 8.1</b> Proposed copper-catalyzed alkynylation of $\alpha$ -bromocarbonyls .....	135
<b>Figure 8.2</b> Proposed photoredox/Ni dual-catalytic synthesis of ynamides .....	136
<b>Figure 8.3</b> Proposed synthesis of a macrocyclic alkynyl sulfide .....	138
<b>Figure 8.4</b> Palladium-mediated peptide and protein cross-linking .....	138
<b>Figure 10.1</b> Mechanistic considerations.....	205
<b>Figure 10.2</b> Continuous flow reactor set-up used for the visible-light-mediated synthesis of alkynyl sulfides .....	219
<b>Figure 10.3</b> Continuous flow reactor - light source outside homemade PFA coil (13 mL, 1 mm I.D.). Blue LED ribbon was purchased from Creative Lighting Solutions, LLC. <i>Specifications:</i> 1210 series, electric blue ( $\lambda_{\text{max}} = 465$ nm), 12 volt DC, 3.6 watts/meter. ....	219
<b>Figure 10.4</b> Continuous flow reactor set-up used for the visible-light-mediated synthesis of macrocyclic alkynyl sulfide .....	240

## List of Schemes

<b>Scheme 1.1</b> The importance of conformation in RCM .....	10
<b>Scheme 1.2</b> Attempts to synthesize Pro-Ala-Ala-Phe-Leu macrocycle <b>1.21</b> .....	11
<b>Scheme 1.3</b> Synthesis of macrolactone <b>1.23</b> via RCM .....	13
<b>Scheme 1.4</b> Synthesis of macrolactone <b>1.25</b> and epothilone C ( <b>1.26</b> ) .....	14
<b>Scheme 1.5</b> Synthesis of macrocyclic triazole <b>1.28</b> .....	15
<b>Scheme 1.6</b> Synthesis of macrocyclic iodotriazole <b>1.30</b> .....	15
<b>Scheme 2.1</b> Castro-Stephens coupling of diphenylacetylene <b>2.3</b> .....	20
<b>Scheme 2.2</b> Palladium-catalyzed syntheses of diphenylacetylene <b>2.3</b> .....	20
<b>Scheme 2.3</b> Synthesis of dynemicin A analog precursor <b>2.17</b> .....	23
<b>Scheme 2.4</b> Synthesis of <i>ansa</i> -macrolide <b>2.20</b> .....	24
<b>Scheme 2.5</b> Synthesis of penarolide sulfate A1 precursor <b>2.23</b> .....	25
<b>Scheme 2.6</b> Synthesis of macrocycle <b>2.26</b> .....	25
<b>Scheme 2.7</b> Synthesis of macrocycle <b>2.28</b> .....	26
<b>Scheme 2.8</b> Synthesis of shape-persistent macrocycle <b>2.31</b> .....	27
<b>Scheme 2.9</b> Iron-catalyzed coupling of diphenylacetylene <b>2.3</b> .....	28
<b>Scheme 2.10</b> Iron-catalyzed <i>N</i> -arylation using different FeCl <sub>3</sub> commercial sources .....	28
<b>Scheme 2.11</b> Copper-catalyzed coupling of diphenylacetylene <b>2.3</b> reported by Miura .....	29
<b>Scheme 2.12</b> Copper-catalyzed coupling of diphenylacetylene <b>2.3</b> reported by Bolm .....	30
<b>Scheme 3.1</b> Total synthesis of ( <i>S</i> )-zearealane using a Cu-catalyzed macrocyclic Sonogashira-type coupling .....	42
<b>Scheme 3.2</b> (Top) Possible mechanism for the Cu-catalyzed macrocyclic Sonogashira-type cross-coupling; (Bottom) Preliminary mechanistic investigations .....	44
<b>Scheme 4.1</b> Seminal contributions to organic photoredox catalysis .....	50
<b>Scheme 4.2</b> Seminal contributions to modern organic photoredox catalysis .....	51
<b>Scheme 4.3</b> Seminal contributions to metallaphotoredox catalysis .....	54
<b>Scheme 4.4</b> Initial reports of metallaphotoredox catalysis using nickel .....	55
<b>Scheme 4.5</b> Dual photoredox/Ni-catalyzed C-O, C-N and C-S cross-couplings .....	57
<b>Scheme 4.6</b> Bis-thiol-ene macrocyclization of peptide <b>4.60</b> .....	59
<b>Scheme 4.7</b> Visible-light-mediated macrocyclization of peptide <b>4.63</b> .....	60

<b>Scheme 5.1</b> Initial synthesis of alkynyl sulfides .....	72
<b>Scheme 5.2</b> One-pot synthesis of alkynyl sulfides using trichloroethylene .....	73
<b>Scheme 5.3</b> Initial synthesis of alkynyl sulfides using disulfides .....	73
<b>Scheme 5.4</b> Synthesis of alkynyl sulfides using mixed disulfides .....	74
<b>Scheme 5.5</b> Synthesis of alkynyl sulfides using thiobromides.....	75
<b>Scheme 5.6</b> Synthesis of alkynyl sulfides using Bunte salts .....	75
<b>Scheme 5.7</b> Synthesis of alkynyl sulfides using EBX-based reagents .....	77
<b>Scheme 5.8</b> Synthesis of alkynyl sulfides using chloroalkynes .....	78
<b>Scheme 5.9</b> Synthesis of alkynyl sulfides using bromoalkynes and palladium catalysis .....	78
<b>Scheme 5.10</b> Synthesis of alkynyl sulfides using bromoalkynes and nickel catalysis.....	79
<b>Scheme 5.11</b> Synthesis of alkynyl sulfides from nucleophilic thioalkynylation.....	80
<b>Scheme 5.12</b> Initial synthesis of alkynyl sulfides from electrophilic thioalkynylation .....	80
<b>Scheme 5.13</b> Modern synthesis of alkynyl sulfides from electrophilic thioalkynylation .....	81
<b>Scheme 5.14</b> Iridium-catalyzed hydrosilylation of alkynyl sulfides .....	82
<b>Scheme 5.15</b> Silylzincation of alkynyl sulfides .....	82
<b>Scheme 5.16</b> Hydroallylation of alkynyl sulfides .....	83
<b>Scheme 5.17</b> Hydrofluorination of alkynyl sulfides.....	83
<b>Scheme 5.18</b> Hydrozirconation of alkynyl sulfides .....	84
<b>Scheme 5.19</b> Synthesis of ketene dithioacetals from alkynyl sulfides.....	84
<b>Scheme 5.20</b> Synthesis of $\alpha$ -arylated thioesters from alkynyl sulfides.....	85
<b>Scheme 5.21</b> Iridium-catalyzed [3+2] cycloaddition of alkynyl sulfides.....	85
<b>Scheme 5.22</b> Ruthenium-catalyzed [3+2] cycloaddition of alkynyl sulfides.....	86
<b>Scheme 5.23</b> Brønsted acid-mediated [2+2+2] cycloaddition of alkynyl sulfides.....	86
<b>Scheme 5.24</b> Gold-catalyzed annulation from alkynyl sulfides.....	87
<b>Scheme 5.25</b> Lewis acid-catalyzed annulation from alkynyl sulfides .....	88
<b>Scheme 6.1</b> Substrate scope. Yields after chromatography. ....	97
<b>Scheme 6.2</b> Diversification/functionalization of alkynyl sulfides. <sup>15</sup> .....	98
<b>Scheme 6.3</b> Dual catalytic synthesis of a 19-membered macrocyclic alkynyl sulfide.....	99
<b>Scheme 7.1</b> Attempt at coupling an alkyl bromoalkyne photochemically .....	105
<b>Scheme 7.2</b> Ullmann-type copper-catalyzed S-arylation .....	110
<b>Scheme 7.3</b> Copper-catalyzed S-vinylation .....	111

<b>Scheme 7.4</b> Oxidative copper-catalyzed S-alkynylation.....	111
<b>Scheme 7.5</b> Decarboxylative copper-catalyzed S-alkynylation .....	112
<b>Scheme 7.6</b> Cu-catalyzed coupling of alkyl bromoalkyne <b>7.2</b> under nitrogen atmosphere ...	115
<b>Scheme 7.7</b> Widening the scope of aryl-substituted bromoalkynes.....	123
<b>Scheme 7.8</b> Formation of a silyl-substituted alkynyl sulfide .....	124
<b>Scheme 7.9</b> Preliminary scope of alkyl-substituted bromoalkynes.....	125
<b>Scheme 7.10</b> Formation of a bis(thio-substituted)alkyne.....	126
<b>Scheme 7.11</b> Preliminary scope of thiols .....	127

## List of Abbreviations

4CzIPN	2,4,5,6-Tetra(9 <i>H</i> -carbazol-9-yl)isophthalonitrile
Å	Angstrom
abs	Absorbance
Ac	Acetate
Acr	Acridinium
ADMET	Acyclic diene metathesis
Anthr	Anthracenyl
aq	Aqueous
atm	Atmosphere (pressure)
bathocup	Bathocuproine
bathophen	Bathophenanthroline
BINOL	1,1'-Binaphthalene-2,2'-diol
Biquin	2,2'-Biquinoline
Boc	<i>tert</i> -Butyloxycarbonyl
Brettphos	2-(Dicyclohexylphosphino)3,6-dimethoxy-2',4',6'-triisopropyl-1,1'-biphenyl
bpy	2,2'-Bipyridine
bpz	2,2'-Bipyrazine
Bn	Benzyl
br	Broad
Bu	Butyl
Bz	Benzoyl
<i>c</i>	Speed of light
C	Celsius
cat	Catalytic
CFL	Compact fluorescent lamp
COD	1,5-Cyclooctadiene
CM	Cross metathesis
Cp	Cyclopentadienyl
Cp*	Pentamethylcyclopentadienyl
CPBA	Chloroperoxybenzoic acid
CuAAC	Copper-catalyzed azide-alkyne cycloaddition
CuAiAc	Copper-catalyzed azide-iodoalkyne cycloaddition
Cy	Cyclohexyl
Cz	Carbazolyl
Δ	Heat
ΔH	Enthalpy
ΔS	Entropy
δ	Chemical shift
d	Doublet
Da	Dalton
dap	2,9-Bis( <i>p</i> -anisyl)-1,10-phenanthroline
DABCO	1,4-Diazabicyclo[2.2.2]octane
dba	Dibenzylideneacetone



DCB	Dichlorobenzenes
DCC	<i>N,N'</i> -Dicyclohexylcarbodiimide
DCE	1,2-Dichloroethane
DCM	Dichloromethane
DDQ	2,3-Dichloro-5,6-dicyano-1,4-benzoquinone
dF(CF <sub>3</sub> )ppy	3,5-Difluoro-2-[5-(trifluoromethyl)-2-pyridinyl-N]phenyl-C
DFT	Density-functional theory
DHP	Diethyl 1,2,6-trimethyl-1,4-dihydropyridine-3,5-dicarboxylate
DIAD	Diisopropyl azodicarboxylate
DIPEA	<i>N,N</i> -Diisopropylethylamine
DMA	<i>N,N</i> -Dimethylacetamide
DMAP	4-Dimethylaminopyridine
dme	Dimethoxyethane
DMEA	<i>N,N'</i> -Dimethylethanolamine
DMEDA	<i>N,N'</i> -Dimethylethylenediamine
DMF	<i>N,N</i> -Dimethylformamide
DMPA	<i>N,N'</i> -Dimethyl-1,3-propanediamine
dmbpy	4,4'-Dimethyl-2,2'-bipyridine
dmphen	2,9-Dimethyl-1,10-phenanthroline
DMSO	Dimethylsulfoxide
DOS	Diversity-oriented synthesis
dr	Diastereomeric ratio
dtbbpy	4,4'-Di- <i>tert</i> -butyl-2,2'-bipyridine
E	Electrophile
E	Energie
EBX	Ethynylbenziodoxolone
ee	Enantiomeric excess
er	Enantiomeric ratio
EDC	1-Ethyl-3-(3-dimethylaminopropyl)carbodiimide
Et	Ethyl
equiv	Equivalents
ESI	Electrospray ionisation mass spectrometry
f	Fluorescence
FEP	Fluorinated ethylene propylene
FG	Functional group
g	Gram
glyme	Dimethoxyethane
h	Hours
<i>h</i>	Planck constant
HCV	Hepatitis C virus
HEPES	4-(2-Hydroxyethyl)-1-piperazineethanesulfonic acid
hex	Hexyl
HOMO	Highest occupied molecular orbital
HPLC	High pressure liquid chromatography
HRMS	High-resolution mass spectrometry
hv	Light irradiation

<i>i</i>	<i>iso</i>
ic	Internal conversion
isc	Intersystem crossing
intra	Intramolecular
inter	Intermolecular
IR	Infrared
IUPAC	International Union of Pure and Applied Chemistry
J	Joule
<i>J</i>	Coupling constant
k	Rate
kg	Kilogram
$\lambda$	Wavelength
$\lambda_{\text{em}}$	Emission wavelength
$\lambda_{\text{max}}$	Maximal absorption wavelength
L	Ligand
LC	Liquid chromatography
LED	Light-emitting diode
Leu	Leucine
LUMO	Lowest unoccupied molecular orbital
Lys	Lysine
m/z	Mass on charge
m	Meter
m	Multiplet
<i>m</i>	<i>meta</i>
M	Molar
Me	Methyl
Mes	Mesityl
MET	$\sigma$ -Bond metathesis
MHz	Megahertz
$\mu\text{L}$	Microliter
min	Minute
mL	Milliliter
mm	Millimeter
mM	Millimolar
mmol	Millimole
MLCT	Metal to ligand charge transfer
mol	Mole
MOM	Methoxymethyl
mg	Milligram
MS	Mass spectrometry
Ms	Methanesulfonyl
<i>n</i>	<i>normal</i>
NBS	<i>N</i> -Bromosuccinimide
NCS	<i>N</i> -Chlorosuccinimide
neo	2,9-Dimethyl-1,10-phenanthroline

NIR	Near-infrared
NIS	<i>N</i> -Iodosuccinimide
nm	Nanometer
NMP	<i>N</i> -Methyl-2-pyrrolidone
NMR	Nuclear magnetic resonance
ns	Nanosecond
Nu	Nucleophile
<i>o</i>	<i>ortho</i>
OA	Oxidative addition
p	Phosphorescence
<i>p</i>	<i>para</i>
PBS	Phosphate-buffered saline
PC	Photocatalyst
PCC	Pyridinium chlorochromate
Ph	Phenyl
PFA	Perfluoroalcoxyalane
Pfp	Pentafluorophenyl
phen	1,10-Phenanthroline
phtha	Phthalimide
Pic	2-(Aminomethyl)pyridine
pin	Pinacolato
PMP	<i>para</i> -Methoxyphenyl
ppm	Parts per million
ppy	2-Phenylpyridinato- $C^2,N$
pKa	Acid dissociation constant at logarithmic scale
Pr	Propyl
q	Quartet
rac	Racemic
rt	Room temperature
RCAM	Ring-closing alkyne metathesis
RCM	Ring-closing metathesis
RE	Reductive elimination
ROMP	Ring-opening metathesis polymerisation
RuAAC	Ruthenium-catalyzed azide-alkyne cycloaddition
s	Second
s	Singlet
SA	Slow addition
SCE	Saturated calomel electrode
SET	Single-electron transfer
SPM	Shape-persistent macrocycle
t	Triplet
t	Time
<i>t</i>	<i>tert</i>
TBD	1,5,7-Triazabicyclo[4.4.0]dec-5-ene
TBS	<i>tert</i> -Butyldimethylsilyl
terpy	2,2';6',2''-Terpyridine

TEMPO	(2,2,6,6-Tetramethylpiperidin-1-yl)oxyl
TES	Triethylsilyl
Tf	Triflate
TFA	Trifluoroacetic acid
THF	Tetrahydrofuran
TIPS	Triisopropylsilyl
TLC	Thin-layer chromatography
TMEDA	Tetramethylethylene diamine
TMG	1,1,3,3-Tetramethylguanidine
tmphen	3,4,7,8-Tetramethyl-1,10-phenanthroline
TMS	Trimethylsilyl
TOF	Time-of-flight mass spectrometry
Tres / $t_r$	Residence time
Trp	Tryptophan
Trt	Trityl
TS	Transition state
TTTA	Tris(4-trimethylsilylmethyl-1,2,3-triazolylmethyl)amine
UV	Ultraviolet
V	Volt
v/v	Volume/volume
vis	Visible
vs	<i>versus</i>
W	Watt
Xantphos	4,5-Bis(diphenylphosphino)-9,9-dimethylxanthene
Xphos	2-Dicyclohexylphosphino-2',4',6'-triisopropylbiphenyl

*To my Family,*

*True success is self-discovery.*

– Marco Pierre White

# Acknowledgments

*If I have seen further than others, it is by standing upon the shoulders of giants.* – Isaac Newton

My nine-year journey at *Université de Montréal* has certainly been the most exhilarating and difficult experience of my life to date. When I began my undergraduate studies in chemistry, I can honestly say that I struggled to find what I wanted for myself and my future. Little did I know at the time, that uncertainty would ultimately fade away thanks to the countless individuals I have crossed paths with throughout the years. I owe these people, some giant (literally), and some not so giant, an immense debt of gratitude for all they have contributed to my personal, academic and professional lives.

Firstly, I would like to express my sincere gratitude to my research supervisor Prof. Shawn K. Collins. Thank you for your continuous support, your patience, motivation, and guidance throughout the entirety of my Ph.D. studies. More importantly however, thank you for believing in me since the very beginning of my journey. I am incredibly grateful for the unexpected opportunity that you gave me to work initially as an intern in your research group in 2010. The experience gathered during the course of that internship not only confirmed my passion for organic chemistry, but it also opened my eyes to the realm of academic research. I am equally grateful for the opportunity that you gave me to join your research group as a graduate student in 2012. Admittedly, my graduate studies were not always smooth sailing. Nevertheless, you always found a way to keep challenging me by proposing all kinds of crazy chemistry ideas. With hindsight, in doing so, you gave me eventually the confidence needed to suggest and to try out ideas of my own. I will certainly miss spending all those hours with you drawing ideas on your office's whiteboard. Thank you for placing your trust and confidence in my abilities to tackle the numerous projects we ventured on over the years. I could not have imagined having a better supervisor and mentor for my Ph.D. studies.

Secondly, I would like to acknowledge all the Collins group members I have interacted with throughout the years. There is no way I can thank you enough for being my caring and dysfunctional second family. I would like to start off by expressing my gratitude to the *old gang*,

Michael Holtz-Mulholland (aka Mike), Augusto Hernandez-Perez (aka Tito), Anne-Catherine Bédard (aka Anne-4), Mylène de Léséleuc, and Michael Raymond (aka Maddawg), for molding me into the chemist I am today. Tito and Anne-4, thank you for being my laboratory mentors and great friends. Your help and guidance were so precious to me. Both of you laid the foundation of my lab skills. More importantly, you exemplified hard work, perseverance and rigor on a daily basis. I have tried emulating your work ethic every day since. I owe a great deal of my success to the both of you. I also cherish so many wonderful memories with both of you inside and outside the lab. Mike, you have been a great organometallics mentor to me. I learned so much from your wide-ranging knowledge. I particularly enjoyed discussing with you as foodies. In a similar vein, thank you for introducing and teaching me everything there is to know about scotch whiskies. They have been at the center of many great conversations between you and me over the years. Mylène, thank you for putting up with me as an office neighbor and as a lab mate. I greatly appreciate all the time you took out of your own to answer all my questions and help me with my assignments. Your attention to detail was very much valued, especially during the preparation of our group's manuscripts. Also, even if it was not an easy mission, thank you for accompanying me on the Collins presentation template revolution all the way! Maddawg, thank you as well for putting up with me as an office neighbor and helping me out with all my assignments. I cherish our experience at the BOSS conference and our following tour of Europe. You were a great traveling partner! I also enjoyed our epic meals and great conversations outside the lab throughout the years.

I would also like to express my gratitude to the *new gang* I leave behind, Antoine Caron, Shawn Parisien-Collette (aka Junior), Éric Godin, Émilie Morin, Clémentine Minozzi (aka Clem), Jean-Christophe Grenier-Petel (aka J-C), Johann Sosoe (aka Da Real JS), Christina Gagnon, and Sacha Nguyen, for continuously upping our group's game. It has been a pleasure working with such a diverse group of talented individuals. My time as the senior group member has certainly been enriched by your unique contributions and knowledge. I hope I have been of some help to all of you in any way, shape, or form. I am confident our group's research projects will be in good hands if you continue to challenge and push each other in order to conquer new chemical frontiers. Antoine, thank you for conveying your general good humor to our group on a daily basis. You are a force to be reckoned with when you put your mind to it! While I have



gone through many ups and downs inside and outside the lab, I appreciate all those times we spent together figuring out stuff about life around several pints of ale at McCarold's. Junior, you too are a force to be reckoned with! You have become a great asset to our group, and I would like to thank you for all your helpful input on my latest projects. We have additionally had the good fortune of travelling together all over the world to present our research. I will keep fond memories from those trips. Also, I would obviously like to thank you for introducing me, and the group, to so many new board games (and cocktails!) over the years. Éric, thank you for being a great colleague, hood neighbor and badminton challenger for the past few years. Your quick wit made sure that my explanations to your questions were clear and double-checked at all times! I am especially appreciative of your constructive suggestions and ideas in group meetings. I would also like to thank you for taking on the *Cu-catalyzed synthesis of alkynyl sulfides* project. I am confident that it is in good hands, and that it will make a great paper in the not too distant future! Émilie, thank you for staying true to yourself and for bringing a much-needed breeze of gentleness to the group. I would like to thank you as well for putting up with me at every chemical and disposables order. I enjoyed having you as my personal cultural guide over the years. Watching a Shakespeare play with you in London was certainly one of the highlights from our trip in the UK! Clem, I have watched you grow as a chemist since the first day you joined the group as my intern. Your resilience throughout the internship inspired me greatly. Thankfully, I believe that both of us matured significantly in the process. We have since collaborated on several projects, and I cannot thank you enough for being such a dedicated co-worker and a great friend. J-C, I have enjoyed working with you on a photochemistry project. Behind your quiet demeanor lies a hard worker. I hope you represent our group's dual-catalysis clique well in the months to come! Also, thank you for teaching me everything there is to know about craft and microbrewed beers. Da Real JS, you possess all the traits required to *climb the ladder to success, escalator style* (– Notorious B.I.G.). I have witnessed your awakening initially as a student of mine, then as my intern, and now as my colleague. You are unquestionably a wholehearted force of nature. I want to thank you for being such a receptive and hard-working intern. Your path to becoming a graduate student in our group has taught me a great deal about strength of character. Christina, even though you are a biochemist, your bubblyness and sassiness blended seamlessly in our group. I hope that your background will serve you well in the group's ambitious enzyme-related chemistry! Also, thank you for taking

good care of my old lab hood! Sacha, our paths were cut short, but from what I hear you have integrated the group nicely. Keep up the good work and good luck in your future endeavors!

I would also like to express my gratitude to the many interns I have engaged with over the years, Florence Josse, Youssef Sanogo, Julien Masset, Amaury Dubart, Alexandre Lévesque, Patrick Chartier, Corentin Cruché (aka Coco), Mathieu Morency, Xavier Abel-Snape, Florian D'Ambra, and Milan Vander Wee. Your various backgrounds and unique personalities have contributed distinct flavors to the group. I hope your experiences in the Collins group were as enriching as mine. Coco, thank you for being such a dedicated and hard-working intern. Your contributions to the *photochemical synthesis of alkynyl sulfides* project was very much appreciated. It gave me great pleasure to watch you progress into a true researcher during your time in our group. You definitely have what it takes to become a skilful graduate student! Mathieu, thank you too for being such a dedicated and hard-working intern. Your desire to learn anything and everything was extremely stimulating as your supervisor. I am delighted that you made great strides as a synthetic chemist over the summer, and I am confident your determination will serve you well in your future endeavors.

I would also like to express my gratitude to the group members who guided me during my first internship, Marie-Ève Mayer, Philippe Bolduc, Tatiana Le Gall, and Anna Vlassova. Thank you all for your patience, kindness, and joviality throughout my entire experience in the group. More importantly, thank you for giving me a glimpse into the grad school world!

I would also like to express my gratitude to Vanessa Kairouz, an honorary member of the Collins group, for her long-standing friendship since the very beginning of my chemistry journey. We have shared many good times together. I have certainly enjoyed our complicity throughout the years! I am glad that we were able to design a new undergraduate flow experiment together in recent times. Hopefully our *J. Chem. Educ.* manuscript will be published in the not too distant future!

In addition, I would like to acknowledge the countless past and current members from the Lebel, Charette, Schmitzer, Masson, Pelletier, and Hanessian groups that I have interacted with throughout the years. Thank you all for your fellowship and good advice. Many of you

(you know who you are!) have become delightful friends of mine. I would like to thank these people for making my graduate studies even more memorable!

I must also acknowledge all the people who continuously make using our department's facilities possible from day to day. I would like to thank the teams from the *Regional Centre of NMR Spectroscopy*, the *Regional Mass Spectrometry Centre*, the *X-Ray Diffraction Laboratory*, the *Machine Shop*, and the *Continuous Flow Synthesis Laboratory* for their help and patience over the years. I would also like to thank the administrative staff for always making sure my records were in order throughout the entirety of my undergraduate and graduate studies.

I am additionally grateful for the numerous scholarships I have received over the years from the *Département de chimie*, the *Faculté des études supérieures et postdoctorales*, the *Faculté des arts et des sciences*, the *Centre in Green Chemistry and Catalysis*, and the *NSERC CREATE Program in Continuous Flow Science*. These scholarships have allowed me not only to maintain focus on my studies and research, but also to participate in informative chemistry conferences around the world.

On a more personal note, I would like to acknowledge my amazing group of friends (you too know who you are!). I'm truly grateful to have such authentic and caring friendships, many of which stemmed from elementary and high school! Thank you all for listening, encouraging me, offering me advice, and supporting me since the very beginning. You have certainly helped me maintain some form of sanity through this entire experience!

I would also like to acknowledge the love of my life: Lilliam Schulz Bechara. I am so lucky that chemistry, oddly enough, enabled us to cross paths along my academic journey! You are truly one of the most kind-hearted, thoughtful and witty people I have ever known. I sincerely thank you, and your family, for supporting me unconditionally. I would especially like to thank you for being so patient and understanding with me during the last months of my Ph.D. studies. Thank you for your part in my journey. The best is yet to come!

Lastly, I would like to acknowledge the most influential people in my life: my family. You, Liana Buttino (aka mom), Robert Santandrea (aka dad), Randy Santandrea (aka brother), my grand-parents, my aunts, my uncles, my cousins, and my extended families, have all played a pivotal role in my success. I am so grateful to all of you for giving me unconditional love and

support throughout my entire academic journey. Brother, our relationship has matured in many ways over the years, for example, you referring to me as a nerd no longer makes me upset! But in all seriousness, thank you for putting up with me through the stressful and difficult times. You helped me realize that there is more to life than just school and work. I remind myself of that fact every day. Also, thank you for sharing your passion for photography with me. My group has certainly benefited from it thanks to you! Mom and dad, there are few words that can adequately describe my gratitude toward both of you. Thank you for believing in me and giving me the liberty to choose what I desired. Although my research remained vague to you over the years, you were willing to support any decision I made. Thank you for your selfless love and care, as well as the many sacrifices you made to shape my life. Thank you for always being there for me and for guiding me on the right path.

# 1. Introduction to Macrocycles

## 1.1 Importance and Applications of Macrocycles

Macrocycles are medium to large ring compounds that intersect between small organic molecules and larger biomolecules such as proteins (Figure 1.1).<sup>1</sup> Formally, macrocycles are defined by IUPAC as a cyclic molecule possessing at least twelve atoms on the main ring's scaffold,<sup>2</sup> although considering eight- to eleven-membered rings macrocycles is unsettled in the literature nowadays. Macrocycles are commonly found in natural products and in pharmaceutical molecules. Interestingly, about 20 % of all known natural products from terrestrial and marine sources possess a macrocyclic core, although their cyclization biogenesis patterns are not fully understood.<sup>3</sup> Macrocycles combine appealing attributes from both the small and the larger molecule spheres, because they can be synthesized with relative control like small molecule drugs, and they can possibly bind to specific sites of biomolecules as they occupy unique chemical space.<sup>4</sup> Unsurprisingly, macrocycles are now utilized in a wide array of fields such as medicinal chemistry, aroma chemistry, supramolecular chemistry, materials science, and biology.

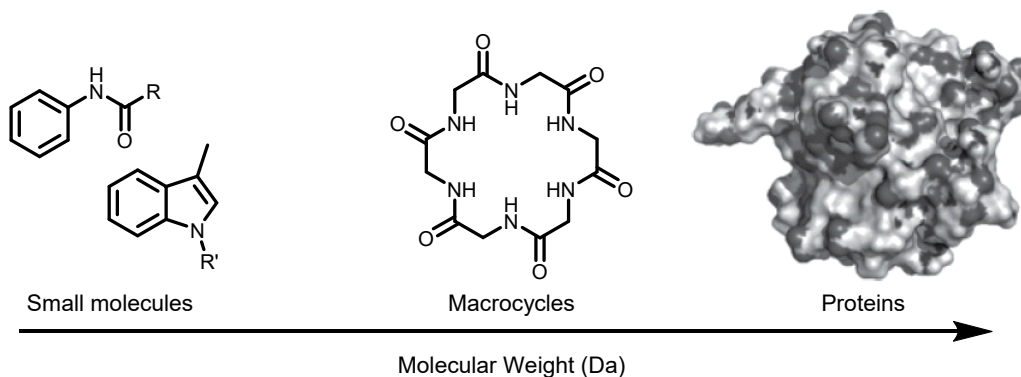


**Figure 1.1** Macrocycles at the intersection of small molecules and larger biomolecules

### 1.1.1 Medicinal Chemistry

Macrocycles that are used in medicinal chemistry need to account for two closely related factors: structural preorganization, which minimizes the entropic costs upon binding onto a biomolecule, and flexibility, which permits steric adjustments to the desired active site.<sup>1b</sup> Medicinal chemists tend to design orally-active drug candidates around Lipinski's "rule of five" as guidelines for identifying pharmaceutically-desirable compounds.<sup>5</sup> It predicts that good absorption or permeation is more likely when there are no more than five hydrogen-bond donors, ten hydrogen-bond acceptors, a molecular weight less than 500 and a calculated Log P less than five. Other guidelines such as having ten or less rotatable bonds, and a polar surface area equal or less than 140 Å, have emerged as better suited parameters for producing drug candidates.<sup>6</sup> Larger biologically active macrocycles do not satisfy Lipinski's molecular weight criterion. The integration of macrocyclic structures in medicine has yet to be fully exploited despite their known therapeutic potential.

Many macrocyclic natural products, including erythromycin A (**1.1**) and epothilone B (**1.2**), and their respective analogues, have been used successfully as drugs (Figure 1.2).<sup>7</sup> Erythromycin A, a potent antibiotic utilized around the world, is now produced biosynthetically on industrial scales, because the chemical synthesis of the compound is considered economically non-viable.<sup>8</sup> Total syntheses of epothilone B, an anticancer drug, have been achieved,<sup>9</sup> but have also not provided an economically viable alternative to fermentation.

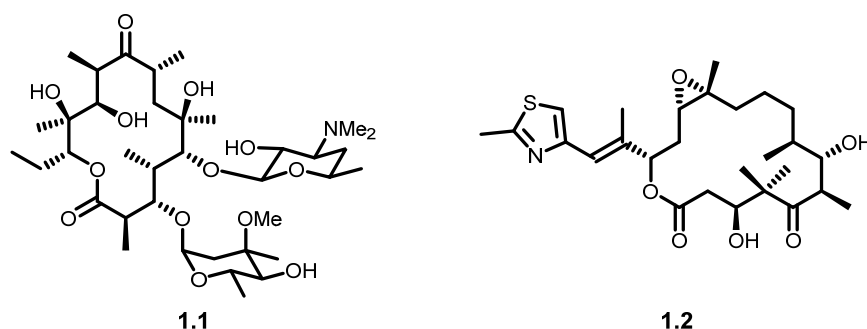


**Figure 1.2** Structures of erythromycin A (**1.1**) and epothilone B (**1.2**)

Other types of macrocyclic drugs include cyclic peptides, some of which are also natural products. Peptide-based macrocycles hold many pharmacokinetic advantages in comparison to their linear counterparts.<sup>10</sup> Macrocyclization has been used in peptide chemistry as an efficient

way of restricting conformation, reducing polarity, increasing proteolytic stability, and improving druggability.<sup>4, 11</sup> Cyclic peptides are relatively straightforward to synthesize because of their modular assembly from amino acid building blocks. Cyclic peptides are considered desirable molecules for producing drug candidates.<sup>12</sup> Tyrocidine (**1.3**), a naturally-occurring cyclodecapeptide, was used in therapeutics as early as 1939 for its antibacterial activity (Figure 1.3).<sup>13</sup> Later in 1941, tyrocidine was mixed with gramicidin S (**1.4**), another macrocyclic peptide, to produce the first commercialized antibiotic, tyrothricin, which is still in use today.

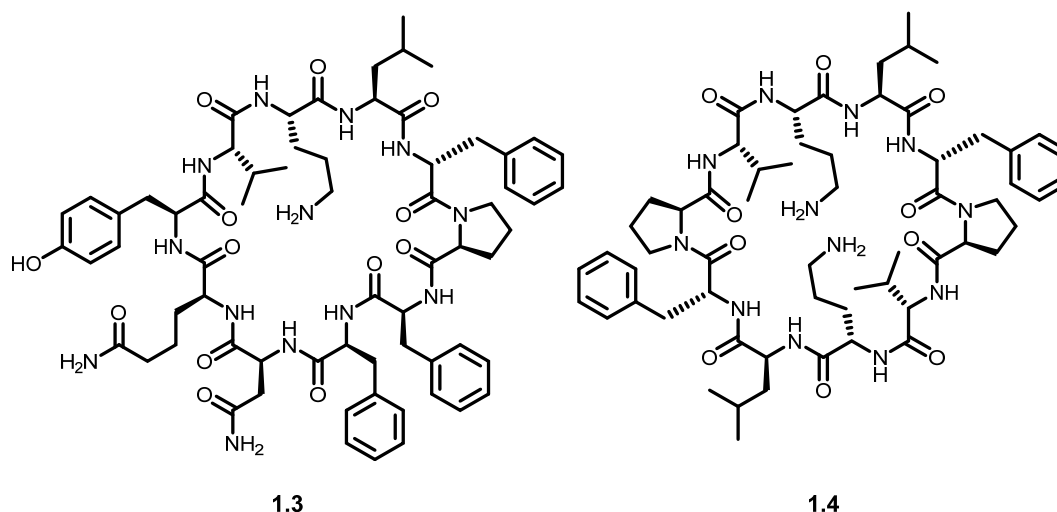


**Figure 1.3** Structures of tyrocidine (**1.3**) and gramicidin S (**1.4**)

Chemical insight from both macrocyclic natural products and cyclic peptides has given rise to numerous families of synthetic macrocycles over the last few decades. The macrocycles have mostly been designed and synthesized in an academic setting, though some pharmaceutical drug discovery groups have successfully completed the total syntheses of biologically active macrocycles.<sup>14</sup> The synthesis of macrocycle BILN 2061 (**1.5**) was first disclosed in 2003 (Figure 1.4).<sup>15</sup> It exhibited potent and competitive inhibition of the NS3 proteases of hepatitis C virus genotypes 1a and 1b and was the first of its class in human trials.<sup>16</sup> Potent tripeptide mimetics were initially identified through extensive NMR and X-ray studies, but it was found that the rigidification of their scaffold by an intramolecular linkage produced macrocyclic inhibitors displaying desirable drug-like properties and improved NS3 protease inhibition in cells.<sup>17</sup> Although its development was ceased in phase 1b clinical trials because of toxicity in

animals, BILN 2061 has paved the way for the design of new macrocyclic inhibitors for hepatitis C.

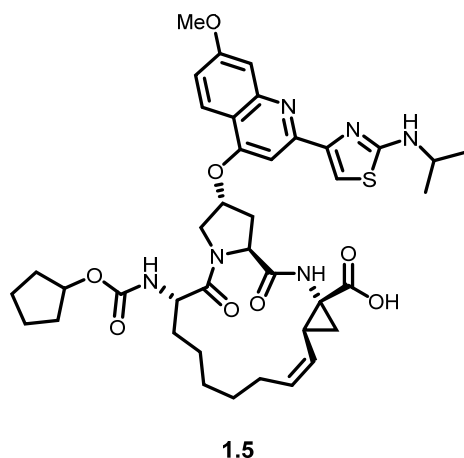


**Figure 1.4** Structure of BILN 2061 (**1.5**)

### 1.1.2 Aroma Chemistry

Aroma chemistry is omnipresent in most of today's manufacturing industries. It consists of synthesizing and employing aroma compounds for different purposes. Aroma chemicals are a class of compounds that possess an odor, either pleasant or unpleasant, and are commercially known as fragrances or flavors, in which case the latter influences the sense of taste.<sup>18</sup> Aroma chemicals generally have relatively low molecular weights, which contributes to their desired volatility. Among the various types of aroma compounds are musks. Musks encompass three structurally distinct compounds: nitro-containing musks, polycyclic musks and macrocyclic musks.

Musks have been used for over a century because of their desirable sweet and fruity smells, but not all have maintained industrial popularity. Nitro-containing musks such as **1.6** (Figure 1.5) were eventually found to be explosive and toxic,<sup>19</sup> and have since been restricted or banned from cosmetic usage in most countries. An alternative to nitro-containing musks were polycyclic musks like **1.7**, but it produced weaker scents and were found problematic with poor biodegradability.<sup>19b</sup>



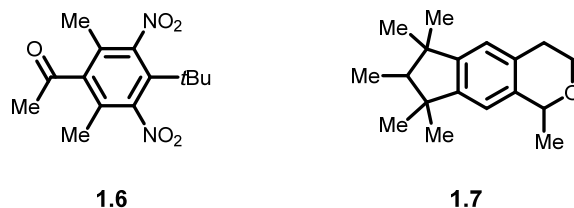


**Figure 1.5** Structures of musk ketone **1.6** and polycyclic musk **1.7**

Macrocyclic musks offer some unique olfactory properties and superior biodegradability when compared to nitro-containing and polycyclic musks.<sup>20</sup> Some macrocyclic musks were extracted early on from natural sources such as animals and plants (Figure 1.6). Macrocyclic ketones like muscone<sup>21</sup> (**1.8**) are generally found in animal glands, while macrolactones are naturally found in plants. Their synthesis remained however a challenge on an industrial scale up until the early nineties. Since then, optimized syntheses have enabled the production of popular macrocyclic musks such as exaltolide (**1.9**) and isoambrettolide (**1.10**) on metric-ton scales.<sup>22</sup>

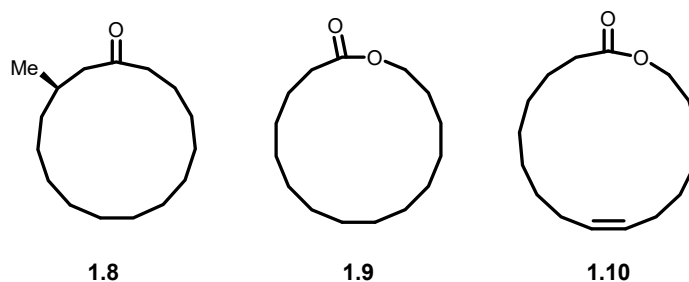


**Figure 1.6** Structures of muscone (**1.8**), exaltolide (**1.9**) and isoambrettolide (**1.10**)

### 1.1.3 Supramolecular Chemistry

Macrocycles are ubiquitous in supramolecular chemistry. They often are heteroatom-rich macrocycles with the possibility of interacting with smaller or larger molecules through host-guest interactions.<sup>23</sup> The 1987 Nobel Prize in Chemistry was awarded to Cram,<sup>24</sup> Lehn<sup>25</sup> and Pedersen<sup>26</sup> for "their development and use of molecules with structure-specific interactions of high selectivity". Their pioneering work that merited the Nobel Prize was based primarily on the synthesis of macrocycles including crown ethers, cryptands, and others (Figure 1.7).

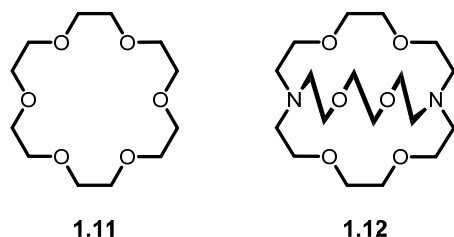


**Figure 1.7** Structures of 18-crown-6 (**1.11**) and [2.2.2]cryptand (**1.12**)

More recently, the 2016 Nobel Prize in Chemistry was awarded to Sauvage,<sup>27</sup> Stoddart<sup>28</sup> and Feringa<sup>29</sup> for "the design and synthesis of molecular machines". The Nobel Laureates' important contributions on mechanically bonded molecules could arguably not have been made possible without the seminal work by Sauvage, and later by Stoddart, on the template-directed synthesis of catenanes (Figure 1.8).<sup>30</sup> Prior to their findings, the synthetic routes to the synthesis of [2]catenanes (**1.13**), two noncovalently interlocked macrocyclic structures, were too low-yielding or too arduous.

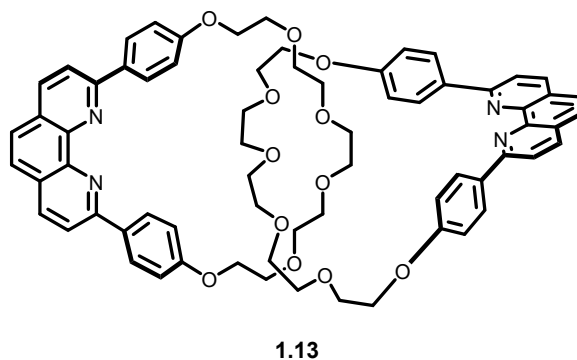


**Figure 1.8** Example of a [2]catenane

Macrocycles have remained closely linked to other supramolecular applications as they have played a pivotal role in the expansion of organic synthesis, molecular electronics and materials science.<sup>31</sup> For instance, shape-persistent macrocycles based on acetylenic scaffoldings have attracted immense attention because of their unique symmetrical structures and novel properties (Figure 1.9).<sup>32</sup> In comparison to flexible macrocycles, shape-persistent macrocycles are designed to be more conformationally rigid to facilitate their assembly into highly organized supramolecular systems. Hence, some conjugated macrocyclic structures have been used as building blocks for nanotubes or 2D porous materials.<sup>33</sup>

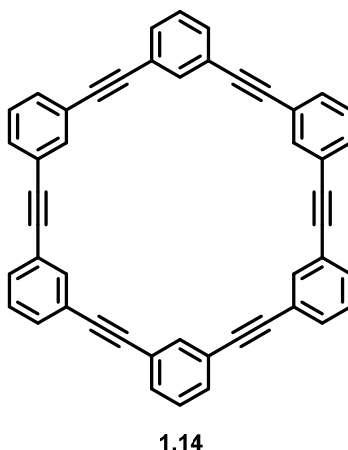


**Figure 1.9** Example of a shape-persistent macrocyclic framework (1.14)

## 1.2 Synthetic Challenges in Macrocyclization Reactions

As mentioned in Section 1.1, macrocycles have impacted multiple fields over the past decades. However, their utilization has yet to be fully exploited. A limiting factor is certainly the challenge associated with their synthesis. The scientific community's hesitance to develop syntheses integrating a key macrocyclization step is however, not unwarranted. Thermodynamic constraints such as entropy and enthalpy, as well as reactive conformations, need to be considered when planning the synthesis of macrocycles.

### 1.2.1 Kinetic Aspects

Early work by Ruzicka<sup>34</sup> and Ziegler<sup>35</sup> illustrated that the synthesis of macrocycles through conventional methods, that involve an intramolecular head-to-tail reaction between two functional groups of an acyclic precursor, was in competition with intermolecular oligomerization. An intramolecular reaction is first order in the reagent concentration, given that it is an unimolecular reaction, and an intermolecular, or oligomerization, pathway is therefore second order as it is a bimolecular reaction (Figure 1.10). Consequently, low substrate concentrations should be applied to favor the desired intramolecular pathway over the intermolecular pathway.<sup>36</sup> Interestingly, high dilution conditions had already been utilized by Ruggli in 1912 for the synthesis of a 12-membered ring.<sup>37</sup>

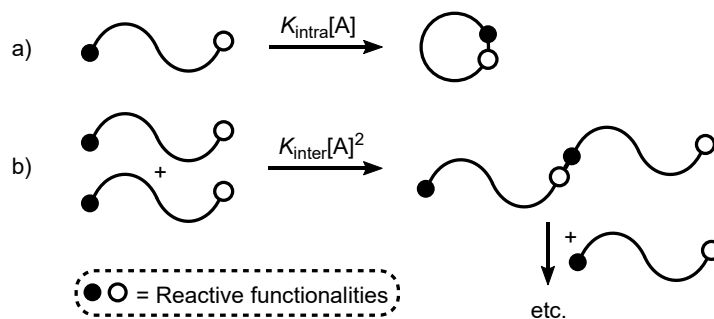


**Figure 1.10** Reaction rates of intramolecular (a) and intermolecular (b) processes

Kinetics and activation parameters for the synthesis of lactones (**1.16**) from  $\omega$ -bromoalkylcarboxylates (**1.15**) were seminally studied by Illuminati, Gali and Mandolini (Figure 1.11).<sup>38</sup> They calculated the rate of intramolecular cyclization as a function of the ring size for a series of lactones. The more favorable kinetic constants ( $k_{\text{intra}}$ ) for the transformation were found to lead to four- to six-membered rings, while the less favorable kinetic constants correspond to the formation of eight- to twelve-membered rings. Moreover, cyclization rates did not differ significantly for twelve- or greater membered lactones, which are comparable to rates of three- and seven-membered rings.

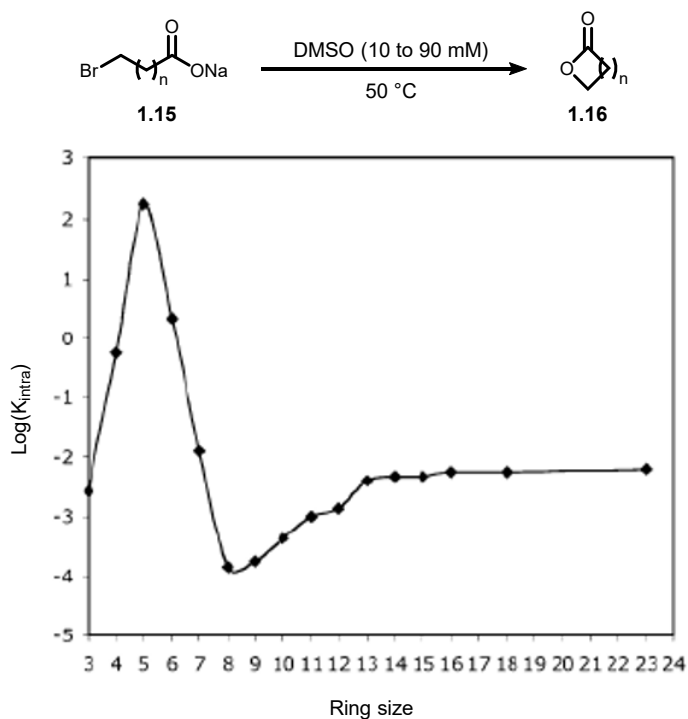


**Figure 1.11** Rate of lactone formation as function of ring size

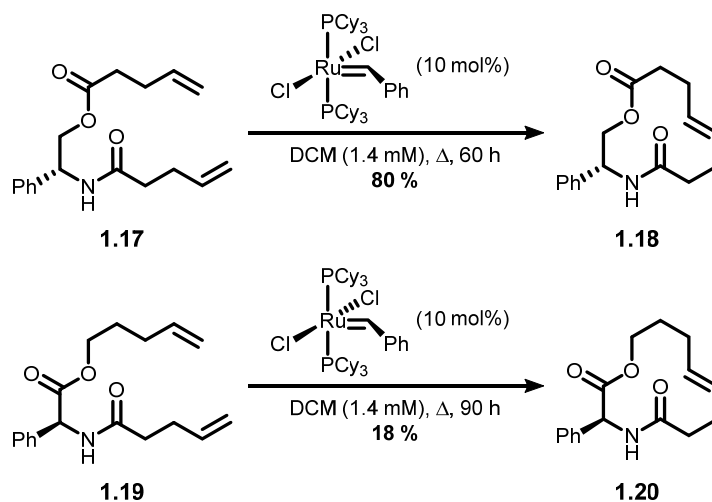
It has been rationalized that cyclization rates are the result of both the open chain initial state (entropic factor) and the activation energy of the transition state, which mirrors the structure of the cyclic product (enthalpic factor).<sup>39</sup> Entropically, the probability term ( $\Delta S^\ddagger$ ), which is the probability of an encounter between two reactive functionalities, decreases as the number of atoms between them increases (*i.e.* above twelve-membered rings), while enthalpically, the highest strains (highest  $\Delta H^\ddagger$  values) are observed for eight- to twelve-membered ring.<sup>40</sup> It is thought that entropic factors prevail for above twelve-membered rings, as the steric strain is released for larger macrocycles, whereas the enthalpic factor outweighs the entropic factors for eight- to twelve-membered rings. Three types of strain can influence the formation of a macrocycle: 1) Pitzer strain, or torsional strain, due to imperfect staggered conformations between adjacent atoms in the ring; 2) Baeyer strain due to deformation of the ring bond angles, and 3) Prelog strain, or transannular strain, due to interactions between atoms across the ring.<sup>41</sup>

The aforementioned considerations in macrocyclization reactions have challenged synthetic chemists to develop other strategies, complementary to high dilution techniques, to favor the rate of intramolecular cyclization. For instance, a slow addition process is often employed to achieve high dilution. The method consists of slowly adding a linear precursor, with or without additional reagents or catalysts, into the reaction mixture by means of a syringe pump. The technique is quite effective as it maintains low concentrations of the linear precursor at any given time in the reaction mixture, all while using less solvent. Slow addition processes are often performed for small- to medium-scale reactions, but less so for large-scale transformations as the setup can be tedious and cumbersome. Solid-phase synthesis is another strategy to artificially attain high dilution conditions. Although it is generally used to prepare peptides and oligonucleotides,<sup>42</sup> it can also serve for macrocyclization purposes.<sup>43</sup> The system exploits pseudodilution effects caused from the low concentration of a reagent's or a catalyst's active sites in a phase separate from the one containing the macrocyclic precursor. Lastly, a phase separation strategy can similarly bypass the need for slow addition and high dilution conditions to perform macrocyclization reactions.<sup>44</sup> Its control of dilution effects is achieved by sequestering the catalytic system from the macrocyclic precursor in biphasic media. By doing so, the effective concentration of the acyclic substrate at the interface of both liquid phases

would be low and mimic concentrations achieved by high dilution techniques without the need for large quantities of solvents.

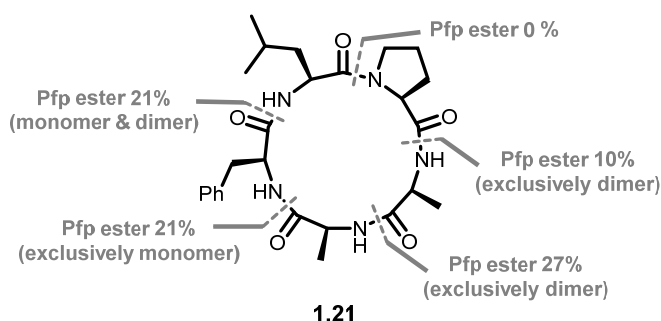
### 1.2.2 Reactive Conformation

The kinetic aspects described in section 1.2.1 do not consider macrocyclic precursors that contain various substitutions and functional groups along their backbones. It is more difficult to predict the macrocyclization outcome of such linear precursors as they can spatially preorganize in conformations that might affect, favorably or unfavorably, the rate of cyclization. Therefore, ring size becomes a less critical indicator of the macrocyclization result, and a more significant factor becomes the ease with which the macrocyclic precursor can adopt the favored reactive conformation.<sup>45</sup> A conformation-directed macrocyclization reaction was specifically developed by Schreiber as proof of concept (Scheme 1.1). Ring-closing metathesis (RCM) of conformationally-tailored diene precursor **1.17** in the presence of Grubbs' catalyst provided macrocycle **1.18**, possessing minimal transannular and torsional strain according to X-ray crystallographic analysis, in 80 % yield.<sup>46</sup> Displacing the structure of the ester led to a conformationally nonideal macrocyclization precursor **1.19**, which only provided 18 % of strained macrocycle **1.20** under identical catalyst loadings.



**Scheme 1.1** The importance of conformation in RCM

It can be particularly daring to predict the macrocyclization outcome of more complex molecules like cyclic peptides. Schmidt and Langners's work on sequence dependency in forming 15-membered macropeptides exemplifies the challenges faced in the process.<sup>47</sup> The Pro-Ala-Ala-Phe-Leu macrocycle **1.21** consists of five amide linkages, all of which are possible macrolactamization disconnections (Scheme 1.2). Macrocyclization was attempted at all five sites using a pentafluorophenyl (Pfp) ester activation strategy. Depending on the amide linkage that was formed in the ring-closing step, wide variability in reaction selectivity was observed. Whereas the desired monomeric product was formed in some cases, the cyclic dimer, or no product, was also formed in others.



**Scheme 1.2** Attempts to synthesize Pro-Ala-Ala-Phe-Leu macrocycle **1.21**

While some macrocyclic precursors naturally adopt predetermined conformations, synthetic chemists have also developed several strategies to favor the rate of intramolecular cyclization based upon conformational control. The alternative strategies to high dilution techniques improve the efficiency of macrocyclization by structurally modifying a macrocyclic precursor. Doing so forces the adoption of a reactive conformation that favors end-to-end interactions of the substrate, thus enabling the ring-closing step. For example, conformational control can be achieved using covalently linked auxiliaries through  $\pi$ - $\pi$  interactions.<sup>48</sup> Efficient as it may be, the method requires additional synthetic steps for the addition and removal of the auxiliary, and is substrate-limited. The *gem*-dialkyl effect, commonly referred to as the Thorpe-Ingold effect, is the name given to the acceleration of a cyclization due to the replacement of hydrogen atoms with alkyl groups on the carbons tethering the two reacting centers.<sup>49</sup> While the strategy has been applied successfully toward the formation of small- and medium-sized rings, it has had limited influence on the cyclization of large rings.<sup>50</sup> Other examples exploiting supramolecular interactions and not necessitating covalent attachment of an auxiliary have also

been reported. Macrocyclizations have been made possible through  $\pi$ - $\pi$  interactions,<sup>51</sup> templated metal ion chelation<sup>52</sup> and planned intramolecular hydrogen bonding.<sup>53</sup> Even though such approaches are more economical in step count, they are mainly substrate-limited.

## 1.3 Employing Catalysis for Macrocycle Synthesis

Despite the growing interest in macrocycles for drug discovery over the past ten years, research aimed at developing novel and sustainable macrocyclization methods has been limited. More often than not, synthetic chemists rely mostly on traditional macrocyclization reactions when planning the ring-closing step toward a desired macrocycle. In this context, macrolactonizations,<sup>54</sup> macrolactamizations,<sup>12b</sup> Wittig-type olefinations<sup>55</sup> and Mitsunobu alkylations<sup>56</sup> remain very much in use today. The concept of sustainability in organic synthesis has gained in importance, and may be considered to minimize the amount of waste generated when employing excess reagent-based methods such as the above-mentioned established protocols.<sup>57</sup> Alternatively, catalysis-based macrocyclizations may offer more environmentally benign reaction conditions by reducing stoichiometric waste by-products and facilitating purification to isolate the desired product. The most widely used catalytic macrocyclization reactions are ring-closing olefin metathesis, copper-catalyzed azide-alkyne cycloadditions and palladium-catalyzed cross-couplings.

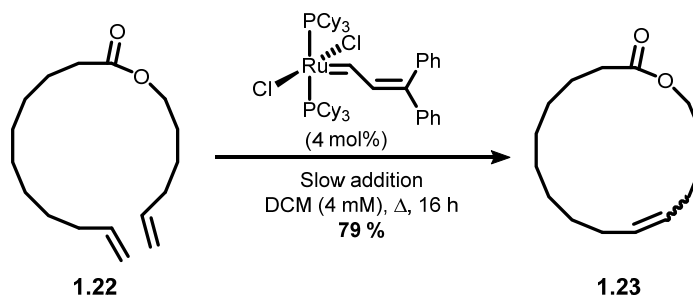
### 1.3.1 Ring-Closing Metathesis

Olefin metathesis is defined as a chemical reaction between two carbon-carbon double bonds from which the double-bonding atom groups change places with one another. The carbon-carbon bond-forming transformation is versatile and efficient. Its use has led to a wealth of applications over the past three decades.<sup>58</sup> Olefin metathesis reactions can be divided into four main categories: cross metathesis (CM), ring-opening metathesis polymerization (ROMP), acyclic diene metathesis polymerization (ADMET) and ring-closing metathesis (RCM).

RCM has played a significant role in synthesizing small- to medium-sized carbocyclic and heterocyclic compounds.<sup>59</sup> The transformation, which relies generally on ruthenium catalysis, has been successfully applied to the synthesis of both natural and unnatural macrocyclic products.<sup>60</sup> The first macrocyclic RCM reaction was reported by Fürstner toward

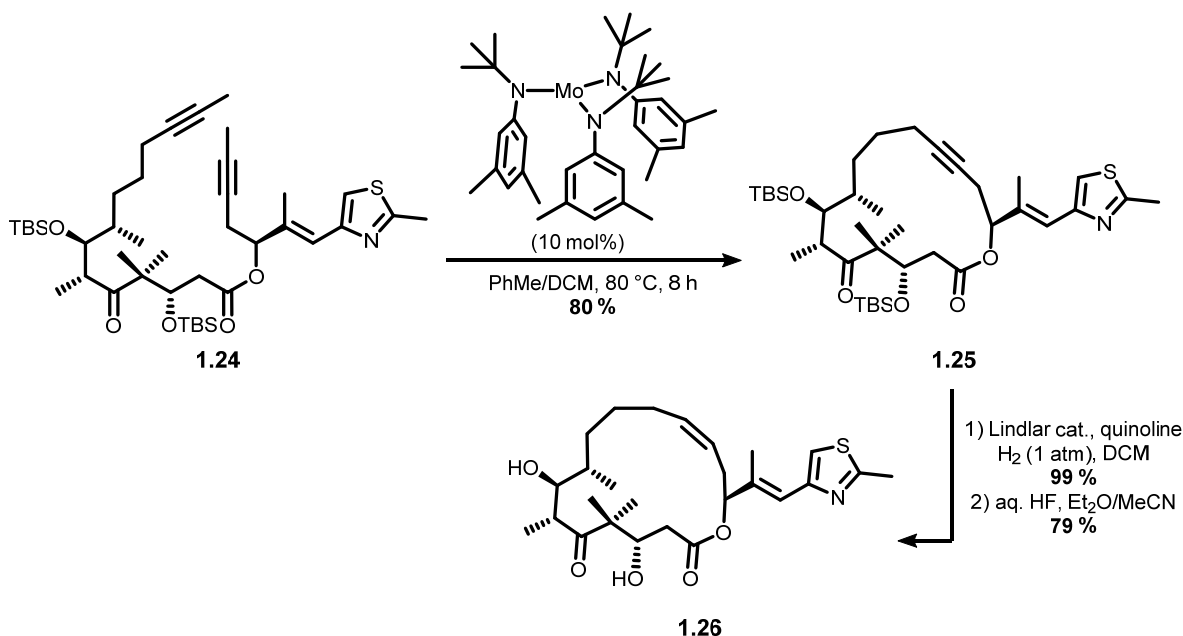


the synthesis of a cyclic precursor of exaltolide (**1.9**, see Section 1.1.2).<sup>61</sup> When diene **1.22** was submitted to a ruthenium catalyst in dichloromethane (4 mM) at reflux, the desired cyclic alkene **1.23** was generated in 79 % yield (Scheme 1.3). The authors further demonstrated that the methodology could be applied to the synthesis of other 15- to 21-membered macrocycles.



**Scheme 1.3** Synthesis of macrolactone **1.23** via RCM

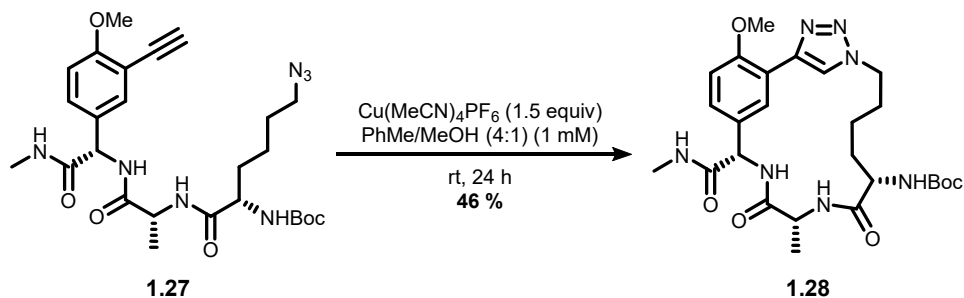
Macrocycles have also been synthesized using alkyne metathesis. After its discovery, alkyne metathesis was scarcely used in organic synthesis in comparison to olefin metathesis. Nevertheless, seminal work from Fürstner showcased the power and utility of ring-closing alkyne metathesis (RCAM)<sup>62</sup> by solving a stereochemical problem that could not be addressed directly by RCM. RCM usually provided macrocyclic olefins as mixtures of the (*E*)- and (*Z*)-isomers, the ratio of which highlighted the poor selectivity toward the (*Z*)-isomer. The selectivity issue was resolved through sequential RCAM and semi-reduction reactions, which gave access to a stereoselective route to (*Z*)-olefins.<sup>63</sup> The strategy was later applied toward the synthesis of epothilone C (**1.26**, Scheme 1.4).<sup>64</sup> Diyne **1.24** was converted to 16-membered macrocycle **1.25** in 80 % yield using a molybdenum amido complex in a toluene/dichloromethane mixture at 80 °C. Epothilone C was obtained in 79 % yield by means of a Lindlar reduction of cycloalkyne **1.25**, followed by a deprotection of silyl ether groups under aqueous hydrogen fluoride conditions. More recently, macrocyclic products have been directly and efficiently accessed through catalyst-controlled stereoselective RCM methodologies.<sup>65</sup>



**Scheme 1.4** Synthesis of macrolactone **1.25** and epothilone C (**1.26**)

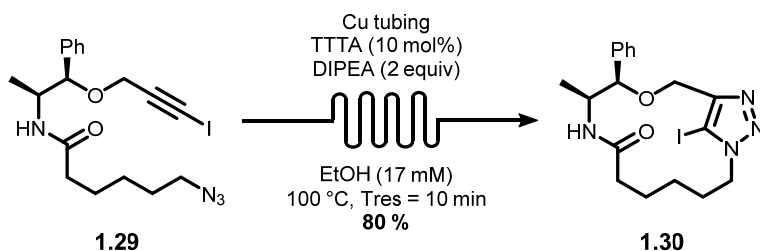
### 1.3.2 Copper-Catalyzed Azide-Alkyne Cycloaddition

The copper-catalyzed azide-alkyne cycloaddition (CuAAC), commonly referred to as a Cu-catalyzed Huisgen cycloaddition, is a straight-forward, robust and reliable transformation that has been exploited in many chemical disciplines.<sup>66</sup> The [3+2] cycloaddition's chemical orthogonality and versatility have allowed its use in drug discovery,<sup>67</sup> pharmacology<sup>68</sup> and materials science.<sup>69</sup> CuAAC is considered as "click" chemistry, because it meets the criteria associated with very efficient chemical transformations:<sup>70</sup> modular, wide in scope, high yielding, generating only inoffensive by-products, stereospecific, mild reaction conditions, using readily available starting materials and reagents, and enabling effective product isolation. Unsurprisingly, CuAAC is gaining increasing importance in the macrocycle field, due in part to the 1,2,3-triazole adduct serving as a *trans* amide bond isostere.<sup>71</sup> For example, a vancomycin-inspired tripeptide mimic **1.28** was synthesized in 46 % yield using CuAAC of precursor **1.27** under mild conditions (Scheme 1.5).<sup>72</sup>



**Scheme 1.5** Synthesis of macrocyclic triazole **1.28**

Macrocyclic CuAACs have been transposed to continuous flow chemistry in an effort to improve the macrocyclization outcome.<sup>73</sup> James reported the synthesis of 12- to 31-membered 5-iodo-1,2,3-triazole-containing macrocycles under continuous flow conditions.<sup>74</sup> The copper azide-iodoalkyne cycloaddition (CuAiAC) was achieved by using tris((1-*tert*-butyl-1*H*-1,2,3-triazolyl)methyl)amine (TTTA) as ligand and DIPEA as base (Scheme 1.6). Acyclic precursor **1.29** was converted to macrocycle **1.30** in 80 % yield following a ten-minute residence time in the copper reactor of the continuous flow apparatus. The resulting macrocyclic iodotriazoles could serve as a point of diversification because the iodide can be successfully reacted in palladium-catalyzed cross-coupling reactions.



**Scheme 1.6** Synthesis of macrocyclic iodotriazole **1.30**

## 1.4 Conclusions

Natural and unnatural macrocycles are ubiquitous in most fields including medicinal, aroma and supramolecular chemistry. Although their use has yet to be fully exploited because of certain kinetic and geometric constraints, chemists have successfully developed strategies such as high dilution and conformational control to overcome the recognized synthetic boundaries. However, chemists tend to rely on established stoichiometric-reagent-based macrocyclization reactions when designing a synthetic route toward a desired macrocycle.

Efficient and reliable catalytic macrocyclizations, such as RCM and CuAAC, are leading the way toward the development of more novel and sustainable approaches for macrocycle synthesis.<sup>75</sup> Additional transition-metal-catalyzed reactions toward macrocycles are expected to favor macrocyclization to evolve more useful and powerful chemistry.

## 1.5 Bibliography

1. (a) Mallinson, J.; Collins, I. *Future Med. Chem.* **2012**, *4*, 1409-1438; (b) Driggers, E. M.; Hale, S. P.; Lee, J.; Terrett, N. K. *Nat. Rev. Drug Discov.* **2008**, *7*, 608-624.
2. McNaught, A. D.; Wilkinson, A. IUPAC. Compendium of Chemical Terminology, 2nd ed. (the "Gold Book"). Blackwell Scientific Publications: Oxford, 2014; p 870.
3. Frank, A. T.; Farina, N. S.; Sawwan, N.; Wauchope, O. R.; Qi, M.; Brzostowska, E. M.; Chan, W.; Grasso, F. W.; Haberfield, P.; Greer, A. *Molec. Divers.* **2007**, *11*, 115-118.
4. Marsault, E.; Peterson, M. L. *J. Med. Chem.* **2011**, *54*, 1961-2004.
5. Lipinski, C. A.; Lombardo, F.; Dominy, B. W.; Feeney, P. J. *Adv. Drug Deliv. Rev.* **2001**, *46*, 3-26.
6. (a) Veber, D. F.; Johnson, S. R.; Cheng, H.-Y.; Smith, B. R.; Ward, K. W.; Kopple, K. D. *J. Med. Chem.* **2002**, *45*, 2615-2623; (b) Doak, B. C.; Zheng, J.; Dobritsch, D.; Kihlberg, J. *J. Med. Chem.* **2016**, *59*, 2312-2327.
7. Gaynor, M.; Mankin, A. S. *Curr. Top. Med. Chem.* **2003**, *3*, 949-960.
8. Wu, J.; Zhang, Q.; Deng, W.; Qian, J.; Zhang, S.; Liu, W. *Appl. Environ. Microbiol.* **2011**, *77*, 7508-7516.
9. (a) Nicolaou, K. C.; Winssinger, N.; Pastor, J.; Ninkovic, S.; Sarabia, F.; He, Y.; Vourloumis, D.; Yang, Z.; Li, T.; Giannakakou, P.; Hamel, E. *Nature* **1997**, *387*, 268-272; (b) Su, D.-S.; Meng, D.; Bertinato, P.; Balog, A.; Sorensen, E. J.; Danishefsky, S. J.; Zheng, Y.-H.; Chou, T.-C.; He, L.; Horwitz, S. B. *Angew. Chem. Int. Ed.* **1997**, *36*, 757-759; (c) Wang, J.; Sun, B.-F.; Cui, K.; Lin, G.-Q. *Org. Lett.* **2012**, *14*, 6354-6357.
10. Maher, S.; Brayden, D. J. *Drug Discov. Today Technol.* **2012**, *9*, e113-e119.
11. (a) Bockus, A. T.; McEwen, C. M.; Lokey, R. S. *Curr. Top. Med. Chem.* **2013**, *13*, 821-836; (b) Horswill, A. R.; Benkovic, S. J. *Cell Cycle* **2005**, *4*, 552-555.
12. (a) Yudin, A. K. *Chem. Sci.* **2015**, *6*, 30-49; (b) White, C. J.; Yudin, A. K. *Nat. Chem.* **2011**, *3*, 509-524; (c) Zhang, X.; Lu, G.; Sun, M.; Mahankali, M.; Ma, Y.; Zhang, M.; Hua, W.; Hu, Y.; Wang, Q.; Chen, J.; He, G.; Qi, X.; Shen, W.; Liu, P.; Chen, G. *Nat. Chem.* **2018**, 10.1038/s41557-018-0006-y.
13. Joo, S. H. *Biomol. Ther.* **2012**, *20*, 19-26.
14. Godin, É.; Bédard, A.-C.; Raymond, M.; Collins, S. K. *J. Org. Chem.* **2017**, *82*, 7576-7582.
15. Lamarre, D.; Anderson, P. C.; Bailey, M.; Beaulieu, P.; Bolger, G.; Bonneau, P.; Bös, M.; Cameron, D. R.; Cartier, M.; Cordingley, M. G.; Faucher, A.-M.; Goudreau, N.; Kawai, S. H.; Kukolj, G.; Lagacé, L.; LaPlante, S. R.; Narjes, H.; Poupart, M.-A.; Rancourt, J.; Sentjens, R. E.; St George, R.; Simoneau, B.; Steinmann, G.; Thibeault, D.; Tsantrizos, Y. S.; Weldon, S. M.; Yong, C.-L.; Llinàs-Brunet, M. *Nature* **2003**, *426*, 186-189.
16. Faucher, A.-M.; Bailey, M. D.; Beaulieu, P. L.; Brochu, C.; Duceppe, J.-S.; Ferland, J.-M.; Ghio, E.; Gorys, V.; Halmos, T.; Kawai, S. H.; Poirier, M.; Simoneau, B.; Tsantrizos, Y. S.; Llinàs-Brunet, M. *Org. Lett.* **2004**, *6*, 2901-2904.

17. Llinàs-Brunet, M.; Bailey, M. D.; Bolger, G.; Brochu, C.; Faucher, A.-M.; Ferland, J. M.; Garneau, M.; Ghiron, E.; Gorys, V.; Grand-Maitre, C.; Halmos, T.; Lapeyre-Paquette, N.; Liard, F.; Poirier, M.; Rhéaume, M.; Tsantrizos, Y. S.; Lamarre, D. *J. Med. Chem.* **2004**, *47*, 1605-1608.
18. Fahlbusch, K.-G.; Hammerschmidt, F.-J.; Panten, J.; Pickenhagen, W.; Schatkowski, D.; Bauer, K.; Garbe, D.; Surburg, H. Flavors and Fragrances. In *Ullmann's Encyclopedia of Industrial Chemistry*, Wiley-VCH: Weinheim, 2003; pp 73-198.
19. (a) Suter-Eichenberger, R.; Altorfer, H.; Lichtensteiger, W.; Schlumpf, M. *Chemosphere* **1998**, *36*, 2747-2762; (b) Luckenbach, T.; Epel, D. *Environ. Health Perspect.* **2005**, *113*, 17-24.
20. Belsito, D.; Bickers, D.; Bruze, M.; Calow, P.; Dagli, M. L.; Fryer, A. D.; Greim, H.; Miyachi, Y.; Saurat, J. H.; Sipes, I. G. *Food Chem. Toxicol.* **2011**, *49*, S219-S241.
21. Sokolov, V. E.; Kagan, M. Z.; Vasilieva, V. S.; Prihodko, V. I.; Zinkevich, E. P. *J. Chem. Ecol.* **1987**, *13*, 71-83.
22. Williams, A. S. *Synthesis* **1999**, 1707-1723.
23. Yang, H.; Yuan, B.; Zhang, X.; Scherman, O. A. *Acc. Chem. Res.* **2014**, *47*, 2106-2115.
24. Cram, D. J. *Angew. Chem. Int. Ed.* **1988**, *27*, 1009-1020.
25. Lehn, J.-M. *Angew. Chem. Int. Ed.* **1988**, *27*, 89-112.
26. Pedersen, C. J. *Angew. Chem. Int. Ed.* **1988**, *27*, 1021-1027.
27. Sauvage, J.-P. *Angew. Chem. Int. Ed.* **2017**, *56*, 11080-11093.
28. Stoddart, J. F. *Angew. Chem. Int. Ed.* **2017**, *56*, 11094-11125.
29. Feringa, B. L. *Angew. Chem. Int. Ed.* **2017**, *56*, 11060-11078.
30. Barnes, J. C.; Mirkin, C. A. *Proc. Natl. Acad. Sci. U.S.A.* **2017**, *114*, 620-625.
31. Diederich, F.; Stang, P. J.; Tykwinski, R. R. *Modern Supramolecular Chemistry: Strategies for Macrocyclic Synthesis*. Wiley-VCH: Weinheim, 2008.
32. (a) Iyoda, M.; Yamakawa, J.; Rahman, M. J. *Angew. Chem. Int. Ed.* **2011**, *50*, 10522-10553; (b) Zhang, W.; Moore, J. S. *Angew. Chem. Int. Ed.* **2006**, *45*, 4416-4439.
33. Höger, S. *Chem. Eur. J.* **2004**, *10*, 1320-1329.
34. Ruzicka, L.; Stoll, M.; Schinz, H. *Helv. Chim. Acta* **1926**, *9*, 249-264.
35. Ziegler, K.; Eberle, H.; Ohlinger, H. *Justus Liebigs Ann. Chem.* **1933**, *504*, 94-130.
36. Martí-Centelles, V.; Pandey, M. D.; Burguete, M. I.; Luis, S. V. *Chem. Rev.* **2015**, *115*, 8736-8834.
37. Ruggli, P. *Justus Liebigs Ann. Chem.* **1912**, *392*, 92-100.
38. (a) Galli, C.; Illuminati, G.; Mandolini, L. *J. Am. Chem. Soc.* **1973**, *95*, 8374-8379; (b) Illuminati, G.; Mandolini, L. *Acc. Chem. Res.* **1981**, *14*, 95-102.
39. Galli, C.; Mandolini, L. *Eur. J. Org. Chem.* **2000**, *2000*, 3117-3125.
40. Illuminati, G.; Mandolini, L.; Masci, B. *J. Am. Chem. Soc.* **1977**, *99*, 6308-6312.
41. Allinger, N. L.; Tribble, M. T.; Miller, M. A.; Wertz, D. H. *J. Am. Chem. Soc.* **1971**, *93*, 1637-1648.
42. Früchtel, J. S.; Jung, G. *Angew. Chem. Int. Ed.* **1996**, *35*, 17-42.
43. Trost, B. M.; Warner, R. W. *J. Am. Chem. Soc.* **1982**, *104*, 6112-6114.
44. Bédard, A.-C.; Collins, S. K. *J. Am. Chem. Soc.* **2011**, *133*, 19976-19981.
45. Blankenstein, J.; Zhu, J. *Eur. J. Org. Chem.* **2005**, *2005*, 1949-1964.
46. Lee, D.; Sello, J. K.; Schreiber, S. L. *J. Am. Chem. Soc.* **1999**, *121*, 10648-10649.
47. Schmidt, U.; Langner, J. *J. Pept. Res.* **1997**, *49*, 67-73.
48. El-Azizi, Y.; Schmitzer, A.; Collins, S. K. *Angew. Chem. Int. Ed.* **2006**, *45*, 968-973.

49. Beesley, R. M.; Ingold, C. K.; Thorpe, J. F. *J. Chem. Soc., Trans.* **1915**, 107, 1080-1106.
50. (a) Jung, M. E.; Piizzi, G. *Chem. Rev.* **2005**, 105, 1735-1766; (b) Galli, C.; Giovannelli, G.; Illuminati, G.; Mandolini, L. *J. Org. Chem.* **1979**, 44, 1258-1261.
51. Bolduc, P.; Jacques, A.; Collins, S. K. *J. Am. Chem. Soc.* **2010**, 132, 12790-12791.
52. (a) Pedersen, C. J. *J. Am. Chem. Soc.* **1967**, 89, 7017-7036; (b) McCallien, D. W. J.; Sanders, J. K. M. *J. Am. Chem. Soc.* **1995**, 117, 6611-6612.
53. (a) Marsden, J. A.; Miller, J. J.; Haley, M. M. *Angew. Chem. Int. Ed.* **2004**, 43, 1694-1697; (b) Miller, S. J.; Blackwell, H. E.; Grubbs, R. H. *J. Am. Chem. Soc.* **1996**, 118, 9606-9614.
54. Parenty, A.; Moreau, X.; Niel, G.; Campagne, J. M. *Chem. Rev.* **2013**, 113, PR1-PR40.
55. Myśliwiec, D.; Lis, T.; Gregoliński, J.; Stepień, M. *J. Org. Chem.* **2015**, 80, 6300-6312.
56. Swamy, K. C. K.; Kumar, N. N. B.; Balaraman, E.; Kumar, K. V. P. P. *Chem. Rev.* **2009**, 109, 2551-2651.
57. Beach, E. S.; Cui, Z.; Anastas, P. T. *Energy Environ. Sci.* **2009**, 2, 1038-1049.
58. (a) Chauvin, Y. *Angew. Chem. Int. Ed.* **2006**, 45, 3740-3747; (b) Schrock, R. R. *Angew. Chem. Int. Ed.* **2006**, 45, 3748-3759; (c) Grubbs, R. H. *Angew. Chem. Int. Ed.* **2006**, 45, 3760-3765.
59. Grubbs, R. H.; Miller, S. J.; Fu, G. C. *Acc. Chem. Res.* **1995**, 28, 446-452.
60. (a) Gradillas, A.; Pérez-Castells, J. *Angew. Chem. Int. Ed.* **2006**, 45, 6086-6101; (b) Nicolaou, K. C.; Bulger, P. G.; Sarlah, D. *Angew. Chem. Int. Ed.* **2005**, 44, 4490-4527.
61. Fürstner, A.; Langemann, K. *J. Org. Chem.* **1996**, 61, 3942-3943.
62. Fürstner, A. *Angew. Chem. Int. Ed.* **2013**, 52, 2794-2819.
63. (a) Fürstner, A.; Seidel, G. *Angew. Chem. Int. Ed.* **1998**, 37, 1734-1736; (b) Fürstner, A.; Guth, O.; Rumbo, A.; Seidel, G. *J. Am. Chem. Soc.* **1999**, 121, 11108-11113.
64. Fürstner, A.; Mathes, C.; Grela, K. *Chem. Commun.* **2001**, 1057-1059.
65. (a) Yu, M.; Wang, C.; Kyle, A. F.; Jakubec, P.; Dixon, D. J.; Schrock, R. R.; Hoveyda, A. H. *Nature* **2011**, 479, 88-93; (b) Shen, X.; Nguyen, T. T.; Koh, M. J.; Xu, D.; Speed, A. W. H.; Schrock, R. R.; Hoveyda, A. H. *Nature* **2017**, 541, 380-385.
66. Hein, J. E.; Fokin, V. V. *Chem. Soc. Rev.* **2010**, 39, 1302-1315.
67. Kolb, H. C.; Sharpless, K. B. *Drug Discov. Today* **2003**, 8, 1128-1137.
68. Agalave, S. G.; Maujan, S. R.; Pore, V. S. *Chem. Asian J.* **2011**, 6, 2696-2718.
69. Xi, W.; Scott, T. F.; Kloxin, C. J.; Bowman, C. N. *Adv. Funct. Mater.* **2014**, 24, 2572-2590.
70. Kolb, H. C.; Finn, M. G.; Sharpless, K. B. *Angew. Chem. Int. Ed.* **2001**, 40, 2004-2021.
71. (a) Thirumurugan, P.; Matosiuk, D.; Jozwiak, K. *Chem. Rev.* **2013**, 113, 4905-4979; (b) Valverde, I. E.; Bauman, A.; Kluba, C. A.; Vomstein, S.; Walter, M. A.; Mindt, T. L. *Angew. Chem. Int. Ed.* **2013**, 52, 8957-8960.
72. Zhang, J.; Kemmink, J.; Rijkers, D. T. S.; Liskamp, R. M. J. *Org. Lett.* **2011**, 13, 3438-3441.
73. (a) Bogdan, A. R.; James, K. *Chem. Eur. J.* **2010**, 16, 14506-14512; (b) Chouhan, G.; James, K. *Org. Lett.* **2011**, 13, 2754-2757; (c) Bogdan, A. R.; Jerome, S. V.; Houk, K. N.; James, K. *J. Am. Chem. Soc.* **2012**, 134, 2127-2138.
74. Bogdan, A. R.; James, K. *Org. Lett.* **2011**, 13, 4060-4063.
75. Santandrea, J.; Bédard, A.-C.; de Léséleuc, M.; Raymond, M.; Collins, S. K. Alternative Strategies for the Construction of Macrocycles. In *Practical Medicinal Chemistry with Macrocycles*, John Wiley & Sons, Inc.: 2017; pp 307-337.

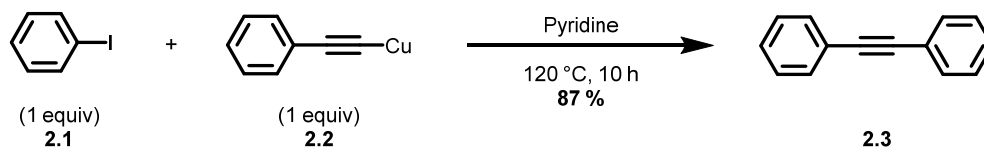
## 2. Introduction to the Sonogashira Reaction

Forming carbon-carbon bonds is challenging. Olefin metathesis (Section 1.3.1) and palladium-catalyzed cross-couplings have been developed over the past few decades as useful synthetic tools for chemists to construct small to large molecules through carbon-carbon bond formation. The utility of palladium-catalyzed cross-couplings, some of which were recognized with the 2010 Nobel Prize in Chemistry,<sup>1</sup> is primarily due to their high selectivity for predictable bond formation between coupling partners. The Sonogashira reaction is among the most widely used palladium-catalyzed cross-couplings in organic synthesis today.<sup>1c</sup> The coupling is formally utilized to access C(sp<sup>2</sup>)-C(sp) bonds from aryl or alkenyl halides or triflates and terminal alkynes. Standard reaction conditions typically involve a palladium(0) and copper(I) catalytic system and a stoichiometric amount of base.

The following chapter will describe the discovery and evolution of the palladium-catalyzed alkynylation. As the Sonogashira reaction gives access to arylalkynes and conjugated enynes, which are precursors of natural products, pharmaceuticals and molecular organic materials,<sup>2</sup> selected macrocyclic examples of the abovementioned classes of molecules will also be presented. Recently, there has been growing interest in first-row transition metal catalysis for cross-couplings.<sup>3</sup> As such, palladium-free variants of the Sonogashira reaction involving iron and copper catalysis will also be introduced.

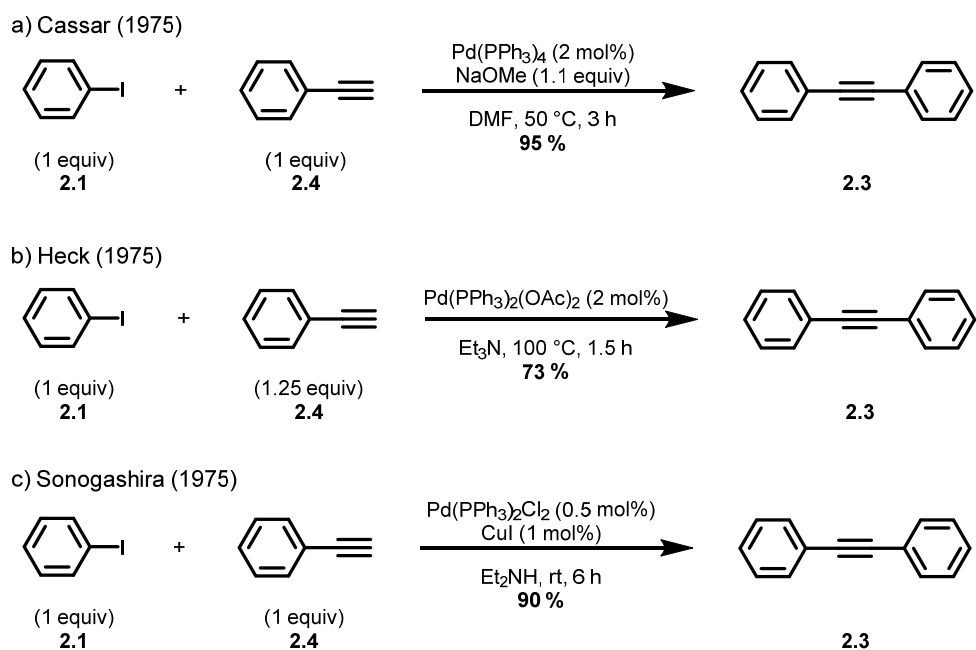
### 2.1 Discovery and Evolution of C(sp<sup>2</sup>)-C(sp) Couplings

The first transition-metal-catalyzed alkynylation of C(sp<sup>2</sup>) bonds was reported by Castro and Stephens in 1963.<sup>4</sup> It enabled the synthesis of diarylacetylenes (**2.3**) by the coupling of stoichiometric aryl iodides (**2.1**) and copper(I) arylacetylides (**2.2**) in a refluxing amine base (Scheme 2.1). The reaction has however been scarcely applied in organic synthesis since its discovery.<sup>5</sup> Though high temperatures and handling of hazardous copper acetylides were required, the Castro-Stephens coupling had undoubtedly paved the way to more efficient C(sp<sup>2</sup>)-C(sp) bond-forming reactions.



**Scheme 2.1** Castro-Stephens coupling of diphenylacetylene **2.3**

Improved C(sp<sup>2</sup>) alkynylation conditions were reported independently by Cassar<sup>6</sup> and Heck<sup>7</sup> in 1975. Cassar's procedure utilized catalytic amounts of palladium(0) triphenylphosphine complexes in the presence of a slight excess of sodium methoxide as base and DMF as solvent (Scheme 2.2a). Aryl iodides such as **2.1**, as well as other aryl and vinyl bromides, converted readily with terminal alkynes (**2.4**) under eight hours when heated (40-100 °C). The method gave access to several aromatic and vinylic acetylenic compounds like diphenylacetylene **2.3** in yields ranging from 50 to 95 %. Similarly, Heck's procedure utilized a catalytic amount of a palladium(II) complex in either triethylamine or piperidine as solvent and as base (Scheme 2.2b). Aryl iodides and bromides, as well as several vinyl bromides, could be converted to aryl acetylenes in under three hours at 100 °C (73 % for **2.3**).



**Scheme 2.2** Palladium-catalyzed syntheses of diphenylacetylene **2.3**



Later in the same year, Sonogashira reported that the addition of a catalytic amount of a copper salt enabled the alkynylation reaction to proceed at room temperature.<sup>8</sup> The improved protocol required catalytic amounts of a palladium(II) complex and of copper(I) iodide in diethylamine as solvent and as base (Scheme 2.2c). Aryl iodides, bromopyridines and vinyl bromides could be readily converted with aryl or alkyl alkynes in three to six hours in yields ranging from 27 to 98 % (90 % for **2.3**). The milder reaction conditions were also functional group tolerant, relatively insensitive to water and technically simple, making the Sonogashira reaction arguably the most popular and reliable procedure for the alkynylation of aryl or alkenyl electrophiles.

Although the coupling is experimentally simple to perform, some caution must be undertaken to insure success. For instance, since catalytic copper salts are utilized to generate copper acetylide intermediates in situ, purging the reaction mixture with an inert gas to remove oxygen is key, as it promotes the formation of homocoupling products of the terminal alkyne (Glaser product) in the presence of copper.<sup>9</sup> Since its discovery, Sonogashira's original protocol has been extensively modified and improved to overcome some of its inherent challenges,<sup>10</sup> such as the abovementioned undesired homocoupling of the terminal alkyne and the difficulty of effectively coupling aryl bromides and chlorides under mild reaction conditions. The drawbacks have to some extent been resolved by the development of numerous palladium precatalysts that operate with, or without, a copper cocatalyst.<sup>2, 10</sup>

In his original report,<sup>8</sup> Sonogashira proposed a mechanism that involved two interdependent catalytic cycles (Figure 2.1). The process would initiate with the reduction of the Pd(II) precatalyst to the believed Pd(0) active catalytic species (**2.5**). Subsequent oxidative addition of the Pd center into the electrophile's (**2.6**) carbon-halogen bond would generate Pd(II) intermediate **2.7**. A transmetalation between Pd(II) intermediate **2.7** and Cu(I) acetylide **2.10**, formed in presence of copper **2.8**, terminal alkyne **2.9** and base, would then occur to furnish a new Pd(II) intermediate (**2.11**). Lastly, reductive elimination of intermediate **2.11** would provide the desired compound (**2.12**) and regenerate active Pd(0) catalyst **2.5**. Although the proposed mechanism is still widely accepted today, it is not fully understood.

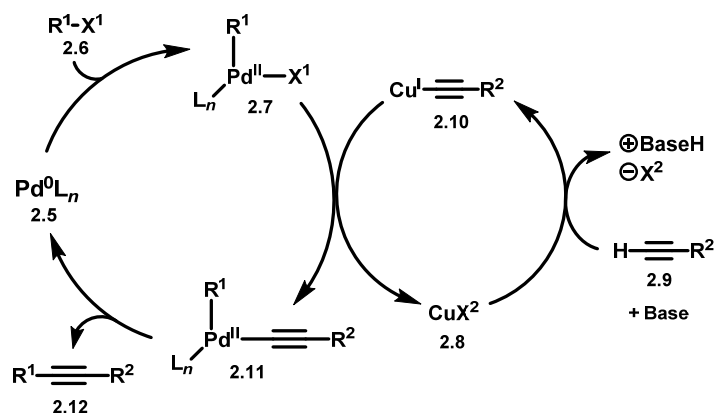


**Figure 2.1** Original proposed mechanism for the Sonogashira coupling

In recent years, some effort has been devoted toward the elucidation of the mechanism of the Sonogashira reaction. However, as analyzing the combined action of two metal catalysts can be quite challenging, computational studies have mainly focused on the mechanism of copper-free Sonogashira reactions.<sup>11</sup> In 2017, a thorough mechanistic investigation into the copper-cocatalyzed Sonogashira reaction was reported by means of DFT calculations.<sup>12</sup> The study essentially revealed that an anion-coordinated copper(I) acetylide (**2.13**) is more kinetically and thermodynamically favored than the generally accepted neutral copper(I) acetylide (**2.10**) to be the actual active species during transmetalation, which was also found to be the rate-determining step. Following the results from the computationally modeled coupling between iodobenzene **2.1** and phenylacetylene **2.4**, where  $[\text{Pd}(\text{PPh}_3)_2]$ , CuI, and  $\text{Cs}_2\text{CO}_3$  were used as catalyst, cocatalyst and base respectively, the originally proposed Sonogashira mechanism could be modified (Figure 2.2).

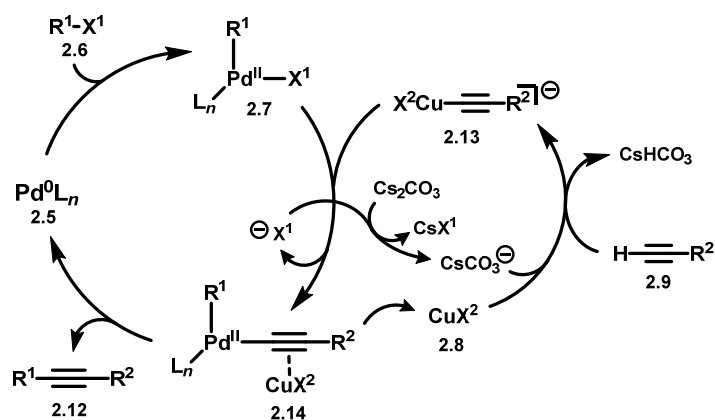


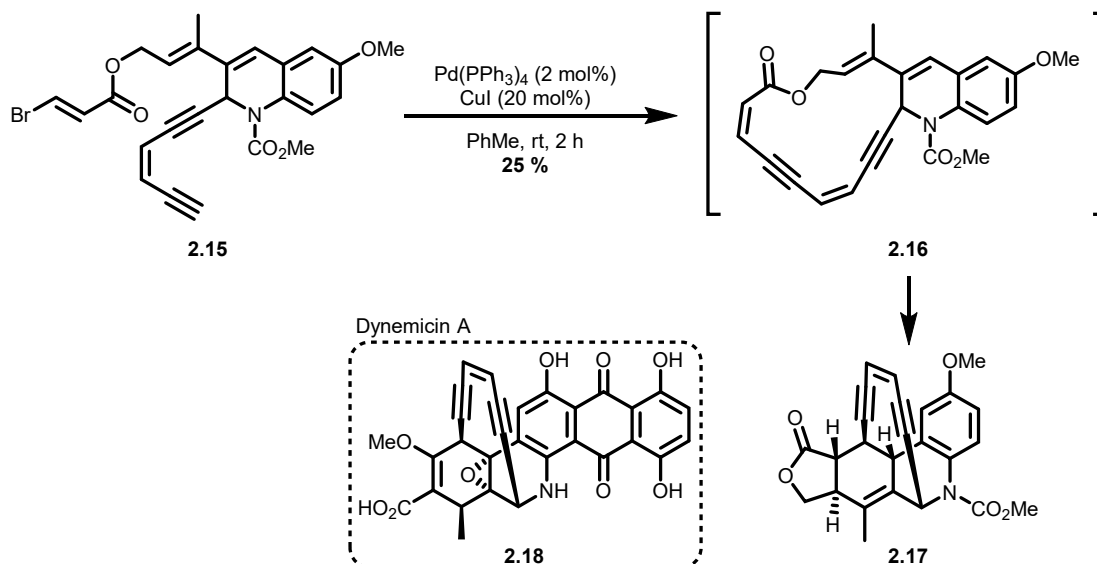
**Figure 2.2** Modified proposed mechanism of the Sonogashira coupling

## 2.2 Applications Toward Macrocyclization

Palladium-catalyzed reactions have expectedly been utilized in the synthesis of various classes of macrocycles. In recent literature, the most commonly found palladium-catalyzed couplings for macrocycle synthesis are the Suzuki-Miyaura, Stille, Heck, Tsuji-Trost and Sonogashira reactions.<sup>13</sup> The Sonogashira reaction generates versatile C(sp<sup>2</sup>)-C(sp) bonds useful for both natural and nonnatural product synthesis.<sup>14</sup>

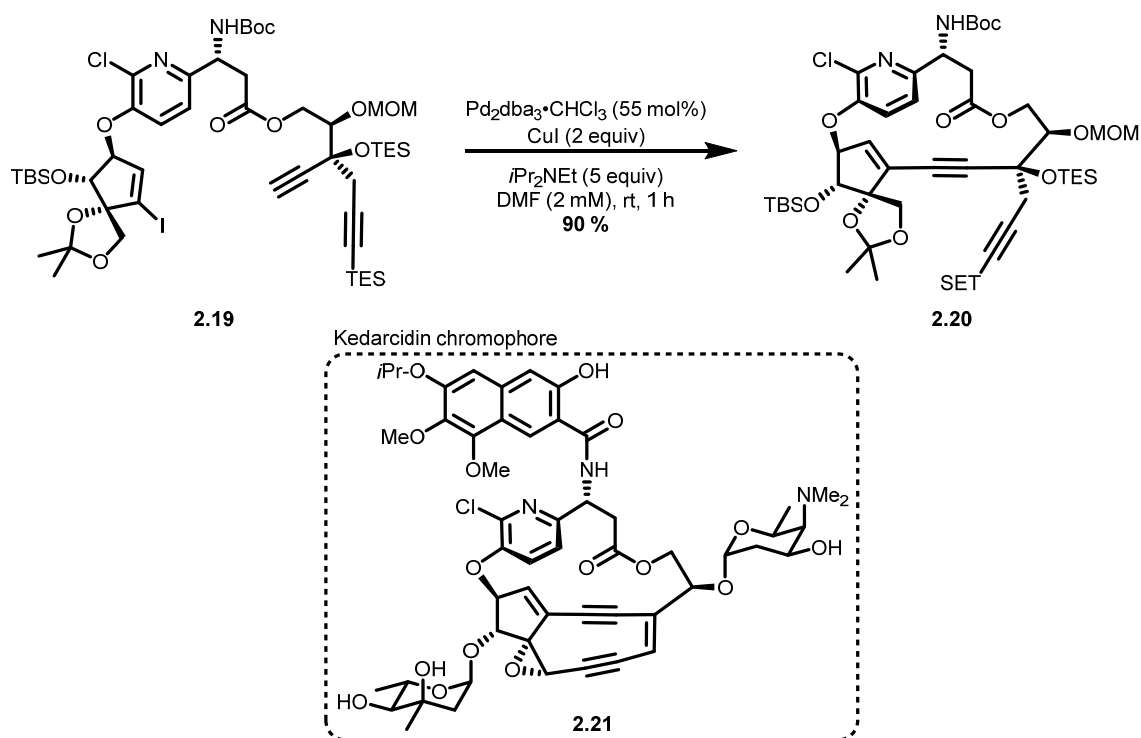
### 2.2.1 Synthesis of Macrocyclic Natural Products

The infrequent use of the Sonogashira reaction in total synthesis may be attributed to the rarity of conjugated-alkyne-containing natural products, such as metabolite dynemicin A (**2.18**, Scheme 2.3). Initially, dynemicin A attracted organic chemists' attention more for its intriguing structure than for its biological properties. Accordingly, many total syntheses of dynemicin A and of its analogues were undertaken.<sup>15</sup> The construction of the cyclic (Z)-enediynes functional group was achieved through various approaches, including consecutive intramolecular Sonogashira and transannular Diels-Alder reactions (Scheme 2.3).<sup>15a</sup> When acyclic precursor **2.15** was submitted to catalytic amounts of Pd(PPh<sub>3</sub>)<sub>4</sub> and CuI in toluene at room temperature, macrocyclic intermediate **2.16** was formed, and reacted subsequently via a transannular Diels-Alder reaction to provide compound **2.17** in 25 % yield.



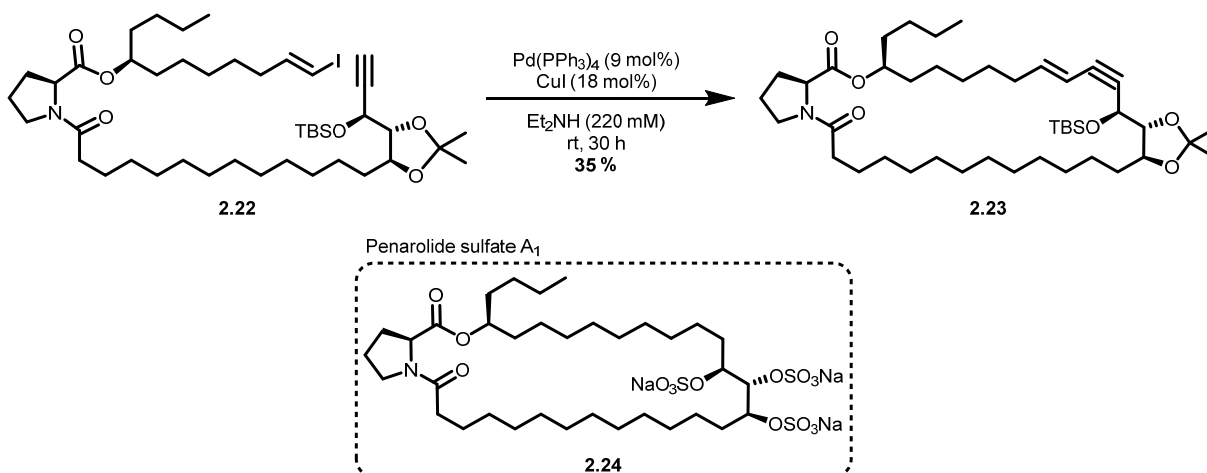
**Scheme 2.3** Synthesis of dynemicin A analog precursor **2.17**

The Sonogashira reaction has also been utilized toward the synthesis of the *ansa*-macrolide moiety (**2.20**) of kerdarcidin chromophore **2.21** (Scheme 2.4).<sup>16</sup> When a high catalyst loading of Pd<sub>2</sub>dba<sub>3</sub>·CHCl<sub>3</sub> and a stoichiometric amount of CuI were applied, cyclization precursor **2.19** was readily converted to macrocycle **2.20** in 90 % yield in degassed DMF (2 mM).



**Scheme 2.4** Synthesis of *ansa*-macrolide **2.20**

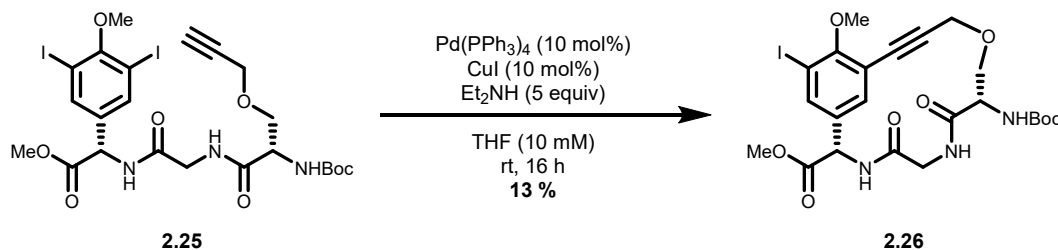
Lastly, an intramolecular Sonogashira coupling was utilized in the synthesis of  $\alpha$ -glucosidase inhibitor penarolide sulfate A<sub>1</sub> (**2.24**, Scheme 2.5).<sup>17</sup> As natural product **2.24** does not contain any alkenes or alkynes, successive Sonogashira and hydrogenation reactions were found to efficiently furnish the 30-membered macrocyclic core. When catalytic amounts of Pd(PPh<sub>3</sub>)<sub>4</sub> and CuI were applied, cyclic precursor **2.22** was converted to macrocycle **2.23** in 35 % yield in diethylamine (220 mM).



**Scheme 2.5** Synthesis of penarolide sulfate A1 precursor **2.23**

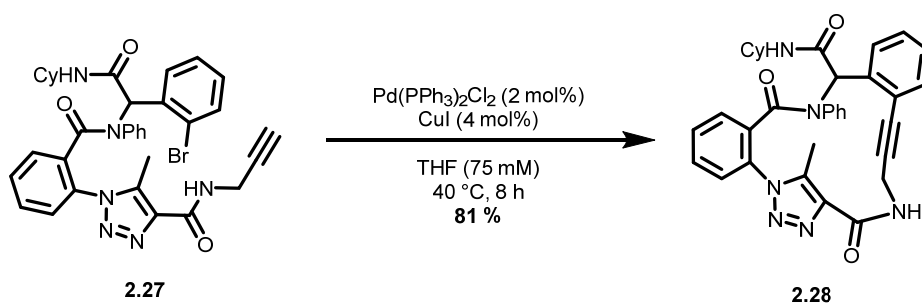
### 2.2.2 Synthesis of Macrocyclic Nonnatural Products

The Sonogashira reaction has been more broadly applied in the synthesis of nonnatural macrocycles such as resorcylic acid lactone analogues and constrained cyclic peptides.<sup>18</sup> For example, the coupling has been utilized to access rigidified 15-membered peptidic macrocycles based on the central ring system of vancomycin.<sup>18d</sup> The cyclization of linear tripeptides such as **2.25** was initially achieved through an intramolecular Sonogashira reaction to provide the corresponding macrocycles (Scheme 2.6). Catalytic amounts of  $\text{Pd(PPh}_3)_4$  and  $\text{CuI}$  were used in the presence of excess diethylamine as base and THF as solvent (10 mM) to provide macrocycle **2.26** in 13 % yield. Although the desired macrocycles could be generated, the intramolecular coupling provided low yields in all cases (13-27 %). It prompted the authors to opt for an alternative sequential intermolecular Sonogashira and macrolactamization route.



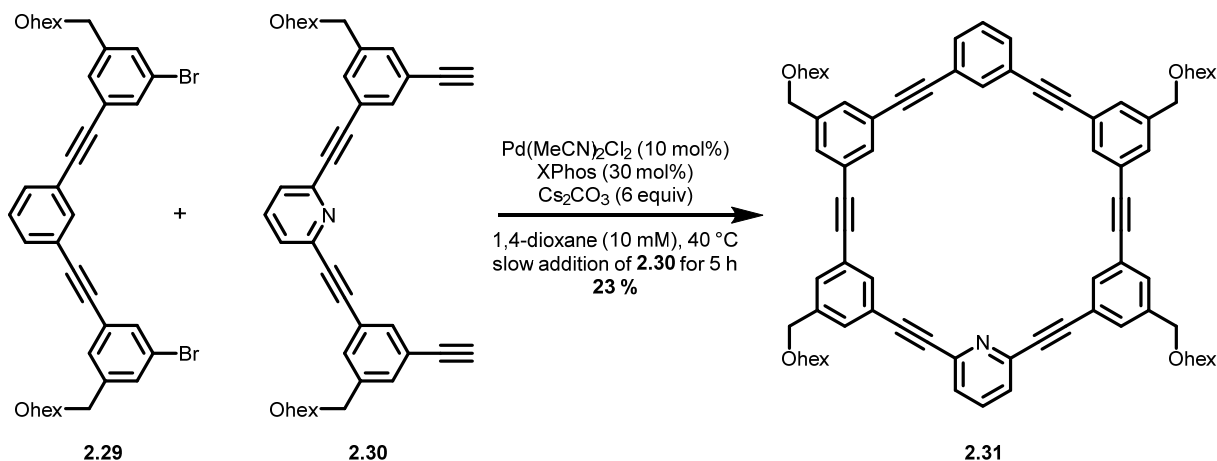
**Scheme 2.6** Synthesis of macrocycle **2.26**

As macrocyclic Sonogashira couplings do not always produce high yields of the desired macrocycles, strategies such as conformational control have been applied to improve the macrocyclization outcome. For instance, the synthesis of benzannulated chiral macrocycles embedded in carbohydrate templates has been shown to greatly improve the macrocyclization yields.<sup>19</sup> Reactive conformations can also be attained when using *ortho*-disubstituted-arene-containing precursors such as **2.27** (Scheme 2.7).<sup>20</sup> Low catalyst loadings of Pd(PPh<sub>3</sub>)<sub>2</sub>Cl<sub>2</sub> and CuI were employed in heated THF (75 mM) in the presence of cyclization precursor **2.27** to afford macrocycle **2.28** in 81 % yield.



**Scheme 2.7** Synthesis of macrocycle **2.28**

Lastly, intramolecular Sonogashira reactions have been greatly applied toward the synthesis of shape-persistent macrocycles (SPMs) and other macrocyclic functional materials.<sup>14c, 21</sup> For SPMs based on acetylenic scaffoldings, intermolecular Sonogashira reactions are usually employed to generate the required cyclization precursors for the subsequent intramolecular Sonogashira coupling. Pyridine-containing SPM **2.31** was synthesized following a similar approach from dibromide **2.29** and diyne **2.30** (Scheme 2.8).<sup>21a</sup> The two-component double Sonogashira-type cyclization was optimal when catalytic amounts of Pd(MeCN)<sub>2</sub>Cl<sub>2</sub> and XPhos were used in the presence of cesium carbonate in heated 1,4-dioxane (10 mM). Thus, SPM **2.31** was formed in 23 % yield by means of the slow addition of diyne **2.30** into the reaction mixture.



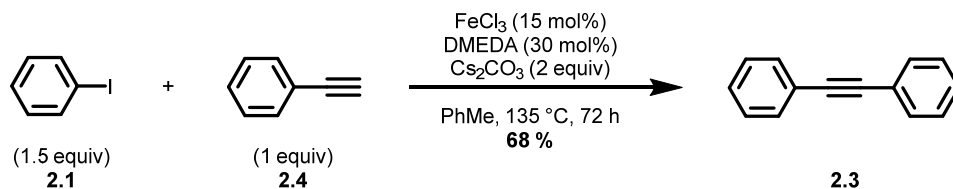
**Scheme 2.8** Synthesis of shape-persistent macrocycle **2.31**

## 2.3 Development of a Palladium-Free Variant

Recently, there has been growing interest in alternative metal sources for cross-coupling because of the high cost and low abundance of precious metals such as palladium. A resurgence of first-row transition-metal-catalyzed reactions has thus been observed over the past decade due to their low cost, low toxicity and synthetic versatility.<sup>3</sup> Most palladium-catalyzed cross-couplings, including the Sonogashira reaction, now possess first-row metal counterparts.<sup>22</sup>

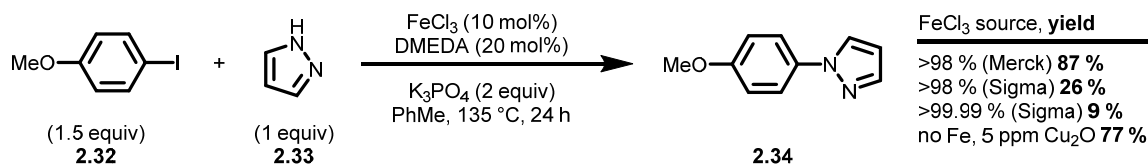
### 2.3.1 Iron-Catalyzed Sonogashira-Type Coupling

In 2008, Bolm reported the first iron-catalyzed  $\text{C}(\text{sp}^2)\text{-C}(\text{sp})$  coupling in an effort to use less expensive and more sustainable catalysts in the Sonogashira reaction (Scheme 2.9).<sup>23</sup> The novel conditions followed the successful iron-catalyzed arylation of nitrogen nucleophiles,<sup>24</sup> phenols<sup>25</sup> and thiols.<sup>26</sup> The alkynylation relied on a catalytic amount of  $\text{FeCl}_3$  as catalyst and DMEDA as ligand to promote the coupling between aryl iodides (**2.1**) and terminal alkynes (**2.4**). When the substrates were submitted to the catalyst system in the presence of cesium carbonate as base in refluxing toluene for 72 hours, the desired acetylenic products were obtained in yields ranging from 15-99 %. The reaction time was found to be a key parameter, as compound **2.3** was isolated in 95 % yield after five days, compared to 68 % yield after three days in the surveyed reaction conditions.



**Scheme 2.9** Iron-catalyzed coupling of diphenylacetylene **2.3**

However, it was later revealed that some commercial iron catalysts contained trace copper, which may account for the activity.<sup>27</sup> Earlier metal salt purity dependency observations prompted Buchwald and Bolm to investigate if trace amounts of copper impurities contained in commercial iron catalysts were indeed catalyzing the reactions. Thus, several sources of FeCl<sub>3</sub> (from >98-99.99 % metal purity) were surveyed for different heteroatom arylations with aryl iodides (Scheme 2.10). For instance, *N*-arylation of pyrazole (**2.33**) was achieved in 87 % when using FeCl<sub>3</sub> from Merck (>98 % metal purity) in the presence of aryl iodide **2.32**. Decreased yields of **2.34** were observed when using different sources of FeCl<sub>3</sub> from Sigma-Aldrich (26 % and 9 % yield from >98 % and >99.99 % metal purity respectively). Lastly, when 5 ppm of Cu<sub>2</sub>O were added to the reaction in the absence of FeCl<sub>3</sub>, compound **2.34** was isolated in 77 %.



**Scheme 2.10** Iron-catalyzed *N*-arylation using different FeCl<sub>3</sub> commercial sources

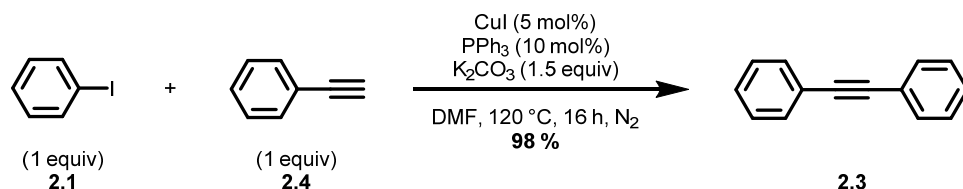
Although the previous observations indicated that the outcome of iron-catalyzed reactions were greatly affected by trace quantities of copper, iron-catalyzed alkynylations operating with,<sup>28</sup> and without,<sup>29</sup> a copper cocatalyst have re-emerged in recent times. While the latest iron-catalyzed Sonogashira-type couplings readily give access to diarylacetylenes, the protocols are generally substrate-limited with regards to aliphatic terminal alkynes.

### 2.3.2 Copper-Catalyzed Sonogashira-Type Coupling

In 1993, Miura reported the first copper-catalyzed Sonogashira-type cross-coupling (Scheme 2.11).<sup>30</sup> A combination of CuI as catalyst and PPh<sub>3</sub> as ligand was utilized, in the presence of potassium carbonate in either DMF or DMSO at 120 °C under N<sub>2</sub>, to couple aryl



and vinyl iodides with terminal alkynes. When aryl iodide **2.1** and alkyne **2.4** were submitted to the optimal reaction conditions, diphenylacetylene (**2.3**) was isolated in 98 % yield. More importantly, the methodology enabled aryl and vinyl iodides to convert smoothly with various aliphatic terminal alkynes between five to 48 hours.



**Scheme 2.11** Copper-catalyzed coupling of diphenylacetylene **2.3** reported by Miura

In the report, Miura proposed a mechanism for the copper-catalyzed Sonogashira-type cross-coupling (Figure 2.3). It was thought that a  $\text{PPh}_3$ -coordinated copper(I) acetylide **2.36** would initially be generated in situ from  $\text{CuI}$  (**2.8**), the terminal alkyne (**2.9**) and the base. Following ligand disassociation, copper(I) acetylide intermediate **2.37** would react with an aryl halide (**2.6**) through a four-centered transition state (**2.38**), to produce the coupled product (**2.12**) and regenerate copper(I) catalyst **2.35**.

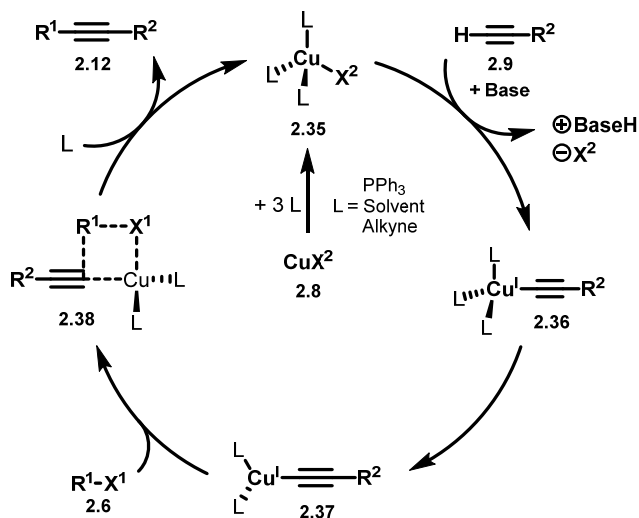


**Figure 2.3** Miura's proposed mechanism for copper-catalyzed alkynylation reaction

Since Miura's work on the copper-catalyzed Sonogashira-type cross-coupling, much effort has been made in fine-tuning the reaction conditions.<sup>31</sup> However, the mechanistic aspects for the copper-only-catalyzed transformation remain elusive. In 2010, Bolm initially reported



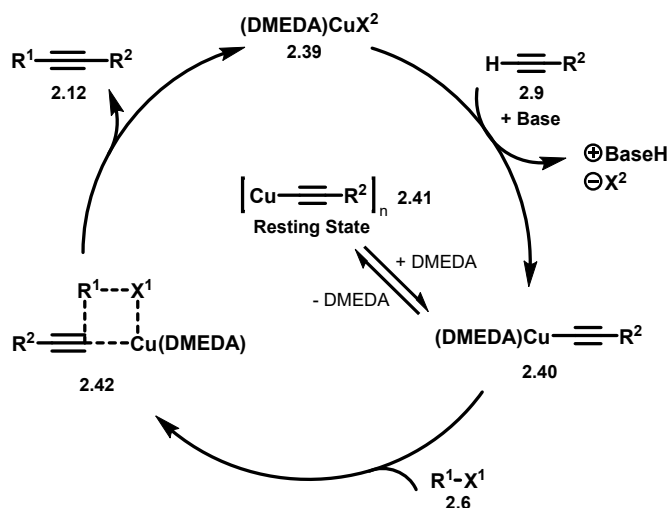


**Figure 2.4** Bolm's proposed mechanism for copper-catalyzed alkynylation reaction

## 2.4 Conclusions

Since its discovery in 1975, the Sonogashira reaction has become one of the most widely used palladium-catalyzed cross-couplings in organic synthesis. The coupling's mild reaction conditions, high functional group tolerance, relative insensitivity to water, experimental simplicity, as well as its ability to generate versatile C(sp<sup>2</sup>)-C(sp) bonds, all have warranted its use in both natural and nonnatural product synthesis. Although the Sonogashira coupling has been used infrequently toward macrocyclic natural products, it has enabled the synthesis of various classes of macrocycles for drug discovery and materials science. First-row transition metal catalysis for cross-couplings, such as iron- and copper-catalyzed variants of the Sonogashira reaction, are also becoming more widespread in the search of more sustainable synthetic methods. The use of low-cost and high-abundance transition metals is desirable. They might also allow chemists to explore uncharted chemical transformations and their mechanisms.

## 2.5 Research Goals

Macrocyclization reactions are useful in chemical synthesis. Efficient and reliable catalytic methods, such as RCM (Section 1.3.1), CuAAC (Section 1.3.2) and palladium-catalyzed cross-couplings (Section 2.2), are sought-after in the context of green chemistry. Desirable transformations use first-row transition metals such as copper, because they are more

environmentally benign compared to the high-cost and low-abundance precious metals like palladium. Considering that first-row transition metal analogues of palladium-catalyzed macrocyclic cross-couplings were absent from the synthetic toolbox, we sought to develop a novel copper-catalyzed Sonogashira-type cross-coupling for the formation of nonnatural macrocycles under the following considerations:

- 1) A copper catalytic system using inexpensive commercially available reagents.
- 2) Conformationally unbiased cyclization precursors to better evaluate the performance of the catalytic system.
- 3) Simplicity in terms of setup to avoid the use of tedious slow addition techniques.
- 4) Synthesize macrocycles relevant to medicinal chemistry, such as resorcylic acid lactones, with various ring sizes and functional groups.
- 5) The synthesis of a known biologically active macrocycle.

## 2.6 Bibliography

1. (a) Suzuki, A. *Angew. Chem. Int. Ed.* **2011**, *50*, 6722-6737; (b) Negishi, E.-i. *Angew. Chem. Int. Ed.* **2011**, *50*, 6738-6764; (c) Johansson Seechurn, C. C. C.; Kitching, M. O.; Colacot, T. J.; Snieckus, V. *Angew. Chem. Int. Ed.* **2012**, *51*, 5062-5085.
2. Chinchilla, R.; Nájera, C. *Chem. Rev.* **2007**, *107*, 874-922.
3. Zweig, J. E.; Kim, D. E.; Newhouse, T. R. *Chem. Rev.* **2017**, *117*, 11680-11752.
4. Stephens, R. D.; Castro, C. E. *J. Org. Chem.* **1963**, *28*, 3313-3315.
5. (a) Castro, C. E.; Havlin, R.; Honwad, V. K.; Malte, A. M.; Moje, S. W. *J. Am. Chem. Soc.* **1969**, *91*, 6464-6470; (b) Batu, G.; Stevenson, R. *J. Org. Chem.* **1980**, *45*, 1532-1534; (c) White, J. D.; Sundermann, K. F.; Wartmann, M. *Org. Lett.* **2002**, *4*, 995-997.
6. Cassar, L. *J. Organomet. Chem.* **1975**, *93*, 253-257.
7. Dieck, H. A.; Heck, F. R. *J. Organomet. Chem.* **1975**, *93*, 259-263.
8. Sonogashira, K.; Tohda, Y.; Hagihara, N. *Tetrahedron Lett.* **1975**, *16*, 4467-4470.
9. Siemsen, P.; Livingston, R. C.; Diederich, F. *Angew. Chem. Int. Ed.* **2000**, *39*, 2632-2657.
10. Chinchilla, R.; Nájera, C. *Chem. Soc. Rev.* **2011**, *40*, 5084-5121.
11. (a) Sikk, L.; Tammiku-Taul, J.; Burk, P. *Organometallics* **2011**, *30*, 5656-5664; (b) García-Melchor, M.; Pacheco, M. C.; Nájera, C.; Lledós, A.; Ujaque, G. *ACS Catal.* **2012**, *2*, 135-144.
12. Wang, X.; Song, Y.; Qu, J.; Luo, Y. *Organometallics* **2017**, *36*, 1042-1048.
13. Ronson, T. O.; Unsworth, W. P.; Fairlamb, I. J. S. Palladium-Catalyzed Synthesis of Macrocycles. In *Practical Medicinal Chemistry with Macrocycles*, John Wiley & Sons, Inc.: 2017; pp 281-305.

14. (a) Nicolaou, K. C.; Bulger, P. G.; Sarlah, D. *Angew. Chem. Int. Ed.* **2005**, *44*, 4442-4489; (b) Wang, D.; Gao, S. *Org. Chem. Front.* **2014**, *1*, 556-566; (c) Zhang, W.; Moore, J. S. *Angew. Chem. Int. Ed.* **2006**, *45*, 4416-4439.
15. (a) Porco, J. A.; Schoenen, F. J.; Stout, T. J.; Clardy, J.; Schreiber, S. L. *J. Am. Chem. Soc.* **1990**, *112*, 7410-7411; (b) Shair, M. D.; Yoon, T.-y.; Danishefsky, S. J. *Angew. Chem. Int. Ed.* **1995**, *34*, 1721-1723; (c) Myers, A. G.; Fraley, M. E.; Tom, N. J.; Cohen, S. B.; Madar, D. J. *Chem. Biol.* **1995**, *2*, 33-43; (d) Myers, A. G.; Tom, N. J.; Fraley, M. E.; Cohen, S. B.; Madar, D. J. *J. Am. Chem. Soc.* **1997**, *119*, 6072-6094.
16. Koyama, Y.; Lear, M. J.; Yoshimura, F.; Ohashi, I.; Mashimo, T.; Hiram, M. *Org. Lett.* **2005**, *7*, 267-270.
17. Mohapatra, D. K.; Bhattasali, D.; Gurjar, M. K.; Khan, M. I.; Shashidhara, K. S. *Eur. J. Org. Chem.* **2008**, *2008*, 6213-6224.
18. (a) Krauss, J.; Unterreitmeier, D.; Neudert, C.; Bracher, F. *Arch. Pharm.* **2005**, *338*, 605-608; (b) Spivey, A. C.; McKendrick, J.; Srikan, R.; Helm, B. A. *J. Org. Chem.* **2003**, *68*, 1843-1851; (c) Balraju, V.; Reddy, D. S.; Periasamy, M.; Iqbal, J. *J. Org. Chem.* **2005**, *70*, 9626-9628; (d) ten Brink, H. T.; Rijkers, D. T. S.; Liskamp, R. M. J. *J. Org. Chem.* **2006**, *71*, 1817-1824; (e) Song, Z. J.; Tellers, D. M.; Journet, M.; Kuethe, J. T.; Lieberman, D.; Humphrey, G.; Zhang, F.; Peng, Z.; Waters, M. S.; Zewge, D.; Nolting, A.; Zhao, D.; Reamer, R. A.; Dormer, P. G.; Belyk, K. M.; Davies, I. W.; Devine, P. N.; Tschaen, D. M. *J. Org. Chem.* **2011**, *76*, 7804-7815.
19. (a) Hussain, A.; Yousuf, S. K.; Kumar, D.; Lambu, M.; Singh, B.; Maity, S.; Mukherjee, D. *Adv. Synth. Catal.* **2012**, *354*, 1933-1940; (b) Hussain, A.; Yousuf, S. K.; Sharma, D. K.; Mallikharjuna Rao, L.; Singh, B.; Mukherjee, D. *Tetrahedron* **2013**, *69*, 5517-5524.
20. Niu, T.-f.; Sun, M.; Lv, M.-f.; Yi, W.-b.; Cai, C. *Org. Biomol. Chem.* **2013**, *11*, 7232-7238.
21. (a) Yamasaki, R.; Shigeto, A.; Saito, S. *J. Org. Chem.* **2011**, *76*, 10299-10305; (b) Schmitt, M.; Ammon, H. *Synlett* **1999**, *6*, 750-752; (c) Miki, K.; Fujita, M.; Inoue, Y.; Senda, Y.; Kowada, T.; Ohe, K. *J. Org. Chem.* **2010**, *75*, 3537-3540; (d) Odermatt, S.; Alonso-Gómez, J. L.; Seiler, P.; Cid, M. M.; Diederich, F. *Angew. Chem. Int. Ed.* **2005**, *44*, 5074-5078; (e) Chen, G.; Wang, L.; Thompson, D. W.; Zhao, Y. *Org. Lett.* **2008**, *10*, 657-660.
22. (a) Han, F.-S. *Chem. Soc. Rev.* **2013**, *42*, 5270-5298; (b) Mako, T. L.; Byers, J. A. *Inorg. Chem. Front.* **2016**, *3*, 766-790; (c) Corcoran, E. B.; Pirnot, M. T.; Lin, S.; Dreher, S. D.; DiRocco, D. A.; Davies, I. W.; Buchwald, S. L.; MacMillan, D. W. C. *Science* **2016**, *353*, 279-283.
23. Carril, M.; Correa, A.; Bolm, C. *Angew. Chem. Int. Ed.* **2008**, *47*, 4862-4865.
24. (a) Correa, A.; Bolm, C. *Angew. Chem. Int. Ed.* **2007**, *46*, 8862-8865; (b) Correa, A.; Bolm, C. *Adv. Synth. Catal.* **2008**, *350*, 391-394; (c) Correa, A.; Elmore, S.; Bolm, C. *Chem. Eur. J.* **2008**, *14*, 3527-3529.
25. Bistri, O.; Correa, A.; Bolm, C. *Angew. Chem. Int. Ed.* **2008**, *47*, 586-588.
26. Correa, A.; Carril, M.; Bolm, C. *Angew. Chem. Int. Ed.* **2008**, *47*, 2880-2883.
27. Buchwald, S. L.; Bolm, C. *Angew. Chem. Int. Ed.* **2009**, *48*, 5586-5587.
28. (a) Petuker, A.; El-Tokhey, M.; Reback, M. L.; Mallick, B.; Apfel, U.-P. *ChemistrySelect* **2016**, *1*, 2717-2721; (b) Rao Volla, C. M.; Vogel, P. *Tetrahedron Lett.* **2008**, *49*, 5961-5964; (c) Huang, H.; Jiang, H.; Chen, K.; Liu, H. *J. Org. Chem.* **2008**, *73*, 9061-9064; (d) Mao, J.; Xie, G.; Wu, M.; Guo, J.; Ji, S. *Adv. Synth. Catal.* **2008**, *350*, 2477-2482.

29. (a) Sindhu, K. S.; Thankachan, A. P.; Thomas, A. M.; Anilkumar, G. *ChemistrySelect* **2016**, *1*, 556-559; (b) Yang, J.; Shen, G.; Chen, D. *Synth. Commun.* **2013**, *43*, 837-847; (c) Sawant, D. N.; Tambade, P. J.; Wagh, Y. S.; Bhanage, B. M. *Tetrahedron Lett.* **2010**, *51*, 2758-2761.
30. Okuro, K.; Furuune, M.; Enna, M.; Miura, M.; Nomura, M. *J. Org. Chem.* **1993**, *58*, 4716-4721.
31. (a) Gujadhur, R. K.; Bates, C. G.; Venkataraman, D. *Org. Lett.* **2001**, *3*, 4315-4317; (b) Thathagar, M. B.; Beckers, J.; Rothenberg, G. *Green Chem.* **2004**, *6*, 215-218; (c) Ma, D.; Liu, F. *Chem. Commun.* **2004**, 1934-1935; (d) Saejueng, P.; Bates, C. G.; Venkataraman, D. *Synthesis* **2005**, *2005*, 1706-1712; (e) Li, J.-H.; Li, J.-L.; Wang, D.-P.; Pi, S.-F.; Xie, Y.-X.; Zhang, M.-B.; Hu, X.-C. *J. Org. Chem.* **2007**, *72*, 2053-2057; (f) Monnier, F.; Turtaut, F.; Duroire, L.; Taillefer, M. *Org. Lett.* **2008**, *10*, 3203-3206; (g) Zuidema, E.; Bolm, C. *Chem. Eur. J.* **2010**, *16*, 4181-4185; (h) Zou, L.-H.; Johansson, A. J.; Zuidema, E.; Bolm, C. *Chem. Eur. J.* **2013**, *19*, 8144-8152; (i) Liu, Y.; Blanchard, V.; Danoun, G.; Zhang, Z.; Tlili, A.; Zhang, W.; Monnier, F.; Van Der Lee, A.; Mao, J.; Taillefer, M. *ChemistrySelect* **2017**, *2*, 11599-11602; (j) Thomas, A. M.; Sujatha, A.; Anilkumar, G. *RSC Adv.* **2014**, *4*, 21688-21698.

### 3. Cu(I)-Catalyzed Macrocyclic Sonogashira-Type Cross-Coupling

Jeffrey Santandrea, Anne-Catherine Bédard and Shawn K. Collins\*

Department of Chemistry and Centre for Green Chemistry and Catalysis,  
Université de Montréal, CP 6128 Station Downtown, Montréal, Québec, Canada, H3C 3J7

*Organic Letters* **2014**, *16*, 3892-3895.

Reproduced with permission from the American Chemical Society

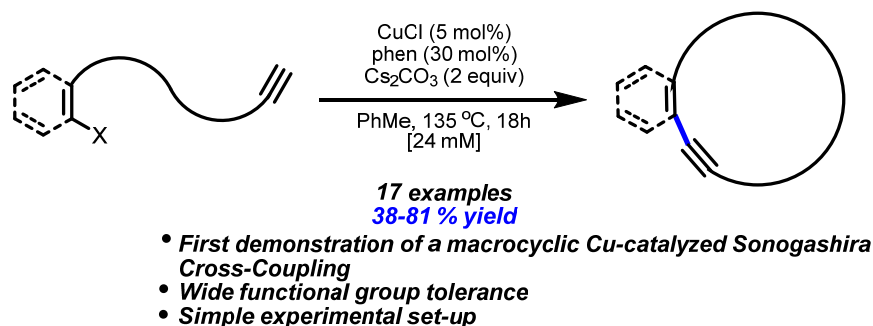
Permanent link to the article (DOI): [10.1021/o1501898b](https://doi.org/10.1021/o1501898b)

#### Contributions:

- Jeffrey Santandrea participated in the design of the experiments, did all the experimental work in the optimization and in the macrocycle scope, participated in the synthesis of (*S*)-zearalane and contributed to the writing of the manuscript.
- Anne-Catherine Bédard participated in the synthesis of (*S*)-zearalane and contributed to the writing of the manuscript.
- Shawn K. Collins participated in the design of the experiments and the writing of the manuscript.

### 3.1 Abstract

A macrocyclic Cu-catalyzed Sonogashira-type cross-coupling reaction has been developed that employs an operationally simple CuCl/phen/Cs<sub>2</sub>CO<sub>3</sub> catalyst system. Macrocyclizations can be performed at relatively high concentrations without the need for slow addition techniques and form macrocycles with various ring sizes and functional groups. The optimized protocol was employed in the synthesis of (*S*)-zearalane, demonstrating applicability toward the synthesis of a macrocycle with known biological activity.



### 3.2 Introduction

As applications of macrocycles continue to emerge in diverse fields,<sup>1</sup> the development of strategies for the synthesis of macrocycles has attracted increased interest. While the design of conformational control techniques and solutions for the control of dilution effects have emerged, the discovery of catalysts and/or catalytic transformations remains a challenging aspect in macrocyclization chemistry. The development of catalysis is particularly critical for macrocyclization via the formation of carbon–carbon bonds. In a recent account of the synthesis of the drug candidate vaniprevir,<sup>2</sup> various Pd-catalyzed cross-coupling strategies were investigated for macrocyclization via carbon–carbon bond formation; an intramolecular Sonogashira cross-coupling<sup>3</sup> was plagued by various difficulties that made it unappealing in the context of drug discovery efforts (Figure 3.1).<sup>4</sup> The Sonogashira cross-coupling traditionally employs a Pd-based catalyst and a Cu-based additive (catalytic or stoichiometric), and high catalyst loadings are often used to improve macrocyclizations. Consequently, the high cost and toxicity of Pd combined with the high dilution often necessary can render macrocyclic Sonogashira reactions problematic. In addition, the coupling of terminal alkynes and



aryl/alkenyl electrophiles can be complicated by competing alkyne dimerization resulting in low yields in many macrocyclization reactions. One avenue for an improved macrocyclic process would involve developing a Cu-catalyzed variant that would include lower costs, lower toxicity, and greater availability relative to Pd-based strategies.<sup>5</sup> Current Cu-catalyzed reactions<sup>6</sup> inspired by the original Castro–Stephens cross-coupling<sup>7</sup> (CuI/PPh<sub>3</sub>, Cu(neo)(PPh<sub>3</sub>), and [Cu-(DMEDA)<sub>2</sub>]Cl<sub>2</sub>) focus on couplings of aryl alkynes, with little emphasis placed on aliphatic alkynes and no reports of intramolecular variants. Herein we report the development of an efficient macrocyclic Cu(I)-catalyzed macrocyclic Sonogashira-type cross-coupling process, with high functional group tolerance and demonstrate its applicability to the synthesis of biologically active natural products.

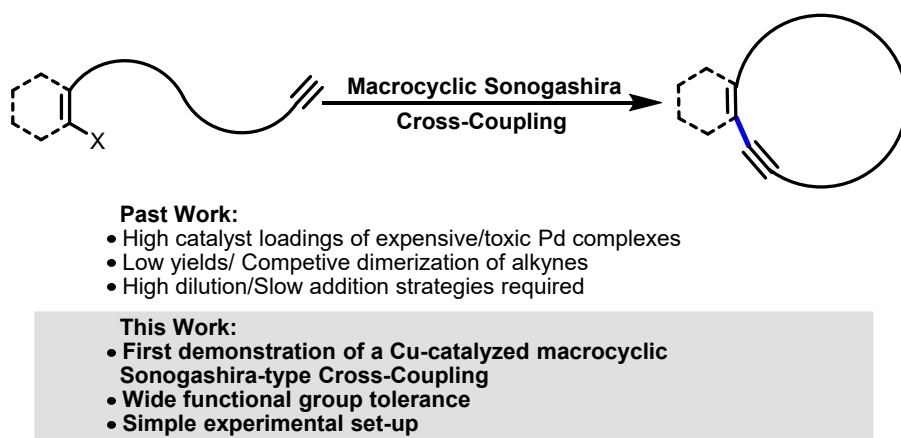


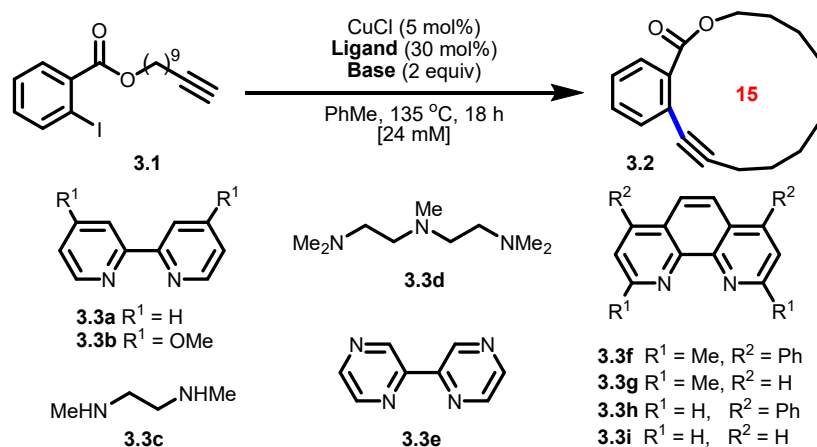
**Figure 3.1** Macrocyclic Sonogashira cross-coupling processes

### 3.3 Results and Discussion

To investigate the development of a macrocyclic Sonogashira cross-coupling, the cyclization of the iodoarene **3.1** to afford the 15-membered macrolactone **3.2** was selected as a model macrocyclization. The acyclic precursor **3.1** possesses a long, flexible alkyl chain with little conformational bias toward cyclization. As such, it is not surprising that Bracher et al. reported that the cyclization of alkyne **3.1** to form benzolactone **3.2** was challenging, requiring high catalyst loadings (Pd(PPh<sub>3</sub>)<sub>2</sub>Cl<sub>2</sub> (35 mol%), CuI (1.5 equiv)) and providing low yields (15 %).<sup>3f</sup> Attempts at improving the process through modification of the ligand or the Pd source did not improve the yield of benzolactone **3.2**.<sup>8</sup> Consequently, the use of Cu-based catalysis for

the intramolecular Sonogashira-type cross-coupling of alkyl alkynes and aryl iodides was investigated for the first time.

**Table 3.1** Optimization of a Cu(I)-catalyzed macrocyclic Sonogashira-type cross-coupling



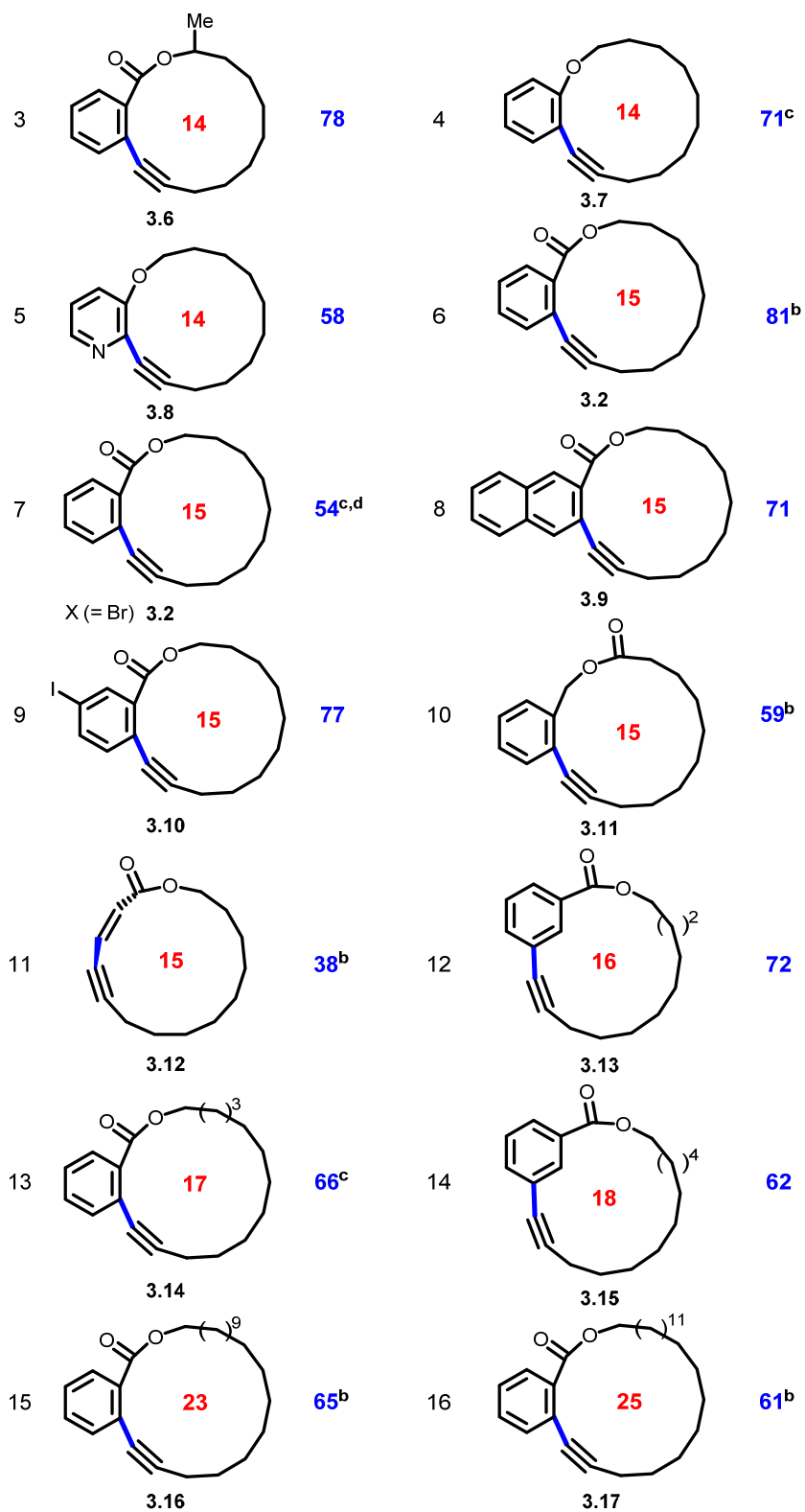
Entry	Ligand	Base	Yield <b>3.2</b> (%) <sup>a</sup>	Recovered <b>3.1</b> (%) <sup>a</sup>
1	<b>3.3a</b>	Cs <sub>2</sub> CO <sub>3</sub>	25	38
2	<b>3.3b</b>	Cs <sub>2</sub> CO <sub>3</sub>	25	<5
3	<b>3.3c<sup>b</sup></b>	Cs <sub>2</sub> CO <sub>3</sub>	30	19
4	<b>3.3c<sup>c</sup></b>	Cs <sub>2</sub> CO <sub>3</sub>	58	<5
5	<b>3.3d</b>	Cs <sub>2</sub> CO <sub>3</sub>	30	19
6	<b>3.3f</b>	Cs <sub>2</sub> CO <sub>3</sub>	32	48
7	<b>3.3g</b>	Cs <sub>2</sub> CO <sub>3</sub>	58	19
8	<b>3.3e</b>	Cs <sub>2</sub> CO <sub>3</sub>	73	<5
9	<b>3.3h</b>	Cs <sub>2</sub> CO <sub>3</sub>	78	<5
10	<b>3.3i</b>	Cs <sub>2</sub> CO <sub>3</sub>	78	<5
11	<b>3.3i</b>	Cs <sub>2</sub> CO <sub>3</sub>	81 <sup>d</sup>	<5
12	<b>3.3i</b>	K <sub>2</sub> CO <sub>3</sub>	70	32
13	<b>3.3i</b>	K <sub>3</sub> PO <sub>4</sub>	63	46

<sup>a</sup>Yields following chromatography. Reactions run on 0.12 mmol scale. Temperature refers to the temperature of the oil bath. <sup>b</sup>In place of CuCl, the preformed catalyst [Cu(DMEDA)<sub>2</sub>]Cl<sub>2</sub> (5 mol%) was used without any other added ligand. <sup>c</sup>In place of CuCl, the preformed catalyst [Cu(DMEDA)<sub>2</sub>]Cl<sub>2</sub> (5 mol %) was used. <sup>d</sup>Using 20 mol% of **3.3i**.

Optimization of the macrocyclic Cu-catalyzed Sonogashira cross-coupling involved the macrocyclization of alkyne **3.1** using CuCl as a Cu source with various other amine-based ligands (Table 3.1). Furthermore, Cs<sub>2</sub>CO<sub>3</sub> was selected as base and toluene at 135 °C (oil bath temperature) as solvent. When CuCl was investigated for the macrocyclization of iodide **3.1** using 2,2'-bipyridine **3.3a** or the more electron-donating ligand **3.3b**, a 25 % yield of the desired macrocycle **3.2** was obtained, along with significant amounts of starting material **3.1** (38 %). Using the preformed catalyst [Cu(DMEDA)<sub>2</sub>]Cl<sub>2</sub> (5 mol%) developed by Bolm et al. afforded a low yield of **3.2** as well (30 %); however, employing [Cu(DMEDA)<sub>2</sub>]Cl<sub>2</sub> with 30 mol% added **3.3c** provided an increased yield of 58 %. Similarly higher yields of the macrocycle resulted when employing the neocuproine **3.3g** or bipyrazine ligand **3.3e** (58 % and 73 % of **3.2** respectively); however, the most efficient ligands surveyed were bathophenanthroline **3.3h** and 1,10-phenanthroline (phen) **3.3i**, which afforded the macrocycle **3.2** in an identical 78 % yield. The ligand loading of phen (**3.3i**) was subsequently investigated, and catalyst loadings of 20 → 30 mol % afforded the best yields.<sup>8</sup> Conducting the macrocyclization in the absence of phen resulted in only 19 % of the desired macrocycle **3.2**. When the reaction was repeated in the absence of CuCl or Cs<sub>2</sub>CO<sub>3</sub>, no reaction was observed.<sup>9</sup> Exchanging the Cs<sub>2</sub>CO<sub>3</sub> base for other bases (K<sub>2</sub>CO<sub>3</sub>, K<sub>3</sub>PO<sub>4</sub>) did not afford improvements in the yield of macrocycle **3.2**. Decreasing the concentration led to very slow reactions and low yields of desired macrocycle **3.2**.<sup>8</sup> As CuCl/phen/Cs<sub>2</sub>CO<sub>3</sub> was identified as a promising catalyst system, the synthesis of various macrocycles with varying ring sizes and functionality was explored (Table 3.2).

**Table 3.2** Scope of the Cu(I)-catalyzed macrocyclic Sonogashira-type cross-coupling

Entry	Macrocycle	Yield (%) <sup>a</sup>	Entry	Macrocycle	Yield (%) <sup>a</sup>
1	 3.4	46	2	 3.5	83

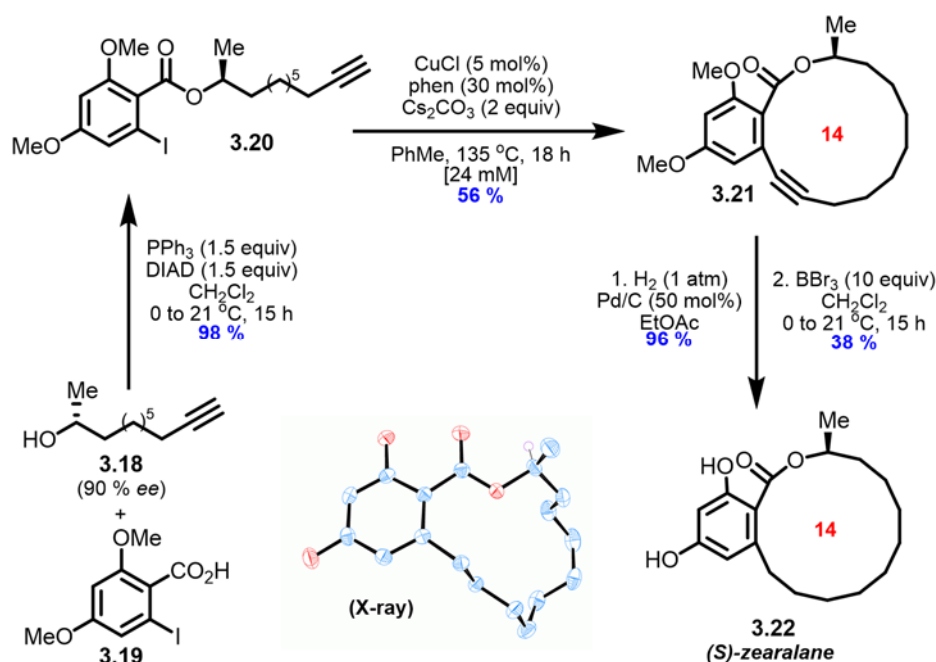


<sup>a</sup>Isolated yields following chromatography. Ring size of the macrocycles are indicated in red. <sup>b</sup>Using 20 mol % of phen. <sup>c</sup>Reaction time was 48 h.

A 10-membered macrolactone **3.4** could be prepared in modest yield (46 %) demonstrating the viability of the method for forming strained macrocycles. An analogous 13-membered macrocycle **3.5** could be formed in higher yield (83 %, entry 2). A variety of 14-membered macrocycles were also prepared (entries 3 → 5): the benzolactone **3.6** was cyclized in 78 % yield. Replacing the ester functionality of **3.6** with an ether afforded the macrocycle **3.7** in 71 % yield. A pyridine-containing analogue **3.8** was also prepared in good yield (58 %). The 15-membered macrocycle **3.2** was prepared in 81 % yield, and the macrocyclization could easily be scaled up to gram scale (~2.5 mmol, 75 %, 48 h). The macrocycle **3.2** could also be prepared from the corresponding aryl bromide. Although the yield was slightly lower (54 %), the Cu-catalyzed macrocyclic Sonogashira-type coupling represents a rare example of such a transformation from a corresponding aryl bromide.<sup>10</sup> The aryl iodide moiety could be extended to naphthalene-derived motifs, and the corresponding macrocycle **3.9** was isolated in good yield (71 %). The macrocycle **3.10** was formed from a corresponding aryl diiodide. Interestingly, macrocyclization was observed with complete selectivity to afford the 15-membered **3.10** in 77 % yield. The macrocyclization was also tolerant to varying the position of the ester unit, as in the 15-membered macrocycle **3.11** (59 % yield). Macrocyclization to form the enyne containing 15-membered macrolactone **3.12** was hampered by the stability of the corresponding starting material. While the macrocycle **3.12** could be isolated in 38 % yield (entry 11), the  $\beta$ -iodo alkenyl ester was sensitive to the basic conditions employed. Macrocyclization to form *meta*-substituted benzolactones occurred in good yields; the 16- and 18-membered macrocycles **3.13** and **3.15** were obtained in 72 % and 62 % yields respectively (entries 12 and 14). Finally, the synthesis of larger rings was explored (entries 13, 15, and 16). The 17-membered macrocycle **3.14** was prepared in 66 % yield, while the analogous 23- and 25-membered benzolactones **3.16** and **3.17** were obtained in 65 % and 61 % yield, respectively.

To further demonstrate the utility of the Cu-catalyzed macrocyclic Sonogashira-type strategy, the polyketide-derived product (*S*)-zearalane was prepared, which has been reported to have interesting anabolic, estrogenic, anthelmintic, and immunomodulating properties (Scheme 3.1).<sup>11</sup> The enantioenriched secondary alcohol **3.18**, prepared via known procedures, underwent Mitsunobu-type coupling with known acid **3.19** to provide the ester **3.20** (98 % yield).<sup>12</sup> Attempts at conducting the macrocyclization of ester **3.20** using known Pd-based

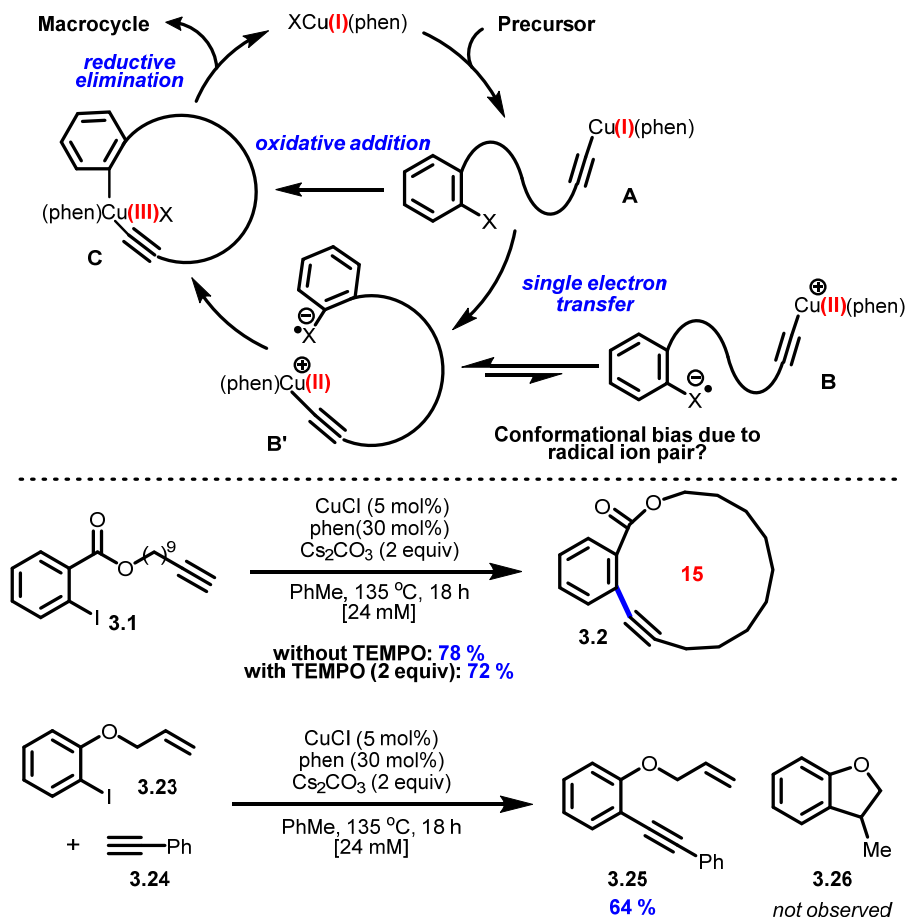
cross-coupling conditions ( $\text{Pd}(\text{PPh}_3)_2\text{Cl}_2$  (5 mol %),  $\text{CuI}$  (10 mol %), THF, 18 h) were unsuccessful. When using slow addition and high dilution ([24 or 2.4 mM]), Sonogashira cross-coupling of alkyne **3.20** did not afford any of the desired product **3.21**, despite 100 % consumption of the starting material **3.20**. In contrast, treating ester **3.20** with the catalytic system afforded the 14-membered macrolactone **3.21** in 56 % yield. Hydrogenation of the aryl alkyne (96 % yield) and subsequent  $\text{BBr}_3$ -mediated cleavage of the methyl ethers afforded (*S*)-zearalane **3.22** in 36 % yield over two steps. X-ray quality crystals of (*S*)-zearalane were obtained from slow diffusion of a  $\text{CH}_2\text{Cl}_2$  solution into hexanes, and subsequent analysis<sup>13</sup> confirmed the macrocyclic structure of **3.22** (Scheme 3.1).



**Scheme 3.1** Total synthesis of (*S*)-zearalane using a Cu-catalyzed macrocyclic Sonogashira-type coupling

The mechanisms of existing Cu-catalyzed Sonogashira-type cross-couplings have not all been studied in detail, and many imply similar mechanistic proposals that have been described for related Cu-catalyzed C–O, C–N, and C–X bond formations.<sup>14</sup> Recently, Bolm et al. have put forth some mechanistic evidence for intermolecular Cu-catalyzed couplings.<sup>15</sup> A likely first step would involve in situ formation of copper acetylide **A** (Scheme 3.2). Bolm reported experimental evidence for the importance of excess ligand to promote the formation of species

such as copper acetylide **A** versus other polymeric Cu acetylide complexes.<sup>15</sup> Bolm also reported computational studies suggesting against the formation of a high energy Cu(III)-intermediate **C** via direct oxidative addition. Alternatively, single electron transfer (SET) could generate the radical anion **B** or **B'**. The formation of a radical ion pair may help to induce a conformational preference which is conducive to the formation of Cu(III)-intermediate **C**. Preliminary investigations reveal a strong solvent dependence for the macrocyclization. When the cyclization (**3.1** → **3.2**, CuCl (5 mol%), phen (30 mol%), Cs<sub>2</sub>CO<sub>3</sub> (2 equiv), 135 °C) was carried out in nonpolar solvents the yields were typically higher (PhMe: 78 %; PhCl: 74 %; xylenes: 72 %) than in polar solvents (DMF: <5 %; dioxane: 57 %) which favor disassociation in the proposed radical ion pair. As radical ion pairs are not commonly invoked in mechanisms of the Pd-catalyzed Sonogashira, it is possible that these mechanistic differences are partially responsible for the efficiency of the Cu-catalyzed strategy. Similar SET pathways for Cu-intermediates have been proposed for photocatalytic Sonogashira cross-couplings.<sup>16</sup> Formation of a carbon centered radical from **B** was investigated: macrocyclization of alkyne **3.1** in the presence of TEMPO as a radical trap still proceeded in high yield (72 % vs 78 % in the absence of TEMPO) (Scheme 3.2). In addition, submitting the allylated iodophenol **3.23** to the optimized conditions for cross-coupling did not afford any of the cyclized **3.26**.<sup>17</sup> This is in contrast to recently reported Cu-catalyzed photoinduced C–N bond formation in which C–I bond cleavage was observed.<sup>18</sup> The final step would involve reductive elimination from **C** and regeneration of the active catalyst.<sup>19</sup>



**Scheme 3.2** (Top) Possible mechanism for the Cu-catalyzed macrocyclic Sonogashira-type cross-coupling; (Bottom) Preliminary mechanistic investigations

### 3.4 Conclusions

In summary, a Cu-catalyzed macrocyclic Sonogashira-type cross-coupling reaction has been developed that outperforms other Pd-catalyzed protocols. Utilization of an operationally simple  $\text{CuCl}/\text{phen}/\text{Cs}_2\text{CO}_3$  catalyst system promotes macrocyclization at relatively high concentrations without the need for slow addition techniques and does not afford homodimerization side products. The macrocyclizations are efficient even when employing alkyl alkyne coupling partners which have rarely been reported. Macrocycles with various ring sizes (10- to 25-membered rings), functional groups, and arene substituents (poly- and heteroaromatic) are accessible using the optimized conditions. The protocol described herein demonstrates that copper can replace the conventional, expensive, and toxic Pd-catalyzed



macrocyclic Sonogashira cross-coupling reactions. The synthesis of biologically active (*S*)-zearalane has been demonstrated and suggests that further application in the synthesis of other natural products and compounds of medicinal interest is possible.

### Supporting Information

Experimental procedures and characterization data for all new compounds. This material is available free of charge via the Internet at <http://pubs.acs.org>.

### Corresponding Author

\*E-mail: [shawn.collins@umontreal.ca](mailto:shawn.collins@umontreal.ca)

### Notes

The authors declare no competing financial interest.

### Acknowledgments

The authors acknowledge the Natural Sciences and Engineering Research Council of Canada (NSERC), Université de Montréal, and the Centre for Green Chemistry and Catalysis for generous funding. A.-C.B. thanks NSERC for a Vanier graduate scholarship.

## 3.5 Bibliography

1. (a) Vendeville, S.; Cummings, M. D. *Annu. Rep. Med. Chem.* **2013**, 48, 371; (b) Yu, X.; Sun, D. *Molecules* **2013**, 18, 6230; (c) Wolfson, W. *Chem. Biol.* **2012**, 19, 1356; (d) White, C. J.; Yudin, A. K. *Nat. Chem.* **2011**, 3, 509; (e) Gross, D. E.; Zang, L.; Moore, J. S. *Pure Appl. Chem.* **2012**, 84, 869.
2. Kong, J.; Chen, C. y.; Balsells-Padros, J.; Cao, Y.; Dunn, R. F.; Dolman, S. J.; Janey, J.; Hongmei Li, H.; Zacuto, M. J. *J. Org. Chem.* **2012**, 77, 3820.
3. (a) Hussain, A.; Khalid, S.; Kumar, D. Y.; Lambu, M.; Singh, B.; Maity, S.; Mukherjee, D. *Adv. Synth. Catal.* **2012**, 354, 1933; (b) Hussain, A.; Rao, M.; Sharma, D. K.; Tripathi, A. K.; Singh, B.; Mukherjee, D. *RSC Adv.* **2013**, 3, 19899; (c) Spivey, A. C.; McKendrick, J.; Srikanan, R. *J. Org. Chem.* **2003**, 68, 1843; (d) Balraju, V.; Reddy, D. S.; Periasamy, M.; Iqbal, J. *J. Org. Chem.* **2005**, 70, 9626; (e) Yamasaki, R.; Shigeto, A.; Saito, S. *J. Org. Chem.* **2011**, 76, 10299; (f) Krauss, J.; Unterreitmeier, D.; Neudert, C.; Bracher, F. *Arch. Pharm. Chem. Life Sci.* **2005**, 338, 605; (g) Gallego, D.; Bruck, A.; Irran, E.; Meier, F.; Kaupp, M.; Driess, M.; Hartwig, J. F. *J. Am. Chem. Soc.* **2013**, 135, 15617.

4. Marsault, E.; Peterson, M. L. *J. Med. Chem.* **2011**, *54*, 1961.
5. (a) Okuro, K.; Furuune, M.; Miura, M.; Nomura, M. *Tetrahedron Lett.* **1992**, *16*, 5363; (b) Sonogashira, K.; Tohda, Y.; Hagihara, N. *Tetrahedron Lett.* **1975**, 4467; (c) Sonogashira, K. *Metal-Catalyzed Cross Coupling Reactions*. 2007; p 203; (d) Chinchilla, R.; Najera, C. *Chem. Soc. Rev.* **2011**, *40*, 5084; (e) Sonogashira, K. *J. Organomet. Chem.* **2002**, 653, 46.
6. (a) Okuro, K.; Furuune, M.; Enna, M.; Miura, M.; Nomura, M. *J. Org. Chem.* **1993**, *58*, 4716; (b) Li, J. H.; Li, J. L.; Wang, D. P.; Pi, S. F.; Xie, Y. X.; Zhang, M. B.; Hu, X. C. *J. Org. Chem.* **2007**, *72*, 2053; (c) Monnier, F.; Turtaut, F. O.; Duroure, L.; Taillefer, M. *Org. Lett.* **2008**, *10*, 3203; (d) Saejueng, P.; Bates, C. G.; Venkataraman, D. *Synthesis* **2005**, *10*, 1706; (e) Carril, M.; Correa, A.; Bolm, C. *Angew. Chem., Int. Ed.* **2008**, *47*, 4862; (f) Zuidema, E.; Bolm, C. *Chem.—Eur. J.* **2010**, *16*, 4181; (g) Thathagar, M. B.; Beckers, J.; Rothenberg, G. *Green Chem.* **2004**, *6*, 215; (h) Gujadhur, R. K.; Bates, C. G.; Venkataraman, D. *Org. Lett.* **2001**, *3*, 4315.
7. Stephens, R. D.; Castro, C. E. *J. Org. Chem.* **1963**, *28*, 3313.
8. For a full description of the attempts to catalyze **3.1**→**3.2** using Pd-catalysis, as well as more details concerning optimization of catalyst loadings and concentrations, see the Supporting Information.
9. Gonda, Z.; Tolnai, G. L.; Novák, Z. *Chem.—Eur. J.* **2010**, *16*, 11822.
10. (a) Thakur, K. G.; Jaseer, E. A.; Naidu, A. B.; Sekar, G. *Tetrahedron Lett.* **2009**, *50*, 2865; (b) Mao, J.; Guo, J.; Ji, S. j.; Mao, J. *J. Mol. Catal. A: Chem.* **2008**, *284*, 85; (c) Yang, D.; Li, B.; Yang, H.; Fu, H.; Hu, L. *Synlett* **2011**, *5*, 702.
11. (a) Stob, M.; Baldwin, R.; Tuite, J.; Andrews, F. N.; Gillette, K. G. *Nature* **1962**, *196*, 1318; (b) Fürstner, A.; Thiel, O. R.; Kindler, N.; Bartkowska, B. *J. Org. Chem.* **2000**, *65*, 7990; (c) Bracher, F.; Krauß, J. *Eur. J. Org. Chem.* **2001**, 4701.
12. (a) Marshall, J. A.; Wang, X. J. *J. Org. Chem.* **1991**, *56*, 4913; (b) Mikula, H.; Skrinjar, P.; Sohr, B.; Ellmer, D.; Hametner, C.; Frohlich, J. *Tetrahedron* **2013**, *69*, 10322.
13. CCDC 999557 (**3.22**) contains the supplementary crystallographic data. These data can be obtained free of charge from The Cambridge Crystallographic DataCentre via [www.ccdc.cam.ac.uk/data\\_request/cif](http://www.ccdc.cam.ac.uk/data_request/cif).
14. (a) Jones, G. O.; Liu, P.; Houk, K. N.; Buchwald, S. L. *J. Am. Chem. Soc.* **2010**, *132*, 6205; (b) Casitas, A.; Ribas, X. *Chem. Sci.* **2013**, *4*, 2301.
15. Liang-Hua Zou, L. H.; Johansson, A. J.; Zuidema, E.; Bolm, C. *Chem.—Eur. J.* **2013**, *19*, 8144.
16. Sagadevan, A.; Hwang, K. C. *Adv. Synth. Catal.* **2012**, *354*, 3421.
17. (a) Tye, J. W.; Weng, Z.; Johns, A. M.; Incarvito, C. D.; Hartwig, J. F. *J. Am. Chem. Soc.* **2008**, *130*, 9971; (b) Sperotto, E.; van Klink, G. P. M.; Koten, G.; de Vries, J. G. *Dalton Trans.* **2010**, *39*, 10338.
18. Creutz, S. E.; Lotito, K. J.; Fu, G. C.; Peters, J. C. *Science* **2012**, *338*, 647.
19. King, A. E.; Huffman, L. M.; Casitas, A.; Ribas, X.; Stahl, S. S. *J. Am. Chem. Soc.* **2010**, *132*, 12068.

## 4. Introduction to Photochemistry

In 1912, Ciamician wrote the now famous article "The Photochemistry of the Future".<sup>1</sup> He recognized the potential of utilizing solar energy, envisioning chemical industries that could manufacture chemicals in a similar way that plants photosynthesize carbohydrates using sunlight. The photochemist concluded his perspective by stating that *"if in a distinct future the supply of coal becomes completely exhausted, civilization will not be checked by that, for life and civilization will continue as long as the sun shines!"* Light is indeed an abundant, inexpensive, clean and safe natural energy source.<sup>2</sup> However, most organic compounds do not absorb in the visible region of the solar spectrum, but rather absorb in the UV range. The limited absorption range reduces the scope of organic compounds able to be activated under visible light irradiation, which in turn limits the range of photochemical transformations in industrial settings.<sup>3</sup> The design of efficient UV photoreactors has allowed chemists to utilize UV light in synthesis,<sup>4</sup> but encompasses drawbacks such as high-power consumption, expensive specialized glassware and protective gear. Alternatively, visible light irradiation is desirable in industry because it does not suffer from the same drawbacks.<sup>5</sup> Significant advances in visible light photocatalysis have been made over the past decade.<sup>6</sup> On irradiation with visible light, numerous photocatalysts now enable a larger scope of organic compounds to react photochemically.<sup>7</sup>

The following chapter will introduce the fundamental principles of photochemistry, as well as the utilization of photocatalysis in organic synthesis. Selected examples of photoredox catalysis and photoredox/nickel dual catalysis will be illustrated. Some photochemical macrocyclization protocols that have emerged in recent years will be presented. Lastly, the utilization of continuous flow photochemistry will be introduced.

### 4.1 Principles of Photochemistry

Photochemistry involves the study of chemical reactions and physical changes resulting from light absorption by atoms and molecules. Light can be polychromatic having a distribution of photons of different wavelengths, or monochromatic possessing a distribution of photons limited to a single wavelength. Photochemical transformations occur generally with the

absorption of visible or UV light irradiations (200-700 nm). Infrared and microwave irradiations are too low in energy to promote a photochemical reaction (Figure 4.1).

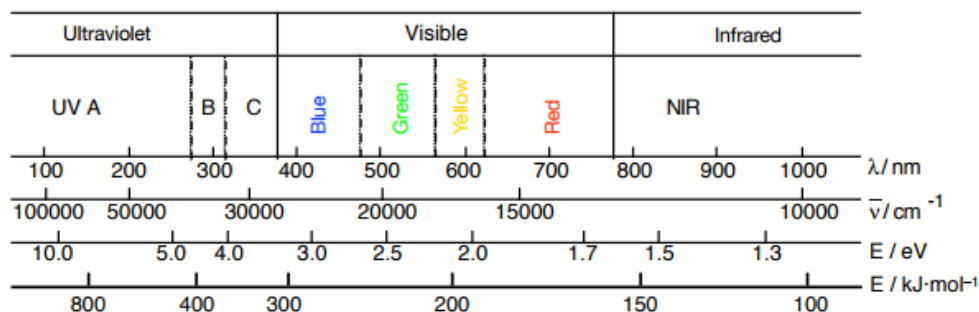


**Figure 4.1** Electromagnetic spectrum

The wavelength of light corresponds to the energy of a photon as described by the Planck-Einstein relation (Equation 4.1), where  $\lambda$  is the wavelength (m),  $E$  is the photon energy (J),  $h$  is Planck's constant ( $6.62 \times 10^{-34}$  J s),  $c$  is the speed of light ( $3.00 \times 10^8$  m s<sup>-1</sup>), and  $\nu$  is the frequency (s<sup>-1</sup>).

$$E = h\nu = \frac{hc}{\lambda} \quad (4.1)$$

The absorption of a photon by a reactant molecule, such as a photocatalyst, generally provides the required activation energy to promote transformations that are not accessible thermally.<sup>8</sup> The electronic states of a molecule, and the transitions between them, during a photochemical process can be illustrated in a Jablonski diagram (Figure 4.2). For example, a transition-metal-based photocatalyst (**PC**) can absorb a photon (abs) to promote a metal-to-ligand charge transfer (MLCT) to a higher energy vibrational level. Numerous singlet excited states (**\*PC** <sup>1</sup>MLCT<sub>n</sub>) may be attained before relaxing to the lowest spin-allowed vibrational level of the first singlet excited state (**\*PC** <sup>1</sup>MLCT<sub>1</sub>) via internal conversion ( $k_{ic}$ ). The **\*PC** <sup>1</sup>MLCT<sub>1</sub> can then pursue several deactivation pathways. Firstly, **\*PC** <sup>1</sup>MLCT<sub>1</sub> can regenerate **PC** either by a non-radiative pathway ( $k_{ic}$ ) or by a spin-allowed radiative pathway (fluorescence,  $k_f$ ). Secondly, **\*PC** <sup>1</sup>MLCT<sub>1</sub> can convert to the lowest energy triplet state (**\*PC** <sup>3</sup>MLCT<sub>1</sub>) through intersystem crossing ( $k_{isc}$ ). The **\*PC** <sup>3</sup>MLCT<sub>1</sub> is typically longer-lived because the transition from the triplet excited state to the singlet ground state is spin forbidden. **\*PC** <sup>3</sup>MLCT<sub>1</sub> can finally regenerate **PC** either by a non-radiative pathway ( $k_{ic}$ ) or by radiative

deactivation (phosphorescence,  $k_p$ ). Furthermore,  $^*PC\ ^3MLCT_1$  can be quenched by a chemical reagent, which would lead to diminished phosphorescence toward **PC**. Moreover, in the case where  $^*PC\ ^3MLCT_1$  is quenched by a substrate through single-electron transfer (SET) or energy transfer (ET) processes, productive photocatalytic transformations can ensue (Section 4.2).

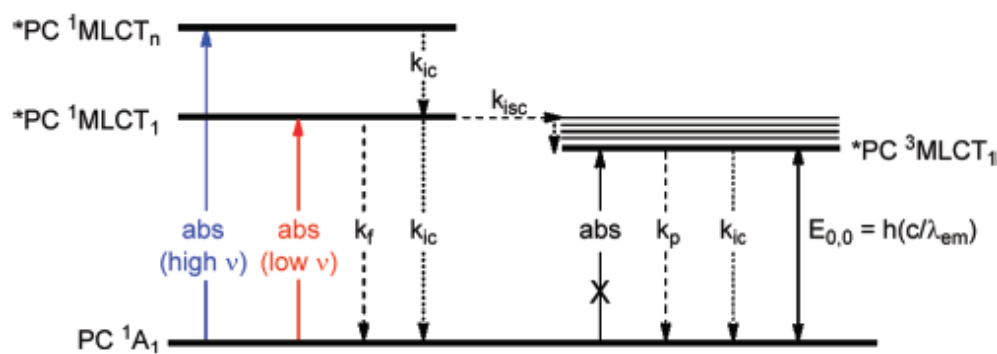


**Figure 4.2** Generalized Jablonski diagram of photocatalysts.  $k_f$ ,  $k_{ic}$ ,  $k_{isc}$ , and  $k_p$  are the rate constants for fluorescence, internal conversion, intersystem crossing, and phosphorescence, respectively and  $\lambda_{em}$  is the maximum emission wavelength of the photocatalyst. Reprinted with permission from ref 8. Copyright 2012 American Chemical Society.

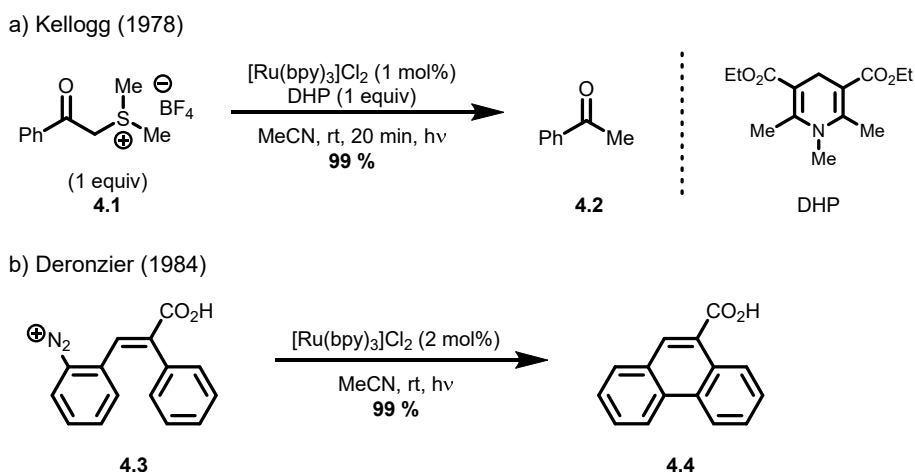
## 4.2 Photocatalysis

Photocatalysis is a term that describes a process in which light is used to activate a catalyst that accelerates the rate of a reaction without being consumed as a reactant. When light is absorbed by a photocatalyst, its triplet excited state can enable photocatalytic transformations through two different pathways.<sup>3</sup> The first pathway corresponds to energy transfer, in which the catalyst generates an excited state of a reactant. The second pathway corresponds to electron transfer, in which the catalyst acts either as an electron donor or acceptor. The latter pathway involves reactions such as visible light photoredox catalysis, which has had significant impact in synthetic chemistry over the past decade, due to potential to enable development of numerous novel organic reactions.

### 4.2.1 Photoredox Catalysis

Photoredox catalysis was first reported in 1978 by Kellogg,<sup>9</sup> who demonstrated that the photomediated reduction of sulfonium ions (**4.1**) to the corresponding alkanes (**4.2**) and

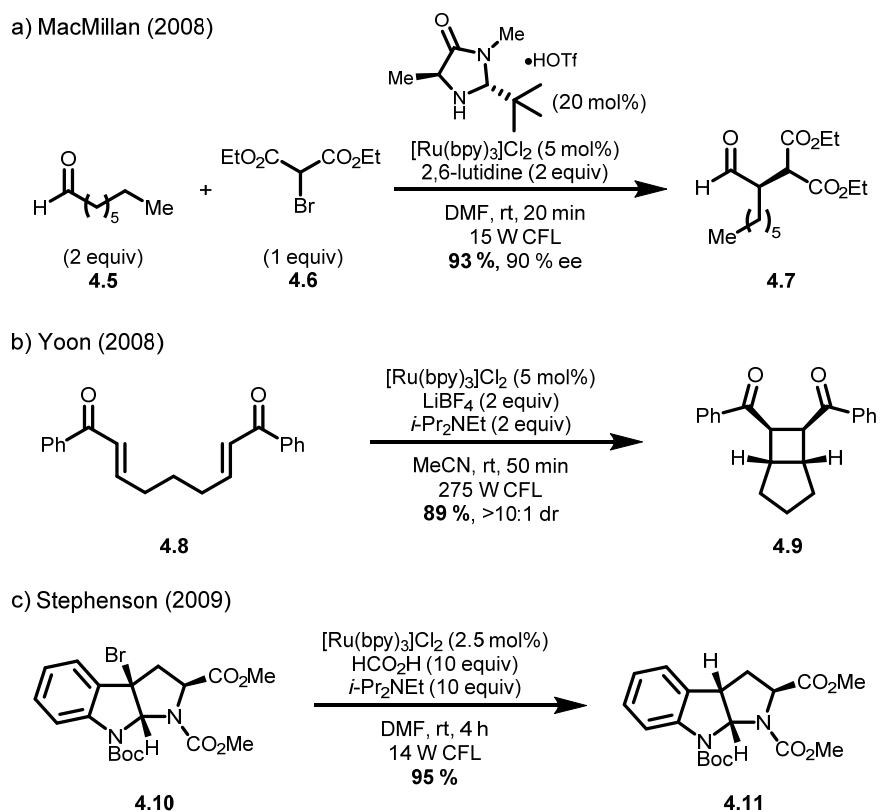
thioethers could be accelerated by the addition of a catalytic amount of  $[\text{Ru}(\text{bpy})_3]\text{Cl}_2$  in the presence of a terminal reductant (Scheme 4.1a). In 1984, the first redox-neutral photoredox-catalyzed process was reported by Deronzier,<sup>10</sup> who found that the Pschorr reaction could be catalyzed by  $[\text{Ru}(\text{bpy})_3]\text{Cl}_2$  to generate phenanthrene **4.4** quantitatively (Scheme 4.1b). In the same year, Deronzier reported the first oxidative photoredox-catalyzed process. Aryldiazonium salts were used as terminal oxidants in the presence of ruthenium(II) polypyridyl complexes for the conversion of benzylic alcohols to the corresponding aldehydes.<sup>11</sup> Other notable contributions to photoredox catalysis were subsequently reported by Fukuzumi and Tanaka,<sup>12</sup> Pac,<sup>13</sup> and Okada.<sup>14</sup>



**Scheme 4.1** Seminal contributions to organic photoredox catalysis

Despite the early demonstration of the utility of photoredox catalysis in organic synthesis, it remained unexploited by the scientific community until the late 2000s.<sup>15</sup> Photoredox catalysis in organic synthesis ultimately resurfaced in 2008, as contributions from MacMillan, Yoon and Stephenson underscored the potential of photocatalysis for method development.<sup>16</sup> MacMillan reported initially an enantioselective intermolecular  $\alpha$ -alkylation of aldehydes by merging photoredox catalysis and organocatalysis (Scheme 4.2a).<sup>16a</sup> Enantioenriched  $\alpha$ -alkylated aldehydes (**4.7**) were obtained upon visible light irradiation of  $[\text{Ru}(\text{bpy})_3]\text{Cl}_2$  in the presence of an aldehyde (**4.5**), an alkyl bromide (**4.6**) and an organocatalyst. It was found that  $[\text{Ru}(\text{bpy})_3]\text{Cl}_2$  enabled the generation of electron-deficient radicals from alkyl halides (**4.6**), which then combined with catalytically generated enamines in a highly enantioselective manner. Yoon concurrently reported a photoredox-catalyzed intramolecular

[2+2] enone cycloaddition reaction (Scheme 4.2b).<sup>16b</sup> It was found that bis(enone) **4.8** underwent efficient cyclization upon visible light irradiation in the presence of [Ru(bpy)<sub>3</sub>]Cl<sub>2</sub> as photocatalyst and LiBF<sub>4</sub> as Lewis acid. The *meso* diastereoisomer of cyclobutane-containing bicycle dione **4.9** was generated in 89 % yield with excellent stereoselectivity. Shortly thereafter in 2009, Stephenson reported a photoredox-mediated reductive dehalogenation protocol for benzylic and  $\alpha$ -acyl halides (Scheme 4.2c).<sup>16c</sup> For example, upon visible light irradiation of a catalytic amount of [Ru(bpy)<sub>3</sub>]Cl<sub>2</sub> in the presence of bromopyrroloindoline **4.10**, *i*-Pr<sub>2</sub>NEt and formic acid, debrominated product **4.11** was obtained in 95 % yield. The dehalogenation procedure was conducted photochemically without the use of toxic tin reagents.



**Scheme 4.2** Seminal contributions to modern organic photoredox catalysis

Visible-light-mediated photoredox catalysis has since grown into a prominent field of research.<sup>7</sup> Most photoredox-mediated transformations are enabled using transition-metal- and organic-based photocatalysts, such as **4.12-4.19** (Figure 4.3). Photocatalysts have been tuned to obtain specific photophysical properties including specific absorption and emission wavelengths, redox potentials and excited-state lifetimes. The growing diversity of

photocatalysts has widened the range of synthetic transformations accessible through photoredox catalysis.<sup>7a-g</sup>

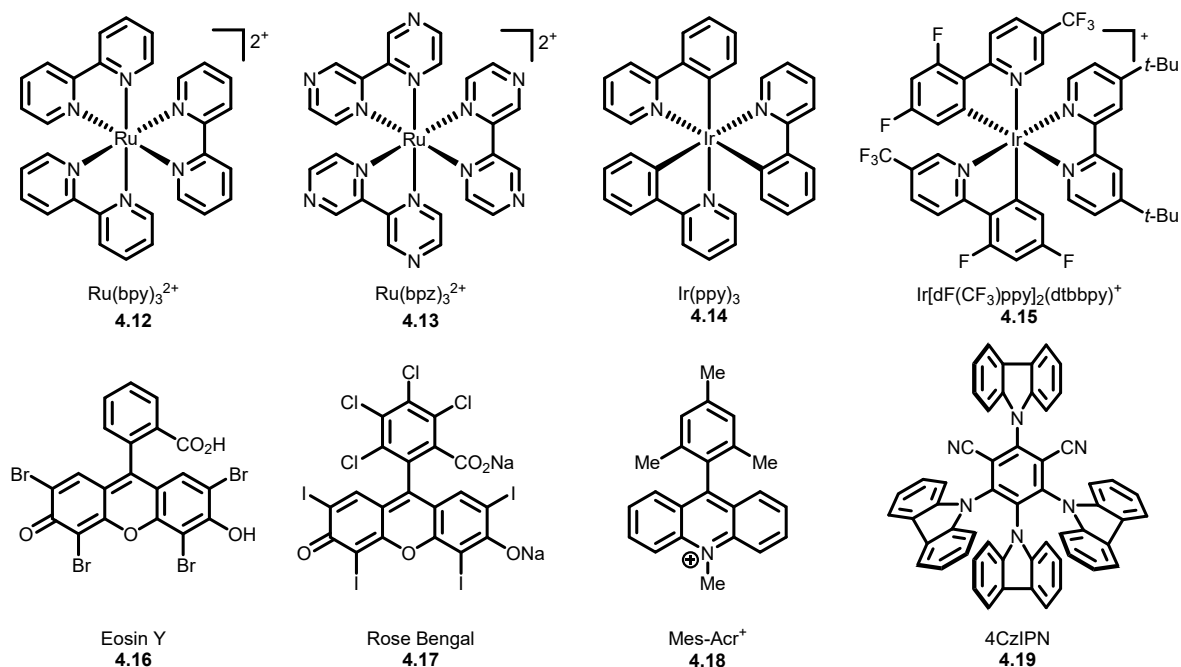


**Figure 4.3** Common metal-based and organic-based photoredox catalysts

Photocatalyst reactivity is mediated by oxidative- and reductive-type quenching mechanisms (Figure 4.4).<sup>8</sup> For example, excitation of Ru(bpy)<sub>3</sub><sup>2+</sup> (**4.12**) by visible light ( $\lambda_{\text{max}} = 452 \text{ nm}$ ) promotes a singlet excited state <sup>\*</sup>Ru(bpy)<sub>3</sub><sup>2+</sup> (**4.20**) via MLCT. In the case of Ru(bpy)<sub>3</sub><sup>2+</sup>, the electronic transitions occur from the t<sub>2g</sub> orbital of the metal (HOMO) to the  $\pi^*$  orbital of one of its bipyridyl ligands (LUMO). When the triplet excited state (<sup>3</sup>MLCT) is attained via intersystem crossing, the LUMO-promoted electron spin is parallel to that of the electron remaining in the t<sub>2g</sub> orbital of the metal. As mentioned in Section 4.1, returning from the triplet excited state to the singlet ground state is forbidden by the spin rule, which explains in part the relatively long excited-state lifetime of <sup>\*</sup>Ru(bpy)<sub>3</sub><sup>2+</sup> (1100 ns). Consequently, long-lived excited states facilitate participation in redox-type processes. If the photocatalyst is in the presence of a compatible electron acceptor (A), <sup>\*</sup>Ru(bpy)<sub>3</sub><sup>2+</sup> ( $E_{1/2}^{\text{II/III}} = -0.81 \text{ V vs SCE}$ ) will be oxidized by releasing an electron from its  $\pi^*$  orbital to convert into Ru(bpy)<sub>3</sub><sup>3+</sup> (**4.21**) ( $E_{1/2}^{\text{III/II}} = +1.29 \text{ V vs SCE}$ ). If the photocatalyst is in the presence of a compatible electron donor (D),



$^*\text{Ru}(\text{bpy})_3^{2+}$  ( $E_{1/2}^{*\text{III/I}} = +0.77 \text{ V}$  vs SCE) will be reduced by adding an electron to its incomplete  $t_{2g}$  octet to convert into  $\text{Ru}(\text{bpy})_3^{3+}$  (4.22) ( $E_{1/2}^{\text{I/II}} = -1.33 \text{ V}$  vs SCE).

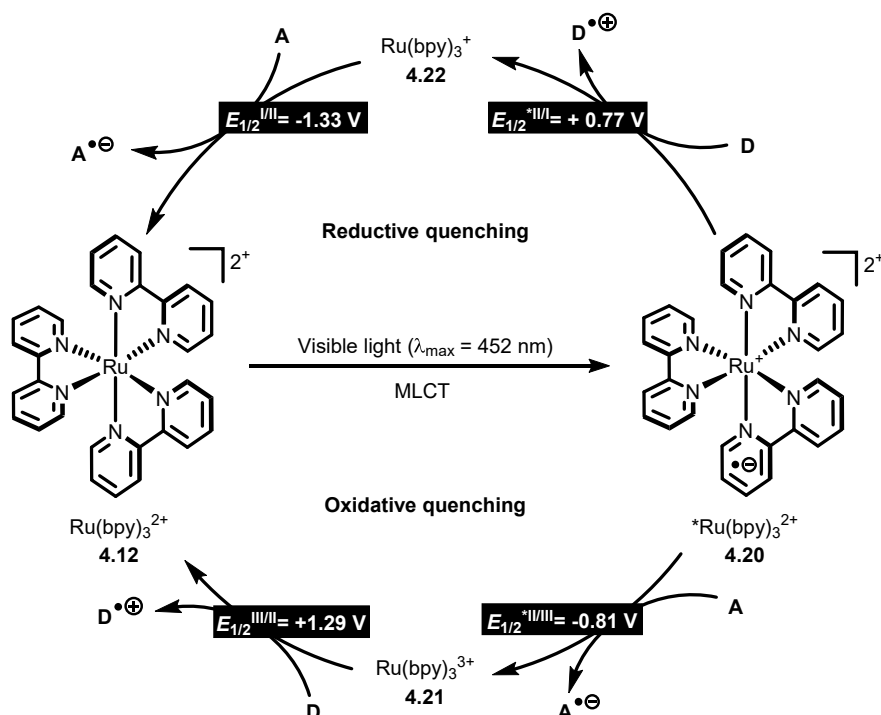
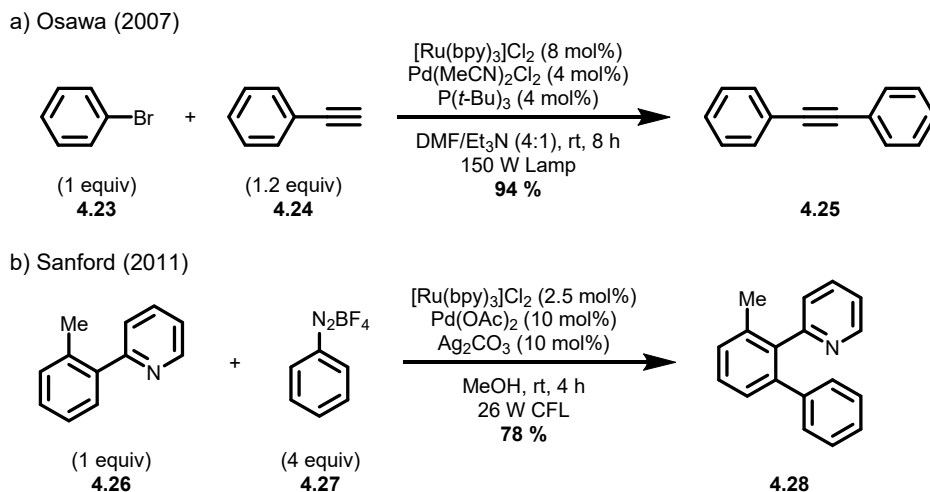


**Figure 4.4** Oxidative and reductive quenching cycles of  $^*\text{Ru}(\text{bpy})_3^{2+}$

### 4.2.2 Photoredox/Nickel Dual Catalysis

Photoredox catalysis has been successfully combined with organocatalysis to develop innovative synthetic transformations.<sup>7a-g</sup> Recently, another dual catalysis approach has emerged which combines photoredox catalysis with transition metal catalysis, also known as metallaphotoredox catalysis. Like previous multicatalytic strategies, metallaphotoredox catalysis has allowed synthetic chemists to further develop novel reaction manifolds<sup>7f, 17</sup> by enabling metal catalysts to readily undergo one-electron oxidation state changes, which characteristically possess small kinetic barriers. The first application of metallaphotoredox catalysis was reported in 2007 by Osawa,<sup>18</sup> who demonstrated that  $[\text{Ru}(\text{bpy})_3]\text{Cl}_2$  in combination with a palladium catalyst could promote a Sonogashira-type coupling between aryl bromides (4.23) and terminal alkynes (4.24) under visible light irradiation at room temperature (Scheme 4.3a). The novel strategy was not mechanistically understood, and was unused in organic synthesis until the report from Sanford in 2011.<sup>19</sup> Aryl radicals, generated

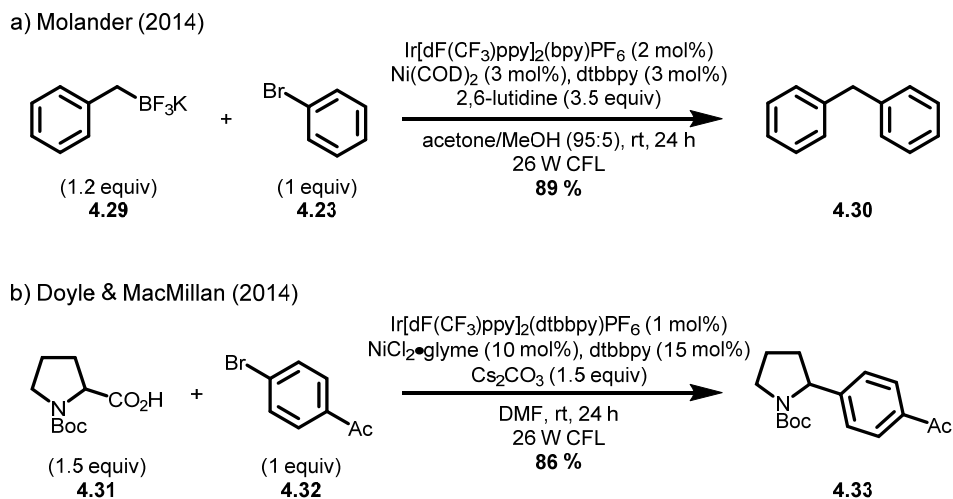
photochemically were reasoned to reduce phenyldiazonium salts (**4.27**) in the presence of  $[\text{Ru}(\text{bpy})_3]\text{Cl}_2$  to initiate a reaction with the palladium(II) complex and cause C-H activation of the substrate (**4.26**) by a one-electron oxidation of the palladium(III)-aryl complex (Scheme 4.3b). Following single-electron transfer, the palladium(III)-aryl species could be photochemically oxidized, which would then lead to C-H arylation of 2-arylpyridines (**4.28**) ensuing from reductive elimination of a palladium(IV)-aryl complex.



**Scheme 4.3** Seminal contributions to metallaphotoredox catalysis

The concept of merging visible-light photoredox catalysis with palladium catalysis to generate a carbon-carbon bond gave rise to the development of new synthetically useful transformations. Metallaphotoredox catalysis involving copper and gold as transition-metal catalysts were later reported by Sanford,<sup>20</sup> Glorius<sup>21</sup> and Toste<sup>22</sup> among others. Another breakthrough in metallaphotoredox catalysis was made in 2014 by Molander,<sup>23</sup> Doyle and MacMillan,<sup>24</sup> who reported concomitantly that nickel catalysis could be merged with visible-light photoredox catalysis to enable cross-coupling of  $\text{C}(\text{sp}^3)$  bonds (Scheme 4.4). The first set of conditions reported by Molander enabled the formation of a  $\text{C}(\text{sp}^2)\text{-C}(\text{sp}^3)$  bond from potassium alkoxyalkyl- and benzyltrifluoroborates (**4.29**) with aryl bromides (**4.23**) under visible light irradiation at room temperature (Scheme 4.4a).<sup>23</sup> The coupling was achieved by using an iridium-based photocatalyst in the presence of  $\text{Ni}(\text{COD})_2$  as catalyst and 4,4'-di-*tert*-butyl-2,2'-dipyridyl (dtbbpy) as ligand. The second set of conditions reported by Doyle and MacMillan also enabled the formation of a  $\text{C}(\text{sp}^2)\text{-C}(\text{sp}^3)$  bond under visible light irradiation,

but was made between carboxylic acid precursors (**4.31**) and aryl halides (**4.32**) (Scheme 4.4b).<sup>24</sup> The latter coupling was achieved by using an iridium-based photocatalyst in the presence of  $\text{NiCl}_2\cdot\text{glyme}$  as catalyst and dtbbpy as ligand.



**Scheme 4.4** Initial reports of metallaphotoredox catalysis using nickel

The ability of nickel catalysts to readily undergo one-electron oxidation state changes was previously reported by Weix<sup>25</sup> and Fu.<sup>26</sup> In Molander's report,<sup>23</sup> nickel catalysis was exploited to circumvent some limitations imposed by two-electron oxidation state changes involved in organoboron-based cross-coupling reactions. For example, the single-electron-mediated transmetalation involving nickel possesses a smaller kinetic barrier than a conventional transmetalation pathway.<sup>27</sup> In combination with visible light photoredox catalysis, nickel catalysis can perform the rate-limiting transmetalation step in a cross-coupling through the oxidation of an organometallic nucleophile, such as an alkyltrifluoroborate, by way of a low-barrier single-electron transfer processes.<sup>28</sup> Excited Ir(III) photocatalyst **4.35** was used to oxidize radical precursor **4.29** to generate a nucleophilic radical coupling partner (**4.37**) (Figure 4.5). Separately, Ni(0) complex **4.38** could undergo oxidative addition into the aryl halide **4.23** to generate Ni(II)-aryl species **4.39**, which could intercept radical **4.37** to generate Ni(III) complex **4.40**. Following reductive elimination, desired product **4.30** is formed and subsequent single-electron transfer from Ir(II) species **4.36** to Ni(I) complex **4.41** closes both catalytic cycles. Doyle and MacMillan<sup>24</sup> postulated analogous catalytic pathways, in which the alkyl radical species is generated by a sequential carboxylate oxidation and rapid loss of  $\text{CO}_2$ . The

decarboxylative coupling is attractive because carboxylic acid precursors are widely available and bench-stable. Such precursors had been used in previous photoredox-mediated transformations due to their capacity to generate carbon-centered radicals via decarboxylation.<sup>7f</sup>

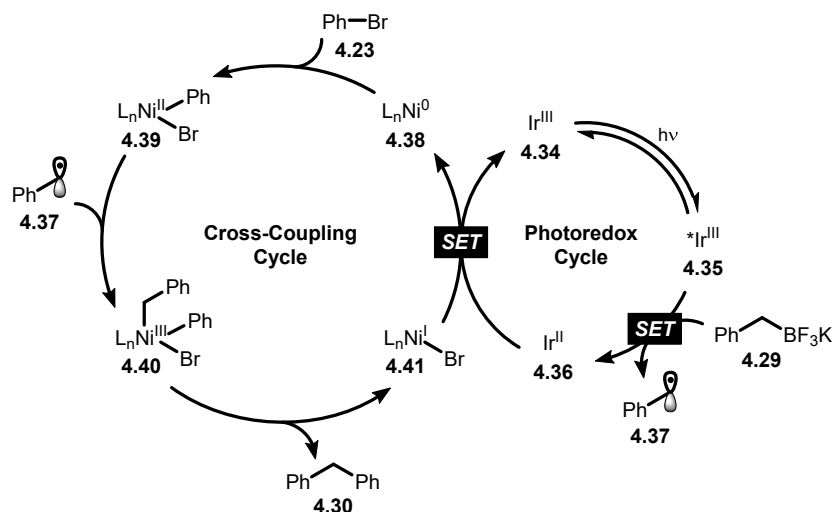
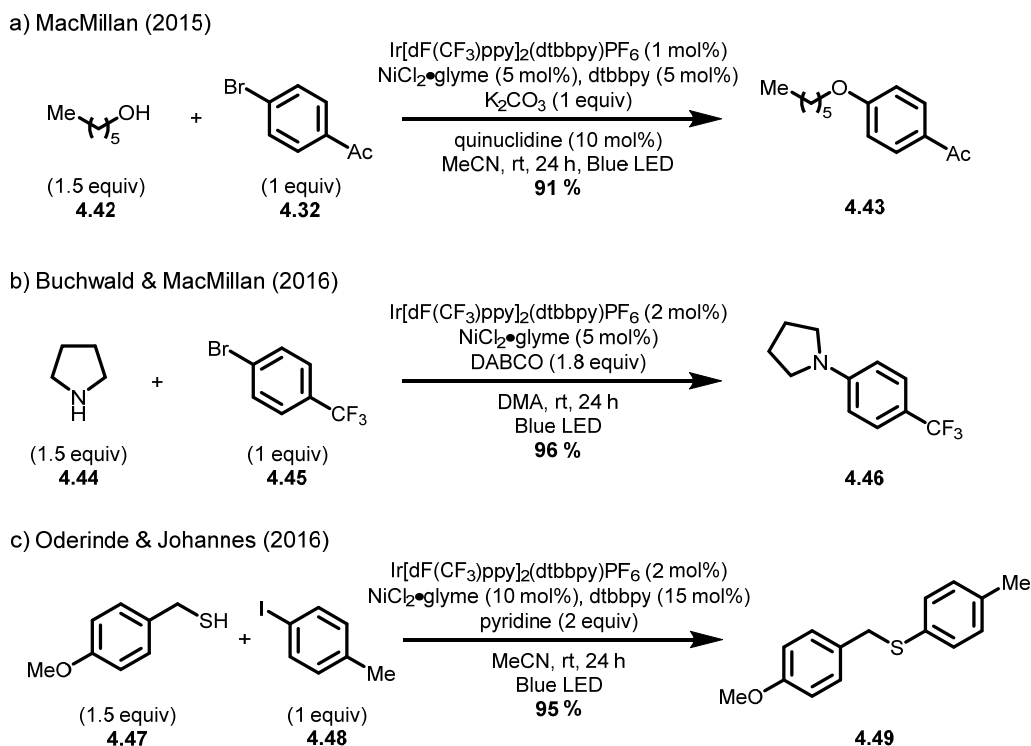


**Figure 4.5** Molander's proposed mechanism for photoredox/Ni-catalyzed cross-coupling

Along with the formation of carbon-carbon bonds, metallaphotoredox catalysis has enabled access to carbon-heteroatom bonds. The versatility of the photochemical dual catalytic strategy has been demonstrated in the formation of carbon-oxygen,<sup>29</sup> carbon-nitrogen<sup>30</sup> and carbon-sulfur bonds.<sup>31</sup> Aryl ethers (**4.43**) were efficiently produced from primary and secondary alcohols (**4.42**) and aryl bromides (**4.32**) using photochemical reaction conditions (Scheme 4.5a).<sup>29</sup> Amines (**4.44**) and aryl bromides (**4.45**) reacted to generate anilines (**4.46**) using similar metallaphotoredox conditions (Scheme 4.5b).<sup>30a</sup> Thiols (**4.47**) were photochemically cross-coupled with aryl iodides (**4.48**) to produce aryl thioethers (**4.49**) via thiyl radical intermediates (Scheme 4.5c).<sup>31a</sup> Chapter 6 presents another visible-light-mediated C-S coupling (C(sp)-S) which was developed in parallel to the latter discovery.



**Scheme 4.5** Dual photoredox/Ni-catalyzed C-O, C-N and C-S cross-couplings

Following a thorough mechanistic investigation, Oderinde and Johannes proposed that C-S bond formation occurred by a distinct mechanistic pathway from that of the nickel-catalyzed cross-couplings of carbon-centered radicals. The carbon-sulfur coupling did not proceed with  $\text{Ni}(\text{COD})_2$ , regardless of the presence or the absence of molecular oxygen (Figure 4.6).<sup>31a</sup> Electrochemical studies were utilized to rationalize the cross-coupling's dependence on the oxidation state of the nickel catalyst. Essentially, cyclic voltammetry of  $\text{NiCl}_2\cdot\text{dtbbpy}$  (**4.55**) in MeCN showed an irreversible two-electron reduction peak corresponding to the  $\text{Ni}^{\text{II}}/\text{Ni}^0$  couple at -1.34 V versus saturated calomel electrode (SCE). However, the  $\text{Ni}^{\text{II}}/\text{Ni}^0$  couple reduction potential of  $\text{NiCl}_2\cdot\text{dtbbpy}$  fell within the margin of error of the reduction potential of reducing Ir(II) species **4.52** ( $E_{1/2}^{\text{red}} [\text{Ir}^{\text{III}}/\text{Ir}^{\text{II}}] = -1.37$  V versus SCE in MeCN), making the reduction of the Ni(II) precatalyst to the corresponding Ni(0) complex thermodynamically unlikely. Alternatively, Ir(II) species **4.52** should thermodynamically and kinetically favor the reduction of the Ni(II) precatalyst to the corresponding Ni(I) complex (**4.56**), because reduction potentials of  $\text{Ni}^{\text{II}}/\text{Ni}^{\text{I}}$  couples were previously measured between -0.57 and -0.88 V (versus SCE in DMF/THF).<sup>32</sup> In light of the experimental results, a mechanistically distinct process for the

photochemical dual-catalytic C-S cross-coupling was proposed (Figure 4.6).<sup>31a</sup> Excited Ir(III) photocatalyst **4.51** ( $E_{1/2}^{\text{red}} [\text{*Ir}^{\text{III}}/\text{Ir}^{\text{II}}] = +1.21$  V versus SCE in MeCN) could readily oxidize thiol **4.47** ( $E_{1/2}^{\text{ox}} = +0.83$  V versus SCE in MeCN for benzyl thiol)<sup>33</sup> to generate a thiyl radical (**4.54**) after deprotonation ( $\text{pK}_{\text{a}} = 2.4$  for benzyl thiol radical cation).<sup>33a</sup> A single-electron transfer between Ni(II) precatalyst **4.55** and Ir(II) species **4.52** would provide the Ni(I) catalyst **4.56**, which may intercept thiyl radical **4.54** to generate Ni(II)-sulfide complex **4.57**. Another single-electron transfer between Ni(II)-sulfide complex **4.57** and Ir(II) species **4.52** would deliver Ni(I)-sulfide complex **4.58** and regenerate Ir(III) photocatalyst **4.50**. Ni(I)-sulfide complex **4.58** could undergo oxidative addition into the aryl iodide (**4.48**) to generate Ni(III)-complex **4.59**. Following reductive elimination, thioether **4.49** would be formed and Ni(I) complex **4.56** would be regenerated.

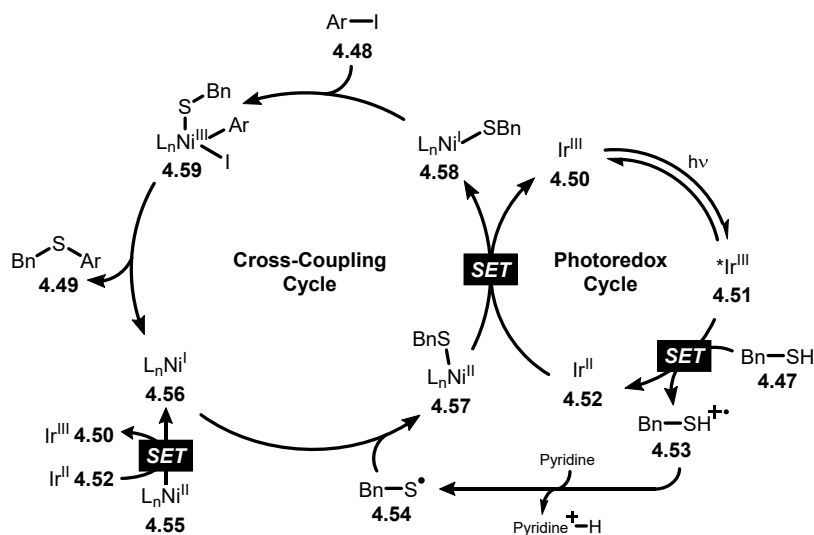


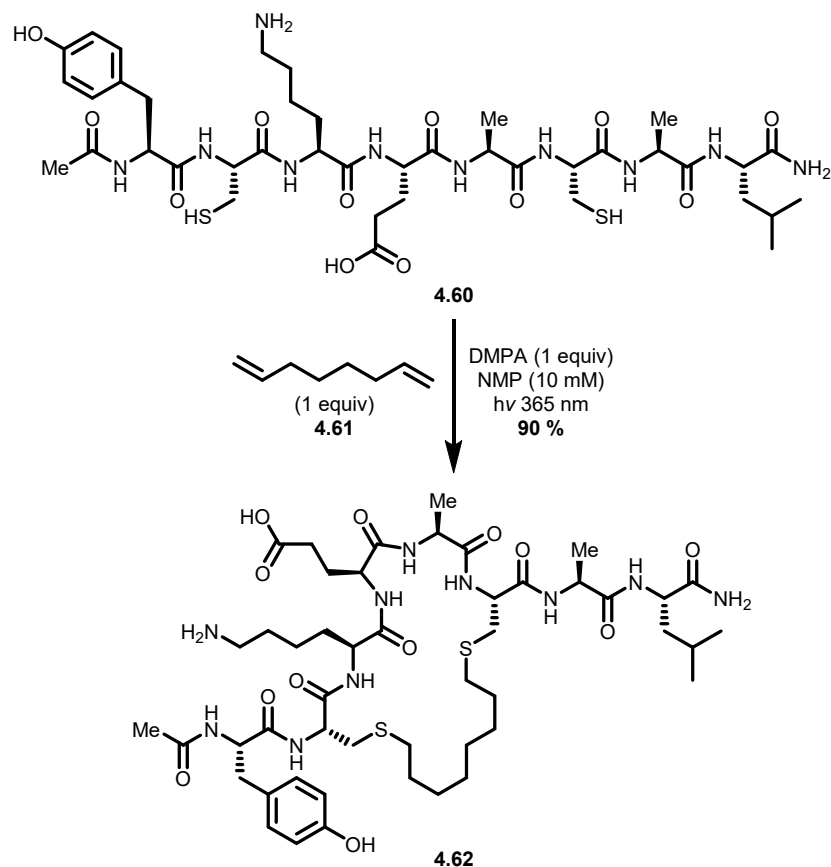
**Figure 4.6** Proposed mechanism for photochemical dual-catalytic C-S cross-coupling

### 4.3 Applications Toward Macrocyclization

Photochemistry has been scarcely applied to macrocycle synthesis. As mentioned in Chapter 1, macrocyclization reactions are generally performed under high dilution conditions to disfavor unwanted oligomerization reactions. However, dilute media can make efficient light penetration challenging, resulting in ineffective light-mediated macrocyclization. Until recently, only UV-mediated photochemical macrocyclizations have been reported.<sup>34</sup> Visible light photoredox catalysis has now enabled visible-light-mediated macrocycle synthesis.<sup>35</sup>

### 4.3.1 UV-Mediated Thiol-Ene Reaction

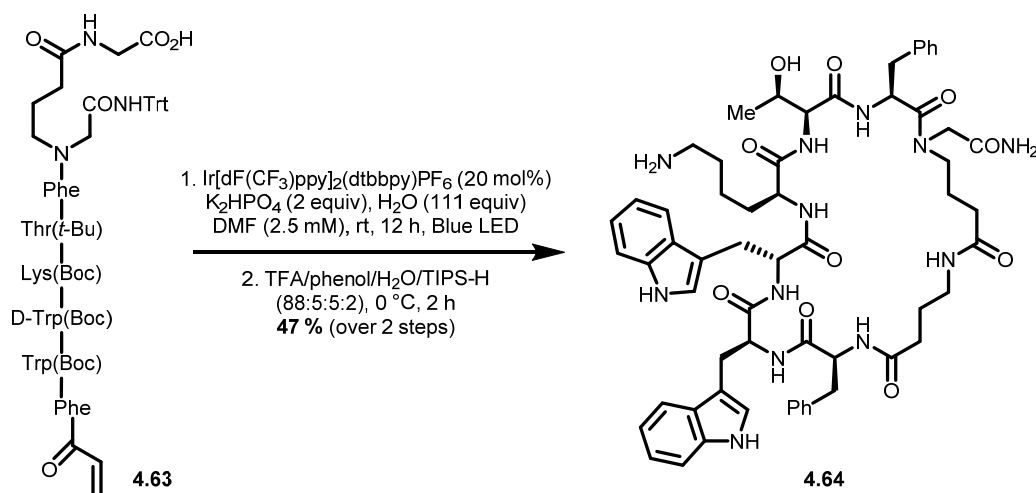
The most commonly performed UV-mediated macrocyclization reaction is the thiol-ene coupling.<sup>34e, 34f</sup> The thiol-ene reaction enables the formation of a robust thioether linkage. A favored reaction in biofunctionalization and materials science, the coupling between a thiol and an alkene is considered a "click" process because it is efficient and chemoselective.<sup>36</sup> The thiol-ene coupling has been applied for native peptide macrocyclization.<sup>34e</sup> Two cysteine residues of unprotected peptides (**4.60**) reacted with dienes (**4.61**) under UV irradiation to generate macrocycles, such as **4.62** in the presence of DMPA as radical initiator and NMP as solvent (10 mM) (Scheme 4.6).



**Scheme 4.6** Bis-thiol-ene macrocyclization of peptide **4.60**

### 4.3.2 Photoredox-Mediated Decarboxylation/Cyclization

In 2017, a visible-light-mediated macrocyclization based on well-studied photoinduced decarboxylations was reported by MacMillan.<sup>35</sup> Recognizing that decarboxylative conjugate addition could enable formation of carbon-carbon bonds,  $\alpha$ -amino carboxylates were used to generate nucleophilic C(sp<sup>3</sup>) radicals via single-electron transfer decarboxylation. The methodology was applied with peptides bearing a C-terminal carboxylate and a N-terminal Michael acceptor, in the presence of Ir[dF(CF<sub>3</sub>)ppy]<sub>2</sub>(dtbbpy)PF<sub>6</sub> as photoredox catalyst and K<sub>2</sub>HPO<sub>4</sub> as base. Upon visible-light irradiation of precursor **4.63** in DMF (2.5 mM), macrocycle **4.64** was obtained in 47 % isolated yield after acid-mediated deprotection (Scheme 4.7).



**Scheme 4.7** Visible-light-mediated macrocyclization of peptide **4.63**

## 4.4 Continuous Flow Chemistry

Continuous flow chemistry has been successfully implemented in organic synthesis over the past decade.<sup>37</sup> An appropriate tool for producing large volumes of a product uniformly, consistently, and reliably in both large scale manufacturing and preparative laboratory scale, continuous flow chemistry is recognized as a viable and sustainable alternative to batch chemistry that offers increased safety and energy efficiency.<sup>38</sup> Although most pharmaceutical and fine-chemical production is currently accomplished using batch processing, continuous flow



technology is increasingly being applied in process development toward commercially relevant compounds.<sup>39</sup>

#### 4.4.1 Description of Parameters and Equipment

Continuous flow chemistry presents several advantages over batch chemistry, including efficient heat transfer, effective mixing and scalable reproducibility.<sup>37</sup> In typical batch reactions, reagents are simultaneously added to a reactor fitted with means for temperature and pressure control, and mixing. The mixing and reaction conditions are applied for the entirety of the desired reaction time prior to workup. Batch reactions often suffer from variable parameters across time and space, because concentration and temperature gradients are known to influence reaction kinetics. Continuous flow processes entail steadily adding reagents to a reactor via tubing by means of a pump. Such processes maintain advantageously constant parameters, such that each molecule may react under the same reaction conditions throughout the process. Continuous flow systems define reaction times as the average time the reaction mixture spends inside a reactor for full conversion, which is termed as the residence time. The flow rate (mL/min) of a continuous flow reaction dictates the residence time (min) of the reaction mixture in the reactor (mL). A continuous flow process can be optimized by modifying either the flow rate or the reactor volume to fine-tune the desired residence time.

In order to achieve reliable and reproducible reaction parameters, continuous flow systems are generally composed of several key features (Figure 4.7).<sup>40</sup> The first component includes the reservoirs, such as reagent bottles and injection loops, which are carefully chosen depending on the scale of the reaction. The next component is the pumping module. A high-pressure gear pump or HPLC pump are typically utilized for systems that require high back pressures (30-180 bar). A syringe pump can alternatively be employed for systems run at lower back pressures. If needed, a mixer can be incorporated to mix the reagents before entering the reactor, or at any point in the process that would require additional reagents or mixing. The following component of the continuous flow system is the reactor, where the chemical transformation occurs. Depending on the desired reactivity profile, coils, microchips or cartridges can be used as reactors. Synthetic transformations are generally performed in coils made from PFA (perfluoro alkoxy alkane), FEP (perfluoro ethylene propylene), stainless steel,

or copper tubing. To cool, heat (-80 to +350 °C), or irradiate by UV or visible light the reaction, the appropriate coil must be selected accordingly. The next component is the back-pressure regulator, which is used to maintain gaseous phases in solution throughout the continuous flow process. A back-pressure regulator is essential when solvents are superheated or when reaction mixtures expulse stoichiometric amounts of gas by-products. Finally, a collection vial or an automated fraction collector is used to retrieve the entirety or portions of the reaction mixture. In-line purification and analysis instrumentation can be included in the continuous process to further enhance the multi-step continuous flow syntheses.<sup>37c, 37d, 39a, 41</sup>

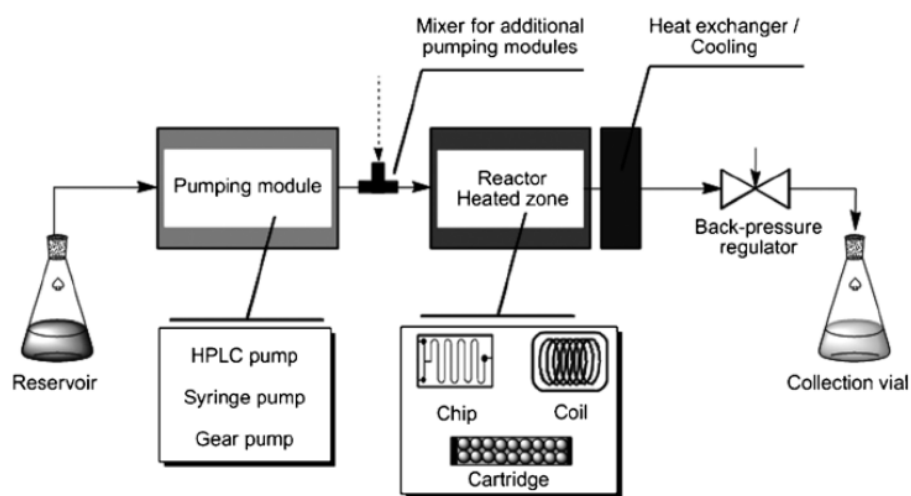


**Figure 4.7** General schematic diagram of high-temperature/high-pressure continuous flow conditions

#### 4.4.2 Merging Continuous Flow Chemistry and Photochemistry

Photochemical processes are often restrained by deficient photon absorption into reaction media. This inherent limitation can be explained by the Beer-Lambert law, which dictates that the photonic flux decreases exponentially with depth in a given reaction medium. Photoredox reactions performed in round bottom flasks or vials, experience sufficient irradiation only within two millimeters of the vessel wall.<sup>42</sup> In 2017, an efficient small-scale batch photochemical reactor was designed by Davies and MacMillan to overcome photon-limited regimes.<sup>43</sup> The photoreactor was developed to be a standard tool for photochemical transformations, and provided significant rate accelerations in various previously reported

visible-light-mediated photoredox reactions. Although the photoreactor enabled enhanced light exposure for small-scale photocatalytic processes ( $< 0.8$  mmol), it was not designed for large-scale synthesis. Alternatively, continuous flow techniques may be employed for photochemical processes, because they offer enhanced photonic flux without scale-limitations.<sup>44</sup> Continuous flow systems utilize generally small internal diameter tubing ( $\leq 1.0$  mm). The path length through which light must travel is considerably shorter than that of a conventional reaction vessel. As a result, photochemical transformations benefit from high surface-area-to-volume ratios in continuous flow photoreactors.

Among the earliest examples of continuous flow photochemistry, in the beginning of the 2000s, Jensen<sup>45</sup> and Kitamura<sup>46</sup> reported applications of UV light irradiation onto microchip reactors to enhance photon transfer, and consequently reaction rate. Afterwards, a practical continuous flow UV photoreactor was developed by Booker-Milburn to enable preparative synthetic organic photochemistry (Figure 4.8).<sup>47</sup> The newly designed photoreactor utilized transparent FEP tubing around a cylindrical water-cooled framework within which was placed the UV light source. The simplicity of the design exemplified that reactors could be easily constructed and customized according to the photochemical transformation.<sup>44a</sup> Since then, numerous UV-mediated chemical transformations, such as photocycloadditions,<sup>47-48</sup> photorearrangements,<sup>49</sup> photocyclizations,<sup>50</sup> photodecarboxylations,<sup>51</sup> and photooxidations,<sup>52</sup> have been facilitated using continuous flow chemistry. In addition, UV light irradiation in a continuous flow process has notably been utilized in an efficient and readily scalable synthesis of the anti-malaria drug artemisinin.<sup>53</sup>

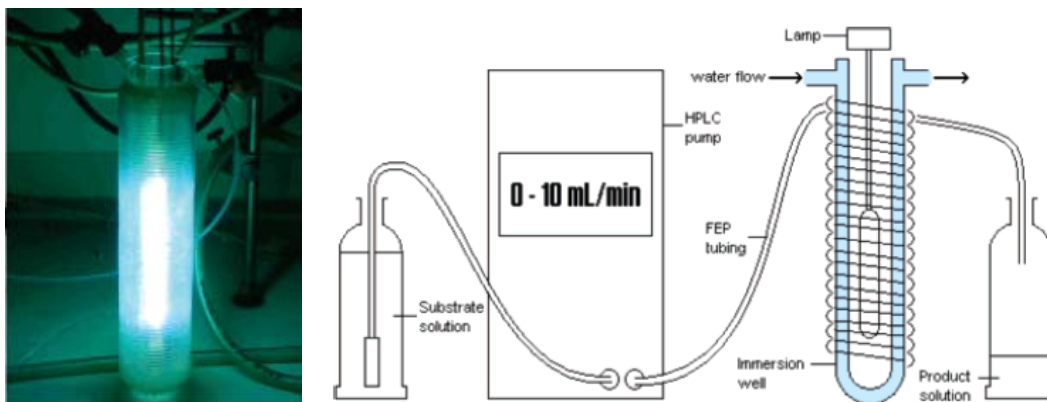


**Figure 4.8** Continuous flow UV photoreactor developed by Booker-Milburn. Reprinted with permission from ref 47. Copyright 2005 American Chemical Society.

Previously, the benefits of continuous flow chemistry were primarily being exploited for UV-mediated transformations. Nonetheless, as visible light photoredox catalysis was blooming in organic synthesis, continuous flow chemistry was eventually recognized as a tool to improve the long reaction times, and poor scalability, often observed for visible light photoredox-catalyzed transformations performed in batch. Continuous flow photochemistry employing visible light irradiation was independently investigated by Seeberger,<sup>54</sup> Gagné,<sup>55</sup> Stephenson and Jamison<sup>56</sup> in 2012. The reported photoreactor designs differed with regards to the tubing's composition and length, but all shared similar blue LED irradiation sources (Figure 4.9). The newly designed visible light photoreactors enabled various ruthenium- and iridium-catalyzed photoredox processes to proceed with short residence times and high reproducibility.<sup>54-56</sup> Continuous flow chemistry has since been increasingly applied for visible light photocatalysis. Continuous flow systems are characteristically modular. They can easily accommodate various light sources, such as simple and inexpensive CFLs and LEDs. In combination with such light sources, suitable photocatalysts have enabled visible-light-mediated photoredox transformations under continuous flow conditions. For example, transition-metal-based photocatalysts containing ruthenium,<sup>57</sup> iridium,<sup>58</sup> copper,<sup>59</sup> and iron,<sup>60</sup> have been effectively applied in visible light continuous flow processes. Recently, organic-based photocatalysts have also been utilized for single-electron photoredox pathways.<sup>7g</sup> Organic dyes such as eosin Y,<sup>61</sup> rose bengal,<sup>62</sup> and xanthenes,<sup>63</sup> which typically display better solubility profiles than metal-

based photocatalysts, have shown promise for visible-light-mediated reactions in continuous flow systems.

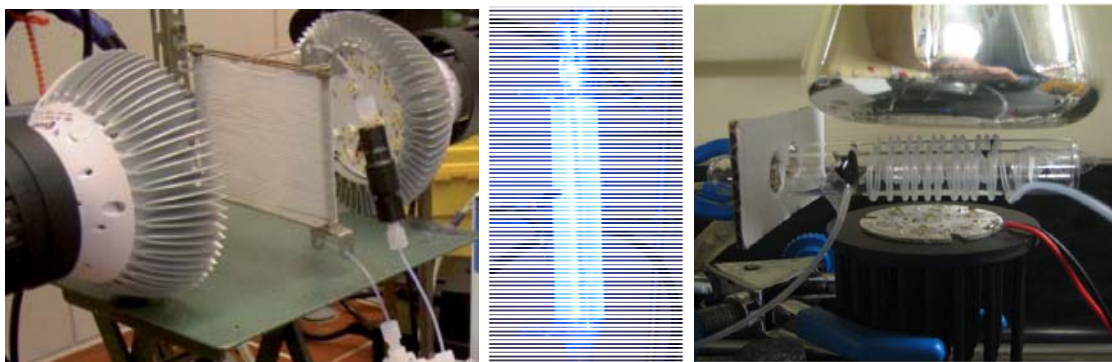


**Figure 4.9** Continuous flow visible light photoreactors developed by: a) Seeberger; b) Gagné; c) Stephenson and Jamison. Reprinted with permission from ref 54. Copyright 2012 The Royal Society of Chemistry. Reprinted with permission from ref 55 & 56. Copyright 2012 John Wiley and Sons

## 4.5 Conclusions

Photocatalysis is a valuable synthetic tool. Light is abundant, renewable and green. Photocatalysis allows chemists to photochemically produce chemicals using a sustainable energy source with potential to reduce toxic by-products. Although visible-light-induced organic photochemistry was historically outshined by UV-mediated transformations, visible-light-mediated photoredox catalysis has re-emerged into a prominent field of research, enabling the discovery of countless novel synthetic transformations including approaches that merge photoredox catalysis respectively with organo- and transition metal catalysis. Although photochemical processes were often limited by the ability to efficiently transfer photons into a given reaction medium, new technologies have overcome such issues associated with insufficient photon fluxes and reproducibility. Continuous flow techniques are now well-suited for efficient and scalable photochemical synthetic transformations using UV and visible light.

## 4.6 Bibliography

1. Ciamician, G. *Science* **1912**, 36, 385-394.
2. (a) Fagnoni, M.; Dondi, D.; Ravelli, D.; Albini, A. *Chem. Rev.* **2007**, 107, 2725-2756; (b) Yoon, T. P.; Ischay, M. A.; Du, J. *Nat. Chem.* **2010**, 2, 527-532.
3. Schultz, D. M.; Yoon, T. P. *Science* **2014**, 343, 1239176.
4. (a) Hölz, K.; Lietard, J.; Somoza, M. M. *ACS Sustainable Chem. Eng.* **2017**, 5, 828-834; (b) Bach, T.; Hehn, J. P. *Angew. Chem. Int. Ed.* **2011**, 50, 1000-1045; (c) Hoffmann, N. *Chem. Rev.* **2008**, 108, 1052-1103.
5. Douglas, J. J.; Sevrin, M. J.; Stephenson, C. R. J. *Org. Process Res. Dev.* **2016**, 20, 1134-1147.
6. König, B. *Eur. J. Org. Chem.* **2017**, 2017, 1979-1981.
7. (a) Narayanam, J. M.; Stephenson, C. R. *Chem. Soc. Rev.* **2011**, 40, 102-113; (b) Prier, C. K.; Rankic, D. A.; MacMillan, D. W. *Chem. Rev.* **2013**, 113, 5322-5363; (c) Gentry, E. C.; Knowles, R. R. *Acc. Chem. Res.* **2016**, 49, 1546-1556; (d) Hernandez-Perez, A. C.; Collins, S. K. *Acc. Chem. Res.* **2016**, 49, 1557-1565; (e) Reiser, O. *Acc. Chem. Res.* **2016**, 49, 1990-1996; (f) Shaw, M. H.; Twilton, J.; MacMillan, D. W. C. *J. Org. Chem.* **2016**, 81, 6898-6926; (g) Romero, N. A.; Nicewicz, D. A. *Chem. Rev.* **2016**, 116, 10075-10166; (h) Marzo, L.; Pagire, S. K.; Reiser, O.; König, B. *Angew. Chem. Int. Ed.* **2018**, 57, 10034-10072.
8. Tucker, J. W.; Stephenson, C. R. J. *J. Org. Chem.* **2012**, 77, 1617-1622.
9. (a) Hedstrand, D. M.; Kruizinga, W. H.; Kellogg, R. M. *Tetrahedron Lett.* **1978**, 19, 1255-1258; (b) Van Bergen, T. J.; Hedstrand, D. M.; Kruizinga, W. H.; Kellogg, R. M. *J. Org. Chem.* **1979**, 44, 4953-4962.
10. Cano-Yelo, H.; Deronzier, A. *J. Chem. Soc., Perkin Trans. 2* **1984**, 1093-1098.
11. Cano-Yelo, H.; Deronzier, A. *Tetrahedron Lett.* **1984**, 25, 5517-5520.
12. (a) Hironaka, K.; Fukuzumi, S.; Tanaka, T. *J. Chem. Soc., Perkin Trans. 2* **1984**, 1705-1709; (b) Fukuzumi, S.; Koumitsu, S.; Hironaka, K.; Tanaka, T. *J. Am. Chem. Soc.* **1987**, 109, 305-316; (c) Fukuzumi, S.; Mochizuki, S.; Tanaka, T. *J. Phys. Chem.* **1990**, 94, 722-726.
13. (a) Pac, C.; Ihama, M.; Yasuda, M.; Miyauchi, Y.; Sakurai, H. *J. Am. Chem. Soc.* **1981**, 103, 6495-6497; (b) Pac, C.; Miyauchi, Y.; Ishitani, O.; Ihama, M.; Yasuda, M.; Sakurai, H. *J. Org. Chem.* **1984**, 49, 26-34; (c) Ishitani, O.; Ihama, M.; Miyauchi, Y.; Pac, C. *J. Chem. Soc., Perkin Trans. 1* **1985**, 1527-1531; (d) Ishitani, O.; Pac, C.; Sakurai, H. *J. Org. Chem.* **1983**, 48, 2941-2942; (e) Ishitani, O.; Yanagida, S.; Takamuku, S.; Pac, C. *J. Org. Chem.* **1987**, 52, 2790-2796.
14. (a) Okada, K.; Okamoto, K.; Morita, N.; Okubo, K.; Oda, M. *J. Am. Chem. Soc.* **1991**, 113, 9401-9402; (b) Okada, K.; Okamoto, K.; Oda, M. *J. Am. Chem. Soc.* **1988**, 110, 8736-8738; (c) Okada, K.; Okamoto, K.; Oda, M. *J. Chem. Soc., Chem. Commun.* **1989**, 1636-1637; (d) Okada, K.; Okubo, K.; Morita, N.; Oda, M. *Tetrahedron Lett.* **1992**, 33, 7377-7380; (e) Okada, K.; Okubo, K.; Morita, N.; Oda, M. *Chem. Lett.* **1993**, 22, 2021-2024.
15. Teplý, F. *Collect. Czech. Chem. Commun.* **2011**, 76, 859-917.
16. (a) Nicewicz, D. A.; MacMillan, D. W. C. *Science* **2008**, 322, 77-80; (b) Ischay, M. A.; Anzovino, M. E.; Du, J.; Yoon, T. P. *J. Am. Chem. Soc.* **2008**, 130, 12886-12887; (c) Narayanam, J. M. R.; Tucker, J. W.; Stephenson, C. R. J. *J. Am. Chem. Soc.* **2009**, 131, 8756-8757.

17. (a) Skubi, K. L.; Blum, T. R.; Yoon, T. P. *Chem. Rev.* **2016**, *116*, 10035-10074; (b) Twilton, J.; Le, C.; Zhang, P.; Shaw, M. H.; Evans, R. W.; MacMillan, D. W. C. *Nat. Rev. Chem.* **2017**, *1*, 1-18.
18. Osawa, M.; Nagai, H.; Akita, M. *Dalton Trans.* **2007**, 827-829.
19. Kalyani, D.; McMurtrey, K. B.; Neufeldt, S. R.; Sanford, M. S. *J. Am. Chem. Soc.* **2011**, *133*, 18566-18569.
20. Ye, Y.; Sanford, M. S. *J. Am. Chem. Soc.* **2012**, *134*, 9034-9037.
21. Sahoo, B.; Hopkinson, M. N.; Glorius, F. *J. Am. Chem. Soc.* **2013**, *135*, 5505-5508.
22. Shu, X.-z.; Zhang, M.; He, Y.; Frei, H.; Toste, F. D. *J. Am. Chem. Soc.* **2014**, *136*, 5844-5847.
23. Tellis, J. C.; Primer, D. N.; Molander, G. A. *Science* **2014**, *345*, 433-436.
24. Zuo, Z.; Ahneman, D. T.; Chu, L.; Terrett, J. A.; Doyle, A. G.; MacMillan, D. W. C. *Science* **2014**, *345*, 437-440.
25. (a) Everson, D. A.; Shrestha, R.; Weix, D. J. *J. Am. Chem. Soc.* **2010**, *132*, 920-921; (b) Everson, D. A.; Jones, B. A.; Weix, D. J. *J. Am. Chem. Soc.* **2012**, *134*, 6146-6159; (c) Biswas, S.; Weix, D. J. *J. Am. Chem. Soc.* **2013**, *135*, 16192-16197.
26. (a) Zultanski, S. L.; Fu, G. C. *J. Am. Chem. Soc.* **2011**, *133*, 15362-15364; (b) Dudnik, A. S.; Fu, G. C. *J. Am. Chem. Soc.* **2012**, *134*, 10693-10697; (c) Zultanski, S. L.; Fu, G. C. *J. Am. Chem. Soc.* **2013**, *135*, 624-627; (d) Schley, N. D.; Fu, G. C. *J. Am. Chem. Soc.* **2014**, *136*, 16588-16593.
27. (a) Lin, X.; Phillips, D. L. *J. Org. Chem.* **2008**, *73*, 3680-3688; (b) Phapale, V. B.; Guisán-Ceinos, M.; Buñuel, E.; Cárdenas, D. J. *Chem. Eur. J.* **2009**, *15*, 12681-12688; (c) Breitenfeld, J.; Ruiz, J.; Wodrich, M. D.; Hu, X. *J. Am. Chem. Soc.* **2013**, *135*, 12004-12012.
28. Tellis, J. C.; Kelly, C. B.; Primer, D. N.; Jouffroy, M.; Patel, N. R.; Molander, G. A. *Acc. Chem. Res.* **2016**, *49*, 1429-1439.
29. Terrett, J. A.; Cuthbertson, J. D.; Shurtleff, V. W.; MacMillan, D. W. C. *Nature* **2015**, *524*, 330-334.
30. (a) Corcoran, E. B.; Pirnot, M. T.; Lin, S.; Dreher, S. D.; DiRocco, D. A.; Davies, I. W.; Buchwald, S. L.; MacMillan, D. W. C. *Science* **2016**, *353*, 279-283; (b) Oderinde, M. S.; Jones, N. H.; Juneau, A.; Frenette, M.; Aquila, B.; Tentarelli, S.; Robbins, D. W.; Johannes, J. W. *Angew. Chem. Int. Ed.* **2016**, *55*, 13219-13223; (c) Tasker, S. Z.; Jamison, T. F. *J. Am. Chem. Soc.* **2015**, *137*, 9531-9534; (d) Mao, R.; Frey, A.; Balon, J.; Hu, X. *Nat. Catal.* **2018**, *1*, 120-126.
31. (a) Oderinde, M. S.; Frenette, M.; Robbins, D. W.; Aquila, B.; Johannes, J. W. *J. Am. Chem. Soc.* **2016**, *138*, 1760-1763; (b) Jouffroy, M.; Kelly, C. B.; Molander, G. A. *Org. Lett.* **2016**, *18*, 876-879.
32. Amatore, C.; Gaubert, F.; Jutand, A.; Utley, J. H. P. *J. Chem. Soc., Perkin Trans. 2* **1996**, 2447-2452.
33. (a) Bordwell, F. G.; Zhang, X.-M.; Satish, A. V.; Cheng, J. P. *J. Am. Chem. Soc.* **1994**, *116*, 6605-6610; (b) Pavlishchuk, V. V.; Addison, A. W. *Inorg. Chim. Acta* **2000**, *298*, 97-102.
34. (a) Pfaffenbach, M.; Roller, A.; Gaich, T. *Chem. Eur. J.* **2016**, *22*, 8444-8447; (b) Nishikawa, K.; Yoshimi, Y.; Maeda, K.; Morita, T.; Takahashi, I.; Itou, T.; Inagaki, S.; Hatanaka, M. *J. Org. Chem.* **2013**, *78*, 582-589; (c) Griesbeck, A. G.; Heinrich, T.; Oelgemöller, M.; Lex, J.; Molis, A. *J. Am. Chem. Soc.* **2002**, *124*, 10972-10973; (d) Yoon, U. C.; Jin, Y. X.; Oh, S. W.; Park, C. H.; Park, J. H.; Campana, C. F.; Cai, X.; Duesler, E.

- N.; Mariano, P. S. *J. Am. Chem. Soc.* **2003**, *125*, 10664-10671; (e) Wang, Y.; Chou, D. H. *C. Angew. Chem. Int. Ed.* **2015**, *54*, 10931-10934; (f) Aimetti, A. A.; Shoemaker, R. K.; Lin, C.-C.; Anseth, K. S. *Chem. Commun.* **2010**, *46*, 4061-4063.
35. McCarver, S. J.; Qiao, J. X.; Carpenter, J.; Borzilleri, R. M.; Poss, M. A.; Eastgate, M. D.; Miller, M. M.; MacMillan, D. W. *C. Angew. Chem. Int. Ed.* **2017**, *56*, 728-732.
  36. Hoyle, C. E.; Bowman, C. N. *Angew. Chem. Int. Ed.* **2010**, *49*, 1540-1573.
  37. (a) Plutschack, M. B.; Pieber, B.; Gilmore, K.; Seeberger, P. H. *Chem. Rev.* **2017**, *117*, 11796-11893; (b) Movsisyan, M.; Delbeke, E. I. P.; Berton, J. K. E. T.; Battilocchio, C.; Ley, S. V.; Stevens, C. V. *Chem. Soc. Rev.* **2016**, *45*, 4892-4928; (c) Britton, J.; Raston, C. L. *Chem. Soc. Rev.* **2017**, *46*, 1250-1271; (d) Webb, D.; Jamison, T. F. *Chem. Sci.* **2010**, *1*, 675-680; (e) Hartman, R. L.; McMullen, J. P.; Jensen, K. F. *Angew. Chem. Int. Ed.* **2011**, *50*, 7502-7519.
  38. Newman, S. G.; Jensen, K. F. *Green Chem.* **2013**, *15*, 1456-1472.
  39. (a) Adamo, A.; Beingessner, R. L.; Behnam, M.; Chen, J.; Jamison, T. F.; Jensen, K. F.; Monbaliu, J.-C. M.; Myerson, A. S.; Revalor, E. M.; Snead, D. R.; Stelzer, T.; Weeranoppanant, N.; Wong, S. Y.; Zhang, P. *Science* **2016**, *352*, 61-67; (b) Gutmann, B.; Cantillo, D.; Kappe, C. O. *Angew. Chem. Int. Ed.* **2015**, *54*, 6688-6728; (c) Porta, R.; Benaglia, M.; Puglisi, A. *Org. Process Res. Dev.* **2016**, *20*, 2-25; (d) Baumann, M.; Baxendale, I. R. *Beilstein J. Org. Chem.* **2015**, *11*, 1194-1219.
  40. Britton, J.; Jamison, T. F. *Nat. Protoc.* **2017**, *12*, 2423-2446.
  41. Perera, D.; Tucker, J. W.; Brahmabhatt, S.; Helal, C. J.; Chong, A.; Farrell, W.; Richardson, P.; Sach, N. W. *Science* **2018**, *359*, 429-434.
  42. (a) Shvydkiv, O.; Gallagher, S.; Nolan, K.; Oelgemöller, M. *Org. Lett.* **2010**, *12*, 5170-5173; (b) Su, Y.; Straathof, N. J. W.; Hessel, V.; Noël, T. *Chem. Eur. J.* **2014**, *20*, 10562-10589.
  43. Le, C. C.; Wismer, M. K.; Shi, Z.-C.; Zhang, R.; Conway, D. V.; Li, G.; Vachal, P.; Davies, I. W.; MacMillan, D. W. C. *ACS Cent. Sci.* **2017**, *3*, 647-653.
  44. (a) Cambié, D.; Bottecchia, C.; Straathof, N. J. W.; Hessel, V.; Noël, T. *Chem. Rev.* **2016**, *116*, 10276-10341; (b) Garlets, Z. J.; Nguyen, J. D.; Stephenson, C. R. J. *Isr. J. Chem.* **2014**, *54*, 351-360; (c) Knowles, J. P.; Elliott, L. D.; Booker-Milburn, K. I. *Beilstein J. Org. Chem.* **2012**, *8*, 2025-2052.
  45. Lu, H.; Schmidt, M. A.; Jensen, K. F. *Lab Chip* **2001**, *1*, 22-28.
  46. Ueno, K.; Kitagawa, F.; Kitamura, N. *Lab Chip* **2002**, *2*, 231-234.
  47. Hook, B. D. A.; Dohle, W.; Hirst, P. R.; Pickworth, M.; Berry, M. B.; Booker-Milburn, K. I. *J. Org. Chem.* **2005**, *70*, 7558-7564.
  48. (a) Takahide, F.; Yoshiko, H.; Naoya, K.; Ilhyong, R. *Chem. Lett.* **2004**, *33*, 1430-1431; (b) Lainchbury, M. D.; Medley, M. I.; Taylor, P. M.; Hirst, P.; Dohle, W.; Booker-Milburn, K. I. *J. Org. Chem.* **2008**, *73*, 6497-6505.
  49. (a) Zhang, Y.; Blackman, M. L.; Leduc, A. B.; Jamison, T. F. *Angew. Chem. Int. Ed.* **2013**, *52*, 4251-4255; (b) Baumann, M.; Baxendale, I. R. *React. Chem. Eng.* **2016**, *1*, 147-150.
  50. (a) McQuade, D. T.; O'Brien, A. G.; Dorr, M.; Rajaratnam, R.; Eisold, U.; Monnanda, B.; Nobuta, T.; Lohmannsroben, H.-G.; Meggers, E.; Seeberger, P. H. *Chem. Sci.* **2013**, *4*, 4067-4070; (b) Caron, A.; Hernandez-Perez, A. C.; Collins, S. K. *Org. Process Res. Dev.* **2014**, *18*, 1571-1574; (c) Parisien-Collette, S.; Cruché, C.; Abel-Snape, X.; Collins, S. K. *Green Chem.* **2017**, *19*, 4798-4803.



51. (a) Belluau, V.; Noeureuil, P.; Ratzke, E.; Skvortsov, A.; Gallagher, S.; Motti, C. A.; Oelgemöller, M. *Tetrahedron Lett.* **2010**, *51*, 4738-4741; (b) Shvydkiv, O.; Nolan, K.; Oelgemöller, M. *Beilstein J. Org. Chem.* **2011**, *7*, 1055-1063.
52. (a) Wootton, R. C. R.; Fortt, R.; de Mello, A. J. *Org. Process Res. Dev.* **2002**, *6*, 187-189; (b) Park, C. Y.; Kim, Y. J.; Lim, H. J.; Park, J. H.; Kim, M. J.; Seo, S. W.; Park, C. P. *RSC Adv.* **2015**, *5*, 4233-4237; (c) Loonov, K. N.; Lopes, J.; Barlog, M.; Astrova, E. V.; Malkov, A. V.; Lapkin, A. A. *Org. Process Res. Dev.* **2014**, *18*, 1443-1454; (d) Lumley, E. K.; Dyer, C. E.; Pamme, N.; Boyle, R. W. *Org. Lett.* **2012**, *14*, 5724-5727.
53. (a) Lévesque, F.; Seeberger, P. H. *Angew. Chem. Int. Ed.* **2012**, *51*, 1706-1709; (b) Triemer, S.; Gilmore, K.; Vu, G. T.; Seeberger, P. H.; Seidel-Morgenstern, A. *Angew. Chem. Int. Ed.* **2018**, *57*, 5525-5528.
54. Bou-Hamdan, F. R.; Seeberger, P. H. *Chem. Sci.* **2012**, *3*, 1612-1616.
55. Andrews, R. S.; Becker, J. J.; Gagné, M. R. *Angew. Chem. Int. Ed.* **2012**, *51*, 4140-4143.
56. Tucker, J. W.; Zhang, Y.; Jamison, T. F.; Stephenson, C. R. J. *Angew. Chem. Int. Ed.* **2012**, *51*, 4144-4147.
57. (a) Konieczynska, M. D.; Dai, C.; Stephenson, C. R. J. *Org. Biomol. Chem.* **2012**, *10*, 4509-4511; (b) Wang, X.; Cuny, G. D.; Noël, T. *Angew. Chem. Int. Ed.* **2013**, *52*, 7860-7864; (c) Straathof, N. J. W.; Gemoets, H. P. L.; Wang, X.; Schouten, J. C.; Hessel, V.; Noël, T. *ChemSusChem* **2014**, *7*, 1612-1617; (d) Beatty, J. W.; Douglas, J. J.; Cole, K. P.; Stephenson, C. R. J. *Nat. Commun.* **2015**, *6*, 7919.
58. (a) Nguyen, J. D.; D'Amato, E. M.; Narayanam, J. M. R.; Stephenson, C. R. J. *Nat. Chem.* **2012**, *4*, 854; (b) Nguyen, J. D.; Rei, Dai, C.; Stephenson, C. R. J. *Chem. Commun.* **2013**, *49*, 4352-4354; (c) Beatty, J. W.; Stephenson, C. R. J. *J. Am. Chem. Soc.* **2014**, *136*, 10270-10273; (d) Rackl, D.; Kreitmeier, P.; Reiser, O. *Green Chem.* **2016**, *18*, 214-219; (e) Yayla, H. G.; Peng, F.; Mangion, I. K.; McLaughlin, M.; Campeau, L.-C.; Davies, I. W.; DiRocco, D. A.; Knowles, R. R. *Chem. Sci.* **2016**, *7*, 2066-2073.
59. (a) Hernandez-Perez, A. C.; Vlassova, A.; Collins, S. K. *Org. Lett.* **2012**, *14*, 2988-2991; (b) Bédard, A.-C.; Vlassova, A.; Hernandez-Perez, A. C.; Bessette, A.; Hanan, G. S.; Heuft, M. A.; Collins, S. K. *Chem. Eur. J.* **2013**, *19*, 16295-16302; (c) Hernandez-Perez, A. C.; Collins, S. K. *Angew. Chem. Int. Ed.* **2013**, *52*, 12696-12700.
60. Parisien-Collette, S.; Hernandez-Perez, A. C.; Collins, S. K. *Org. Lett.* **2016**, *18*, 4994-4997.
61. (a) Talla, A.; Driessen, B.; Straathof, N. J. W.; Milroy, L. G.; Brunsveld, L.; Hessel, V.; Noël, T. *Adv. Synth. Catal.* **2015**, *357*, 2180-2186; (b) Straathof, N.; Osch, D.; Schouten, A.; Wang, X.; Schouten, J.; Hessel, V.; Noël, T. *J. Flow Chem.* **2014**, *4*, 12-17; (c) Cantillo, D.; de Frutos, O.; Rincón, J. A.; Mateos, C.; Kappe, C. O. *Org. Lett.* **2014**, *16*, 896-899; (d) Bottecchia, C.; Rubens, M.; Gunnou, S. B.; Hessel, V.; Madder, A.; Noël, T. *Angew. Chem. Int. Ed.* **2017**, *56*, 12702-12707.
62. (a) Rueping, M.; Vila, C.; Bootwicha, T. *ACS Catal.* **2013**, *3*, 1676-1680; (b) Penders, I. G. T. M.; Amara, Z.; Horvath, R.; Rossen, K.; Poliakoff, M.; George, M. W. *RSC Adv.* **2015**, *5*, 6501-6504.
63. (a) Cantillo, D.; de Frutos, O.; Rincón, J. A.; Mateos, C.; Kappe, C. O. *J. Org. Chem.* **2014**, *79*, 8486-8490; (b) Kumarasamy, E.; Raghunathan, R.; Jockusch, S.; Ugrinov, A.; Sivaguru, J. *J. Am. Chem. Soc.* **2014**, *136*, 8729-8737.

## 5. Introduction to Alkynyl Sulfides

Alkynes are versatile building blocks for chemical synthesis.<sup>1</sup> Alkynes are generally prepared from carbonyl compounds using various procedures such as the Corey-Fuchs reaction and the Seyferth-Gilbert homologation.<sup>2</sup> Terminal and internal alkynes can participate in a wide range of transformations including the Sonogashira coupling (Chapter 2), nucleophilic and electrophilic additions, alkyne metathesis, hydroboration, oxidative cleavage, and cycloadditions. Such transformations have enabled the rapid and efficient assembly of fragments to generate molecules of higher structural complexity. The development of versatile reagents such as heteroatom-substituted alkynes has had impact upon organic synthesis by enabling the design of new chemical transformations. The following chapter will introduce heteroatom-substituted alkynes and their applications in synthesis. Chapters 6 and 7 will focus specifically on alkynyl sulfides, reviewing their synthesis and recent synthetic applications.

### 5.1 Heteroatom-Substituted Alkynes

While IUPAC does not provide a formal definition of a heteroatom, heteroatom-substituted alkynes are primarily referred to as alkynes connected to either nitrogen, oxygen, phosphorus or sulfur (Figure 5.1).



**Figure 5.1** Common heteroatom-substituted alkynes

Heteroatom-substituted alkynes constitute a class of alkynes that have still not been fully explored since their discovery in the mid-twentieth century. Such alkynes possess interesting properties due to electron-rich heteroatom polarization at the triple bond. Reactive alkynes such as ynamines, alkynyl ethers, alkynyl phosphines, and alkynyl sulfides enable transformations to proceed with increased chemo-, regio-, and stereoselectivities which are not generally observed using conventional alkynes (Figure 5.2).

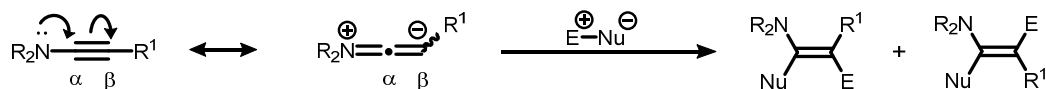


**Figure 5.2** Predictable regioselectivity from ynamines

Over the past decade, ynamides have experienced a resurgence of interest due to the development of efficient methods to access nitrogen-substituted alkynes.<sup>3</sup> Although ynamines were considered highly reactive reagents, their usefulness was hindered by limited stability and rapid hydrolysis. Electron-deficient ynamines, commonly referred to as ynamides, exhibit increased stability and maintain strong polarization of the alkyne. The synthesis and applications of ynamides have evolved into a significant field of research.<sup>4</sup> Alkynyl ethers<sup>5</sup> and alkynyl phosphines<sup>6</sup> have also been recently employed in synthesis in spite of stability issues. To overcome such issues, alkynyl ethers have been generated in situ and used in tandem bond-forming reactions.<sup>7</sup> In contrast, alkynyl sulfides (thioalkynes) are relatively stable compounds that possess reactivity complementary to ynamides. Despite the prominence of sulfur in biomolecules<sup>8</sup> and materials,<sup>9</sup> few practical and efficient methods have until recently given access to alkynyl sulfides, limiting their synthetic potential. Alkynyl sulfides are recognized as versatile sulfur-containing building blocks. New strategies for their synthesis and applications have surfaced and developed into a rapidly growing field of research.

## 5.2 Approaches Toward Synthesis of Alkynyl Sulfides

Alkynyl sulfides have been reported as early as the late 1950s, but have had, until recently, limited use in organic synthesis because of insufficient practical and efficient methods to access sulfur-substituted alkynes. Considering both components are inherently nucleophilic, the umpolung of either the sulfur or the alkyne is generally required to efficiently generate alkynyl sulfides. Other strategies, including dehydrohalogenations, and nucleophilic and electrophilic thioalkynylations, have been developed to access alkynyl sulfides (Figure 5.3).

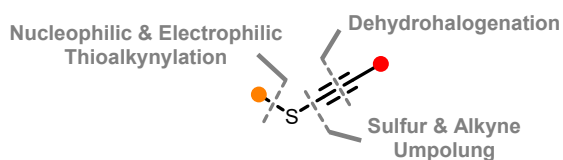
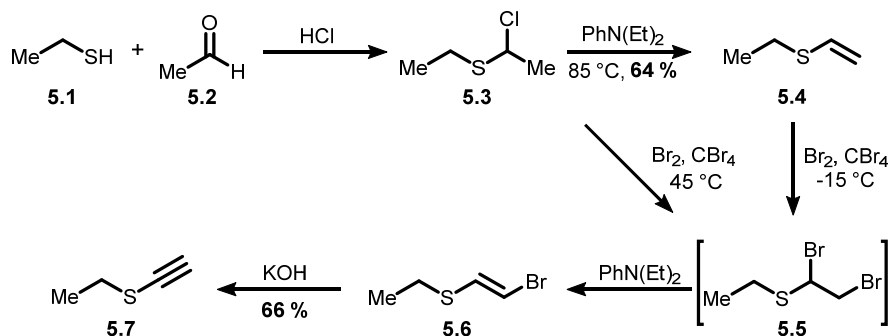


**Figure 5.3** Synthetic disconnections toward alkynyl sulfides

### 5.2.1 Dehydrohalogenation

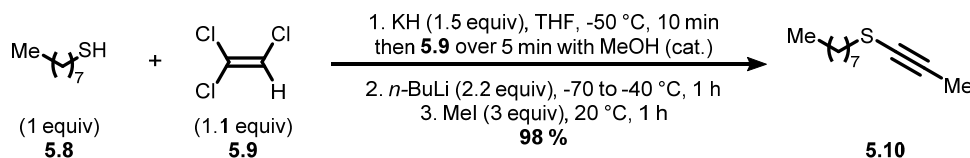
The first synthesis of alkynyl sulfides was reported by Arens in 1956.<sup>10</sup> The synthetic route commenced by formation of ethyl- $\alpha$ -chloroethyl-thioether **5.3** from ethanethiol (**5.1**) and acetaldehyde (**5.2**) under acidic conditions (Scheme 5.1). Next, thioether **5.3** was dissolved in diethylaniline and heated at 85 °C to generate ethyl-vinyl-thioether **5.4** in 64 % yield. Key precursor ethyl- $\beta$ -bromovinyl-thioether **5.6** could be obtained from two different sequences. The first path involved successive treatment of **5.4** with bromine in carbon tetrabromide at -15 °C to generate dibromide **5.5**, followed by elimination using diethylaniline. Upon complete addition of the base, the mixture was heated at 70 °C for 30 minutes, and work-up ensued to provide vinyl bromide **5.6** in 81 % yield. The second path involved the direct bromination of ethyl- $\alpha$ -chloroethyl-thioether **5.3** using bromine in heated carbon tetrabromide (45 °C), which would also give rise to intermediate **5.5**. The reaction mixture was then added dropwise to diethylaniline at 80 °C, and after work-up, precursor **5.6** was isolated in 70 % yield. Lastly, ethyl- $\beta$ -bromovinyl-thioether **5.6** was mixed with potassium hydroxide and was then heated to generate alkynyl sulfide **5.7** in 66 % yield via dehydrohalogenation.



**Scheme 5.1** Initial synthesis of alkynyl sulfides

A one-pot base-mediated elimination approach was later reported by Greene in 1995.<sup>11</sup> A free thiol (**5.8**) in the presence of potassium hydride at -50 °C, was treated with trichloroethylene (**5.9**) and a catalytic amount of methanol to generate a dichloroacetylene intermediate in situ. Once the gas evolution was complete at room temperature, the reaction mixture was treated with *n*-butyllithium at -70 °C, and after 30 minutes, the mixture was warmed to -40 °C. Lastly, the iodomethane was added dropwise to the reaction mixture, and it was stirred for one hour at room temperature to generate the desired alkynyl sulfide (**5.10**) in 98 %.

Compatible electrophiles included primary alkyl iodides and chlorotrimethylsilane. As such, the methodology gave access to a wide scope of *S*-alkyl and *S*-aryl alkynyl sulfides from the corresponding thiols. Similarly, the approach was later applied in the synthesis of camphor-derived chelating thiols for asymmetric Pauson-Khand reactions.<sup>12</sup>



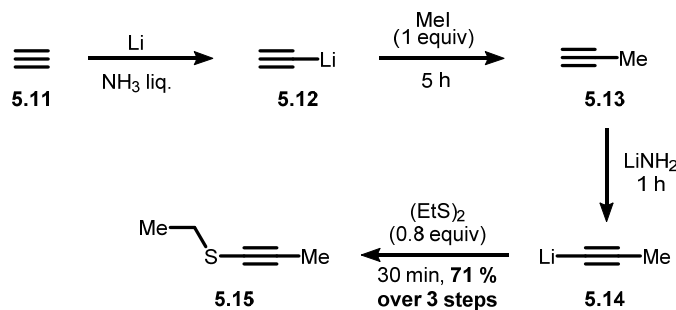
**Scheme 5.2** One-pot synthesis of alkynyl sulfides using trichloroethylene

## 5.2.2 Sulfur Umpolung

Since the early 1960s, alkynyl sulfides were commonly synthesized by a sulfur umpolung strategy, in which an organometallic acetylide served as the nucleophile and a pre-activated thiol as the electrophile to form a new C(sp)-S bond.

### 5.2.2.1 Disulfides

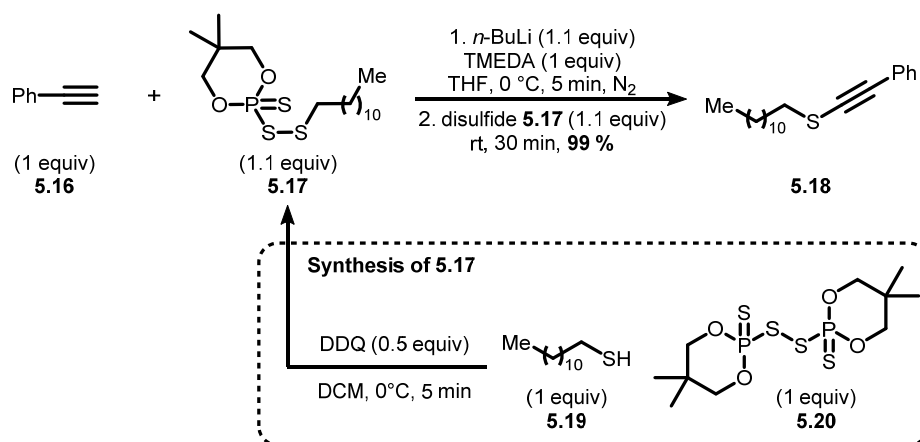
Disulfides have been used as a source of prefunctionalized thiol electrophiles.<sup>13</sup> Initially applied by Arens in 1961 to generate internal-alkyne-containing alkynyl sulfides (**5.15**),<sup>13a</sup> the synthetic route (Scheme 5.3) consisted of treating propyne (**5.11**) with lithium amide in liquid ammonia to generate lithium acetylide **5.12**, followed by reaction with diethyl disulfide to provide functionalized alkynyl sulfide **5.15** in 71 % yield.



**Scheme 5.3** Initial synthesis of alkynyl sulfides using disulfides

More recently, 5,5-dimethyl-2-thioxo-1,3,2-dioxaphosphorinan-2-disulfanyl derivatives (e.g. **5.17**) have been developed to promote the formation of alkynyl sulfides (Scheme 5.4).<sup>14</sup>

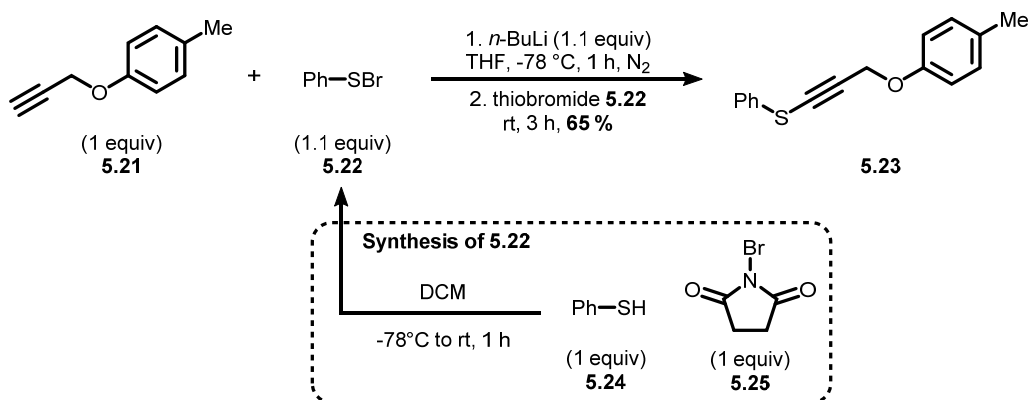
The electrophilic sulfur species are readily accessed from bis-(5,5-dimethyl-2-thioxo-1,3,2-dioxaphosphorinan-2-yl) disulfide **5.20** in the presence of a thiol (**5.19**) and DDQ, and are suggested to be more stable than the analogous symmetrical disulfides. With the electrophilic precursor (**5.17**) in hand, a THF solution of an organolithium acetylide was prepared from a terminal alkyne (**5.16**) using *n*-butyllithium in the presence of TMEDA. A solution of disulfide **5.17** was then added to generate alkynyl sulfide **5.18** in 99 % yield. The method could also provide alkynyl sulfides bearing hydroxyl, carboxyl and protected amino groups.



**Scheme 5.4** Synthesis of alkynyl sulfides using mixed disulfides

### 5.2.2.2 Thiobromides

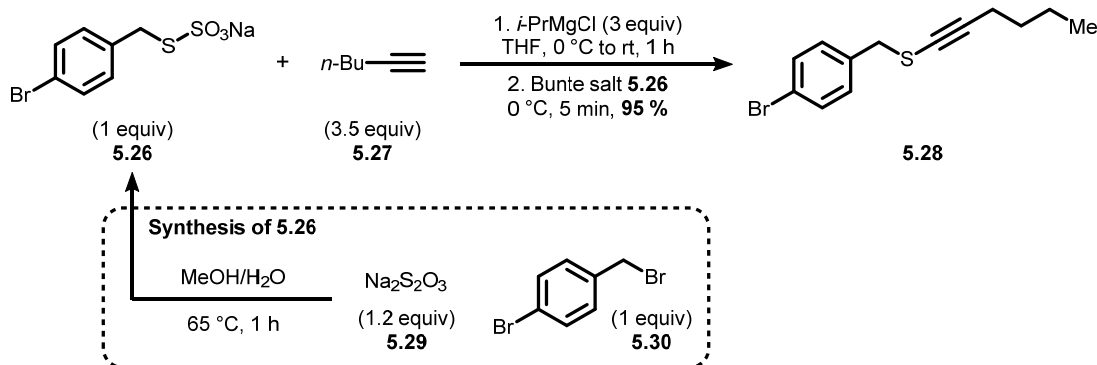
Other sulfur-based electrophiles have also been applied for the synthesis of alkynyl sulfides. For instance, thiobromides (**5.22**) were used toward the preparation of 3-halo-4-chalcogen-2*H*-benzopyrans.<sup>15</sup> To introduce the alkynyl sulfide moiety, the lithium acetylide species was initially generated from a terminal alkyne (**5.21**) using *n*-butyllithium (Scheme 5.5). Thiobromide **5.22** was then added to provide alkynyl sulfide **5.23** in 65 % yield. While only two examples using electrophilic sulfur species were reported, the method could also implicate electrophilic selenium and tellurium substrates.



**Scheme 5.5** Synthesis of alkynyl sulfides using thiobromides

### 5.2.2.3 Bunte Salts

Bunte salts (e.g. **5.26**) are conveniently prepared between sodium thiosulfate (**5.29**) and alkyl halides (**5.30**). Bunte salts are easy-to-handle odorless crystalline solids which have recently been used as an electrophilic sulfur source to form alkynyl sulfides (Scheme 5.6).<sup>16</sup> For example, when Bunte salt **5.26** was treated with a Grignard reagent, alkynyl sulfide **5.28** was generated in 95 % yield.



**Scheme 5.6** Synthesis of alkynyl sulfides using Bunte salts

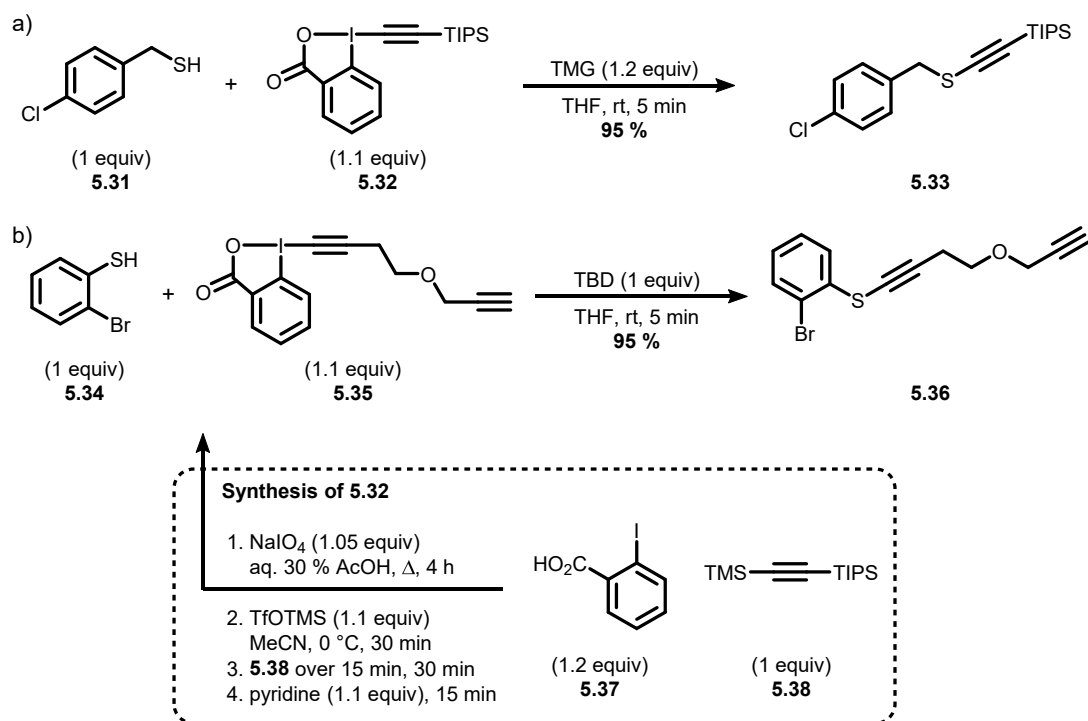
### 5.2.3 Alkyne Umpolung

Over the past decade, alkynyl sulfides have been synthesized using an alkyne umpolung strategy, consisting of using a free thiol as nucleophile and a prefunctionalized alkyne as electrophile to form the new C(sp)-S bond.

### 5.2.3.1 Ethynyl Benziiodoxolones

An efficient procedure utilizing a hypervalent-iodine-based alkyne-transfer reagent (**5.32**) for synthesizing TIPS-substituted alkynyl sulfides was reported by Waser in 2013 (Scheme 5.7a).<sup>17</sup> While ethynyl benziiodoxolone (EBX) reagents such as **5.32** are usually obtained after several synthetic steps, they are air stable solids and allow for long-term storage on multi-gram scale. Thiols (**5.31**) reacted rapidly with TIPS-EBX reagent **5.32** in the presence of 1,1,3,3-tetramethylguanidine (TMG) as base. TIPS-protected alkynyl sulfides (e.g. **5.33**) were produced in high yields from a wide scope of thiol substrates. A methodology allowing for the functionalization of thiols with multiple electrophilic alkyne-transfer reagents was later developed.<sup>18</sup> Switching from TMG to 1,5,7-triazabicyclo[4.4.0]dec-5-ene (TBD) as base enabled the utilization of different EBX reagents, bearing aliphatic- and mesityl-substituted alkynes, with a broad scope of thiols (Scheme 5.7b). For example, thiol **5.34** reacted chemoselectively with EBX reagent **5.35** to provide alkyne-substituted alkynyl sulfide **5.36** in 95 % yield. The high efficiency of the transformation was also rationalized through thorough computational studies.<sup>18-19</sup> They revealed two distinct mechanistic pathways ( $\alpha$ - or  $\beta$ -additions) which were dependant on the nature of the EBX reagent.

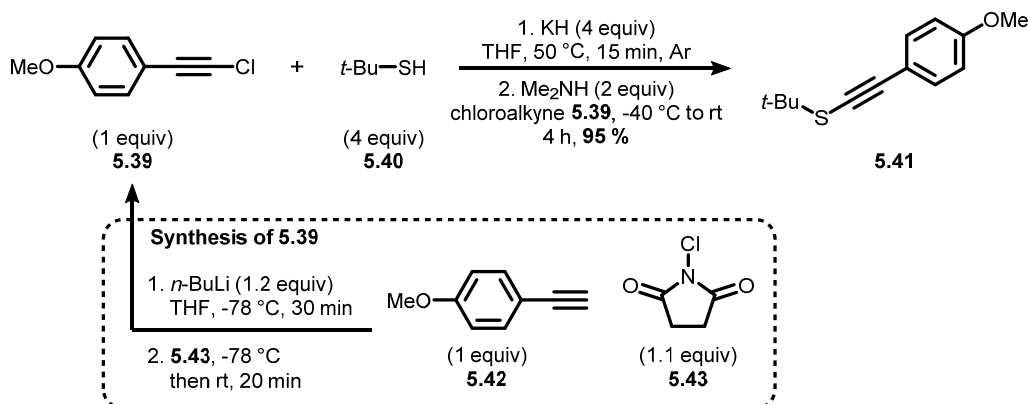




**Scheme 5.7** Synthesis of alkynyl sulfides using EBX-based reagents

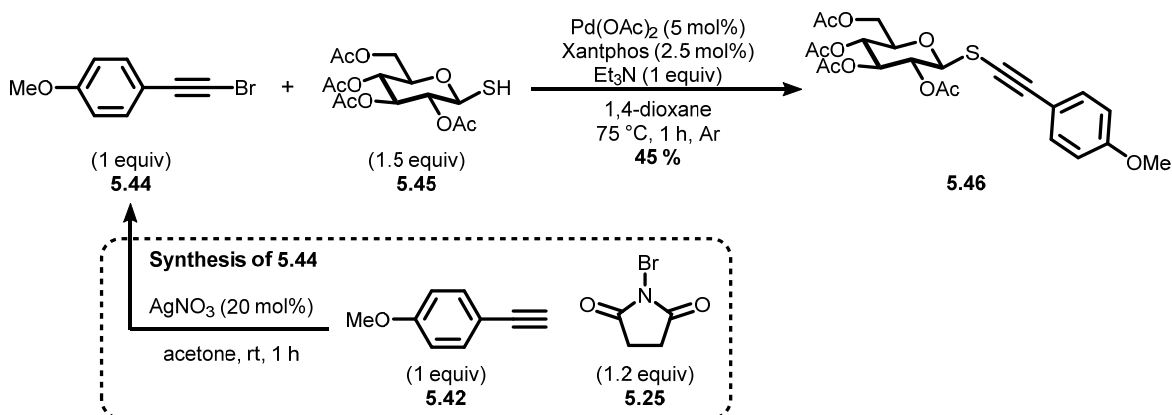
### 5.2.3.2 Haloalkynes

Haloalkynes have been applied in recent years for the synthesis of alkynyl sulfides. Haloalkynes were typically generated via alkyne deprotonation, followed by trapping with a halogenating reagent. Several mild and convenient methods to prepare haloalkynes efficiently have since emerged, making their use more appealing in organic synthesis.<sup>20</sup> Chloroalkynes (e.g **5.39**) displayed good reactivity with thiolate salts to generate alkynyl sulfides (Scheme 5.8).<sup>21</sup> For example, alkynyl sulfide **5.41** was obtained from chloroalkyne **5.39** upon addition of a thiolate which was generated from thiol **5.40**. It was postulated that an addition-elimination mechanism may occur.<sup>22</sup> While alkynyl sulfides were readily generated when using chloroalkynes, using bromoalkynes and iodoalkynes led to the formation of the corresponding vinyl sulfides when exposed to potassium thiolate salts. The difference in reactivity between the haloalkynes may result from an alternative mechanism,<sup>23</sup> where the first step involves a nucleophilic substitution at the halogen, rather than at the carbon atom.<sup>24</sup>



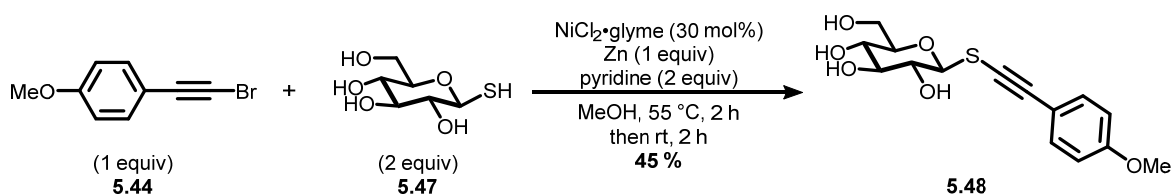
**Scheme 5.8** Synthesis of alkynyl sulfides using chloroalkynes

Bromoalkynes have also been used in combination with transition metals to generate thioglycoside-derived alkynyl sulfides. In 2013, Alami and Messaoudi reported that  $\beta$ -alkynylthioglycosides (**5.46**) can be prepared using palladium catalysis (Scheme 5.9).<sup>25</sup> Employing  $\text{Pd}(\text{OAc})_2$  as catalyst, Xantphos as ligand, and triethylamine as base enabled the coupling between *O*-acetylated  $\beta$ -thioglucopyranose **5.45** and bromoalkyne **5.44** to provide alkynyl sulfide **5.46** in 45 % yield. The C(sp)-S bond-forming methodology was later improved by applying a highly active G3-Xantphos-palladium precatalyst.<sup>26</sup> The modified reaction conditions, which were mainly applied for thioglycoside arylations, also facilitated the formation of  $\beta$ -alkynylthioglycosides at room temperature.



**Scheme 5.9** Synthesis of alkynyl sulfides using bromoalkynes and palladium catalysis

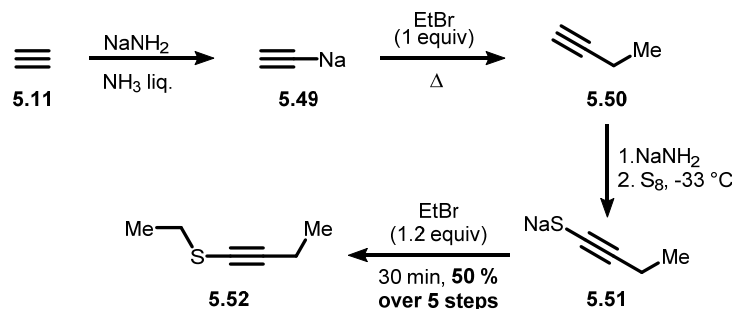
Alami and Messaoudi also reported that thioglycoside-derived alkynyl sulfides (**5.48**) can be generated from nickel catalysis (Scheme 5.10).<sup>27</sup> Employing  $\text{NiCl}_2\cdot\text{glyme}$  as precatalyst, pyridine as ligand and base, and zinc powder as reductant enabled the coupling of unprotected 1-thio- $\beta$ -D-glucopyranose **5.47** with bromoalkyne **5.44** at room temperature. Crucially, the active  $\text{Ni}(0)$  catalyst had to be prepared prior to the addition of both coupling partners. The presumed  $[\text{Ni}^0(\text{glyme})(\text{pyridine})]$  catalyst was prepared in situ in two hours from a mixture of  $\text{NiCl}_2\cdot\text{glyme}$ , zinc powder and pyridine. Following the addition of **5.44** and **5.47**, alkynyl sulfide **5.48** was obtained in 45 % yield.



**Scheme 5.10** Synthesis of alkynyl sulfides using bromoalkynes and nickel catalysis

#### 5.2.4 Nucleophilic Thioalkynylation

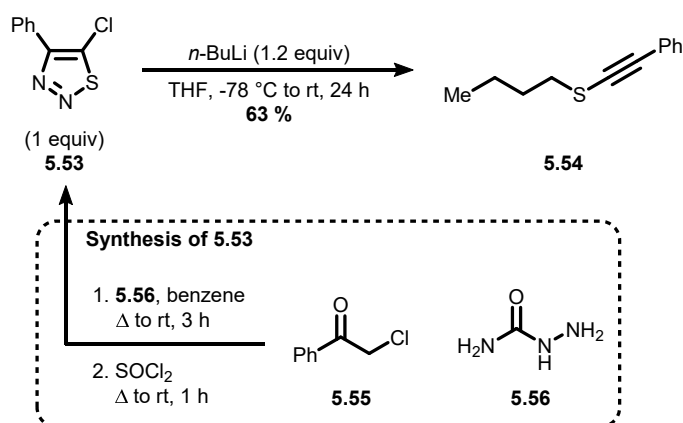
Nucleophilic thioalkynylation approaches have also been used to synthesize alkynyl sulfides. They consist of functionalizing an organometallic acetylide with sulfur powder to form an alkynyl thiolate which reacts with an electrophilic species. The approach was widely applied in the early 1960s,<sup>28</sup> as using sulfur powder was considered a more economical route to alkynyl sulfides than utilizing thiols or disulfides. The synthetic route commenced with the formation of terminal alkyne **5.50**, similarly to a previous approach (Schemes 5.3 & 5.11).<sup>28a</sup> Sodium acetylide **5.51** was then generated using sodium amide and sulfur powder, to which was added ethyl bromide to provide alkynyl sulfide **5.52** in 50 % yield over five steps. The procedure was also applied toward the synthesis of alkynyl selenides and tellurides. While the nucleophilic thioalkynylation approach has since been scarcely applied in synthesis,<sup>29</sup> it has recently been simplified as a one-pot procedure.<sup>30</sup>



**Scheme 5.11** Synthesis of alkynyl sulfides from nucleophilic thioalkynylation

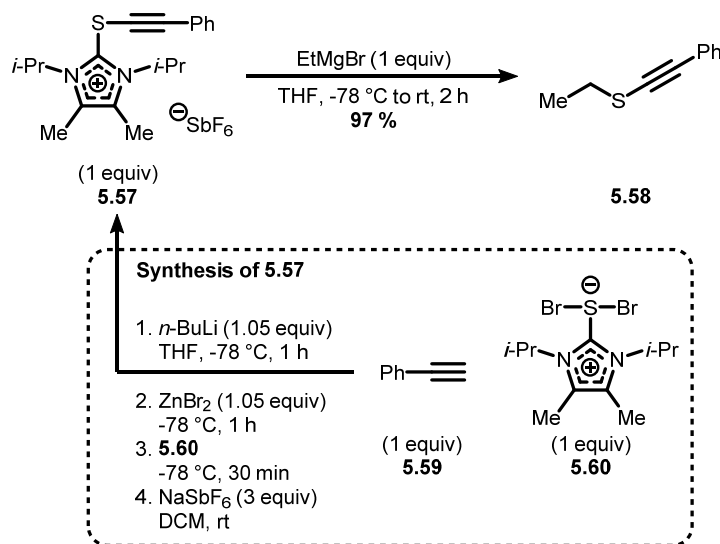
### 5.2.5 Electrophilic Thioalkynylation

Electrophilic thioalkynylation approaches have been developed to synthesize alkynyl sulfides. They generally consist of using an organometallic reagent as nucleophile and a thioalkyne-transfer reagent as electrophile to form the new C(sp)-S bond. One report was based on the ring-opening of 5-chloro-1,2,3-thiadiazoles (**5.53**) by Grignard and organolithium reagents (Scheme 5.12).<sup>31</sup> 4,5-Disubstituted 1,2,3-thiadiazoles (**5.53**) were prepared from  $\alpha$ -chloromethylene ketones (**5.55**) using the Hurd–Mori protocol. For example, when 5-chloro-4-phenylthiadiazole **5.53** was treated with *n*-butyllithium, alkynyl sulfide **5.54** was provided in 63 % yield. It was proposed that organometallic reagents attack at the sulfur atom of 1,2,3-thiadiazoles (**5.53**), concertedly expelling nitrogen and a leaving group to produce alkynyl sulfides.



**Scheme 5.12** Initial synthesis of alkynyl sulfides from electrophilic thioalkynylation

Few methods have since been developed using the electrophilic thioalkynylation approach. Following the design of novel electrophilic group-transfer reagents based on dihalo(imidazolium)sulfuranes (**5.60**),<sup>32</sup> Alcarazo reported an efficient synthesis of alkynyl sulfides using alkynylthioimidazolium salts (**5.57**).<sup>33</sup> Electrophilic thioalkyne precursors (e.g. **5.57**), which are generated from sulfurane **5.60** and zinc acetylides, are light- and air-stable compounds (Scheme 5.13). When alkynylthioimidazolium salt **5.57** was treated with a Grignard reagent, alkynyl sulfide **5.58** was generated in 97 % yield.



**Scheme 5.13** Modern synthesis of alkynyl sulfides from electrophilic thioalkynylation

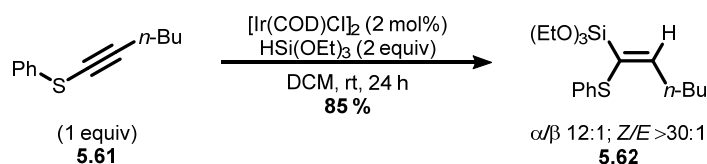
### 5.3 Synthetic Applications of Alkynyl Sulfides

Alkynyl sulfides are versatile building blocks that have been utilized to construct various sulfur-containing compounds since the 1960s.<sup>34</sup> The more reactive triple bond from the electron-rich sulfur atom has provided novel chemical transformations including nucleophilic additions, cycloadditions, and annulations. Selected synthetic applications of alkynyl sulfides from the last five years will be presented in the following section.

## 5.3.1 Nucleophilic Additions

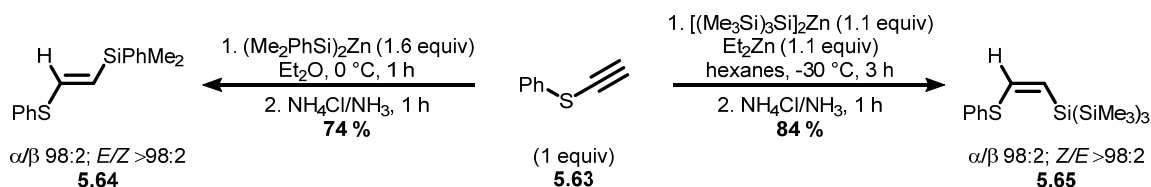
### 5.3.1.1 Hydrosilylation

It was shown by Sun and co-workers that internal alkynyl sulfides can participate in hydrosilylation reactions to generate vinylsilane compounds (**5.62**) in regio- and stereoselective fashion (Scheme 5.14).<sup>35</sup> For example, alkynyl sulfide **5.61** reacted in the presence of triethoxysilane and a catalytic amount of  $[\text{Ir}(\text{COD})\text{Cl}]_2$  to produce vinyl sulfide **5.62** in 85 % yield at room temperature. The iridium-based catalyst enabled the hydrosilylation of diverse alkynyl sulfides with a range of silanes in high  $\alpha$ -regioselectivity and *Z*-stereoselectivity. Sun and co-workers had previously reported the first mild hydrosilylation of alkynyl sulfides using  $[\text{Cp}^*\text{Ru}(\text{MeCN})_3]\text{PF}_6$  as catalyst.<sup>36</sup> Although the methodology could be applied to various internal alkynyl sulfides, only the bulky and expensive silane  $(\text{TMSO})_3\text{SiH}$  gave good yields.



**Scheme 5.14** Iridium-catalyzed hydrosilylation of alkynyl sulfides

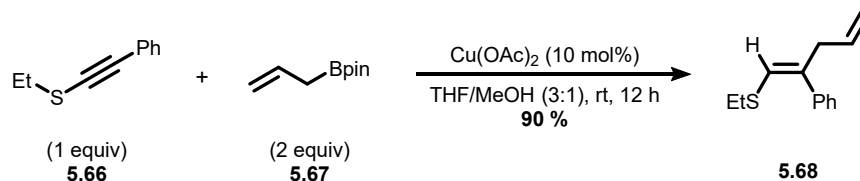
Stereodivergent silylzincations of terminal alkynyl sulfides have also been developed to generate exclusive  $\beta$ -silyl-substituted vinyl sulfides with tunable stereoselectivity.<sup>37</sup> For example, alkynyl sulfide **5.63** reacted with  $(\text{Me}_2\text{PhSi})_2\text{Zn}$  to afford vinyl sulfide **5.64** in 74 % yield with high *E*-stereoselectivity following hydrolysis (Scheme 5.15). Alternatively, using alkynyl sulfide **5.63** in the presence of  $[(\text{Me}_3\text{Si})_3\text{Si}]_2\text{Zn}$  and  $\text{Et}_2\text{Zn}$  afforded vinyl sulfide **5.65** in 84 % yield with high *Z*-stereoselectivity. Reacting the silylzincation intermediates with  $\text{CuCN}\cdot 2\text{LiCl}$  and allyl bromide provided the corresponding  $\alpha$ -allyl- $\beta$ -silyl-substituted vinyl sulfides.



**Scheme 5.15** Silylzincation of alkynyl sulfides

### 5.3.1.2 Hydroallylation

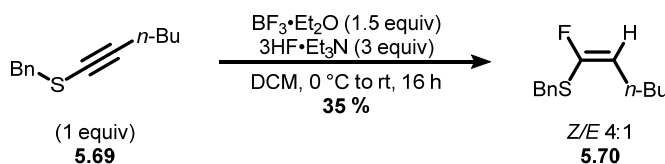
Recently, a regio- and stereoselective alkynyl sulfide hydroallylation protocol was reported by Zhu and Kong.<sup>38</sup> For example, alkynyl sulfide **5.66** reacted with allylboronate **5.67** and a catalytic amount of Cu(OAc)<sub>2</sub> to provide trisubstituted vinyl sulfide **5.68** in 90 % yield (Scheme 5.16). The copper-based catalyst enabled the hydroallylation of various alkynyl sulfides with many allylation reagents in high  $\beta$ -regioselectivity and *E*-stereoselectivity.



**Scheme 5.16** Hydroallylation of alkynyl sulfides

### 5.3.1.3 Hydrohalogenation

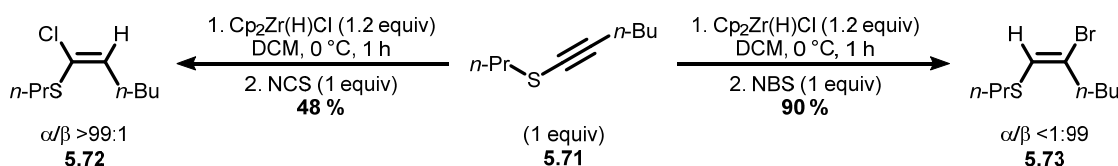
Alkynyl sulfides can also be functionalized by halogens. O'Hagan reported that internal alkynyl sulfides participated in Lewis acid-promoted hydrofluorination reactions to generate  $\alpha$ -fluorovinyl sulfides (**5.70**).<sup>39</sup> For example, alkynyl sulfide **5.69** reacted in the presence of BF<sub>3</sub>•Et<sub>2</sub>O and 3HF•Et<sub>3</sub>N to afford  $\alpha$ -fluorovinyl sulfide **5.70** in 35 % yield (Scheme 5.17). The procedure provided *Z*-hydrofluorination products with generally good stereoselectivity.



**Scheme 5.17** Hydrofluorination of alkynyl sulfides

Other halogens can be employed to generate halogenated vinyl sulfides. Zheng found that internal alkynyl sulfides could readily undergo hydrozirconation to provide  $\alpha$ -thiovinyl zirconocenes as intermediates toward halogenated vinyl sulfides (Scheme 5.18).<sup>40</sup> For example, alkynyl sulfide **5.71** reacted with Schwartz's reagent (Cp<sub>2</sub>Zr(H)Cl) to give the corresponding  $\alpha$ -thiovinyl zirconocene species, which reacted with NCS to provide  $\alpha$ -chlorovinyl sulfide **5.72** in

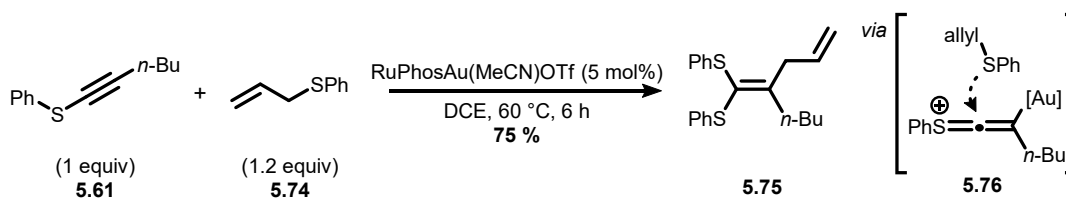
48 % yield. Alternatively, the zirconocene species could be quenched with NBS to produce  $\beta$ -bromovinyl sulfide **5.73** in 90 % yield. The difference in regioselectivity between electrophilic sources of chlorine and bromine was rationalized due to steric hindrance. Additionally, it was found that treating  $\alpha$ -thiovinyl zirconocene intermediates with saturated ammonium chloride provided the corresponding (*Z*)-vinyl sulfides.



**Scheme 5.18** Hydrozirconation of alkynyl sulfides

#### 5.3.1.4 Synthesis of Ketene Dithioacetals

Shi reported that gold catalysis could activate alkynyl sulfides toward the synthesis of ketene dithioacetals (**5.75**).<sup>41</sup> Alkynyl sulfide **5.61** reacted with allylic thioether **5.74** in the presence of RuPhosAu(MeCN)OTf as catalyst to give acyclic ketene dithioacetals **5.75** in 75 % yield (Scheme 5.19). The gold-based catalyst has enabled the synthesis of diverse acyclic ketene dithioacetals from various internal alkynyl sulfides and allylic aryl thioethers in generally good yield. An alkynyl sulfide (**5.61**) was proposed to react with the gold complex to generate a sulfonium intermediate (**5.76**) which would serve as electrophile. A thioether (**5.74**) acting as nucleophile would add onto the  $\alpha$ -position of the sulfonium-gold species to provide the desired product (**5.75**) upon allyl migration.



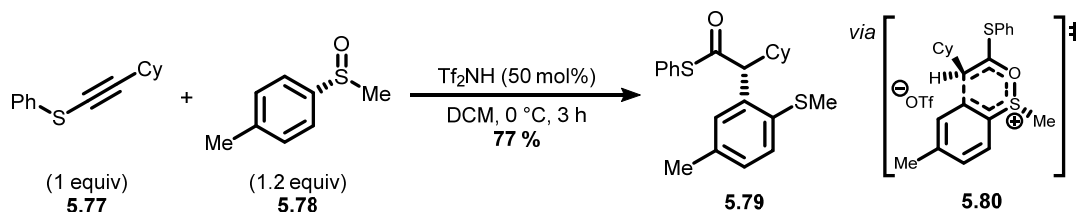
**Scheme 5.19** Synthesis of ketene dithioacetals from alkynyl sulfides

#### 5.3.1.5 1,4-Chirality Transfer

Alkynyl sulfides were found to participate in asymmetric redox arylations with chiral sulfoxides.<sup>42</sup> Maulide reported the first 1,4-chirality transfer from sulfur to carbon through a



sulfonium [3,3]-sigmatropic rearrangement to access  $\alpha$ -arylated thioesters (Scheme 5.20). For example, alkynyl sulfide **5.77** reacted with chiral sulfoxide **5.78** in the presence of  $\text{Tf}_2\text{NH}$  as catalyst to afford  $\alpha$ -arylated thioester **5.79** in 77 % yield and 91:9 e.r. The transformation has allowed various internal alkynyl sulfides, as well as multiple ynamides, to react with *S*-aryl chiral sulfoxides. The use of (*R*)-configured sulfoxides led mainly to the (*R*)-configured products. A correlation between the steric bulk of the alkynyl sulfide substituent and enantioselectivity for the  $\alpha$ -arylated thioesters was observed.

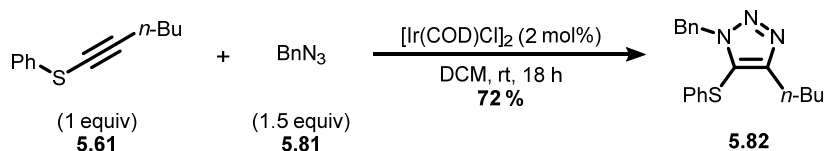


**Scheme 5.20** Synthesis of  $\alpha$ -arylated thioesters from alkynyl sulfides

## 5.3.2 Cycloadditions

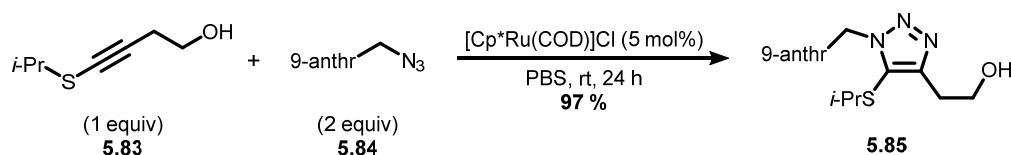
### 5.3.2.1 [3+2] Cycloaddition

Sun and Jia reported that internal alkynyl sulfides can participate in azide-alkyne cycloadditions to generate 1,4-disubstituted 1,2,3-triazoles (**5.82**) with exclusive 1,5-regioselectivity (Scheme 5.21).<sup>43</sup> For example, alkynyl sulfide **5.61** reacted with benzyl azide (**5.81**) in the presence of a catalytic amount of  $[\text{Ir}(\text{COD})\text{Cl}]_2$  to give triazole **5.82** in 72 % yield. The iridium-based catalyst, unlike conventional ruthenium- and copper-based catalytic systems, enabled the azide-alkyne cycloaddition of diverse internal alkynyl sulfides with several azides to generate 5-thio-1,2,3-triazoles. Investigations to rationalize the 1,5-regioselectivity of the iridium-catalyzed cycloaddition were performed using computational studies.<sup>44</sup>



**Scheme 5.21** Iridium-catalyzed [3+2] cycloaddition of alkynyl sulfides

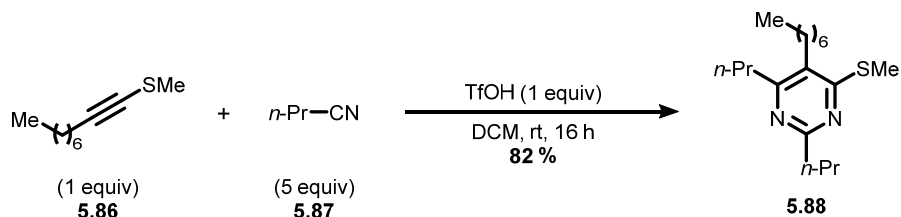
López and Mascareñas reported that internal alkynyl sulfides can partake in azide-alkyne cycloadditions in aqueous media in the presence of biomolecules.<sup>45</sup> A ruthenium-based catalyst enabled the azide-alkyne cycloaddition of various internal alkynyl sulfides and azides to generate 5-thio-1,2,3-triazoles (**5.85**) in aqueous mixtures such as phosphate-buffered saline, cell lysates, and fetal bovine serum (Scheme 5.22). For example, alkynyl sulfide **5.83** reacted with fluorogenic anthracenyl-azide **5.84** and a catalytic amount of [Cp\*Ru(COD)]Cl in phosphate-buffered saline (PBS) to afford triazole **5.85** in 97 % yield. The ruthenium-based system displayed better biocompatibility than previously reported iridium-based system,<sup>43</sup> and could be performed orthogonally with copper-catalyzed azide–terminal alkyne cycloadditions.



**Scheme 5.22** Ruthenium-catalyzed [3+2] cycloaddition of alkynyl sulfides

### 5.3.2.2 [2+2+2] Cycloaddition

Maulide found that internal alkynyl sulfides could participate in metal-free intermolecular [2+2+2] cycloaddition reactions with nitriles to provide pyrimidines (**5.88**) in a regioselective manner (Scheme 5.23).<sup>46</sup> The Brønsted acid-mediated cycloaddition enabled the reaction of a wide scope of internal alkynyl sulfides and nitriles to generate tetrasubstituted pyrimidines. For example, alkynyl sulfide **5.86** reacted with nitrile **5.87** in the presence of TfOH to give pyrimidine **5.88** in 82 % yield. The procedure was also compatible with ynamides.

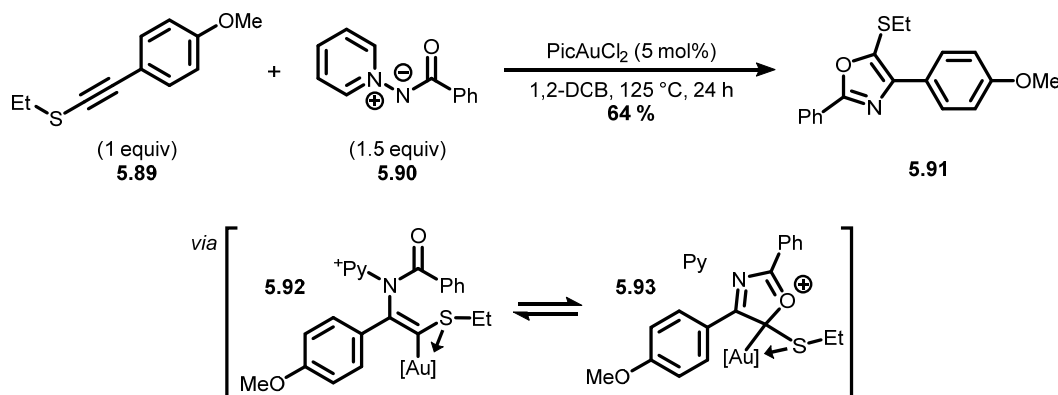


**Scheme 5.23** Brønsted acid-mediated [2+2+2] cycloaddition of alkynyl sulfides

### 5.3.3 Annulations

#### 5.3.3.1 Synthesis of Oxazoles

Davies reported that gold catalysis could activate alkynyl sulfides toward the synthesis of oxazoles (**5.91**).<sup>47</sup> Alkynyl sulfide **5.89** reacted with aminide **5.90** in the presence of PicAuCl<sub>2</sub> as catalyst to provide 5-thio-oxazole **5.91** in 64 % yield (Scheme 5.24). The gold-based catalyst enabled the synthesis of other trisubstituted oxazoles from various electron-rich internal alkynyl sulfides and *N*-acyl pyridinium *N*-aminides in high 5-thio-regioselectivity. The observed regioselectivity was reasoned to arise from a  $\beta$ -centered carbocation vinyl gold species, generated from the alkynyl sulfide, rather than from a sulfonium-gold species. The latter species would lead to the unwanted 4-thio-oxazole regioisomers. Maintaining stabilizing Au-S interactions, a favored  $\beta$ -addition of the nitrenoid would ensue and lead to the intramolecular formation of an aured heterocycle species (**5.93**) via a vinyl gold carbenoid (**5.92**). Desired 5-thio-oxazoles would finally be obtained following aromatization.

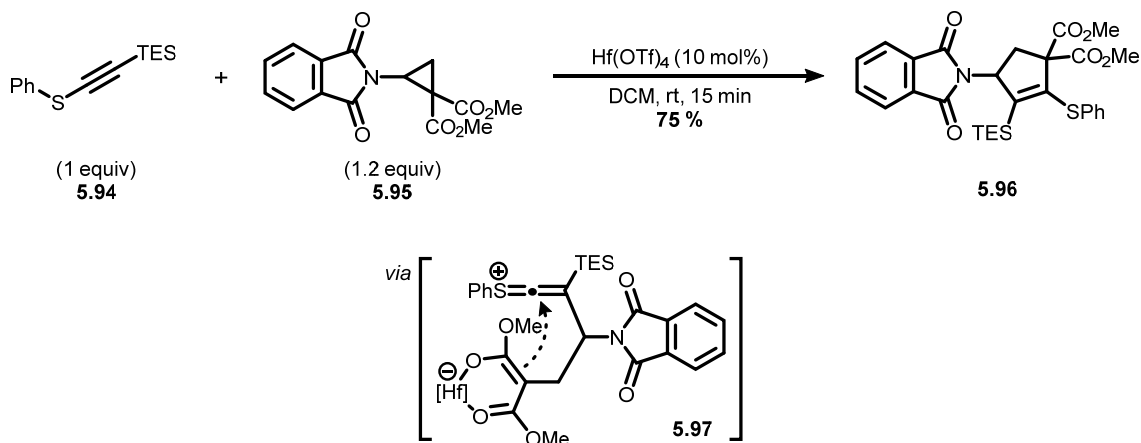


**Scheme 5.24** Gold-catalyzed annulation from alkynyl sulfides

#### 5.3.3.2 Synthesis of 1-Thio-cyclopenten-3-amines

Waser found that silyl-substituted alkynyl sulfides could participate in annulation reactions with donor-acceptor cyclopropanes to provide 1-thio-cyclopenten-3-amines (**5.96**).<sup>48</sup> For example, alkynyl sulfide **5.94** reacted with cyclopropane **5.95** in the presence of catalytic Hf(OTf)<sub>4</sub> in dichloromethane to give cyclopentene **5.96** in 75 % yield (Scheme 5.25). The Lewis acid-catalyzed annulation allowed a variety of triethylsilyl-substituted alkynyl sulfides and phthalimide-substituted cyclopropanes to form 1-thio-cyclopenten-3-amines with high

regioselectivity. A nucleophilic  $\beta$ -addition of a hafnium-activated cyclopropane onto an alkynyl sulfide was proposed to generate a sulfonium intermediate (**5.97**). The steric effects of the silyl group would favor an  $\alpha$ -addition of the malonate anion, rather than the phthalimide carbonyl oxygen onto the thioketene to produce the desired annulation product.



**Scheme 5.25** Lewis acid-catalyzed annulation from alkynyl sulfides

## 5.4 Conclusions

Unlike common transformations involving thiols, such as oxidative S-S bond formation, thiol alkylation and ene reactions to make  $\text{C}(\text{sp}^3)\text{-S}$  bonds and thiol arylation and yne reactions to produce  $\text{C}(\text{sp}^2)\text{-S}$  bonds, strategies to access alkynyl sulfides remained underexplored for many decades. Several umpolung-type strategies have been recently developed to form proficiently  $\text{C}(\text{sp})\text{-S}$  bonds. As alkynyl sulfides have become attainable, they have been increasingly used as building blocks to prepare various sulfur-containing compounds by transformations such as nucleophilic additions, cycloadditions, and annulations. Interest in alkynyl sulfides, such as ynamides, can be attributed to their versatility and relative stability, but several aspects of their reactivity remain to be explored. Innovative transformations using heteroatom-substituted alkynes are expected in the coming years.

## 5.5 Research Goals

As reviewed in Chapter 5, alkynyl sulfides represent a versatile class of alkynes. Several methods enable the efficient formation of alkynyl sulfides, but procedures are often performed

under strongly basic conditions, and require the prefunctionalization of either the thiol or the alkyne. An efficient synthesis of alkynyl sulfides was reported by Waser.<sup>17-18</sup> The alkyne umpolung strategy using ethynyl benziodoxolone reagents gave rapidly and efficiently access to silyl-, alkyl- and mesityl-substituted alkynyl sulfides under mild reaction conditions. However, the method was generally incompatible with aryl-substituted alkynes. A complementary methodology (Chapter 6) to give access to aryl-substituted alkynyl alkynes under the following considerations:

- 1) A chemoselective C(sp)-S coupling compatible with a wide scope of thiols and aryl bromoalkynes, which are more readily prepared than EBX-type reagents.
- 2) Dual catalysis using photochemistry to synthesize the alkynyl sulfides, based of reports by Noël,<sup>49</sup> Oderinde and Johannes<sup>50</sup> that visible-light-mediated photoredox catalysis could readily generate reactive thiyl radicals from thiols in appropriate conditions (see Chapter 4).
- 3) A rapid reproducible continuous flow process amenable to scale-up featuring a photochemical reaction that benefits from improved light penetration (see Chapter 4).
- 4) Organic-based photocatalysts to improve solubility relative to metal-based photocatalysts.
- 5) Subsequent functionalization to demonstrate the utility of the alkynyl sulfides as versatile building blocks.
- 6) A photochemical-mediated macrocyclization with high dilution in high yield.

## 5.6 Bibliography

1. Trost, B. M.; Tracy, J. S. *Isr. J. Chem.* **2018**, *58*, 18-27.
2. Habrant, D.; Rauhala, V.; Koskinen, A. M. P. *Chem. Soc. Rev.* **2010**, *39*, 2007-2017.
3. (a) DeKorver, K. A.; Li, H.; Lohse, A. G.; Hayashi, R.; Lu, Z.; Zhang, Y.; Hsung, R. P. *Chem. Rev.* **2010**, *110*, 5064-5106; (b) Evano, G.; Coste, A.; Jouvin, K. *Angew. Chem. Int. Ed.* **2010**, *49*, 2840-2859.
4. (a) Evano, G.; Blanchard, N.; Compain, G.; Coste, A.; Demmer, C. S.; Gati, W.; Guissart, C.; Heimbürger, J.; Henry, N.; Jouvin, K.; Karthikeyan, G.; Laouiti, A.; Lecomte, M.; Martin-Mingot, A.; Métayer, B.; Michelet, B.; Nitelet, A.; Theunissen, C.; Thibaudeau, S.; Wang, J.; Zarca, M.; Zhang, C. *Chem. Lett.* **2016**, *45*, 574-585; (b) Gao, Y.; Wu, G.; Zhou, Q.; Wang, J. *Angew. Chem. Int. Ed.* **2018**, *57*, 2716-2720; (c) Zeng, X.; Li, J.; Ng, C. K.; Hammond, G. B.; Xu, B. *Angew. Chem. Int. Ed.* **2018**, *57*, 2924-2928; (d) Baldassari, L. L.; de la Torre, A.; Li, J.; Lüdtke, D. S.; Maulide, N. *Angew. Chem. Int. Ed.* **2017**, *56*, 15723-15727; (e) Wang, T.; Hoye, T. R. *J. Am. Chem. Soc.* **2016**, *138*, 13870-13873.

5. (a) Gray, V. J.; Wilden, J. D. *Org. Biomol. Chem.* **2016**, *14*, 9695-9711; (b) Zhang, W.; Ready, J. M. *J. Am. Chem. Soc.* **2016**, *138*, 10684-10692; (c) Hari Babu, M.; Dwivedi, V.; Kant, R.; Sridhar Reddy, M. *Angew. Chem. Int. Ed.* **2015**, *54*, 3783-3786; (d) Alford, J. S.; Davies, H. M. L. *J. Am. Chem. Soc.* **2014**, *136*, 10266-10269; (e) Minami, Y.; Shiraishi, Y.; Yamada, K.; Hiyama, T. *J. Am. Chem. Soc.* **2012**, *134*, 6124-6127.
6. (a) Rawe, B. W.; Scott, M. R.; Brown, C. M.; MacKenzie, H. K.; Gates, D. P. *Macromolecules* **2017**, *50*, 8916-8927; (b) Chen, Y.-T.; Krytchankou, I. S.; Karttunen, A. J.; Grachova, E. V.; Tunik, S. P.; Chou, P.-T.; Koshevoy, I. O. *Organometallics* **2017**, *36*, 480-489; (c) Wang, T.; Chen, S.; Shao, A.; Gao, M.; Huang, Y.; Lei, A. *Org. Lett.* **2015**, *17*, 118-121; (d) Krishna, H.; Caruthers, M. H. *J. Am. Chem. Soc.* **2012**, *134*, 11618-11631.
7. Minehan, T. G. *Acc. Chem. Res.* **2016**, *49*, 1168-1181.
8. Minghao, F.; Bingqing, T.; Steven, H. L.; Xuefeng, J. *Curr. Top. Med. Chem.* **2016**, *16*, 1200-1216.
9. Hoyle, C. E.; Lowe, A. B.; Bowman, C. N. *Chem. Soc. Rev.* **2010**, *39*, 1355-1387.
10. Arens, J. F.; Doornbos, T. *Recl. Trav. Chim. Pays-Bas* **1956**, *75*, 481-486.
11. Nebois, P.; Kann, N.; Greene, A. E. *J. Org. Chem.* **1995**, *60*, 7690-7692.
12. Marchueta, I.; Montenegro, E.; Panov, D.; Poch, M.; Verdaguer, X.; Moyano, A.; Pericàs, M. A.; Riera, A. *J. Org. Chem.* **2001**, *66*, 6400-6409.
13. (a) Nooi, J. R.; Arens, J. F. *Recl. Trav. Chim. Pays-Bas* **1961**, *80*, 244-256; (b) Chandanshive, J. Z.; Bonini, B. F.; Gentili, D.; Fochi, M.; Bernardi, L.; Franchini, M. C. *Eur. J. Org. Chem.* **2010**, *2010*, 6440-6447; (c) Mohan, B.; Hwang, S.; Woo, H.; Park, K. H. *Synthesis* **2015**, *47*, 3741-3745; (d) Bieber, L. W.; da Silva, M. F.; Menezes, P. H. *Tetrahedron Lett.* **2004**, *45*, 2735-2737; (e) Braga, A. L.; Reckziegel, A.; Menezes, P. H.; Stefani, H. A. *Tetrahedron Lett.* **1993**, *34*, 393-394.
14. Doroszuk, J.; Musiejuk, M.; Demkowicz, S.; Rachon, J.; Witt, D. *RSC Adv.* **2016**, *6*, 105449-105453.
15. Godoi, B.; Sperança, A.; Back, D. F.; Brandão, R.; Nogueira, C. W.; Zeni, G. *J. Org. Chem.* **2009**, *74*, 3469-3477.
16. Reeves, J. T.; Camara, K.; Han, Z. S.; Xu, Y.; Lee, H.; Busacca, C. A.; Senanayake, C. H. *Org. Lett.* **2014**, *16*, 1196-1199.
17. Frei, R.; Waser, J. *J. Am. Chem. Soc.* **2013**, *135*, 9620-9623.
18. Frei, R.; Wodrich, M. D.; Hari, D. P.; Borin, P.-A.; Chauvier, C.; Waser, J. *J. Am. Chem. Soc.* **2014**, *136*, 16563-16573.
19. Wodrich, M. D.; Caramenti, P.; Waser, J. *Org. Lett.* **2016**, *18*, 60-63.
20. Wu, W.; Jiang, H. *Acc. Chem. Res.* **2014**, *47*, 2483-2504.
21. Chowdhury, R. M.; Wilden, J. D. *Org. Biomol. Chem.* **2015**, *13*, 5859-5861.
22. (a) Ziegler, G. R.; Welch, C. A.; Orzech, C. E.; Kikkawa, S.; Miller, S. I. *J. Am. Chem. Soc.* **1963**, *85*, 1648-1651; (b) Ni, Z.; Wang, S.; Mao, H.; Pan, Y. *Tetrahedron Lett.* **2012**, *53*, 3907-3910.
23. Zefirov, N. S.; Makhon'kov, D. I. *Chem. Rev.* **1982**, *82*, 615-624.
24. Arens, J. F. *Recl. Trav. Chim. Pays-Bas* **1963**, *82*, 183-188.
25. Brachet, E.; Brion, J. D.; Alami, M.; Messaoudi, S. *Adv. Synth. Catal.* **2013**, *355*, 2627-2636.
26. Bruneau, A.; Roche, M.; Hamze, A.; Brion, J. D.; Alami, M.; Messaoudi, S. *Chem. Eur. J.* **2015**, *21*, 8375-8379.
27. Brachet, E.; Brion, J. D.; Alami, M.; Messaoudi, S. *Chem. Eur. J.* **2013**, *19*, 15276-15280.

28. (a) Brandsma, L.; Wijers, H.; Arens, J. F. *Recl. Trav. Chim. Pays-Bas* **1962**, *81*, 583-584; (b) Brandsma, L.; Wijers, H. E.; Jonker, C. *Recl. Trav. Chim. Pays-Bas* **1964**, *83*, 208-216; (c) Wijers, H. E.; Montijn, P. P.; Brandsma, L.; Arens, J. F. *Recl. Trav. Chim. Pays-Bas* **1965**, *84*, 1284-1288.
29. (a) Miyaura, N.; Yanagi, T.; Suzuki, A. *Chem. Lett.* **1979**, *8*, 535-536; (b) Schaumann, E.; Lindstaedt, J. *Chem. Ber.* **1983**, *116*, 1728-1738.
30. Zheng, W.; Zheng, F.; Hong, Y.; Hu, L. *Heteroat. Chem* **2012**, *23*, 105-110.
31. Voets, M.; Smet, M.; Dehaen, W. *J. Chem. Soc., Perkin Trans. 1* **1999**, 1473-1476.
32. Talavera, G.; Peña, J.; Alcarazo, M. *J. Am. Chem. Soc.* **2015**, *137*, 8704-8707.
33. Peña, J.; Talavera, G.; Waldecker, B.; Alcarazo, M. *Chem. Eur. J.* **2017**, *23*, 75-78.
34. (a) Bos, L. B.; Arens, J. F. *Recl. Trav. Chim. Pays-Bas* **1963**, *82*, 157-171; (b) Brandsma, L.; Wijers, H. E.; Arens, J. F. *Recl. Trav. Chim. Pays-Bas* **1963**, *82*, 1040-1046; (c) Drenth, W.; Nieuwdorp, G. H. E. *Recl. Trav. Chim. Pays-Bas* **1969**, *88*, 307-312.
35. Song, L. J.; Ding, S.; Wang, Y.; Zhang, X.; Wu, Y. D.; Sun, J. *J. Org. Chem.* **2016**, *81*, 6157-6164.
36. Ding, S.; Song, L. J.; Wang, Y.; Zhang, X.; Chung, L. W.; Wu, Y. D.; Sun, J. *Angew. Chem. Int. Ed.* **2015**, *54*, 5632-5635.
37. (a) Fopp, C.; Isaac, K.; Romain, E.; Chemla, F.; Ferreira, F.; Jackowski, O.; Oestreich, M.; Perez-Luna, A. *Synthesis* **2017**, *49*, 724-735; (b) Fopp, C.; Romain, E.; Isaac, K.; Chemla, F.; Ferreira, F.; Jackowski, O.; Oestreich, M.; Perez-Luna, A. *Org. Lett.* **2016**, *18*, 2054-2057.
38. Kong, W.; Che, C.; Kong, L.; Zhu, G. *Tetrahedron Lett.* **2015**, *56*, 2780-2782.
39. Bello, D.; O'Hagan, D. *Beilstein J. Org. Chem.* **2015**, *11*, 1902-1909.
40. Zheng, W.; Hong, Y.; Wang, P.; Zheng, F.; Zhang, Y.; Wang, W. *Tetrahedron Lett.* **2013**, *54*, 3643-3646.
41. Ye, X.; Wang, J.; Ding, S.; Hosseini, S.; Wojtas, L.; Akhmedov, N. G.; Shi, X. *Chem. Eur. J.* **2017**, *23*, 10506-10510.
42. Kaldre, D.; Maryasin, B.; Kaiser, D.; Gajsek, O.; Gonzalez, L.; Maulide, N. *Angew. Chem. Int. Ed.* **2017**, *56*, 2212-2215.
43. Ding, S.; Jia, G.; Sun, J. *Angew. Chem. Int. Ed.* **2014**, *53*, 1877-1880.
44. Luo, Q.; Jia, G.; Sun, J.; Lin, Z. *J. Org. Chem.* **2014**, *79*, 11970-11980.
45. Destito, P.; Couceiro, J. R.; Faustino, H.; Lopez, F.; Mascarenas, J. L. *Angew. Chem. Int. Ed.* **2017**, *56*, 10766-10770.
46. Xie, L. G.; Niyomchon, S.; Mota, A. J.; Gonzalez, L.; Maulide, N. *Nat. Commun.* **2016**, *7*, 10914.
47. Reddy, R. J.; Ball-Jones, M. P.; Davies, P. W. *Angew. Chem. Int. Ed.* **2017**, *56*, 13310-13313.
48. Racine, S.; Hegedüs, B.; Scopelliti, R.; Waser, J. *Chem. Eur. J.* **2016**, *22*, 11997-12001.
49. Talla, A.; Driessen, B.; Straathof, N. J. W.; Milroy, L. G.; Brunsveld, L.; Hessel, V.; Noël, T. *Adv. Synth. Catal.* **2015**, *357*, 2180-2186.
50. Oderinde, M. S.; Frenette, M.; Robbins, D. W.; Aquila, B.; Johannes, J. W. *J. Am. Chem. Soc.* **2016**, *138*, 1760-1763.

## 6. Photochemical Dual-Catalytic Synthesis of Alkynyl Sulfides

Jeffrey Santandrea, Clémentine Minozzi, Corentin Cruché and Shawn K. Collins\*

Department of Chemistry and Centre for Green Chemistry and Catalysis,  
Université de Montréal, CP 6128 Station Downtown, Montréal, Québec, Canada, H3C 3J7

*Angewandte Chemie International Edition* **2017**, 56, 12255-12259.

Reproduced with permission from John Wiley and Sons  
Permanent link to the article (DOI): [10.1002/anie.201705903](https://doi.org/10.1002/anie.201705903)

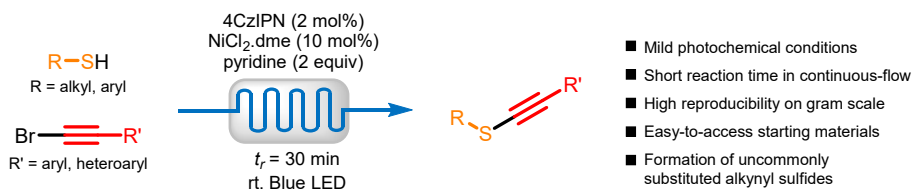
### Contributions:

- Jeffrey Santandrea participated in the design of the experiments, did all the experimental work to optimize the aryl alkyne substrate scope, and macrocyclization reactions, participated in the examination of the thiol substrate scope and the diversification reactions, and contributed to the writing of the manuscript.
- Clémentine Minozzi participated in exploring the thiol substrate scope and contributed to the writing of the manuscript.
- Corentin Cruché participated in exploring the thiol substrate scope and the diversification reactions, and contributed to the writing of the manuscript.
- Shawn K. Collins participated in the design of the experiments and writing of the manuscript.



## 6.1 Abstract

A photochemical dual-catalytic cross-coupling to form alkynyl sulfides via C(sp)-S bond formation is described. The cross-coupling of thiols and bromoalkynes is promoted by a soluble organic carbazole-based photocatalyst using continuous flow techniques. Synthesis of alkynyl sulfides bearing a wide range of electronically and sterically diverse aromatic alkynes and thiols can be achieved in good to excellent yields (50-96 %). The simple continuous flow setup also allows for short reaction times (30 min) and high reproducibility on gram scale. In addition, we report the first application of photoredox/nickel dual catalysis towards macrocyclization, as well as the first example of the incorporation of an alkynyl sulfide functional group into a macrocyclic scaffold.



## 6.2 Introduction

Carbon-sulfur bonds have an important role in the chemical sciences.<sup>1</sup> The functionalization of thiols has long served as a key tool in medicinal chemistry and chemical biology, but is now playing a prominent role in modern materials science.<sup>2</sup> As such, there is an increasing demand to expand the set of thiol-based coupling reactions that are chemoselective, tolerant of complex functionality and provide facile access to new functional group architectures. Interest in heteroatom-substituted alkynes has focused mainly on nitrogen-substituted alkynes (ynamides) or alkynyl ethers.<sup>3</sup> However, the prominence of carbon-sulfur bonds in molecules of interest in both medicine and material science has recently led to the development of thio-alkynylation methodologies.<sup>4</sup> The direct substitution of an alkyne by a sulfur provides a fascinating arrangement of functional groups, as the electron-rich sulfur atom permits conjugation with its lone pair(s) to afford enhanced reactivity to the triple bond as well as a handle for modulation of physical properties and desired applications. Alkynyl sulfides can be obtained in chemoselective fashion through the use of Umpolung-type strategies: the C-S bond can be formed through manipulation of a leaving group on sulfur, typically employing a

copper- or a rhodium-catalyzed coupling with disulfides<sup>5</sup> or by nucleophilic displacement of a sulfur-halogen functionality or Bunte salts (Figure 6.1A).<sup>6</sup> Direct oxidative coupling of thiols and terminal alkynes is also possible via copper catalysis, but competing homocoupling of both the alkyne and the thiol can be problematic.<sup>7</sup> Consequently, novel routes to the alkynylation of thiols continue to be reported, such as a recent disclosure of a transition-metal-free protocol using ethynyl benziodoxolone (EBX) reagents to promote the C-S bond formation (Figure 6.1B).<sup>8</sup> The base-mediated strategy is highly efficient for accessing alkyl-<sup>8b</sup> and silyl-substituted<sup>8c</sup> alkynyl sulfides, but aryl alkynes were found to be generally incompatible. Thiols and alkynes can also be employed as reaction partners in the photochemical thiol-yne click reaction to form C(sp<sup>2</sup>)-S bonds,<sup>9</sup> while C(sp<sup>3</sup>)-S bonds can also be formed photochemically from thiols and alkenes via thiol-ene coupling (Figure 6.1C).<sup>10</sup> Surprisingly, photochemical methods for the synthesis of alkynyl sulfides (forming C(sp)-S bonds) are absent from the toolbox of synthetic chemists.<sup>11</sup> Herein, we describe a complementary photochemical continuous flow alkynylation of thiols employing dual photocatalysis to generate structurally diverse and complex alkynyl sulfides (Figure 6.1D).

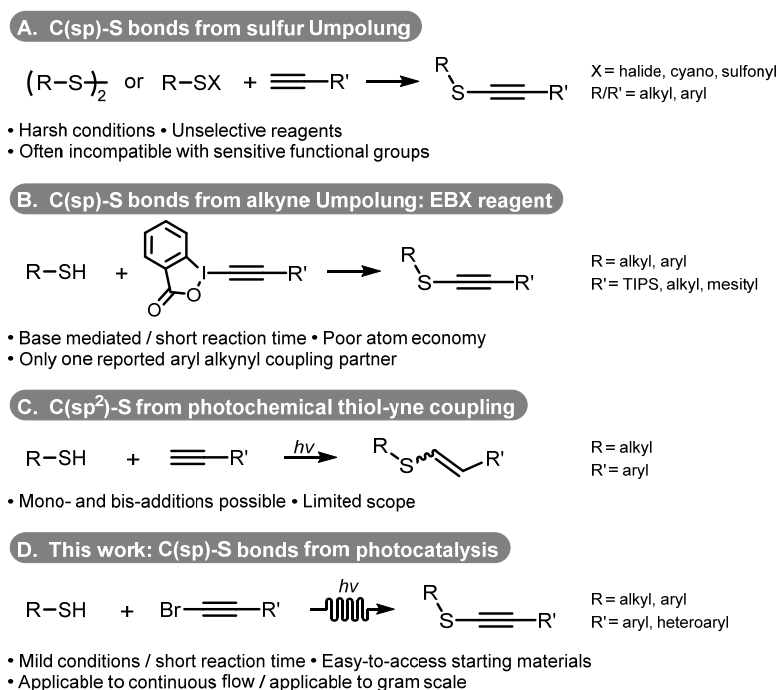


**Figure 6.1** Selected examples of carbon-sulfur bond forming reactions between thiols and alkynes

## 6.3 Results and Discussion

Investigation into a photochemical synthesis of alkynyl sulfides focused on exploiting dual catalysis involving a Ni-catalyzed cross-coupling and photocatalysis (Table 6.1). In addition, the present work placed an emphasis on the use of continuous flow conditions to provide optimal photon flux and more practical scale-up potential.<sup>12</sup> Important targets also included exploiting inexpensive, readily accessible photocatalysts with good solubility profiles. As such, method development began using 4CzIPN, an organic carbazole-based sensitizer reported by Zhang.<sup>13</sup> The model cross-coupling employed the 4-chlorobenzylthiol **6.1a** and bromoalkyne **6.2a** using the 4CzIPN photocatalyst under blue LED irradiation. A solvent mixture of MeCN:DMF (23:1) (50 mM), was found to be optimal and afforded the desired alkynyl sulfide **6.3a** in 96 % yield in a residence time of 30 minutes within the flow apparatus (Table 6.1). In addition, only traces of **6.3a** were found in the absence of light, 4CzIPN or pyridine. No additional bipyridine-based ligand was found to be necessary, in contrast to other photoredox/nickel dual catalyzed transformations.<sup>14</sup> Organic photocatalyst eosin Y, and transition-metal-based complexes of Ir, Ru and Cu only provided the desired product in low yields.<sup>15</sup> Finally, irradiation using a 23 W energy saving light bulb also provided a good yield of alkynyl sulfide **6.3a** (82 %).<sup>15</sup>

**Table 6.1** Control reactions for photoredox/Ni dual-catalyzed C-S coupling

Reaction scheme showing the synthesis of alkynyl sulfide **6.3a** from thiol **6.1a** and bromoalkyne **6.2a** using 4CzIPN photocatalyst and NiCl<sub>2</sub>·dme catalyst in MeCN/DMF (23:1) solvent mixture under blue LED irradiation.

Reagents: 4CzIPN (2 mol%), NiCl<sub>2</sub>·dme (10 mol%), pyridine (2 equiv), MeCN/DMF (23:1) (0.05 M), *t<sub>r</sub>* = 30 min (433 μL/min), rt, Blue LED.

Products: **6.3a** (R<sup>1</sup> = 4-ClBn, R<sup>2</sup> = PMP).

Structure of 4CzIPN is shown in a dashed box.

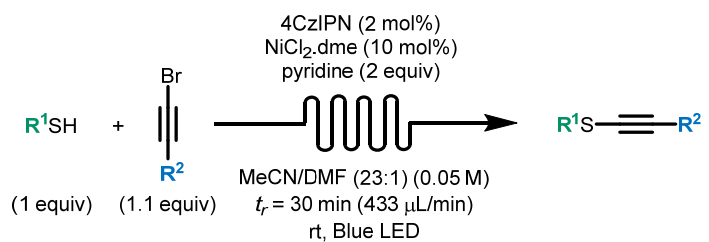
Entry	Variation from standard conditions	Yield (%) <sup>a</sup>
1	none	96
2	no light (dark)	<5
3	no 4CzIPN	<5
4	no NiCl <sub>2</sub> ·dme	28
5	no pyridine	<5

<sup>a</sup>Yield determined by <sup>1</sup>H NMR spectroscopy using anisole as an internal standard.

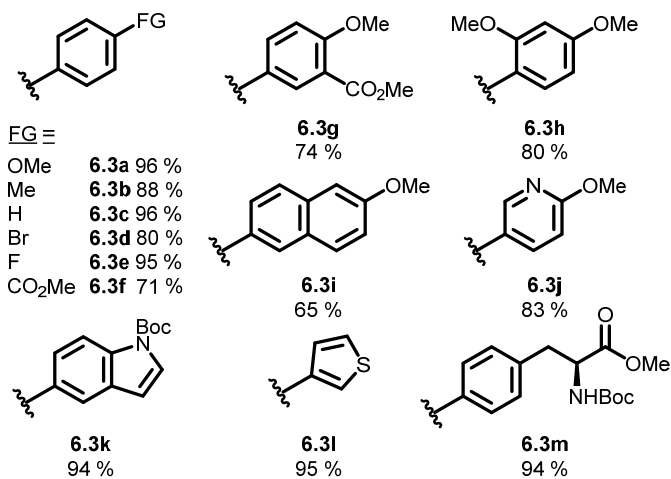
PMP = *p*-methoxyphenyl.

With optimized conditions, the scope of the coupling was first explored with respect to the alkyne (Scheme 6.1). With regards to electronic effects, the dual-catalyzed photocatalytic cross-coupling was tolerant of electron-donating or neutral substituents (OMe **6.3a**, Me **6.3b**, H **6.3c**) on the aromatic alkyne, affording high yields of alkynyl sulfide products (88-96%). Electron-withdrawing substituents (Br **6.3d**, F **6.3e**, CO<sub>2</sub>Me **6.3f**) on the aromatic alkyne cross-coupling partners also reacted smoothly (71-95 % yields). Di-substituted aromatic alkynes were also competent partners, providing good yields of thioalkynes **6.3g** and **6.3h**, even with groups in the ortho-positions of the aromatic (74 and 80 % respectively). Gratifyingly, a number of more complex alkynes underwent coupling to form the desired C-S bonds in high yields. For example, alkynes bearing a substituted naphthyl (**6.3i**, 65 %), pyridine (**6.3j**, 83 %), indole (**6.3k**, 94 %) and thiophene (**6.3l**, 95 %) all provided the products in good to excellent yields. To our delight, phenylalanine-substituted thioalkyne **6.3m** was synthesized in excellent yield (94 %), thus illustrating the feasibility of incorporating alkynyl sulfides in a peptidic scaffold. The scope of the dual-catalyzed photocatalytic cross-coupling to form thioalkynes was next explored with regards to the thiol coupling partner (Scheme 6.1). Electron-rich benzylic thiols reacted smoothly under optimized conditions to generate **6.3n** and **6.3o** (80 and 91 % respectively). A primary alkyl thiol bearing a halogen underwent productive coupling (**6.3p**, 61 %). Boc-protected cysteine also underwent coupling to provide the thioalkyne amino acid **6.3q** in 75 % yield. Secondary alkyl thiols were also competent reaction partners, as the cyclohexyl substituted alkynyl sulfide **6.3r** was isolated in 66 % yield. An enantiomerically pure secondary thiol was employed under photochemical conditions to generate **6.3s** in 70 % yield without loss of the optical activity. Functionalization of captopril afforded the corresponding alkynyl sulfide derivative **6.3t** in 62 % yield. Furthermore, a thioglucose derivative was also successfully coupled to furnish **6.3u** in 50 % yield. Aromatic thiols provided the corresponding alkynyl sulfides **6.3v** and **6.3w** in 96 and 78 % yield respectively. As well, two complex heterocyclic thiols afforded the cross-coupling products in good to excellent yields (**6.3x** and **6.3y**,<sup>16</sup> 52 and 95 %). Note that all of the substrate scope was explored in continuous flow at

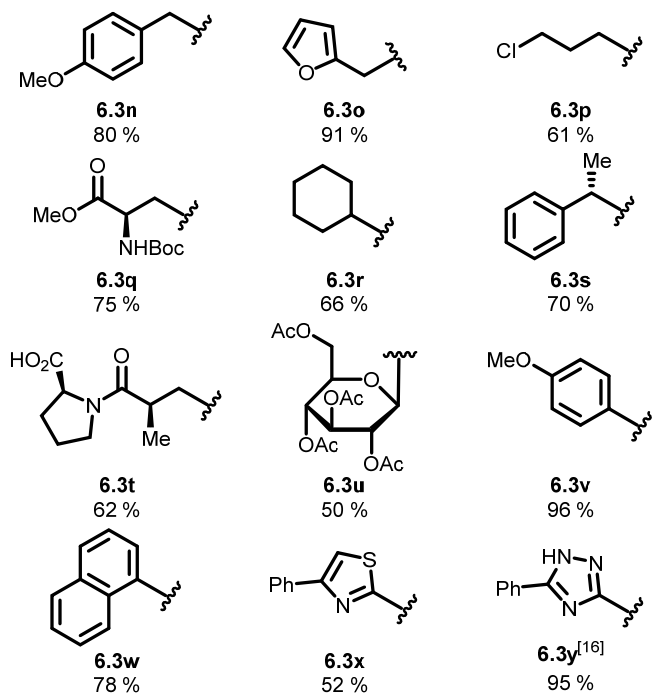
short residence times (30 min), but reactions can be run in batch with longer reaction times (4 h) although yields diminish upon scale-up.<sup>15</sup>



**R<sup>2</sup> Scope (R<sup>1</sup> = 4-ClBn)**

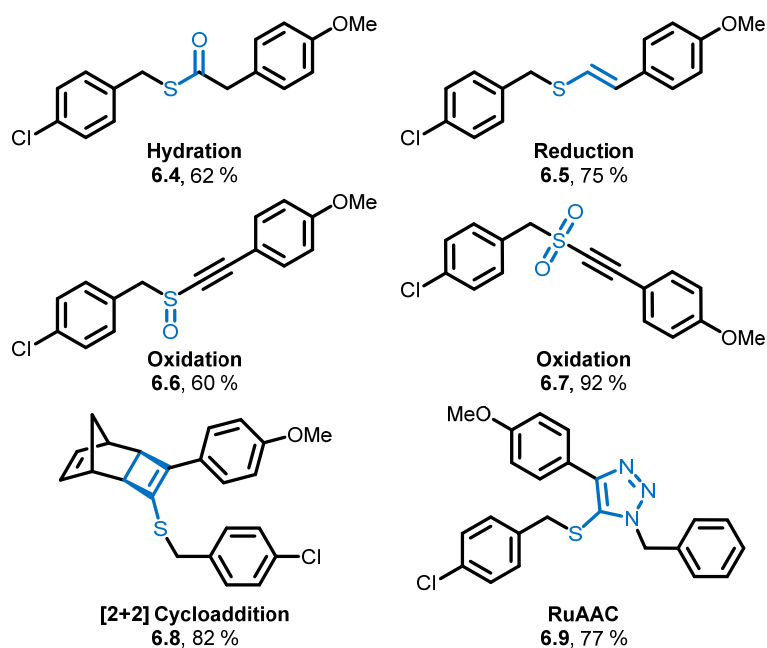


**R<sup>1</sup> Scope (R<sup>2</sup> = PMP)**



**Scheme 6.1** Substrate scope. Yields after chromatography.

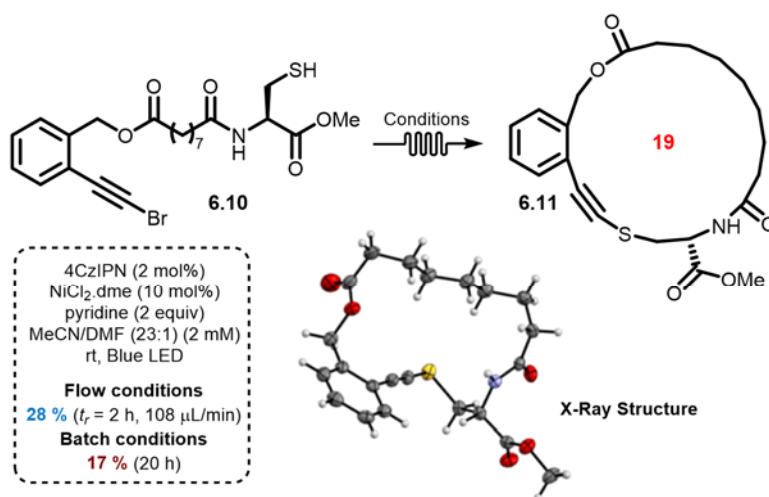
To demonstrate the versatility of alkynyl sulfides as synthons, a series of functionalizing transformations were performed (Scheme 6.2). First, the model thioalkyne **6.3a** was prepared on gram scale using the photocatalytic dual-catalyzed cross-coupling. Even upon scale-up, the method was highly reproducible, affording thioalkyne **6.3a** in 90 % yield.<sup>15</sup> Next, diversification using the alkyne unit was pursued. The thioalkyne **6.3a** could undergo hydration upon treatment with *p*TsOH/SiO<sub>2</sub> to afford the corresponding thioester **6.4** (62 %).<sup>17</sup> Reduction using LiAlH<sub>4</sub> affords the (*E*)-thiovinyl ether **6.5** (75 % yield). It is to be noted that (*Z*)-thiovinyl ethers can be obtained using a weaker hydride source in the presence of CuBr.<sup>18</sup> The sulfur atom of the alkynyl sulfide can also undergo oxidation to the corresponding sulfoxide (**6.6**) and sulfone (**6.7**), and such activated alkynes have already been demonstrated as valuable building blocks able to undergo conjugate additions.<sup>19</sup> Cycloadditions could also be used to install additional structural complexity: a Ru-catalyzed [2+2] cycloaddition provided the norbornene-adduct **6.8** in 82 % yield.<sup>20</sup> A Ru-catalyzed azide-alkyne cycloaddition afforded the corresponding triazole **6.9** in 77 % yield;<sup>21</sup> alkynyl sulfides are representative of a small class of internal alkynes known to undergo selective azide-alkyne cycloaddition.<sup>22</sup>



**Scheme 6.2** Diversification/functionalization of alkynyl sulfides.<sup>15</sup>

Given the successful synthesis of the alkynyl sulfide cross-coupling with cysteine, the possible application to the preparation of macrocyclic peptide-like structures was envisioned.

To the best of our knowledge, dual-catalysis employing photochemistry/Ni-catalysis has yet to be exploited in the context of macrocyclization. Photochemical macrocyclizations are rare; notable examples include the thiol-ene reaction,<sup>23</sup> in which a cyclization occurred on solid support<sup>23b</sup> (2 examples, 30 % average yield) and a recent decarboxylative photoredox macrocyclization (18 examples, 43 % average yield).<sup>24</sup> Macrocyclizations in batch normally require highly dilute reaction mixtures which make efficient light penetration a significant challenge. As such, it was hoped that the continuous flow protocol developed herein, would aid in the development of a novel macrocyclization protocol. Macrocyclic precursor **6.10** was prepared and submitted to the optimized catalyst system, albeit at a reduced concentration (2 mM). Gratifyingly, the desired 19-membered ring **6.11** was isolated in 28 % yield (2 h residence time) and an improvement was observed over a batch process (17 %, 20 h). X-ray quality crystals of **6.11** were obtained and subsequent analysis<sup>25</sup> confirmed the macrocyclic structure (Scheme 6.3).



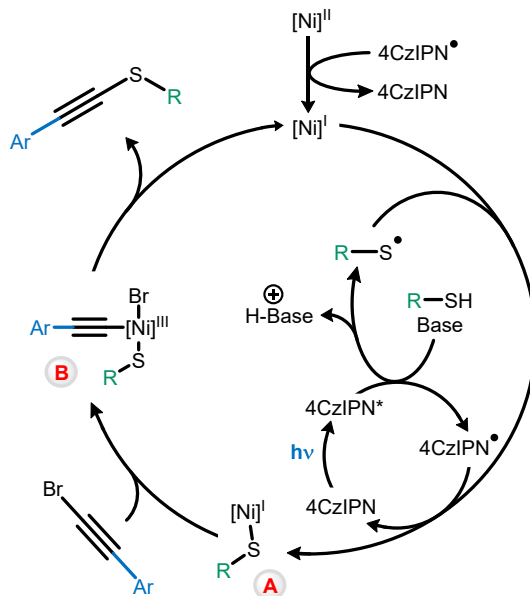
**Scheme 6.3** Dual catalytic synthesis of a 19-membered macrocyclic alkynyl sulfide.

Recently, other dual catalytic systems have been reported for C-S bond formation,<sup>11</sup> but do not report the synthesis of alkynyl sulfides. The mechanism proposed involves generation of the thiyl radical being trapped by a nickel species (**A**, Figure 6.2, *top*). Subsequent oxidative addition forms **B** and reductive elimination results in C-S bond formation. The failure of aliphatic alkynes to react under the developed reaction conditions could be explained by

problematic oxidative addition of the alkynyl halide (**A**→**B**, Figure 6.2, *top*). For example, the groups of Ranu<sup>26</sup> and Li<sup>27</sup> demonstrated that a nickel-based catalyst system could not undergo oxidative addition with an aliphatic alkynyl bromide. It is important to note that the photochemical synthesis of alkynyl sulfides proceeded in the absence of nickel to provide 28 % of **6.3a** (Table 6.1, entry 4). A possible explanation would consist of photochemical generation of the thiyl radical and addition to the alkyne to form the stabilized radical **C** (Figure 6.2, *bottom*).<sup>28</sup> Trapping of the radical with another thiol results in propagation and formation of vinyl bromide **D**.<sup>29</sup> Subsequent base-mediated elimination would form the desired alkynyl sulfide.



**Top: Plausible mechanism with nickel**



**Bottom: Plausible mechanism without nickel**

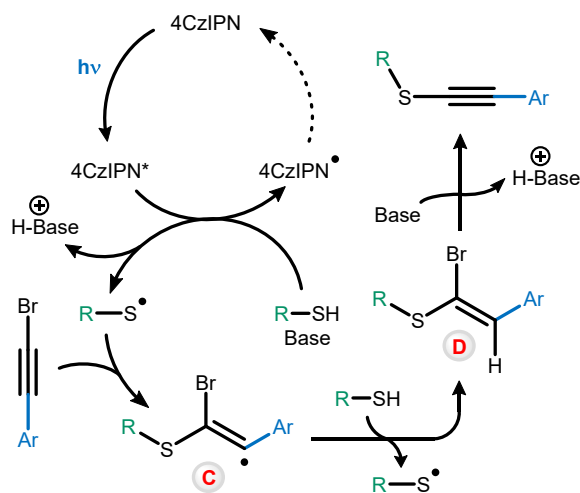


**Figure 6.2** Mechanistic proposals for the synthesis of alkynyl sulfides.

## 6.4 Conclusions

In summary, a novel photochemical dual-catalytic cross-coupling to form alkynyl sulfides has been developed. The method provides the first photochemical route to C(sp)-S bond architectures, and should complement existing photochemical functionalizations as the thiol-ene (C(sp<sup>3</sup>)-S bond) and thiol-yne (C(sp<sup>2</sup>)-S bond) reactions, which have been established as

important tools in the chemical sciences. The method exploits a readily available and soluble organic photocatalyst that permits exploiting continuous flow techniques. As such, facile and rapid (30 min residence time) synthesis of thioalkynes on gram scale is possible, and a wide range of electronically and sterically diverse aromatic alkynes and thiols are viable coupling partners. In addition, the first dual-catalytic macrocyclization was achieved to prepare a 19-membered macrocycle, which represents, to the best of our knowledge, the first incorporation of the thioalkyne moiety into a macrocyclic scaffold. Considering the utility for new chemoselective and functional group-tolerant thiol-based coupling reactions, the method will provide access to new thioalkyne architectures for application in medicinal chemistry, chemical biology, and materials science.

### **Acknowledgments**

The authors acknowledge the Natural Sciences and Engineering Research Council of Canada (NSERC), the NSERC CREATE program in Continuous Flow Science, the Canadian Foundation for Innovation for financial support for continuous flow infrastructure and the Centre for Green Chemistry and Catalysis (CGCC) for funding. Ms. Vanessa Kairouz is thanked for assistance concerning continuous flow protocols.

### **Conflict of Interests**

The authors declare no conflict of interest.

### **Keywords**

Alkynyl sulfides, continuous flow, dual catalysis, macrocycles, photocatalysis.

### **Corresponding Author**

\*E-mail: shawn.collins@umontreal.ca

### **Supporting information for this article can be found under:**

<https://doi.org/10.1002/anie.201705903>.

## 6.5 Bibliography

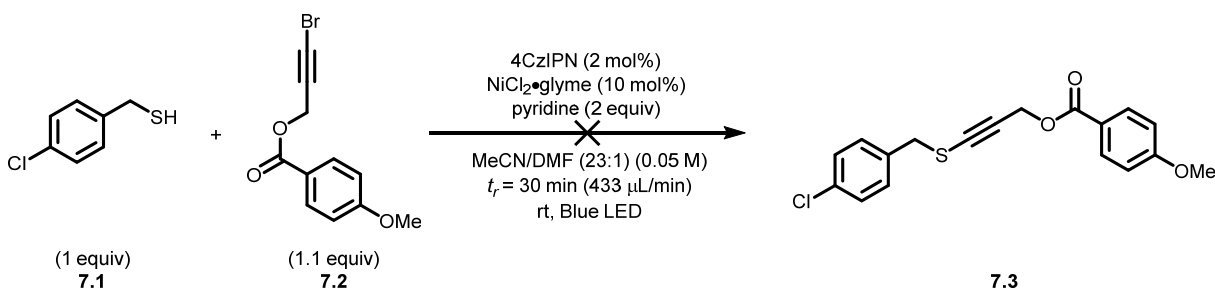
- (a) Ghaderi, A. *Tetrahedron* **2016**, *72*, 4758-4782; (b) Shen, C.; Zhang, P.; Sun, Q.; Bai, S.; Hor, T. S. A.; Liu, X. *Chem. Soc. Rev.* **2015**, *44*, 291-314.
- Boyd, D. A. *Angew. Chem. Int. Ed.* **2016**, *55*, 15486-15502.
- (a) Evano, G.; Blanchard, N.; Compain, G.; Coste, A.; Demmer, C. S.; Gati, W.; Guissart, C.; Heimbürger, J.; Henry, N.; Jouvin, K.; Karthikeyan, G.; Laouiti, A.; Lecomte, M.; Martin-Mingot, A.; Métayer, B.; Michelet, B.; Nitelet, A.; Theunissen, C.; Thibaudeau, S.; Wang, J.; Zarca, M.; Zhang, C. *Chem. Lett.* **2016**, *45*, 574-585; (b) Xie, L.-G.; Niyomchon, S.; Mota, A. J.; González, L.; Maulide, N. *Nat. Commun.* **2016**, *7*, 10914; (c) Kaldre, D.; Maryasin, B.; Kaiser, D.; Gajsek, O.; González, L.; Maulide, N. *Angew. Chem. Int. Ed.* **2017**, *56*, 2212-2215; (d) Minehan, T. G. *Acc. Chem. Res.* **2016**, *49*, 1168-1181.
- (a) Peña, J.; Talavera, G.; Waldecker, B.; Alcarazo, M. *Chem. Eur. J.* **2017**, *23*, 75-78; (b) Doroszuk, J.; Musiejuk, M.; Demkowicz, S.; Rachon, J.; Witt, D. *RSC Adv.* **2016**, *6*, 105449-105453; (c) Chowdhury, R. M.; Wilden, J. D. *Org. Biomol. Chem.* **2015**, *13*, 5859-5861.
- (a) Sujatha, A.; Thomas, A. M.; Thankachan, A. P.; Anilkumar, G. *Arkivoc* **2015**, *1*, 1-28; (b) Fang, Z.; He, W.; Cai, M.; Lin, Y.; Zhao, H. *Tetrahedron Lett.* **2015**, *56*, 6463-6467; (c) Mohan, B.; Hwang, S.; Woo, H.; Park, K. H. *Synthesis* **2015**, *47*, 3741-3745.
- Reeves, J. T.; Camara, K.; Han, Z. S.; Xu, Y.; Lee, H.; Busacca, C. A.; Senanayake, C. H. *Org. Lett.* **2014**, *16*, 1196-1199.
- Yang, Y.; Dong, W.; Guo, Y.; Rioux, R. M. *Green Chem.* **2013**, *15*, 3170-3175.
- (a) Wodrich, M. D.; Caramenti, P.; Waser, J. *Org. Lett.* **2016**, *18*, 60-63; (b) Frei, R.; Wodrich, M. D.; Hari, D. P.; Borin, P.-A.; Chauvier, C.; Waser, J. *J. Am. Chem. Soc.* **2014**, *136*, 16563-16573; (c) Frei, R.; Waser, J. *J. Am. Chem. Soc.* **2013**, *135*, 9620-9623.
- (a) Zaleskiy, S. S.; Shlapakov, N. S.; Ananikov, V. P. *Chem. Sci.* **2016**, *7*, 6740-6745; (b) Lowe, A. B. *Polymer* **2014**, *55*, 5517-5549; (c) Dénès, F.; Pichowicz, M.; Povie, G.; Renaud, P. *Chem. Rev.* **2014**, *114*, 2587-2693.
- (a) Calce, E.; De Luca, S. *Chem. Eur. J.* **2017**, *23*, 224-233; (b) Scanlan, E.; Corcé, V.; Malone, A. *Molecules* **2014**, *19*, 19137; (c) Lowe, A. B. *Polymer Chemistry* **2014**, *5*, 4820-4870; (d) Hoyle, C. E.; Bowman, C. N. *Angew. Chem. Int. Ed.* **2010**, *49*, 1540-1573.
- (a) Oderinde, M. S.; Frenette, M.; Robbins, D. W.; Aquila, B.; Johannes, J. W. *J. Am. Chem. Soc.* **2016**, *138*, 1760-1763; (b) Jouffroy, M.; Kelly, C. B.; Molander, G. A. *Org. Lett.* **2016**, *18*, 876-879.
- (a) Cambié, D.; Bottecchia, C.; Straathof, N. J. W.; Hessel, V.; Noël, T. *Chem. Rev.* **2016**, *116*, 10276-10341; (b) Plutschack, M. B.; Pieber, B.; Gilmore, K.; Seeberger, P. H. *Chem. Rev.* **2017**, *117*, 11796-11893.
- Luo, J.; Zhang, J. *ACS Catal.* **2016**, *6*, 873-877.
- (a) Skubi, K. L.; Blum, T. R.; Yoon, T. P. *Chem. Rev.* **2016**, *116*, 10035-10074; (b) Tellis, J. C.; Kelly, C. B.; Primer, D. N.; Jouffroy, M.; Patel, N. R.; Molander, G. A. *Acc. Chem. Res.* **2016**, *49*, 1429-1439.
- See the Supporting Information for details.
- Alkynyl sulfide **6.3 y** is unstable and decomposes neat and in solution at room temperature. See the Supporting Information for details.

17. Braga, A. L.; Martins, T. L. C.; Silveira, C. C.; Rodrigues, O. E. D. *Tetrahedron* **2001**, *57*, 3297-3300.
18. (a) Vermeer, P.; de Graaf, C.; Meijer, J. *Recl. Trav. Chim. Pays-Bas* **1974**, *93*, 24-25; (b) Song, L.-J.; Ding, S.; Wang, Y.; Zhang, X.; Wu, Y.-D.; Sun, J. *J. Org. Chem.* **2016**, *81*, 6157-6164.
19. Back, T. G.; Clary, K. N.; Gao, D. *Chem. Rev.* **2010**, *110*, 4498-4553.
20. Riddell, N.; Tam, W. *J. Org. Chem.* **2006**, *71*, 1934-1937.
21. Ding, S.; Jia, G.; Sun, J. *Angew. Chem. Int. Ed.* **2014**, *53*, 1877-1880.
22. Luo, Q.; Jia, G.; Sun, J.; Lin, Z. *J. Org. Chem.* **2014**, *79*, 11970-11980.
23. (a) Wang, Y.; Chou, D. H.-C. *Angew. Chem. Int. Ed.* **2015**, *54*, 10931-10934; (b) Aimetti, A. A.; Shoemaker, R. K.; Lin, C.-C.; Anseth, K. S. *Chem. Commun.* **2010**, *46*, 4061-4063.
24. McCarver, S. J.; Qiao, J. X.; Carpenter, J.; Borzilleri, R. M.; Poss, M. A.; Eastgate, M. D.; Miller, M. M.; MacMillan, D. W. C. *Angew. Chem. Int. Ed.* **2017**, *56*, 728-732.
25. CCDC 1550775 contains the supplementary crystallographic data for this paper. These data can be obtained free of charge from The Cambridge Crystallographic Data Centre.
26. Mukherjee, N.; Kundu, D.; Ranu, B. C. *Chem. Commun.* **2014**, *50*, 15784-15787.
27. (a) Mo, S.; Shao, X.-B.; Zhang, G.; Li, Q.-H. *RSC Adv.* **2017**, *7*, 27243-27247; (b) Li, Q.-H.; Ding, Y.; Yang, X.-J. *Chin. Chem. Lett.* **2014**, *25*, 1296-1300.
28. Nakatani, S.; Yoshida, J.-i.; Isoe, S. *J. Chem. Soc., Chem. Commun.* **1992**, 880-881.
29. It should be noted that attempts at generating **D** via coupling of a 1,1-dibromoalkene failed to produce any desired product. See the Supporting Information for details.

## 7. Cu(I)-Catalyzed Synthesis of Alkynyl Sulfides

### 7.1 Expanding the Scope of Reactivity

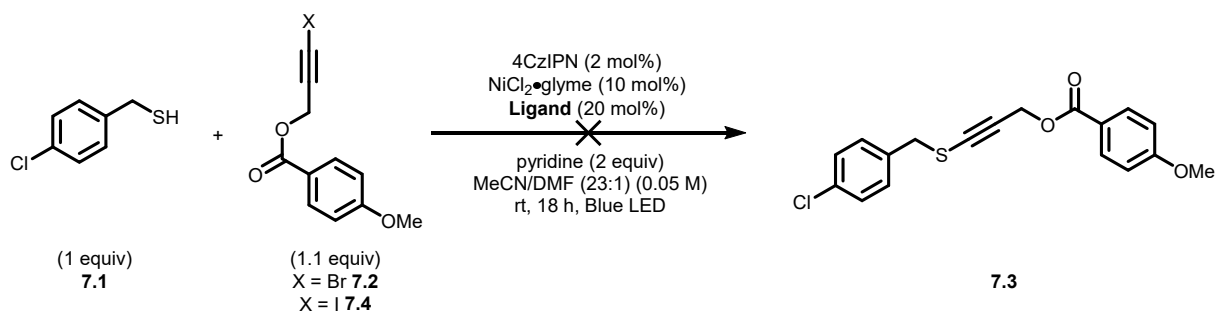
During the development of the work presented in Chapter 6, it was found that alkyl-substituted bromoalkyne **7.2** did not react photochemically with thiol **7.1** under previously reported conditions<sup>1</sup> to provide alkyl-substituted alkynyl sulfide **7.3** (Scheme 7.1).



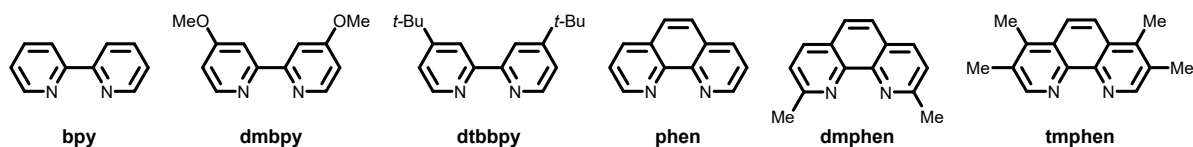
**Scheme 7.1** Attempt at coupling an alkyl bromoalkyne photochemically

In an effort to promote the coupling between thiol **7.1** and alkyl bromoalkyne **7.2**, different diamine ligands were surveyed (Table 7.1). The electronic properties of the nickel complex were varied to favour oxidative addition with less activated bromoalkyne **7.2**. Several bipyridine- and phenanthroline-based ligands were screened in the photochemical conditions. However, irradiating the reaction mixtures overnight in batch did not provide the desired alkynyl sulfide **7.3** (Table 7.1, entries 1-6). Bromoalkyne precursor **7.2** was replaced by iodoalkyne **7.4** in the photochemical reaction in the presence of diamine ligands, because a C(sp)-I bond was reasoned to be more prone to oxidative addition; however, no desired alkynyl sulfide **7.3** was formed (Table 7.1, entries 7-12). Instead, the thiol was converted to the corresponding disulfide quantitatively.

**Table 7.1** Screening of diamine ligands



Ligand



Entry	X	Ligand	<b>7.3</b> (%) <sup>a</sup>
1	Br	bpy	0
2	Br	dmbpy	0
3	Br	dtbbpy	0
4	Br	phen	0
5	Br	dmphen	0
6	Br	tmphen	0
7	I	bpy	0
8	I	dmbpy	0
9	I	dtbbpy	0
10	I	phen	0
11	I	dmphen	0
12	I	tmphen	0

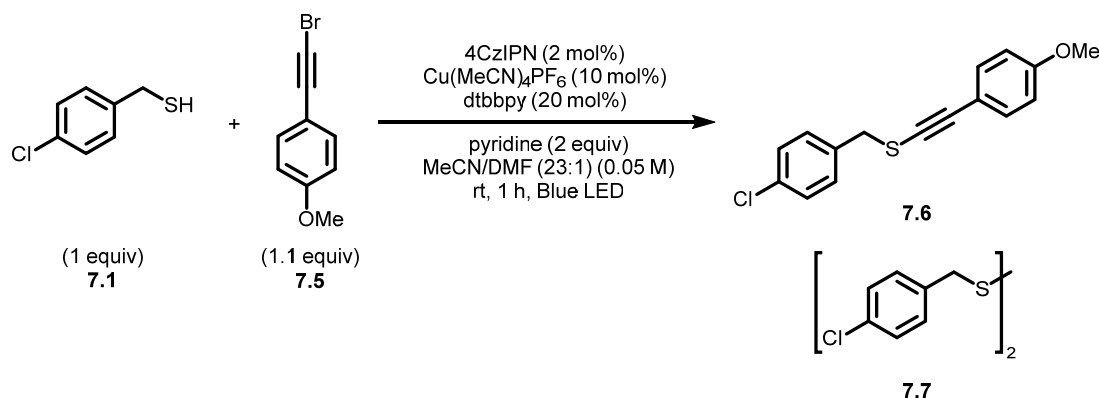
<sup>a</sup> Yield determined by <sup>1</sup>H NMR spectroscopy using 4-nitrobenzaldehyde as an internal standard.

Reactions performed on 0.237 mmol scale.

## 7.1.1 Initial Breakthrough: From Nickel to Copper

### 7.1.1.1 Cu-catalyzed coupling of an aryl bromoalkyne

After unsuccessful attempts to couple thiol **7.1** and alkyl bromoalkyne **7.2** in a dual photoredox-nickel-catalyzed process, the nickel catalyst was exchanged with other transition metal-based catalysts to enable C(sp)-S coupling. Thiol **7.1** was used with aryl bromoalkyne **7.5** to assess catalyst performance. Copper complexes are known to react with bromoalkynes,<sup>2</sup> and were applied instead of NiCl<sub>2</sub>•glyme in the photochemical dual-catalytic system. After one hour of irradiation at room temperature, copper-based catalyst Cu(MeCN)<sub>4</sub>PF<sub>6</sub>, in the presence of 4CzIPN as photocatalyst, dtbbpy as ligand, and pyridine as base generated alkynyl sulfide **7.6** in 65 % yield (Table 7.2, entry 1). Control experiments were subsequently performed to evaluate the necessity of each component in the reaction mixture (Table 7.2, entries 2-6). In the absence of photocatalyst 4CzIPN, alkynyl sulfide **7.6** was obtained in 73 % yield. Employing thiol **7.1** and bromoalkyne **7.5** in the absence of either the copper catalyst, the ligand, or the base led to diminished formation of alkynyl sulfide **7.6**. Performing the reaction in the absence of light did not affect the yield of the reaction. In light of the control experiments, the copper-catalyzed C(sp)-S bond-forming reaction was concluded not to be photochemical.

**Table 7.2** Initial Cu-catalyzed coupling of an aryl bromoalkyne and control experiments

Entry	Variation from conditions	Conversion <b>7.5</b> (%) <sup>a</sup>	Yield <b>7.6</b> (%) <sup>a</sup>	Yield <b>7.7</b> (%) <sup>a</sup>
1	None	88	65	39
2	No 4CzIPN	94	73	32
3	No Cu(MeCN) <sub>4</sub> PF <sub>6</sub>	19	<5	88
4	No dtbbpy	44	17	73
5	No pyridine	51	21	77
6	No light (dark)	87	64	38

<sup>a</sup> Determined by <sup>1</sup>H NMR spectroscopy using 4-nitrobenzaldehyde as an internal standard. Reactions performed on 0.237 mmol scale.

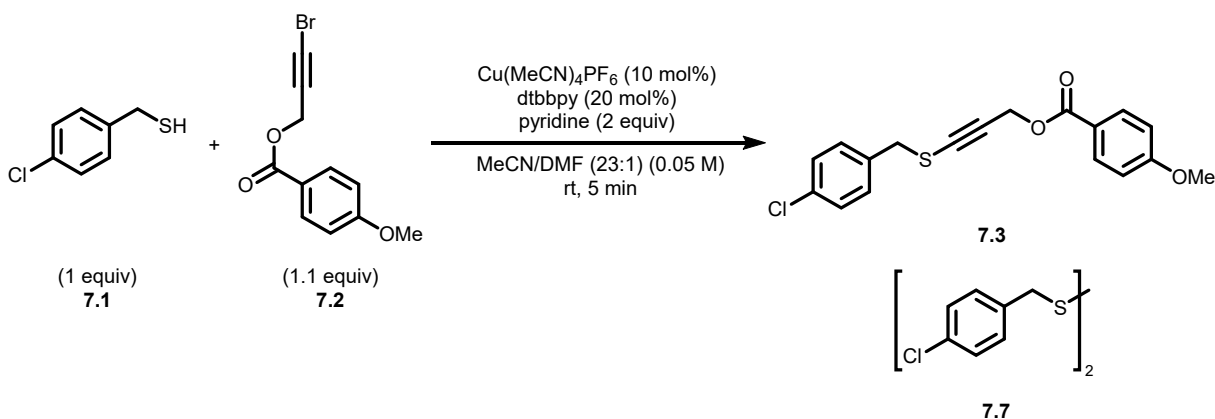
#### 7.1.1.2 Cu-catalyzed coupling of an alkyl bromoalkyne

Following the promising results using aryl bromoalkyne **7.5** and copper catalysis, an attempt using alkyl bromoalkyne **7.2** was made with unoptimized conditions. After five minutes at room temperature, thiol **7.1** and alkyl bromoalkyne **7.2** provided alkynyl sulfide **7.3** in 59 % yield upon exposure to Cu(MeCN)<sub>4</sub>PF<sub>6</sub> as catalyst, dtbbpy as ligand, and pyridine as base (Table 7.3, entry 1). The abovementioned result was the first successful coupling of an alkyl-based bromoalkyne during our reaction development. Control experiments were subsequently performed to evaluate the necessity of each component in the reaction mixture (Table 7.3, entries 2-6). Employing thiol **7.1** and bromoalkyne **7.2** in the absence of either the copper catalyst or the ligand resulted in no productive conversion. In the absence of base, alkynyl sulfide **7.3** was



obtained in 27 % yield, along with 68 % yield of disulfide **7.7**. In addition, removing DMF from the reaction mixture did not affect the yield of alkynyl sulfide **7.3**. Moreover, employing iodoalkyne **7.4** instead of bromoalkyne **7.2** in analogous conditions provided 24 % yield of alkynyl sulfide **7.3** and 72 % yield of disulfide **7.7** (Table 7.3, entry 6). Although alkynyl sulfide **7.3** was synthesized in moderate yield, the results presented the first feasible means to C(sp)-S couple thiols with both alkyl-, and aryl-substituted bromoalkynes.

**Table 7.3** Initial Cu-catalyzed coupling of an alkyl bromoalkyne and control experiments



Entry	Variation from conditions	Conversion <b>7.2</b> (%) <sup>a</sup>	Yield <b>7.3</b> (%) <sup>a</sup>	Yield <b>7.7</b> (%) <sup>a</sup>
1	None	62	59	41
2	No Cu(MeCN) <sub>4</sub> PF <sub>6</sub>	<5	0	0
3	No dtbbpy	<5	0	0
4	No pyridine	41	27	68
5	No DMF	65	60	38
6	Iodoalkyne instead of bromoalkyne	80	24	72

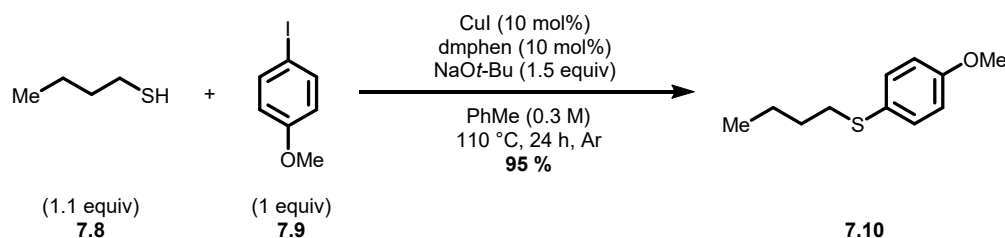
<sup>a</sup> Determined by <sup>1</sup>H NMR spectroscopy using 4-nitrobenzaldehyde as an internal standard. Reactions performed on 0.237 mmol scale.

## 7.1.2 Copper-Catalyzed C-S Couplings

Copper catalysis has previously been applied toward the coupling of thiols with numerous electrophiles.<sup>3</sup> The most common copper-catalyzed C-S bond-forming reactions encompass arylations and vinylations. Recently, alkynyl sulfides have also been generated through copper catalysis.

### 7.1.2.1 S-Arylation

Thioethers have been the subject of much scrutiny in recent years,<sup>4</sup> as the formation of C-S bonds is of great interest in the fields of organic synthesis and drug discovery.<sup>5</sup> The copper-catalyzed arylation of thiols has been mainly achieved using methods such as the Ullmann-type reaction,<sup>6</sup> the Chan-Lam reaction,<sup>7</sup> and the Stadler-Ziegler reaction.<sup>8</sup> For example, an efficient procedure utilizing copper catalysis to generate aryl-substituted thioethers (**7.10**) from thiols and aryl iodides was reported by Venkataraman (Scheme 7.2),<sup>6</sup> who found that employing CuI as catalyst, dmphen as ligand, and sodium *tert*-butoxide as base enabled the coupling between thiol **7.8** and aryl iodide **7.9**. Thioether **7.10** was obtained in 95 % yield after 24 hours in toluene at 110 °C. Several studies to elucidate the mechanism of copper-catalyzed Ullmann-type arylations have been attempted. Many factors concerning the oxidation states of the metal and intermediates remain uncertain.<sup>9</sup> Mechanistic considerations involving C-S bond-forming reactions will be discussed in Section 7.4.

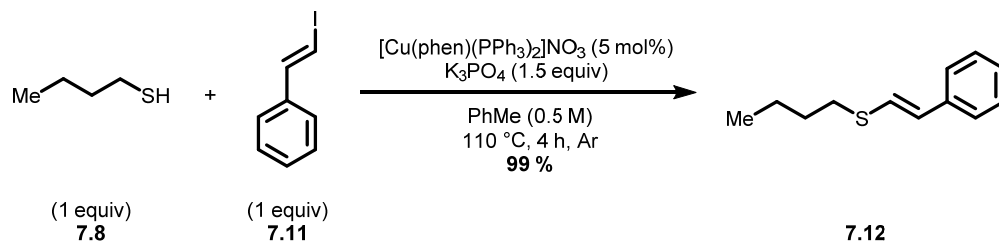


**Scheme 7.2** Ullmann-type copper-catalyzed S-arylation

### 7.1.2.2 S-Vinylation

A copper-catalyzed vinylation of thiols was also developed by Venkataraman (Scheme 7.3).<sup>10</sup> For example, vinyl sulfides (e.g. **7.12**) were readily obtained from thiols (e.g. **7.8**) and vinyl iodides (e.g. **7.11**) in the presence of [Cu(phen)(PPh<sub>3</sub>)<sub>2</sub>]NO<sub>3</sub> as catalyst and K<sub>3</sub>PO<sub>4</sub> as base.

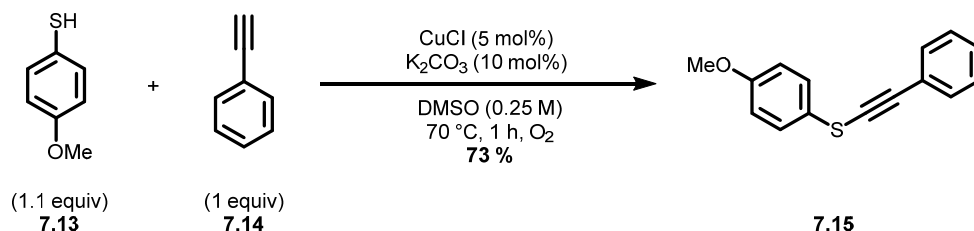
Vinyl sulfide **7.12** was obtained in 99 % yield after four hours in toluene at 110 °C. Both (*E*)- and (*Z*)-vinyl iodides were well tolerated and reacted to generate the corresponding vinyl sulfides in high stereoselectivity.



**Scheme 7.3** Copper-catalyzed S-vinylation

### 7.1.2.3 S-Alkynylation

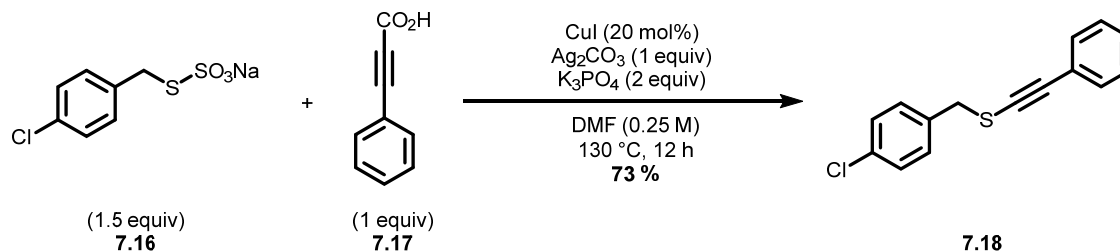
In recent years, copper catalysis has been exploited in aerobic cross-dehydrogenative couplings of thiols and terminal alkynes for the synthesis of alkynyl sulfides.<sup>11</sup> Such processes were developed as an alternative to methods that required the prefunctionalization of coupling partners. For example, Yang and Rioux reported that utilizing catalytic amounts of CuCl and K<sub>2</sub>CO<sub>3</sub> under an atmosphere of O<sub>2</sub> in the presence of thiol **7.13** and alkyne **7.14** to form alkynyl sulfide **7.15** in 73 % yield (Scheme 7.4).<sup>11a</sup> Effective for the coupling of thiophenols, the procedure lacked generality with aliphatic and heteroaromatic thiols. In addition, competing side-reactions, such as the homocoupling of the terminal alkyne or thiol, were observed in some cases.



**Scheme 7.4** Oxidative copper-catalyzed S-alkynylation

Copper catalysis has allowed coupling of prefunctionalized thiols with terminal<sup>12</sup> and pre-activated alkynes,<sup>13</sup> which may avoid use of malodorous and air-sensitive thiols. Yi reported in 2018 a copper-catalyzed decarboxylative coupling to generate alkynyl sulfides (Scheme 7.5).<sup>13a</sup> For example, alkynyl sulfide **7.18** was obtained in 73 % yield from Bunte salt

**7.16** and alkynyl carboxylic acid **7.17** in the presence of CuI as catalyst, K<sub>3</sub>PO<sub>4</sub> as base and Ag<sub>2</sub>CO<sub>3</sub> as oxidant after twelve hours in DMF at 130 °C. Selenium-derived Bunte salts could also be submitted to the copper-catalyzed protocol to form the corresponding alkynyl selenides.



**Scheme 7.5** Decarboxylative copper-catalyzed S-alkynylation

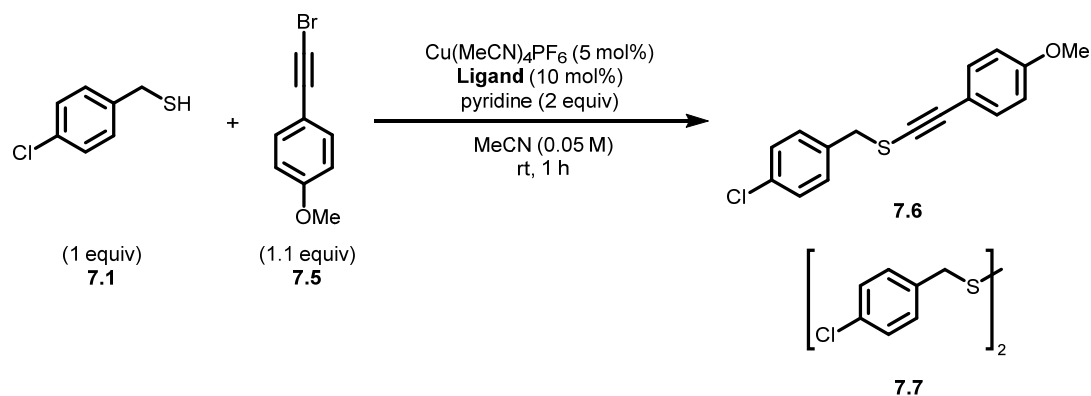
### 7.1.3 Preliminary Screening of Reaction Parameters with Model Aromatic Alkynyl Bromide

Preliminary results demonstrated that both alkyl- and aryl-substituted alkynyl sulfides were prepared under copper catalysis. Screening of reaction parameters were next explored using model thiol **7.1** and aryl bromoalkyne **7.5**.

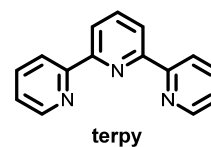
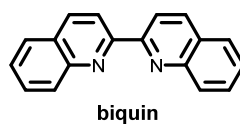
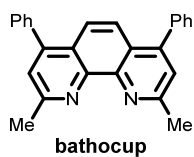
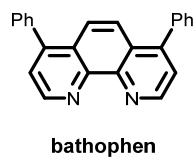
#### 7.1.3.1 Effect of Ligand

The first screened parameter was the ligand. The reaction conditions involved thiol **7.1** (1 equiv) and bromoalkyne **7.5** (1.1 equiv) in the presence of Cu(MeCN)<sub>4</sub>PF<sub>6</sub> (5 mol%), a ligand (10 mol%) and pyridine (2 equiv) in MeCN at room temperature for one hour. By lowering Cu(MeCN)<sub>4</sub>PF<sub>6</sub> and dtbbpy loadings, from 10 to 5 mol% and from 20 to 10 mol% respectively, alkynyl sulfide **7.6** was obtained in 70 % yield. Other bipyridyl-based ligands provided alkynyl sulfide **7.6** in similar yields (Table 7.4, entries 2-3). Although most reactions in Table 7.4 were stirred for one hour, TLC analysis indicated that thiol **7.1** was fully consumed after five minutes in the presence of dtbbpy, and after 15 minutes in the presence of bpy and dmbpy. Several phenanthroline-based ligands were screened, yielding alkynyl sulfide **7.6** in ranges from 0 to 42 % and disulfide **7.7** in ranges from 0 to 68 % (Table 7.4, entries 4-8). Moreover, diamine ligand biquin, as well as triamine ligand terpy did not enable reaction of thiol **7.1** and bromoalkyne **7.5** into the desired product (Table 7.4, entries 9-10).

**Table 7.4** Ligand screening toward formation of alkynyl sulfide **7.6**



Ligand



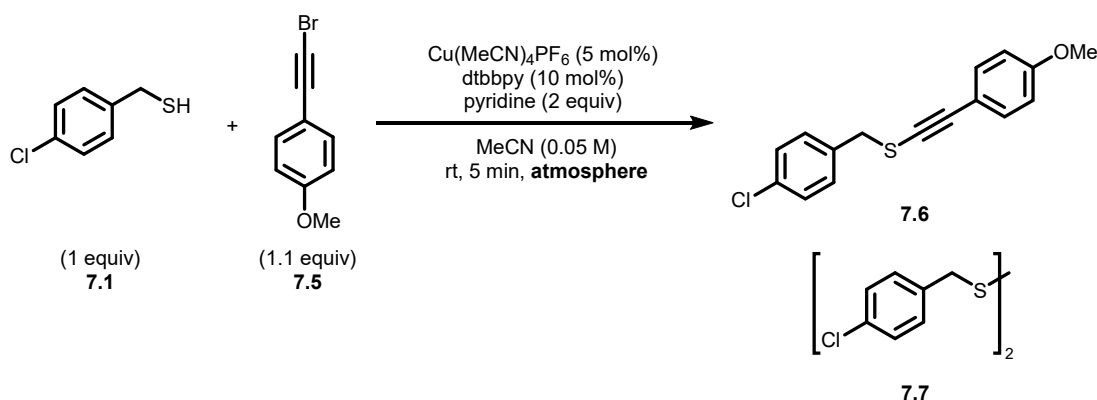
Entry	Ligand	Conversion <b>7.5</b> (%) <sup>a</sup>	Yield <b>7.6</b> (%) <sup>a</sup>	Yield <b>7.7</b> (%) <sup>a</sup>
1	dtbbpy <sup>b</sup>	74	70	28
2	bpy <sup>c</sup>	70	69	27
3	dmbpy <sup>c</sup>	74	70	32
4	phen	40	35	68
5	tmphen	43	27	72
6	bathophen	49	42	55
7	dmphen	<5	0	0
8	bathocup	<5	0	0
9	biquin	<5	0	0
10	terpy	<5	0	0

<sup>a</sup> Determined by <sup>1</sup>H NMR spectroscopy using 4-nitrobenzaldehyde as an internal standard. <sup>b</sup> Reaction time was 5 minutes. <sup>c</sup> Reaction time was 15 minutes. Reactions performed on 0.237 mmol scale.

### 7.1.3.2 Effect of Atmosphere

The formation of alkynyl sulfide **7.6** was often accompanied by undesired disulfide **7.7** and unreacted bromoalkyne **7.5**. To inhibit formation of disulfide **7.7**, two inert atmospheres were evaluated with thiol **7.1** (1 equiv) and bromoalkyne **7.5** (1.1 equiv) in the presence of Cu(MeCN)<sub>4</sub>PF<sub>6</sub> (5 mol%), dtbbpy (10 mol%) and pyridine (2 equiv) in MeCN at room temperature for five minutes. Purging of the solvent and reaction vessel by rigorous bubbling of an inert gas considerably diminished the formation of disulfide **7.7** (Table 7.5, entry 1 vs entries 2-3). Performing the C(sp)-S coupling under nitrogen or argon also improved alkynyl sulfide **7.6** formation to 94 and 88 % yields respectively.

**Table 7.5** Atmosphere screening toward formation of alkynyl sulfide **7.6**

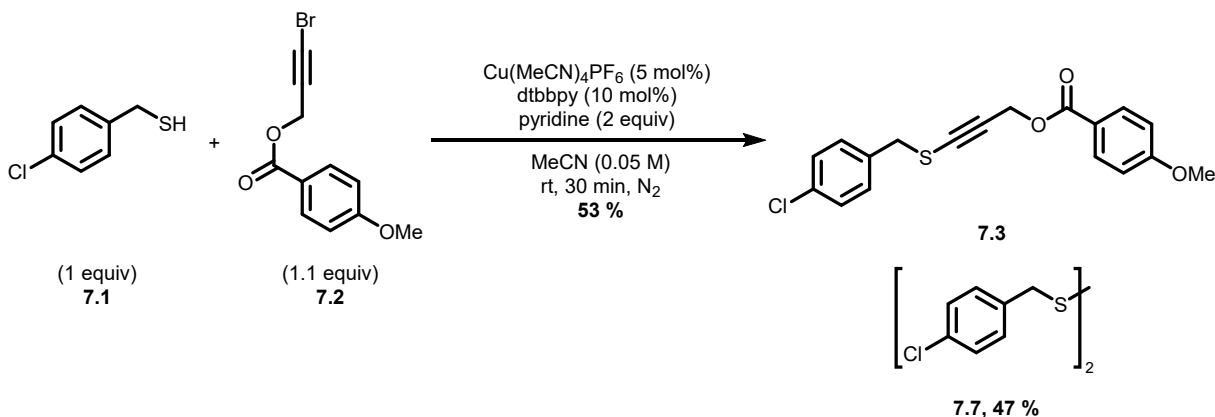


Entry	Atmosphere	Conversion <b>7.5</b> (%) <sup>a</sup>	Yield <b>7.6</b> (%) <sup>a</sup>	Yield <b>7.7</b> (%) <sup>a</sup>
1	air	74	70	28
2	N <sub>2</sub>	95	94	8
3	Ar	89	88	12

<sup>a</sup> Determined by <sup>1</sup>H NMR spectroscopy using 4-nitrobenzaldehyde as an internal standard. Reactions performed on 0.237 mmol scale.

## 7.2 Screening of Reaction Parameters for Coupling with Model Alkyl Alkynyl Bromide

Preliminary screening of reaction conditions between thiol **7.1** and aryl bromoalkyne **7.5** was followed by optimization of the C(sp)-S coupling using alkyl bromoalkyne **7.2**; however, the improved conditions under a nitrogen atmosphere gave only 53 % yield of alkynyl sulfide **7.3**, along with disulfide **7.7** (47 %) and unreacted bromoalkyne **7.2** (56 %) (Scheme 7.6). Analysis by TLC indicated that thiol **7.1** was consumed after 30 minutes. Apparently, the nitrogen atmosphere alone did not inhibit formation of disulfide **7.7** and the reaction rate was slower for coupling alkyl than aryl bromoalkynes. More reaction parameters were screened to improve the efficiency of coupling of thiol **7.1** with alkyl bromoalkyne **7.2**.



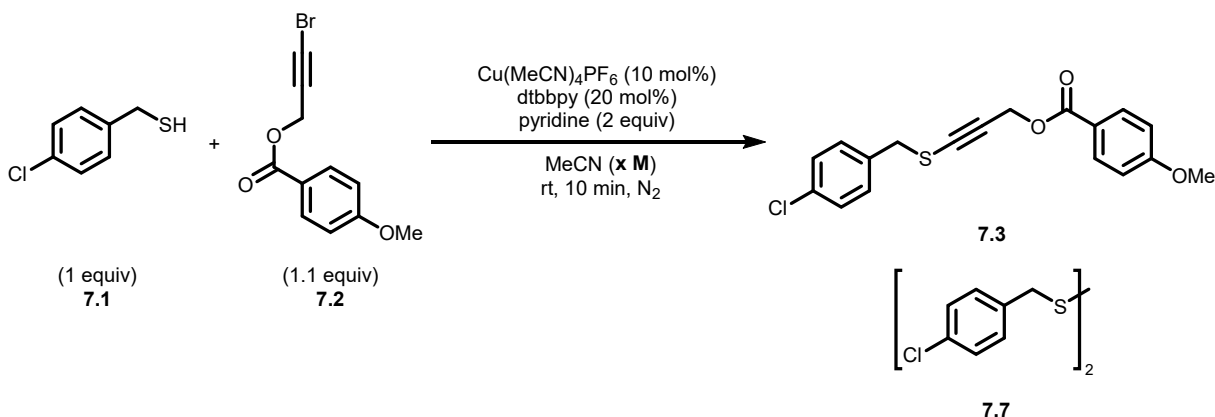
**Scheme 7.6** Cu-catalyzed coupling of alkyl bromoalkyne **7.2** under nitrogen atmosphere

### 7.2.1 Effect of Concentration

The concentration was initially screened at a higher catalyst loading using thiol **7.1** (1 equiv) and alkyl bromoalkyne **7.2** (1.1 equiv) in the presence of Cu(MeCN)<sub>4</sub>PF<sub>6</sub> (10 mol%), dtbbpy (20 mol%) and pyridine (2 equiv) in MeCN at room temperature for ten minutes. Alkynyl sulfide **7.3** and disulfide **7.7** were obtained in 75 % and 25 % yields respectively at 0.05, 0.10 and 0.20 M (Table 7.6, entries 1-3). Lowering the concentration from 0.05 M to 0.025 M provided alkynyl sulfide **7.3** and disulfide **7.7** in 65 % and 36 % yield respectively (Table 7.6, entry 4). At 0.05 M, higher catalyst loadings enabled thiol conversion in a shorter

reaction time (10 min) providing considerable amounts of disulfide **7.7** and unreacted bromoalkyne **7.2**.

**Table 7.6** Concentration screening toward formation of alkynyl sulfide **7.3**



Entry	Concentration (M)	Conversion <b>7.2</b> (%) <sup>a</sup>	Yield <b>7.3</b> (%) <sup>a</sup>	Yield <b>7.7</b> (%) <sup>a</sup>
1	0.05	84	75	25
2	0.10	88	76	27
3	0.20	86	76	25
4	0.025	78	65	36

<sup>a</sup> Determined by  $^1\text{H}$  NMR spectroscopy using 3-chlorotoluene as an internal standard. Reactions performed on 0.237 mmol scale.

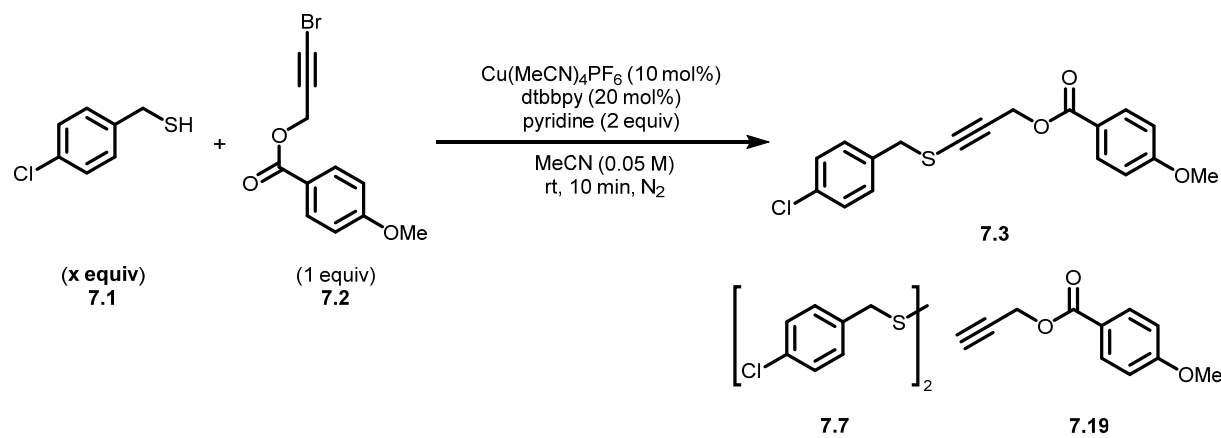
### 7.2.2 Effect of Reagent Stoichiometry

In an effort to fully convert alkyl bromoalkyne **7.2** toward alkynyl sulfide **7.3**, the stoichiometry between thiol **7.1** and bromoalkyne **7.2** was inversed. The reaction conditions involved thiol **7.1** in excess and bromoalkyne **7.2** (1 equiv) in the presence of  $\text{Cu}(\text{MeCN})_4\text{PF}_6$  (10 mol%), dtbbpy (20 mol%) and pyridine (2 equiv) in MeCN at room temperature for ten minutes. When 1.1 equivalents of thiol **7.1** were reacted with 1.0 equivalent of bromoalkyne **7.2**, alkynyl sulfide **7.3** was obtained in 78 % yield, along with disulfide **7.7** (28 %) and terminal alkyne **7.19** (19 %) (Table 7.7, entry 1). Using 1.2 equivalents of thiol **7.1** with bromoalkyne **7.2** provided alkynyl sulfide **7.3** in 88 % yield, as well as disulfide **7.7** (35 %) and terminal alkyne **7.19** (13 %) (Table 7.7, entry 3). Diminishing catalyst loading with 1.1 or 1.2 equivalents



of thiol **7.1** did not improve the yield of the desired product (Table 7.7, entries 2 & 4). However, lower catalyst loadings with a larger excess of thiol **7.1** provided alkynyl sulfide **7.3** in yields ranging from 90 to 94 % (Table 7.7, entries 5-7). Although the desired product was prepared in satisfactory yields, the reaction conditions leading to them were not ideal. Indeed, it was decided that the optimization would carry on utilizing 1.2 equivalents of thiol **7.2**, as higher reagent loadings would be considered wasteful and unappealing.

**Table 7.7** Stoichiometry screening toward formation of alkynyl sulfide **7.3**

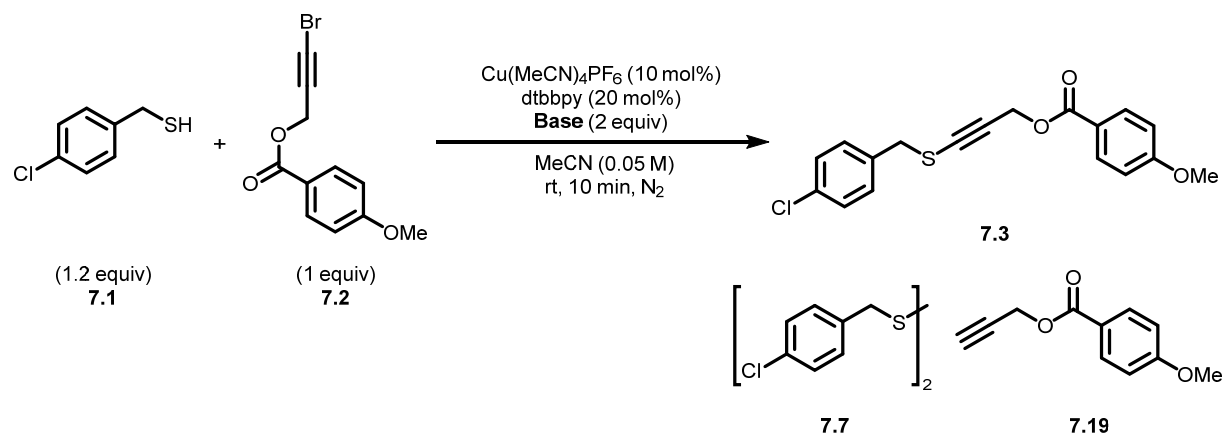


Entry	Equivalents of <b>7.1</b>	Conversion <b>7.2</b> (%) <sup>a</sup>	Yield <b>7.3</b> (%) <sup>a</sup>	Yield <b>7.7</b> (%) <sup>a</sup>	Yield <b>7.19</b> (%) <sup>a</sup>
1	1.1	100	78	28	19
2 <sup>b</sup>	1.1	86	65	36	21
3	1.2	100	88	35	13
4 <sup>b</sup>	1.2	100	83	40	18
5 <sup>b</sup>	1.4	100	90	45	8
6 <sup>b</sup>	1.6	100	94	55	6
7 <sup>b</sup>	1.8	100	93	53	<5

<sup>a</sup> Determined by  $^1\text{H}$  NMR spectroscopy using 3-chlorotoluene as an internal standard. <sup>b</sup>  $\text{Cu}(\text{MeCN})_4\text{PF}_6$  (5 mol%) and dtbbpy (10 mol%). Reactions performed on 0.237 mmol scale.

### 7.2.3 Effect of Base

A variety of organic bases were employed to evaluate whether alkyl bromoalkyne **7.2** could be fully converted to alkynyl sulfide **7.3** without generating corresponding alkyne side-product **7.19**. As such, the reaction conditions involved thiol **7.1** (1.2 equiv) and bromoalkyne **7.2** (1 equiv) in the presence of Cu(MeCN)<sub>4</sub>PF<sub>6</sub> (10 mol%), dtbbpy (20 mol%) and a base (2 equiv) in MeCN at room temperature for ten minutes. Relatively stronger bases, such as Et<sub>3</sub>N, DIPEA and TMG, afforded alkynyl sulfide **7.3** in lower yields than pyridine (Table 7.8, entries 1-4). The substituted pyridine 2,6-lutidine afforded alkynyl sulfide **7.3** in the best yield (98 %) and minimized disulfide **7.7** (19 %) and terminal alkyne **7.19** formation (Table 7.8, entry 5). The relatively weaker pyridine bases 2-picoline and 3-pyridylcarbinol generated trace amounts of terminal alkyne **7.19**, but provided lower yields of alkynyl sulfide **7.3** and higher amounts of disulfide **7.7** (Table 7.8, entries 6-7). Lastly, DABCO failed to give **7.3** and produced mostly disulfide **7.7** and alkyne **7.19** (Table 7.8, entry 8).

**Table 7.8** Base screening toward formation of alkynyl sulfide **7.3**

Entry	Base	Conversion <b>7.2</b> (%) <sup>a</sup>	Yield <b>7.3</b> (%) <sup>a</sup>	Yield <b>7.7</b> (%) <sup>a</sup>	Yield <b>7.19</b> (%) <sup>a</sup>
1	pyridine	100	88	35	16
2	$\text{Et}_3\text{N}$	60	11	88	52
3	DIPEA	58	18	87	<5
4	TMG	77	<5	>95	36
5	2,6-lutidine	100	98	18	<5
6	2-picoline	80	84	38	<5
7	3-pyridylcarbinol	66	65	54	<5
8	DABCO	52	<5	>95	48

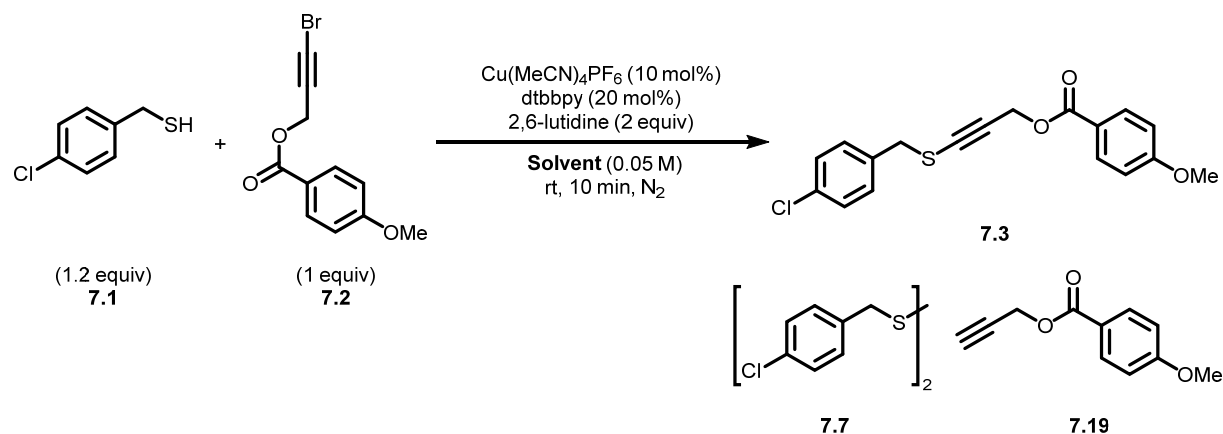
<sup>a</sup> Determined by  $^1\text{H}$  NMR spectroscopy using 3-chlorotoluene as an internal standard. Reactions performed on 0.237 mmol scale.

### 7.2.4 Effect of Solvent

Polar and non-polar solvents were utilized to assess their compatibility with the catalyst system. The reaction conditions involved thiol **7.1** (1.2 equiv) and bromoalkyne **7.2** (1 equiv) in the presence of  $\text{Cu}(\text{MeCN})_4\text{PF}_6$  (10 mol%), dtbbpy (20 mol%) and 2,6-lutidine (2 equiv) in various solvents at room temperature for ten minutes. Performing the reaction in a non-polar solvent like PhMe afforded alkynyl sulfide **7.3** in 98 % yield (Table 7.9, entry 2). When thiol **7.1** and bromoalkyne **7.2** were submitted in polar aprotic solvents such as EtOAc, THF, DMF

and acetone, alkynyl sulfide **7.3** was obtained in yields ranging between 91 and 98 % (Table 7.9, entries 3-6). Lastly, polar protic solvent MeOH provided alkynyl sulfide **7.3** in lower yield (71 %), along with disulfide **7.7** (19 %) and alkyne **7.19** (10 %) (Table 7.9, entry 7). While the copper catalyst system was tolerant of all screened aprotic solvents, homogeneous conditions were observed only in MeCN and DMF.

**Table 7.9** Solvent screening toward formation of alkynyl sulfide **7.3**



Entry	Solvent	Conversion <b>7.2</b> (%) <sup>a</sup>	Yield <b>7.3</b> (%) <sup>a</sup>	Yield <b>7.7</b> (%) <sup>a</sup>	Yield <b>7.19</b> (%) <sup>a</sup>
1	MeCN	100	98	18	<5
2	PhMe	100	98	19	<5
3	EtOAc	100	98	22	<5
4	THF	100	95	18	<5
5	DMF	100	95	25	<5
6	Acetone	100	91	26	<5
7	MeOH	83	71	19	10

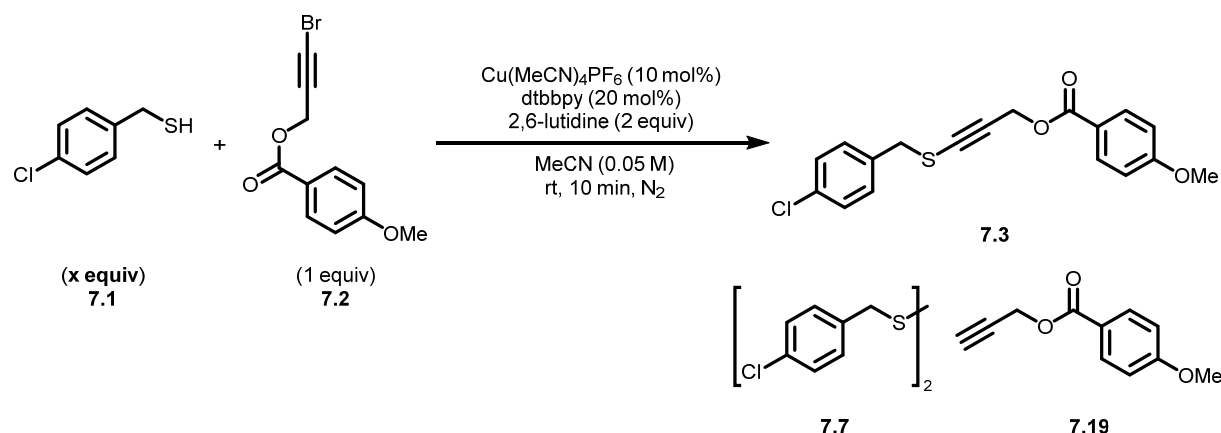
<sup>a</sup> Determined by  $^1\text{H}$  NMR spectroscopy using 3-chlorotoluene as an internal standard. Reactions performed on 0.237 mmol scale.

### 7.2.5 Fine-Tuning of Reagent Stoichiometry

Replacing pyridine by 2,6-lutidine as base allowed for bromoalkyne **7.2** to be fully converted with thiol **7.1** toward alkynyl sulfide **7.3**. The effect of lowering the amount of thiol

on the yield of alkynyl sulfide **7.3** was then investigated. The reaction conditions involved thiol **7.1** and bromoalkyne **7.2** (1 equiv) in the presence of Cu(MeCN)<sub>4</sub>PF<sub>6</sub> (10 mol%), dtbbpy (20 mol%) and 2,6-lutidine (2 equiv) in MeCN at room temperature for ten minutes. When 1.1 equivalents of thiol **7.1** were reacted with 1.0 equivalent of bromoalkyne **7.2**, alkynyl sulfide **7.3** was essentially obtained quantitatively, along with disulfide **7.7** (12 %) (Table 7.10, entry 2). Using 1.0 equivalent of thiol **7.1** with bromoalkyne **7.2** provided alkynyl sulfide **7.3** in 90 % yield, as well as disulfide **7.7** (16 %) (Table 7.10, entry 3). Although it was possible to reduce the amount of thiol **7.1** to 1.0 equivalent and maintain high yields of alkynyl sulfide **7.3**, using 1.1 equivalents of the thiol afforded better reproducibility in terms of conversion and yield.

**Table 7.10** Fine-tuning of conditions toward formation of alkynyl sulfide **7.3**



Entry	Equivalents of <b>7.1</b>	Conversion <b>7.2</b> (%) <sup>a</sup>	Yield <b>7.3</b> (%) <sup>a</sup>	Yield <b>7.7</b> (%) <sup>a</sup>	Yield <b>7.19</b> (%) <sup>a</sup>
1	1.2	100	98	18	<5
2	1.1	100	99	12	<5
3	1.0	94	90	16	<5

<sup>a</sup> Determined by <sup>1</sup>H NMR spectroscopy using 3-chlorotoluene as an internal standard. Reactions performed on 0.237 mmol scale.

It is to be noted that the results summarized in Section 7.2 were obtained following a specific procedure (see Chapter 11 for details). The first components added to the reaction vessel were the bromoalkyne, the ligand and the base. The reaction mixture was colorless prior to the addition of the copper salt (Figure 7.1, A). Upon the addition of the copper precatalyst into

reaction mixture **A**, the immediate formation of a Cu(I)-dtbbpy species was visible from the change of the colorless liquid to dark orange (Figure 7.1, **A**→**B**). As the reaction mixture gradually evolved, the dark orange colour changed to light green (Figure 7.1, **B**→**C**) indicative of an oxidation state change from resting Cu(I)-dtbbpy species to Cu(II)-dtbbpy species.<sup>14</sup>

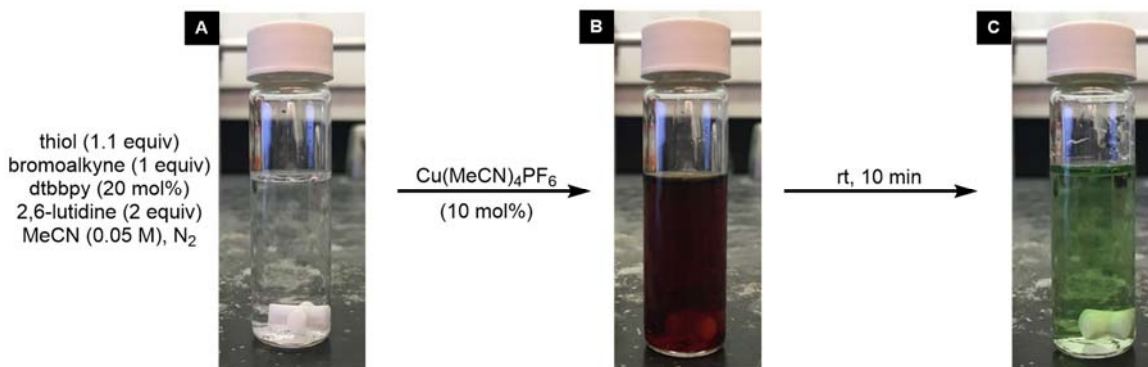


**Figure 7.1** Observed electrochromism during formation of alkynyl sulfides

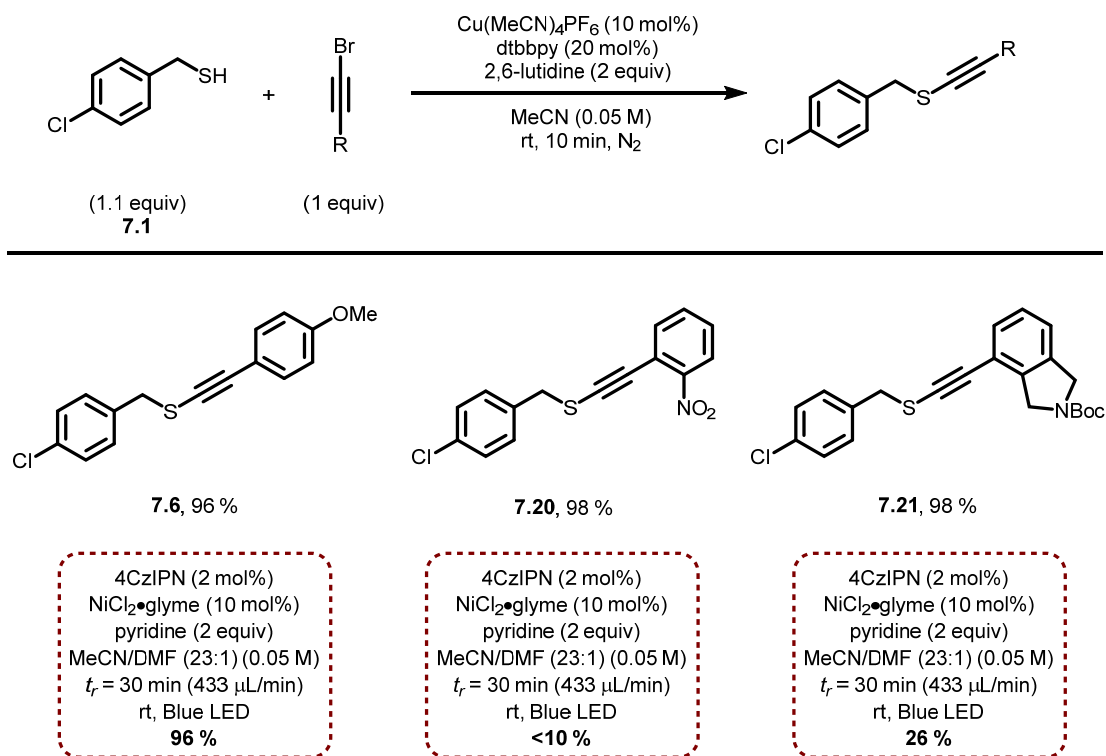
## 7.3 Preliminary Substrate Scope

With optimized C(sp)-S coupling conditions in hand, various coupling partners including aryl-, silyl-, and alkyl-substituted bromoalkynes were employed with thiol **7.1**. In addition, a less common heteroatom-substituted bromoalkyne was utilized to generate a bis(heteroatom-substituted)acetylene. Primary, secondary and tertiary thiols were also tested in the presence of bromoalkyne **7.2**.

### 7.3.1 Aryl-Substituted Alkynyl Bromide Coupling Partners

As Section 7.2 was dedicated to the C(sp)-S coupling optimization of alkyl bromoalkyne **7.2** with thiol **7.1**, aryl bromoalkyne **7.5** had not been tested in the improved reaction conditions. As such, bromoalkyne **7.5** (1 equiv) and thiol **7.1** (1.1 equiv) were submitted to a mixture of Cu(MeCN)<sub>4</sub>PF<sub>6</sub> (10 mol%), a dtbbpy (20 mol%) and 2,6-lutidine (2 equiv) in MeCN (0.05 M) (Scheme 7.7). After stirring the mixture at room temperature for five minutes, alkynyl sulfide **7.6** was isolated in 96 % yield. The yield was comparable to that obtained in previously reported photochemical conditions,<sup>1</sup> albeit in a shorter reaction time (5 min vs 30 min). While the methodology described in Chapter 6 was efficient for the coupling of various aryl- and heteroaryl-substituted bromoalkynes, the photochemical conditions were not compatible with

nitro groups (**7.20**, <10 %) and benzylic amines (**7.21**, 26 %) (Scheme 7.7). It was thus believed that the copper-catalyzed procedure might allow the coupling of bromoalkynes bearing such functional groups. When a nitro-containing bromoalkyne was submitted to the new protocol, alkynyl sulfide **7.20** was isolated in 98 % yield. Similarly, alkynyl sulfide **7.21** was isolated in 98 % yield following the coupling of a bromoalkyne-bearing isoindoline reacted with thiol **7.1**.

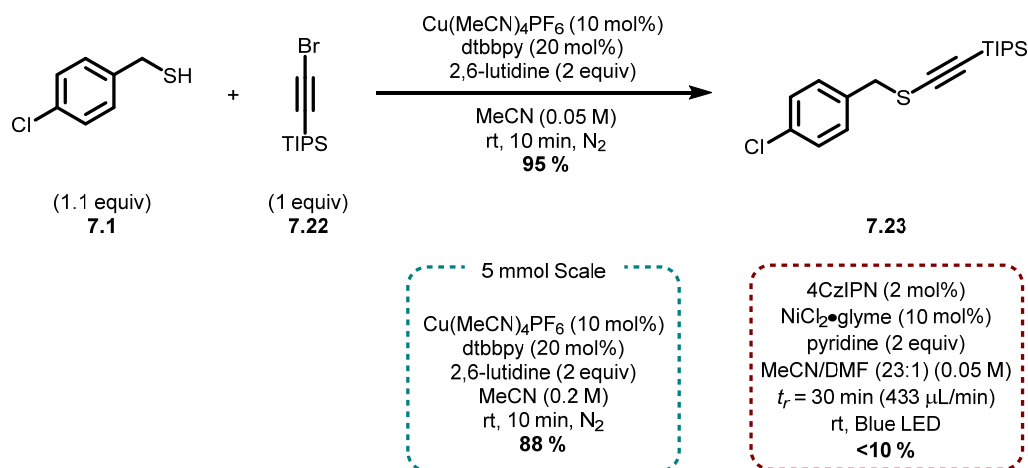


**Scheme 7.7** Widening the scope of aryl-substituted bromoalkynes

### 7.3.2 Silyl-Substituted Alkynyl Bromide Coupling Partners

The previously reported photochemical C(sp)-S coupling was also incompatible with silyl-substituted bromoalkynes (**7.22**, <10 %) (Scheme 7.8). As alkyl-substituted bromoalkyne **7.2** reacted efficiently using the copper catalyst system, it was hoped that it might enable the coupling of a TIPS-substituted bromoalkyne as well. Submitting bromoalkyne **7.22** to the new reaction conditions readily provided alkynyl sulfide **7.23** in 95 % isolated yield. Moreover, the coupling between thiol **7.1** and bromoalkyne **7.22** was performed on a 5 mmol scale at a 0.20 M concentration. Accordingly, alkynyl sulfide **7.23** was obtained in 88 % isolated yield

(Scheme 7.8). The copper catalyst system's reproducibility from small to large scale was thus demonstrated.

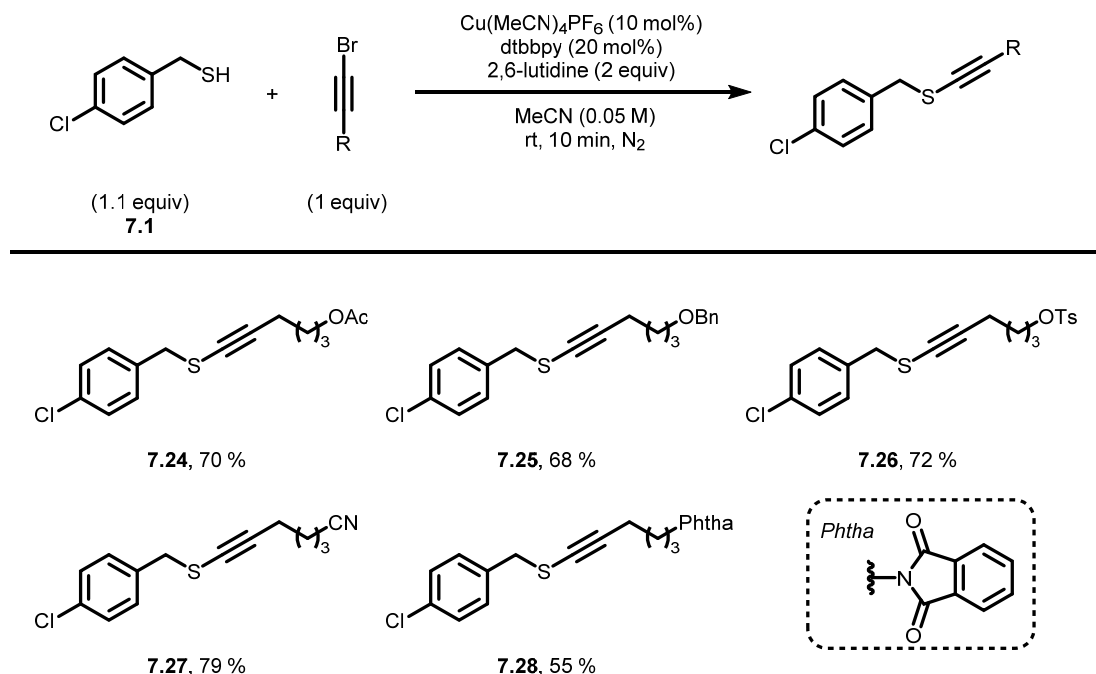


**Scheme 7.8** Formation of a silyl-substituted alkynyl sulfide

### 7.3.3 Alkyl-Substituted Alkynyl Bromide Coupling Partners

Following the successful coupling of alkyl bromoalkyne **7.2** with thiol **7.1**, other alkyl-substituted bromoalkynes were additionally tested in the copper-catalyzed conditions (Scheme 7.9). Bromoalkynes functionalized with several hydroxyl protecting groups were tested. As such, acetyl-, benzyl-, and tosyl-protected bromoalkynes were submitted to the optimized reaction conditions and enabled the formation of alkynyl sulfides **7.24-7.26** in yields ranging from 68 % to 72 %. To be noted, an analogous hydroxyl-containing alkyl bromoalkyne was initially employed with thiol **7.1** but did not productively convert to its corresponding alkynyl sulfide. While TLC analysis indicated that the corresponding bromoalkyne was fully converted, it led to a complex reaction mixture. In addition, when a nitrile-containing bromoalkyne was reacted with thiol **7.1**, alkynyl sulfide **7.27** was obtained in 79 % isolated yield. Furthermore, a phthalimide-substituted bromoalkyne was found to be compatible, as alkynyl sulfide **7.28** was prepared in 55 % yield.

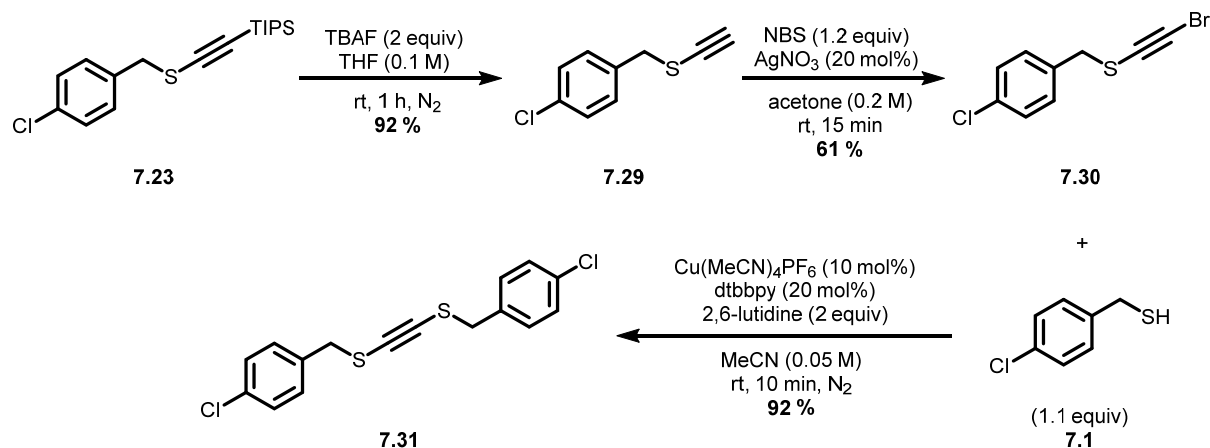




**Scheme 7.9** Preliminary scope of alkyl-substituted bromoalkynes

### 7.3.4 Heteroatom-Substituted Alkynyl Bromide Coupling Partners

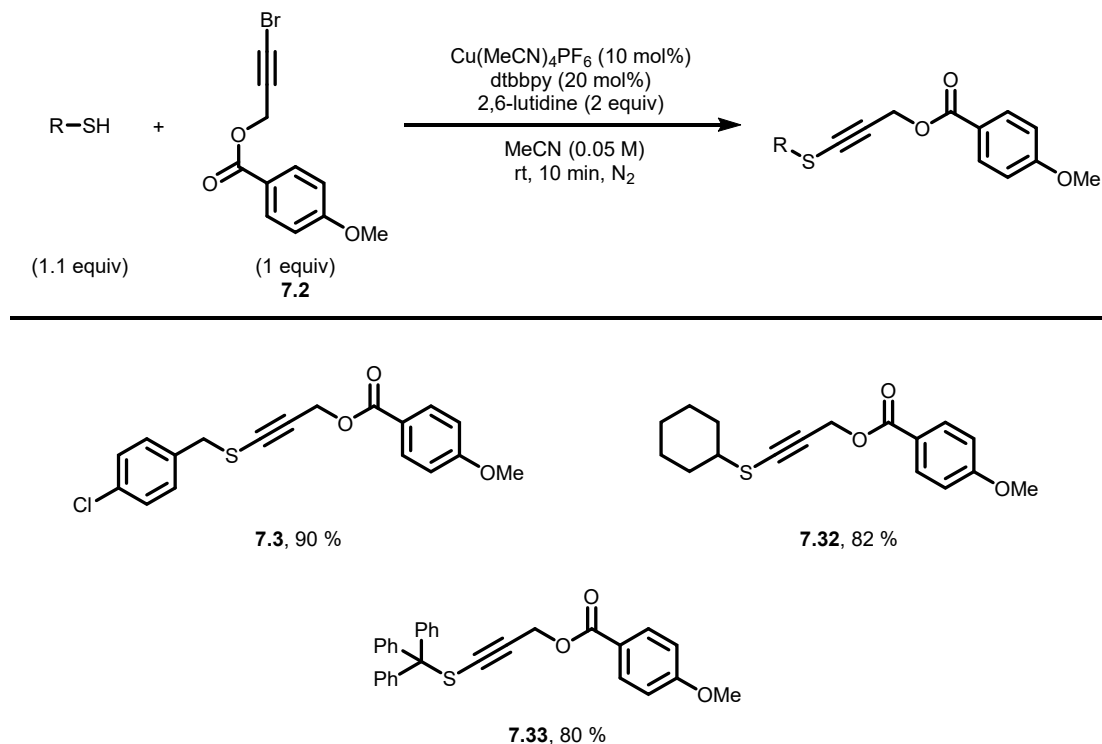
Few methods to generate bis(heteroatom-substituted)acetylenes have been reported.<sup>15</sup> It was thus wondered if the developed copper-catalyzed methodology would allow to access such compounds. The synthesis began with the TBAF-mediated silyl deprotection of alkynyl sulfide **7.23** (Scheme 7.10). Stirring the reaction mixture for one hour at room temperature in THF afforded terminal alkynyl sulfide **7.29** in 92 % yield. Then, alkynyl sulfide **7.29** was brominated in the presence of NBS and catalytic  $\text{AgNO}_3$  in acetone for 15 minutes at room temperature. As a result, bromoalkyne **7.30** was isolated in 61 % following purification. With bromoalkyne **7.33** finally in hand, it was submitted with thiol **7.1** in the optimized catalytic system to provide bis(thio-substituted)alkyne **7.31** in 92 % yield. The preliminary result represented, to the best of our knowledge, the simplest synthetic route toward bis(thio-substituted)alkynes.



**Scheme 7.10** Formation of a bis(thio-substituted)alkyne

### 7.3.5 Thiol Coupling Partners

The parameter screenings in Section 7.2 were solely completed with model thiol **7.1** and alkyl bromoalkyne **7.2**. In addition, the experimental yields were usually determined by  $^1\text{H}$  NMR spectroscopy using an internal standard. Consequently, the isolation of alkynyl sulfide **7.3** had not been accomplished previously (99 % NMR yield). As such, benzylic thiol **7.1** and bromoalkyne **7.2** were submitted once again to the optimal reaction conditions. Following chromatography, alkynyl sulfide **7.3** was finally isolated in 90 % yield (Scheme 7.11). Next, cyclohexanethiol was treated with bromoalkyne **7.2** to the copper-catalyzed system to provide alkynyl sulfide **7.32** in 82 % yield. In addition, when the methodology was applied between triphenylmethanethiol and bromoalkyne **7.2**, alkynyl sulfide **7.33** was generated in 80 % yield. The preceding result was noteworthy as tertiary thiols did not take part in C(sp)-S coupling in the photochemical conditions described in Chapter 6.



**Scheme 7.11** Preliminary scope of thiols

## 7.4 Plausible Mechanisms for Cu-Catalyzed C-S Cross-Couplings

Copper catalysis has been utilized since the early 1900s toward the formation of C-X (X = N, O, and S) bonds. Ullmann-type couplings leading to C-N and C-O bonds have been widely studied, but have not been fully understood.<sup>9</sup> Conversely, less effort has been made for corresponding C-S bond-forming reactions. Copper-catalyzed cross-couplings are thought to proceed via one of four accepted mechanistic pathways, namely oxidative addition/reductive elimination (OA/RE), halogen atom transfer (HAT), single electron transfer (SET), and  $\sigma$ -bond metathesis (MET) (Figure 7.2).<sup>9</sup> Mechanisms like halogen atom transfer or single electron transfer are based on one-electron redox processes, which typically involve the redox couple Cu(I)/Cu(II) and radical intermediates. Two-electron redox processes like oxidative addition/reductive elimination generally involve a Cu(I)/Cu(III) catalytic cycle. Metathesis mechanisms in which the copper species remain in their Cu(I) oxidation state involve the formation of four-membered cyclic transition states.

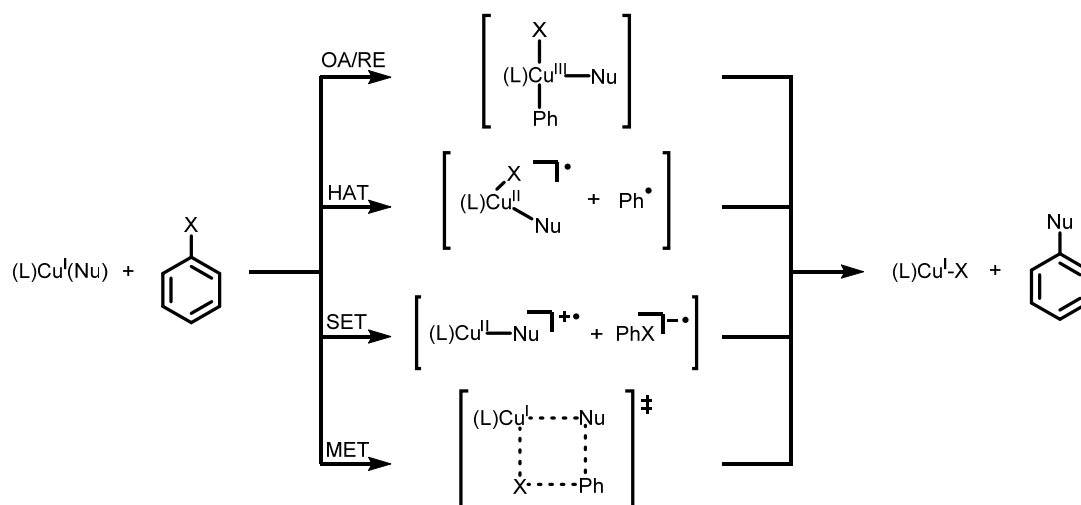


**Figure 7.2** Possible mechanistic pathways for copper-catalyzed Ullmann-type reactions

### 7.4.1 C(sp<sup>2</sup>)-S Bonds: Ullmann-Type Arylations

The mechanisms of copper-catalyzed S-arylations have mostly been studied through computational methods.<sup>16</sup> The typical model system involves thiophenol (**7.34**) and iodobenzene (**7.35**) in the presence of CuI as catalyst, phenanthroline or 2,2'-bipyridine as ligand, and various bases and solvents (Figure 7.3).

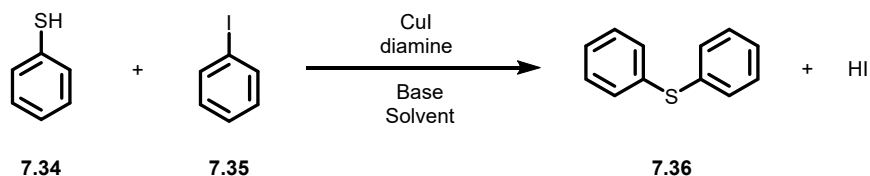


**Figure 7.3** General model system for copper-catalyzed C-S arylation studies

Despite the uncertainty surrounding the distinct aryl halide activation pathways, a consensus has been reached that the active catalyst involved in the catalytic cycle should be a Cu(I) species.<sup>16-17</sup> The starting point for all mechanisms would be the formation of complex **7.37** once CuI is added into a solution containing a strongly binding ancillary ligand such as phenanthroline or 2,2'-bipyridine (Figure 7.4). Complex **7.38** would be a diamine-ligated Cu(I)-thiophenolato intermediate, which would be generated between complex **7.37** and thiophenol **7.34** in the presence of a base. Complex **7.38** would be thermodynamically favored over complex **7.37** according to calculations.<sup>16a, 16c</sup> An equilibrium between neutral complex **7.38** and

its ionic forms **7.39** and **7.40** following disproportionation has also been observed computationally<sup>16a</sup> and experimentally.<sup>17</sup> Interestingly, the disproportionation event was found to be unfavorable in nonpolar solvents, while it becomes favored when the dielectric constant of the solvent increases.

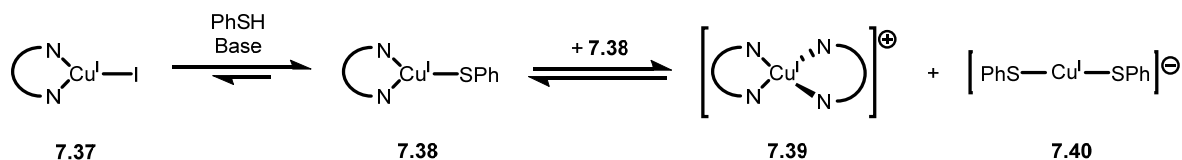


**Figure 7.4** Equilibriums of possible copper species in solution

Next, proposed mechanisms for the copper-catalyzed C-S arylation reaction, such as oxidative addition, halogen atom transfer, single electron transfer, and  $\sigma$ -bond metathesis, were computationally investigated between iodobenzene **7.35** and either complex **7.38** or complex **7.40**. It was found in all cases that single electron transfer and  $\sigma$ -bond metathesis mechanistic pathways possessed high activation barriers, rendering them kinetically unfavorable.<sup>16</sup> Depending of the operated calculation method, the alternative oxidative addition<sup>16b-d</sup> and halogen atom transfer<sup>16a</sup> aryl halide activation pathways were found to be consistently more favorable as they both possessed lower activation barriers.

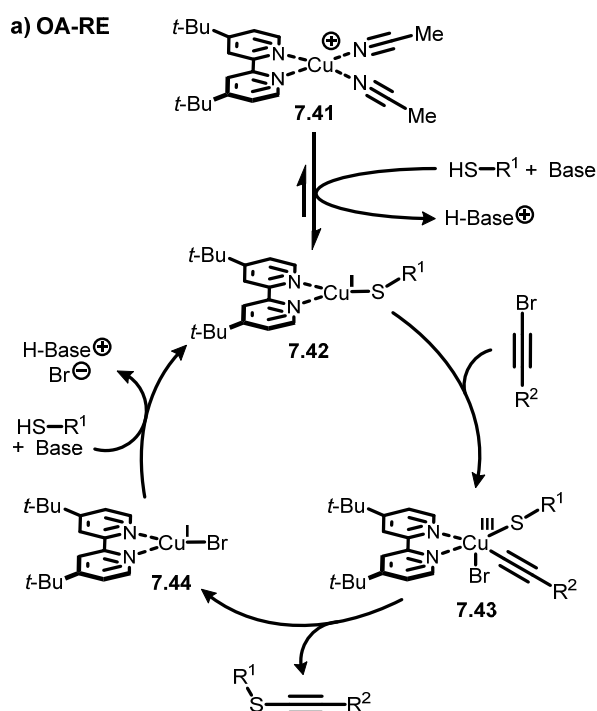
## 7.4.2 C(sp)-S Bonds

While the aforementioned computational studies on the copper-catalyzed reactions only involved the arylation of thiols, similar oxidative addition and halogen atom transfer mechanisms could be implied for the alkynylation of thiols. When considering either oxidative addition/reductive elimination or halogen atom transfer mechanisms for the copper-catalyzed thiol alkynylation, the initial steps leading to the formation of complex **7.41** would be the same (Figure 7.5). As such, dtbbpy-ligated Cu(I) intermediate **7.42** would be generated between complex **7.41** and a thiol in the presence of base.

In the case of an oxidative addition/reductive elimination mechanistic pathway, Cu(I) complex **7.42** would then undergo an oxidative addition into the bromoalkyne's carbon-halogen bond to generate penta-coordinated Cu(III) intermediate **7.43** (Figure 7.5a). Lastly, reductive

elimination of intermediate **7.43** would provide the desired alkynyl sulfide and regenerate active Cu(I) catalyst **7.42** in the presence of a thiol and a base.

In the case of a halogen atom transfer mechanistic pathway, a bromoalkyne would transfer its bromine atom to Cu(I) complex **7.42**, which would lead to the formation of Cu(II) complex **7.45** and alkynyl radical **7.46** (Figure 7.5b). The resulting alkynyl radical can either directly attack the sulfur atom of complex **7.45** to form the alkynyl sulfide or recombine with the generated Cu(II) complex **7.45** to form Cu(III) intermediate **7.43**. Reductive elimination of intermediate **7.43** would then provide the alkynyl sulfide and regenerate active Cu(I) catalyst **7.42** in the presence of a thiol and a base. To be noted, we do not have any experimental or computational evidence to favor either mechanism at this time.



b) HAT

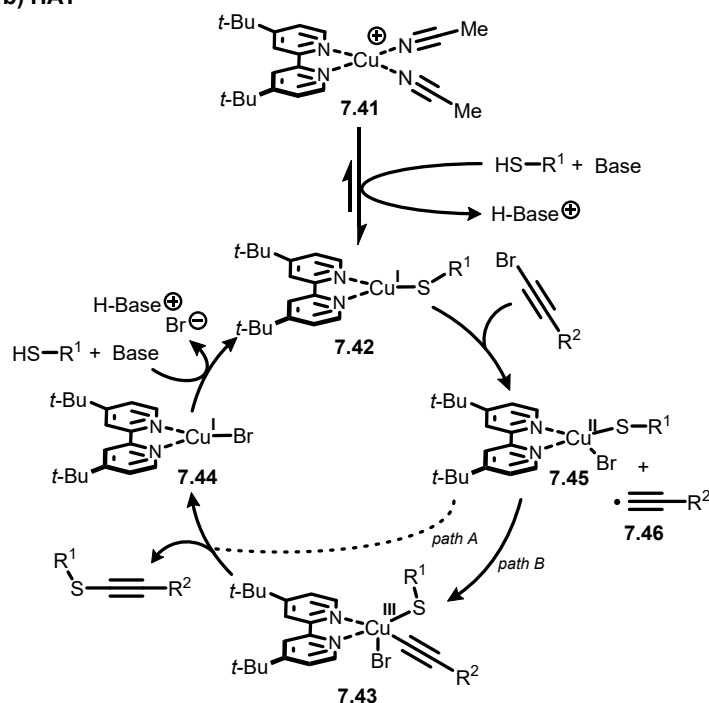


**Figure 7.5** Proposed mechanism for copper-catalyzed S-alkynylation

## 7.5 Conclusions

The work summarized in Chapter 7 was dedicated to developing a method that would enable the coupling of thiols with aryl- and alkyl-substituted bromoalkynes, as the photoredox/nickel dual-catalytic conditions developed in Chapter 6 did not allow the coupling of thiols with alkyl-substituted bromoalkynes. It was initially thought that performing the photochemical reaction in the presence of a ligand would vary the electronic properties of the nickel complex for it to engage in oxidative addition with less activated alkyl-substituted haloalkynes, but the approach did not succeed. Afterwards, a breakthrough was made when replacing the nickel-based catalyst by a copper-based catalyst. As control experiments determined that the copper-catalyzed C-S coupling was not photochemical, the screening of reaction parameters ensued. A thorough screening process eventually led to improved reaction conditions which enabled high yields of alkynyl sulfides from corresponding thiols and aryl/alkyl bromoalkynes. The  $\text{Cu}(\text{MeCN})_4\text{PF}_6/\text{dtbbpy}/2,6\text{-lutidine}$  catalyst system is performed at room temperature under ten minutes, and unlike previously reported copper-catalyzed

couplings, is operationally simple. Importantly, the new catalyst system is compatible with aryl-, alkyl-, silyl-, and heteroatom-substituted bromoalkynes. In addition, the copper-catalyzed coupling was successfully applied toward the synthesis of an alkynyl sulfide on a 5 mmol scale, thus demonstrating reproducibility from small to large scale. While no mechanistic investigations were pursued, it can be imagined, based on computational studies provided for copper-catalyzed S-arylations, that the copper-catalyzed S-alkynylation protocol also proceeds either via oxidative addition/reductive elimination or halogen atom transfer pathways.

## 7.7 Bibliography

1. Santandrea, J.; Minozzi, C.; Cruché, C.; Collins, S. K. *Angew. Chem. Int. Ed.* **2017**, *56*, 12255-12259.
2. (a) Gong, T. J.; Yu, S. H.; Li, K.; Su, W.; Lu, X.; Xiao, B.; Fu, Y. *Chem. Asian J.* **2017**, *12*, 2884-2888; (b) Cornelissen, L.; Lefrancq, M.; Riant, O. *Org. Lett.* **2014**, *16*, 3024-3027; (c) Zhang, Y.; Hsung, R. P.; Tracey, M. R.; Kurtz, K. C.; Vera, E. L. *Org. Lett.* **2004**, *6*, 1151-1154.
3. Sujatha, A.; Thomas, A. M.; Thankachan, A. P.; Anilkumar, G. *Arkivoc* **2015**, *1*, 1-28.
4. (a) Liu, B.; Lim, C.-H.; Miyake, G. M. *J. Am. Chem. Soc.* **2017**, *139*, 13616-13619; (b) Bottecchia, C.; Rubens, M.; Gunnoo, S. B.; Hessel, V.; Maddar, A.; Noël, T. *Angew. Chem. Int. Ed.* **2017**, *56*, 12702-12707; (c) Oderinde, M. S.; Frenette, M.; Robbins, D. W.; Aquila, B.; Johannes, J. W. *J. Am. Chem. Soc.* **2016**, *138*, 1760-1763.
5. (a) Kondo, T.; Mitsudo, T.-a. *Chem. Rev.* **2000**, *100*, 3205-3220; (b) Dunbar, K. L.; Scharf, D. H.; Litomska, A.; Hertweck, C. *Chem. Rev.* **2017**, *117*, 5521-5577; (c) Wimmer, A.; König, B. *Beilstein J. Org. Chem.* **2018**, *14*, 54-83; (d) Minghao, F.; Bingqing, T.; Steven, H. L.; Xuefeng, J. *Curr. Top. Med. Chem.* **2016**, *16*, 1200-1216.
6. Bates, C. G.; Gujadhur, R. K.; Venkataraman, D. *Org. Lett.* **2002**, *4*, 2803-2806.
7. Xu, H.-J.; Zhao, Y.-Q.; Feng, T.; Feng, Y.-S. *J. Org. Chem.* **2012**, *77*, 2878-2884.
8. Li, Y.; Pu, J.; Jiang, X. *Org. Lett.* **2014**, *16*, 2692-2695.
9. Sambiagio, C.; Marsden, S. P.; Blacker, A. J.; McGowan, P. C. *Chem. Soc. Rev.* **2014**, *43*, 3525-3550.
10. Bates, C. G.; Saejueng, P.; Doherty, M. Q.; Venkataraman, D. *Org. Lett.* **2004**, *6*, 5005-5008.
11. (a) Yang, Y.; Dong, W.; Guo, Y.; Rioux, R. M. *Green Chem.* **2013**, *15*, 3170-3175; (b) Fang, Z.; He, W.; Cai, M.; Lin, Y.; Zhao, H. *Tetrahedron Lett.* **2015**, *56*, 6463-6467.
12. (a) Mohan, B.; Hwang, S.; Woo, H.; Park, K. H. *Synthesis* **2015**, *47*, 3741-3745; (b) Bieber, L. W.; da Silva, M. F.; Menezes, P. H. *Tetrahedron Lett.* **2004**, *45*, 2735-2737.
13. (a) Liu, F.; Yi, W. *Org. Chem. Front.* **2018**, *5*, 428-433; (b) Braga, A. L.; Reckziegel, A.; Menezes, P. H.; Stefani, H. A. *Tetrahedron Lett.* **1993**, *34*, 393-394.
14. (a) Minozzi, C.; Caron, A.; Grenier-Petel, J.-C.; Santandrea, J.; Collins, S. K. *Angew. Chem. Int. Ed.* **2018**, *57*, 5477-5481; (b) Walesa-Chorab, M.; Banasz, R.; Marcinkowski, D.; Kubicki, M.; Patroniak, V. *RSC Adv.* **2017**, *7*, 50858-50867; (c) Williams, R. M.; Cola, L.



- D.; Hartl, F.; Lagref, J.-J.; Planeix, J.-M.; Cian, A. D.; Hosseini, M. W. *Coord. Chem. Rev.* **2002**, *230*, 253-261.
15. (a) Baganz, H.; Triebsch, W. *Chem. Ber.* **1956**, *89*, 895-898; (b) Stang, P. J.; Zhdankin, V. V. *J. Am. Chem. Soc.* **1990**, *112*, 6437-6438; (c) Stang, P. J.; Zhdankin, V. V. *J. Am. Chem. Soc.* **1991**, *113*, 4571-4576.
  16. (a) Zhang, S.-L.; Fan, H.-J. *Organometallics* **2013**, *32*, 4944-4951; (b) Weng, Z.; He, W.; Chen, C.; Lee, R.; Tan, D.; Lai, Z.; Kong, D.; Yuan, Y.; Huang, K. W. *Angew. Chem. Int. Ed.* **2013**, *52*, 1548-1552; (c) Andrada, D.; Soria-Castro, S.; Caminos, D.; Argüello, J.; Peñéñory, A. *Catalysts* **2017**, *7*, 388; (d) Soria-Castro, S. M.; Andrada, D. M.; Caminos, D. A.; Argüello, J. E.; Robert, M.; Peñéñory, A. B. *J. Org. Chem.* **2017**, *82*, 11464-11473.
  17. (a) Chen, C.; Weng, Z.; Hartwig, J. F. *Organometallics* **2012**, *31*, 8031-8037; (b) Cheng, S.-W.; Tseng, M.-C.; Lii, K.-H.; Lee, C.-R.; Shyu, S.-G. *Chem. Commun.* **2011**, *47*, 5599-5601.

## 8. Conclusions and Perspectives

The present thesis has described the development of novel carbon- (Chapter 3) and sulfur-based (Chapters 6 and 7) alkynylation methodologies through copper and nickel catalysis.

### 8.1 Cu-Catalyzed Macrocyclic Sonogashira-Type Cross-Coupling

#### 8.1.1 Summary

The work presented in Chapter 3 demonstrated that copper catalysis can be employed for the formation of macrocycles from conformationally unbiased linear precursors.<sup>1</sup> The macrocyclic Sonogashira-type cross-coupling exploited a CuCl/phen/Cs<sub>2</sub>CO<sub>3</sub> catalytic system to generate 17 macrocycles with various ring sizes (10- to 25-membered rings) and functional groups in yields ranging between 38-83 %. Also, the method could be performed at relatively high concentrations (24 mM) without the need for slow addition techniques. The optimized reaction conditions were additionally applied toward the synthesis of (*S*)-zearalane, where traditional Sonogashira Pd/Cu co-catalyzed conditions were found to be ineffective for the key ring-closing step.

#### 8.1.2 Future Work

Other more challenging resorcylic acid lactones, constrained cyclic peptides, or shape-persistent macrocycles (Chapters 1 and 2) would be interesting synthetic targets on which to experiment our developed methodology. Additionally, applying our developed copper catalyst system toward the alkynylation of sp<sup>3</sup>-based electrophiles would introduce new synthetic opportunities. The use of electron-deficient radical precursors, such as bromomalonates, and copper acetylides might provide electronically matched coupling partners, as they both can readily participate in single-electron transfer processes. As such, it would be reasonable to assume that copper-catalyzed thermal redox, which might be occurring in Chapter 3, could be extended to other electrophiles.<sup>2</sup> For example, utilizing various substituted  $\alpha$ -bromocarbonyls (**8.1**) in the presence of a terminal alkyne (**8.2**) under copper catalysis would lead to the formation of tertiary or quaternary carbon centers (**8.3**) (Figure 8.1). If the transformation was

possible, the use of copper complexes bearing chiral ligands could be further applied as a means to generate chiral centers with high enantioselectivity.

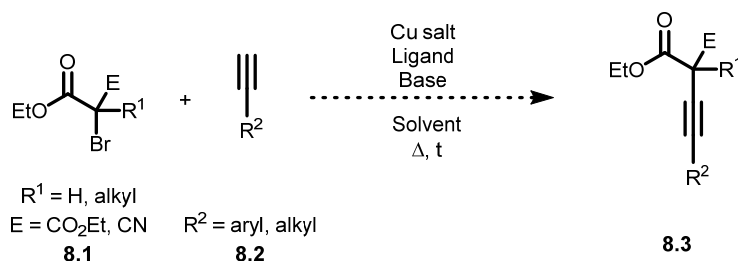


**Figure 8.1** Proposed copper-catalyzed alkynylation of  $\alpha$ -bromocarbonyls

## 8.2 Photoredox/Ni Dual-Catalyzed Synthesis of Alkynyl Sulfides

### 8.2.1 Summary

The work presented in Chapter 6 demonstrated that photoredox and nickel dual catalysis could be employed to generate aryl- and heteroaryl-substituted alkynyl sulfides.<sup>3</sup> The protocol is complementary to previously reported methods as it readily gives access to a distinct class of alkynyl sulfides from easy-to-access starting materials. The C(sp)-S bond-forming coupling was achieved between thiols and aromatic bromoalkynes using a 4CzIPN/NiCl<sub>2</sub>•glyme/pyridine catalytic system under visible-light irradiation at room temperature. As a result, 25 alkynyl sulfides, bearing a wide range of electronically and sterically diverse aromatic alkynes and thiols, were obtained in good to excellent yields (50-96 %). To shorten reaction times, the photochemical reactions were performed in continuous flow conditions using an in-house designed visible-light photoreactor. The reproducibility of the method was also demonstrated from small to large scale, thus illustrating the practicality of continuous flow techniques for photochemical transformations (Chapter 4). Additionally, the versatility of alkynyl sulfides as building blocks (Chapter 5) was further demonstrated by performing several diversification reactions such as a hydration, a reduction, oxidations, and cycloadditions. Our continuous flow methodology was also applied toward the synthesis of a macrocycle. Macrocyclizations are rarely performed in photochemical conditions because of inefficient light penetration into dilute media. It was thought that performing a photochemically-mediated macrocyclization reaction in continuous flow would bypass the photon flux limitation typically experienced in batch. As

a result, a macrocyclic alkynyl sulfide was synthesized using the photochemical dual-catalytic procedure, which represented, to the best of our knowledge, the first example of a macrocyclization exploiting photoredox/nickel dual-catalysis.

### 8.2.2 Future Work

While the methodology presented limitations with regards to alkyl- and silyl-substituted bromoalkynes, further endeavors exploiting our 4CzIPN/ $\text{NiCl}_2\cdot\text{glyme}$ /pyridine photocatalytic system could include the synthesis of other heteroatom-substituted alkynes. Oderinde and Johannes recently reported that anilines could participate with aryl halides in a photoredox-nickel dual-catalytic process via aniline radical intermediates.<sup>4</sup> If such intermediates could be photochemically generated from an analogous 4CzIPN/ $\text{NiCl}_2\cdot\text{glyme}$ /pyridine system in the presence of haloalkynes, it would lead to the formation of aryl-substituted ynamines (Figure 8.2).

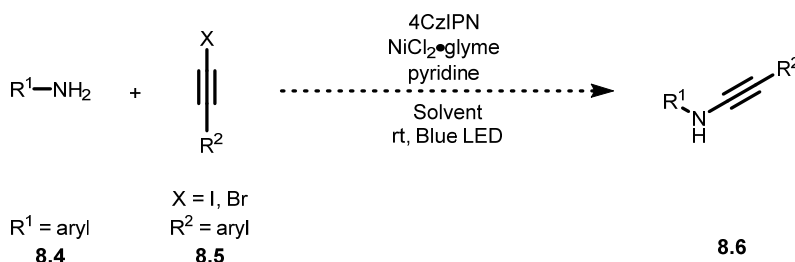


**Figure 8.2** Proposed photoredox/Ni dual-catalytic synthesis of ynamides

It would also be interesting to apply our photochemical C(sp)-S coupling in tandem photochemical-thermal reactions using continuous flow chemistry. As continuous flow systems are modular,<sup>5</sup> our designed photochemical reactor could be readily connected in series with a variety of thermal reactors.<sup>6</sup> For example, a multistep flow synthesis of thio-adducts would be achieved from a consecutive photochemical C(sp)-S coupling and cycloaddition reaction.

## 8.3 Cu-Catalyzed Synthesis of Alkynyl Sulfides

### 8.3.1 Summary

The work presented in Chapter 7 demonstrated that copper catalysis could be employed to generate aryl-, alkyl-, silyl-, and heteroatom-substituted alkynyl sulfides. As such, the copper-

catalyzed protocol solves some shortcomings from the work in Chapter 6, such as using alkyl- and silyl-substituted bromoalkynes, and tertiary thiol coupling partners. Thus, the improved  $\text{Cu}(\text{MeCN})_4\text{PF}_6/\text{dtbbpy}/2,6\text{-lutidine}$  catalyst system establishes itself as the first general and efficient method to access all classes of alkynyl sulfides from readily accessible thiols and bromoalkynes. Initial reaction development determined that the copper-catalyzed  $\text{C}(\text{sp})\text{-S}$  coupling was not photochemical and could be performed at room temperature. Pursuing a screening of reaction parameters additionally led to improved conditions which gave access to alkynyl sulfides in high yields under ten minutes. The method was also found to be reproducible from small to large scale. A preliminary substrate scope illustrated that the improved protocol could generate aryl-substituted alkynyl sulfides bearing nitro and benzylic amine functional groups from their corresponding bromoalkyne. Such bromoalkynes were found to be incompatible in the photochemical conditions described in Chapter 6. In addition, five alkyl-substituted alkynyl sulfides, bearing functional groups such as protected hydroxy groups, nitriles and phthalimides, were successfully synthesized in good yield. Furthermore, the methodology efficiently led to a TIPS-substituted alkynyl sulfide and a bis(thio-substituted)alkyne in excellent yield. Lastly, the copper-catalyzed protocol was tolerant of primary, secondary and tertiary thiols.

### 8.3.2 Future Work

Certain aspects of the work presented in Chapter 7 are unfinished. The substrate scope needs to be further explored to properly assess the copper-catalyzed  $\text{C-S}$  coupling's limitations. For instance, aryl- and alkyl-substituted bromoalkynes bearing sensitive and/or sterically hindered functional groups may be considered. In addition, coupling thiols with various heteroatom-substituted bromoalkynes can lead to an underexplored class of compounds.

Macrocyclization applications involving the copper-catalyzed  $\text{C-S}$  coupling would also further develop an uncommon class of compounds. The photocatalyzed formation of thioalkyne-containing macrocycles (Chapter 6) was not ideal, as precursors bearing an aryl bromoalkyne were required. The preparation of such macrocyclic precursors was tedious and limited the structural scope of macrocyclic alkynyl sulfides. Therefore, it would be interesting to explore the macrocyclization using alkyl bromoalkynes, as they would expand the scope of precursors

from readily accessible alkyl alkynes. For instance, simple structures containing a cysteine could be initially made to evaluate the feasibility of our copper-catalyzed C-S coupling in a macrocyclization context (Figure 8.3). Macrocyclic alkynyl sulfides could additionally be useful for the diversity-oriented synthesis (DOS) of macrocycles,<sup>7</sup> as the thioalkyne moiety can serve as a point of diversification (Chapter 5) following ring-closure.

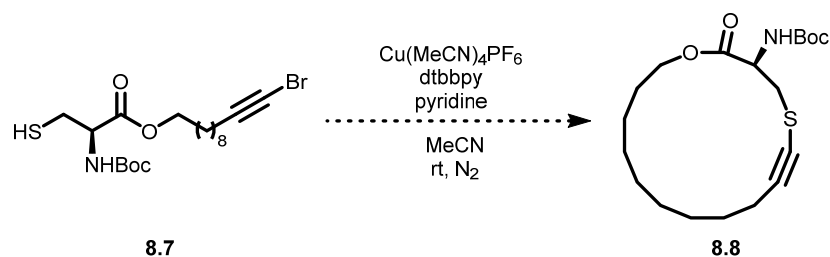


**Figure 8.3** Proposed synthesis of a macrocyclic alkynyl sulfide

In addition, it would be interesting to test the biocompatibility of the C(sp)-S coupling given the wide tolerance of the reaction conditions to different polar solvents. Pentelute and Buchwald have recently demonstrated that selective cross-linking of peptides and proteins from natural amino acid residues was possible using palladium oxidative addition complexes (Figure 8.4).<sup>8</sup> Although the palladium-mediated arylation of cysteine residues is stoichiometric in nature, it produces highly stable linkers which exhibit minimal hydrolysis side reactions. It could be useful to develop an analogous cross-linking strategy from suitably functionalized bromoalkynes using our developed copper-catalyzed C-S coupling as alkynyl sulfides are also resistant to hydrolysis. Another potential application of alkynyl sulfides could involve selective tagging of cysteine residues in peptides.<sup>9</sup>

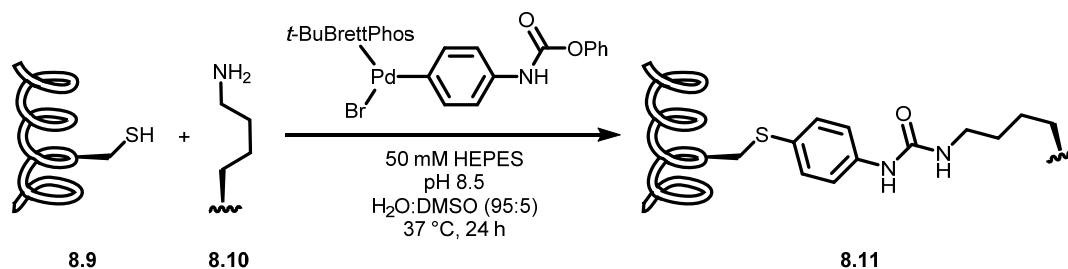


**Figure 8.4** Palladium-mediated peptide and protein cross-linking

## 8.4 Bibliography

1. Santandrea, J.; Bédard, A.-C.; Collins, S. K. *Org. Lett.* **2014**, *16*, 3892-3895.
2. (a) Pan, G. H.; Ouyang, X. H.; Hu, M.; Xie, Y. X.; Li, J. H. *Adv. Synth. Catal.* **2017**, *359*, 2564-2570; (b) Gietter, A. A. S.; Gildner, P. G.; Cinderella, A. P.; Watson, D. A. *Org. Lett.* **2014**, *16*, 3166-3169.
3. Santandrea, J.; Minozzi, C.; Cruché, C.; Collins, S. K. *Angew. Chem. Int. Ed.* **2017**, *56*, 12255-12259.
4. Oderinde, M. S.; Jones, N. H.; Juneau, A.; Frenette, M.; Aquila, B.; Tentarelli, S.; Robbins, D. W.; Johannes, J. W. *Angew. Chem. Int. Ed.* **2016**, *55*, 13219-13223.
5. (a) Britton, J.; Raston, C. L. *Chem. Soc. Rev.* **2017**, *46*, 1250-1271; (b) Adamo, A.; Beingessner, R. L.; Behnam, M.; Chen, J.; Jamison, T. F.; Jensen, K. F.; Monbaliu, J.-C. M.; Myerson, A. S.; Revalor, E. M.; Snead, D. R.; Stelzer, T.; Weeranoppanant, N.; Wong, S. Y.; Zhang, P. *Science* **2016**, *352*, 61-67; (c) Webb, D.; Jamison, T. F. *Chem. Sci.* **2010**, *1*, 675-680.
6. Josland, S.; Mumtaz, S.; Oelgemöller, M. *Chem. Eng. Technol.* **2016**, *39*, 81-87.
7. (a) Guarnieri-Ibanez, A.; Medina, F.; Besnard, C.; Kidd, S. L.; Spring, D. R.; Lacour, J. *Chem. Sci.* **2017**, *8*, 5713-5720; (b) Nie, F.; Kunciw, D. L.; Wilcke, D.; Stokes, J. E.; Galloway, W. R. J. D.; Bartlett, S.; Sore, H. F.; Spring, D. R. *Angew. Chem. Int. Ed.* **2016**, *55*, 11139-11143; (c) Beckmann, H. S. G.; Nie, F.; Hagerman, C. E.; Johansson, H.; Tan, Y. S.; Wilcke, D.; Spring, D. R. *Nat. Chem.* **2013**, *5*, 861; (d) Kopp, F.; Stratton, C. F.; Akella, L. B.; Tan, D. S. *Nat. Chem. Biol.* **2012**, *8*, 358.
8. Kubota, K.; Dai, P.; Pentelute, B. L.; Buchwald, S. L. *J. Am. Chem. Soc.* **2018**, *140*, 3128-3133.
9. (a) Al-Shuaeeb, R. A. A.; Kolodych, S.; Koniev, O.; Delacroix, S.; Erb, S.; Nicolaÿ, S.; Cintrat, J. C.; Brion, J. D.; Cianféroni, S.; Alami, M.; Wagner, A.; Messaoudi, S. *Chem. Eur. J.* **2016**, *22*, 11365-11370; (b) deGruyter, J. N.; Malins, L. R.; Baran, P. S. *Biochemistry* **2017**, *56*, 3863-3873; (c) Embaby, A. M.; Schoffelen, S.; Kofoed, C.; Meldal, M.; Diness, F. *Angew. Chem. Int. Ed.* **2018**, *57*, 8022-8026; (d) Koniev, O.; Leriche, G.; Nothisen, M.; Remy, J.-S.; Strub, J.-M.; Schaeffer-Reiss, C.; Van Dorsselaer, A.; Baati, R.; Wagner, A. *Bioconjugate Chem.* **2014**, *25*, 202-206.

## 9. Supporting Information of Chapter 3

### 9.1 General

Reactions carried out under anhydrous conditions were performed under an inert argon or nitrogen atmosphere in glassware that had previously been dried overnight at 120 °C or flame dried and cooled under a stream of argon or nitrogen.<sup>1</sup> All chemical products were obtained from Sigma-Aldrich Chemical Company or Alfa Aesar, and were reagent quality. The following products were prepared according to their respective literature procedures: hex-5-yn-1-ol<sup>2</sup>, non-8-yn-1-ol<sup>2</sup>, undec-10-yn-1-ol<sup>2</sup>, tridec-12-yn-1-ol<sup>3</sup>, nonadec-18-yn-1-ol<sup>3</sup>, heneicos-20-yn-1-ol<sup>3</sup>, 3-iodo-2-naphthoic acid<sup>4</sup>, 2-iodo-3-hydroxypyridine<sup>5</sup>, (*Z*)-3-iodo-propenoic acid<sup>6</sup> and 2-iodo-4,6-dimethoxybenzoic acid.<sup>7</sup> Technical solvents were obtained from VWR International Co. Anhydrous solvents (CH<sub>2</sub>Cl<sub>2</sub>, Et<sub>2</sub>O, THF, DMF, toluene, and *n*-hexane) were dried and deoxygenated using a GlassContour system (Irvine, CA). Isolated yields reflect the mass obtained following flash column silica gel chromatography. Organic compounds were purified using the method reported by W. C. Still<sup>8</sup> on silica gel obtained from Silicycle Chemical division (40-63 nm; 230-240 mesh). Analytical thin-layer chromatography (TLC) was performed on glass-backed silica gel 60 plates coated with a fluorescence indicator (Silicycle Chemical division, 0.25 mm, F<sub>254</sub>). Visualization of TLC plates was performed by UV (254 nm), KMnO<sub>4</sub> or *p*-anisaldehyde stains. All mixed solvent eluents are reported as v/v solutions. Concentration refers to removal of volatiles at low pressure on a rotary evaporator. All reported compounds were homogeneous by thin layer chromatography (TLC) and by <sup>1</sup>H NMR spectroscopy. NMR spectra were taken in deuterated CDCl<sub>3</sub> using Bruker AV-300 and AV-400 instruments unless otherwise noted. Signals of solvent served as internal standard (CHCl<sub>3</sub>: δ 7.27 for <sup>1</sup>H, δ 77.0 for <sup>13</sup>C). The acquisition parameters are shown on all spectra. The <sup>1</sup>H NMR chemical shifts and

---

<sup>1</sup> Shriver, D. F.; Drezdon, M. A. in *The Manipulation of Air-Sensitive Compounds*; Wiley-VCH: New York, 1986.

<sup>2</sup> Bédard, A.-C.; Collins, S. K. *J. Am. Chem. Soc.* **2011**, *133*, 19976.

<sup>3</sup> Lumbroso, A.; Abermil, N.; Breit, B. *Chem. Sci.* **2012**, *3*, 789.

<sup>4</sup> Uyanik, M.; Akakura, M.; Ishihara, K. *J. Am. Chem. Soc.* **2009**, *131*, 251.

<sup>5</sup> Loidreau, Y.; Marchand, P.; Dubouilh-Benard, C.; Nourrisson, M.-R.; Duflos, M.; Besson, T. *Tetrahedron Lett.* **2012**, *53*, 944.

<sup>6</sup> Suh, Y.-G.; Jung, J.-K.; Seo, S.-Y.; Min, K.-H.; Shin, D.-Y.; Lee, Y.-S.; Kim, S.-H.; Park, H.-J. *J. Org. Chem.* **2002**, *67*, 4127.

<sup>7</sup> Mikula, H.; Skrinjar, P.; Sohr, B.; Ellmer, D.; Hametner, C.; Fröhlich, J. *Tetrahedron* **2013**, *69*, 10322.

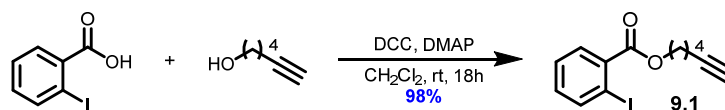
<sup>8</sup> Still, W. C.; Kahn, M.; Mitra, A. *J. Org. Chem.* **1978**, *43*, 2923.



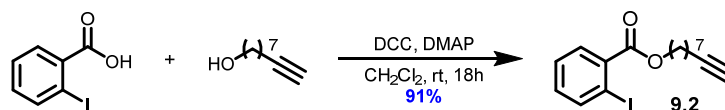
coupling constants were determined assuming first-order behavior. Multiplicity is indicated by one or more of the following: s (singlet), d (doublet), t (triplet), q (quartet), m (multiplet), br (broad); the list of couplings constants ( $J$ ) corresponds to the order of the multiplicity assignment. High resolution mass spectrometry (HRMS) was done by the Centre régional de spectrométrie de masse at the Département de Chimie, Université de Montréal on an Agilent LC-MSD TOF system using ESI mode of ionization unless otherwise noted.

## 9.2 Synthesis of Macrocyclization Precursors

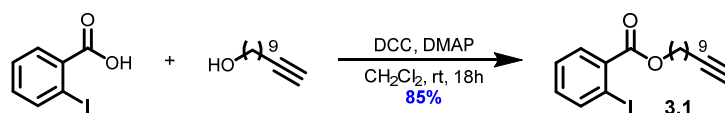
**Steglich Esterification Procedure A:** To a stirred solution of the alcohol (1 equiv.) and the carboxylic acid (1.5 equiv.) in dry dichloromethane (0.1 M), *N,N'*-dicyclohexylcarbodiimide (DCC, 2 equiv.) and 4-methylaminopyridine (DMAP, 3 equiv.) were added at room temperature. The reaction mixture was stirred at room temperature for 18 hours. Upon complete conversion of the starting material, the crude reaction mixture was placed in a freezer for 5 hours to induce the precipitation of the urea, which was subsequently removed by filtration. The filtrate was concentrated under vacuum to provide a residue which was purified by column chromatography on silica-gel to afford the desired product.



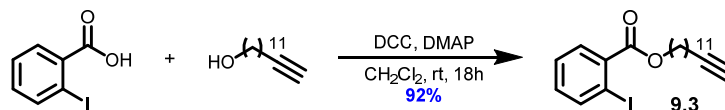
**Hex-5-yn-1-yl 2-iodobenzoate (9.1):** Following Procedure A, hex-5-yn-1-ol (0.089 g, 0.907 mmol, 1.0 equiv.), 2-iodobenzoic acid (0.337 g, 1.36 mmol, 1.5 equiv.), DCC (0.374 g, 1.81 mmol, 2.0 equiv.) and DMAP (0.332 g, 2.72 mmol, 3.0 equiv.) were dissolved in anhydrous dichloromethane (10 mL) in a round bottom flask equipped with a stir bar. After purification by column chromatography (100 % hexanes → 10 % diethyl ether in hexanes), iodide **9.1** was obtained as a colorless oil (0.292 g, 98 % yield). <sup>1</sup>H NMR (400 MHz, CDCl<sub>3</sub>) δ = 8.00 (dd, *J* = 8.0, 1.1 Hz, 1H), 7.80 (dd, *J* = 7.8, 1.7 Hz, 1H), 7.41 (td, *J* = 7.6, 1.2 Hz, 1H), 7.16 (td, *J* = 7.7, 1.7 Hz, 1H), 4.38 (t, *J* = 6.4 Hz, 2H), 2.29 (td, *J* = 7.0, 2.6 Hz, 2H), 1.98 (t, *J* = 2.7 Hz, 1H), 1.89 - 1.97 (m, 2H), 1.68 - 1.77 (m, 2H); <sup>13</sup>C NMR (100 MHz, CDCl<sub>3</sub>) δ = 166.6, 141.3, 135.4, 132.6, 130.1, 127.9, 94.0, 83.8, 68.8, 65.1, 27.6, 25.0, 18.1; HRMS (ESI) *m/z* calculated for C<sub>13</sub>H<sub>14</sub>IO<sub>2</sub> [M+H]<sup>+</sup> 350.9852; found 350.9863.



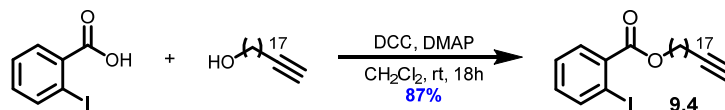
**Non-8-yn-1-yl 2-iodobenzoate (9.2):** Following Procedure A, non-8-yn-1-ol (0.116 g, 0.827 mmol, 1.0 equiv.), 2-iodobenzoic acid (0.308 g, 1.24 mmol, 1.5 equiv.), DCC (0.341 g, 1.66 mmol, 2.0 equiv.) and DMAP (0.303 g, 2.48 mmol, 3.0 equiv.) were dissolved in anhydrous dichloromethane (8 mL) in a round bottom flask equipped with a stir bar. After purification by column chromatography (100 % hexanes → 10 % diethyl ether in hexanes), iodide **9.2** was obtained as a colorless oil (0.278 g, 91 % yield).  $^1\text{H}$  NMR (400 MHz,  $\text{CDCl}_3$ )  $\delta$  = 8.00 (dd,  $J$  = 8.0, 0.8 Hz, 1H), 7.79 (dd,  $J$  = 7.9, 1.5 Hz, 1H), 7.41 (td,  $J$  = 7.6, 1.1 Hz, 1H), 7.16 (td,  $J$  = 7.7, 1.7 Hz, 1H), 4.34 (t,  $J$  = 6.7 Hz, 2H), 2.20 (td,  $J$  = 7.0, 2.7 Hz, 2H), 1.95 (t,  $J$  = 2.7 Hz, 1H), 1.75 - 1.84 (m, 2H), 1.51 - 1.60 (m, 2H), 1.35 - 1.50 (m, 6H);  $^{13}\text{C}$  NMR (75 MHz,  $\text{CDCl}_3$ )  $\delta$  = 166.7, 141.2, 135.6, 132.5, 130.8, 127.9, 93.9, 84.6, 68.2, 65.8, 28.7, 28.6, 28.5, 28.3, 25.9, 18.3; HRMS (ESI)  $m/z$  calculated for  $\text{C}_{16}\text{H}_{20}\text{IO}_2$   $[\text{M}+\text{H}]^+$  371.0503; found 371.0510.



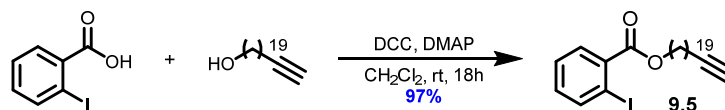
**Undec-10-yn-1-yl 2-iodobenzoate (3.1):** Following Procedure A, undec-10-yn-1-ol (1.00 g, 5.94 mmol, 1.0 equiv.), 2-iodobenzoic acid (2.21 g, 8.91 mmol, 1.5 equiv.), DCC (2.45 g, 11.9 mmol, 2.0 equiv.) and DMAP (2.18 g, 17.8 mmol, 3.0 equiv.) were dissolved in anhydrous dichloromethane (60 mL) in a round bottom flask equipped with a stir bar. After purification by column chromatography (100 % hexanes → 10 % diethyl ether in hexanes), iodide **3.1** was obtained as a colorless oil (2.03 g, 85 % yield).  $^1\text{H}$  NMR (400 MHz,  $\text{CDCl}_3$ )  $\delta$  = 8.00 (dd,  $J$  = 7.9, 0.9 Hz, 1H), 7.79 (dd,  $J$  = 7.8, 1.7 Hz, 1H), 7.41 (td,  $J$  = 7.6, 1.3 Hz, 1H), 7.15 (td,  $J$  = 7.7, 1.6 Hz, 1H), 4.34 (t,  $J$  = 6.7 Hz, 2H), 2.19 (td,  $J$  = 7.0, 2.7 Hz, 2H), 1.95 (t,  $J$  = 2.7 Hz, 1H), 1.74 - 1.83 (m, 2H), 1.49 - 1.58 (m, 2H), 1.28 - 1.49 (m, 10H);  $^{13}\text{C}$  NMR (75 MHz,  $\text{CDCl}_3$ )  $\delta$  = 166.7, 141.2, 135.6, 132.5, 130.8, 127.9, 94.0, 84.7, 68.1, 65.8, 29.3, 29.2, 29.0, 28.7, 28.6, 28.4, 26.0, 18.4; HRMS (ESI)  $m/z$  calculated for  $\text{C}_{18}\text{H}_{24}\text{IO}_2$   $[\text{M}+\text{H}]^+$  399.0816; found 399.0796.



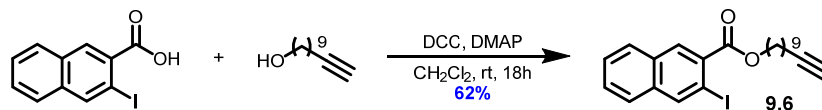
**Tridec-12-yn-1-yl 2-iodobenzoate (9.3):** Following Procedure A, tridec-12-yn-1-ol (0.150 g, 0.764 mmol, 1.0 equiv.), 2-iodobenzoic acid (0.284 g, 1.15 mmol, 1.5 equiv.), DCC (0.315 g, 1.53 mmol, 2.0 equiv.) and DMAP (0.280 g, 2.29 mmol, 3.0 equiv.) were dissolved in anhydrous dichloromethane (8 mL) in a round bottom flask equipped with a stir bar. After purification by column chromatography (100 % hexanes  $\rightarrow$  10 % diethyl ether in hexanes), iodide **9.3** was obtained as a colorless oil (0.300 g, 92 % yield).  $^1\text{H}$  NMR (400 MHz,  $\text{CDCl}_3$ )  $\delta$  = 7.99 (dd,  $J$  = 7.8, 1.0 Hz, 1H), 7.79 (dd,  $J$  = 7.8, 1.7 Hz, 1H), 7.41 (td,  $J$  = 7.6, 1.2 Hz, 1H), 7.15 (td,  $J$  = 7.7, 1.7 Hz, 1H), 4.34 (t,  $J$  = 6.7 Hz, 2H), 2.19 (td,  $J$  = 7.1, 2.7 Hz, 2H), 1.94 (t,  $J$  = 2.7 Hz, 1H), 1.74 - 1.83 (m, 2H), 1.49 - 1.57 (m, 2H), 1.27 - 1.48 (m, 14H);  $^{13}\text{C}$  NMR (100 MHz,  $\text{CDCl}_3$ )  $\delta$  = 166.7, 141.2, 135.6, 132.4, 130.8, 127.9, 93.9, 84.8, 68.0, 65.9, 29.47, 29.46, 29.4, 29.2, 29.1, 28.7, 28.6, 28.5, 26.0, 18.4; HRMS (ESI)  $m/z$  calculated for  $\text{C}_{20}\text{H}_{28}\text{IO}_2$   $[\text{M}+\text{H}]^+$  427.1129; found 427.1128.



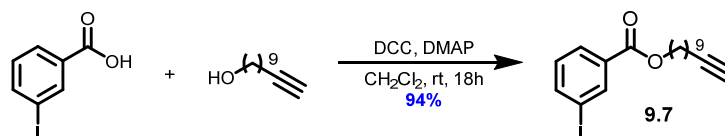
**Nonadec-18-yn-1-yl 2-iodobenzoate (9.4):** Following Procedure A, nonadec-18-yn-1-ol (0.300 g, 1.07 mmol, 1.0 equiv.), 2-iodobenzoic acid (0.398 g, 1.61 mmol, 1.5 equiv.), DCC (0.441 g, 2.14 mmol, 2.0 equiv.) and DMAP (0.392 g, 3.21 mmol, 3.0 equiv.) were dissolved in anhydrous dichloromethane (10 mL) in a round bottom flask equipped with a stir bar. After purification by column chromatography (100 % hexanes  $\rightarrow$  10 % diethyl ether in hexanes), iodide **9.4** was obtained as a white solid (0.475 g, 87 % yield).  $^1\text{H}$  NMR (400 MHz,  $\text{CDCl}_3$ )  $\delta$  = 8.00 (dd,  $J$  = 7.9, 1.1 Hz, 1H), 7.79 (dd,  $J$  = 7.9, 1.7 Hz, 1H), 7.41 (td,  $J$  = 7.6, 1.0 Hz, 1H), 7.15 (td,  $J$  = 7.7, 1.7 Hz, 1H), 4.34 (t,  $J$  = 6.8 Hz, 2H), 2.19 (td,  $J$  = 7.1, 2.7 Hz, 2H), 1.94 (t,  $J$  = 2.7 Hz, 1H), 1.74 - 1.83 (m, 2H), 1.49 - 1.57 (m, 2H), 1.24 - 1.48 (m, 26H);  $^{13}\text{C}$  NMR (100 MHz,  $\text{CDCl}_3$ )  $\delta$  = 166.7, 141.2, 135.6, 132.5, 130.8, 127.9, 94.0, 84.8, 68.0, 65.9, 29.7 (3C), 29.64, 29.63, 29.60, 29.57, 29.5 (2C), 29.2, 29.1, 28.8, 28.6, 28.5, 26.0, 18.4; HRMS (ESI)  $m/z$  calculated for  $\text{C}_{26}\text{H}_{40}\text{IO}_2$   $[\text{M}+\text{H}]^+$  511.2068; found 511.2065.



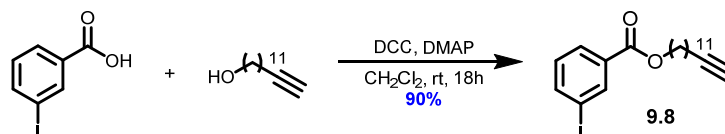
**Henicos-20-yn-1-yl 2-iodobenzoate (9.5):** Following Procedure A, henicos-20-yn-1-ol (0.300 g, 0.972 mmol, 1.0 equiv.), 2-iodobenzoic acid (0.362 g, 1.46 mmol, 1.5 equiv.), DCC (0.401 g, 1.95 mmol, 2.0 equiv.) and DMAP (0.357 g, 2.92 mmol, 3.0 equiv.) were dissolved in anhydrous dichloromethane (10 mL) in a round bottom flask equipped with a stir bar. After purification by column chromatography (100 % hexanes  $\rightarrow$  10 % diethyl ether in hexanes), iodide **9.5** was obtained as a white solid (0.507 g, 97 % yield).  $^1\text{H}$  NMR (400 MHz,  $\text{CDCl}_3$ )  $\delta$  = 8.00 (dd,  $J$  = 8.0, 0.8 Hz, 1H), 7.79 (dd,  $J$  = 7.6, 1.6 Hz, 1H), 7.41 (td,  $J$  = 7.6, 1.1 Hz, 1H), 7.15 (td,  $J$  = 7.7, 1.7 Hz, 1H), 4.34 (t,  $J$  = 6.7 Hz, 2H), 2.19 (td,  $J$  = 7.1, 2.7 Hz, 2H), 1.94 (t,  $J$  = 2.7 Hz, 1H), 1.74 - 1.83 (m, 2H), 1.49 - 1.57 (m, 2H), 1.23 - 1.48 (m, 30H);  $^{13}\text{C}$  NMR (100 MHz,  $\text{CDCl}_3$ )  $\delta$  = 166.7, 141.2, 135.6, 132.5, 130.8, 127.9, 94.0, 84.8, 68.0, 65.9, 29.68 (3C), 29.67 (2C), 29.65, 29.63, 29.60, 29.57, 29.51, 29.50, 29.2, 29.1, 28.8, 28.6, 28.5, 26.0, 18.4; HRMS (ESI)  $m/z$  calculated for  $\text{C}_{28}\text{H}_{44}\text{IO}_2$   $[\text{M}+\text{H}]^+$  539.2381; found 539.2396.



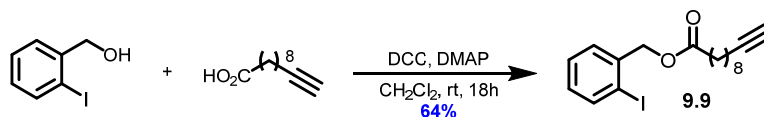
**Undec-10-yn-1-yl 3-iodo-2-naphthoate (9.6):** Following Procedure A, undec-10-yn-1-ol (0.187 g, 1.11 mmol, 1.0 equiv.), 3-iodo-2-naphthoic acid (0.496 g, 1.66 mmol, 1.5 equiv.), DCC (0.457 g, 2.22 mmol, 2.0 equiv.) and DMAP (0.406 g, 3.33 mmol, 3.0 equiv.) were dissolved in anhydrous dichloromethane (10 mL) in a round bottom flask equipped with a stir bar. After purification by column chromatography (100 % hexanes  $\rightarrow$  10 % diethyl ether in hexanes), iodide **9.6** was obtained as a colorless oil (0.308 g, 62 % yield).  $^1\text{H}$  NMR (400 MHz,  $\text{CDCl}_3$ )  $\delta$  = 8.51 (s, 1H), 8.33 (s, 1H), 7.88 (d,  $J$  = 7.7 Hz, 1H), 7.75 (d,  $J$  = 7.9 Hz, 1H), 7.53 - 7.62 (m, 2H), 4.40 (t,  $J$  = 6.8 Hz, 2H), 2.19 (td,  $J$  = 7.1, 2.6 Hz, 2H), 1.95 (t,  $J$  = 2.7 Hz, 1H), 1.79 - 1.88 (m, 2H), 1.47 - 1.58 (m, 4H), 1.28 - 1.46 (m, 8H);  $^{13}\text{C}$  NMR (100 MHz,  $\text{CDCl}_3$ )  $\delta$  = 166.8, 140.6, 135.7, 131.7, 131.6, 131.4, 128.70, 128.69, 127.3, 126.6, 88.6, 84.7, 68.1, 65.9, 29.4, 29.2, 29.0, 28.7, 28.6, 28.5, 26.1, 18.4; HRMS (ESI)  $m/z$  calculated for  $\text{C}_{22}\text{H}_{26}\text{IO}_2$   $[\text{M}+\text{H}]^+$  449.0972; found 449.0970.



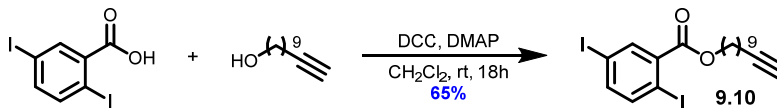
**Undec-10-yn-1-yl 3-iodobenzoate (9.7):** Following Procedure A, undec-10-yn-1-ol (0.250 g, 1.49 mmol, 1.0 equiv.), 3-iodobenzoic acid (0.553 g, 2.23 mmol, 1.5 equiv.), DCC (0.613 g, 2.97 mmol, 2.0 equiv.) and DMAP (0.545 g, 4.46 mmol, 3.0 equiv.) were dissolved in anhydrous dichloromethane (15 mL) in a round bottom flask equipped with a stir bar. After purification by column chromatography (100 % hexanes  $\rightarrow$  10 % diethyl ether in hexanes), iodide **9.7** was obtained as a colorless oil (0.557 g, 94 % yield).  $^1\text{H}$  NMR (400 MHz,  $\text{CDCl}_3$ )  $\delta$  = 8.38 (s, 1H), 8.01 (d,  $J$  = 7.7 Hz, 1H), 7.89 (d,  $J$  = 7.9 Hz, 1H), 7.19 (t,  $J$  = 7.9 Hz, 1H), 4.32 (t,  $J$  = 6.7 Hz, 2H), 2.19 (td,  $J$  = 7.0, 2.5 Hz, 2H), 1.95 (t,  $J$  = 2.6 Hz, 1H), 1.72 - 1.82 (m, 2H), 1.49 - 1.57 (m, 2H), 1.27 - 1.48 (m, 10H);  $^{13}\text{C}$  NMR (75 MHz,  $\text{CDCl}_3$ )  $\delta$  = 165.1, 141.6, 138.4, 132.4, 130.0, 128.7, 93.8, 84.7, 68.1, 65.5, 29.3, 29.1, 29.0, 28.7, 28.6, 28.4, 25.9, 18.4; HRMS (ESI)  $m/z$  calculated for  $\text{C}_{18}\text{H}_{24}\text{IO}_2$   $[\text{M}+\text{H}]^+$  399.0816; found 399.0796.



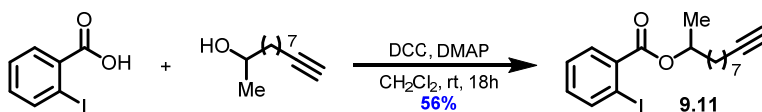
**Tridec-12-yn-1-yl 3-iodobenzoate (9.8):** Following Procedure A, tridec-12-yn-1-ol (0.100 g, 0.509 mmol, 1.0 equiv.), 3-iodobenzoic acid (0.189 g, 0.764 mmol, 1.5 equiv.), DCC (0.210 g, 1.02 mmol, 2.0 equiv.) and DMAP (0.187 g, 1.53 mmol, 3.0 equiv.) were dissolved in anhydrous dichloromethane (5 mL) in a round bottom flask equipped with a stir bar. After purification by column chromatography (100 % hexanes  $\rightarrow$  10 % diethyl ether in hexanes), iodide **9.8** was obtained as a colorless oil (0.196 g, 90 % yield).  $^1\text{H}$  NMR (400 MHz,  $\text{CDCl}_3$ )  $\delta$  = 8.38 (t,  $J$  = 1.7 Hz, 1H), 8.01 (dt,  $J$  = 7.7, 1.4 Hz, 1H), 7.89 (dt,  $J$  = 7.9, 1.5 Hz, 1H), 7.19 (t,  $J$  = 7.9 Hz, 1H), 4.32 (t,  $J$  = 6.7 Hz, 2H), 2.19 (td,  $J$  = 7.1, 2.7 Hz, 2H), 1.94 (t,  $J$  = 2.6 Hz, 1H), 1.72 - 1.81 (m, 2H), 1.49 - 1.56 (m, 2H), 1.26 - 1.48 (m, 14H);  $^{13}\text{C}$  NMR (100 MHz,  $\text{CDCl}_3$ )  $\delta$  = 165.2, 141.6, 138.4, 132.4, 130.0, 128.7, 93.8, 84.8, 68.0, 65.6, 29.48, 29.45 (2C), 29.2, 29.1, 28.7, 28.6, 28.5, 26.0, 18.4; HRMS (ESI)  $m/z$  calculated for  $\text{C}_{20}\text{H}_{28}\text{IO}_2$   $[\text{M}+\text{H}]^+$  427.1129; found 427.1129.



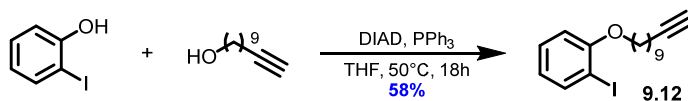
**2-Iodobenzyl undec-10-ynoate (9.9):** Following Procedure A, (2-iodophenyl)-methanol (0.188 g, 0.803 mmol, 1.0 equiv.), 10-undecynoic acid (0.220 g, 1.21 mmol, 1.5 equiv.), DCC (0.332 g, 1.61 mmol, 2.0 equiv.) and DMAP (0.294 g, 2.41 mmol, 3.0 equiv.) were dissolved in anhydrous dichloromethane (8 mL) in a round bottom flask equipped with a stir bar. After purification by column chromatography (100 % hexanes  $\rightarrow$  10 % diethyl ether in hexanes), iodide **9.9** was obtained as a colorless oil (0.205 g, 64 % yield).  $^1\text{H}$  NMR (400 MHz,  $\text{CDCl}_3$ )  $\delta$  = 7.87 (d,  $J$  = 7.7 Hz, 1H), 7.33 - 7.41 (m, 2H), 6.99 - 7.07 (m, 1H), 5.13 (s, 2H), 2.40 (t,  $J$  = 7.6 Hz, 2H), 2.18 (td,  $J$  = 7.1, 2.6 Hz, 2H), 1.94 (t,  $J$  = 2.6 Hz, 1H), 1.63 - 1.73 (m, 2H), 1.48 - 1.55 (m, 2H), 1.27 - 1.44 (m, 8H);  $^{13}\text{C}$  NMR (75 MHz,  $\text{CDCl}_3$ )  $\delta$  = 173.3, 139.5, 138.5, 129.8, 129.5, 128.3, 98.4, 84.7, 69.9, 68.1, 34.2, 29.08, 29.06, 28.9, 28.6, 28.4, 24.9, 18.4; HRMS (ESI)  $m/z$  calculated for  $\text{C}_{18}\text{H}_{24}\text{IO}_2$   $[\text{M}+\text{H}]^+$  399.0816; found 399.0834.



**Undec-10-yn-1-yl 2,5-diiodobenzoate (9.10):** Following Procedure A, undec-10-yn-1-ol (0.229 g, 1.36 mmol, 1.0 equiv.), 2,5-diiodobenzoic acid (0.763 g, 2.04 mmol, 1.5 equiv.), DCC (0.561 g, 2.72 mmol, 2.0 equiv.) and DMAP (0.498 g, 4.08 mmol, 3.0 equiv.) were dissolved in anhydrous dichloromethane (14 mL) in a round bottom flask equipped with a stir bar. After purification by column chromatography (100 % hexanes  $\rightarrow$  10 % diethyl ether in hexanes), iodide **9.10** was obtained as a colorless oil (0.463 g, 65 % yield).  $^1\text{H}$  NMR (400 MHz,  $\text{CDCl}_3$ )  $\delta$  = 8.07 (d,  $J$  = 2.2 Hz, 1H), 7.69 (d,  $J$  = 8.3 Hz, 1H), 7.45 (dd,  $J$  = 8.3, 2.2 Hz, 1H), 4.33 (t,  $J$  = 6.8 Hz, 2H), 2.19 (td,  $J$  = 7.1, 2.7 Hz, 2H), 1.95 (t,  $J$  = 2.7 Hz, 1H), 1.74 - 1.83 (m, 2H), 1.49 - 1.58 (m, 2H), 1.27 - 1.49 (m, 10H);  $^{13}\text{C}$  NMR (100 MHz,  $\text{CDCl}_3$ )  $\delta$  = 165.2, 142.6, 141.3, 139.4, 137.2, 93.3, 93.1, 84.7, 68.1, 66.2, 29.3, 29.1, 29.0, 28.7, 28.5, 28.4, 26.0, 18.4; HRMS (ESI)  $m/z$  calculated for  $\text{C}_{18}\text{H}_{22}\text{I}_2\text{O}_2\text{Na}$   $[\text{M}+\text{Na}]^+$  546.9601; found 546.9620.



**Undec-10-yn-2-yl 2-iodobenzoate (9.11):** Following Procedure A, undec-10-yn-2-ol (0.130 g, 0.77 mmol, 1.0 equiv.), 2-iodobenzoic acid (0.288 g, 1.16 mmol, 1.5 equiv.), DCC (0.317 g, 1.54 mmol, 2.0 equiv.) and DMAP (0.282 g, 2.31 mmol, 3.0 equiv.) were dissolved in anhydrous dichloromethane (8 mL) in a round bottom flask equipped with a stir bar. After purification by column chromatography (100 % hexanes  $\rightarrow$  10 % diethyl ether in hexanes), iodide **9.11** was obtained as a colorless oil (0.168 g, 56 % yield).  $^1\text{H}$  NMR (300 MHz,  $\text{CDCl}_3$ )  $\delta$  = 7.96 (dd,  $J$  = 7.9, 1.1 Hz, 1H), 7.74 (dd,  $J$  = 7.8, 1.7 Hz, 1H), 7.38 (ddd,  $J$  = 7.6, 6.2, 1.2 Hz, 1H), 7.17 – 7.07 (m, 1H), 5.30 – 5.01 (m, 1H), 2.17 (td,  $J$  = 7.0, 2.6 Hz, 2H), 1.92 (dd,  $J$  = 5.4, 2.8 Hz, 1H), 1.82 – 1.39 (m, 8H), 1.36 (d,  $J$  = 6.0, 3H), 1.34 – 1.18 (m, 4H);  $^{13}\text{C}$  NMR (75 MHz,  $\text{CDCl}_3$ )  $\delta$  = 166.2, 141.1, 135.9, 132.2, 130.5, 127.8, 93.8, 84.6, 72.7, 68.1, 35.8, 29.2, 28.9, 28.5, 28.3, 25.3, 19.9, 18.3; HRMS (ESI)  $m/z$  calculated for  $\text{C}_{18}\text{H}_{27}\text{INO}_2$   $[\text{M}+\text{NH}_4]^+$  416.1081; found 416.1084.

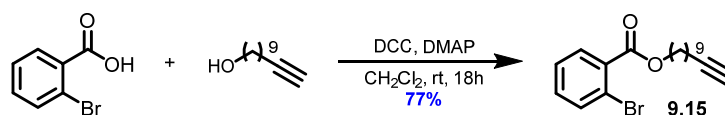


**1-Iodo-2-(undec-10-yn-1-yloxy)benzene (9.12):** To a stirred solution of 2-iodophenol (0.255 g, 1.16 mmol, 1.0 equiv.) in anhydrous tetrahydrofuran (25 mL, 0.05 M), triphenylphosphine (0.304 g, 1.16 mmol, 1.0 equiv.) and undec-10-yn-1-ol (0.195 g, 1.16 mmol, 1.0 equiv.) were added under a nitrogen atmosphere. Diisopropyl azodicarboxylate (0.23 mL, 1.16 mmol, 1.0 equiv.) was then added dropwise to the mixture at room temperature. The reaction mixture was heated at 50 °C for 18 hours, cooled and concentrated under reduced pressure to provide a residue, which was purified by column chromatography on silica-gel (100 % hexanes  $\rightarrow$  5 % diethyl ether in hexanes) to afford iodide **9.12** as a colorless oil (0.249 g, 58 % yield).  $^1\text{H}$  NMR (400 MHz,  $\text{CDCl}_3$ )  $\delta$  = 7.77 (dd,  $J$  = 7.8, 1.6 Hz, 1H), 7.27 - 7.31 (m, 1H), 6.81 (dd,  $J$  = 8.2, 1.1 Hz, 1H), 6.70 (td,  $J$  = 7.5, 1.2 Hz, 1H), 4.01 (t,  $J$  = 6.4 Hz, 2H), 2.19 (td,  $J$  = 7.0, 2.7 Hz, 2H), 1.95 (t,  $J$  = 2.6 Hz, 1H), 1.80 - 1.89 (m, 2H), 1.49 - 1.59 (m, 4H), 1.29 - 1.47 (m, 8H);  $^{13}\text{C}$  NMR (75 MHz,  $\text{CDCl}_3$ )  $\delta$  = 157.6, 139.3, 129.3, 122.2, 112.0, 86.7, 84.7, 69.1, 68.1, 29.4, 29.2, 29.1,

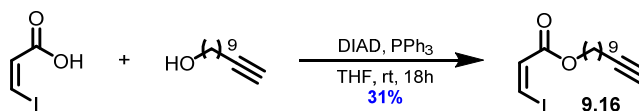




28.7, 28.5, 26.0, 18.4; HRMS (ESI)  $m/z$  calculated for  $C_{16}H_{23}INO$   $[M+H]^+$  372.0819; found 372.0809.



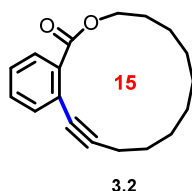
**Undec-10-yn-1-yl 2-bromobenzoate (9.15):** Following Procedure A, undec-10-yn-1-ol (0.279 g, 1.66 mmol, 1.0 equiv.), 2-bromobenzoic acid (0.500 g, 2.49 mmol, 1.5 equiv.), DCC (0.684 g, 3.32 mmol, 2.0 equiv.) and DMAP (0.608 g, 4.97 mmol, 3.0 equiv.) were dissolved in anhydrous dichloromethane (16 mL) in a round bottom flask equipped with a stir bar. After purification by column chromatography (100 % hexanes  $\rightarrow$  10 % diethyl ether in hexanes), bromide **9.15** was obtained as a colorless oil (0.450 g, 77 % yield).  $^1H$  NMR (400 MHz,  $CDCl_3$ )  $\delta$  = 7.78 (dd,  $J$  = 7.5, 1.8 Hz, 1H), 7.66 (dd,  $J$  = 7.8, 1.4 Hz, 1H), 7.29 - 7.41 (m, 2H), 4.34 (t,  $J$  = 6.7 Hz, 2H), 2.19 (td,  $J$  = 7.1, 2.7 Hz, 2H), 1.94 (t,  $J$  = 2.7 Hz, 1H), 1.73 - 1.82 (m, 2H), 1.48 - 1.58 (m, 2H), 1.27 - 1.47 (m, 10H);  $^{13}C$  NMR (75 MHz,  $CDCl_3$ )  $\delta$  = 166.3, 134.3, 132.6, 132.4, 131.2, 127.1, 121.5, 84.7, 68.1, 65.8, 29.3, 29.1, 29.0, 28.7, 28.5, 28.4, 26.0, 18.4; HRMS (ESI)  $m/z$  calculated for  $C_{18}H_{24}BrO_2$   $[M+H]^+$  351.0954; found 351.0963.



**(Z)-undec-10-yn-1-yl 3-iodoacrylate (9.16):** To a stirred solution of (Z)-3-iodo-propenoic acid (0.250 g, 1.26 mmol, 1.0 equiv.) in anhydrous tetrahydrofuran (10 mL, 0.1 M), triphenylphosphine (0.331 g, 1.26 mmol, 1.0 equiv.) and undec-10-yn-1-ol (0.372 g, 2.21 mmol, 1.75 equiv.) were added under a nitrogen atmosphere. Diisopropyl azodicarboxylate (0.25 mL, 1.26 mmol, 1.0 equiv.) was then added dropwise to the reaction mixture at 0 °C. The mixture was allowed to warm to room temperature and stirred for 18 hours. The volume was concentrated under vacuum to provide a residue which was purified by column chromatography on silica-gel (100 % hexanes  $\rightarrow$  5 % diethyl ether in hexanes) to afford vinyl iodide **9.16** as a colorless oil (0.137 g, 31 % yield).  $^1H$  NMR (400 MHz,  $CDCl_3$ )  $\delta$  = 7.44 (d,  $J$  = 9.0 Hz, 1H),

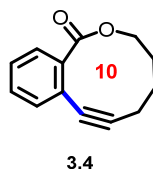
6.91 (d,  $J = 8.9$  Hz, 1H), 4.19 (t,  $J = 6.7$  Hz, 2H), 2.15 - 2.22 (m, 2H), 1.94 (t,  $J = 2.7$  Hz, 1H), 1.64 - 1.73 (m, 2H), 1.49 - 1.57 (m, 2H), 1.27 - 1.45 (m, 10H);  $^{13}\text{C}$  NMR (100 MHz,  $\text{CDCl}_3$ )  $\delta$  = 164.7, 130.0, 94.5, 84.7, 68.1, 64.9, 29.3, 29.1, 29.0, 28.7, 28.5, 28.4, 25.9, 18.4; HRMS (ESI)  $m/z$  calculated for  $\text{C}_{14}\text{H}_{25}\text{INO}_2$   $[\text{M}+\text{NH}_4]^+$  366.0925; found 366.0910.

## 9.3 Synthesis of Macrocycles



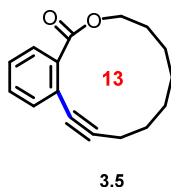
### Representative procedure for the copper-catalyzed macrocyclic coupling:

**Macrolactone 3.2:** To a dried sealable tube equipped with a stir bar, copper(I) chloride (0.006 mmol, 5 mol%), 1,10-phenanthroline (0.024 mmol, 20 mol%) and cesium carbonate (0.24 mmol, 2 equiv.) were added. The macrocyclic precursor (0.12 mmol, 1 equiv.) was added to the sealable tube as a toluene solution (5 mL) in one portion. The aperture of the tube was covered with a rubber septum and the reaction mixture was bubbled with nitrogen for 10 minutes. The septum was then replaced by a Teflon-coated screw cap and the sealed-tube was placed in a pre-heated oil bath at 135 °C. After stirring for 18 hours, the mixture was cooled to room temperature and diluted with ethyl acetate. The resulting solution was filtered through a pad of Celite® and concentrated under vacuum to provide a residue which was purified by column chromatography on silica-gel (100 % hexanes → 10 % diethyl ether in hexanes) to afford macrolactone **3.2** as a white solid (26 mg, 81 % yield). <sup>1</sup>H NMR (400 MHz, CDCl<sub>3</sub>) δ = 7.70 (dd, *J* = 7.8, 1.1 Hz, 1H), 7.50 (dd, *J* = 7.7, 1.0 Hz, 1H), 7.39 (td, *J* = 7.6, 1.4 Hz, 1H), 7.28 - 7.33 (m, 1H), 4.47 - 4.53 (m, 2H), 2.51 - 2.54 (m, 2H), 1.72 - 1.81 (m, 2H), 1.35 - 1.62 (m, 12H); <sup>13</sup>C NMR (100 MHz, CDCl<sub>3</sub>) δ = 167.7, 134.0, 133.9, 130.8, 129.2, 127.1, 123.6, 95.4, 79.1, 63.8, 29.5, 27.6, 27.2, 25.8, 25.7, 25.5, 23.5, 19.0; HRMS (ESI) *m/z* calculated for C<sub>18</sub>H<sub>24</sub>O<sub>2</sub> [M+H]<sup>+</sup> 271.1693; found 271.1702.

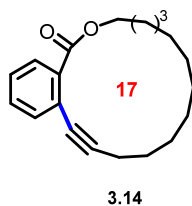


**Macrolactone 3.4:** Following the procedure described above, macrolactone **3.4** was isolated as a colorless oil (11 mg, 46 % yield). <sup>1</sup>H NMR (400 MHz, CDCl<sub>3</sub>) δ = 7.70 - 7.77 (m, 1H), 7.38 -

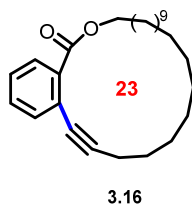
7.45 (m, 1H), 7.31 - 7.37 (m, 2H), 4.45 (dd,  $J = 5.9, 3.5$  Hz, 2H), 2.39 - 2.47 (m, 2H), 1.92 - 2.03 (m, 4H);  $^{13}\text{C}$  NMR (100 MHz,  $\text{CDCl}_3$ )  $\delta = 168.4, 137.3, 131.2, 129.4, 129.2, 127.5, 123.5, 99.2, 82.5, 66.3, 28.8, 28.2, 21.2$ ; HRMS (ESI)  $m/z$  calculated for  $\text{C}_{13}\text{H}_{14}\text{O}_2$   $[\text{M}+\text{H}]^+$  201.0910; found 201.0907.



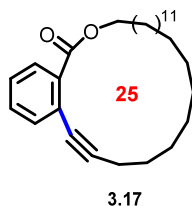
**Macrolactone 3.5:** Following the procedure described above, macrolactone **3.5** was isolated as a white solid (24 mg, 83 % yield).  $^1\text{H}$  NMR (400 MHz,  $\text{CDCl}_3$ )  $\delta = 7.81$  (ddd,  $J = 7.8, 1.5, 0.5$  Hz, 1H), 7.47 - 7.51 (m, 1H), 7.40 (td,  $J = 7.6, 1.5$  Hz, 1H), 7.29 - 7.35 (m, 1H), 4.38 - 4.44 (m, 2H), 2.49 - 2.54 (m, 2H), 1.81 - 1.88 (m, 2H), 1.58 - 1.74 (m, 8H);  $^{13}\text{C}$  NMR (100 MHz,  $\text{CDCl}_3$ )  $\delta = 168.4, 134.2, 133.3, 131.0, 130.3, 127.3, 123.2, 95.5, 79.4, 65.0, 27.8, 27.0, 25.4, 24.77, 24.75, 18.9$ ; HRMS (ESI)  $m/z$  calculated for  $\text{C}_{16}\text{H}_{20}\text{O}_2$   $[\text{M}+\text{H}]^+$  243.1380; found 243.1383.



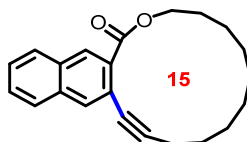
**Macrolactone 3.14:** Following the procedure described above, macrolactone **3.14** was isolated as a white solid (24 mg, 66 % yield).  $^1\text{H}$  NMR (400 MHz,  $\text{CDCl}_3$ )  $\delta = 7.80 - 7.84$  (m, 1H), 7.52 (dd,  $J = 7.8, 0.9$  Hz, 1H), 7.41 (td,  $J = 7.6, 1.5$  Hz, 1H), 7.28 - 7.33 (m, 1H), 4.40 (t,  $J = 6.4$  Hz, 2H), 2.48 - 2.54 (m, 2H), 1.73 - 1.80 (m, 2H), 1.50 - 1.64 (m, 4H), 1.30 - 1.49 (m, 12H);  $^{13}\text{C}$  NMR (100 MHz,  $\text{CDCl}_3$ )  $\delta = 166.8, 134.2, 132.8, 131.1, 129.8, 127.0, 124.3, 95.7, 79.2, 65.1, 28.3, 28.0, 27.5, 27.2, 27.0, 26.9, 26.8, 25.9, 24.2, 19.7$ ; HRMS (ESI)  $m/z$  calculated for  $\text{C}_{20}\text{H}_{28}\text{O}_2$   $[\text{M}+\text{H}]^+$  299.2006; found 299.2009.



**Macrolactone 3.16:** Following the procedure described above, macrolactone **3.16** was isolated as a white solid (30 mg, 65 % yield).  $^1\text{H}$  NMR (400 MHz,  $\text{CDCl}_3$ )  $\delta$  = 7.86 (dd,  $J$  = 7.8, 1.1 Hz, 1H), 7.50 (dd,  $J$  = 7.8, 1.0 Hz, 1H), 7.41 (td,  $J$  = 7.6, 1.4 Hz, 1H), 7.28 - 7.34 (m, 1H), 4.34 (t,  $J$  = 7.0 Hz, 2H), 2.46 (t,  $J$  = 7.2 Hz, 2H), 1.76 – 1.83 (m, 2H), 1.59 - 1.69 (m, 2H), 1.41 - 1.54 (m, 4H), 1.26 - 1.41 (m, 24H);  $^{13}\text{C}$  NMR (100 MHz,  $\text{CDCl}_3$ )  $\delta$  = 167.1, 134.1, 132.7, 131.2, 130.1, 127.1, 124.0, 95.6, 79.2, 65.4, 28.8, 28.7, 28.62, 28.58, 28.5, 28.38, 28.37, 28.3, 28.2, 27.48, 27.45, 27.3, 27.2, 27.1, 25.8, 19.8; HRMS (ESI)  $m/z$  calculated for  $\text{C}_{26}\text{H}_{40}\text{O}_2$   $[\text{M}+\text{H}]^+$  383.2945; found 383.2961.

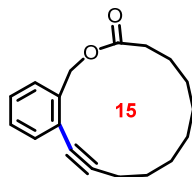


**Macrolactone 3.17:** Following the procedure described above, macrolactone **3.17** was isolated as a white solid (30 mg, 61 % yield).  $^1\text{H}$  NMR (400 MHz,  $\text{CDCl}_3$ )  $\delta$  = 7.87 (dt,  $J$  = 7.8, 0.7 Hz, 1H), 7.50 (dd,  $J$  = 7.8, 1.0 Hz, 1H), 7.41 (td,  $J$  = 7.6, 1.5 Hz, 1H), 7.28 - 7.34 (m, 1H), 4.34 (t,  $J$  = 7.0 Hz, 2H), 2.46 (t,  $J$  = 7.2 Hz, 2H), 1.74 - 1.85 (m, 2H), 1.60 - 1.70 (m, 2H), 1.41 - 1.53 (m, 4H), 1.26 - 1.40 (m, 26H);  $^{13}\text{C}$  NMR (100 MHz,  $\text{CDCl}_3$ )  $\delta$  = 167.1, 134.1, 132.6, 131.2, 130.1, 127.1, 124.1, 95.6, 79.3, 65.4, 28.94, 28.91, 28.89, 28.87, 28.8, 28.69, 28.66, 28.6 (2C), 28.09, 28.05, 28.0, 27.8, 27.73, 27.67, 27.3, 25.9, 19.9; HRMS (ESI)  $m/z$  calculated for  $\text{C}_{28}\text{H}_{42}\text{NaO}_2$   $[\text{M}+\text{Na}]^+$  433.3077; found 433.3076.



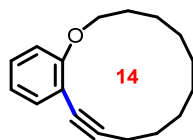
3.9

**Macrolactone 3.9:** Following the procedure described above, macrolactone **3.9** was isolated as a white solid (27 mg, 71 % yield).  $^1\text{H}$  NMR (400 MHz,  $\text{CDCl}_3$ )  $\delta$  = 8.24 (s, 1H), 8.02 (s, 1H), 7.85 (d,  $J$  = 8.1 Hz, 1H), 7.78 (d,  $J$  = 8.0 Hz, 1H), 7.47 - 7.58 (m, 2H), 4.54 - 4.60 (m, 2H), 2.56 (t,  $J$  = 5.7 Hz, 2H), 1.76 - 1.84 (m, 2H), 1.58 - 1.65 (m, 4H), 1.37 - 1.58 (m, 8H);  $^{13}\text{C}$  NMR (100 MHz,  $\text{CDCl}_3$ )  $\delta$  = 167.5, 134.0, 133.8, 131.3, 130.9, 130.1, 128.5, 128.1, 127.2, 127.0, 119.8, 94.4, 79.3, 63.7, 29.6, 27.8, 27.4, 25.9, 25.7, 25.6, 23.6, 19.1; HRMS (ESI)  $m/z$  calculated for  $\text{C}_{22}\text{H}_{26}\text{O}_2$   $[\text{M}+\text{H}]^+$  321.1849; found 321.1857.



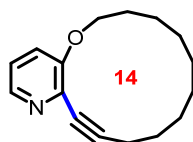
3.11

**Macrolactone 3.11:** Following the procedure described above, macrolactone **3.11** was isolated as a white solid (19 mg, 59 % yield).  $^1\text{H}$  NMR (400 MHz,  $\text{CDCl}_3$ )  $\delta$  = 7.46 - 7.50 (m, 1H), 7.37 - 7.40 (m, 1H), 7.26 - 7.33 (m, 2H), 5.22 (s, 2H), 2.50 (t,  $J$  = 5.7 Hz, 2H), 2.35 - 2.40 (m, 2H), 1.52 - 1.68 (m, 6H), 1.37 - 1.46 (m, 6H);  $^{13}\text{C}$  NMR (100 MHz,  $\text{CDCl}_3$ )  $\delta$  = 173.9, 136.4, 132.7, 131.2, 128.8, 127.7, 125.6, 94.8, 78.6, 65.6, 34.7, 27.3, 26.3, 25.8, 25.7, 25.5, 23.8, 19.3; HRMS (ESI)  $m/z$  calculated for  $\text{C}_{18}\text{H}_{24}\text{O}_2$   $[\text{M}+\text{H}]^+$  271.1693; found 271.1689.



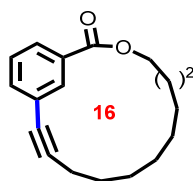
3.7

**Macrolactone 3.7:** Following the procedure described above, macrolactone **3.7** was isolated as a white solid (21 mg, 72 % yield).  $^1\text{H}$  NMR (400 MHz,  $\text{CDCl}_3$ )  $\delta$  = 7.35 (dd,  $J$  = 7.5, 1.6 Hz, 1H), 7.17 - 7.24 (m, 1H), 6.81 - 6.89 (m, 2H), 4.01 (t,  $J$  = 6.0 Hz, 2H), 2.47 (t,  $J$  = 6.6 Hz, 2H), 1.77 - 1.87 (m, 2H), 1.48 - 1.67 (m, 6H), 1.34 - 1.41 (m, 6H);  $^{13}\text{C}$  NMR (100 MHz,  $\text{CDCl}_3$ )  $\delta$  = 159.8, 133.0, 128.7, 120.2, 112.1, 112.0, 94.4, 68.6, 29.80, 29.77, 29.7, 29.53, 29.51, 28.9, 28.8, 26.4, 19.7; HRMS (ESI)  $m/z$  calculated for  $\text{C}_{17}\text{H}_{23}\text{O}$   $[\text{M}+\text{H}]^+$  242.1665; found 242.1659.



3.8

**Macrolactone 3.8:** Following the procedure described above, macrolactone **3.8** was isolated as a white solid (17 mg, 59 % yield).  $^1\text{H}$  NMR (400 MHz,  $\text{CDCl}_3$ )  $\delta$  = 8.12 (dd,  $J$  = 3.6, 2.4 Hz, 1H), 7.12 - 7.16 (m, 2H), 4.02 - 4.09 (m, 2H), 2.55 (dd,  $J$  = 6.8, 4.9 Hz, 2H), 1.80 - 1.88 (m, 2H), 1.59 - 1.70 (m, 6H), 1.44 - 1.58 (m, 6H);  $^{13}\text{C}$  NMR (100 MHz,  $\text{CDCl}_3$ )  $\delta$  = 156.3, 141.3, 134.6, 122.8, 118.3, 95.6, 77.7, 68.5, 27.6, 27.0, 26.9, 26.7, 26.3, 26.1, 24.4, 19.1; HRMS (ESI)  $m/z$  calculated for  $\text{C}_{16}\text{H}_{23}\text{NO}$   $[\text{M}+\text{H}]^+$  244.1696; found 244.1692.

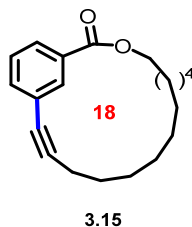


3.13

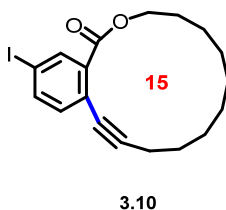
**Macrolactone 3.13:** Following the procedure described above, macrolactone **3.13** was isolated as a white solid (23 mg, 72 % yield).  $^1\text{H}$  NMR (400 MHz,  $\text{CDCl}_3$ )  $\delta$  = 8.30 (t,  $J$  = 1.5 Hz, 1H),



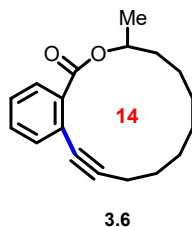
7.92 (dt,  $J = 7.7$ , 1.5 Hz, 1H), 7.42 - 7.49 (m, 1H), 7.34 - 7.42 (m, 1H), 4.34 - 4.41 (m, 2H), 2.41 - 2.48 (m, 2H), 1.82 (dt,  $J = 11.0$ , 5.5 Hz, 2H), 1.57 - 1.77 (m, 8H), 1.41 - 1.57 (m, 4H);  $^{13}\text{C}$  NMR (100 MHz,  $\text{CDCl}_3$ )  $\delta = 165.8, 136.2, 132.5, 130.6, 128.6, 128.1, 124.5, 93.6, 82.1, 66.4, 30.6, 30.1, 29.9, 28.8, 28.4, 28.2, 27.7, 19.2$ ; HRMS (ESI)  $m/z$  calculated for  $\text{C}_{18}\text{H}_{24}\text{O}_2$   $[\text{M}+\text{H}]^+$  271.1693; found 271.1693.



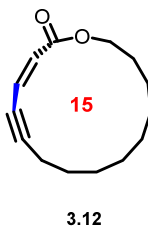
**Macrolactone 3.15:** Following the procedure described above, macrolactone **3.15** was isolated as a white solid (22 mg, 62 % yield).  $^1\text{H}$  NMR (400 MHz,  $\text{CDCl}_3$ )  $\delta = 8.06$  (t,  $J = 1.5$  Hz, 1H), 7.96 (dt,  $J = 7.8$ , 1.5 Hz, 1H), 7.53 (dt,  $J = 7.7$ , 1.4 Hz, 1H), 7.38 (td,  $J = 7.8$ , 0.5 Hz, 1H), 4.31 - 4.39 (m, 2H), 2.42 - 2.51 (m, 2H), 1.70 - 1.79 (m, 2H), 1.54 - 1.69 (m, 6H), 1.37 - 1.54 (m, 10H);  $^{13}\text{C}$  NMR (100 MHz,  $\text{CDCl}_3$ )  $\delta = 165.9, 134.5, 133.3, 130.8, 128.7, 128.5, 124.4, 91.3, 80.8, 64.9, 29.2, 28.8, 28.7, 28.6, 28.3, 28.0, 27.5, 27.1, 25.2, 19.0$ ; HRMS (ESI)  $m/z$  calculated for  $\text{C}_{20}\text{H}_{28}\text{O}_2$   $[\text{M}+\text{H}]^+$  299.2006; found 299.2008.



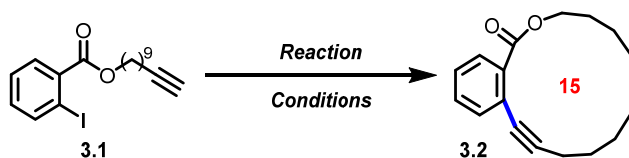
**Macrolactone 3.10:** Following the procedure described above, macrolactone **3.10** was isolated as a white solid (37 mg, 77 % yield).  $^1\text{H}$  NMR (400 MHz,  $\text{CDCl}_3$ )  $\delta = 8.02$  (dd,  $J = 1.9, 0.3$  Hz, 1H), 7.71 (dd,  $J = 8.2, 1.9$  Hz, 1H), 7.21 (d,  $J = 8.2$  Hz, 1H), 4.46 - 4.52 (m, 2H), 2.46 - 2.55 (m, 2H), 1.71 - 1.79 (m, 2H), 1.34 - 1.59 (m, 12H);  $^{13}\text{C}$  NMR (100 MHz,  $\text{CDCl}_3$ )  $\delta = 166.1, 139.7, 138.0, 135.4, 135.3, 123.1, 97.0, 92.0, 78.4, 64.1, 29.4, 27.5, 27.2, 25.8, 25.7, 25.5, 23.5, 19.0$ ; HRMS (ESI)  $m/z$  calculated for  $\text{C}_{18}\text{H}_{23}\text{IO}_2$   $[\text{M}+\text{H}]^+$  397.0659; found 397.0665.



**Macrolactone 3.6:** Following the procedure described above, macrolactone **3.6** was isolated as a white solid (25 mg, 78 % yield).  $^1\text{H}$  NMR (400 MHz,  $\text{CDCl}_3$ )  $\delta$  = 7.65 (dd,  $J$  = 7.7, 1.1 Hz, 1H), 7.47 (dd,  $J$  = 7.7, 1.1 Hz, 1H), 7.38 (td,  $J$  = 7.6, 1.5 Hz, 1H), 7.28 - 7.33 (m, 1H), 5.29 - 5.38 (m, 1H), 2.54 - 2.62 (m, 1H), 2.36 - 2.45 (m, 1H), 1.30 - 1.79 (m, 12H), 1.36 (d,  $J$  = 6.3 Hz, 3H);  $^{13}\text{C}$  NMR (100 MHz,  $\text{CDCl}_3$ )  $\delta$  = 167.7, 134.9, 133.3, 130.4, 128.7, 127.1, 122.8, 95.0, 79.4, 71.3, 34.9, 26.6, 25.9, 25.1, 24.3, 22.3, 20.7, 19.0; HRMS (ESI)  $m/z$  calculated for  $\text{C}_{18}\text{H}_{24}\text{O}_2$   $[\text{M}+\text{H}]^+$  271.1693; found 271.1700.



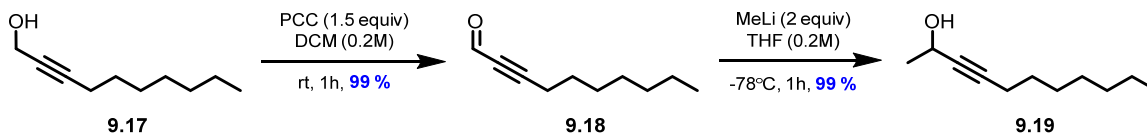
**Macrolactone 3.12:** Following the procedure described above, macrolactone **3.12** was isolated as a colorless oil (10 mg, 38 % yield).  $^1\text{H}$  NMR (400 MHz,  $\text{CDCl}_3$ )  $\delta$  = 6.10 - 6.15 (m, 1H), 5.97 (d,  $J$  = 11.8 Hz, 1H), 4.31 - 4.36 (m, 2H), 2.47 - 2.53 (m, 2H), 1.66 - 1.73 (m, 2H), 1.44 - 1.59 (m, 10H), 1.36 - 1.44 (m, 2H);  $^{13}\text{C}$  NMR (100 MHz,  $\text{CDCl}_3$ )  $\delta$  = 165.8, 128.0, 121.6, 102.8, 77.7, 63.7, 28.9, 27.1, 26.4, 25.8, 25.5, 25.1, 23.5, 19.0; HRMS (ESI)  $m/z$  calculated for  $\text{C}_{14}\text{H}_{20}\text{O}_2\text{Na}$   $[\text{M}+\text{Na}]^+$  243.1356; found 243.1344.

**Table 9.1** Optimization of a macrocyclic Pd-catalyzed Sonogashira cross-coupling

	Conditions	Yield (%) <sup>a,b</sup>
1	Pd(PPh <sub>3</sub> ) <sub>2</sub> Cl <sub>2</sub> (35 mol %), CuI (1.5 eq.), DMEA, 21°C, 12 h, SA [6.5 mM]	15
2	Pd(OAc) <sub>2</sub> (2 mol %), PPh <sub>3</sub> (4 mol %), CuI (4 mol %), NEt <sub>3</sub> (6 eq.), THF, 21°C, 18 h, SA [5 mM]	(48)
3	Pd(OAc) <sub>2</sub> (2 mol %), P( <i>t</i> -Bu) <sub>3</sub> •HBF <sub>4</sub> (4 mol %), CuI (4 mol %), NEt <sub>3</sub> (6 eq.), THF, 21°C, 18 h, [5 mM]	(61)
4	Pd(dppf)Cl <sub>2</sub> (5 mol %), CuI (10 mol %), NEt <sub>3</sub> (6 eq.), THF, 21°C, 18 h, [5 mM]	(12)
5	Pd <sub>2</sub> (dba) <sub>3</sub> (5 mol %), XPhos (10 mol %), CuI (10 mol %), NEt <sub>3</sub> (6 eq.), THF, 21°C, 18 h, [5 mM]	(91)
6	[Cu(DMEDA) <sub>2</sub> ]Cl <sub>2</sub> (5 mol %), DMEDA (30 mol %), Cs <sub>2</sub> CO <sub>3</sub> (2 eq.), 1,4-dioxane, 135°C, 16 h, [24 mM]	52
7	[Cu(DMEDA) <sub>2</sub> ]Cl <sub>2</sub> (5 mol %), DMEDA (30 mol %), Cs <sub>2</sub> CO <sub>3</sub> (2 eq.), PhMe, 135°C, 16 h, [24 mM]	58

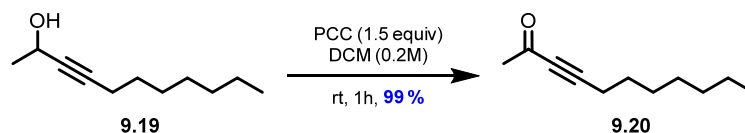
<sup>a</sup> Isolated yields of **3.2** following chromatography. <sup>b</sup> Yields in brackets refer to isolated yields of recovered starting material **3.1**. SA = slow addition; DMEA = dimethylethylamine; DMEDA = *N,N'*-dimethylethylenediamine; XPhos = 2-dicyclohexylphosphino-2',4',6'-triisopropylbiphenyl.

## 9.4 Synthesis of (*S*)-Zearalane

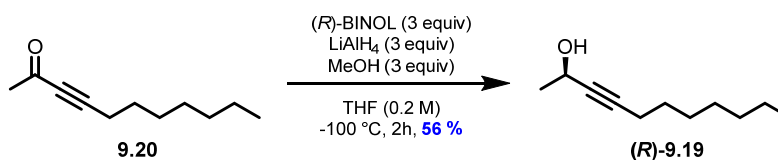


**Dec-2-ynal (9.18):** Dec-2-yn-1-ol (2.0 g, 13.0 mmol, 1.0 equiv.) was dissolved in dichloromethane (8 mL) and treated with pyridinium chlorochromate (4.2 g, 19.5 mmol, 1.5 equiv.) in one portion. The mixture was stirred at room temperature for 1 hour. Silica gel was added to the mixture and the volatiles were removed under vacuum. The resulting solid was then placed onto a short pad of silica-gel and washed with 10 % ethyl acetate in hexanes. Following evaporation of the collected fractions, aldehyde **9.18** was obtained as a colorless oil (1.98 g, 99 % yield) that was used immediately in the next transformation, because aldehyde **9.18** oxidizes readily to the corresponding carboxylic acid even after 18 h in a freezer. **Undec-3-yn-2-ol (9.19):** To a stirred solution of dec-2-ynal (1.98 g, 13.0 mmol, 1.0 equiv.) in anhydrous tetrahydrofuran (65 mL) at -78 °C was added a solution of methyl lithium (1.6 M in diethyl ether, 16.3 mL, 26 mmol, 2.0 equiv.) The mixture was stirred for 1 hour, quenched with water and diluted with ethyl acetate. The organic phase was separated and dried with anhydrous sodium sulfate. The resulting suspension was filtered, and the filtrate was concentrated under vacuum to provide a residue which was purified by column chromatography on silica-gel (20 % ethyl acetate in hexanes) to afford alcohol **9.19** as a colorless oil (2.2 g, 99 % yield). The alcohol was sensitive to oxidation and was kept in the freezer under nitrogen. NMR data was in accordance with what was previously reported.<sup>9</sup>

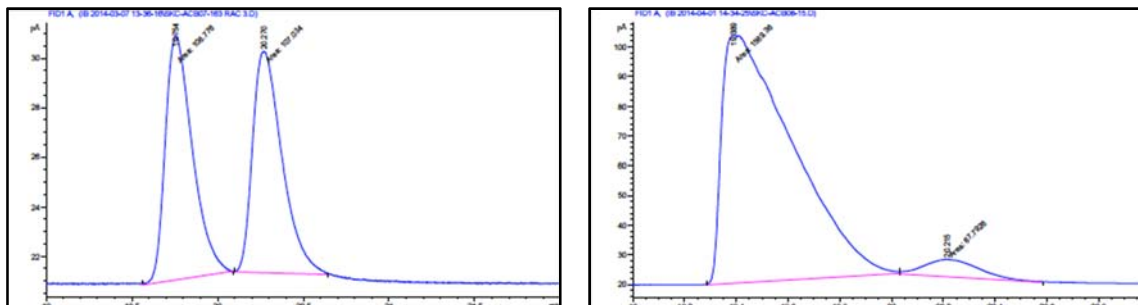
<sup>9</sup> Marshall, J. A.; Wang, X.-J.; *J. Org. Chem.* **1991**, 56, 4913.



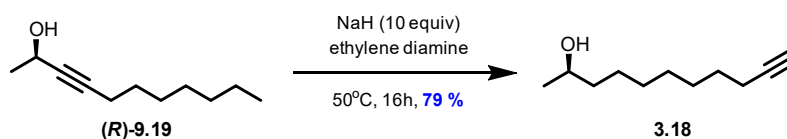
**Undec-3-yn-2-one (9.20):** Undec-3-yn-2-ol (1.0 g, 5.94 mmol, 1.0 equiv.) was dissolved in dichloromethane (30 mL) and pyridinium chlorochromate (1.9 g, 8.92 mmol, 1.5 equiv.) was then added to the reaction in one portion. The mixture was stirred at room temperature for 1 hour. Silica gel was added to the mixture and the volatiles were removed under vacuum. The dry pack was placed onto a short pad of silica-gel and eluted with 10 % ethyl acetate in hexanes. Following evaporation of the collected fractions, ketone **9.20** was obtained as a colorless oil (0.988 g, 99 % yield). NMR data was in accordance with what was previously reported.<sup>9</sup>



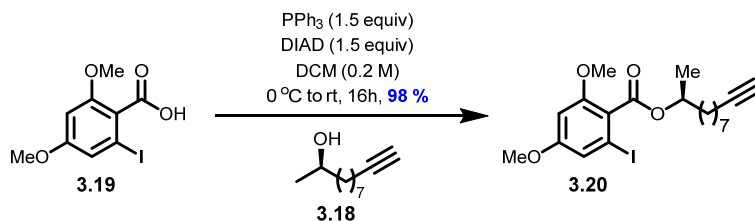
**(R)-Undec-3-yn-2-ol ((R)-9.19):** To a stirred solution of lithium aluminium hydride (0.321 g, 8.37 mmol, 3.0 equiv.) in tetrahydrofuran (15 mL) at 0 °C, (R)-BINOL (2.43 g, 8.47 mmol, 3.0 equiv.) was added dropwise as a tetrahydrofuran solution (2 mL). Methanol (1 M in tetrahydrofuran, 8.47 mL, 3.0 equiv.) was then added dropwise to the mixture. The solution was cooled to - 100 °C and treated dropwise with a solution of undec-3-yn-2-one (0.470 g, 2.8 mmol, 1.0 equiv.) in tetrahydrofuran (3 mL). The resulting mixture was stirred for 2 hours at - 100 °C and quenched with water and diluted with ethyl acetate. The organic phase was separated and dried with anhydrous sodium sulfate. The resulting suspension was filtered, and the filtrate was concentrated under vacuum to provide a residue which was purified by column chromatography on silica-gel (10 % ethyl acetate in hexanes) to afford alcohol **(R)-9.19** as a colorless oil (0.264 g, 56 % yield, 90 % *ee*). NMR data was in accordance with what was previously reported.<sup>8</sup> The enantiomeric purity was determined by GC analysis in comparison with the racemic material ( $\beta$ -dex, L  $\times$  I.D. 30 m  $\times$  0.25 mm,  $d_f$  0.25  $\mu$ m, flow rate: 1.1 mL/min, 120 °C):  $t_R$  of **(R)-9.19**: 19 min (major) and 20 min (minor).



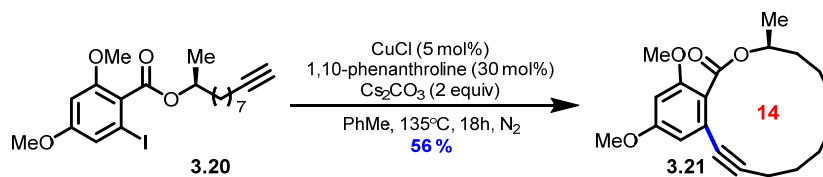
Peak #	Ret. Time	Area %	Peak #	Ret. Time	Area %
1	19.5	50.404	1	19.4	94.765
2	20.3	49.596	2	20.2	5.235



**(R)-Undec-10-yn-2-ol (3.18):** A solution of ethylene diamine (25 mL) at 0 °C was treated with sodium hydride (1.99 g, 49.7 mmol, 10.0 equiv.) in small portions. The mixture was kept under a nitrogen atmosphere and stirred at 0 °C for 30 minutes then warmed to room temperature. When the mixture turned purple, the solution was warmed to 60 °C and stirred for 2 hours. (R)-Undec-3-yn-2-ol (0.836 g, 4.97 mmol, 1.0 equiv.) was then added to the reaction mixture in one portion and stirred at 60 °C for another 16 hours. The crude mixture was cooled to 0 °C and acidified by dropwise addition of 6M HCl until pH ~ 5. The mixture was diluted with ethyl acetate. The organic phase was separated and dried with anhydrous sodium sulfate. The resulting suspension was filtered, and the filtrate was concentrated under vacuum to provide a residue which was purified by column chromatography on silica-gel (20 % ethyl acetate in hexanes) to afford alkyne **3.18** as a colorless oil (0.667 g, 79 % yield). NMR data was in accordance with what was previously reported.<sup>9</sup>

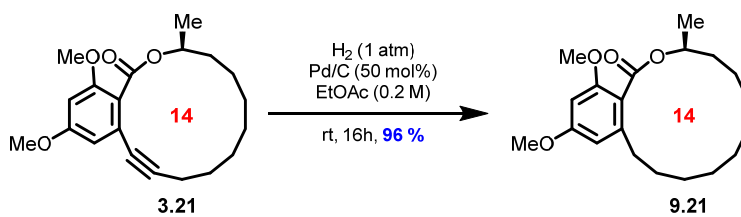


**(S)-Undec-10-yn-2-yl 2-iodo-4,6-dimethoxybenzoate (3.20):** 2-Iodo-4,6-dimethoxybenzoic acid (0.788 g, 2.55 mmol, 1.0 equiv.) and (*R*)-undec-10-yn-2-ol (0.635 g, 3.82 mmol, 1.5 equiv.) were dissolved in anhydrous dichloromethane (13 mL). The stirred solution was cooled to  $0\text{ }^\circ\text{C}$  and triphenylphosphine (1.00 g, 3.82 mmol, 1.5 equiv.) was added followed by diisopropyl azodicarboxylate (0.79 mL, 3.82 mmol, 1.5 equiv.). The mixture was then warmed to room temperature and was stirred for 16 hours. Silica was added to the mixture and the volatiles were removed under vacuum. The resulting solid was placed on a column of silica gel and purified by column chromatography (20 % ethyl acetate in hexanes). Iodide **3.20** was obtained as a colorless oil (1.14 g, 98 % yield).  $^1\text{H}$  NMR (300 MHz,  $\text{CDCl}_3$ )  $\delta$  = 6.88 (d,  $J$  = 2.2 Hz, 1 H), 6.41 (d,  $J$  = 2.0 Hz, 1 H), 5.18-5.12 (m, 1 H), 3.76 (s, 3 H), 3.75 (s, 3 H), 2.16 (dt,  $J$  = 6.9, 2.6 Hz, 2 H), 1.92 (t,  $J$  = 2.6 Hz, 1 H), 1.79 - 1.37 (m, 12 H), 1.34 (d,  $J$  = 6.1 Hz, 3 H);  $^{13}\text{C}$  NMR (75 MHz,  $\text{CDCl}_3$ )  $\delta$  = 167.1, 161.2, 157.5, 123.8, 114.9, 98.8, 92.3, 28.6, 72.5, 68.1, 55.8, 55.6, 35.8, 29.1, 28.9, 28.5, 28.3, 25.2, 19.9, 18.2; HRMS (ESI)  $m/z$  calculated for  $\text{C}_{20}\text{H}_{29}\text{IO}_4$   $[\text{M}+\text{H}]^+$  459.1027; found 459.1040.



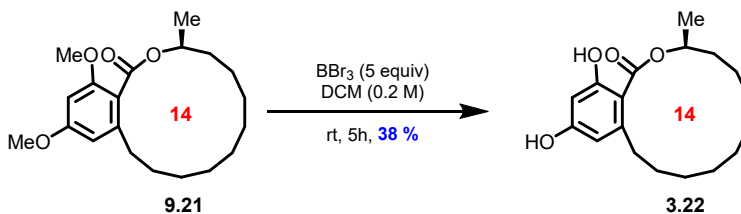
**Macrolactone 3.21:** To a dried sealable tube equipped with a stir bar, copper(I) chloride (0.002 g, 0.006 mmol, 5 mol%), 1,10-phenanthroline (0.018 g, 0.036 mmol, 30 mol%) and cesium carbonate (0.213 g, 0.24 mmol, 2 equiv.) were added. The macrocyclic precursor **3.20** (0.150 g, 0.12 mmol, 1 equiv.) was added to the sealable tube as a toluene solution (14 mL) in one portion. The aperture of the tube was covered with a rubber septum and the reaction mixture was bubbled with nitrogen for 10 minutes. The septum was then replaced by a Teflon-coated screw cap and

the sealed-tube was placed in a pre-heated oil bath at 135 °C. After stirring for 18 hours, the mixture was cooled to room temperature and diluted with ethyl acetate. The resulting solution was filtered through a pad of Celite<sup>®</sup> and concentrated under vacuum to provide a residue which was purified by column chromatography on silica-gel (100 % hexanes → 10 % ethyl acetate in hexanes) to afford macrolactone **3.21** as a white solid (0.061 g, 56 % yield). <sup>1</sup>H NMR (400 MHz, CDCl<sub>3</sub>) δ = 6.54 (d, *J* = 2.3 Hz, 1H), 6.41 (d, *J* = 2.3 Hz, 1H), 5.26 - 5.35 (m, 1H), 3.79 (s, 3H), 3.79 (s, 3H), 2.50 - 2.59 (m, 1H), 2.29 - 2.37 (m, 1H), 1.37 - 1.65 (m, 12H), 1.34 (d, *J* = 6.3 Hz, 3H); <sup>13</sup>C NMR (100 MHz, CDCl<sub>3</sub>) δ = 167.3, 160.8, 157.3, 122.9, 120.6, 107.8, 99.1, 94.0, 78.2, 70.7, 55.9, 55.5, 35.1, 26.5, 26.0, 25.8, 25.0, 22.2, 20.4, 19.1; HRMS (ESI) *m/z* calculated for C<sub>20</sub>H<sub>28</sub>O<sub>4</sub> [M+H]<sup>+</sup> 331.1904; found 331.1909.



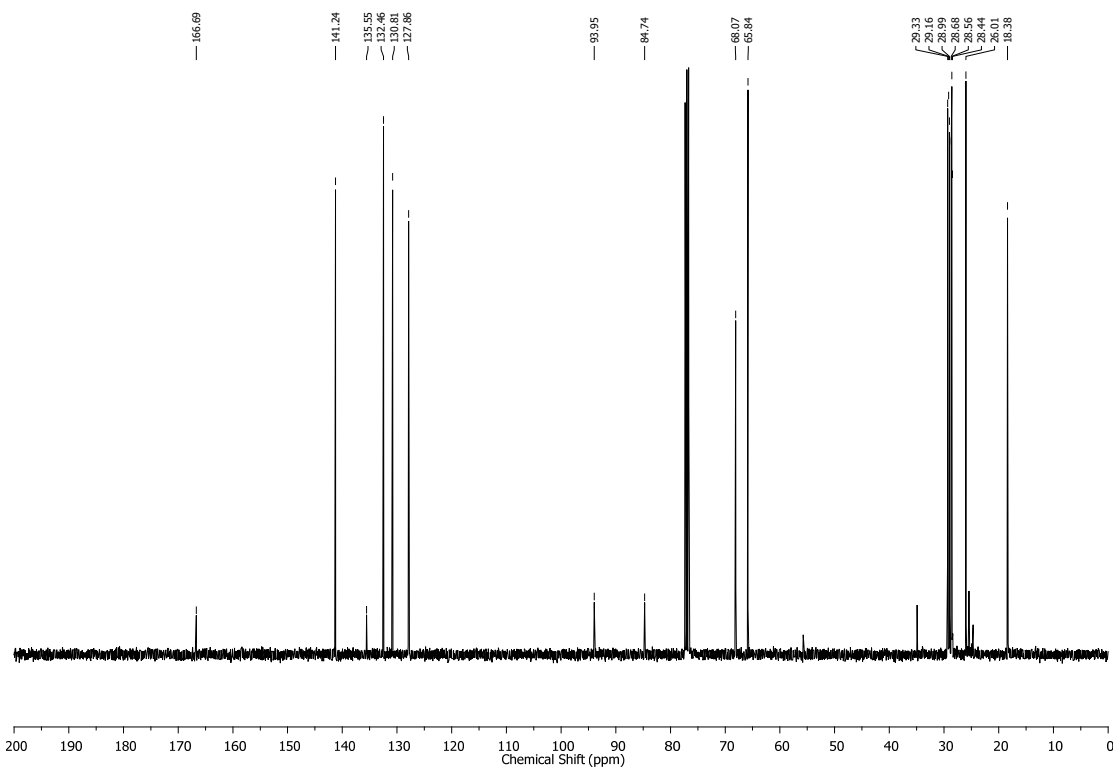
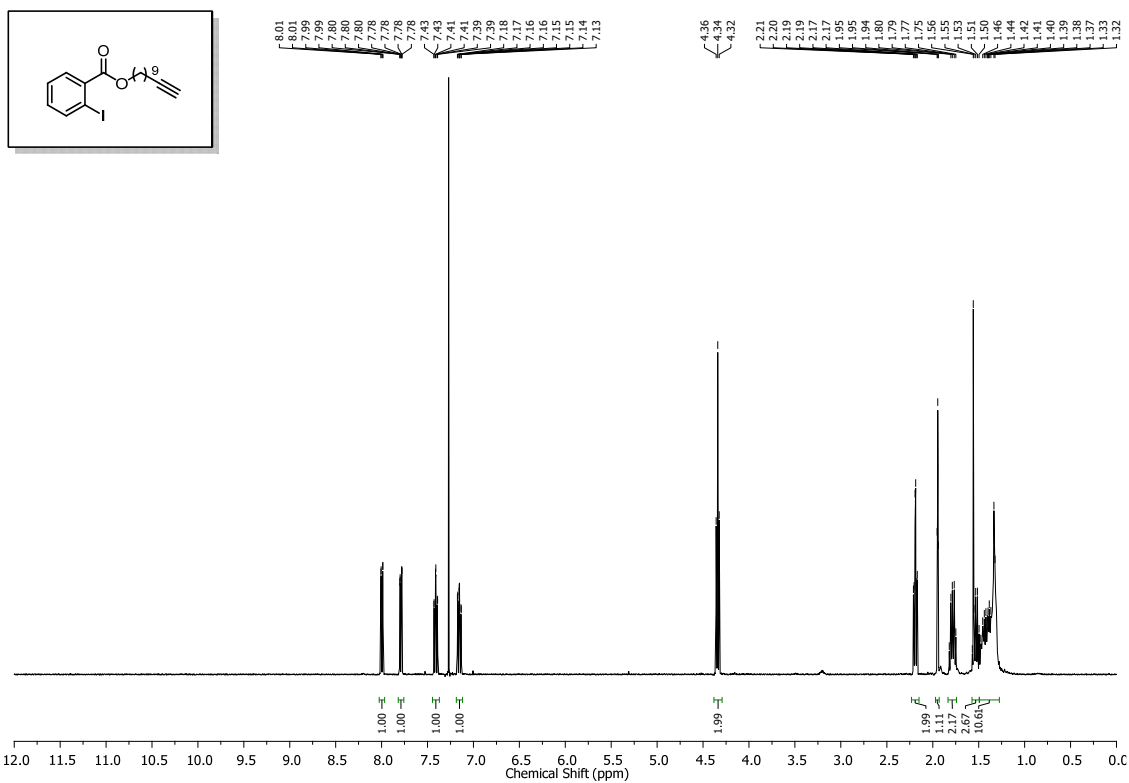
**Macrolactone 9.21:** Macrolactone **3.21** (0.037 g, 0.10 mmol, 1.0 equiv.) was dissolved in ethyl acetate (5 mL). The solution was degassed with nitrogen. Palladium on carbon (0.107 g, 0.05 mmol, 50 mol%) was added to the reaction mixture. The suspension was then bubbled with hydrogen for 5 to 10 minutes and it was stirred under a hydrogen atmosphere (balloon) for an additional 16 hours. The mixture was then filtered on Celite<sup>®</sup> and the filtrate was evaporated under vacuum. Macrolactone **9.21** was obtained as a colorless oil (0.032 g, 96 % yield). <sup>1</sup>H NMR (700 MHz, CDCl<sub>3</sub>) δ = 6.37 (d, *J* = 2.0 Hz, 1 H), 6.31 (d, *J* = 2.1 Hz, 1 H), 5.33 - 5.26 (m, 1 H), 3.80 (s, 3 H), 3.79 (s, 3 H), 2.74 - 2.70 (m, 1 H), 2.49 - 2.44 (m, 1 H), 1.71 - 1.36 (m, 10 H), 1.35 (d, *J* = 6.3 Hz, 3 H), 1.33 - 1.22 (m, 6 H); <sup>13</sup>C NMR (175 MHz, CDCl<sub>3</sub>) δ = 168.6, 161.1, 157.8, 142.6, 117.4, 105.5, 96.3, 70.6, 55.8, 55.3, 34.9, 32.5, 29.8, 27.2, 25.9, 25.6, 25.1, 24.1, 21.9, 20.2; HRMS (ESI) *m/z* calculated for C<sub>20</sub>H<sub>31</sub>O<sub>4</sub> [M+H]<sup>+</sup> 335.2217; found 335.2229.

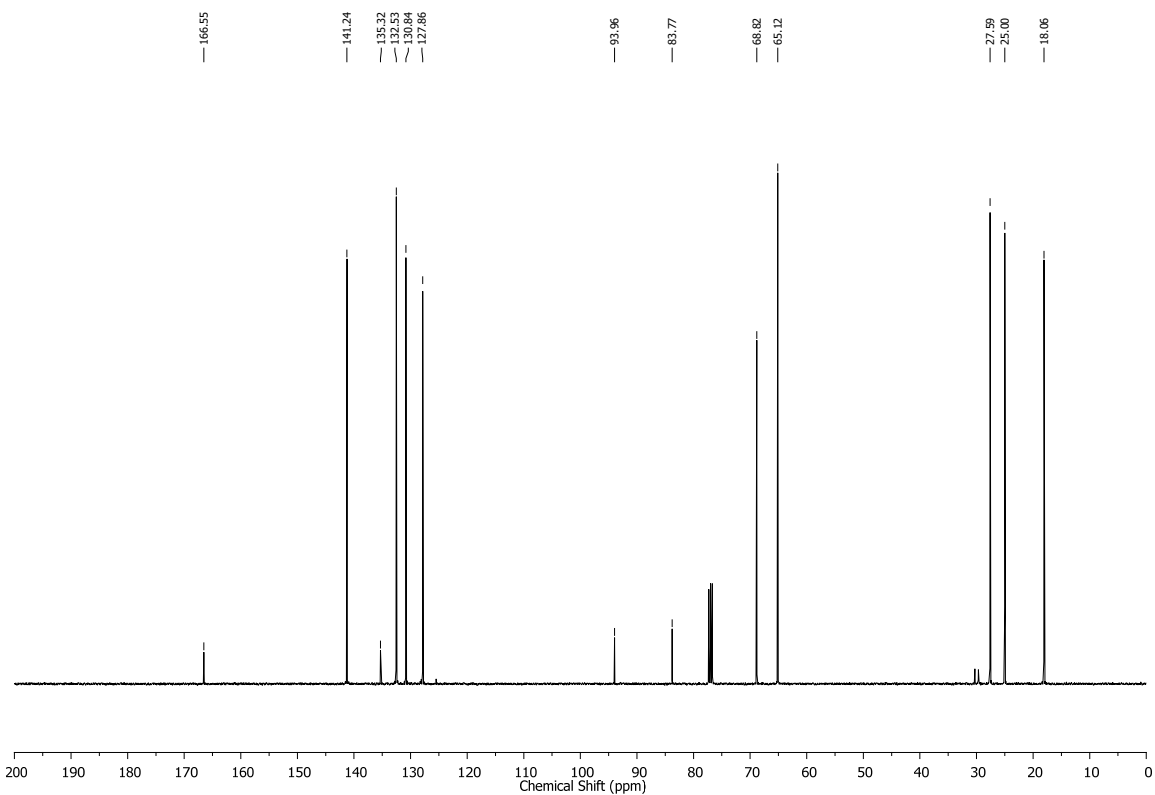
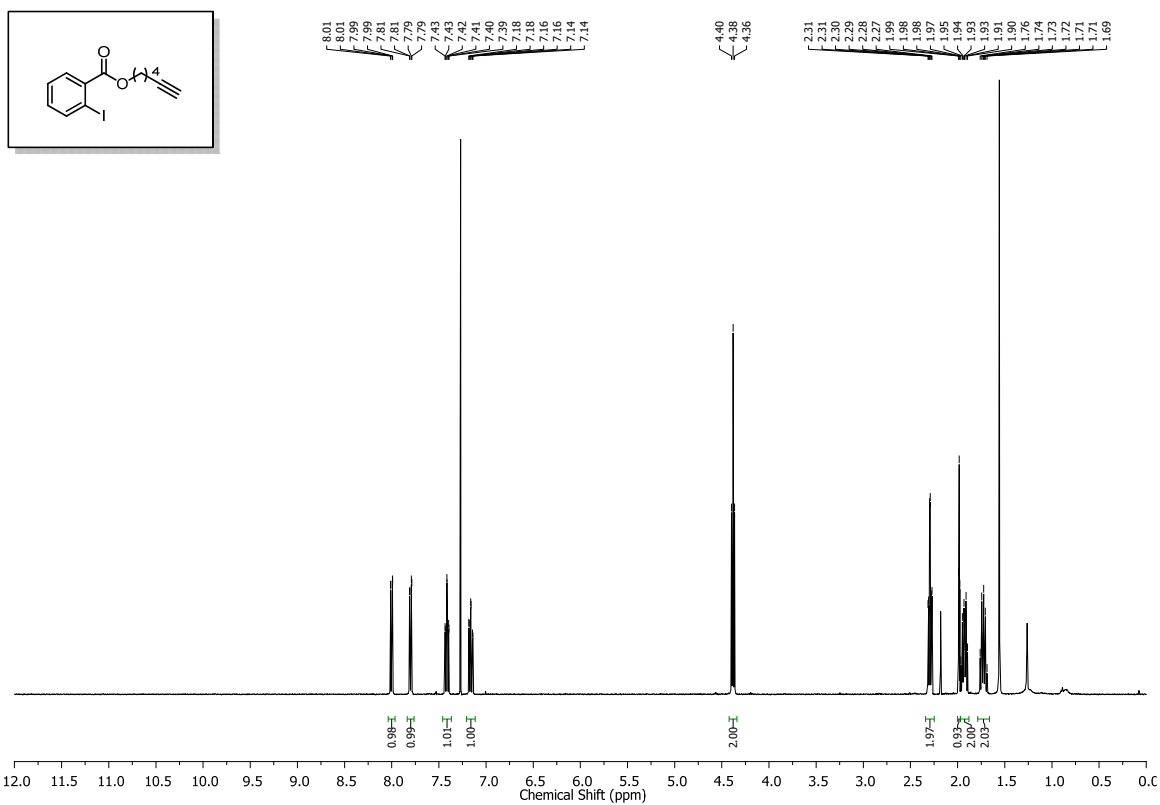


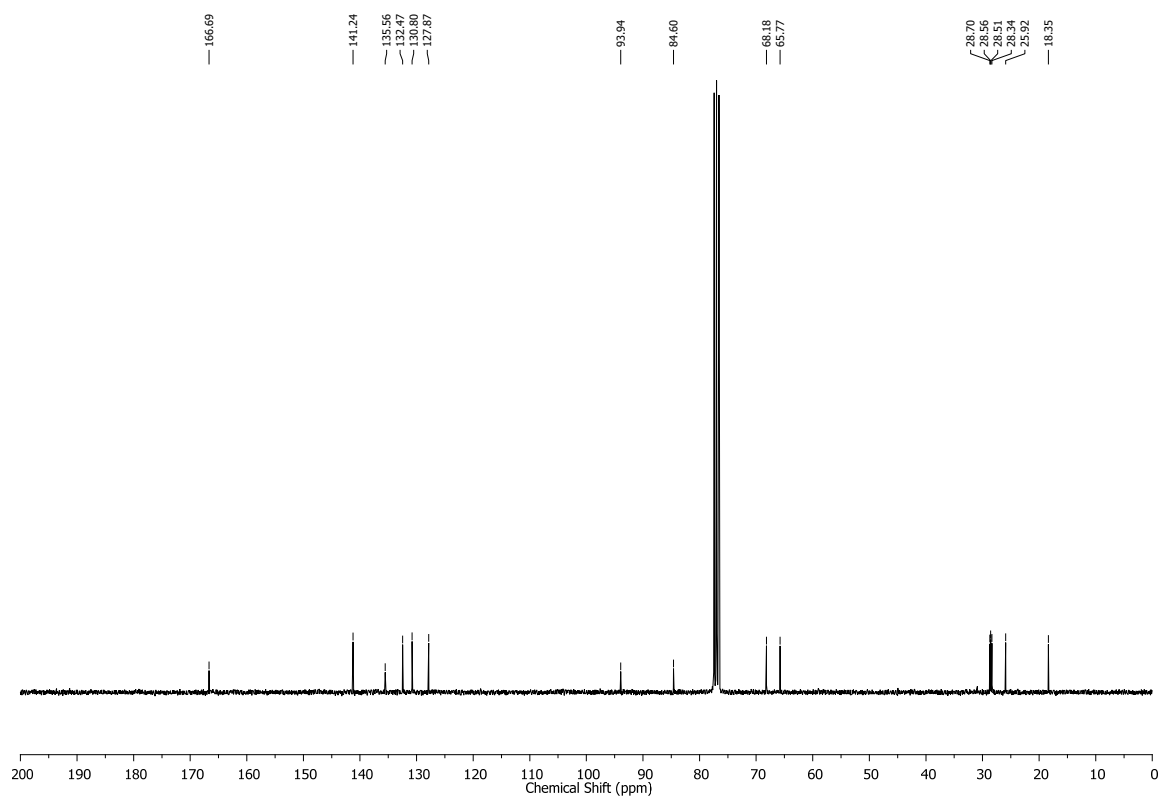
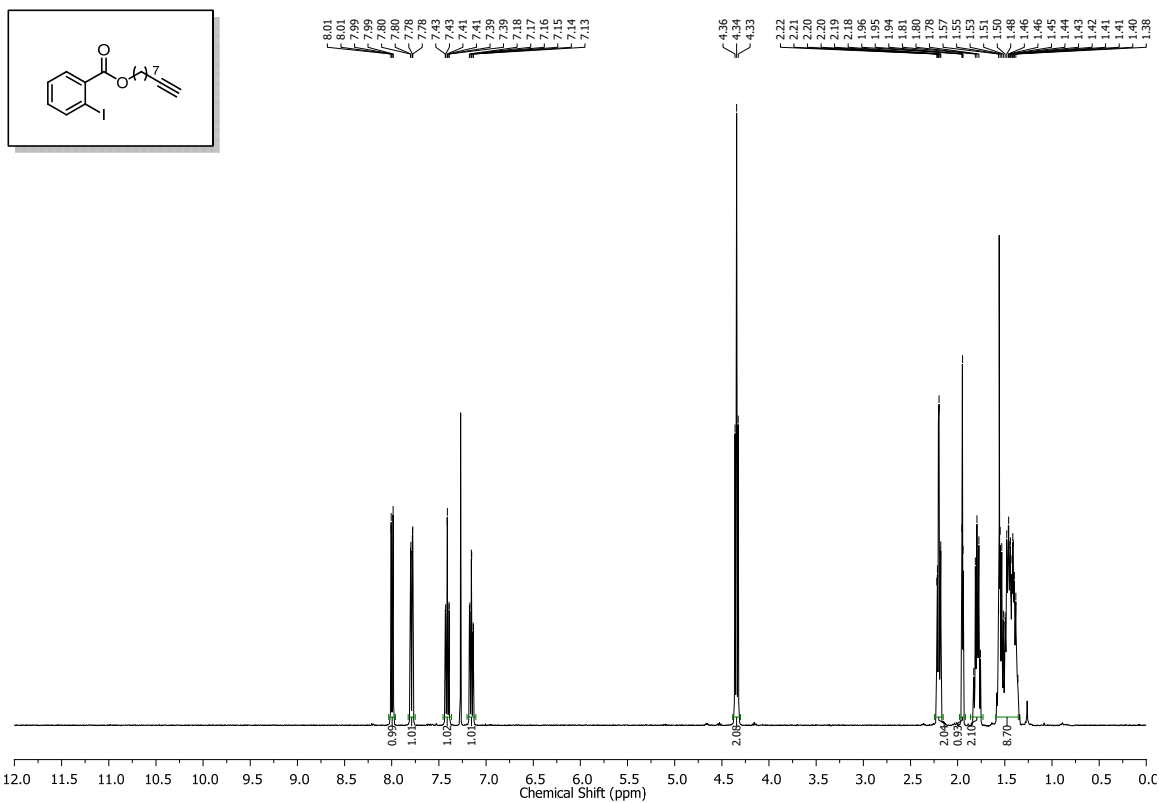


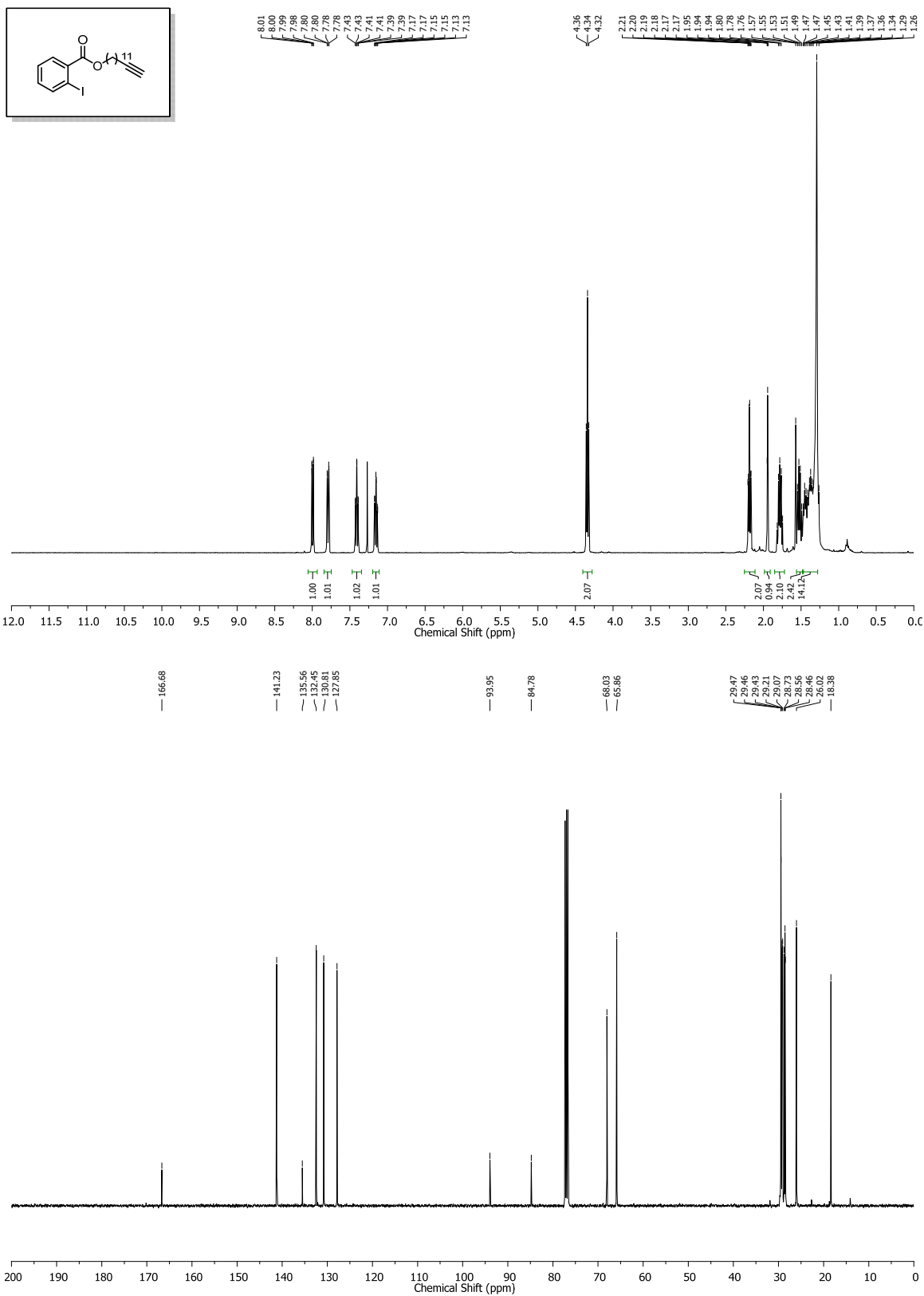
**(S)-Zearalane (3.22):** Macrolactone **9.21** (0.028 g, 0.09 mmol, 1.0 equiv.) was dissolved in anhydrous dichloromethane (1 mL) and cooled to 0 °C. Boron tribromide (1 M in hexanes, 0.425 mL, 0.425 mmol, 5.0 equiv.) was added dropwise to the reaction mixture. The solution was stirred at 0 °C for 30 minutes and was then warmed to room temperature over 5 hours. Sodium hydroxide (1 M) was added to the reaction mixture and stirred for 30 minutes. Dichloromethane and water were added to the mixture. The organic phases were separated and dried with anhydrous sodium sulfate. The resulting suspension was filtered, and the filtrate was concentrated under vacuum to provide a residue which was purified by column chromatography on silica-gel (20 % ethyl acetate in hexanes) to afford (*S*)-zearalane **3.22** as a white solid (0.011 g, 38 % yield). <sup>1</sup>H NMR (400 MHz, CDCl<sub>3</sub>) δ = 12.12 (s, 1 H), 6.28 (d, *J* = 2.7 Hz, 1 H), 6.23 (d, *J* = 2.6 Hz, 1 H), 5.29 - 5.13 (m, 1 H), 5.06 (s, 1 H), 3.28 (dt, *J* = 12.3, 4.0 Hz, 1 H), 2.45 (dt, *J* = 12.5, 4.8 Hz, 1 H), 1.95 - 1.67 (m, 2 H), 1.56 - 1.39 (m, 14 H), 1.37 (d, *J* = 6.2 Hz, 3 H); <sup>13</sup>C NMR (100 MHz, CDCl<sub>3</sub>) δ = 171.7, 165.7, 160.0, 149.2, 110.4, 105.5, 101.5, 73.7, 37.2, 34.8, 31.3, 26.81, 26.76, 26.7, 22.5, 22.2, 21.3; HRMS (ESI) *m/z* calculated for C<sub>18</sub>H<sub>26</sub>NaO<sub>4</sub> [M+Na]<sup>+</sup> 329.1723; found 329.1726. NMR data was in accordance with what was previously reported.<sup>9</sup>

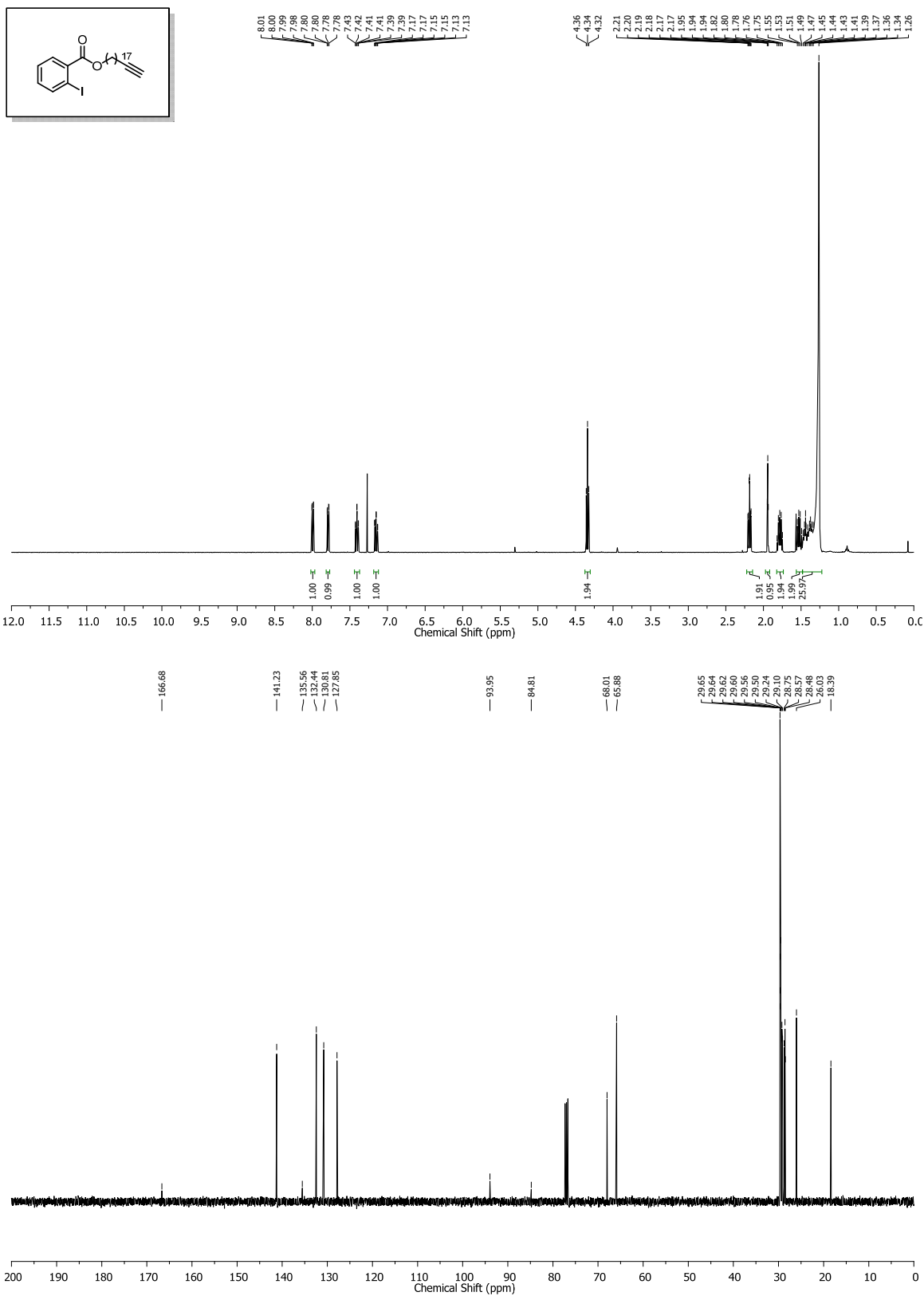
## 9.5 NMR Data for all New Compounds

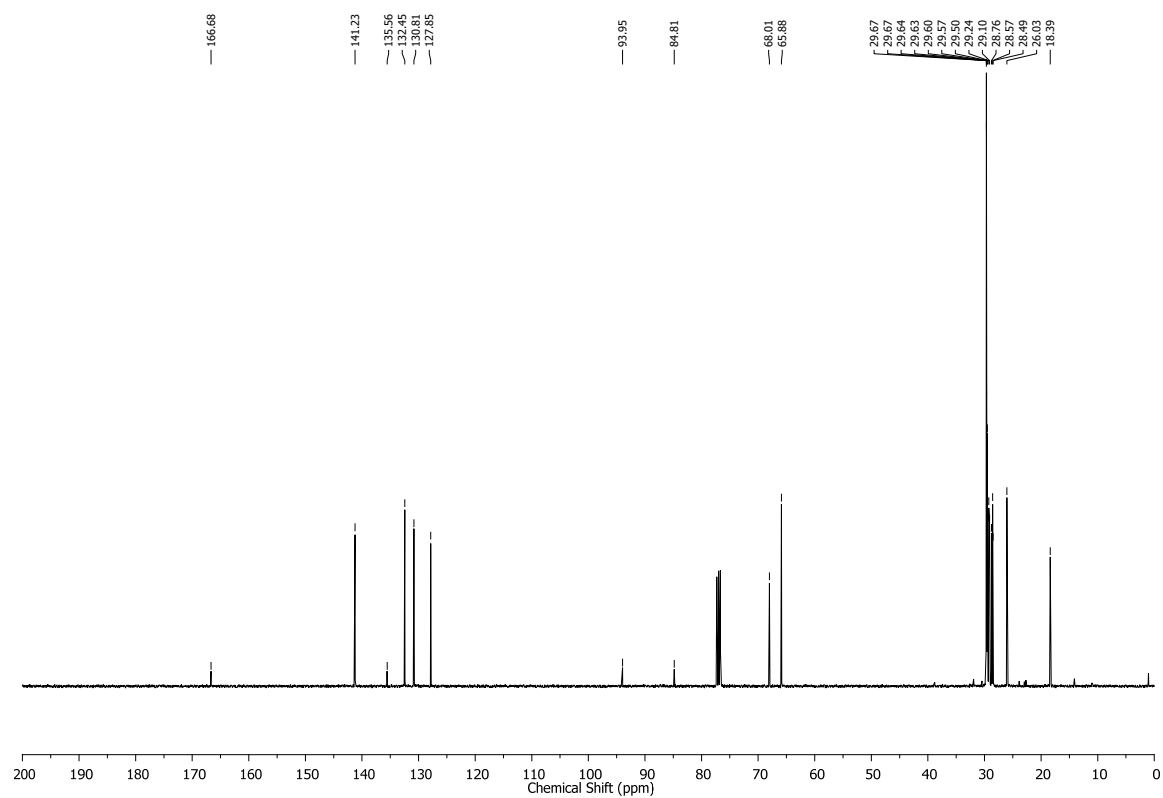
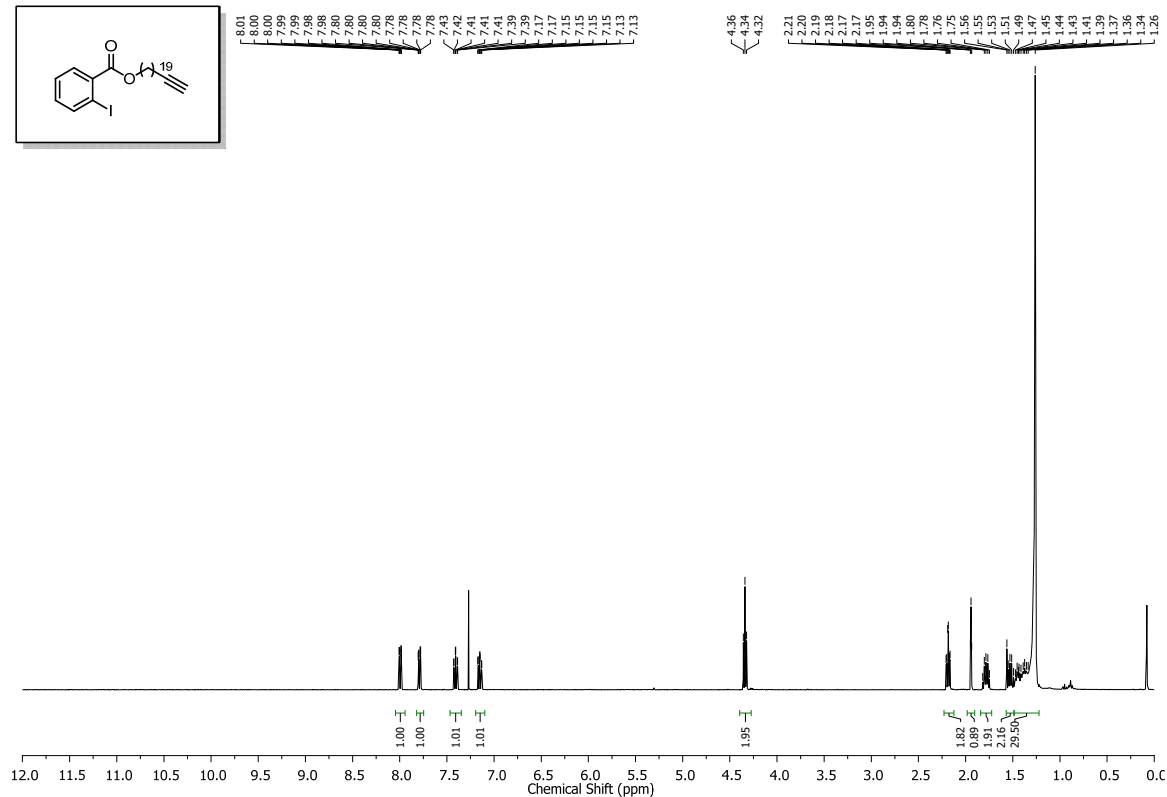


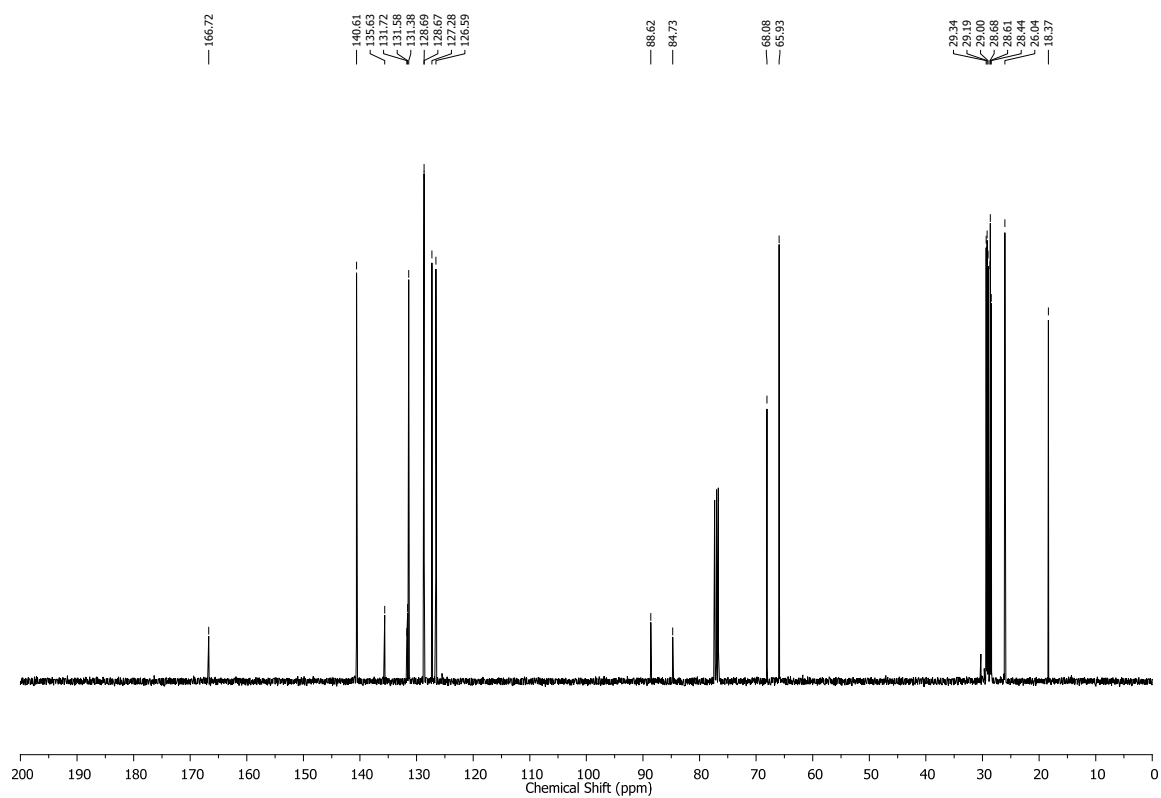
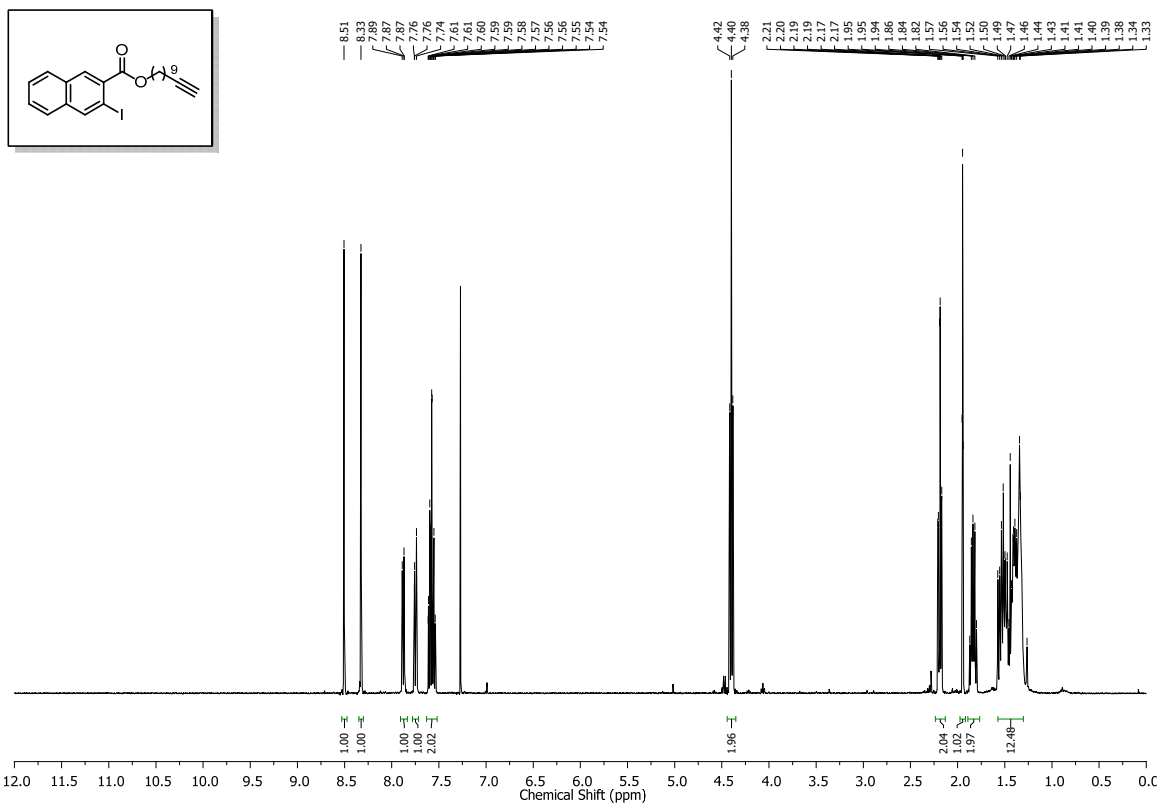




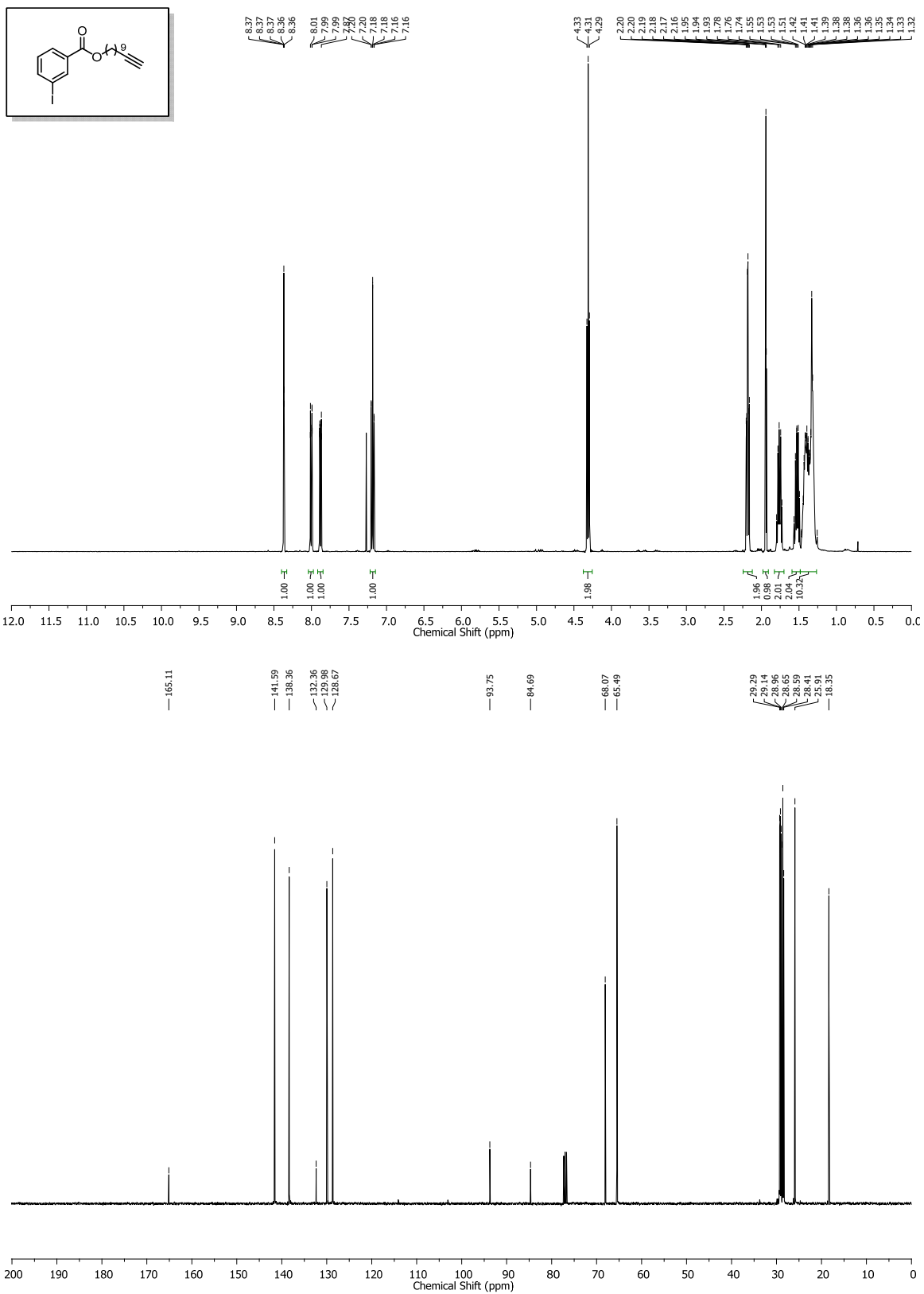


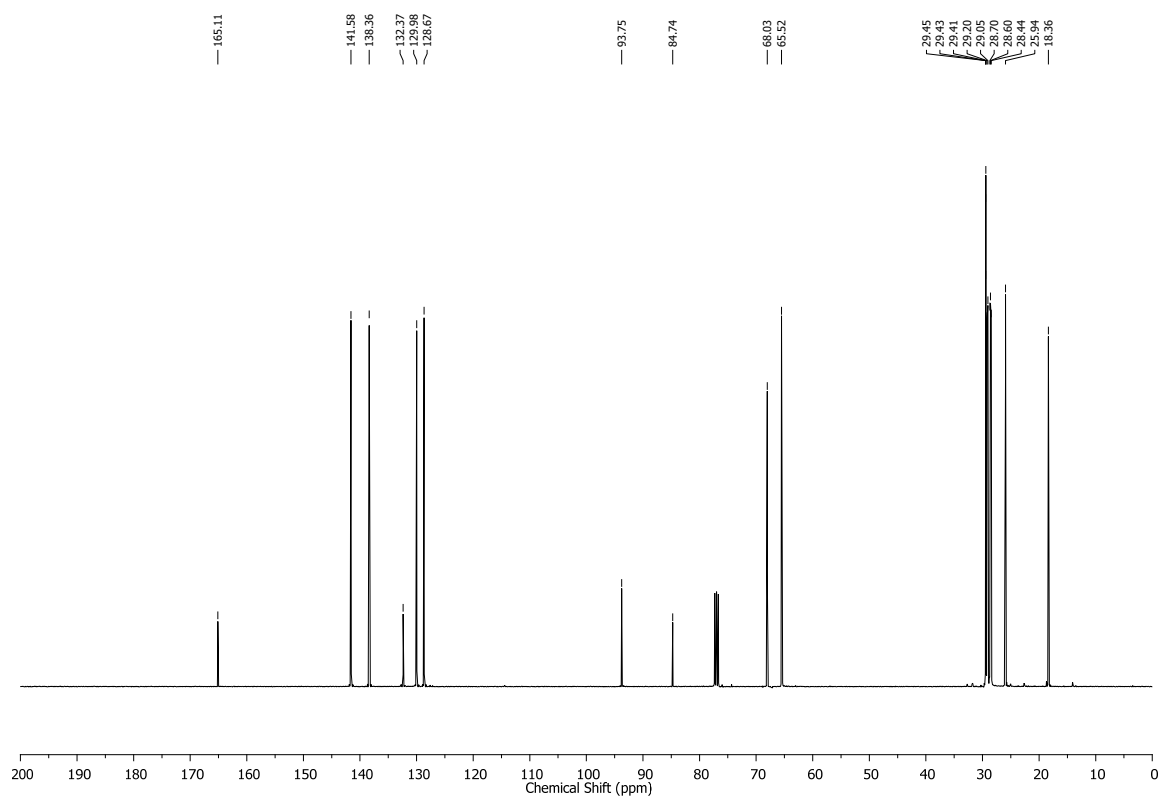
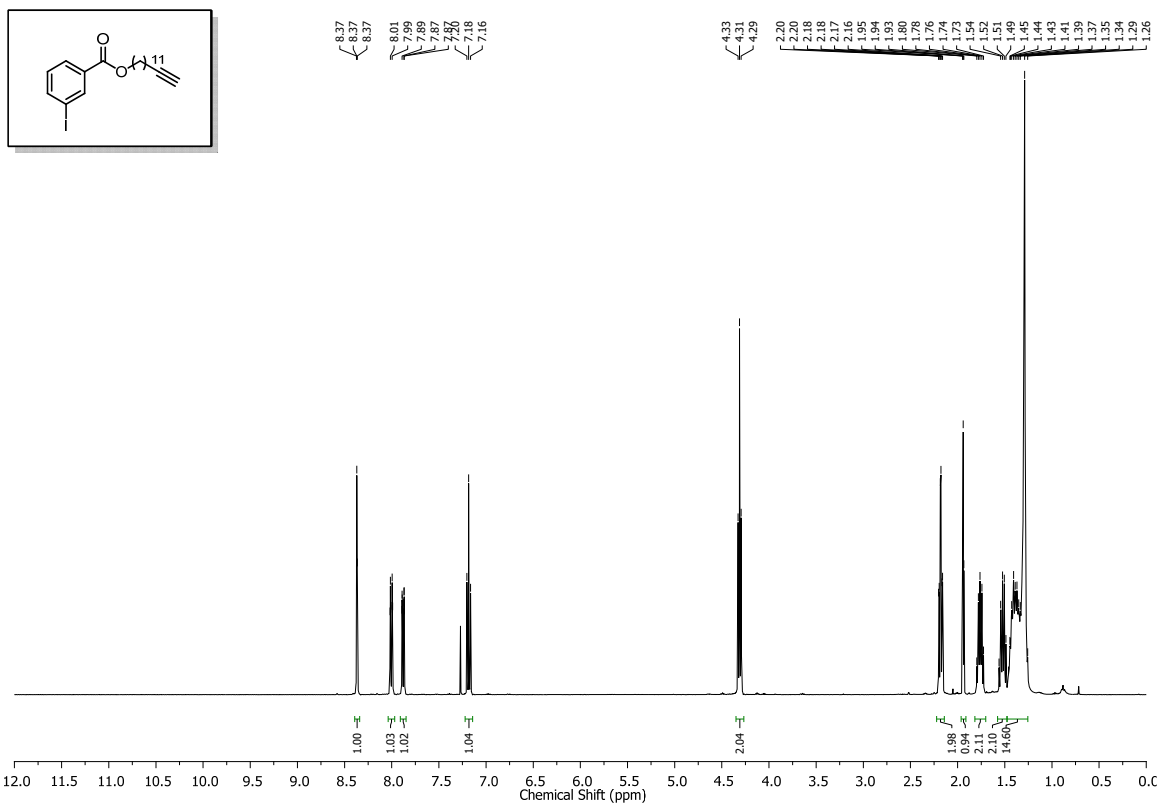


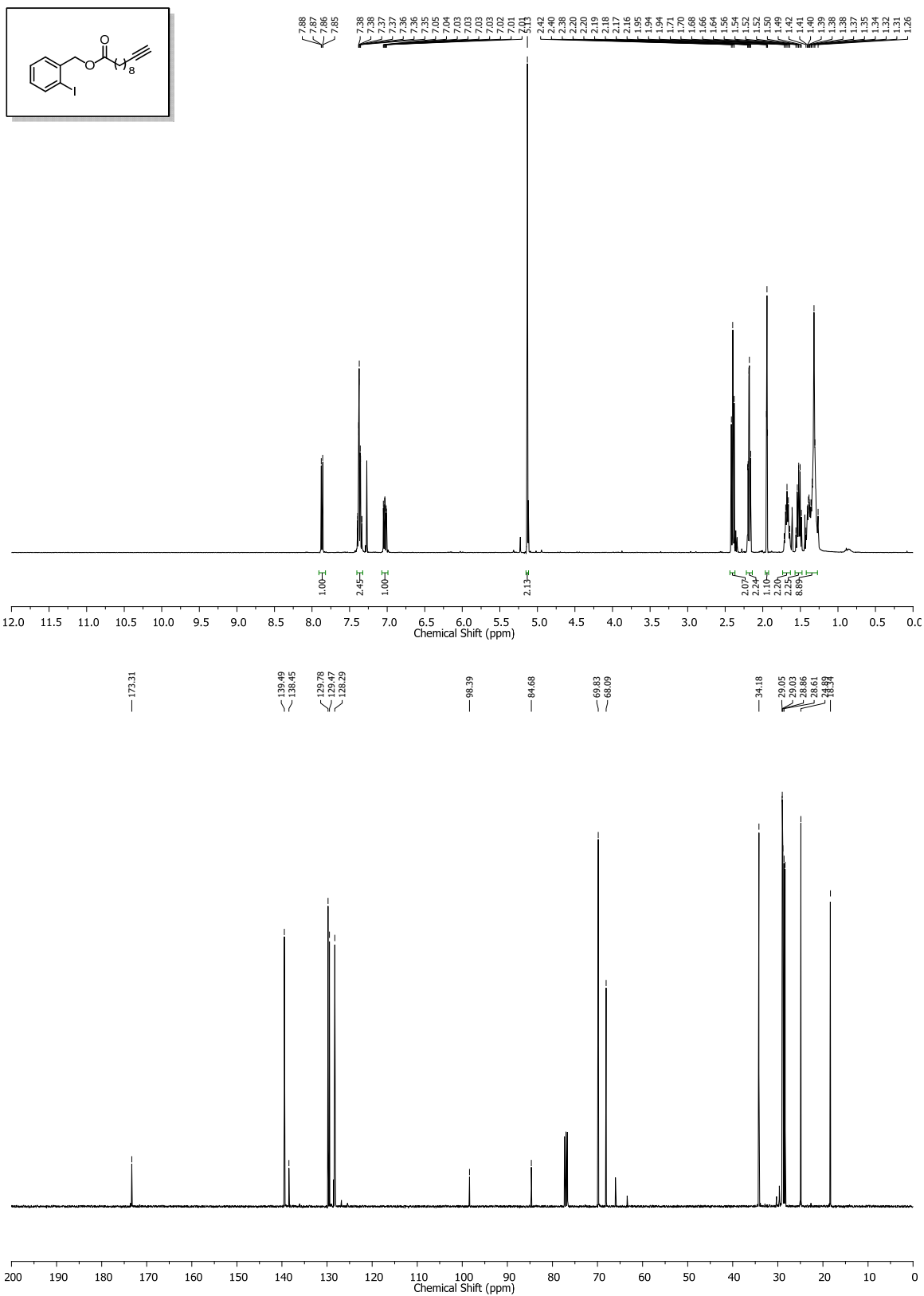


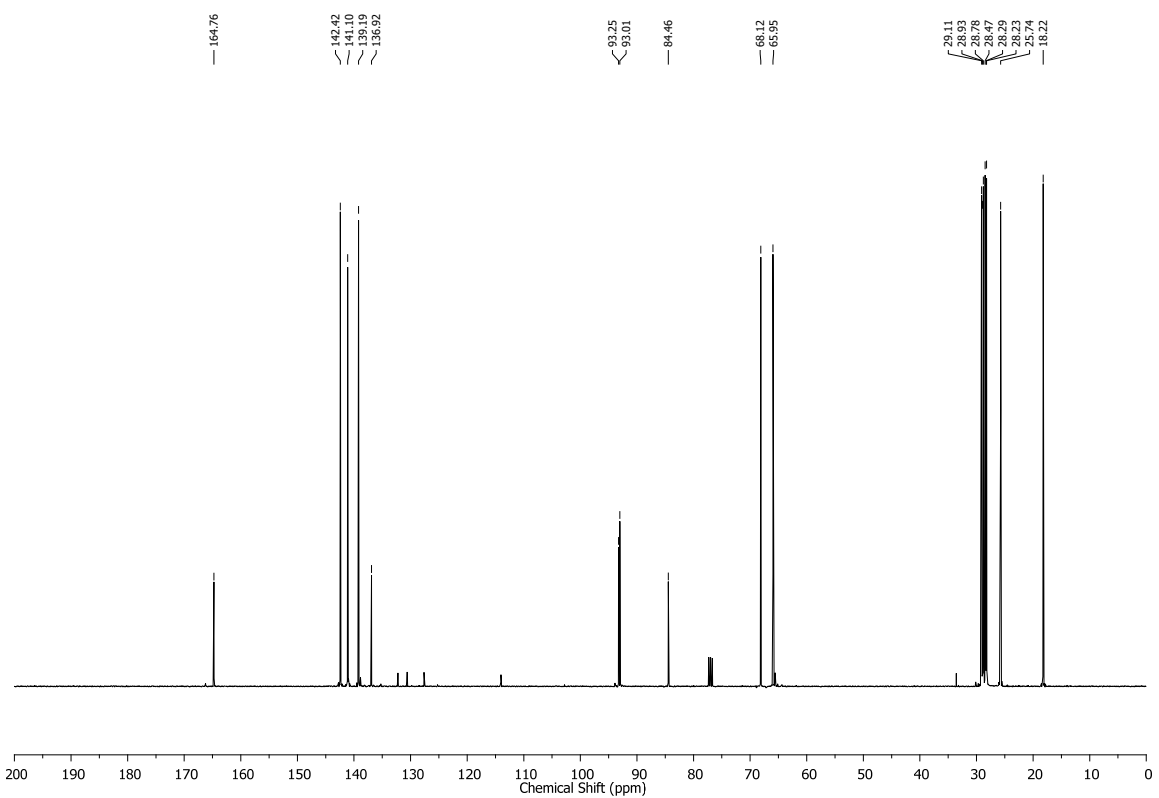
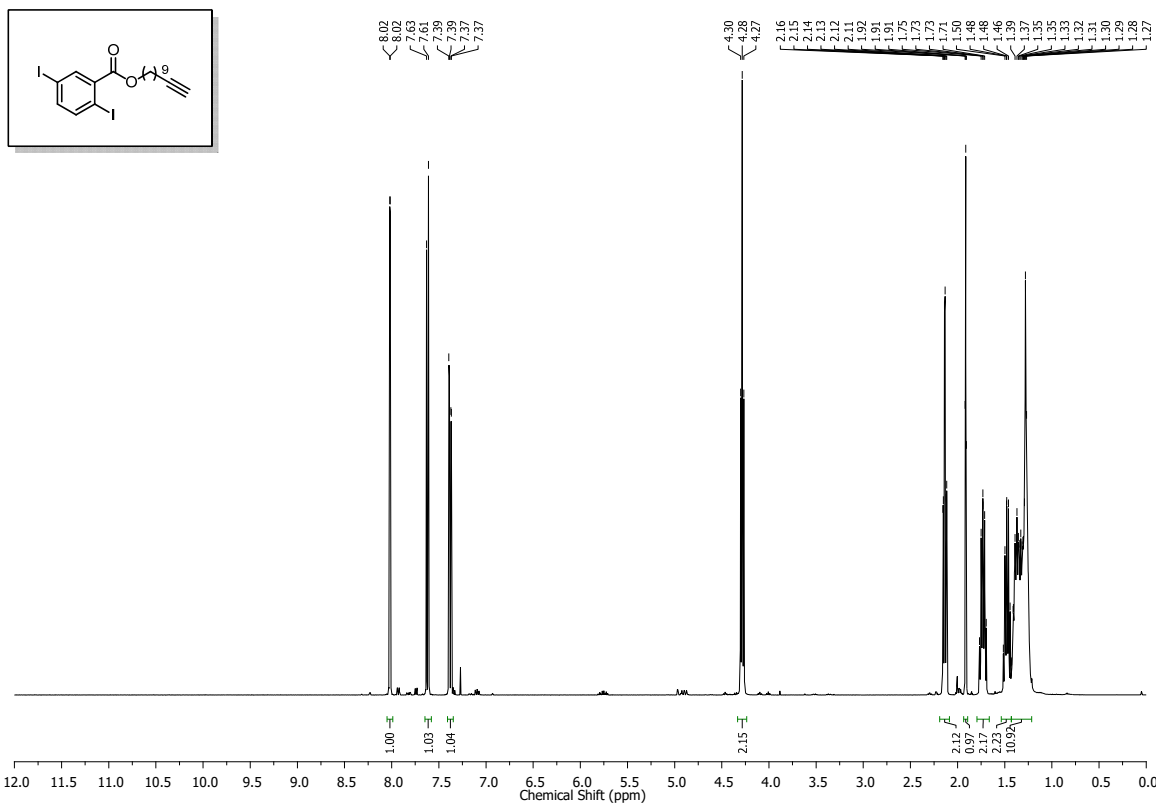


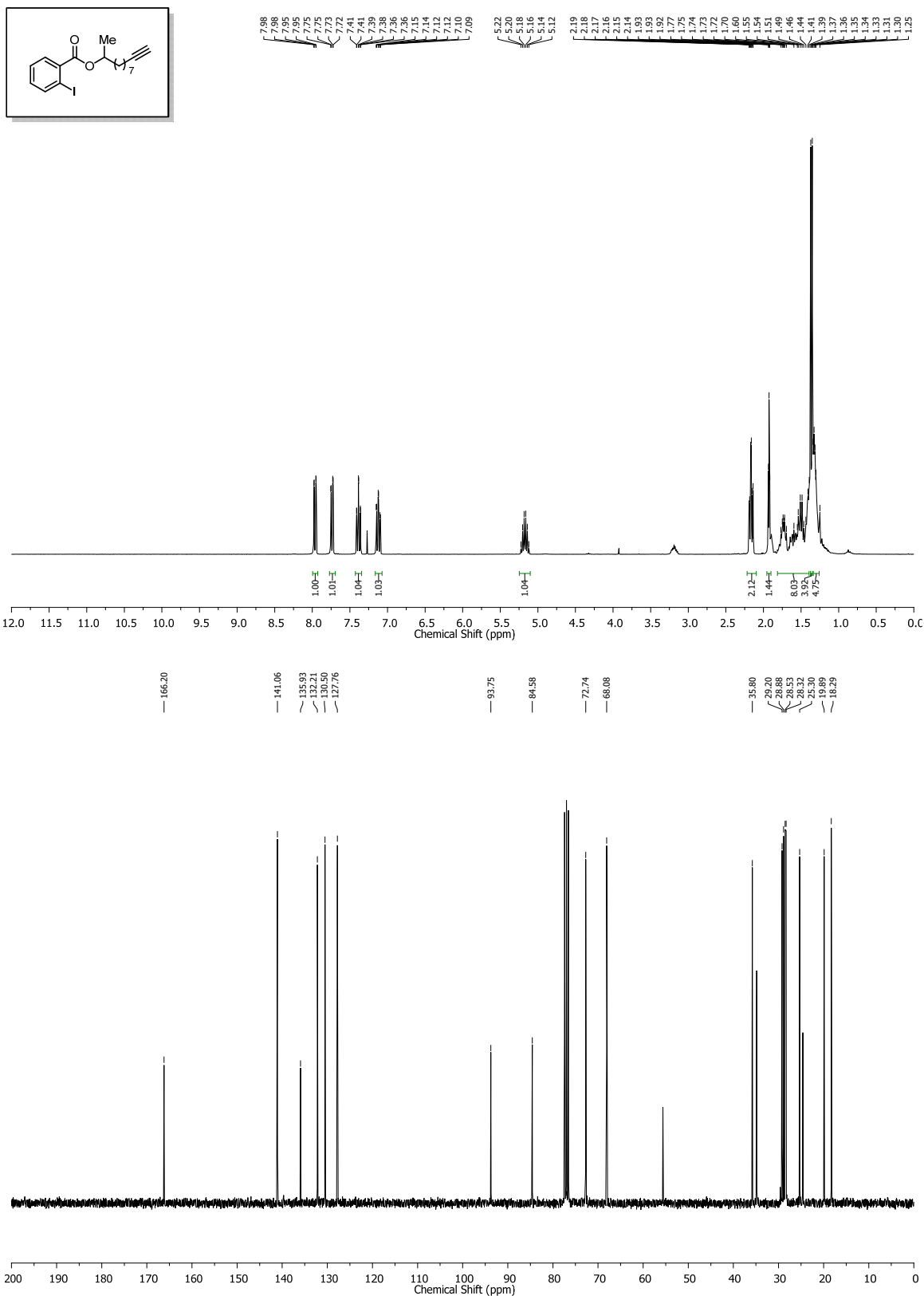


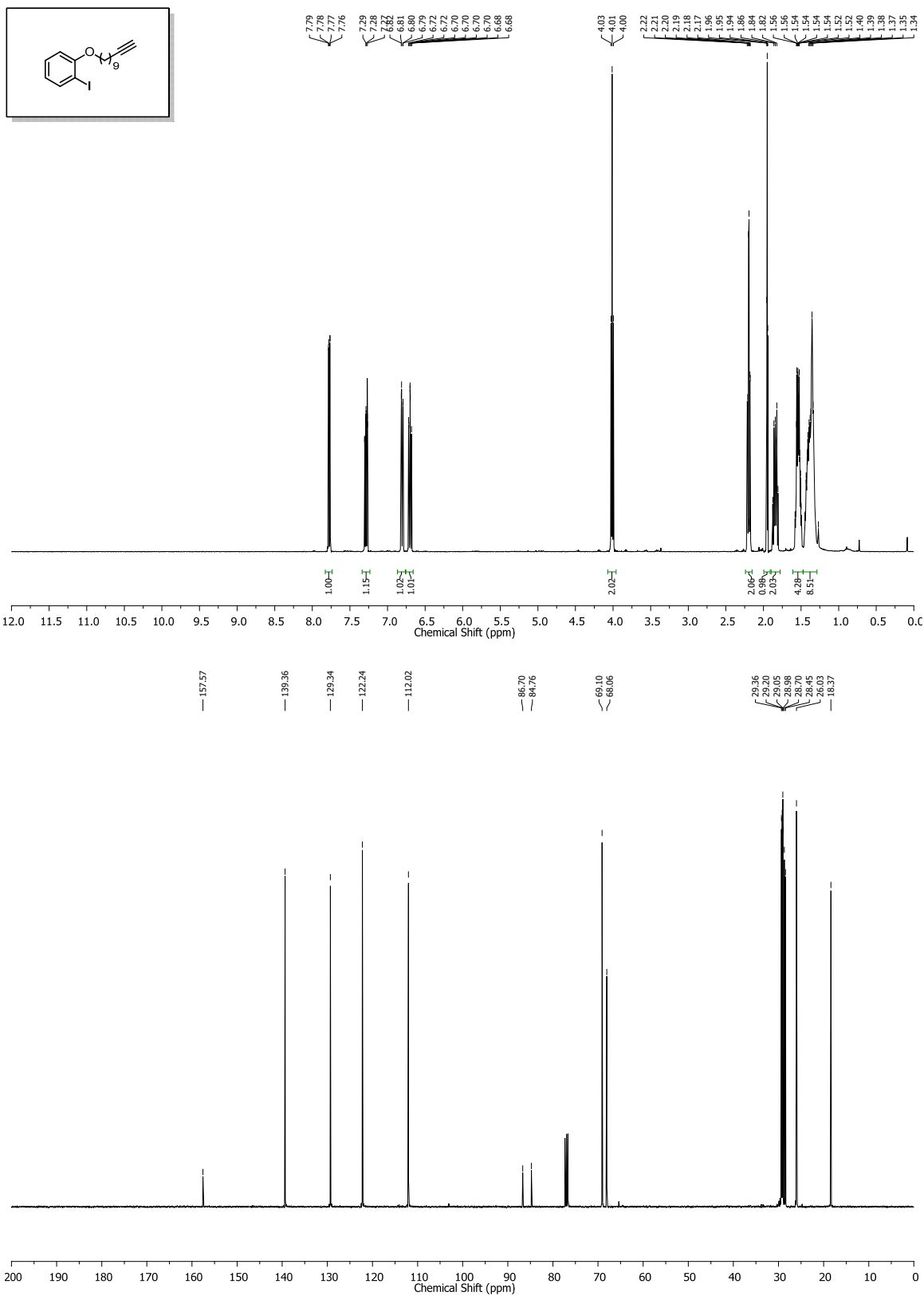


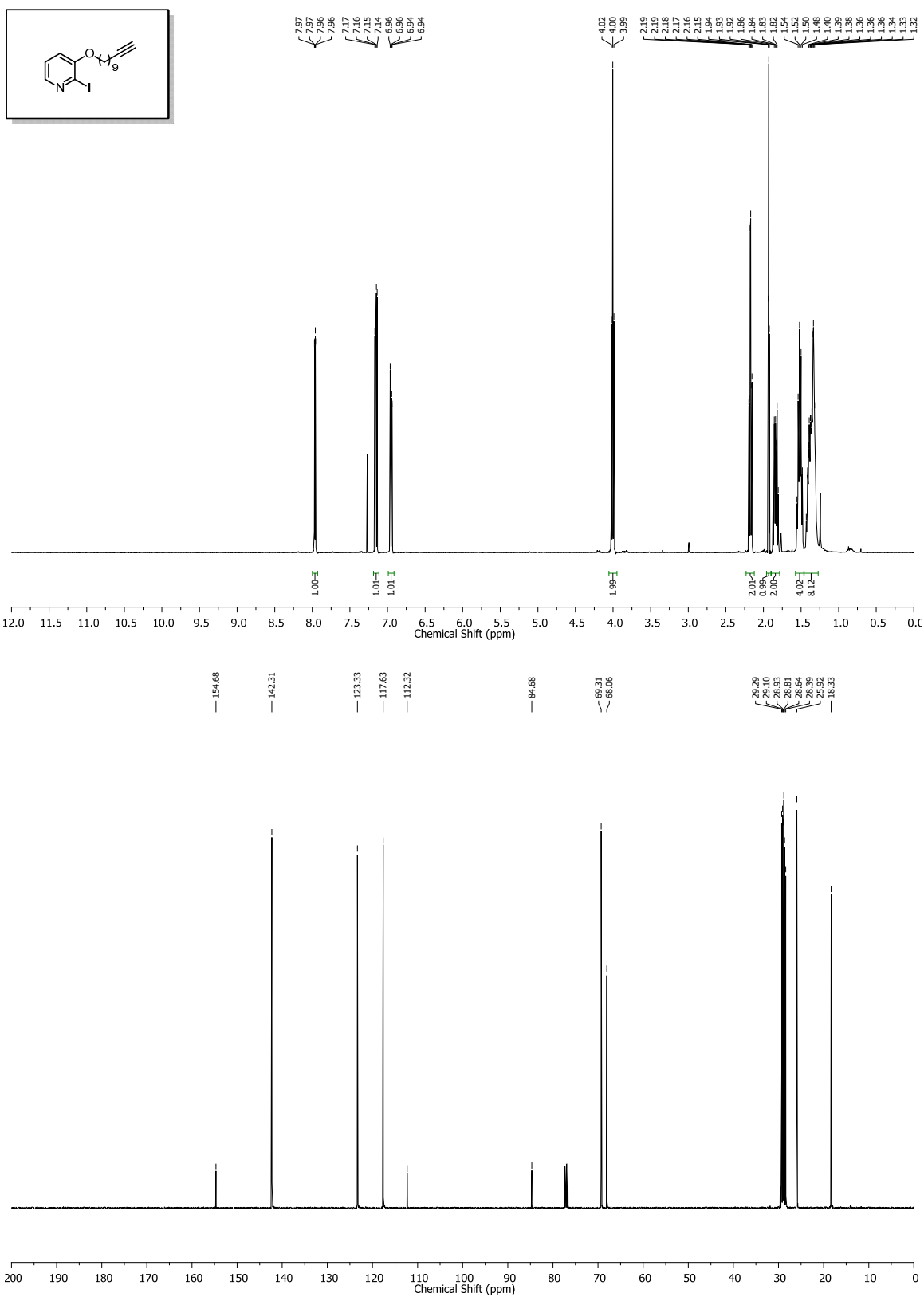


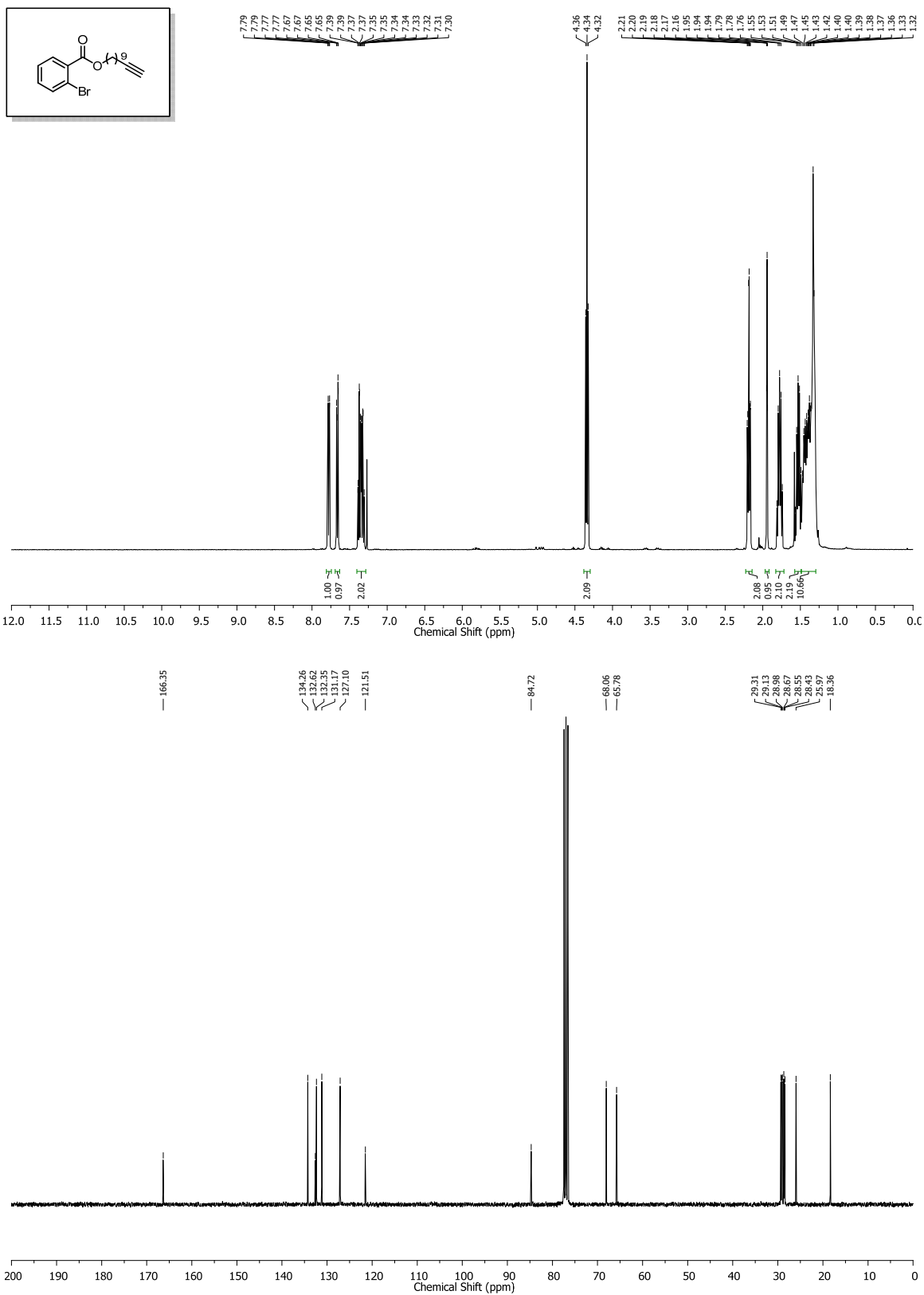




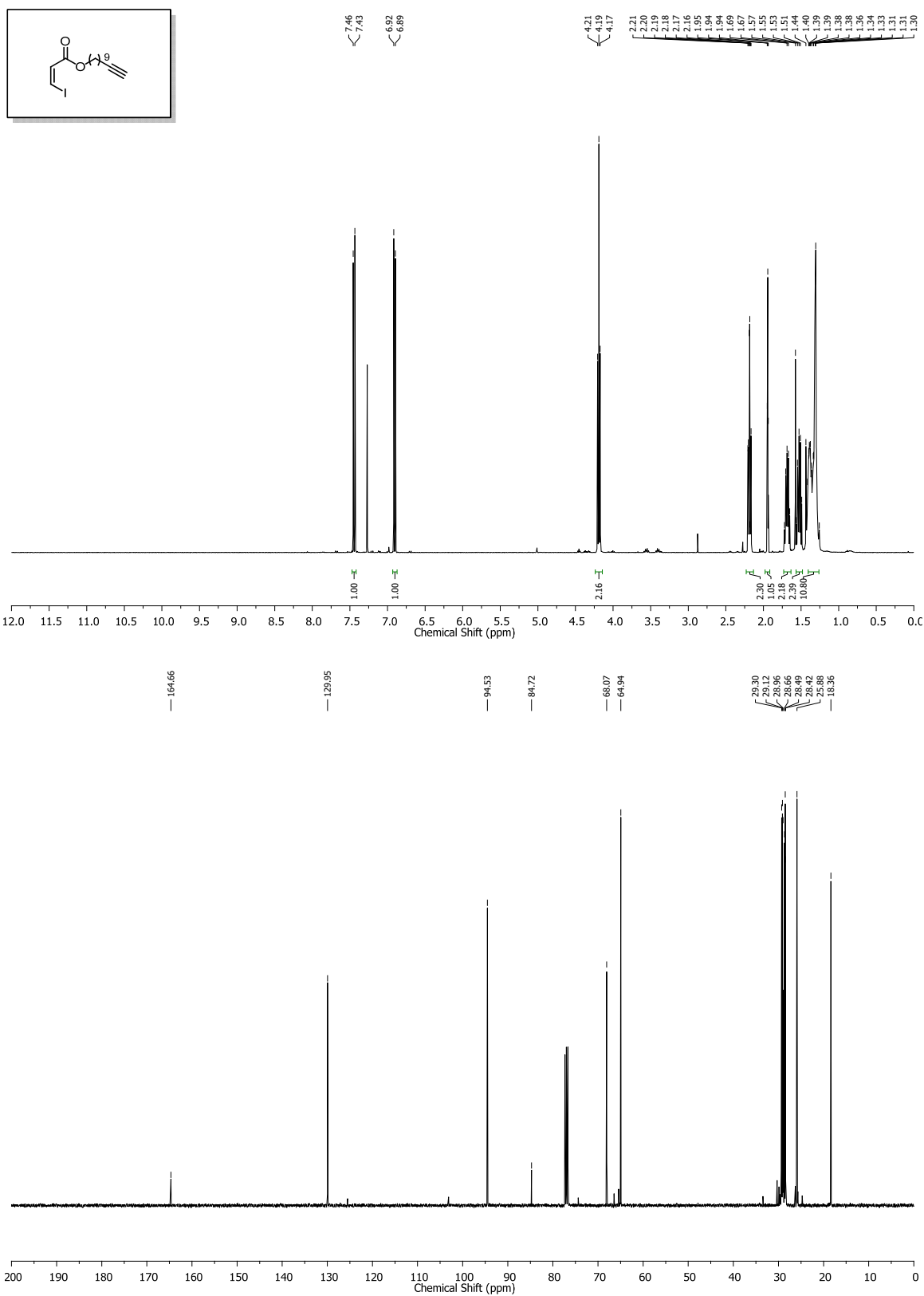


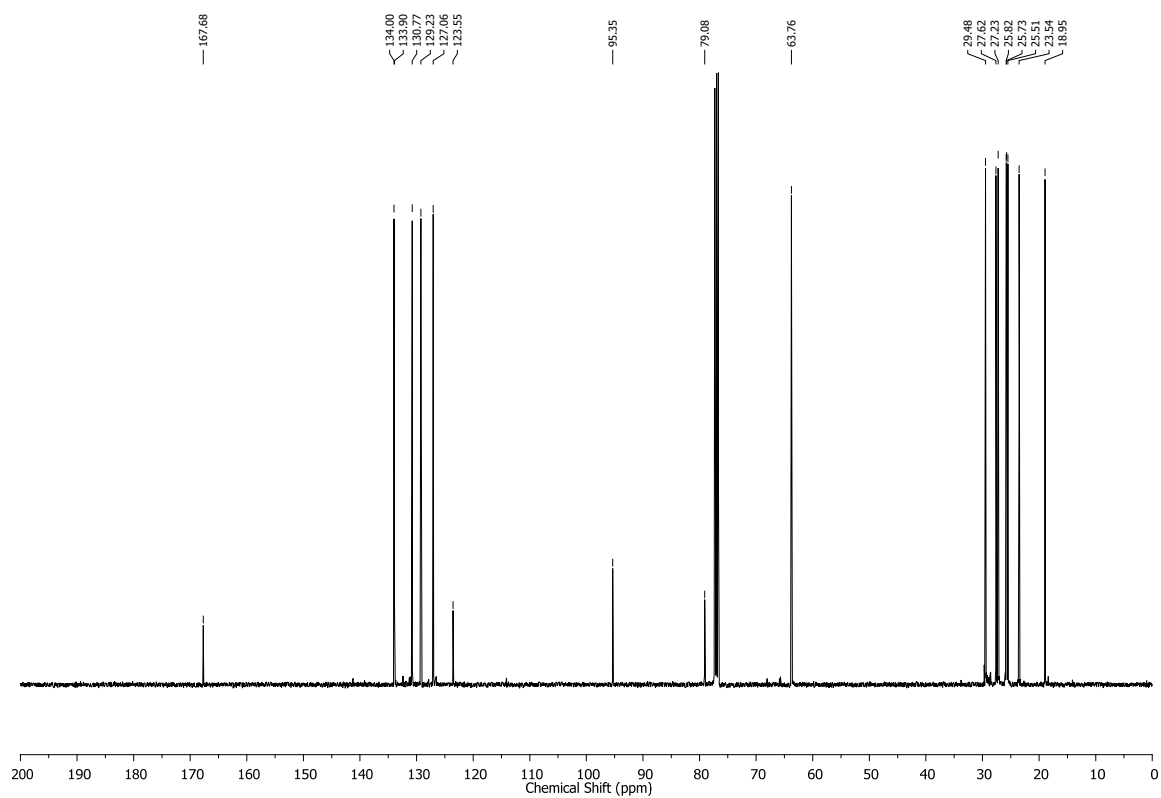
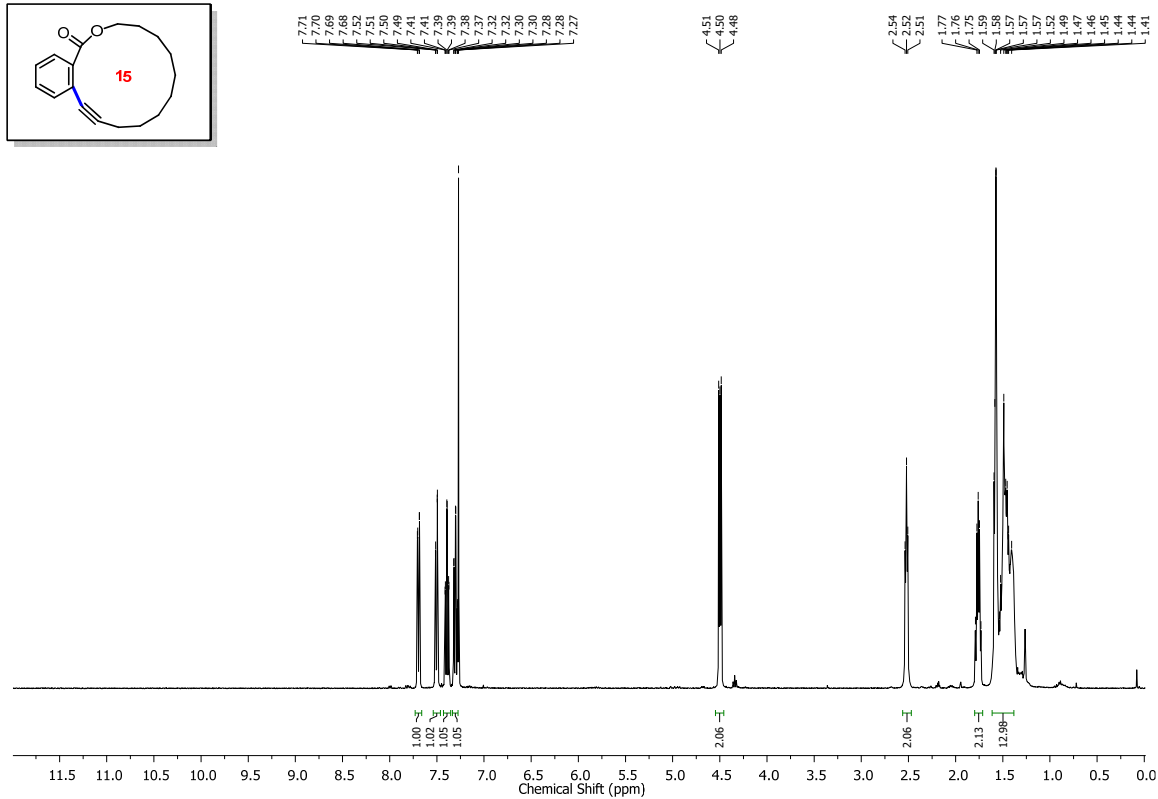
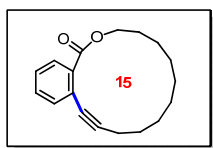


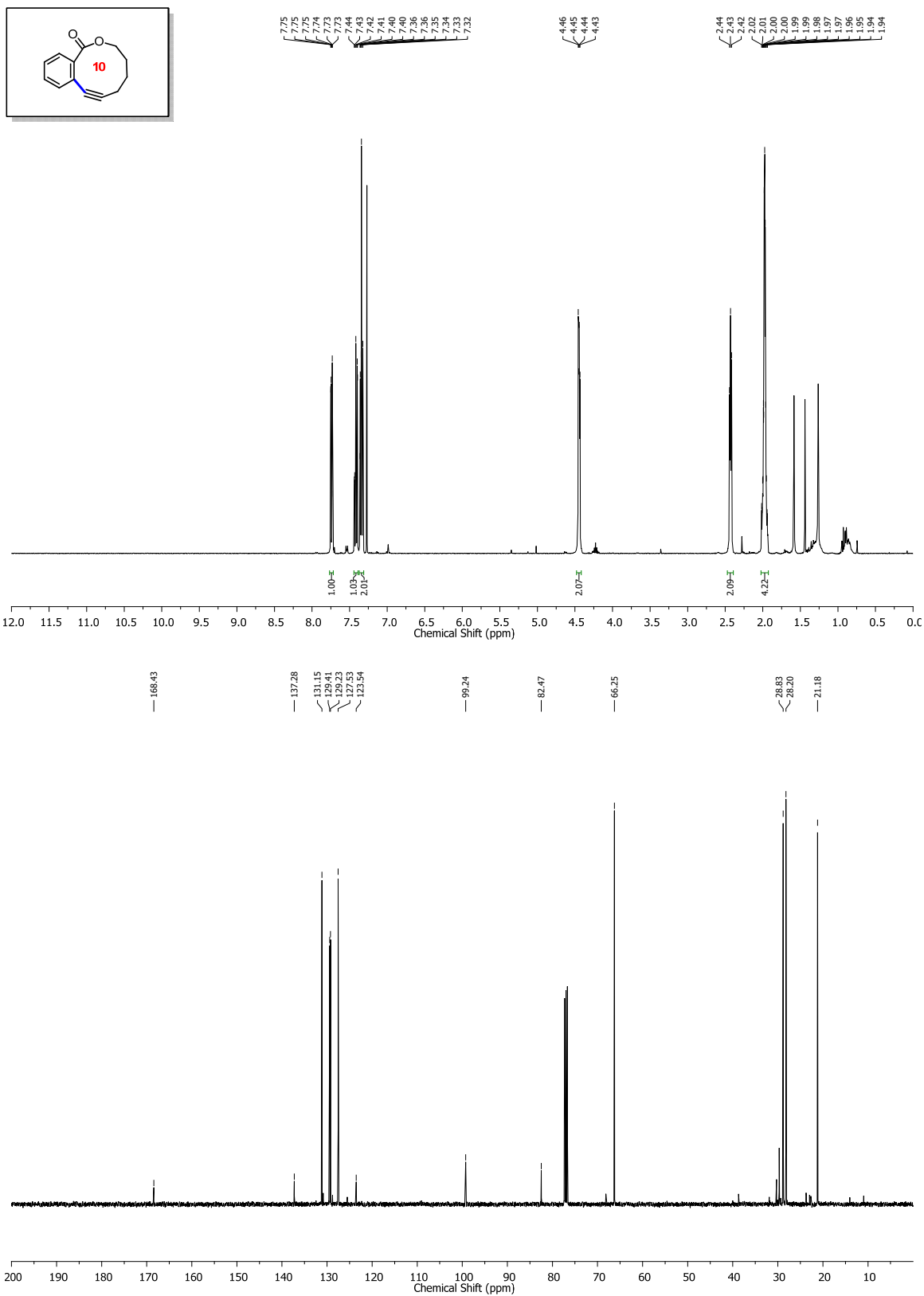


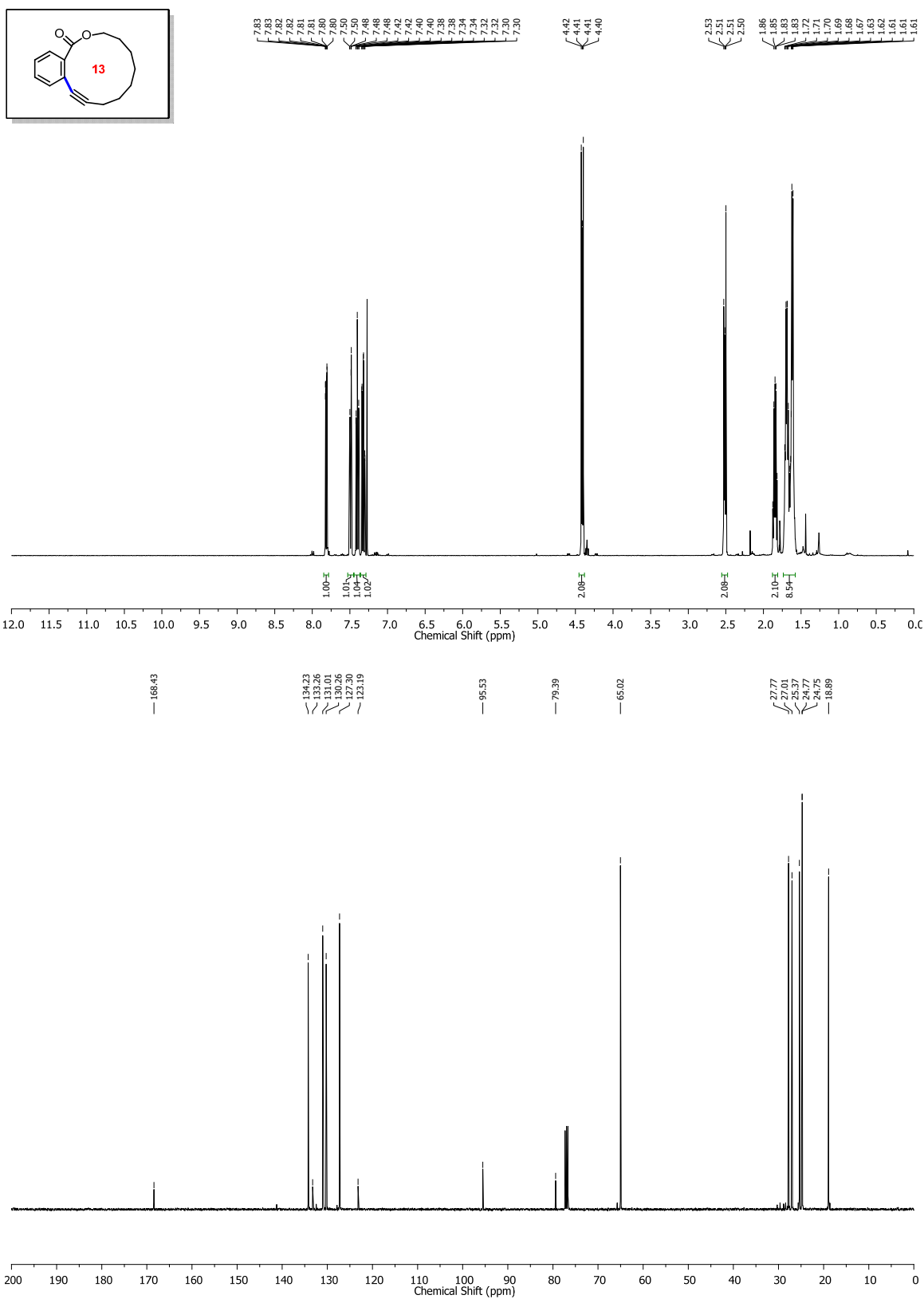


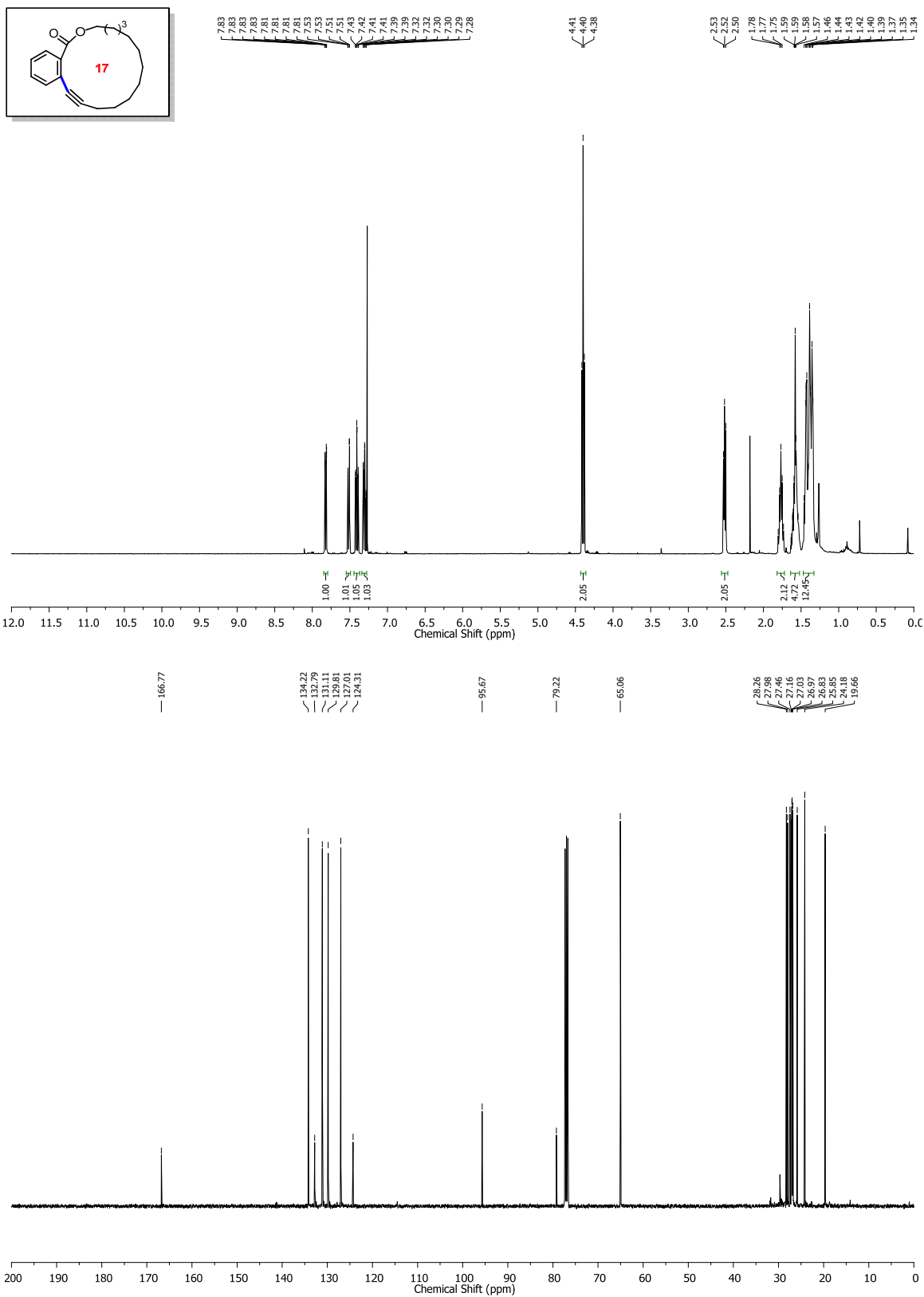


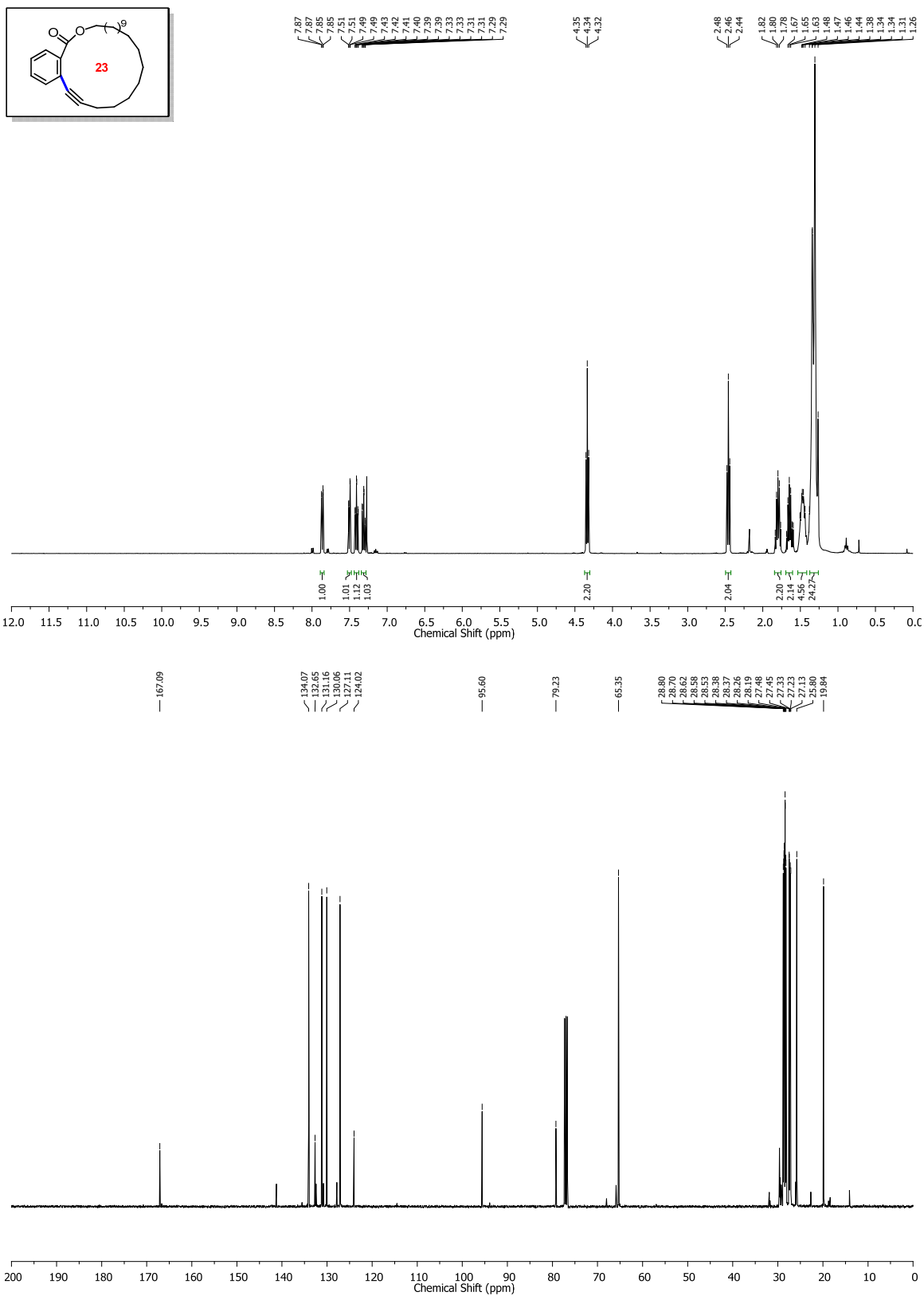


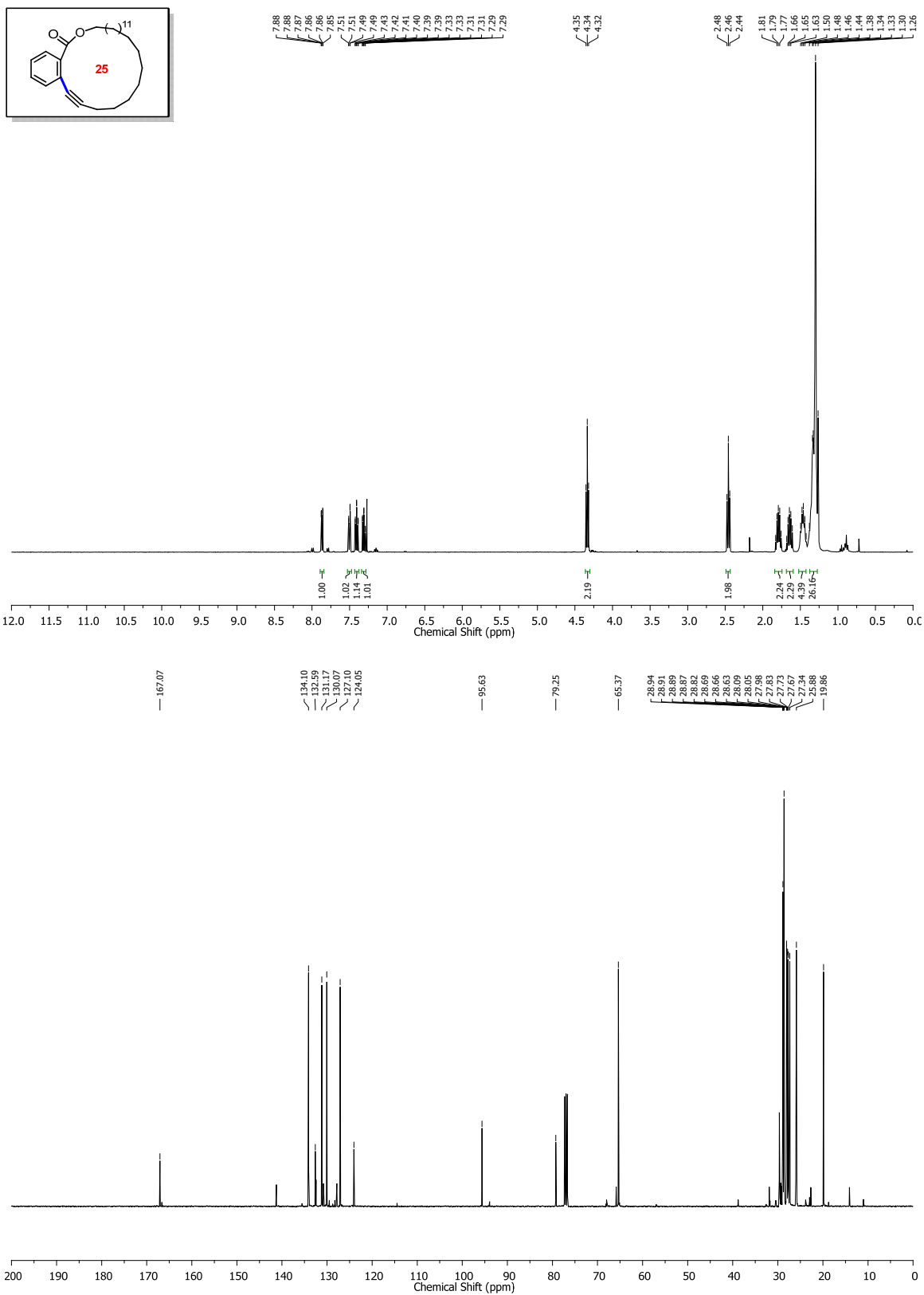


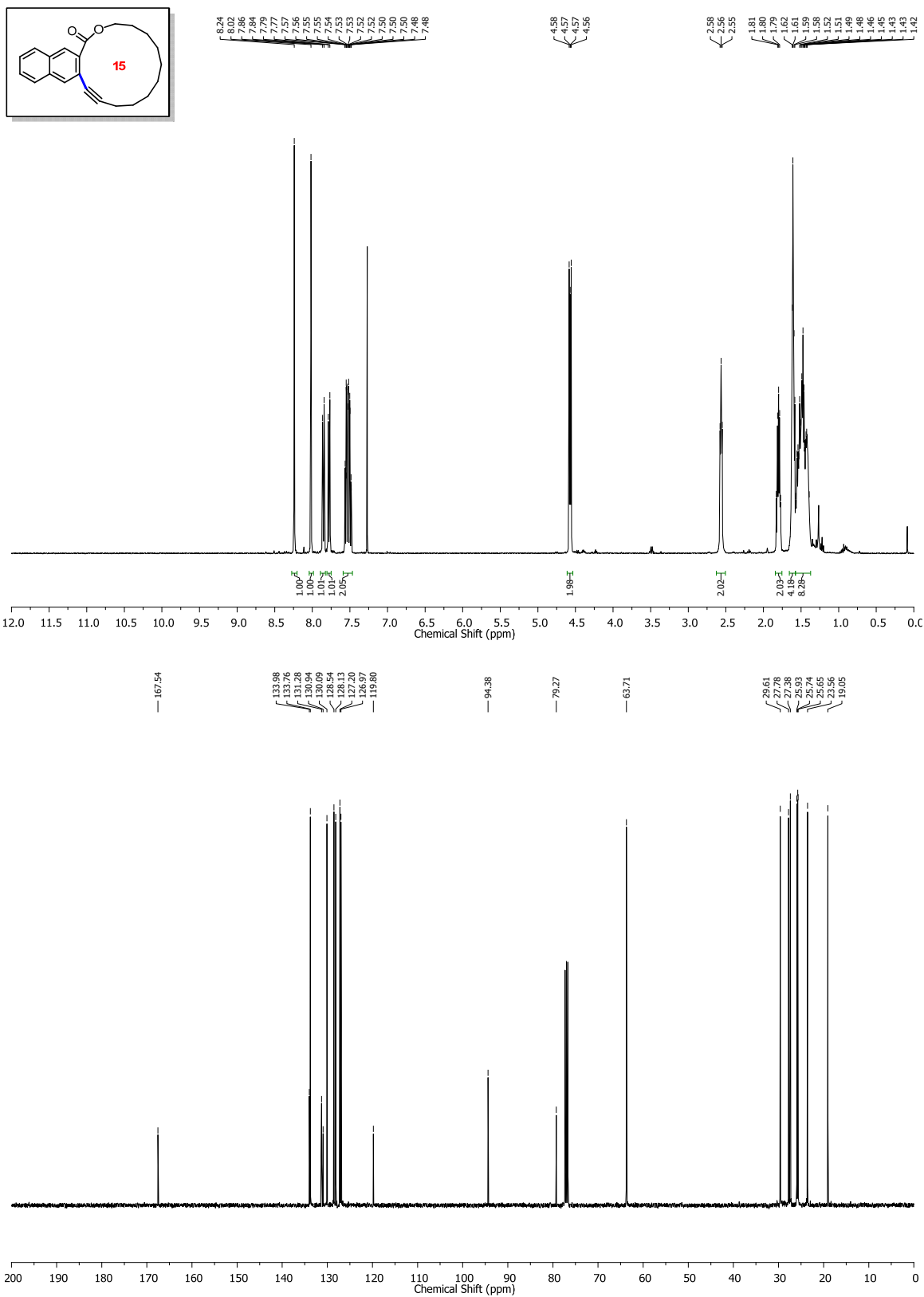




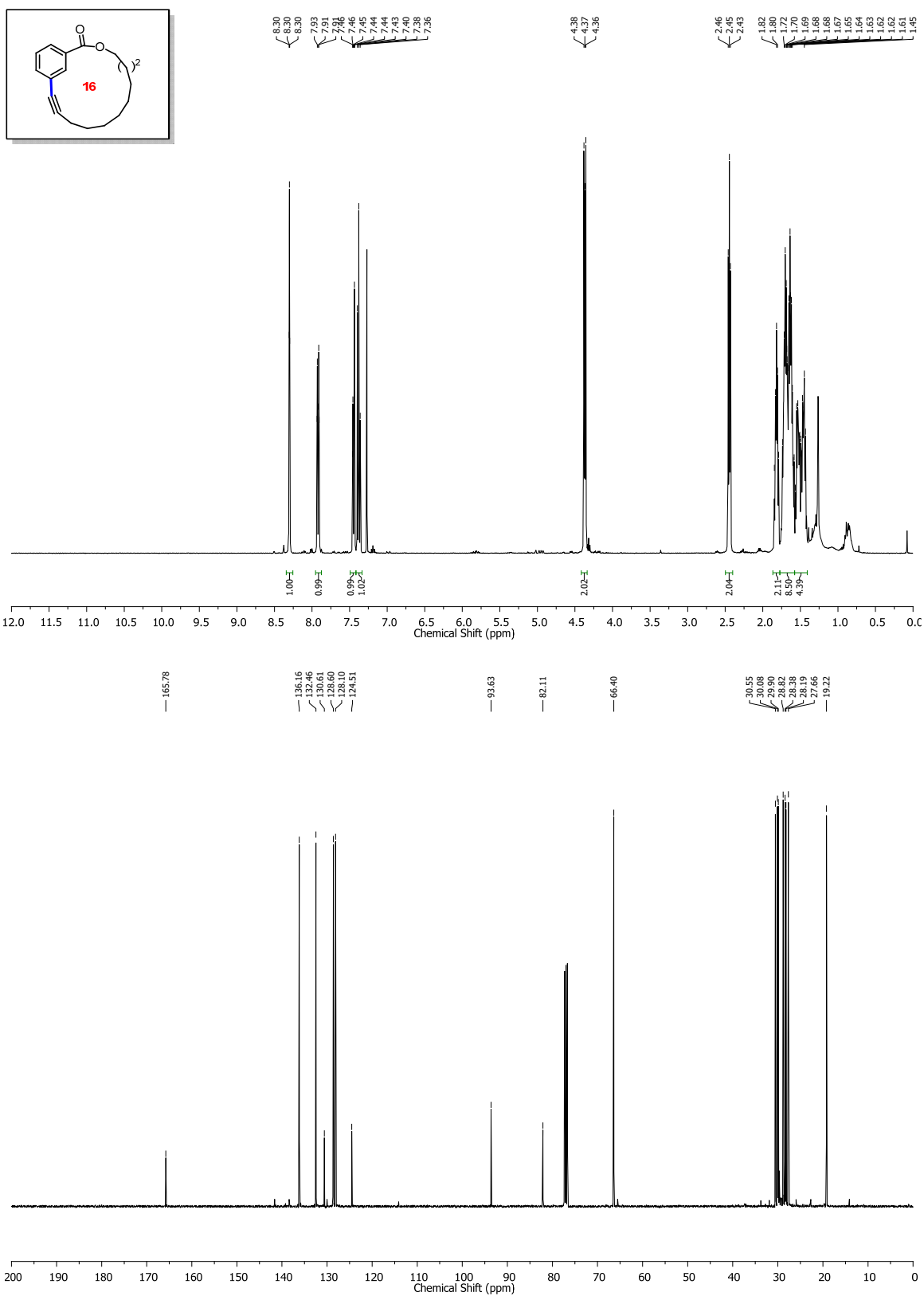


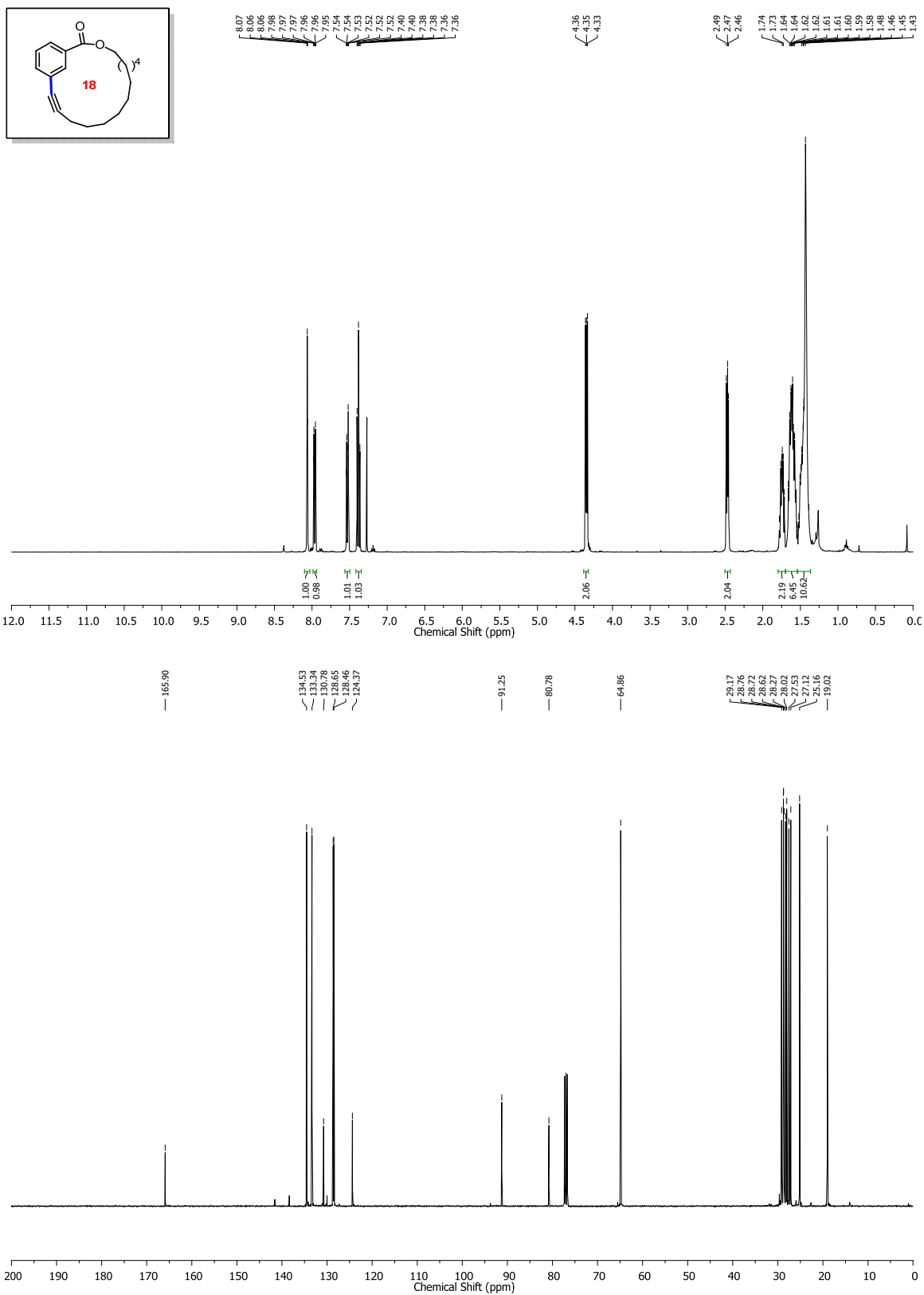


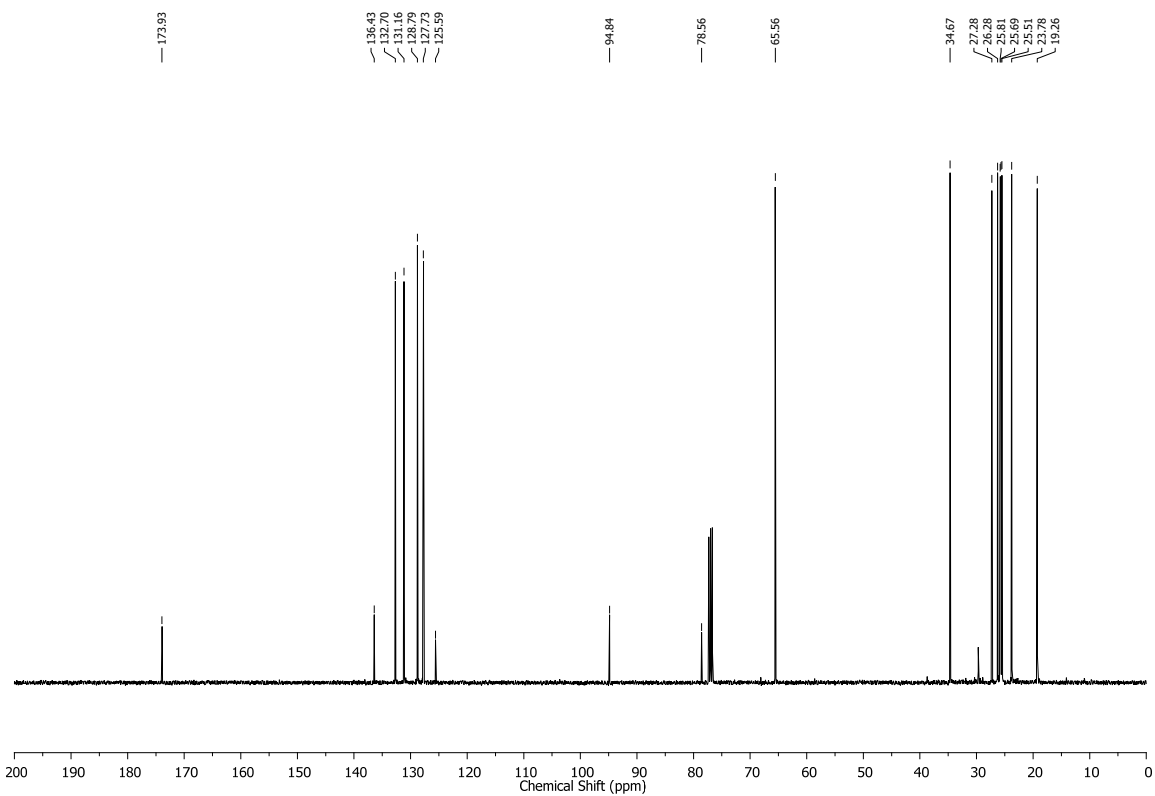
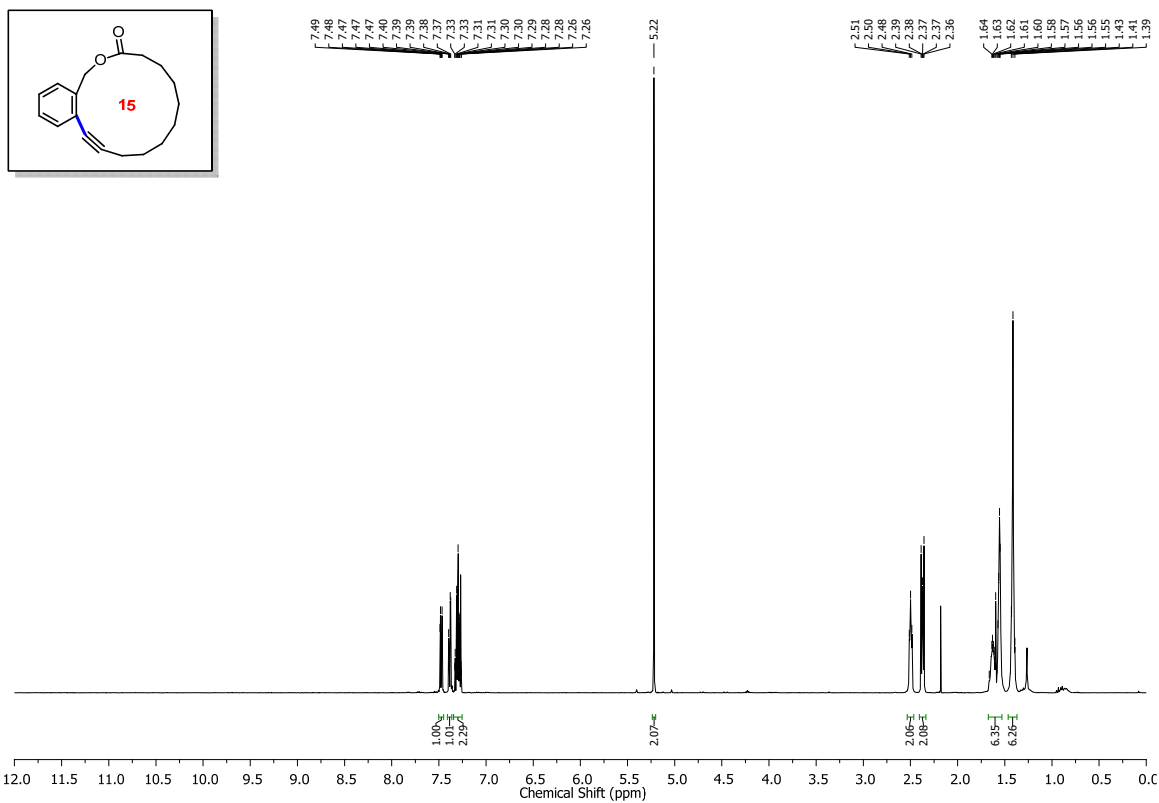


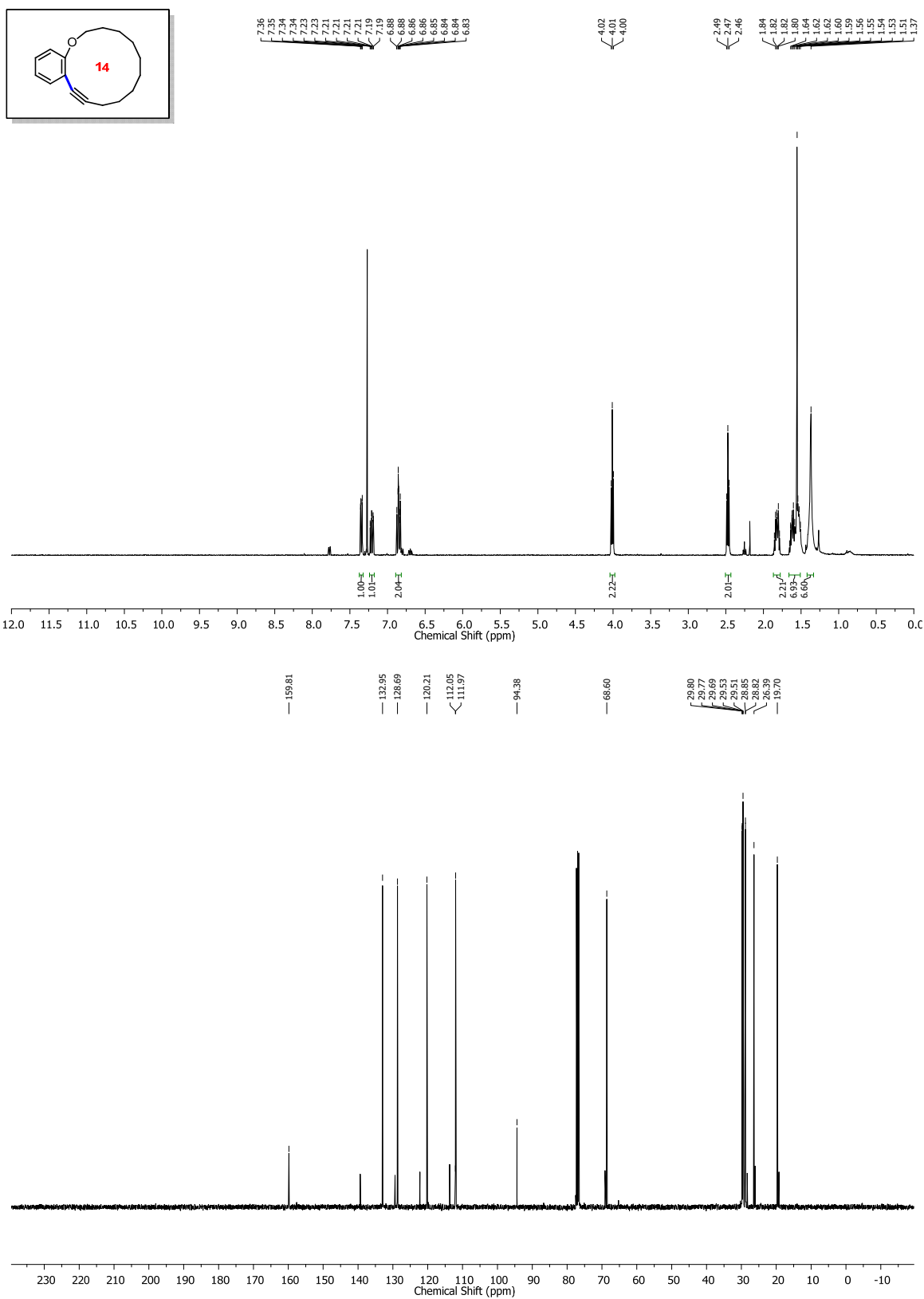


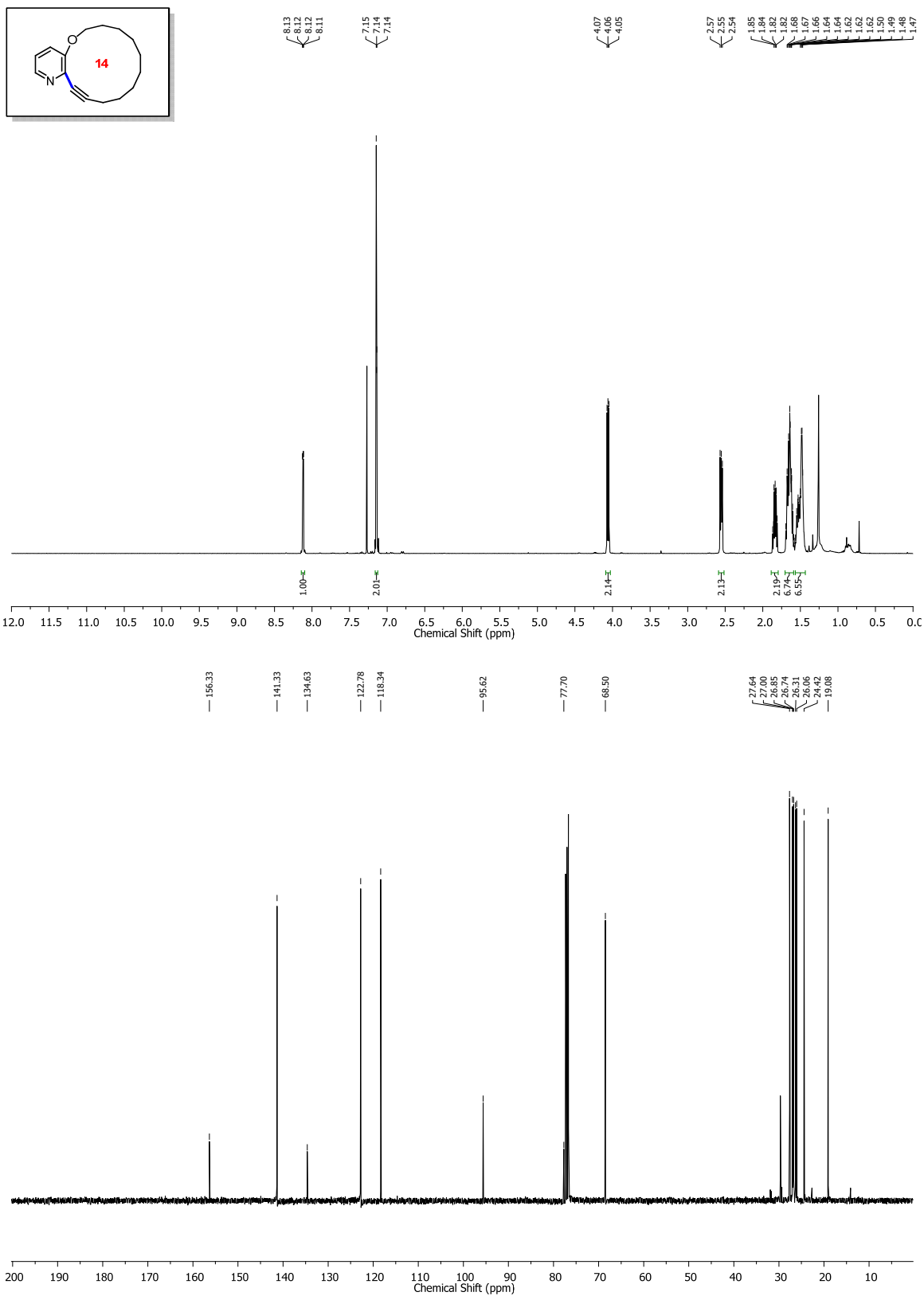


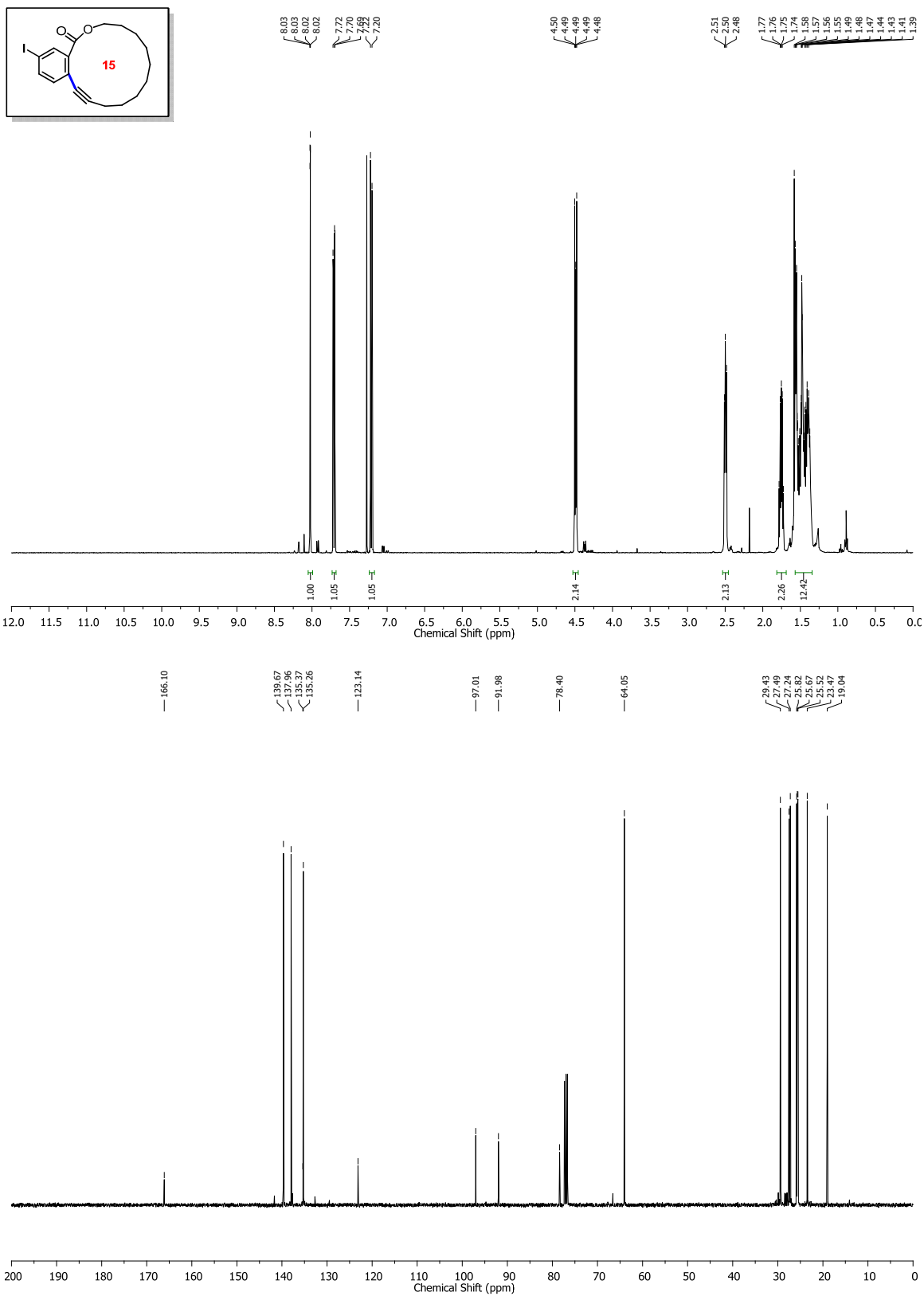


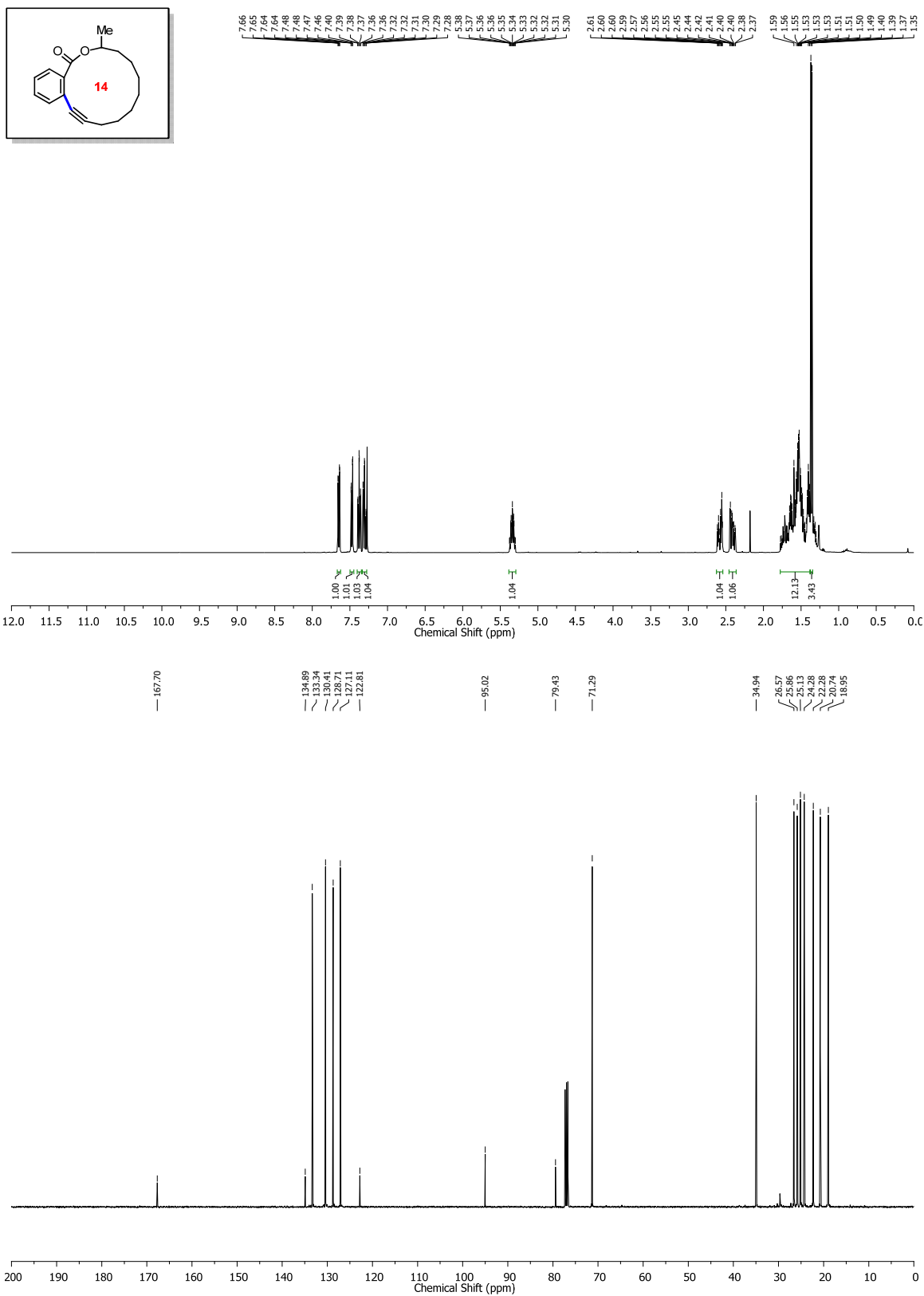


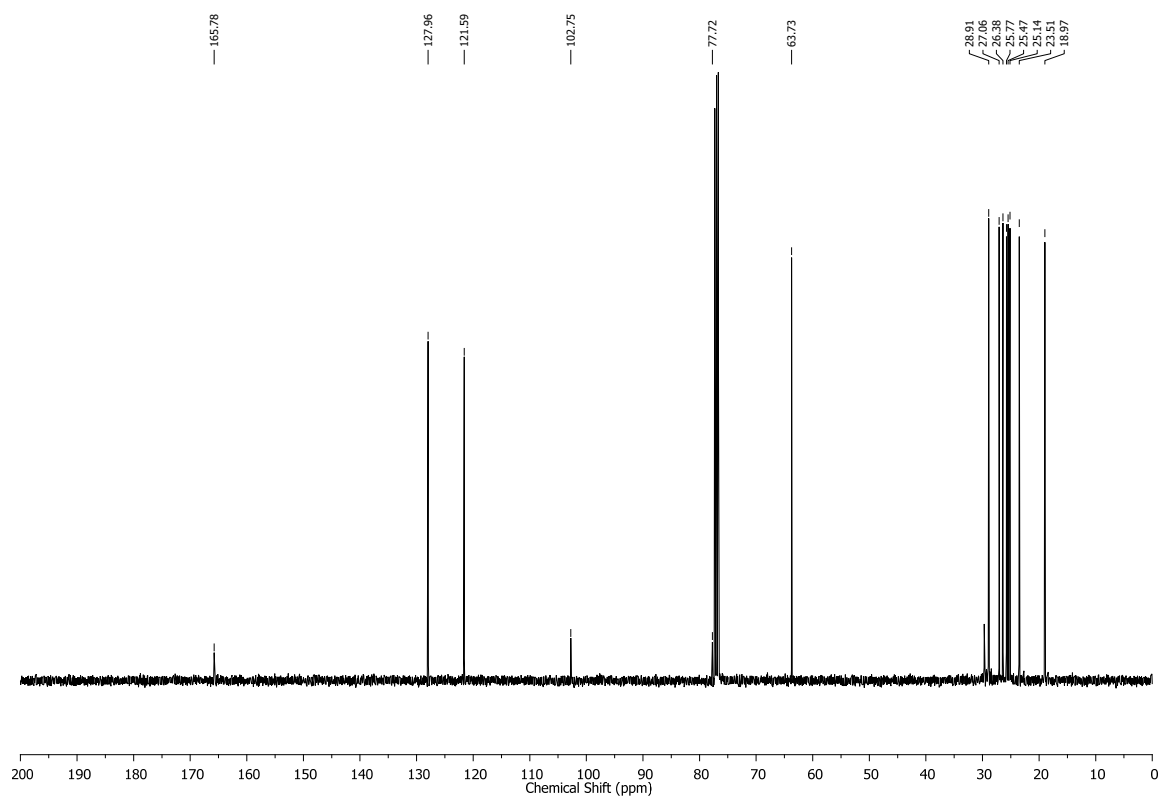
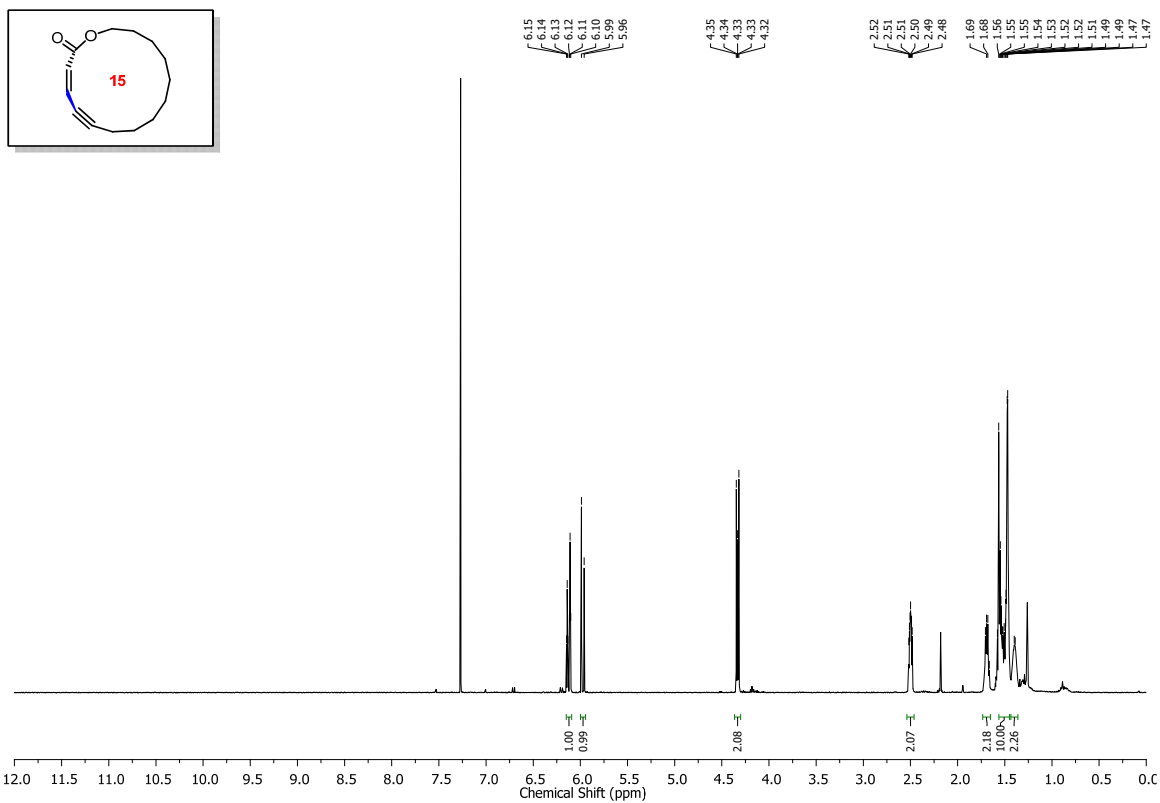




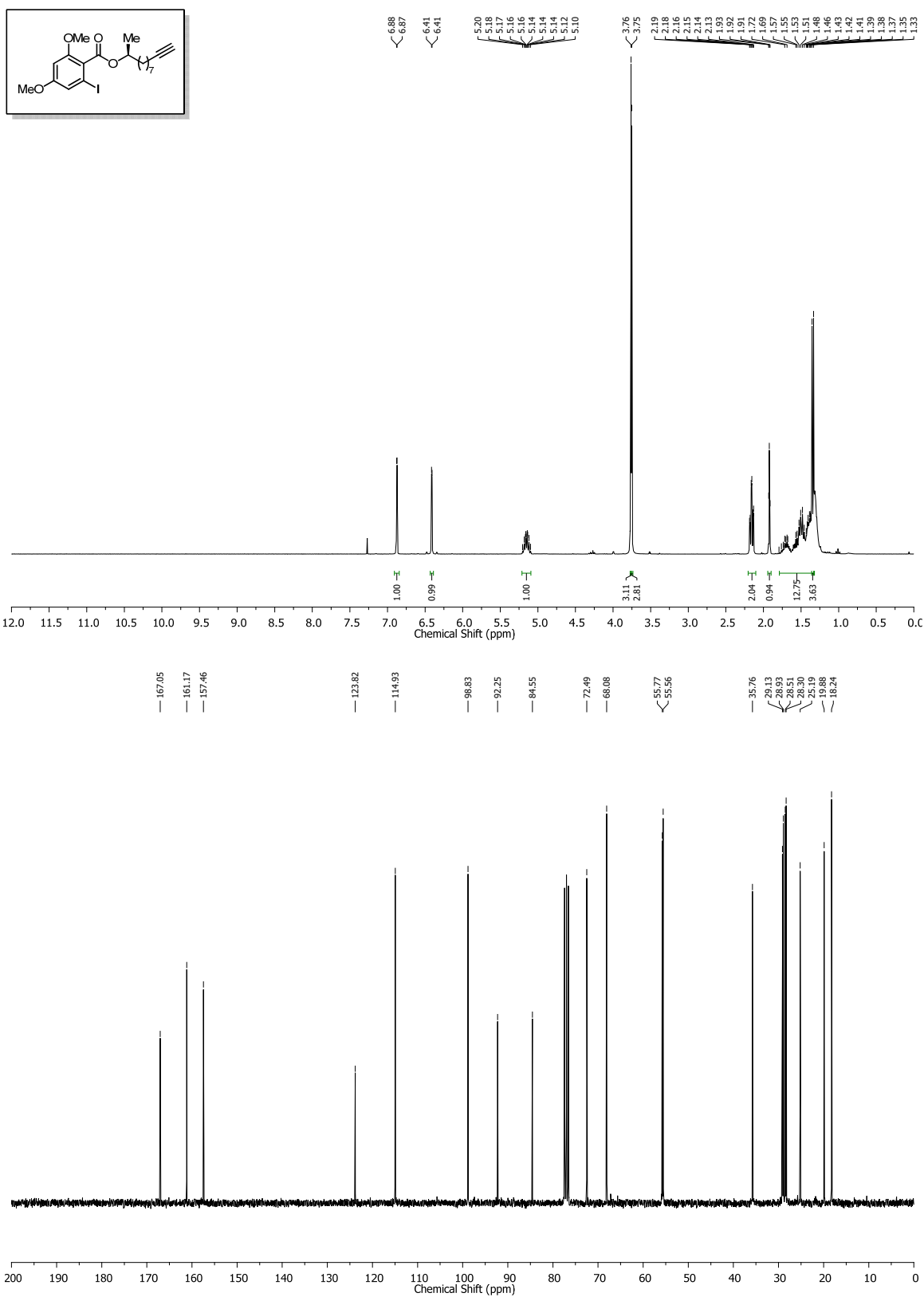


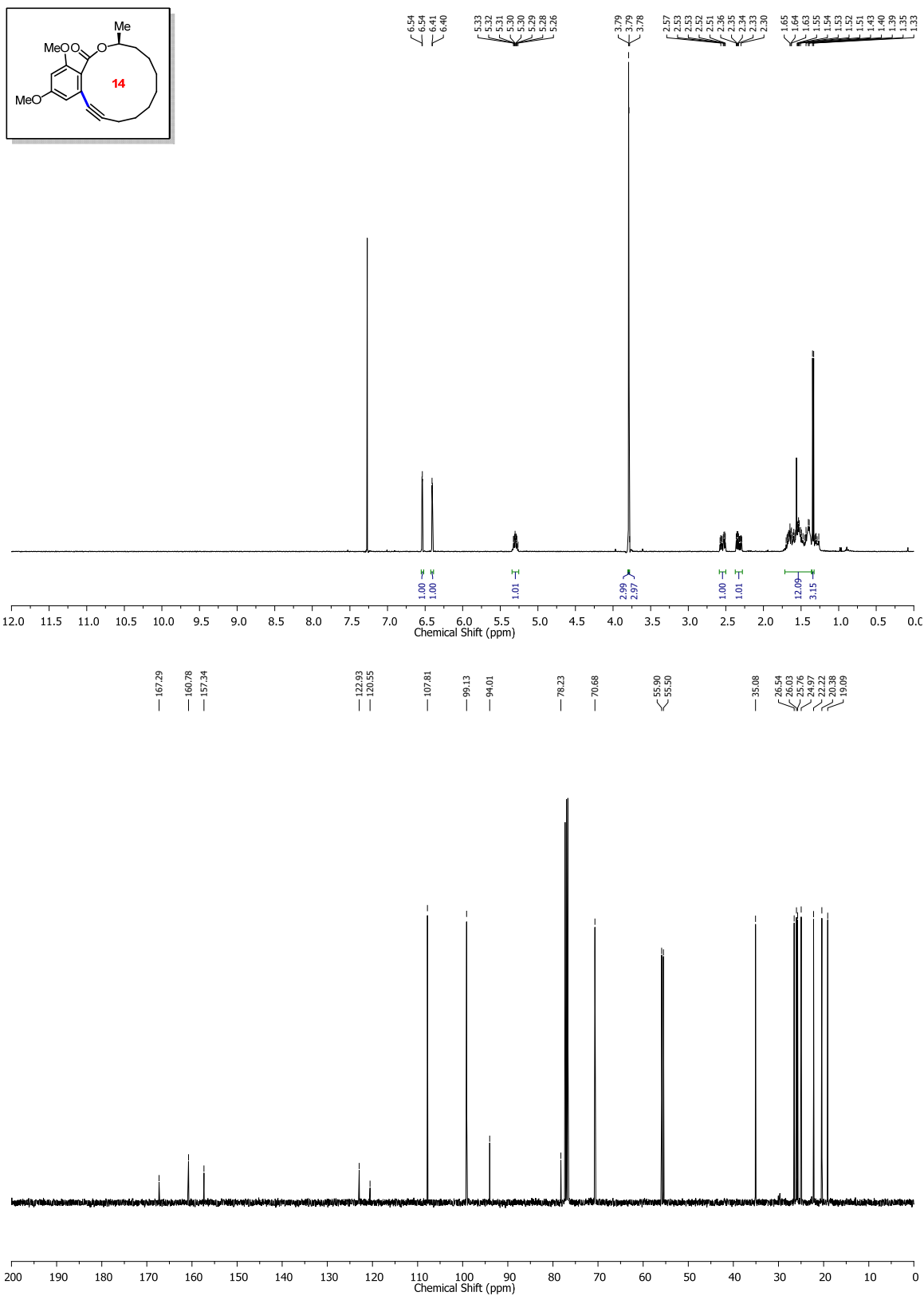


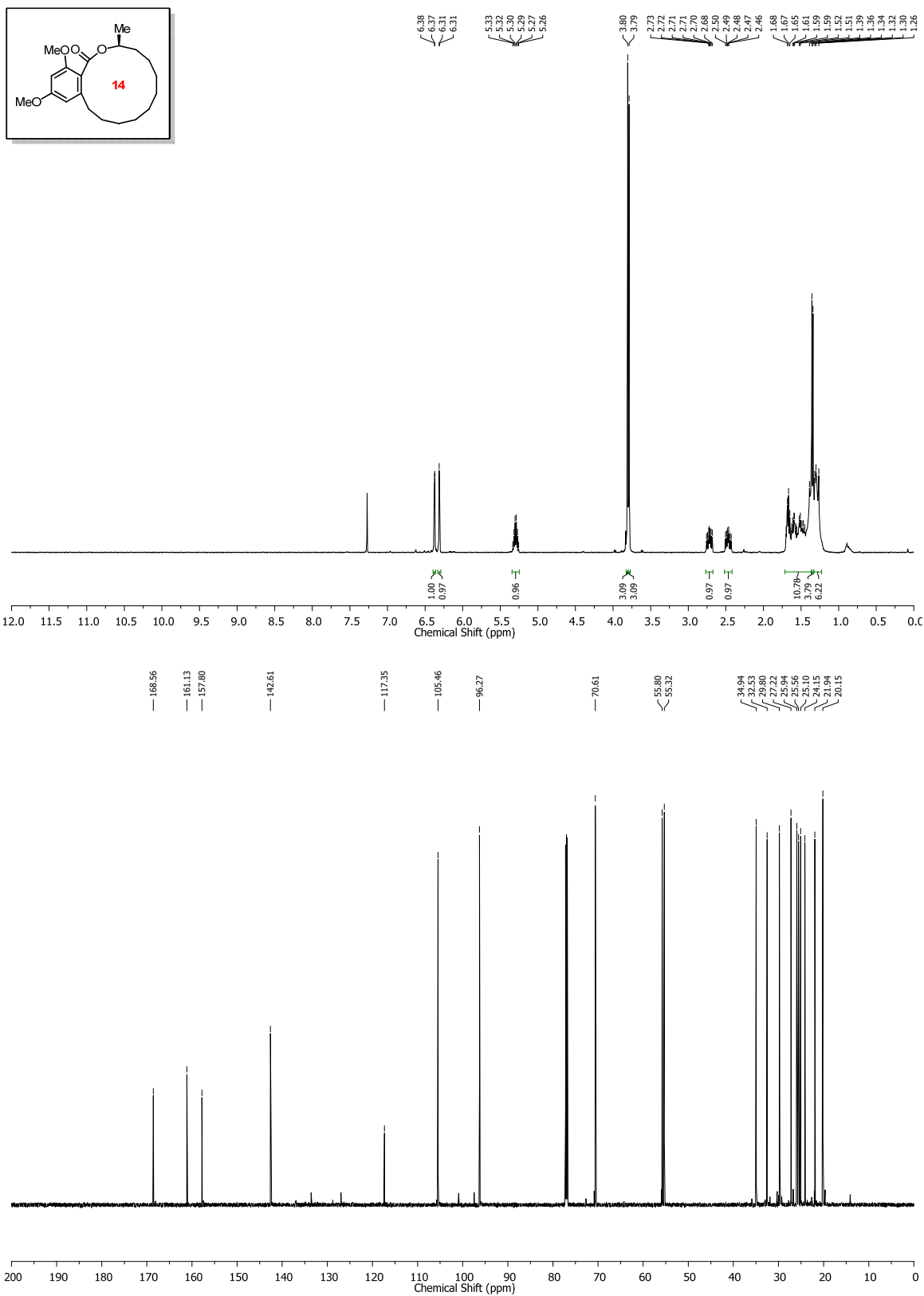


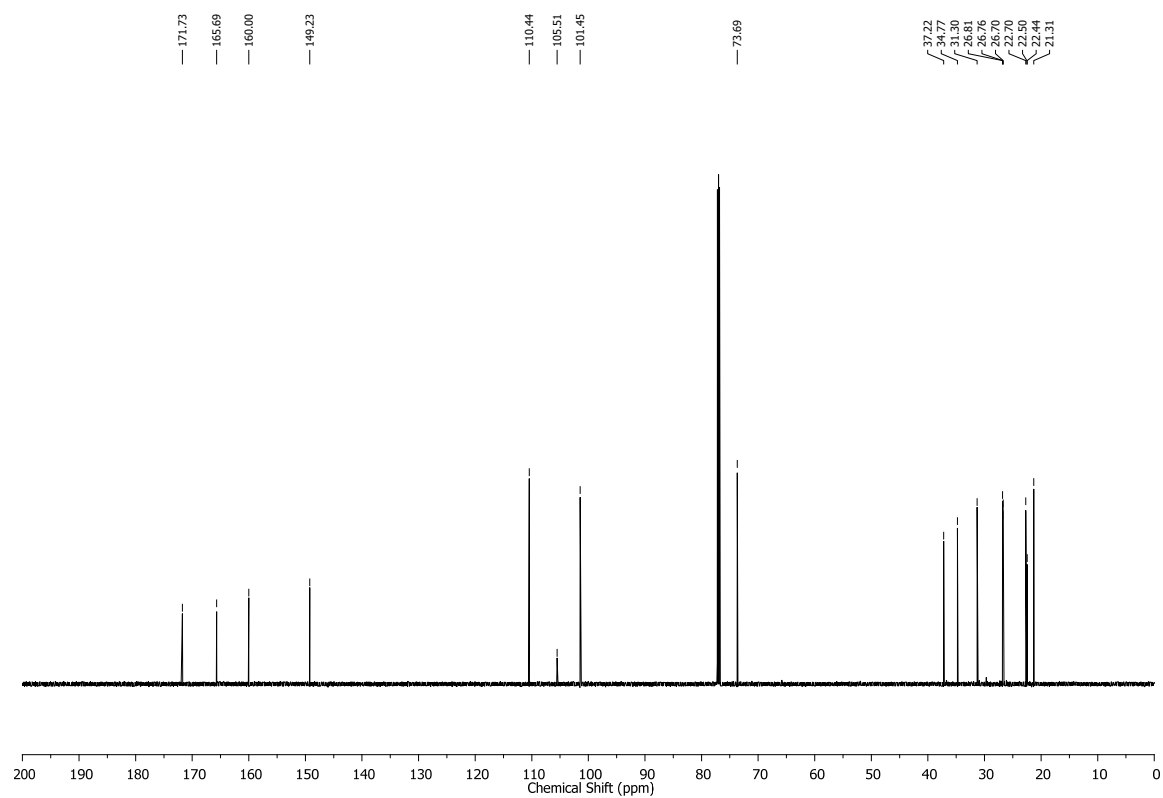
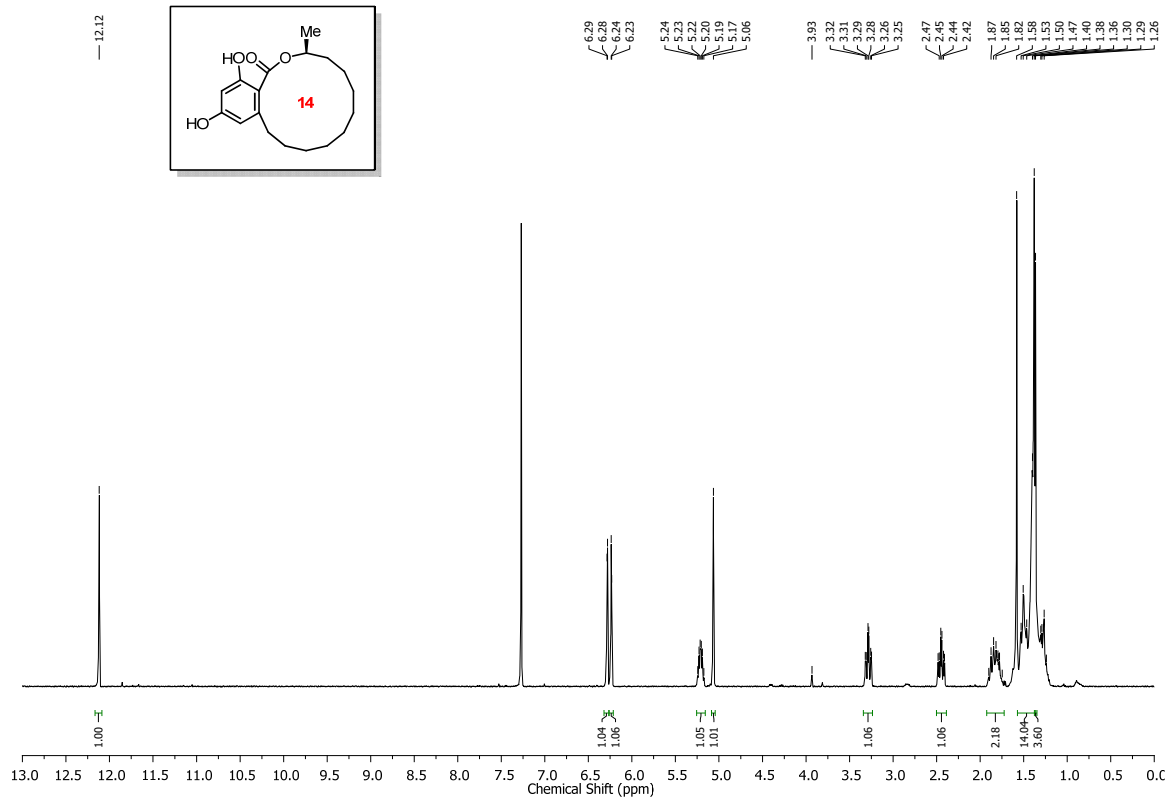












## 10. Supporting Information of Chapter 6

### 10.1 General

Reactions carried out under anhydrous conditions were performed under an inert argon or nitrogen atmosphere in glassware that had previously been dried overnight at 120 °C or flame dried and cooled under a stream of argon or nitrogen.<sup>10</sup> All chemical products were obtained from Sigma-Aldrich Chemical Company or Alfa Aesar, and were reagent quality. The following products were prepared according to their respective literature procedures: 4CzIPN<sup>11</sup>, NiCl<sub>2</sub>·dme<sup>12</sup>, methyl (*tert*-butoxycarbonyl)-*L*-cysteinate<sup>13</sup>, 1-phenylethane-1-thiol<sup>14</sup>, (*S*)-1-phenylethane-1-thiol<sup>5</sup>, 1-(2,2-dibromovinyl)-4-methoxybenzene<sup>15</sup>, 3-bromoprop-2-yn-1-yl benzoate<sup>16</sup> and 4-bromo-2-methylbut-3-yn-2-ol<sup>17</sup>. Technical solvents were obtained from VWR International Co. Anhydrous solvents (CH<sub>2</sub>Cl<sub>2</sub>, Et<sub>2</sub>O, THF, DMF, toluene, and *n*-hexane) were dried and deoxygenated using a GlassContour system (Irvine, CA). Isolated yields reflect the mass obtained following flash column silica gel chromatography. Organic compounds were purified using the method reported by W. C. Still<sup>18</sup> on silica gel obtained from Silicycle Chemical division (40-63 nm; 230-240 mesh). Analytical thin-layer chromatography (TLC) was performed on glass-backed silica gel 60 plates coated with a fluorescence indicator (Silicycle Chemical division, 0.25 mm, F<sub>254</sub>). Visualization of TLC plates was performed by UV (254 nm), KMnO<sub>4</sub> or *p*-anisaldehyde stains. All mixed solvent eluents are reported as v/v solutions. Concentration refers to removal of volatiles at low pressure on a rotary evaporator. All reported compounds were homogeneous by thin layer chromatography (TLC) and by <sup>1</sup>H NMR spectroscopy. NMR spectra were taken in deuterated CDCl<sub>3</sub> using Bruker AV-300, AV-400 and AV-500 instruments unless otherwise noted. Signals of solvent served as internal standard (CHCl<sub>3</sub>: δ 7.27 for <sup>1</sup>H, δ 77.0 for <sup>13</sup>C). The <sup>1</sup>H NMR chemical shifts and coupling constants

---

<sup>10</sup> Shriver, D. F.; Drezdon, M. A. in *The Manipulation of Air-Sensitive Compounds*; Wiley-VCH: New York, 1986.

<sup>11</sup> Luo, J.; Zhang, J. *ACS Catal.* **2016**, 6, 873-877.

<sup>12</sup> Kermagoret, A.; Braunstein, P. *Organometallics* **2008**, 27, 88-99.

<sup>13</sup> Chen, J.; Wu, W.; McNeil, A. J. *Chem. Commun.* **2012**, 48, 7310-7312.

<sup>14</sup> Knope, S.; Kothalawala, N.; Jupally, V. R.; Dass, A.; Bürgi, T. *Chem. Commun.* **2012**, 48, 4630-4632.

<sup>15</sup> Du, W.; Gu, Q.; Li, Y.; Lin, Z.; Yang, D. *Org. Lett.* **2017**, 19, 316-319.

<sup>16</sup> He, L.-Y.; Schulz-Senft, M.; Thiedemann, B.; Linshoeft, J.; Gates, P. J.; Staubitz, A. *Eur. J. Org. Chem.* **2015**, 2498-2502.

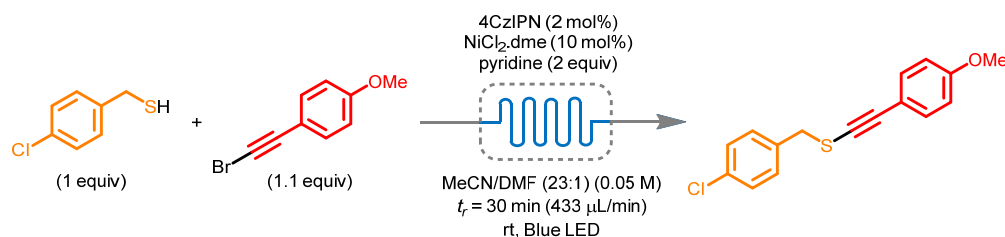
<sup>17</sup> Chen, Z.; Jiang, H.; Li, Y.; Qi, C. *Chem. Commun.* **2010**, 46, 8049-8051.

<sup>18</sup> Still, W. C.; Kahn, M.; Mitra, A. *J. Org. Chem.* **1978**, 43, 2923-2925.

were determined assuming first-order behavior. Multiplicity is indicated by one or more of the following: s (singlet), d (doublet), t (triplet), q (quartet), m (multiplet), br (broad); the list of couplings constants ( $J$ ) corresponds to the order of the multiplicity assignment. High resolution mass spectrometry (HRMS) was done by the Centre régional de spectrométrie de masse at the Département de Chimie, Université de Montréal on an Agilent LC-MSD TOF system using ESI mode of ionization unless otherwise noted.

## 10.2 Optimization/Scale-Up and Mechanism

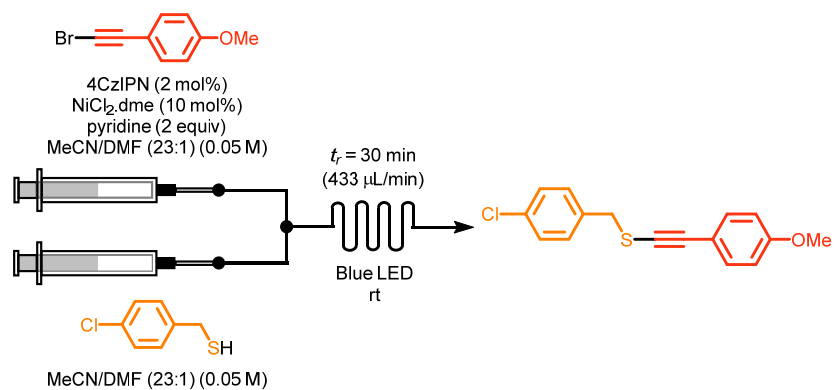
**Table 10.1** Control & optimization experiments



Entry	Variation from standard conditions	Yield <sup>a</sup> (%)
1	None	96
2	with dtbbpy ligand (15 mol%)	95
3	no light (dark)	< 5
4	no 4CzIPN	< 5
5	no NiCl <sub>2</sub> ·dme	28
6	no pyridine	< 5
7	iodo(4-OMe-phenylacetylene)	16
8	chloro(4-OMe-phenylacetylene)	< 5
9	Ir[dF(CF <sub>3</sub> )ppy] <sub>2</sub> (dtbbpy)PF <sub>6</sub>	24
10	Ir(ppy) <sub>2</sub> (dtbbpy)PF <sub>6</sub>	18
11	Ir[dF(CF <sub>3</sub> )ppy] <sub>2</sub> (bpy)PF <sub>6</sub>	46
12	Ru(bpy) <sub>3</sub> (PF <sub>6</sub> ) <sub>2</sub>	15
13	Ru(phen) <sub>3</sub> (PF <sub>6</sub> ) <sub>2</sub>	18
14 <sup>b</sup>	Cu(dap) <sub>2</sub> Cl	22
15 <sup>b</sup>	eosin Y	12
14	26 W CFL instead of blue LED	82
15	Green LED instead of blue LED	16

<sup>a</sup> Yield determined by <sup>1</sup>H NMR spectroscopy using anisole as an internal standard. <sup>b</sup> Green LED were used instead of blue LED.

**Table 10.2** Scale screening



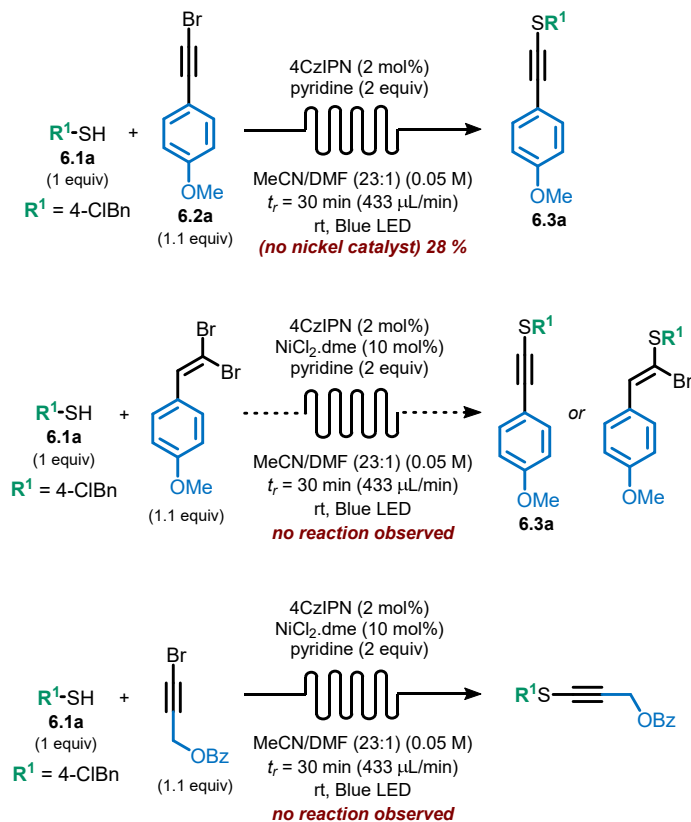
Entry	Scale (mmol)	Yield in Flow <sup>a</sup> (%)	Time in Flow	Yield in Batch <sup>a</sup> (%)	Time in Batch
1	0.24 (65 mg)	96	30 min	92	4 h
2	1.00 (270 mg)	94	30 min	-	-
3	3.00 (780 mg)	90	30 min	-	-
4	5.00 (1.40 g)	90	30 min	26 <sup>b</sup>	4 h

<sup>a</sup> Yield after chromatography. <sup>b</sup> Recovered 64 % bromoalkyne and 71% of the disulfide.

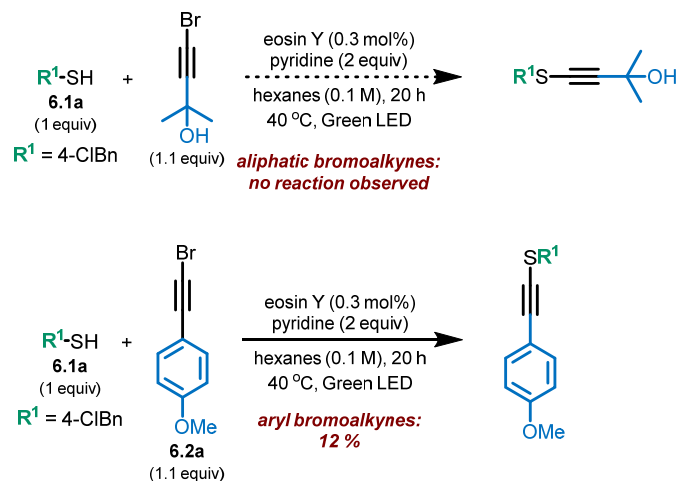


**Figure 10.1** Mechanistic considerations.

### Control Reactions



Addition of thiyl radicals generated by an alternative method also fail to add to aliphatic bromoalkynes (see: S. S. Zalesskiy, N. S. Shlapakov, V. P. Ananikov, *Chem. Sci.* **2016**, 7, 6740-6745):



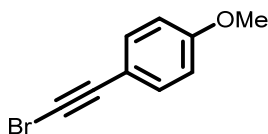
## 10.3 Synthesis of Precursors

**Procedure for Sonogashira Cross-Coupling (A):** To a stirred solution of the aryl iodide (1 equiv.),  $\text{PdCl}_2(\text{PPh}_3)_2$  (5 mol%) and  $\text{CuI}$  (5 mol%) in anhydrous tetrahydrofuran (0.1 M), triethylamine (3 equiv.) was added at room temperature. The reaction mixture was bubbled with nitrogen for 5 minutes and ethynyltrimethylsilane (1.5 equiv.) was then added under nitrogen. The reaction mixture was stirred at room temperature for 18 hours. Upon complete conversion of the starting material, the residue was concentrated under vacuum and purified by column chromatography on silica-gel to afford the desired product.

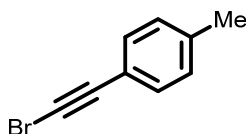
**Procedure for TMS Deprotection (B):** To a stirred solution of the protected aryl alkyne (1 equiv.) in a 1:1 mixture of methanol and tetrahydrofuran (0.2 M), potassium carbonate (2 equiv.) was added at room temperature. The reaction mixture was stirred at room temperature for 1 hour. Upon complete conversion of the starting material, the residue was concentrated under vacuum and purified by column chromatography on silica-gel to afford the desired product.

**Procedure for TMS Deprotection (C):** To a stirred solution of the protected aryl alkyne (1 equiv.) in anhydrous tetrahydrofuran (0.2 M), tetrabutylammonium fluoride (TBAF, 1 M in THF, 2 equiv.) was added at room temperature. The reaction mixture was stirred at room temperature for 15 minutes. Upon complete conversion of the starting material, the residue was concentrated under vacuum and purified by column chromatography on silica-gel to afford the desired product.

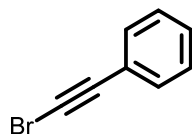
**Procedure for Alkyne Bromination (D):** To a stirred solution of the aryl alkyne (1 equiv.) in acetone (0.2 M), *N*-bromosuccinimide (NBS, 1.2 equiv.) and  $\text{AgNO}_3$  (20 mol%) were added at room temperature. The reaction mixture was stirred at 40 °C for 15-60 minutes. Upon complete conversion of the starting material, the residue was concentrated under vacuum and purified by column chromatography on silica-gel to afford the desired product.



**1-(Bromoethynyl)-4-methoxybenzene (6.2a):** Following Procedure D, 1-ethynyl-4-methoxybenzene (1.04 mL, 8.02 mmol, 1.0 equiv.), NBS (1.72 g, 9.62 mmol, 1.2 equiv.) and AgNO<sub>3</sub> (0.272 g, 1.60 mmol, 20 mol%) were dissolved in acetone (40 mL) in a round bottom flask equipped with a stir bar. After purification by column chromatography (100 % hexanes → 1 % diethyl ether in hexanes), bromide **6.2a** was obtained as a yellow solid (1.35 g, 80 % yield). NMR data was in accordance with what was previously reported.<sup>19</sup>



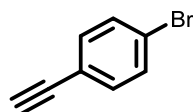
**1-(Bromoethynyl)-4-methylbenzene (6.2b):** Following Procedure D, 1-ethynyl-4-methylbenzene (0.50 mL, 3.94 mmol, 1.0 equiv.), NBS (0.841 g, 4.73 mmol, 1.2 equiv.) and AgNO<sub>3</sub> (0.134 g, 0.788 mmol, 20 mol%) were dissolved in acetone (20 mL) in a round bottom flask equipped with a stir bar. After purification by column chromatography (100 % hexanes), bromide **6.2b** was obtained as a yellow oil (0.588 g, 76 % yield). NMR data was in accordance with what was previously reported.<sup>19</sup>



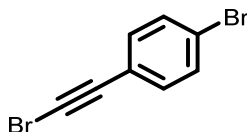
**(Bromoethynyl)benzene (6.2c):** Following Procedure D, ethynylbenzene (0.25 mL, 2.28 mmol, 1.0 equiv.), NBS (0.486 g, 2.73 mmol, 1.2 equiv.) and AgNO<sub>3</sub> (0.077 g, 0.455 mmol, 20 mol%) were dissolved in acetone (11 mL) in a round bottom flask equipped with a stir bar. After purification by column chromatography (100 % hexanes), bromide **6.2c** was obtained as a

<sup>19</sup> Feng, Y.-S.; Xu, Z.-Q.; Mao, L.; Zhang, F.-F.; Xu, H.-J. *Org. Lett.* **2013**, *15*, 1472-1475.

yellow oil (0.33 g, 81 % yield). NMR data was in accordance with what was previously reported.<sup>19</sup>



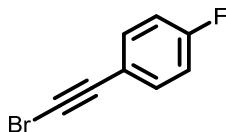
**1-Bromo-4-ethynylbenzene (10.1):** Following Procedure B, ((4-bromophenyl)ethynyl)trimethylsilane (0.500 g, 1.97 mmol, 1.0 equiv.) and potassium carbonate (0.546 g, 3.95 mmol, 2 equiv.) were dissolved in methanol (5 mL) and tetrahydrofuran (5 mL) in a round bottom flask equipped with a stir bar. After purification by column chromatography (100 % hexanes), bromide **10.1** was obtained as a white solid (0.299 g, 84 % yield). NMR data was in accordance with what was previously reported.<sup>20</sup>



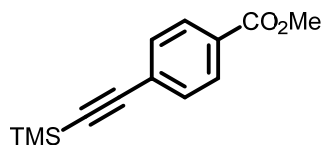
**1-Bromo-4-(bromoethynyl)benzene (6.2d):** Following Procedure D, 1-bromo-4-ethynylbenzene (0.295 g, 1.63 mmol, 1.0 equiv.), NBS (0.349 g, 1.96 mmol, 1.2 equiv.) and AgNO<sub>3</sub> (0.055 g, 0.326 mmol, 20 mol%) were dissolved in acetone (8 mL) in a round bottom flask equipped with a stir bar. After purification by column chromatography (100 % hexanes → 1 % diethyl ether in hexanes), bromide **6.2d** was obtained as a white solid (0.300 g, 71 % yield). NMR data was in accordance with what was previously reported.<sup>19</sup>

---

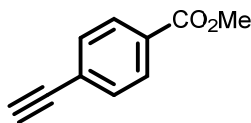
<sup>20</sup> Yasukawa, T.; Miyamura, H.; Kobayashi, S. *Org. Biomol. Chem.* **2011**, *9*, 6208-6210.



**1-(Bromoethynyl)-4-fluorobenzene (6.2e):** Following Procedure D, 1-ethynyl-4-fluorobenzene (0.24 mL, 2.08 mmol, 1.0 equiv.), NBS (0.445 g, 2.50 mmol, 1.2 equiv.) and AgNO<sub>3</sub> (0.071 g, 0.420 mmol, 20 mol%) were dissolved in acetone (10 mL) in a round bottom flask equipped with a stir bar. After purification by column chromatography (100 % hexanes), bromide **6.2e** was obtained as a white solid (0.247 g, 60 % yield). NMR data was in accordance with what was previously reported.<sup>19</sup>



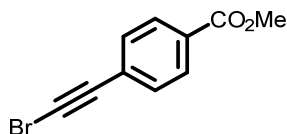
**Methyl 4-((trimethylsilyl)ethynyl)benzoate (10.2):** Following Procedure A, methyl 4-iodobenzoate (0.355 g, 1.28 mmol, 1.0 equiv.), ethynyltrimethylsilane (0.27 mL, 1.92 mmol, 1.5 equiv.), PdCl<sub>2</sub>(PPh<sub>3</sub>)<sub>2</sub> (0.045 g, 0.064 mmol, 5 mol%), CuI (0.012 g, 0.064 mmol, 5 mol%) and triethylamine (0.54 mL, 3.84 mmol, 3.0 equiv.) were dissolved in anhydrous tetrahydrofuran (13 mL) in a round bottom flask equipped with a stir bar. After purification by column chromatography (100 % hexanes → 5 % diethyl ether in hexanes), benzoate **10.2** was obtained as a colorless oil (0.291 g, 98 % yield). NMR data was in accordance with what was previously reported.<sup>21</sup>



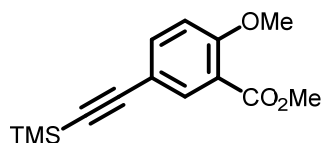
**Methyl 4-ethynylbenzoate (10.3):** Following Procedure B, methyl 4-((trimethylsilyl)ethynyl)benzoate (0.327 g, 1.41 mmol, 1.0 equiv.) and potassium carbonate

<sup>21</sup> Parsons, S. R., Hooper, J. F.; Willis, M. C. *Org. Lett.* **2011**, *13*, 998-1000.

(0.389 g, 2.82 mmol, 2 equiv.) were dissolved in methanol (3.5 mL) and tetrahydrofuran (3.5 mL) in a round bottom flask equipped with a stir bar. After purification by column chromatography (100 % hexanes → 5 % diethyl ether in hexanes), benzoate **10.3** was obtained as a colorless oil (0.151 g, 67 % yield). NMR data was in accordance with what was previously reported.<sup>21</sup>



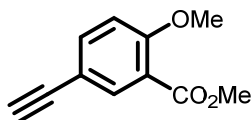
**Methyl 4-(bromoethynyl)benzoate (6.2f):** Following Procedure D, methyl 4-ethynylbenzoate (0.151 g, 0.943 mmol, 1.0 equiv.), NBS (0.201 g, 1.13 mmol, 1.2 equiv.) and AgNO<sub>3</sub> (0.032 g, 0.189 mmol, 20 mol%) were dissolved in acetone (5 mL) in a round bottom flask equipped with a stir bar. After purification by column chromatography (100 % hexanes → 5 % diethyl ether in hexanes), bromide **6.2f** was obtained as a white solid (0.156 g, 70 % yield). NMR data was in accordance with what was previously reported.<sup>22</sup>



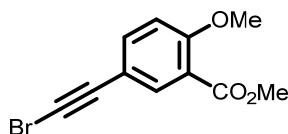
**Methyl 2-methoxy-5-((trimethylsilyl)ethynyl)benzoate (10.4):** Following Procedure A, methyl 5-iodo-2-methoxybenzoate (0.750 g, 2.57 mmol, 1.0 equiv.), ethynyltrimethylsilane (0.53 mL, 3.85 mmol, 1.5 equiv.), PdCl<sub>2</sub>(PPh<sub>3</sub>)<sub>2</sub> (0.090 g, 0.128 mmol, 5 mol%), CuI (0.024 g, 0.128 mmol, 5 mol%) and triethylamine (1.1 mL, 7.71 mmol, 3.0 equiv.) were dissolved in anhydrous tetrahydrofuran (26 mL) in a round bottom flask equipped with a stir bar. After purification by column chromatography (100 % hexanes → 10 % ethyl acetate in hexanes), the

<sup>22</sup> Liang, X.; Gopalaswamy, R.; Navas III, F.; Toone, E. J.; Zhou, P. *J. Org. Chem.* **2016**, *81*, 4393-4398.

benzoate **10.4** was obtained as a white solid (0.661 g, 98 % yield). NMR data was in accordance with what was previously reported.<sup>23</sup>

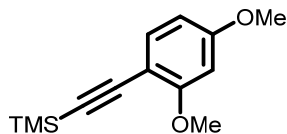


**Methyl 5-ethynyl-2-methoxybenzoate (10.5):** Following Procedure B, methyl 2-methoxy-5-((trimethylsilyl)ethynyl)benzoate (0.700 g, 2.67 mmol, 1.0 equiv.) and potassium carbonate (0.737 g, 5.34 mmol, 2 equiv.) were dissolved in methanol (6.5 mL) and tetrahydrofuran (6.5 mL) in a round bottom flask equipped with a stir bar. After purification by column chromatography (100 % hexanes → 10 % ethyl acetate in hexanes), benzoate **10.5** was obtained as a white solid (0.360 g, 71 % yield). NMR data was in accordance with what was previously reported.<sup>23</sup>

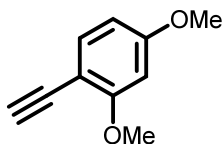


**Methyl 5-(bromoethynyl)-2-methoxybenzoate (6.2g):** Following Procedure D, methyl 5-ethynyl-2-methoxybenzoate (0.200 g, 1.05 mmol, 1.0 equiv.), NBS (0.225 g, 1.26 mmol, 1.2 equiv.) and AgNO<sub>3</sub> (0.036 g, 0.210 mmol, 20 mol%) were dissolved in acetone (5 mL) in a round bottom flask equipped with a stir bar. After purification by column chromatography (100 % hexanes → 10 % ethyl acetate in hexanes), bromide **6.2g** was obtained as a white solid (0.245 g, 87 % yield). <sup>1</sup>H NMR (400 MHz, CDCl<sub>3</sub>) δ = 7.91 (d, *J* = 2.2 Hz, 1H), 7.55 (dd, *J* = 8.7, 2.2 Hz, 1H), 6.93 (d, *J* = 8.8 Hz, 1H), 3.92 (s, 3H), 3.90 (s, 3H); <sup>13</sup>C NMR (100 MHz, CDCl<sub>3</sub>) δ = 165.6, 159.2, 136.9, 135.5, 120.2, 114.6, 112.0, 78.8, 56.1, 52.2, 49.0; HRMS (ESI) *m/z* calculated for C<sub>11</sub>H<sub>10</sub>BrO<sub>3</sub> [M+H]<sup>+</sup> 268.9808; found 268.9813.

<sup>23</sup> Lee, S. H.; Kwon, Y. B.; Yoon, C. M. *Synthetic Communications* **2009**, 39, 4069-4078.



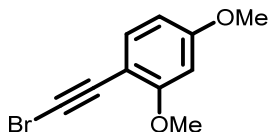
**((2,4-Dimethoxyphenyl)ethynyl)trimethylsilane (10.6):** Following Procedure A, 1-iodo-2,4-dimethoxybenzene (0.542 g, 2.05 mmol, 1.0 equiv.), ethynyltrimethylsilane (0.43 mL, 3.08 mmol, 1.5 equiv.),  $\text{PdCl}_2(\text{PPh}_3)_2$  (0.072 g, 0.103 mmol, 5 mol%), CuI (0.020 g, 0.103 mmol, 5 mol%) and triethylamine (0.86 mL, 6.16 mmol, 3.0 equiv.) were dissolved in anhydrous tetrahydrofuran (20 mL) in a round bottom flask equipped with a stir bar. After purification by column chromatography (100 % hexanes  $\rightarrow$  2.5 % diethyl ether in hexanes), silane **10.6** was obtained as a colorless oil (0.242 g, 50 % yield). NMR data was in accordance with what was previously reported.<sup>24</sup>



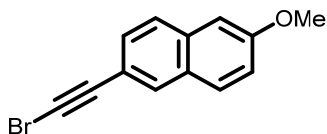
**1-Ethynyl-2,4-dimethoxybenzene (10.7):** Following Procedure B, ((2,4-dimethoxyphenyl)ethynyl)trimethylsilane (0.240 g, 1.02 mmol, 1.0 equiv.) and potassium carbonate (0.282 g, 2.04 mmol, 2 equiv.) were dissolved in methanol (2.5 mL) and tetrahydrofuran (2.5 mL) in a round bottom flask equipped with a stir bar. After purification by column chromatography (100 % hexanes  $\rightarrow$  2.5 % diethyl ether in hexanes), alkyne **10.7** was obtained as a colorless oil (0.162 g, 98 % yield). NMR data was in accordance with what was previously reported.<sup>24</sup>

<sup>24</sup> Mehta, S.; Larock, R. C. *J. Org. Chem.* **2010**, 75, 1652-1658.



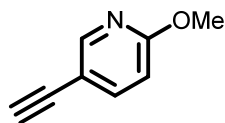


**1-(Bromoethynyl)-2,4-dimethoxybenzene (6.2h):** Following Procedure D, 1-ethynyl-2,4-dimethoxybenzene (0.147 g, 0.908 mmol, 1.0 equiv.), NBS (0.194 g, 1.09 mmol, 1.2 equiv.) and AgNO<sub>3</sub> (0.031 g, 0.182 mmol, 20 mol%) were dissolved in acetone (5 mL) in a round bottom flask equipped with a stir bar. After purification by column chromatography (100 % hexanes → 5 % diethyl ether in hexanes), bromide **6.2h** was obtained as a white solid (0.115 g, 53 % yield). <sup>1</sup>H NMR (400 MHz, CDCl<sub>3</sub>) δ = 7.35 (d, *J* = 8.4 Hz, 1H), 6.46-6.43 (m, 2H), 3.87 (s, 3H), 3.82 (s, 3H); <sup>13</sup>C NMR (75 MHz, CDCl<sub>3</sub>) δ = 161.9, 161.4, 134.8, 104.8, 104.4, 98.4, 76.4, 55.8, 55.4, 51.1; HRMS (ASAP) *m/z* calculated for C<sub>10</sub>H<sub>9</sub>BrO<sub>2</sub> [M<sup>+</sup>] 239.9786; found 239.9791.

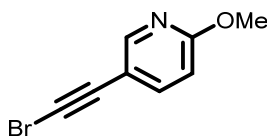


**2-(Bromoethynyl)-6-methoxynaphthalene (6.2i):** Following Procedure D, 2-ethynyl-6-methoxynaphthalene (0.350 g, 1.92 mmol, 1.0 equiv.), NBS (0.409 g, 2.30 mmol, 1.2 equiv.) and AgNO<sub>3</sub> (0.065 g, 0.380 mmol, 20 mol%) were dissolved in acetone (10 mL) in a round bottom flask equipped with a stir bar. After purification by column chromatography (100 % hexanes), bromide **6.2i** was obtained as a white solid (0.288 g, 57 % yield). NMR data was in accordance with what was previously reported.<sup>25</sup>

<sup>25</sup> Urban, C.; Cadoret, F.; Blazejewski, J.-C.; Magnier, E. *Eur. J. Org. Chem.* **2011**, 4862-4867.

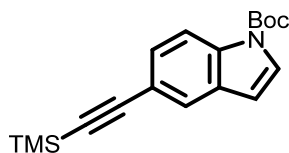


**5-Ethynyl-2-methoxypyridine (10.8):** Following Procedure B, 2-fluoro-5-((trimethylsilyl)ethynyl)pyridine (0.300 g, 1.55 mmol, 1.0 equiv.) and potassium carbonate (0.428 g, 3.10 mmol, 2 equiv.) were dissolved in methanol (16 mL) in a round bottom flask equipped with a stir bar. After purification by column chromatography (100 % hexanes → 5 % diethyl ether in hexanes), alkyne **10.8** was obtained as a colorless oil (0.198 g, 96 % yield). NMR data was in accordance with what was previously reported.<sup>26</sup>

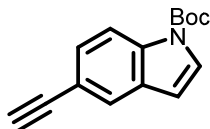


**5-(Bromoethynyl)-2-methoxypyridine (6.2j):** Following Procedure D, 5-ethynyl-2-methoxypyridine (0.187 g, 1.41 mmol, 1.0 equiv.), NBS (0.301 g, 1.69 mmol, 1.2 equiv.) and AgNO<sub>3</sub> (0.048 g, 0.281 mmol, 20 mol%) were dissolved in acetone (7 mL) in a round bottom flask equipped with a stir bar. After purification by column chromatography (100 % hexanes → 5 % diethyl ether in hexanes), bromide **6.2j** was obtained as a white solid (0.243 g, 81 % yield). <sup>1</sup>H NMR (400 MHz, CDCl<sub>3</sub>) δ = 8.28 (d, *J* = 1.9 Hz, 1H), 7.61 (dd, *J* = 8.6, 2.3 Hz, 1H), 6.70 (d, *J* = 9.1 Hz, 1H), 3.95 (s, 3H); <sup>13</sup>C NMR (100 MHz, CDCl<sub>3</sub>) δ = 163.5, 150.6, 141.4, 112.6, 110.7, 77.0, 53.7, 50.9; HRMS (ESI) *m/z* calculated for C<sub>8</sub>H<sub>7</sub>BrNO [M+H]<sup>+</sup> 211.9706; found 211.9700.

<sup>26</sup> Cai, L.; Yang, D.; Sun, Z.; Tao, X.; Cai, L.; Pike, V. W. *Chin. J. Chem.* **2011**, 29, 1059-1062.

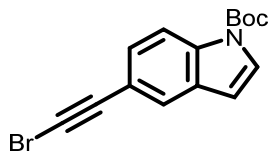


**tert-Butyl 5-((trimethylsilyl)ethynyl)-1H-indole-1-carboxylate (10.9):** Following Procedure A, *tert*-butyl 5-iodo-1H-indole-1-carboxylate (0.620 g, 1.81 mmol, 1.0 equiv.), ethynyltrimethylsilane (0.38 mL, 2.71 mmol, 1.5 equiv.), PdCl<sub>2</sub>(PPh<sub>3</sub>)<sub>2</sub> (0.063 g, 0.090 mmol, 5 mol%), CuI (0.017 g, 0.090 mmol, 5 mol%) and triethylamine (0.76 mL, 5.43 mmol, 3.0 equiv.) were dissolved in anhydrous tetrahydrofuran (18 mL) in a round bottom flask equipped with a stir bar. After purification by column chromatography (100 % hexanes → 2.5 % diethyl ether in hexanes), silane **10.9** was obtained as a colorless oil (0.555 g, 98 % yield). <sup>1</sup>H NMR (400 MHz, CDCl<sub>3</sub>) δ = 8.07 (d, *J* = 8.4 Hz, 1H), 7.70 (s, 1H), 7.60 (d, *J* = 3.7 Hz, 1H), 7.42 (dd, *J* = 8.6, 1.3 Hz, 1H), 6.53 (d, *J* = 3.7 Hz, 1H), 1.68 (s, 9H), 0.27 (s, 9H); <sup>13</sup>C NMR (100 MHz, CDCl<sub>3</sub>) δ = 149.5, 134.9, 130.3, 128.1, 126.7, 124.9, 117.2, 115.0, 107.1, 105.9, 92.4, 84.0, 28.2, 0.07; HRMS (ESI) *m/z* calculated for C<sub>18</sub>H<sub>24</sub>NO<sub>2</sub>Si [M+H]<sup>+</sup> 314.1579; found 314.1571.

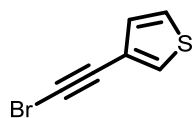


**tert-Butyl 5-ethynyl-1H-indole-1-carboxylate (10.10):** Following Procedure C, *tert*-butyl 5-((trimethylsilyl)ethynyl)-1H-indole-1-carboxylate (0.480 g, 1.53 mmol, 1.0 equiv.) and TBAF (3.0 mL, 3.06 mmol, 2 equiv.) were dissolved in anhydrous tetrahydrofuran (15 mL) in a round bottom flask equipped with a stir bar. After purification by column chromatography (100 % hexanes → 2.5 % diethyl ether in hexanes), alkyne **10.10** was obtained as a colorless oil (0.326 g, 88 % yield). NMR data was in accordance with what was previously reported.<sup>27</sup>

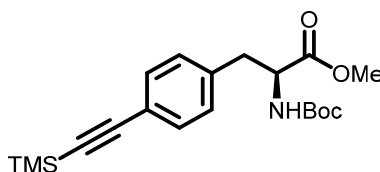
<sup>27</sup> Yu, R. T.; Rovis, T. *J. Am. Chem. Soc.* **2006**, *128*, 12370-12371.



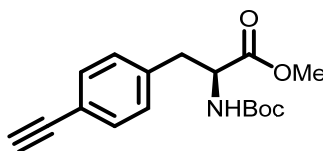
**tert-Butyl 5-(bromoethynyl)-1H-indole-1-carboxylate (6.2k):** Following Procedure D, *tert*-butyl 5-ethynyl-1H-indole-1-carboxylate (0.111 g, 0.460 mmol, 1.0 equiv.), NBS (0.098 g, 0.552 mmol, 1.2 equiv.) and AgNO<sub>3</sub> (0.016 g, 0.092 mmol, 20 mol%) were dissolved in acetone (2 mL) in a round bottom flask equipped with a stir bar. After purification by column chromatography (100 % hexanes → 1 % diethyl ether in hexanes), bromide **6.2k** was obtained as a colorless oil (0.113 g, 77 % yield). <sup>1</sup>H NMR (400 MHz, CDCl<sub>3</sub>) δ = 8.09 (d, *J* = 8.4 Hz, 1H), 7.68 (d, *J* = 1.0 Hz, 1H), 7.62 (d, *J* = 3.7 Hz, 1H), 7.40 (dd, *J* = 8.6, 1.6 Hz, 1H), 6.54 (d, *J* = 3.8 Hz, 1H), 1.68 (s, 9H); <sup>13</sup>C NMR (100 MHz, CDCl<sub>3</sub>) δ = 149.4, 134.9, 130.4, 127.9, 126.9, 124.9, 116.8, 115.1, 107.0, 84.1, 80.6, 47.9, 28.1; HRMS (ASAP) *m/z* calculated for C<sub>15</sub>H<sub>15</sub>BrNO<sub>2</sub> [M+H]<sup>+</sup> 320.0281; found 320.0288.



**3-(Bromoethynyl)thiophene (6.2l):** Following Procedure D, 3-ethynylthiophene (0.20 mL, 2.00 mmol, 1.0 equiv.), NBS (0.427 g, 2.40 mmol, 1.2 equiv.) and AgNO<sub>3</sub> (0.068 g, 0.400 mmol, 20 mol%) were dissolved in acetone (10 mL) in a round bottom flask equipped with a stir bar. After purification by column chromatography (100 % hexanes), bromide **6.2l** was obtained as a colorless oil (0.246 g, 66 % yield). <sup>1</sup>H NMR (400 MHz, CDCl<sub>3</sub>) δ = 7.49 (dd, *J* = 3.0, 1.1 Hz, 1H), 7.28-7.26 (m, 1H), 7.13 (dd, *J* = 5.0, 1.1 Hz, 1H); <sup>13</sup>C NMR (75 MHz, CDCl<sub>3</sub>) δ = 129.8, 129.7, 125.3, 121.6, 75.3, 49.3; HRMS (ASAP) *m/z* calculated for C<sub>6</sub>H<sub>3</sub>BrS [M<sup>+</sup>] 185.9139; found 185.9112.

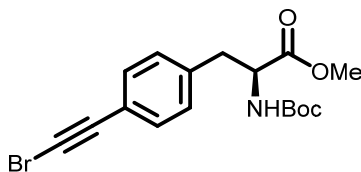


**Methyl (S)-2-((tert-butoxycarbonyl)amino)-3-(4-((trimethylsilyl)ethynyl)phenyl)propanoate (10.11):** Following Procedure A, methyl (S)-2-((tert-butoxycarbonyl)amino)-3-(4-iodophenyl)propanoate (0.500 g, 1.23 mmol, 1.0 equiv.), ethynyltrimethylsilane (0.26 mL, 1.85 mmol, 1.5 equiv.), PdCl<sub>2</sub>(PPh<sub>3</sub>)<sub>2</sub> (0.043 g, 0.062 mmol, 5 mol%), CuI (0.012 g, 0.062 mmol, 5 mol%) and triethylamine (0.51 mL, 3.70 mmol, 3.0 equiv.) were dissolved in anhydrous tetrahydrofuran (12 mL) in a round bottom flask equipped with a stir bar. After purification by column chromatography (100 % hexanes → 7.5 % ethyl acetate in hexanes), silane **10.11** was obtained as an orange oil (0.457 g, 99 % yield). NMR data was in accordance with what was previously reported.<sup>28</sup>



**Methyl (S)-2-((tert-butoxycarbonyl)amino)-3-(4-ethynylphenyl)propanoate (10.12):** Following Procedure C, methyl (S)-2-((tert-butoxycarbonyl)amino)-3-(4-((trimethylsilyl)ethynyl)phenyl)propanoate (0.330 g, 0.875 mmol, 1.0 equiv.) and TBAF (0.92 mL, 0.919 mmol, 1.1 equiv.) were dissolved in anhydrous tetrahydrofuran (8 mL) in a round bottom flask equipped with a stir bar. After purification by column chromatography (100 % hexanes → 15 % ethyl acetate in hexanes), alkyne **10.12** was obtained as an orange solid (0.205 g, 77 % yield). NMR data was in accordance with what was previously reported.<sup>28</sup>

<sup>28</sup> Verlinden, S.; Ballet, S.; Verniest, G. *Eur. J. Org. Chem.* **2016**, 5807-5812.



**Methyl (S)-3-(4-(bromoethynyl)phenyl)-2-((tert-butoxycarbonyl)amino)propanoate (6.2m):** Following Procedure D, methyl (S)-2-((tert-butoxycarbonyl)amino)-3-(4-ethynylphenyl)propanoate (0.200 g, 0.659 mmol, 1.0 equiv.), NBS (0.141 g, 0.791 mmol, 1.2 equiv.) and AgNO<sub>3</sub> (0.022 g, 0.132 mmol, 20 mol%) were dissolved in acetone (3.5 mL) in a round bottom flask equipped with a stir bar. After purification by column chromatography (100 % hexanes → 15 % ethyl acetate in hexanes), bromide **6.2m** was obtained as a white solid (0.224 g, 89 % yield). <sup>1</sup>H NMR (400 MHz, CDCl<sub>3</sub>) δ = 7.38 (d, *J* = 8.1 Hz, 2H), 7.09 (d, *J* = 8.1 Hz, 2H), 4.98-4.96 (m, 1H), 4.60-4.58 (m, 1H), 3.71 (s, 3H), 3.15-3.01 (m, 2H), 1.43 (s, 9H); <sup>13</sup>C NMR (125 MHz, CDCl<sub>3</sub>) δ = 172.1, 155.0, 136.9, 132.1, 129.3, 121.4, 80.1, 79.7, 54.2, 52.3, 49.8, 38.3, 28.3; HRMS (ESI) *m/z* calculated for C<sub>12</sub>H<sub>13</sub>BrNO<sub>2</sub> [M-BOC+H]<sup>+</sup> 282.0124; found 282.0115.

## 10.4 Synthesis of Alkynyl Sulfides

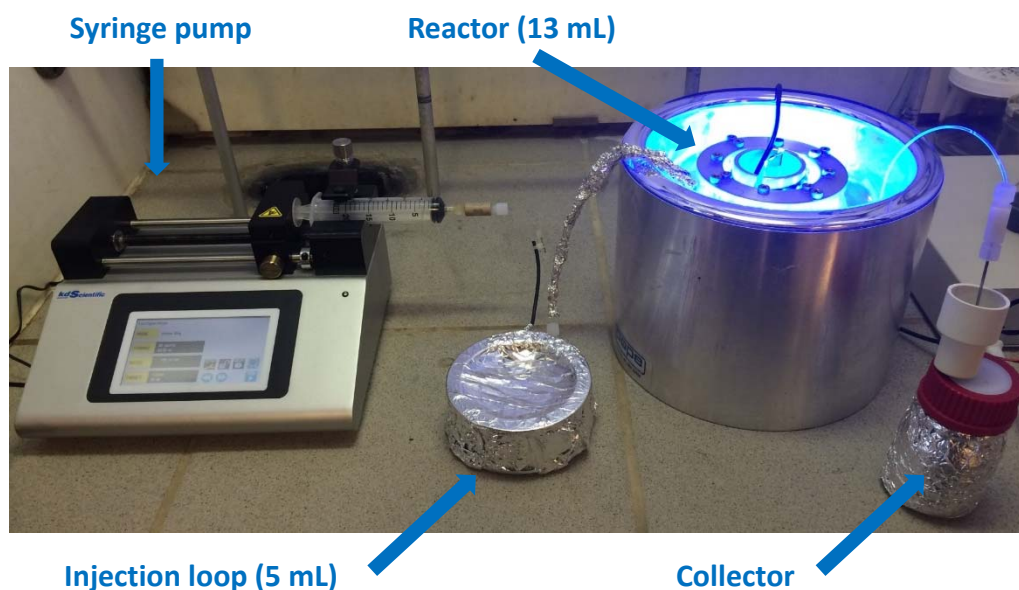


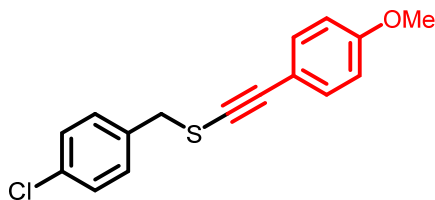
**Figure 10.2** Continuous flow reactor set-up used for the visible-light-mediated synthesis of alkynyl sulfides



**Figure 10.3** Continuous flow reactor - light source outside homemade PFA coil (13 mL, 1 mm I.D.). Blue LED ribbon was purchased from Creative Lighting Solutions, LLC. *Specifications:* 1210 series, electric blue ( $\lambda_{\text{max}} = 465 \text{ nm}$ ), 12 volt DC, 3.6 watts/meter.

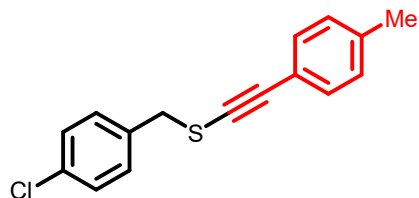
**Representative Procedure for the Photocatalyzed Coupling under Continuous Flow:**

The bromoalkyne (0.261 mmol, 1.1 equiv.), 4CzIPN (0.00474 mmol, 2 mol%) and NiCl<sub>2</sub>·dme (0.0237 mmol, 10 mol%) were added to a 20 mL screw cap vial. A 23:1 mixture of degassed acetonitrile (4.6 mL) and *N,N*-dimethylformamide (0.2 mL) was added to the vial (0.05 M). The reaction mixture was sonicated until complete homogeneity following the addition of pyridine (0.474 mmol, 2 equiv.). The thiol (0.237 mmol, 1.0 equiv.) was then added to the reaction mixture. The solution was injected via a syringe into an aluminium foil-covered 5 mL injection loop. The injection syringe was switched with a syringe containing 20 mL of acetonitrile. The solvent-containing syringe was positioned onto the KD Scientific syringe pump. The pump was turned on at a flow rate of 0.430 mL/min. The reaction mixture was pumped through a 13 mL PFA-coiled reactor irradiated with blue LEDs for a 30 minutes residence time. The collected solution was concentrated under vacuum to provide a residue which was purified by column chromatography on silica-gel.

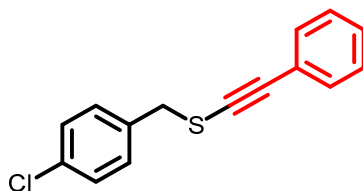


**(4-Chlorobenzyl)((4-methoxyphenyl)ethynyl)sulfane (6.3a):** Following the representative procedure described above, the residue was purified by column chromatography on silica-gel (100 % hexanes → 2.5 % diethyl ether in hexanes) to afford alkynyl sulfide **6.3a** as a white solid (72 mg, 96 % yield). <sup>1</sup>H NMR (400 MHz, CDCl<sub>3</sub>) δ = 7.34-7.15 (m, 6H), 6.83 (d, 2H, *J* = 8.8 Hz), 3.95 (s, 2H), 3.82 (s, 3H); <sup>13</sup>C NMR (75 MHz, CDCl<sub>3</sub>) δ = 159.7, 135.3, 133.5, 133.3, 130.4, 130.2, 128.7, 115.2; 113.9, 94.8, 55.3, 39.7; HRMS (ESI) *m/z* calculated for C<sub>16</sub>H<sub>14</sub>ClOS [M+H]<sup>+</sup> 289.0448; found 289.0447.

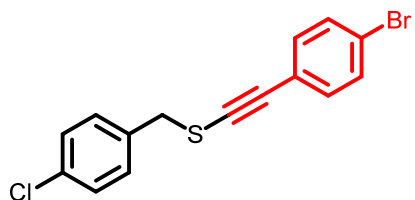




**(4-Chlorobenzyl)(*p*-tolylethynyl)sulfane (6.3b):** Following the representative procedure described above, the residue was purified by column chromatography on silica-gel (100 % hexanes → 1 % diethyl ether in hexanes) to afford alkynyl sulfide **6.3b** as a white solid (57 mg, 88 % yield).  $^1\text{H}$  NMR (400 MHz,  $\text{CDCl}_3$ )  $\delta$  = 7.37-7.27 (m, 6H), 7.13 (d,  $J$  = 7.9 Hz, 2H), 3.98 (s, 2H), 2.37 (s, 3H);  $^{13}\text{C}$  NMR (75 MHz,  $\text{CDCl}_3$ )  $\delta$  = 138.5, 135.3, 133.6, 131.4, 130.6, 130.4, 129.0, 128.7, 120.0, 95.1, 39.6, 21.5; HRMS (ESI)  $m/z$  calculated for  $\text{C}_{16}\text{H}_{14}\text{ClS}$   $[\text{M}+\text{H}]^+$  273.0499; found 273.0492.

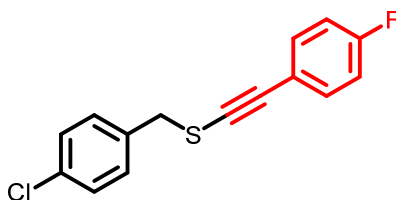


**(4-Chlorobenzyl)(phenylethynyl)sulfane (6.3c):** Following the representative procedure described above, the residue was purified by column chromatography on silica-gel (100 % hexanes → 1 % diethyl ether in hexanes) to afford alkynyl sulfide **6.3c** as a white solid (71 mg, 98 % yield).  $^1\text{H}$  NMR (400 MHz,  $\text{CDCl}_3$ )  $\delta$  = 7.38-7.31 (m, 9H), 3.98 (s, 2H);  $^{13}\text{C}$  NMR (75 MHz,  $\text{CDCl}_3$ )  $\delta$  = 135.2, 133.6, 131.3, 130.4, 128.7, 128.3, 128.2, 123.1, 95.0, 78.6, 39.6; HRMS (ESI)  $m/z$  calculated for  $\text{C}_{15}\text{H}_{12}\text{ClS}$   $[\text{M}+\text{H}]^+$  259.0343; found 259.0345.

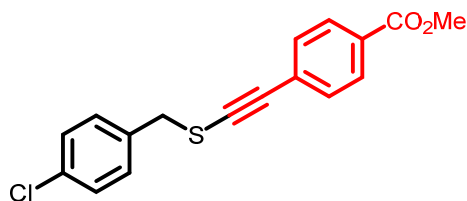


**((4-Bromophenyl)ethynyl)(4-chlorobenzyl)sulfane (6.3d):** Following the representative procedure described above, the residue was purified by column chromatography on silica-gel

(100 % hexanes → 1 % diethyl ether in hexanes) to afford alkynyl sulfide **6.3d** as a white solid (63 mg, 78 % yield).  $^1\text{H}$  NMR (300 MHz,  $\text{CDCl}_3$ )  $\delta$  = 7.43 (d,  $J$  = 8.4 Hz, 2H), 7.36-7.29 (m, 4H), 7.19 (d,  $J$  = 8.4 Hz, 2H), 3.97 (s, 2H);  $^{13}\text{C}$  NMR (75 MHz,  $\text{CDCl}_3$ )  $\delta$  = 135.0, 133.7, 132.7, 131.6, 130.4, 128.7, 122.4, 122.1, 93.9, 80.1, 39.5; HRMS (ESI)  $m/z$  calculated for  $\text{C}_{15}\text{H}_{11}\text{BrClS}$   $[\text{M}+\text{H}]^+$  336.9448; found 336.9448.

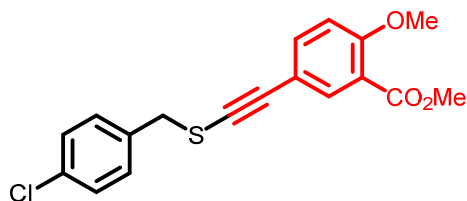


**(4-Chlorobenzyl)((4-fluorophenyl)ethynyl)sulfane (6.3e):** Following the representative procedure described above, the residue was purified by column chromatography on silica-gel (100 % hexanes → 1 % diethyl ether in hexanes) to afford alkynyl sulfide **6.3e** as a white solid (62 mg, 95 % yield).  $^1\text{H}$  NMR (400 MHz,  $\text{CDCl}_3$ )  $\delta$  = 7.35-7.30 (m, 6H), 7.00 (dd,  $J$  = 8.6, 8.6 Hz, 2H), 3.97 (s, 2H);  $^{13}\text{C}$  NMR (75 MHz,  $\text{CDCl}_3$ )  $\delta$  = 162.5 (d,  $J$  = 249.8 Hz), 135.1, 133.7, 133.5 (d,  $J$  = 8.4 Hz), 130.4, 128.7, 119.2 (d,  $J$  = 3.5 Hz), 115.6 (d,  $J$  = 22.1 Hz), 93.8, 78.3 (d,  $J$  = 1.6 Hz), 39.5; HRMS (ESI)  $m/z$  calculated for  $\text{C}_{15}\text{H}_{11}\text{ClFS}$   $[\text{M}+\text{H}]^+$  277.0249; found 277.0247.

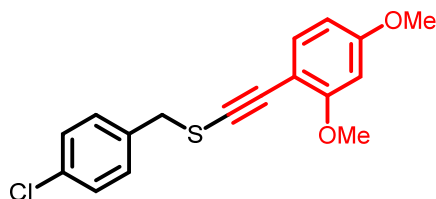


**Methyl 4-(((4-chlorobenzyl)thio)ethynyl)benzoate (6.3f):** Following the representative procedure described above, the residue was purified by column chromatography on silica-gel (100 % hexanes → 5 % diethyl ether in hexanes) to afford alkynyl sulfide **6.3f** as a white solid (53 mg, 71 % yield).  $^1\text{H}$  NMR (400 MHz,  $\text{CDCl}_3$ )  $\delta$  = 7.96 (d,  $J$  = 8.3 Hz, 2H), 7.37-7.30 (m, 6H), 3.99 (s, 2H), 3.92 (s, 3H);  $^{13}\text{C}$  NMR (75 MHz,  $\text{CDCl}_3$ )  $\delta$  = 166.4, 134.9, 134.0, 130.7,

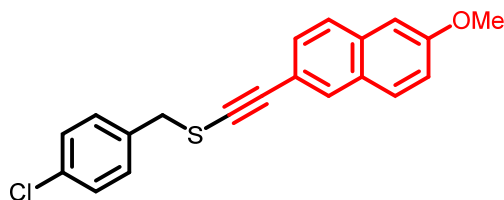
130.4, 129.5, 129.1, 128.8, 127.8, 94.6, 82.6, 52.2, 39.5; HRMS (ESI)  $m/z$  calculated for  $C_{17}H_{14}ClO_2S$   $[M+H]^+$  317.0398; found 317.0408.



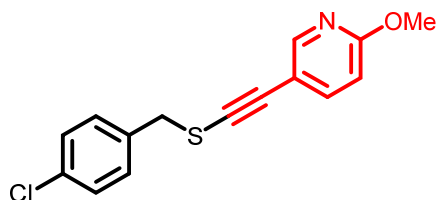
**Methyl 5-(((4-chlorobenzyl)thio)ethynyl)-2-methoxybenzoate (6.3g):** Following the representative procedure described above, the residue was purified by column chromatography on silica-gel (100 % hexanes  $\rightarrow$  % diethyl ether in hexanes) to afford alkynyl sulfide **6.3g** as a white solid (61 mg, 74 % yield).  $^1H$  NMR (400 MHz,  $CDCl_3$ )  $\delta$  = 7.80 (d,  $J$  = 1.8 Hz, 1H), 7.43 (dd,  $J$  = 8.7, 1.8 Hz, 1H), 7.34-7.28 (m, 4H), 6.90 (d,  $J$  = 8.7 Hz, 1H), 3.94 (s, 2H), 3.90 (s, 3H), 3.89 (s, 3H);  $^{13}C$  NMR (100 MHz,  $CDCl_3$ )  $\delta$  = 165.6, 158.9, 136.6, 135.2, 135.1, 133.6, 130.4, 128.7, 120.1, 115.0, 112.0, 93.7, 77.8, 56.1, 52.1, 39.6; HRMS (ESI)  $m/z$  calculated for  $C_{18}H_{16}ClO_3S$   $[M+H]^+$  347.0503; found 347.0520.



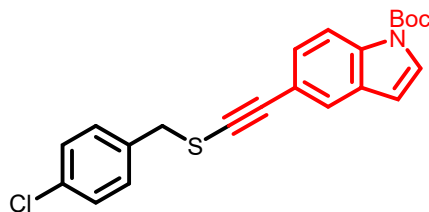
**(4-Chlorobenzyl)((2,4-dimethoxyphenyl)ethynyl)sulfane (6.3h):** Following the representative procedure described above, the residue was purified by column chromatography on silica-gel (100 % hexanes  $\rightarrow$  10 % diethyl ether in hexanes) to afford alkynyl sulfide **6.3h** as a white solid (60 mg, 80 % yield).  $^1H$  NMR (400 MHz,  $CDCl_3$ )  $\delta$  = 7.35-7.30 (m, 4H), 7.25 (d,  $J$  = 8.1 Hz, 1H), 6.45-6.42 (m, 2H), 3.95 (s, 2H), 3.84 (s, 3H), 3.82 (s, 3H);  $^{13}C$  NMR (75 MHz,  $CDCl_3$ )  $\delta$  = 161.5, 161.3, 135.5, 134.6, 133.3, 130.4, 128.5, 104.9, 104.7, 98.3, 91.0, 80.4, 55.7, 55.4, 39.8; HRMS (ESI)  $m/z$  calculated for  $C_{17}H_{16}ClO_2S$   $[M+H]^+$  319.0554; found 319.0560.



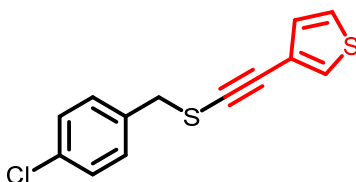
**(4-Chlorobenzyl)((6-methoxynaphthalen-2-yl)ethynyl)sulfane (6.3i):** Following the representative procedure described above, the residue was purified by column chromatography on silica-gel (100 % hexanes  $\rightarrow$  5 % diethyl ether in hexanes) to afford alkynyl sulfide **6.3i** as a white solid (52 mg, 65 % yield).  $^1\text{H}$  NMR (400 MHz,  $\text{CDCl}_3$ )  $\delta$  = 7.79 (s, 1H), 7.68 (d,  $J$  = 9.0 Hz, 1H), 7.65 (d,  $J$  = 8.5 Hz, 1H), 7.37-7.26 (m, 5H), 7.16 (dd,  $J$  = 9.0, 2.5 Hz, 1H), 7.10 (d,  $J$  = 2.2 Hz, 1H), 4.00 (s, 2H), 3.93 (s, 3H);  $^{13}\text{C}$  NMR (75 MHz,  $\text{CDCl}_3$ )  $\delta$  = 158.4, 135.3, 134.1, 133.6, 131.3, 130.5, 129.3, 128.9, 128.7, 128.4, 126.8, 119.4, 118.0, 105.8, 95.5, 78.0, 55.3, 39.7; HRMS (ESI)  $m/z$  calculated for  $\text{C}_{20}\text{H}_{16}\text{OSCl}$   $[\text{M}+\text{H}]^+$  339.0605; found 339.0611.



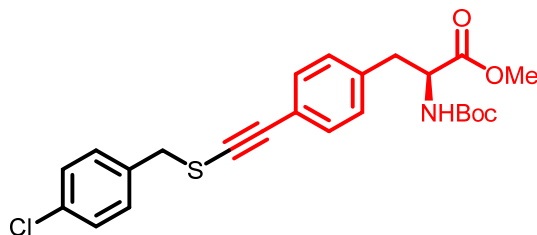
**5-(((4-Chlorobenzyl)thio)ethynyl)-2-methoxypyridine (6.3j):** Following the representative procedure described above, the residue was purified by column chromatography on silica-gel (100 % hexanes  $\rightarrow$  5 % diethyl ether in hexanes) to afford alkynyl sulfide **6.3j** as a white solid (57 mg, 83 % yield).  $^1\text{H}$  NMR (400 MHz,  $\text{CDCl}_3$ )  $\delta$  = 8.19 (d,  $J$  = 1.8 Hz, 1H), 7.50 (dd,  $J$  = 8.6, 2.1 Hz, 1H), 7.33-7.28 (m, 4H), 6.67 (d,  $J$  = 8.6 Hz, 1H), 3.95 (s, 2H), 3.94 (s, 3H);  $^{13}\text{C}$  NMR (75 MHz,  $\text{CDCl}_3$ )  $\delta$  = 163.4, 150.4, 141.3, 135.1, 133.7, 130.4, 128.7, 113.0, 110.6, 91.7, 79.9, 53.6, 39.6; HRMS (ESI)  $m/z$  calculated for  $\text{C}_{15}\text{H}_{13}\text{ClNOS}$   $[\text{M}+\text{H}]^+$  290.0401; found 290.0413.



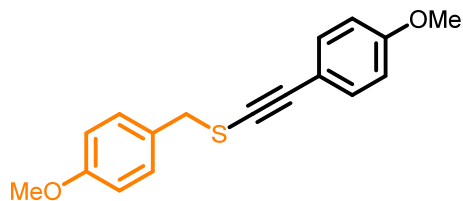
**tert-Butyl 5-(((4-chlorobenzyl)thio)ethynyl)-1H-indole-1-carboxylate (6.3k):** Following the representative procedure described above, the residue was purified by column chromatography on silica-gel (100 % hexanes  $\rightarrow$  2.5 % diethyl ether in hexanes) to afford alkynyl sulfide **6.3k** as a white solid (88 mg, 94 % yield).  $^1\text{H}$  NMR (400 MHz,  $\text{CDCl}_3$ )  $\delta$  = 8.08 (d,  $J$  = 8.4 Hz, 1H), 7.62 (d,  $J$  = 3.7 Hz, 1H), 7.58 (d,  $J$  = 1.0 Hz, 1H), 7.36-7.33 (m, 4H), 7.31 (dd,  $J$  = 8.7, 1.6 Hz, 1H), 6.54 (d,  $J$  = 3.8 Hz, 1H), 3.98 (s, 2H), 1.69 (s, 9 H);  $^{13}\text{C}$  NMR (100 MHz,  $\text{CDCl}_3$ )  $\delta$  = 149.4, 135.3, 134.7, 133.6, 130.6, 130.4, 128.7, 127.8, 126.8, 124.5, 117.2, 115.1, 107.0, 95.6, 84.0, 76.7, 39.7, 28.1; HRMS (ESI)  $m/z$  calculated for  $\text{C}_{22}\text{H}_{21}\text{ClNO}_2\text{S}$   $[\text{M}+\text{H}]^+$  398.0976; found 398.0987.



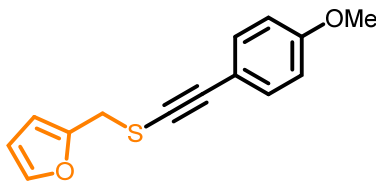
**3-(((4-Chlorobenzyl)thio)ethynyl)thiophene (6.3l):** Following the representative procedure described above, the residue was purified by column chromatography on silica-gel (100 % hexanes  $\rightarrow$  1 % diethyl ether in hexanes) to afford alkynyl sulfide **6.3l** as a white solid (60 mg, 95 % yield).  $^1\text{H}$  NMR (400 MHz,  $\text{CDCl}_3$ )  $\delta$  = 7.40 (dd,  $J$  = 3.0, 1.1 Hz, 1H), 7.34-7.29 (m, 4H), 7.25 (dd,  $J$  = 5.0, 3.0 Hz, 1H), 7.05 (dd,  $J$  = 5.0, 1.1 Hz, 1H), 3.96 (s, 2H);  $^{13}\text{C}$  NMR (125 MHz,  $\text{CDCl}_3$ )  $\delta$  = 135.2, 133.7, 130.4, 129.9, 129.3, 128.7, 125.3, 122.2, 89.9, 78.0, 39.7; HRMS (ESI)  $m/z$  calculated for  $\text{C}_{13}\text{H}_{10}\text{ClS}_2$   $[\text{M}+\text{H}]^+$  264.9907; found 264.9901.



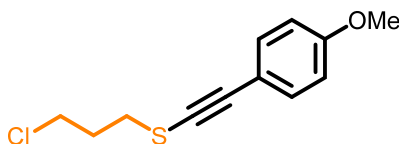
**Methyl (S)-2-(((4-chlorobenzyl)thio)ethynyl)-3-((tert-butoxycarbonyl)amino)propanoate (6.3m):** Following the representative procedure described above, the residue was purified by column chromatography on silica-gel (100 % hexanes  $\rightarrow$  15 % ethyl acetate in hexanes) to afford alkynyl sulfide **6.3m** as a white solid (102 mg, 94 % yield).  $^1\text{H}$  NMR (400 MHz,  $\text{CDCl}_3$ )  $\delta$  = 7.34-7.29 (m, 4H), 7.26 (d,  $J$  = 8.0 Hz, 2H), 7.06 (d,  $J$  = 7.9 Hz, 2H), 4.99-4.97 (m, 1H), 4.58-4.57 (m, 1H), 3.95 (s, 2H), 3.71 (s, 3H), 3.13-3.00 (m, 2H), 1.42 (s, 9H);  $^{13}\text{C}$  NMR (75 MHz,  $\text{CDCl}_3$ )  $\delta$  = 172.1, 155.0, 136.4, 135.2, 133.6, 131.5, 130.4, 129.3, 128.7, 121.8, 94.7, 80.0, 78.7, 54.2, 52.2, 39.6, 38.3, 28.2; HRMS (ESI)  $m/z$  calculated for  $\text{C}_{19}\text{H}_{20}\text{ClNO}_2\text{S}$  [ $\text{M-BOC+H}$ ] $^+$  360.0820; found 360.0835.



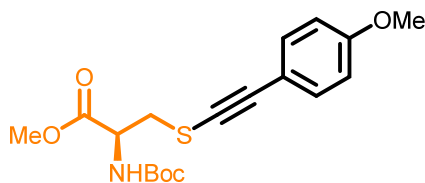
**(4-Methoxybenzyl)((4-methoxyphenyl)ethynyl)sulfane (6.3n):** Following the representative procedure described above, the residue was purified by column chromatography on silica gel (100 % hexanes  $\rightarrow$  2.5 % diethyl ether in hexanes) to afford alkynyl sulfide **6.3n** as a yellow oil (51 mg, 80 % yield).  $^1\text{H}$  NMR (400 MHz,  $\text{CDCl}_3$ )  $\delta$  = 7.34-7.30 (m, 4H), 6.89 (d,  $J$  = 8.6 Hz, 2H), 6.83 (d,  $J$  = 8.9 Hz, 2H), 3.99 (s, 2H), 3.819 (s, 3H), 3.816 (s, 3H);  $^{13}\text{C}$  NMR (75 MHz,  $\text{CDCl}_3$ )  $\delta$  = 159.6, 159.2, 133.3, 130.3, 128.7, 115.5, 114.0, 113.9, 94.2, 77.5, 55.28, 55.27, 40.2; HRMS (ESI)  $m/z$  calculated for  $\text{C}_{17}\text{H}_{18}\text{O}_2\text{S}$  [ $\text{M+H}$ ] $^+$  285.0944; found 285.0933.



**2-((((4-Methoxyphenyl)ethynyl)thio)methyl)furan (6.3o):** Following the representative procedure described above, the residue was purified by column chromatography on silica gel (100 % hexanes  $\rightarrow$  5 % diethyl ether in hexanes) to afford alkynyl sulfide **6.3o** as a yellow oil (53 mg, 91 % yield).  $^1\text{H}$  NMR (400 MHz,  $\text{CDCl}_3$ )  $\delta$  = 7.42 (dd,  $J$  = 1.7, 0.9 Hz, 1H), 7.35 (d,  $J$  = 9.0 Hz, 2H), 6.83 (d,  $J$  = 9.0 Hz, 2H), 6.36-6.34 (m, 2H), 4.04 (s, 2H), 3.81 (s, 3H);  $^{13}\text{C}$  NMR (125 MHz,  $\text{CDCl}_3$ )  $\delta$  = 159.7, 149.7, 142.7, 133.4, 115.3, 113.9, 110.6, 109.0, 94.9, 76.6, 55.3, 33.0; HRMS (ESI)  $m/z$  calculated for  $\text{C}_{14}\text{H}_{13}\text{O}_2\text{S}$   $[\text{M}+\text{H}]^+$  245.0631; found 245.0628.

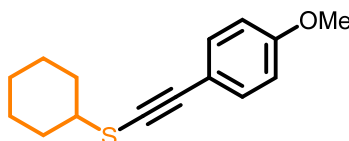


**(3-Chloropropyl)((4-methoxyphenyl)ethynyl)sulfane (6.3p):** Following the representative procedure described above, the residue was purified by column chromatography on silica gel (100 % hexanes  $\rightarrow$  1 % diethyl ether in hexanes) to afford alkynyl sulfide **6.3p** as a yellow oil (35 mg, 61 % yield).  $^1\text{H}$  NMR (400 MHz,  $\text{CDCl}_3$ )  $\delta$  = 7.38 (d,  $J$  = 8.9 Hz, 2H), 6.84 (d,  $J$  = 8.8 Hz, 2H), 3.82 (s, 3H), 3.75 (t,  $J$  = 6.2 Hz, 2H), 2.94 (t,  $J$  = 6.8 Hz, 2H), 2.31-2.25 (m, 2H);  $^{13}\text{C}$  NMR (75 MHz,  $\text{CDCl}_3$ )  $\delta$  = 159.7, 133.4, 115.3, 113.9, 93.2, 76.4, 55.3, 42.8, 32.5, 31.8; HRMS (ESI)  $m/z$  calculated for  $\text{C}_{12}\text{H}_{14}\text{ClOS}$   $[\text{M}+\text{H}]^+$  241.0448; found 241.0452.

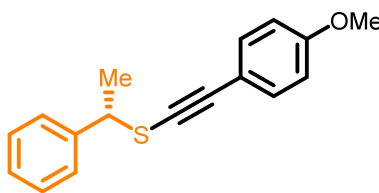


**Methyl *N*-(*tert*-butoxycarbonyl)-*S*-((4-methoxyphenyl)ethynyl)-*D*-cysteinate (6.3q):** Following the representative procedure described above, the residue was purified by column

chromatography on silica-gel (100 % hexanes → 5 % ethyl acetate in hexanes) to afford alkynyl sulfide **6.3q** as a white solid (65 mg, 75 % yield).  $^1\text{H}$  NMR (400 MHz,  $\text{CDCl}_3$ )  $\delta$  = 7.39 (d,  $J$  = 8.9 Hz, 2H), 6.83 (d,  $J$  = 8.9 Hz, 2H), 5.61-5.59 (m, 1H), 4.74-4.72 (m, 1H), 3.82 (s, 3H), 3.73 (s, 3H), 3.32-3.21 (m, 2H), 1.44 (s, 9H);  $^{13}\text{C}$  NMR (125 MHz,  $\text{CDCl}_3$ )  $\delta$  = 170.3, 159.9, 155.0, 133.6, 115.0, 113.9, 92.9, 80.3, 76.1, 55.3, 53.5, 52.7, 38.0, 28.3; HRMS (ESI)  $m/z$  calculated for  $\text{C}_{18}\text{H}_{23}\text{NO}_2\text{SNa}$   $[\text{M}+\text{Na}]^+$  388.1189; found 388.1206.



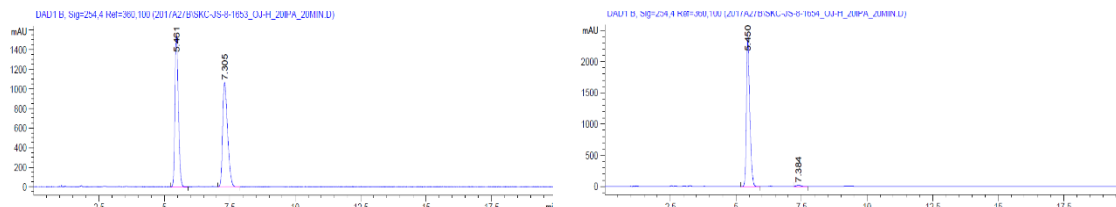
**Cyclohexyl-((4-methoxyphenyl)ethynyl)sulfane (6.3r):** Following the representative procedure described above, the residue was purified by column chromatography on silica gel (100 % hexanes → 1 % diethyl ether in hexanes) to afford alkynyl sulfide **6.3r** as a yellow oil (38 mg, 66 % yield).  $^1\text{H}$  NMR (400 MHz,  $\text{CDCl}_3$ )  $\delta$  = 7.38 (d,  $J$  = 8.9 Hz, 2H), 6.83 (d,  $J$  = 8.9 Hz, 2H), 3.82 (s, 3H), 3.01-2.95 (m, 1H), 2.13-2.09 (m, 2H), 1.85-1.79 (m, 2H), 1.67-1.56 (m, 3H), 1.41-1.30 (m, 3H);  $^{13}\text{C}$  NMR (75 MHz,  $\text{CDCl}_3$ )  $\delta$  = 159.5, 133.3, 115.8, 113.9, 94.0, 76.5, 55.3, 47.7, 33.0, 26.1, 25.4; HRMS (ESI)  $m/z$  calculated for  $\text{C}_{15}\text{H}_{19}\text{OS}$   $[\text{M}+\text{H}]^+$  247.1151; found 247.1156.



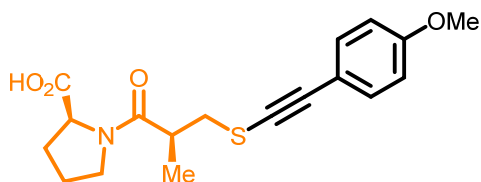
**(S)-((4-Methoxyphenyl)ethynyl)(1-phenylethyl)sulfane (6.3s):** Following the representative procedure described above, the residue was purified by column chromatography on silica gel (100 % hexanes → 1 % diethyl ether in hexanes) to afford alkynyl sulfide **6.3s** as a white solid (45 mg, 70 % yield).  $^1\text{H}$  NMR (400 MHz,  $\text{CDCl}_3$ )  $\delta$  = 7.42-7.28 (m, 7H), 6.83 (d,  $J$  = 8.9 Hz, 2H), 4.34 (q,  $J$  = 7.0 Hz, 1H), 3.82 (s, 3H), 1.81 (d,  $J$  = 7.0 Hz, 3H);  $^{13}\text{C}$  NMR (100 MHz,  $\text{CDCl}_3$ )  $\delta$  = 159.6, 141.5, 133.3, 128.5, 127.8, 127.3, 115.6, 113.9, 95.3, 77.2, 55.3, 48.5, 21.1;



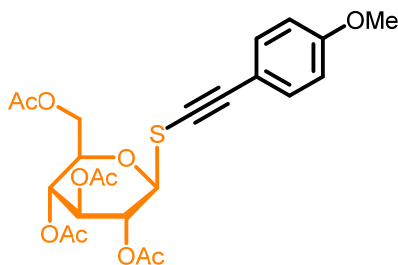
HRMS (ESI)  $m/z$  calculated for  $C_{17}H_{17}OS$   $[M+H]^+$  269.0995; found 269.0985. The enantiomeric purity was determined by SFC analysis in comparison with racemic material (OJ-H, BPR pressure: 150 bar, column temperature: 30 °C, injection volume: 15  $\mu$ L into 20  $\mu$ L loop, solvent: 20 % IPA, signal = 254.4 nm):  $t_R$  of **6.3s**: 5 min (major) and 7 min (minor).



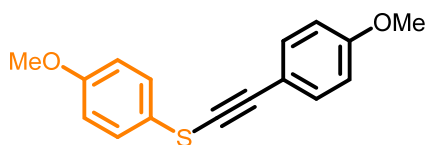
Peak #	Ret. Time	Area %	Peak #	Ret. Time	Area %
1	5.5	50.123	1	5.5	98.937
2	7.3	49.877	2	7.4	1.063



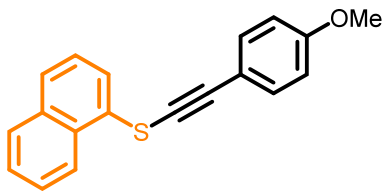
**((S)-3-(((4-Methoxyphenyl)ethynyl)thio)-2-methylpropanoyl)-L-proline (6.3t):** Following the representative procedure described above, the residue was purified by column chromatography on silica gel (100 % dichloromethane  $\rightarrow$  10 % methanol in dichloromethane) to afford alkynyl sulfide **6.3t** as a yellow oil (50 mg, 61 % yield).  $^1H$  NMR (400 MHz,  $CDCl_3$ )  $\delta$  = 10.16 (br s, 1H), 7.34 (d,  $J$  = 8.9 Hz, 2H), 6.83 (d,  $J$  = 8.9 Hz, 2H), 4.58-4.56 (m, 1H), 3.82-3.74 (m, 4H), 3.68-3.62 (m, 1H), 3.21-3.13 (m, 1H), 3.09-3.04 (m, 1H), 2.78 (dd,  $J$  = 12.8, 5.1 Hz, 1H), 2.24-2.10 (m, 2H), 2.04-1.88 (m, 2H), 1.28 (d,  $J$  = 6.7 Hz, 3H);  $^{13}C$  NMR (100 MHz,  $CDCl_3$ )  $\delta$  = 176.8, 174.9, 159.7, 133.3, 130.5, 115.1, 114.0, 93.2, 76.9, 55.2, 47.4, 38.5, 38.3, 28.2, 24.7, 16.8; HRMS (ESI)  $m/z$  calculated for  $C_{18}H_{22}NO_4S$   $[M+H]^+$  348.1264; found 348.1264.



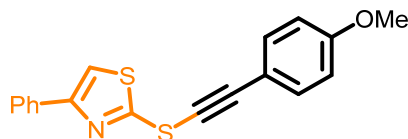
**(2*R*,3*R*,4*S*,5*R*,6*S*)-2-(Acetoxymethyl)-6-(((4-methoxyphenyl)ethynyl)thio)tetrahydro-2*H*-pyran-3,4,5-triyl triacetate (6.3u):** Following the representative procedure described above, the residue was purified by column chromatography on silica gel (100 % dichloromethane → 2.5 % methanol in dichloromethane) to afford alkynyl sulfide **6.3u** as a white solid (56 mg, 50 % yield). <sup>1</sup>H NMR (400 MHz, CDCl<sub>3</sub>) δ = 7.46 (d, *J* = 8.9 Hz, 2H), 6.85 (d, *J* = 8.9 Hz, 2H), 5.35 (dd, *J* = 9.2, 9.2 Hz, 1H), 5.27 (dd, *J* = 9.2, 9.1 Hz, 1H), 5.13 (dd, *J* = 9.8, 9.3 Hz, 1H), 4.60 (d, *J* = 9.4 Hz, 1H), 4.26 (dd, *J* = 12.4, 4.9 Hz, 1H), 4.19 (dd, *J* = 12.4, 2.3 Hz, 1H), 3.82 (s, 3H), 3.81-3.77 (m, 1H), 2.11 (s, 3H), 2.06 (s, 3H), 2.03 (s, 3H), 2.02 (s, 3H); <sup>13</sup>C NMR (125 MHz, CDCl<sub>3</sub>) δ = 170.6, 170.2, 169.3, 169.0, 160.2, 134.1, 114.7, 113.9, 97.1, 84.5, 76.4, 73.9, 70.7, 69.7, 67.8, 62.0, 55.3, 20.69, 20.65, 20.56, 20.53; HRMS (ESI) *m/z* calculated for C<sub>23</sub>H<sub>27</sub>O<sub>10</sub>S [M+H]<sup>+</sup> 495.1319; found 495.1332.



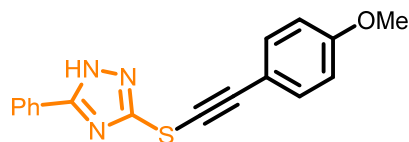
**(4-Methoxyphenyl)((4-methoxyphenyl)ethynyl)sulfane (6.3v):** Following the representative procedure described above, the residue was purified by column chromatography on silica gel (100 % hexanes → 2.5 % diethyl ether in hexanes) to afford alkynyl sulfide **6.3v** as a yellow oil (62 mg, 97 % yield). <sup>1</sup>H NMR (500 MHz, CDCl<sub>3</sub>) δ = 7.45 (d, *J* = 8.9 Hz, 2H), 7.43 (d, *J* = 8.9 Hz, 2H), 6.91 (d, *J* = 8.8 Hz, 2H), 6.86 (d, *J* = 8.9 Hz, 2H), 3.83 (s, 3H), 3.81 (s, 3H); <sup>13</sup>C NMR (125 MHz, CDCl<sub>3</sub>) δ = 159.9, 158.9, 133.6, 132.6, 128.6, 123.5, 115.1, 115.0, 114.6, 114.0, 96.3, 75.0, 55.4, 55.3; HRMS (ESI) *m/z* calculated for C<sub>16</sub>H<sub>15</sub>O<sub>2</sub>S [M+H]<sup>+</sup> 271.0787; found 271.0774.



**((4-Methoxyphenyl)ethynyl)(naphthalen-1-yl)sulfane (6.3w):** Following the representative procedure described above, the residue which was purified by column chromatography on silica-gel (100 % hexanes) to afford alkynyl sulfide **6.3w** as a yellow solid (44 mg, 78 % yield).  $^1\text{H}$  NMR (400 MHz,  $\text{CDCl}_3$ ) 8.14 (d,  $J = 8.2$  Hz, 1H), 7.93 (d,  $J = 7.3$  Hz, 1H), 7.89 (d,  $J = 7.5$  Hz, 1H), 7.77 (d,  $J = 8.2$  Hz, 1H), 7.61 – 7.47 (m, 5H), 6.89 (d,  $J = 8.8$  Hz, 2H), 3.84 (s, 3H);  $^{13}\text{C}$  NMR (125 MHz,  $\text{CDCl}_3$ )  $\delta = 160.1, 133.8$  (2C), 130.6, 130.2, 128.6, 127.3, 126.5, 126.4, 125.9, 125.1, 123.4, 115.0, 114.0, 98.0, 73.5, 55.3; HRMS (ESI)  $m/z$  calculated for  $\text{C}_{19}\text{H}_{15}\text{OS}$   $[\text{M}+\text{H}]^+$  291.0838; found 294.0842.

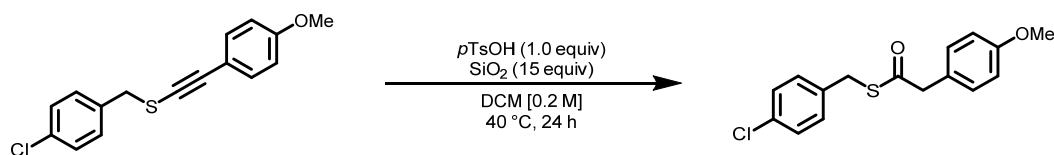


**2-(((4-Methoxyphenyl)ethynyl)thio)-4-phenylthiazole (6.3x):** Following the representative procedure described above, the residue was purified by column chromatography on silica gel (100 % hexanes  $\rightarrow$  5 % diethyl ether in hexanes) to afford alkynyl sulfide **6.3x** as a beige solid (40 mg, 52 % yield).  $^1\text{H}$  NMR (400 MHz,  $\text{CDCl}_3$ )  $\delta = 7.87$  (d,  $J = 7.2$  Hz, 2H), 7.52 (d,  $J = 8.9$  Hz, 2H), 7.45 (s, 1H), 7.43 (dd,  $J = 7.8, 7.3$  Hz, 2H), 7.36-7.33 (m, 1H), 6.91 (d,  $J = 8.9$  Hz, 2H), 3.86 (s, 3H);  $^{13}\text{C}$  NMR (100 MHz,  $\text{CDCl}_3$ )  $\delta = 160.7, 156.9, 134.0, 133.9, 128.7, 128.3, 126.2, 114.2, 114.0, 113.6, 101.5, 77.2, 71.6, 55.4$ ; HRMS (ESI)  $m/z$  calculated for  $\text{C}_{18}\text{H}_{14}\text{NOS}_2$   $[\text{M}+\text{H}]^+$  324.0511; found 324.0510.

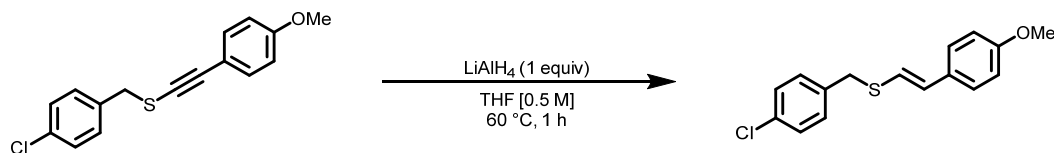


**3-(((4-Methoxyphenyl)ethynyl)thio)-5-phenyl-1H-1,2,4-triazole (6.3y):** Following the representative procedure described above, the residue was purified by column chromatography on silica gel (100 % hexanes  $\rightarrow$  20 % diethyl ether in hexanes) to afford alkynyl sulfide **6.3y** as a beige solid (69 mg, 95 % yield). *Compound 6.3y decomposed quickly both neat and in solution complicating the characterization of the product. As such, characterization was limited to  $^1\text{H}$  NMR and HRMS.*  $^1\text{H}$  NMR (400 MHz,  $\text{CDCl}_3$ )  $\delta$  = 8.27-8.24 (m, 2H), 8.14 (d,  $J$  = 8.9 Hz, 2H), 7.51-7.43 (m, 3H), 7.07 (d,  $J$  = 8.9 Hz, 2H), 6.96 (s, 1H), 3.91 (s, 3H); HRMS (ESI)  $m/z$  calculated for  $\text{C}_{17}\text{H}_{14}\text{N}_3\text{OS}$   $[\text{M}+\text{H}]^+$  308.0852; found 308.0837.

## 10.5 Post-Functionalization Reactions

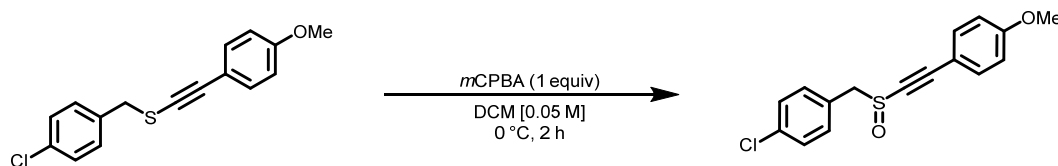


***S*-(4-Chlorobenzyl)-2-(4-methoxyphenyl)ethanethioate (6.4):** (4-Chlorobenzyl)((4-methoxyphenyl)ethynyl)sulfane (0.116 g, 0.400 mmol, 1.0 equiv.) was dissolved in dry dichloromethane (2 mL) and *p*-toluenesulfonic acid (0.068 g, 0.400 mmol, 1.0 equiv.) and SiO<sub>2</sub> (0.400 g, 6.00 mmol, 15 equiv.) were then added in one portion. The mixture was stirred at 60 °C for 12 hours. Silica gel was added to the mixture and the volatiles were removed under vacuum. The residue was placed on a column of silica gel and purified by column chromatography (100 % hexanes → 10 % diethyl ether in hexanes). Thioate **6.4** was obtained as a white solid (0.075 g, 62 % yield). <sup>1</sup>H NMR (400 MHz, CDCl<sub>3</sub>) δ = 7.26-7.19 (m, 6H), 6.88 (d, *J* = 8.6 Hz, 2H), 4.05 (s, 2H), 3.81 (s, 3H), 3.79 (s, 2H); <sup>13</sup>C NMR (100 MHz, CDCl<sub>3</sub>) δ = 197.1, 159.0, 136.0, 133.0, 130.7, 130.2, 128.7, 125.2, 114.1, 55.2, 49.3, 32.8; HRMS (ESI) *m/z* calculated for C<sub>16</sub>H<sub>16</sub>ClO<sub>2</sub>S [M+H]<sup>+</sup> 307.0554; found 307.0563.

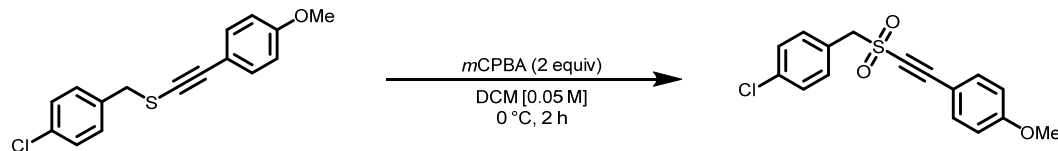


***E*-(4-Chlorobenzyl)(4-methoxystyryl)sulfane (6.5):** (4-Chlorobenzyl)((4-methoxyphenyl)ethynyl)sulfane (0.100 g, 0.346 mmol, 1.0 equiv.) was dissolved in dry tetrahydrofuran (1 mL) and LiAlH<sub>4</sub> (0.013 g, 0.346 mmol, 1.0 equiv.) was then added in one portion. The mixture was stirred at 60 °C for 1 hour and then cooled to 0 °C. 1M HCl was added dropwise to the reaction mixture until a pH ~ 7 was obtained. Diethyl ether was added to the mixture. The organic and aqueous phases were separated. The combined organic phases were dried with anhydrous magnesium sulfate. The resulting suspension was filtered, and the filtrate was concentrated under vacuum to provide a residue which was purified by column chromatography (100 % hexanes → 1 % diethyl ether in hexanes). Vinyl sulfide **6.5** was obtained as a white solid (0.075 g, 75 % yield). <sup>1</sup>H NMR (400 MHz, CDCl<sub>3</sub>) δ = 7.35-7.28 (m,

4H), 7.21 (d,  $J = 8.7$ , 2H), 6.84 (d,  $J = 8.8$  Hz, 2H), 6.52 (d,  $J = 2.4$  Hz, 2H), 3.94 (s, 2H), 3.81 (s, 3H);  $^{13}\text{C}$  NMR (125 MHz,  $\text{CDCl}_3$ )  $\delta = 159.0, 136.0, 133.0, 130.1, 129.6, 129.2, 128.7, 126.9, 120.8, 114.0, 55.2, 37.0$ ; HRMS (ESI)  $m/z$  calculated for  $\text{C}_{16}\text{H}_{16}\text{ClOS}$   $[\text{M}+\text{H}]^+$  291.0605; found 291.0600.

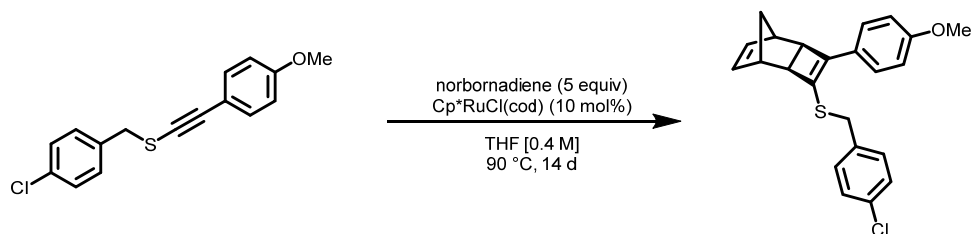


**1-Chloro-4-(((4-methoxyphenyl)ethynyl)sulfinyl)methylbenzene (6.6):** (4-Chlorobenzyl)((4-methoxyphenyl)ethynyl)sulfane (0.250 g, 0.866 mmol, 1.0 equiv.) was dissolved in dry dichloromethane (18 mL) and *m*-CPBA (77% purity, 0.388 g, 1.73 mmol, 2.0 equiv.) was then added in one portion. The mixture was stirred at 0 °C for 2 hours. Silica gel was added to the mixture and the volatiles were removed under vacuum. The residue was placed on a column of silica gel and purified by column chromatography (100 % hexanes  $\rightarrow$  40 % ethyl acetate in hexanes). Sulfoxide **6.6** was obtained as a white solid (0.257 g, 60 % yield).  $^1\text{H}$  NMR (400 MHz,  $\text{CDCl}_3$ )  $\delta = 7.42\text{--}7.33$  (m, 6H), 6.89 (d,  $J = 8.7$  Hz, 2H), 4.35 (d,  $J = 12.6$  Hz, 1H), 4.28 (d,  $J = 12.6$  Hz, 1H), 3.85 (s, 3H);  $^{13}\text{C}$  NMR (75 MHz,  $\text{CDCl}_3$ )  $\delta = 161.5, 134.9, 134.1, 131.9, 128.8, 127.7, 114.3, 111.3, 104.5, 83.7, 61.7, 55.4$ ; HRMS (ESI)  $m/z$  calculated for  $\text{C}_{16}\text{H}_{14}\text{ClO}_2$   $[\text{M}+\text{H}]^+$  305.0398; found 305.0387.

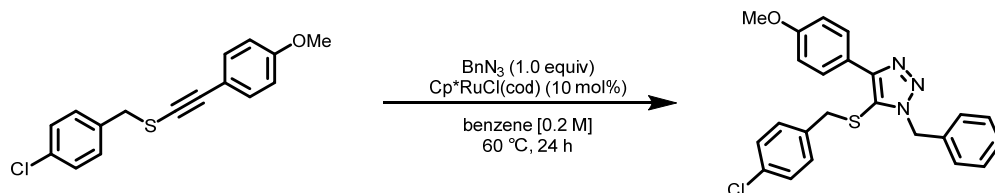


**1-Chloro-4-(((4-methoxyphenyl)ethynyl)sulfonyl)methylbenzene (6.7):** (4-Chlorobenzyl)((4-methoxyphenyl)ethynyl)sulfane (0.250 g, 0.866 mmol, 1.0 equiv.) was dissolved in dry dichloromethane (18 mL) and *m*-CPBA (77% purity, 0.388 g, 1.73 mmol, 2.0 equiv.) was then added in one portion. The mixture was stirred at 0 °C for 2 hours. Silica gel was added to the mixture and the volatiles were removed under vacuum. The residue was placed on a column of silica gel and purified by column chromatography (100 % hexanes  $\rightarrow$  40 % ethyl acetate in hexanes). Sulfone **6.7** was obtained as a white solid (0.257 g, 92 % yield).  $^1\text{H}$  NMR

(400 MHz, CDCl<sub>3</sub>)  $\delta$  = 7.44 (d,  $J$  = 8.9 Hz, 2H), 7.42-7.38 (m, 4H), 6.91 (d,  $J$  = 8.9 Hz, 2H), 4.46 (s, 2H), 3.86 (s, 3H); <sup>13</sup>C NMR (75 MHz, CDCl<sub>3</sub>)  $\delta$  = 162.4, 135.7, 134.8, 132.5, 129.1, 126.0, 114.6, 108.9, 95.7, 81.8, 63.9, 55.5; HRMS (ESI)  $m/z$  calculated for C<sub>16</sub>H<sub>14</sub>ClO<sub>3</sub>S [M+H]<sup>+</sup> 321.0347; found 321.0340.



**(4-Chlorobenzyl)((1*S*,2*R*,5*S*,6*R*)-4-(4-methoxyphenyl)tricyclo[4.2.1.0<sup>2,5</sup>]nona-3,7-dien-3-yl)sulfane (6.8):** (4-Chlorobenzyl)((4-methoxyphenyl)ethynyl)sulfane (0.200 g, 0.693 mmol, 1.0 equiv.) was dissolved in dry tetrahydrofuran (2 mL) and 2,5-norbornadiene (0.35 mL, 3.47 mmol, 5.0 equiv.) was then added in one portion. The solution was transferred into a rubber septum-covered sealable tube containing Cp\*RuCl(cod) (0.026 g, 0.069 mmol, 10 mol%). The reaction mixture was purged with nitrogen for 10 minutes. The septum was then replaced by a Teflon-coated screw cap and the sealed-tube was placed in a pre-heated oil bath at 90 °C. After stirring for 14 days, the mixture was cooled to room temperature and diluted with ethyl acetate. Silica gel was added to the mixture and the volatiles were removed under vacuum. The residue was placed on a column of silica gel and purified by column chromatography (100 % hexanes → 1 % diethyl ether in hexanes). Vinyl sulfide **6.8** was obtained as a beige solid (0.216 g, 82 % yield). <sup>1</sup>H NMR (400 MHz, CDCl<sub>3</sub>)  $\delta$  = 7.40 (d,  $J$  = 8.9 Hz, 2H), 7.35-7.29 (m, 4H), 6.90 (d,  $J$  = 8.8 Hz, 2H), 6.21 (dd,  $J$  = 5.6, 3.0 Hz, 1H), 6.15 (dd,  $J$  = 5.5, 3.0 Hz, 1H), 4.10 (d,  $J$  = 13.5 Hz, 1H), 4.03 (d,  $J$  = 13.5 Hz, 1H), 3.82 (s, 3H), 2.69-2.68 (m, 2H), 2.59-2.58 (m, 1H), 2.52-2.51 (m, 1H), 1.45 (d,  $J$  = 9.2 Hz, 1H), 1.37 (d,  $J$  = 9.2 Hz, 1H); <sup>13</sup>C NMR (100 MHz, CDCl<sub>3</sub>)  $\delta$  = 158.6, 141.0, 136.6, 136.4, 135.4, 133.0, 130.7, 130.0, 128.7, 127.2, 127.0, 113.9, 55.3, 46.4, 43.6, 40.3, 39.8, 39.5, 35.2; HRMS (ESI)  $m/z$  calculated for C<sub>23</sub>H<sub>22</sub>ClOS [M+H]<sup>+</sup> 381.1074; found 381.1091.

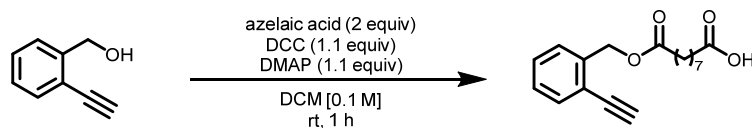


**1-Benzyl-5-((4-chlorobenzyl)thio)-4-(4-methoxyphenyl)-1H-1,2,3-triazole (6.9):**

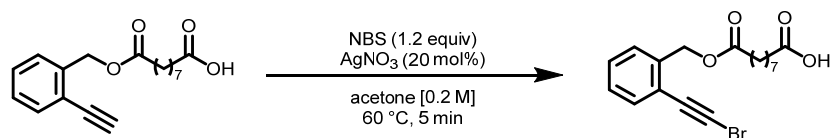
Cp\*RuCl(cod) (0.026 g, 0.069 mmol, 10 mol%) was dissolved in dry benzene (3.5 mL) and (4-chlorobenzyl)((4-methoxyphenyl)ethynyl)sulfane (0.200 g, 0.693 mmol, 1.0 equiv.) and benzyl azide (0.092 g, 0.693 mmol, 1.0 equiv.) were then added in one portion. The reaction mixture was purged with nitrogen for 10 minutes. The mixture was stirred at 60 °C for 24 hours. Silica gel was added to the mixture and the volatiles were removed under vacuum. The residue was placed on a column of silica gel and purified by column chromatography (100 % hexanes → 20 % ethyl acetate in hexanes). Thioether **6.9** was obtained as a beige solid (0.225 g, 77 % yield). <sup>1</sup>H NMR (400 MHz, CDCl<sub>3</sub>) δ = 7.97 (d, *J* = 8.8 Hz, 2H), 7.36-7.27 (m, 5H), 7.03 (d, *J* = 8.4 Hz, 2H), 6.94 (d, *J* = 8.9 Hz, 2H), 6.67 (d, *J* = 8.3 Hz, 2H), 5.38 (s, 2H), 3.85 (s, 3H), 3.40 (s, 2H); <sup>13</sup>C NMR (100 MHz, CDCl<sub>3</sub>) δ = 159.6, 149.7, 135.1, 134.3, 133.4, 129.9, 128.7, 128.4, 128.2, 128.0, 127.7, 122.9, 122.8, 113.7, 55.1, 51.7, 38.9; HRMS (ESI) *m/z* calculated for C<sub>23</sub>H<sub>21</sub>ClN<sub>3</sub>OS [M+H]<sup>+</sup> 422.1088; found 422.1107.



## 10.6 Synthesis of Macrocycle

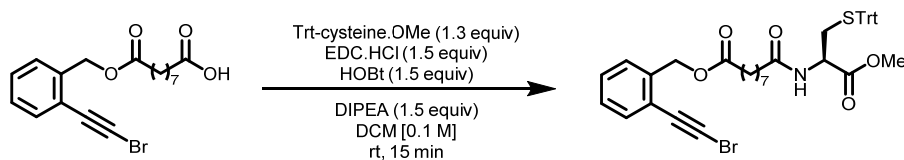


**9-((2-Ethynylbenzyl)oxy)-9-oxononanoic acid (10.13):** To a stirred solution of 2-ethynylbenzyl alcohol (1.00 g, 7.57 mmol, 1.0 equiv.) and azelaic acid (2.85 g, 15.3 mmol, 2.0 equiv.) in dry dichloromethane (75 mL), *N,N'*-dicyclohexylcarbodiimide (DCC, 1.72 g, 8.33 mmol, 1.1 equiv.) and 4-dimethylaminopyridine (DMAP, 1.02 g, 8.33 mmol, 1.1 equiv.) were added at room temperature. The reaction mixture was stirred at room temperature for 1 hour. Upon complete conversion of the starting material, the reaction mixture was placed in a freezer for 5 hours to induce the precipitation of the urea, which was subsequently removed by filtration. The filtrate was concentrated under vacuum to provide a residue which was purified by column chromatography (100 % hexanes  $\rightarrow$  50 % diethyl ether in hexanes). Carboxylic acid **10.13** was obtained as a red oil (1.50 g, 66 % yield).  $^1\text{H}$  NMR (400 MHz,  $\text{CDCl}_3$ )  $\delta$  = 10.77 (br s, 1H), 7.53 (d,  $J$  = 7.7 Hz, 1H), 7.42-7.35 (m, 2H), 7.32-7.27 (m, 1H), 5.30 (s, 2H), 3.31 (s, 1H), 2.41-2.33 (m, 4H), 1.70-1.60 (m, 4H), 1.40-1.30 (m, 6H);  $^{13}\text{C}$  NMR (100 MHz,  $\text{CDCl}_3$ )  $\delta$  = 178.9, 173.5, 138.3, 132.9, 129.0, 128.2, 128.0, 121.4, 82.1, 80.8, 64.3, 34.2, 33.8, 28.9, 28.84, 28.82, 24.9, 24.6; HRMS (ESI)  $m/z$  calculated for  $\text{C}_{18}\text{H}_{21}\text{O}_4$   $[\text{M}-\text{H}]^-$  301.1445; found 301.1446.

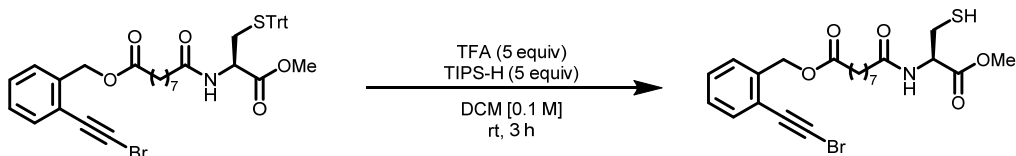


**9-((2-(Bromoethynyl)benzyl)oxy)-9-oxononanoic acid (10.14):** To a stirred solution of 9-((2-ethynylbenzyl)oxy)-9-oxononanoic acid (1.50 g, 4.96 mmol, 1.0 equiv.) in acetone (25 mL), *N*-bromosuccinimide (1.06 g, 5.95 mmol, 1.2 equiv.) and  $\text{AgNO}_3$  (0.169 g, 0.992 mmol, 20 mol%) were added at room temperature. The reaction mixture was stirred at 60 °C for 5 minutes. Upon complete conversion of the starting material, the reaction mixture was concentrated under vacuum to provide a residue which was purified by column chromatography (100 % hexanes  $\rightarrow$  30 % ethyl acetate in hexanes). Bromide **10.14** was obtained as a light-yellow solid (1.37 g, 72 % yield).  $^1\text{H}$  NMR (400 MHz,  $\text{CDCl}_3$ )  $\delta$  = 10.23 (br s, 1H), 7.49 (d,  $J$  = 7.4 Hz, 1H), 7.40-7.33

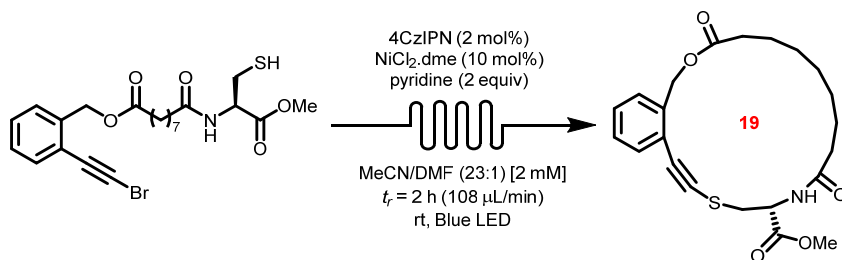
(m, 2H), 7.29 (dd,  $J = 7.5, 2.1$  Hz, 1H), 5.26 (s, 2H), 2.41-2.33 (m, 4H), 1.71-1.60 (m, 4H), 1.40-1.32 (m, 6H);  $^{13}\text{C}$  NMR (75 MHz,  $\text{CDCl}_3$ )  $\delta = 178.7, 173.5, 138.4, 132.8, 128.8, 128.3, 128.0, 122.1, 77.2, 64.3, 54.5, 34.2, 33.8, 28.90, 28.86, 28.8, 24.9, 24.6$ ; HRMS (ESI)  $m/z$  calculated for  $\text{C}_{18}\text{H}_{20}\text{BrO}_4$   $[\text{M}-\text{H}]^-$  379.0551; found 379.0547.



**2-(Bromoethynyl)benzyl (R)-9-((1-methoxy-1-oxo-3-(tritylthio)propan-2-yl)amino)-9-oxononanoate (10.15):** A stirred solution of 9-((2-(bromoethynyl)benzyl)oxy)-9-oxononanoic acid (0.200 g, 0.525 mmol, 1.0 equiv.) and methyl *S*-trityl-*L*-cysteinate (0.258 g, 0.683 mmol, 1.3 equiv.) in dry dichloromethane (5 mL) was treated with *N*-(3-dimethylaminopropyl)-*N'*-ethylcarbodiimide hydrochloride (EDC·HCl, 0.151 g, 0.787 mmol, 1.5 equiv.), 1-hydroxybenzotriazole (HOBt, 0.106 g, 0.787 mmol, 1.5 equiv.) and *N,N*-diisopropylethylamine (DIPEA, 0.14 mL, 0.787 mmol, 1.5 equiv.) were added at room temperature, and stirred at room temperature for 15 minutes. The reaction mixture was neutralized by dropwise addition of 1M HCl. Dichloromethane was added to the mixture. The organic and aqueous phases were separated. The combined organic phases were dried with anhydrous magnesium sulfate. The resulting suspension was filtered, and the filtrate was concentrated under vacuum to provide a residue which was purified by column chromatography (100 % hexanes  $\rightarrow$  40 % ethyl acetate in hexanes). Amide **10.15** was obtained as a white solid (0.302 g, 78 % yield).  $^1\text{H}$  NMR (400 MHz,  $\text{CDCl}_3$ )  $\delta = 7.49$  (d,  $J = 7.3$  Hz, 1H), 7.40-7.33 (m, 8H), 7.31-7.26 (m, 7H), 7.25-7.21 (m, 3H), 5.86 (d,  $J = 7.9$  Hz, 1H), 5.26 (s, 2H), 4.64-4.59 (m, 1H), 3.72 (s, 3H), 2.65 (d,  $J = 5.2$  Hz, 2H), 2.37 (t,  $J = 7.4$  Hz, 2H), 2.15 (t,  $J = 7.3$  Hz, 2H), 1.68-1.59 (m, 4H), 1.37-1.30 (m, 6H);  $^{13}\text{C}$  NMR (100 MHz,  $\text{CDCl}_3$ )  $\delta = 172.6, 171.0, 144.3, 132.8, 129.54, 129.46, 128.9, 128.3, 128.1, 128.0, 126.9, 77.2, 64.3, 52.6, 50.9, 36.4, 34.2, 33.8, 28.99, 28.96$  (2C), 25.4, 24.9; HRMS (ESI)  $m/z$  calculated for  $\text{C}_{41}\text{H}_{42}\text{BrNO}_5\text{SAg}$   $[\text{M}+\text{Ag}]^+$  846.1013; found 846.0997.



**2-(Bromoethynyl)benzyl (R)-9-((3-mercapto-1-methoxy-1-oxopropan-2-yl)amino)-9-oxononanoate (6.10):** To a stirred solution of 2-(bromoethynyl)benzyl (R)-9-((1-methoxy-1-oxo-3-(tritylthio)propan-2-yl)amino)-9-oxononanoate (0.300 g, 0.405 mmol, 1.0 equiv.) in dry dichloromethane (4 mL), trifluoroacetic acid (0.16 mL, 2.02 mmol, 5.0 equiv.) and triisopropylsilane (0.41 mL, 2.02 mmol, 5.0 equiv.) were added at room temperature. The reaction mixture was stirred at room temperature for 3 hours. Upon complete conversion of the starting material, the reaction mixture was concentrated under vacuum to provide a residue which was purified by column chromatography (100 % hexanes  $\rightarrow$  75 % diethyl ether in hexanes). Thiol **6.10** was obtained as a white semi-solid (0.144 g, 71 % yield).  $^1\text{H}$  NMR (400 MHz,  $\text{CDCl}_3$ )  $\delta$  = 7.49 (d,  $J$  = 7.4 Hz, 1H), 7.40-7.33 (m, 2H), 7.29 (dd,  $J$  = 7.4, 2.1 Hz, 1H), 6.37 (d,  $J$  = 6.2 Hz, 1H), 5.26 (s, 2H), 4.92-4.88 (m, 1H), 3.81 (s, 3H), 3.05-3.01 (m, 2H), 2.39 (t,  $J$  = 7.4 Hz, 2H), 2.28 (t,  $J$  = 7.4 Hz, 2H), 1.71-1.62 (m, 4H), 1.39-1.31 (m, 6H), 1.27 (t,  $J$  = 7.1 Hz, 1H);  $^{13}\text{C}$  NMR (100 MHz,  $\text{CDCl}_3$ )  $\delta$  = 173.4, 173.0, 170.6, 138.3, 132.8, 128.8, 128.2, 128.0, 122.0, 77.4, 64.3, 54.5, 53.4, 52.8, 36.3, 34.1, 28.91, 28.86 (2C), 26.8, 25.4, 24.8; HRMS (ESI)  $m/z$  calculated for  $\text{C}_{22}\text{H}_{29}\text{BrNO}_5\text{S}$   $[\text{M}+\text{H}]^+$  498.0944; found 498.0956.



**Macrolactone (6.11):** To a first flask was added 2-(bromoethynyl)benzyl (R)-9-((3-mercapto-1-methoxy-1-oxopropan-2-yl)amino)-9-oxononanoate (0.080 g, 0.160 mmol, 1.0 equiv.). To a second flask were added 4CzIPN (0.0024 g, 0.003 mmol, 2 mol%),  $\text{NiCl}_2 \cdot \text{dme}$  (0.0035 g, 0.016 mmol, 10 mol%) and pyridine (0.026 mL, 0.320 mmol, 2 equiv.). A 23:1 mixture of degassed acetonitrile (38.4 mL) and  $N,N$ -dimethylformamide (1.62 mL) was added to each flask (2 mM). Both reaction mixtures were sonicated until complete homogeneity. Both reaction mixtures

were then transferred into their respective 60 mL syringe. The two syringes were positioned onto the KD Scientific syringe pump (*see Figure 10.4*). The pump was turned on at a flow rate of 54  $\mu\text{L}/\text{min}$ . The reaction mixture was pumped through a 13 mL PFA-coiled reactor irradiated with blue LEDs for a 2-hour residence time. Two new syringes each containing 8 mL of acetonitrile replaced the injection syringes upon complete injection of both injection syringes. The pump was turned on at a flow rate of 54  $\mu\text{L}/\text{min}$ . The collected solution was concentrated under vacuum to provide a residue which was purified by column chromatography (100 % dichloromethane  $\rightarrow$  5 % acetone in dichloromethane). Macrolactone **6.11** was obtained as a white solid (0.019 g, 28 % yield).  $^1\text{H}$  NMR (700 MHz,  $\text{CDCl}_3$ )  $\delta$  = 7.47-7.45 (m, 1H), 7.40-7.39 (m, 1H), 7.32-7.30 (m, 2H), 6.57 (d,  $J$  = 7.2 Hz, 1H), 5.25 (d,  $J$  = 11.7 Hz, 1H), 5.12 (d,  $J$  = 11.7 Hz, 1H), 4.95-4.92 (m, 1H), 3.79 (s, 3H), 3.47 (dd,  $J$  = 13.4, 4.7 Hz, 1H), 3.33 (dd,  $J$  = 13.5, 6.0 Hz, 1H), 2.35 (t,  $J$  = 6.8 Hz, 2H), 2.33-2.30 (m, 1H), 2.28-2.24 (m, 1H), 1.72-1.57 (m, 4H), 1.43-1.26 (m, 6H);  $^{13}\text{C}$  NMR (175 MHz,  $\text{CDCl}_3$ )  $\delta$  = 173.8, 173.1, 170.5, 137.1, 132.1, 130.4, 128.6, 128.4, 123.6, 91.3, 82.5, 65.0, 52.9, 51.7, 37.0, 36.2, 34.3, 27.9, 27.8, 27.3, 25.1, 24.4; HRMS (ESI)  $m/z$  calculated for  $\text{C}_{22}\text{H}_{28}\text{NO}_5\text{S}$   $[\text{M}+\text{H}]^+$  418.1683; found 418.1686.

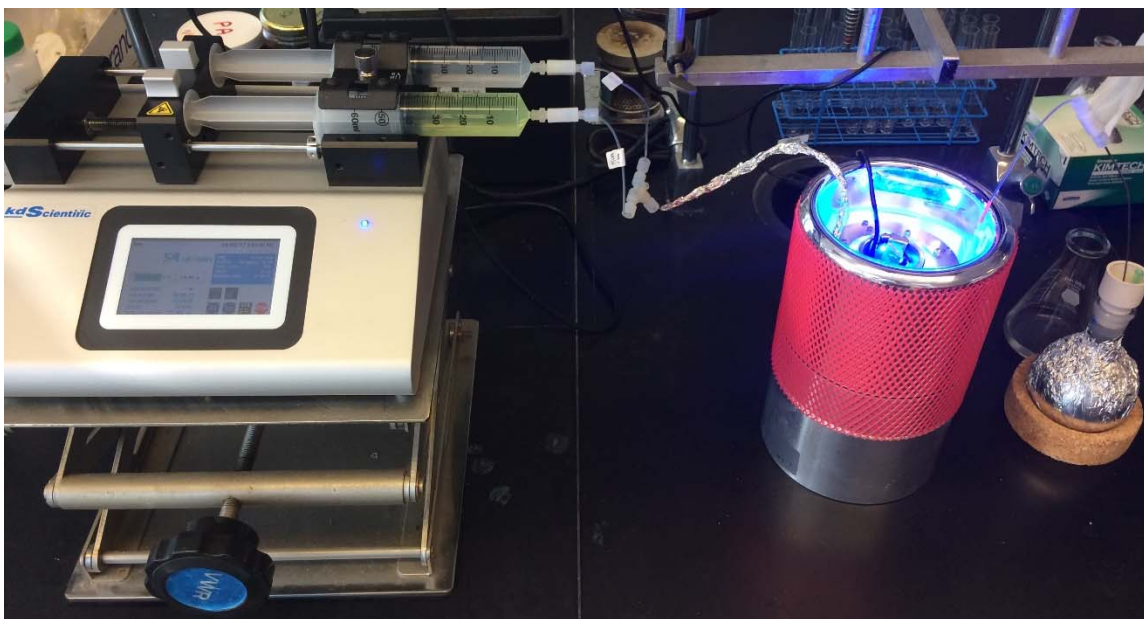
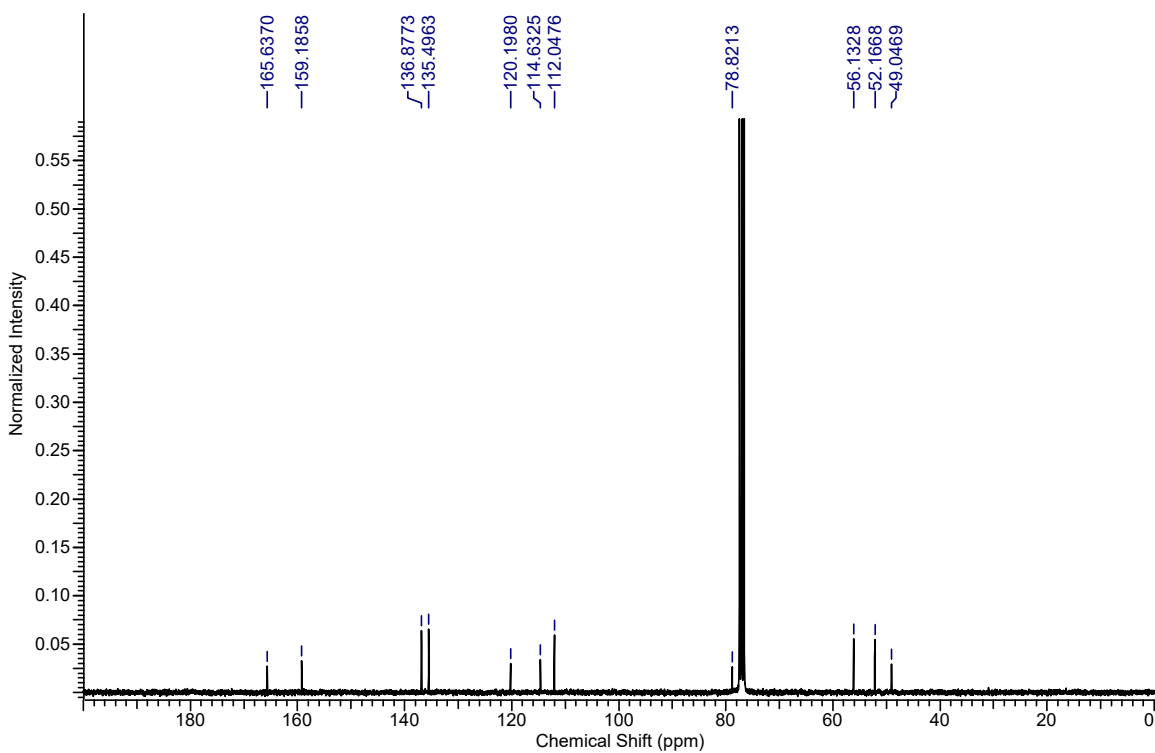
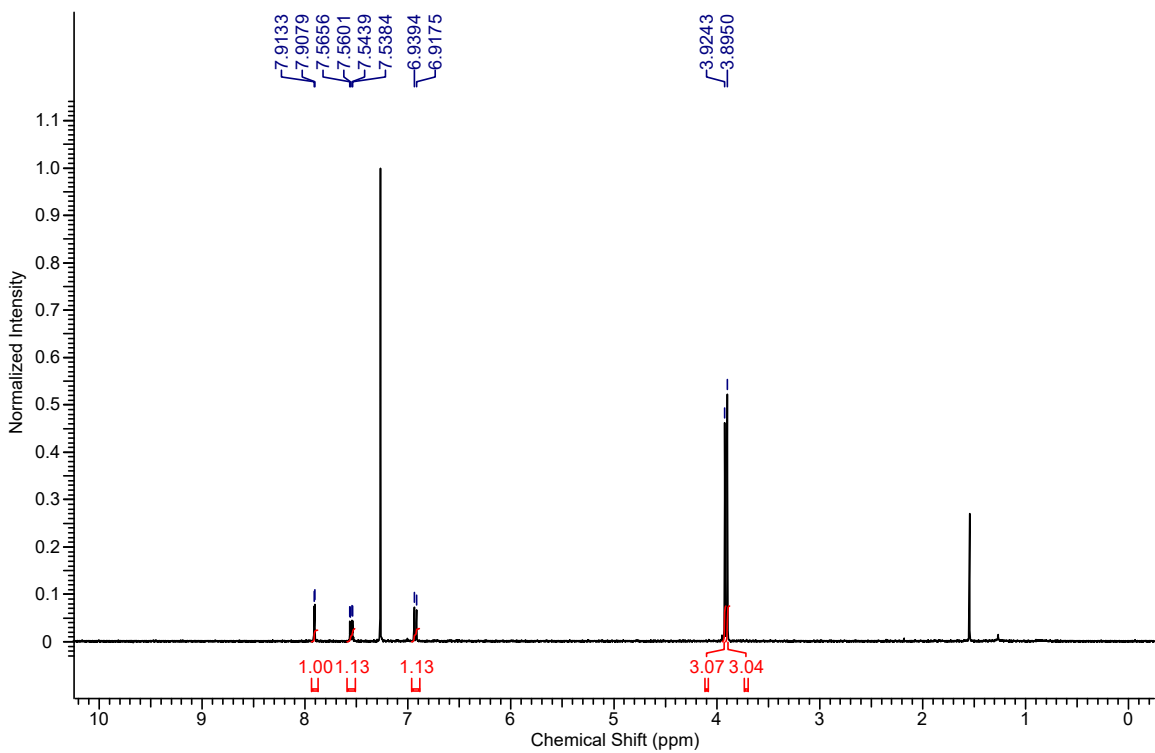


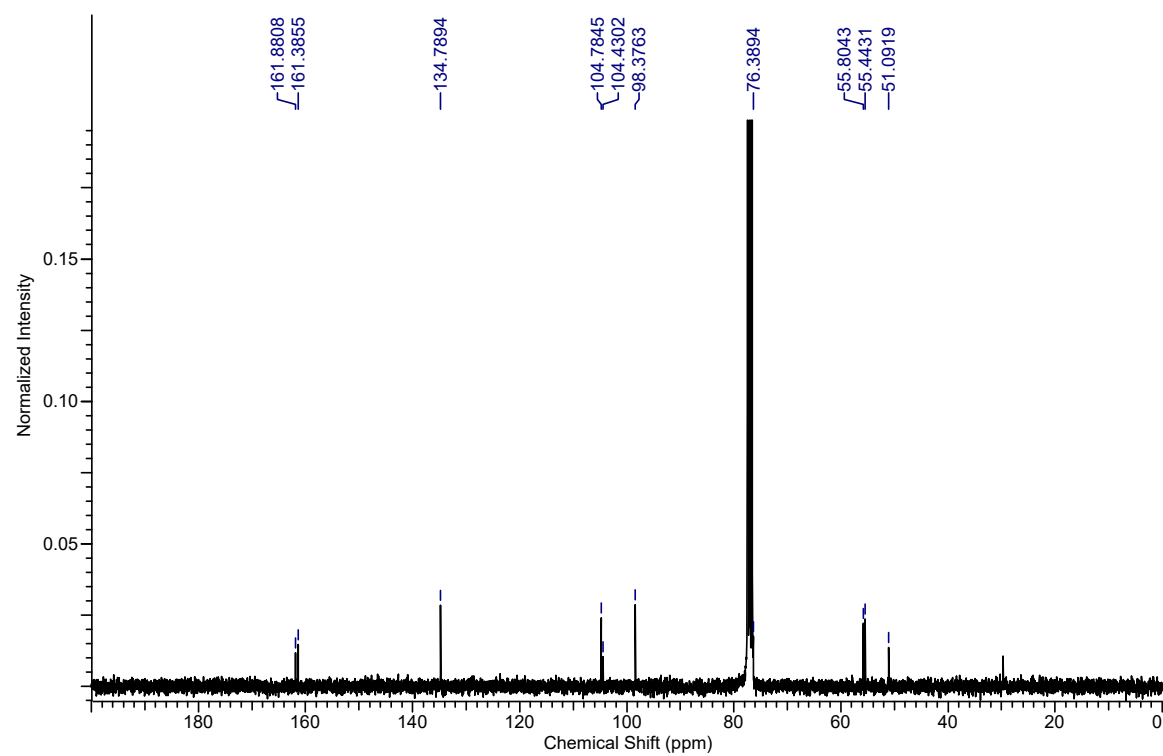
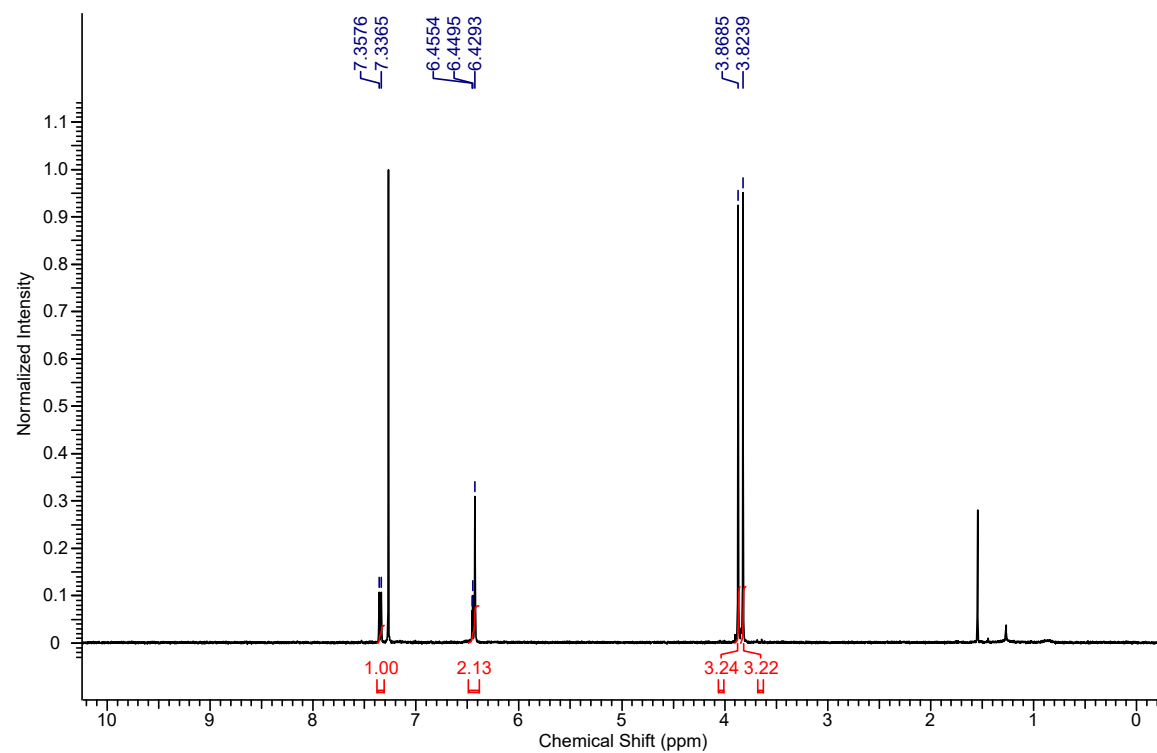
**Figure 10.4** Continuous flow reactor set-up used for the visible-light-mediated synthesis of macrocyclic alkynyl sulfide

## 10.7 NMR Data for all New Compounds

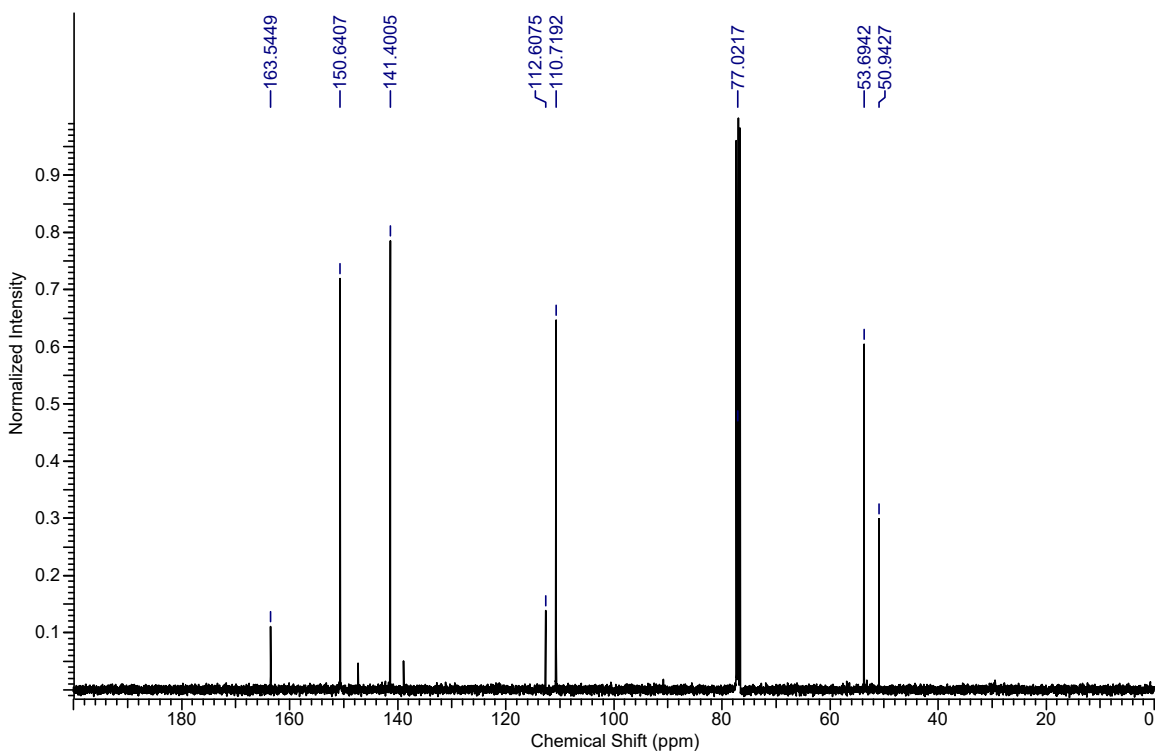
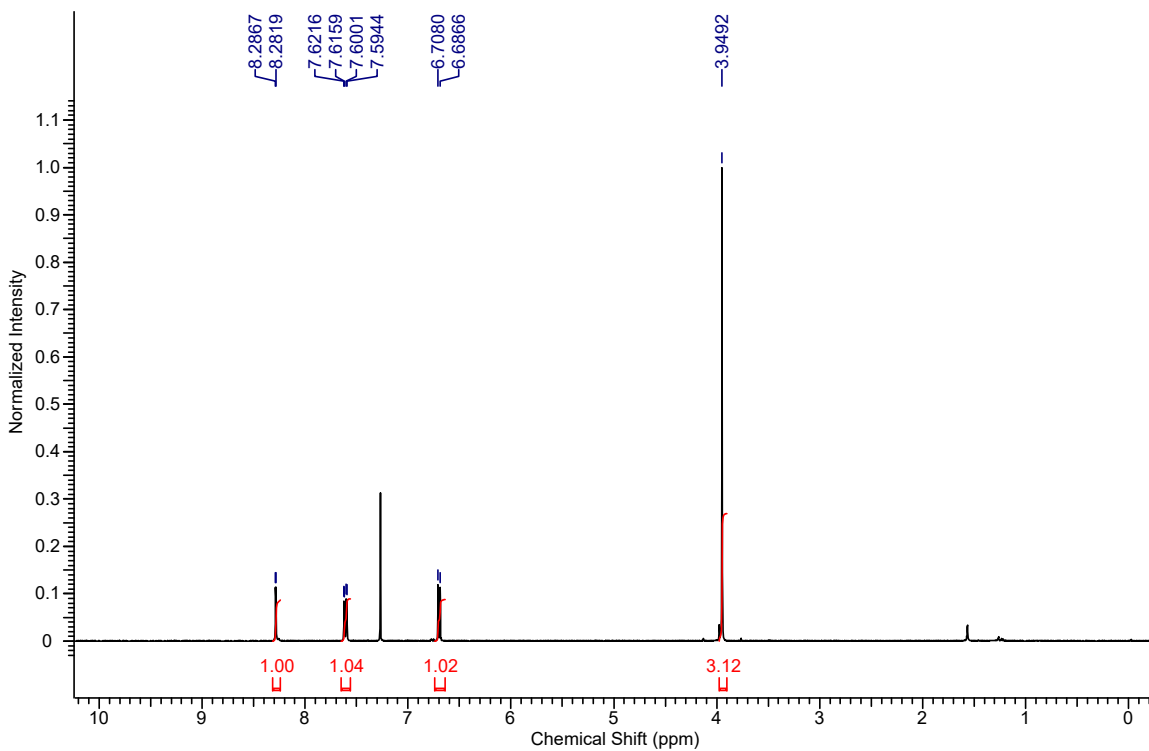
### Methyl 5-(bromoethynyl)-2-methoxybenzoate (6.2g):



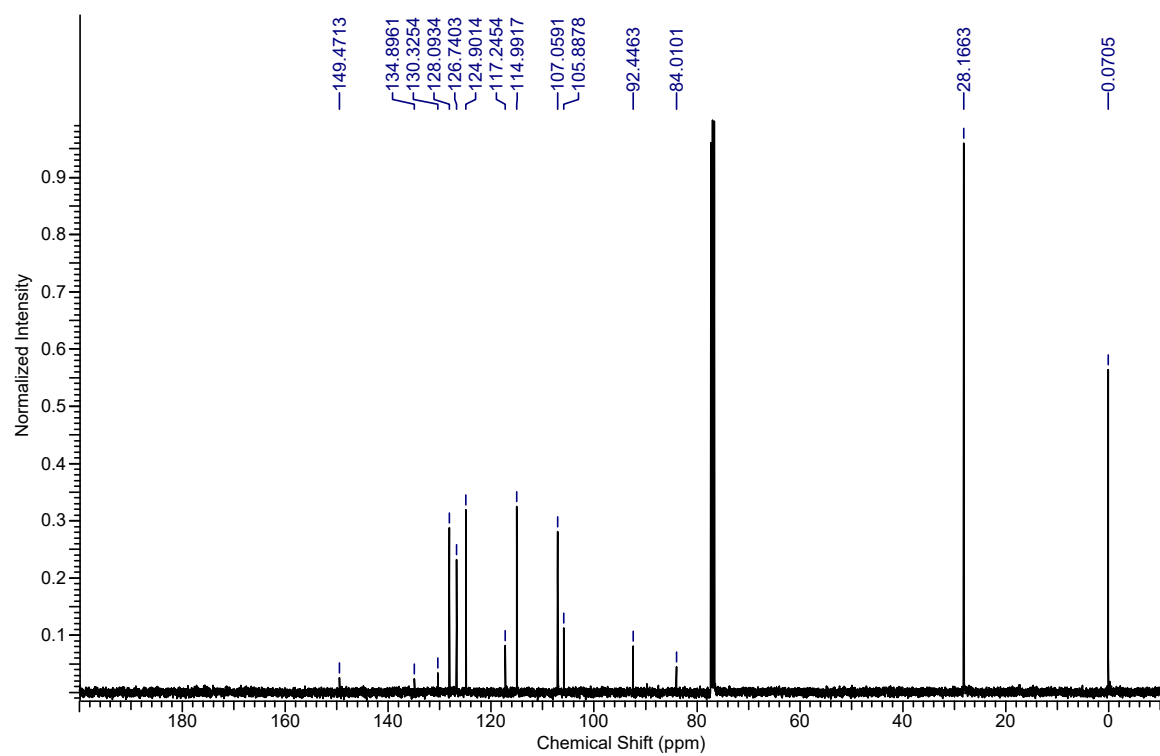
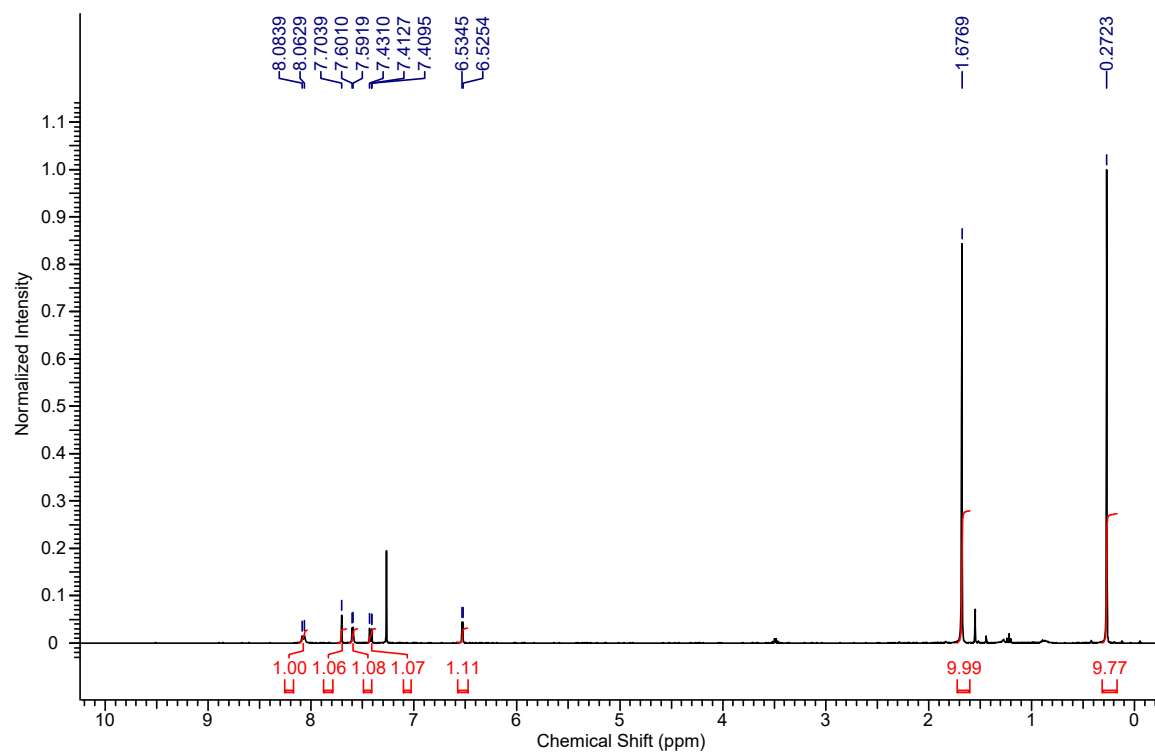
**1-(Bromoethynyl)-2,4-dimethoxybenzene (6.2h):**



**5-(Bromoethynyl)-2-methoxypyridine (6.2j):**

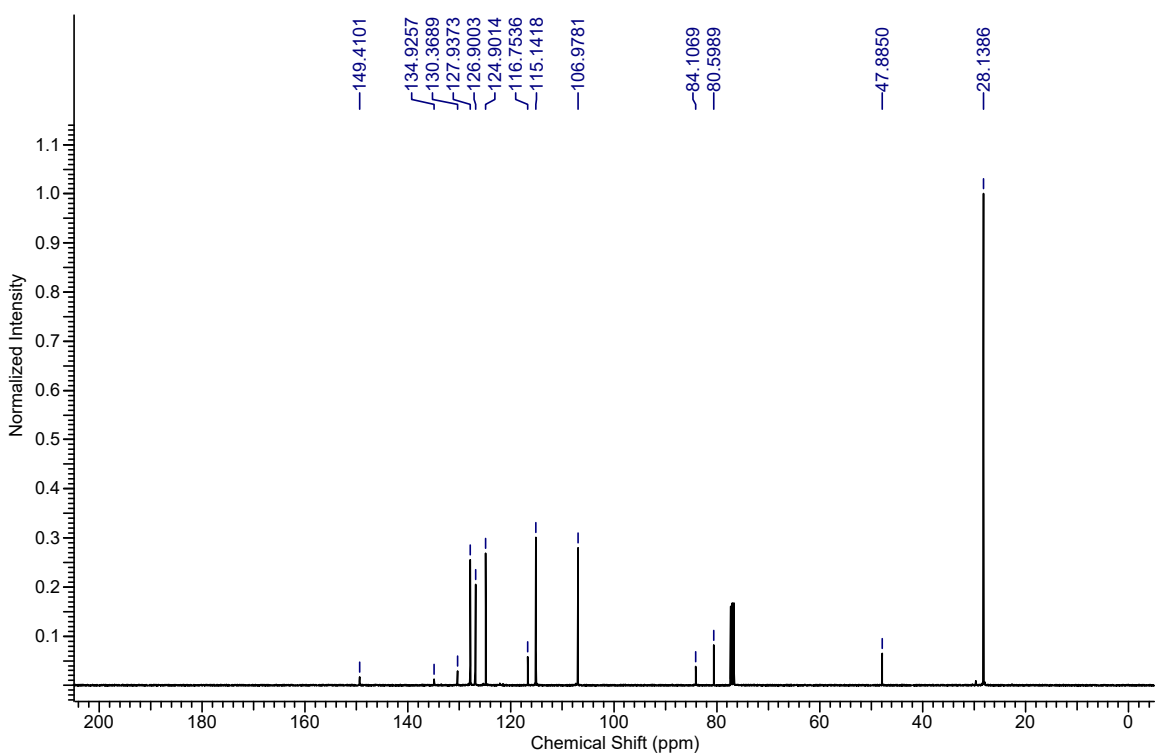
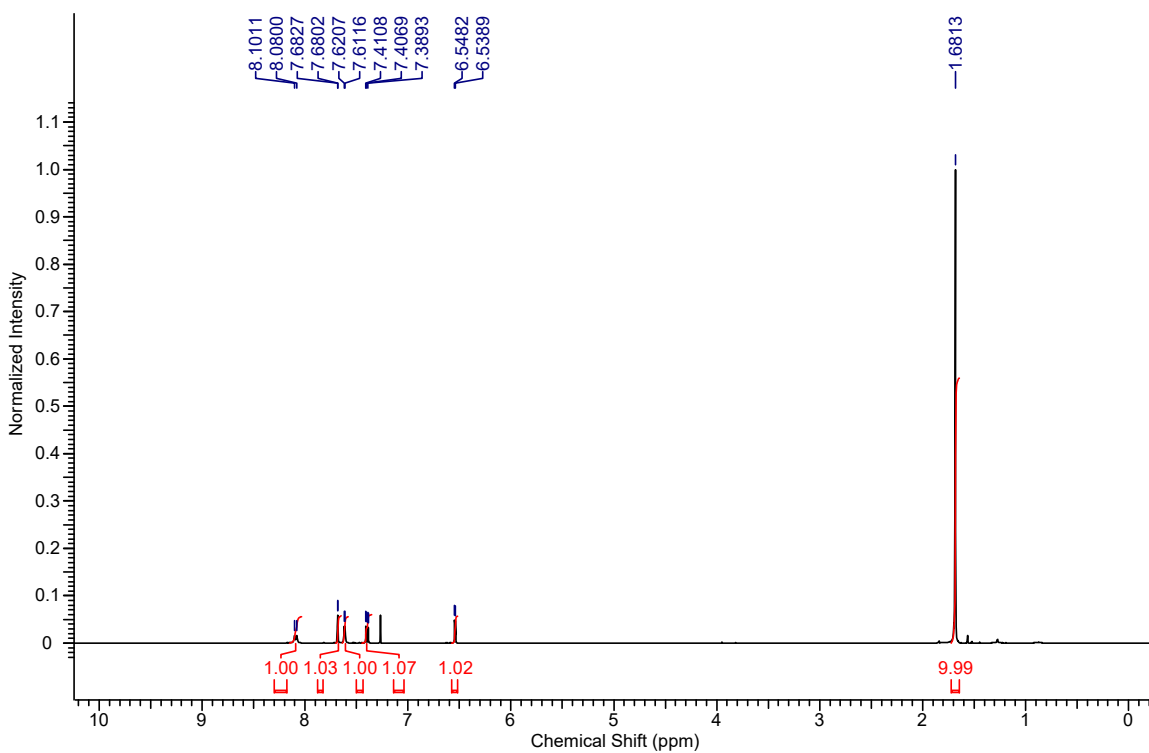


***tert*-Butyl 5-((trimethylsilyl)ethynyl)-1*H*-indole-1-carboxylate (10.9):**

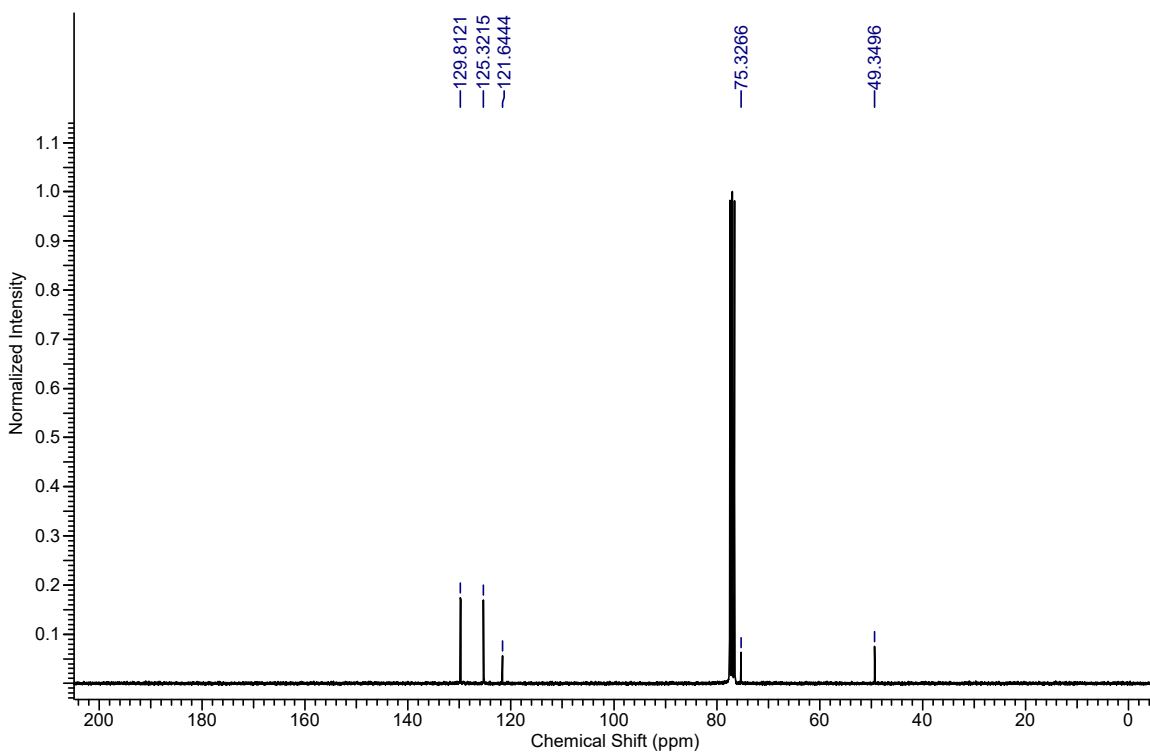
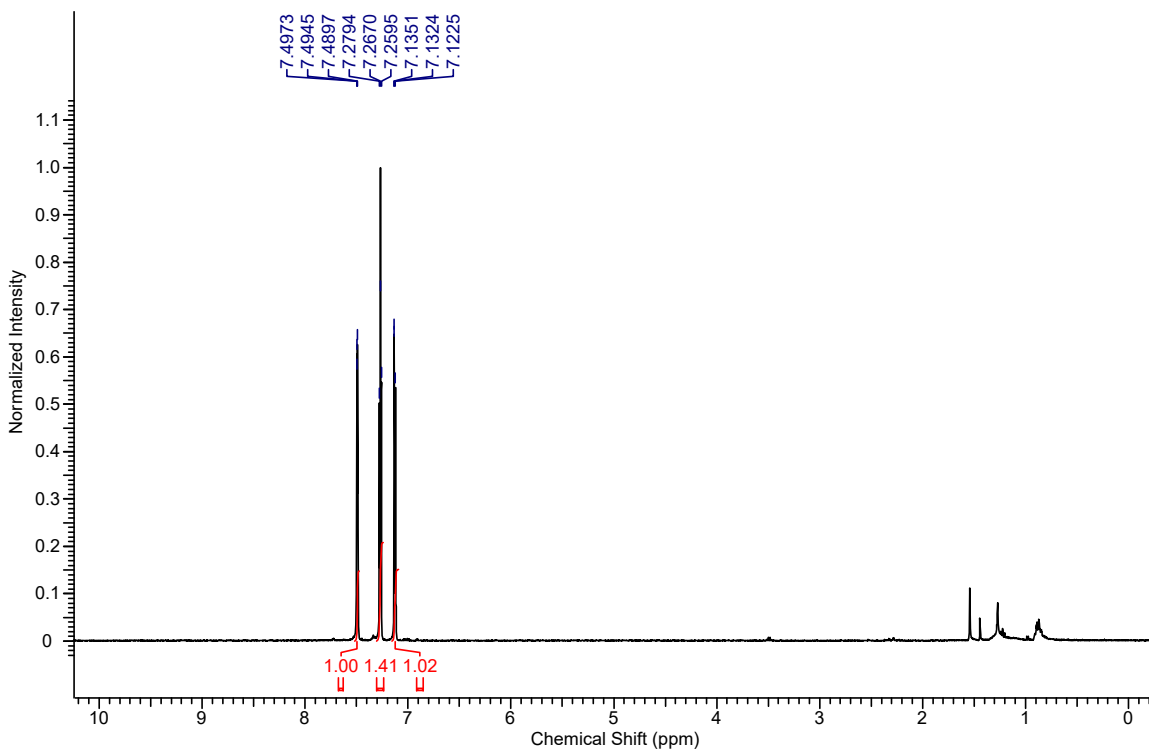




***tert*-Butyl 5-(bromoethynyl)-1*H*-indole-1-carboxylate (6.2k):**

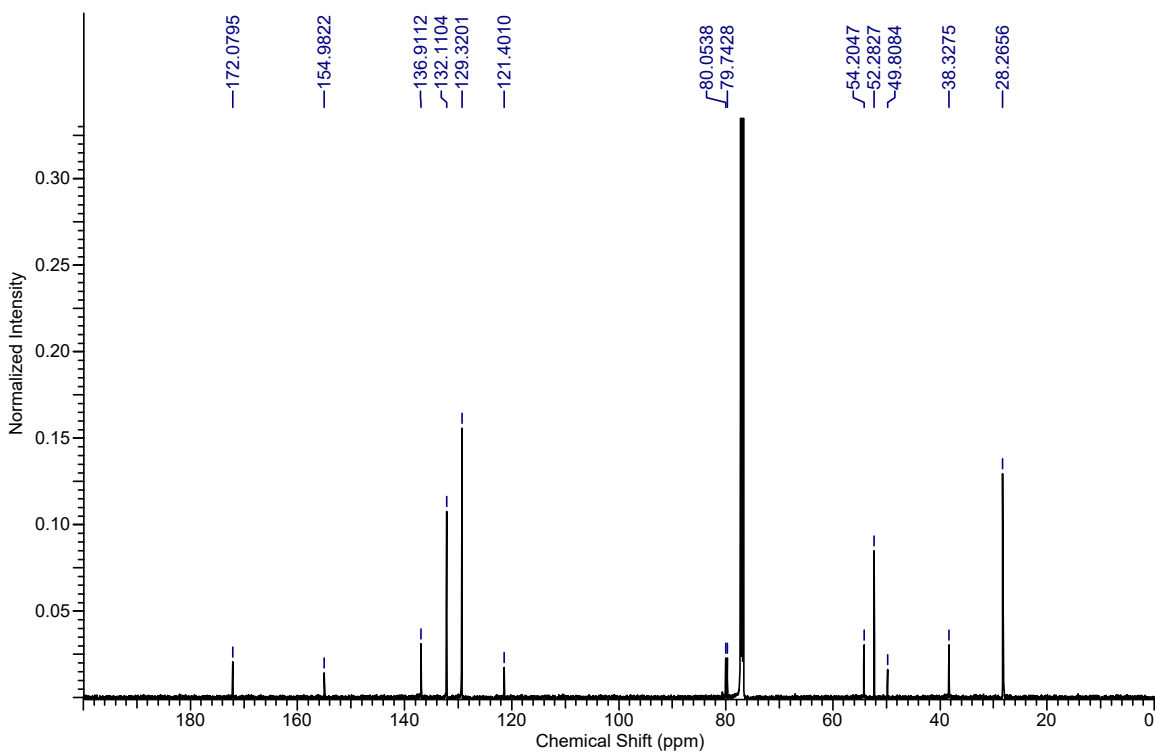
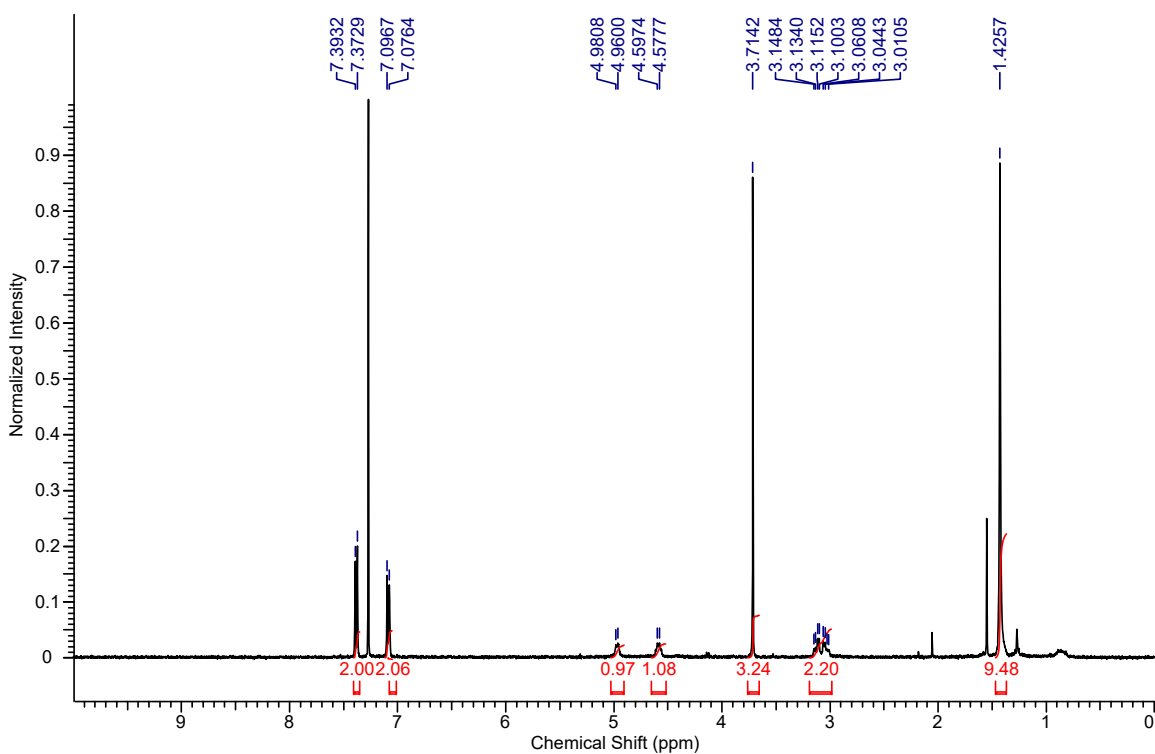


**3-(Bromoethynyl)thiophene (6.2l):**

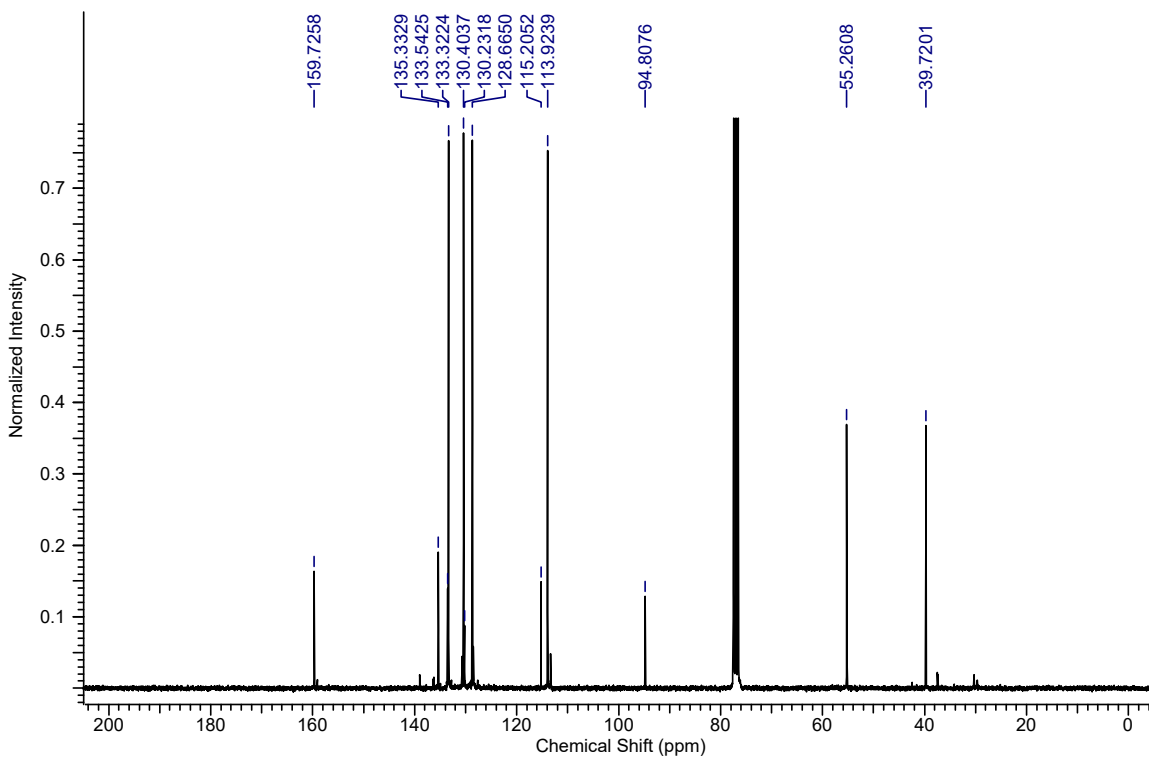
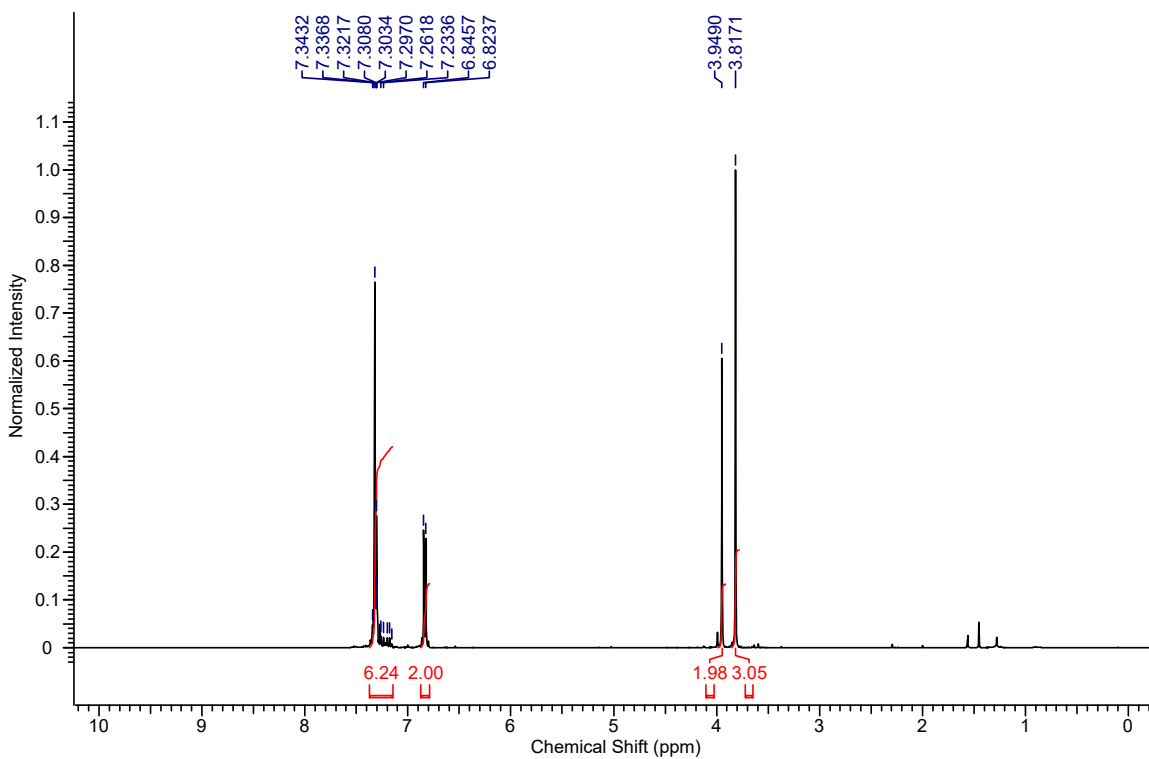


**Methyl  
(6.2m):**

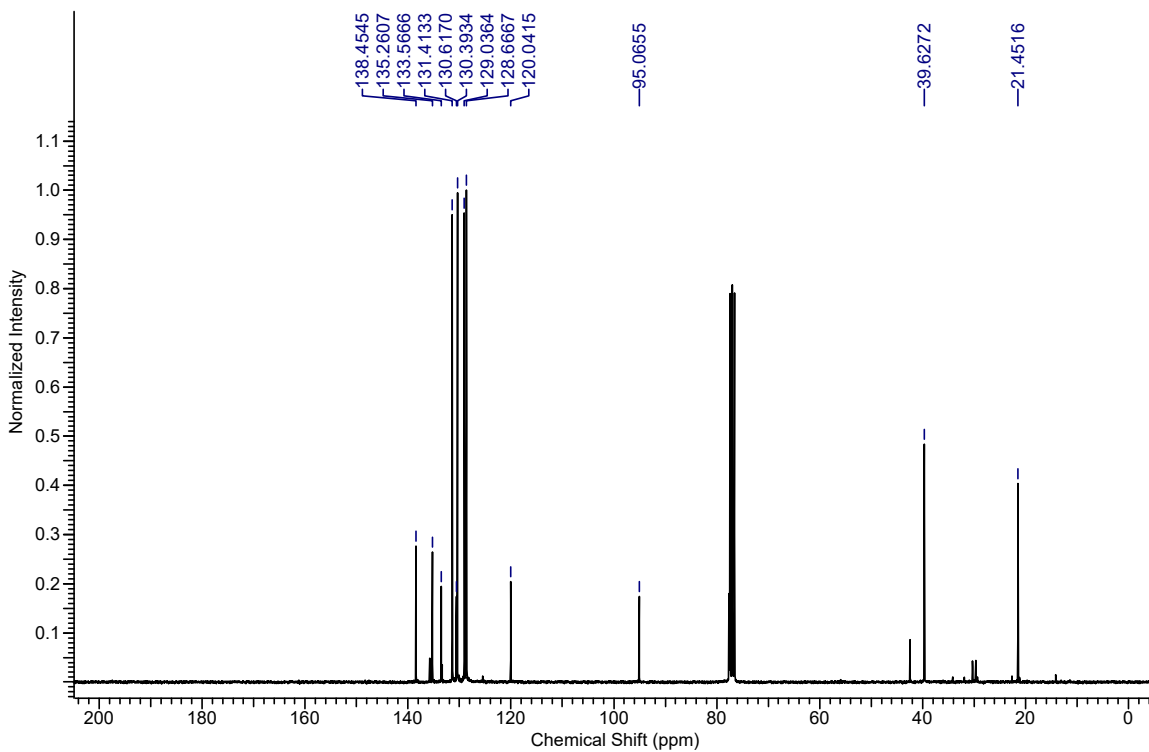
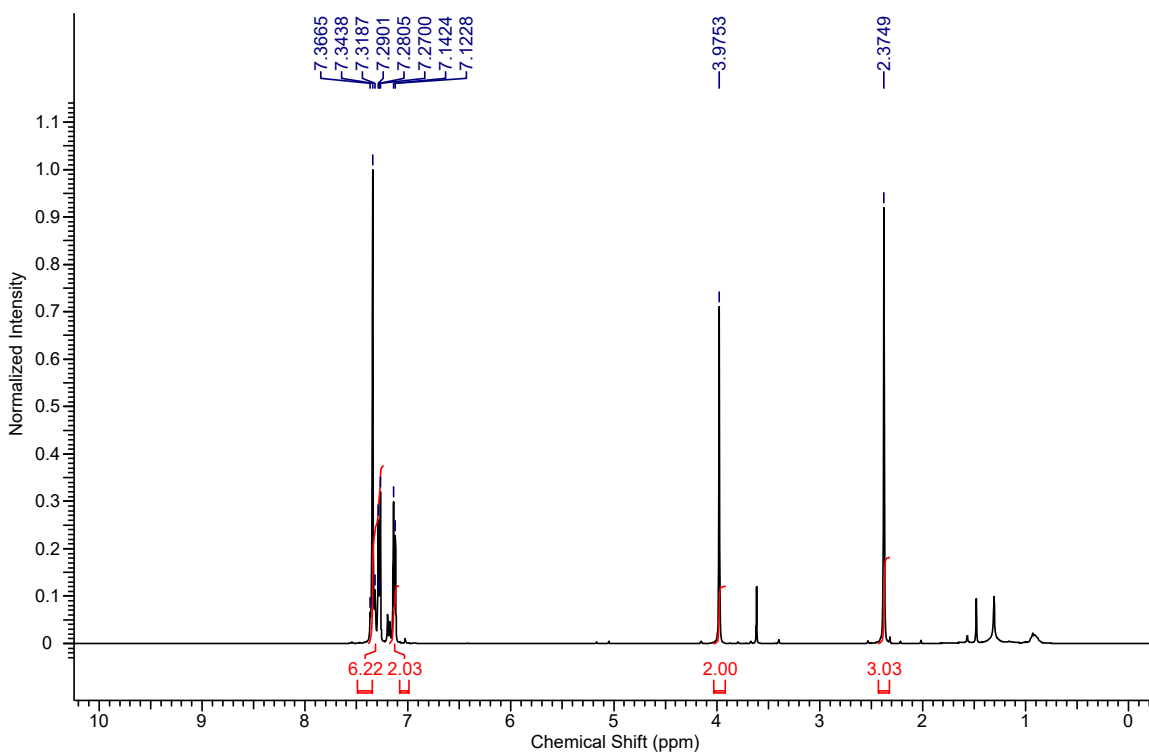
**(S)-3-(4-(bromoethynyl)phenyl)-2-((*tert*-butoxycarbonyl)amino)propanoate**



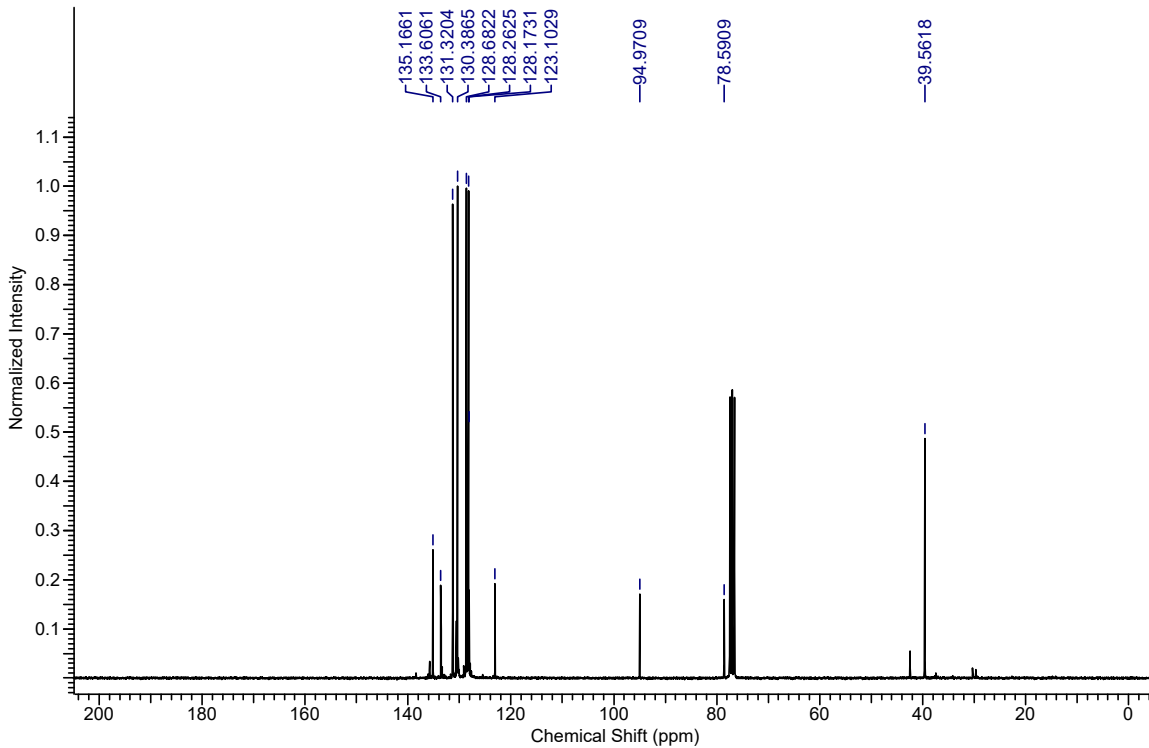
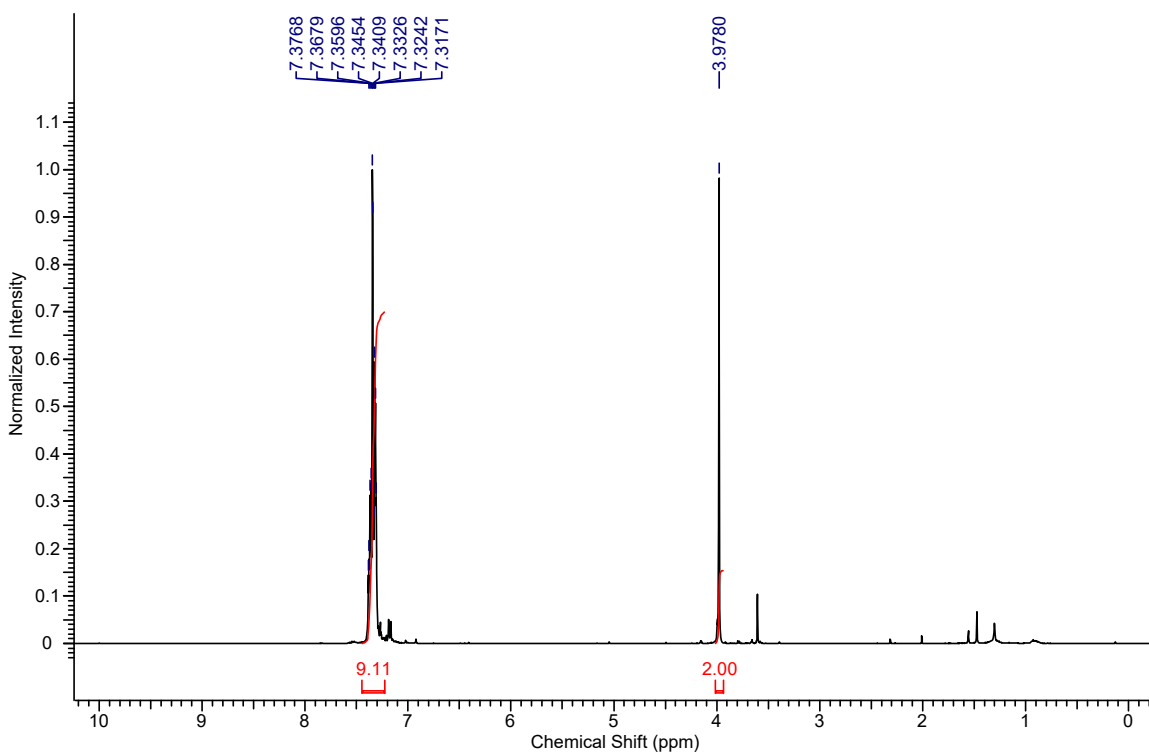
**(4-Chlorobenzyl)((4-methoxyphenyl)ethynyl)sulfane (6.3a):**



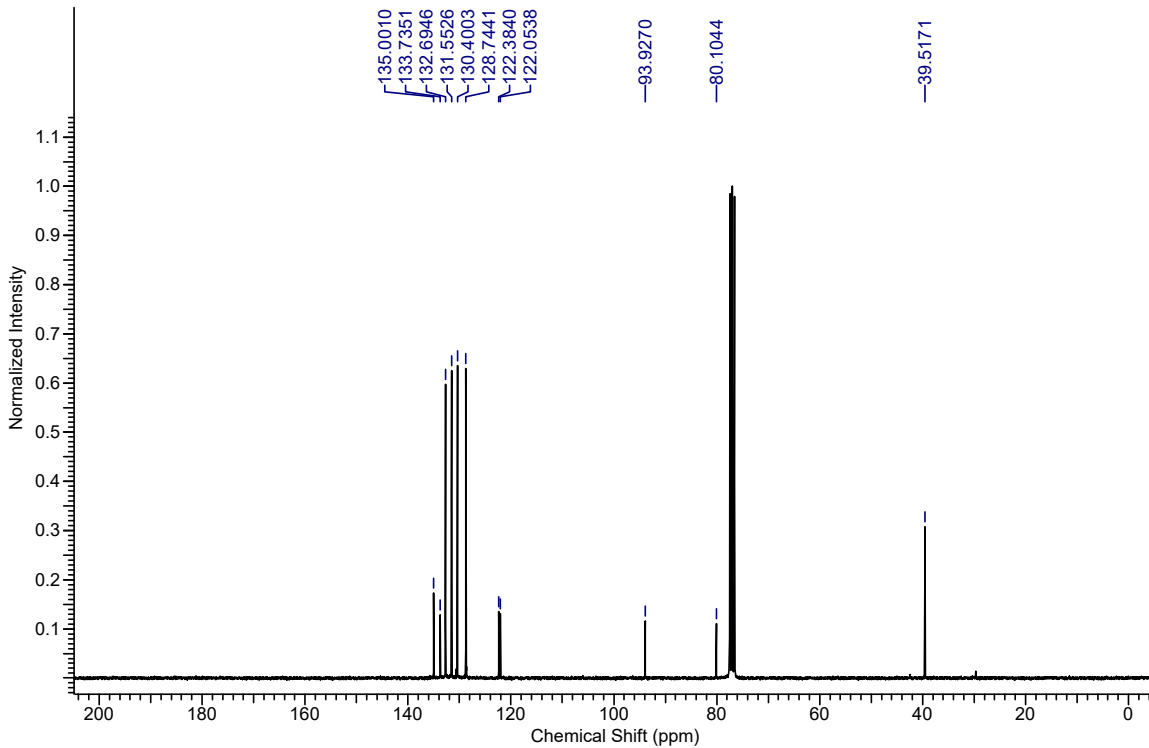
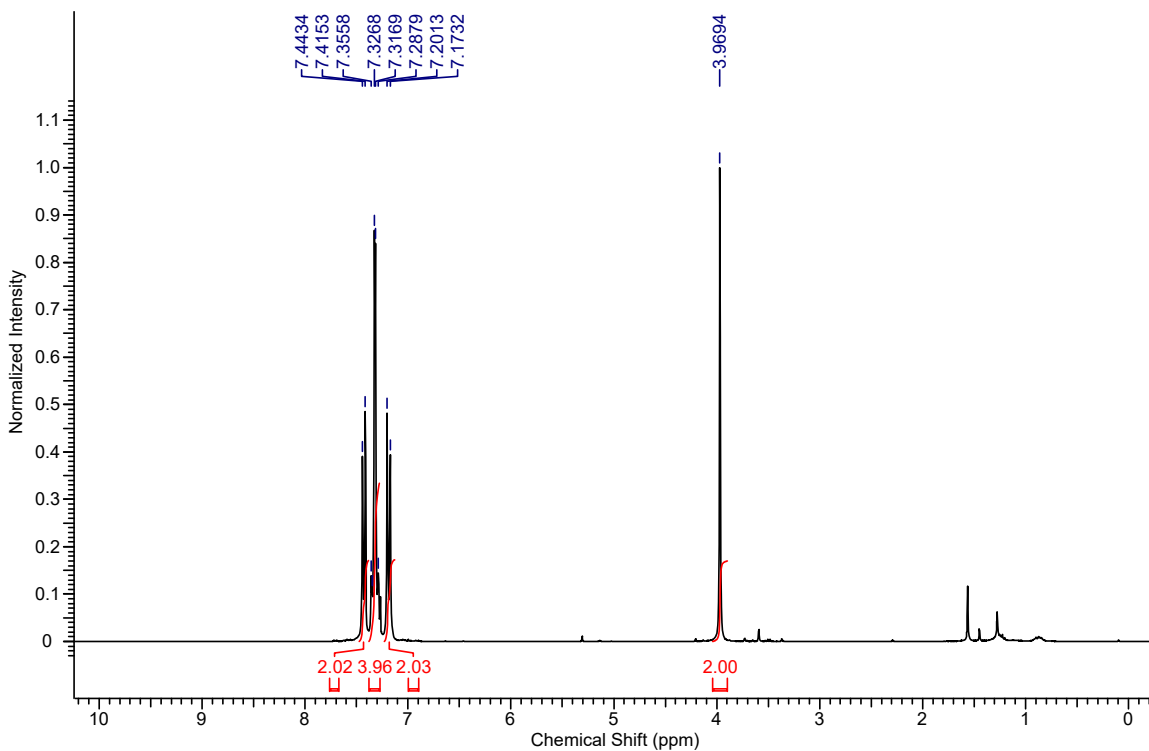
**(4-Chlorobenzyl)(*p*-tolylethynyl)sulfane (6.3b):**



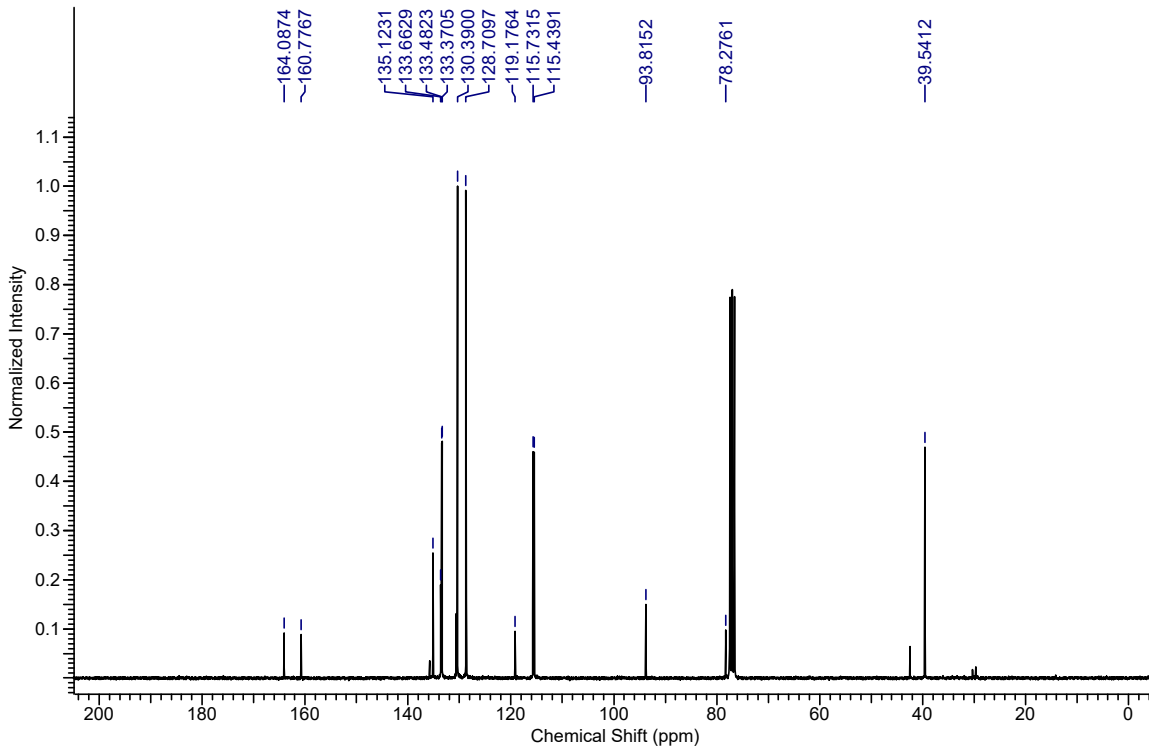
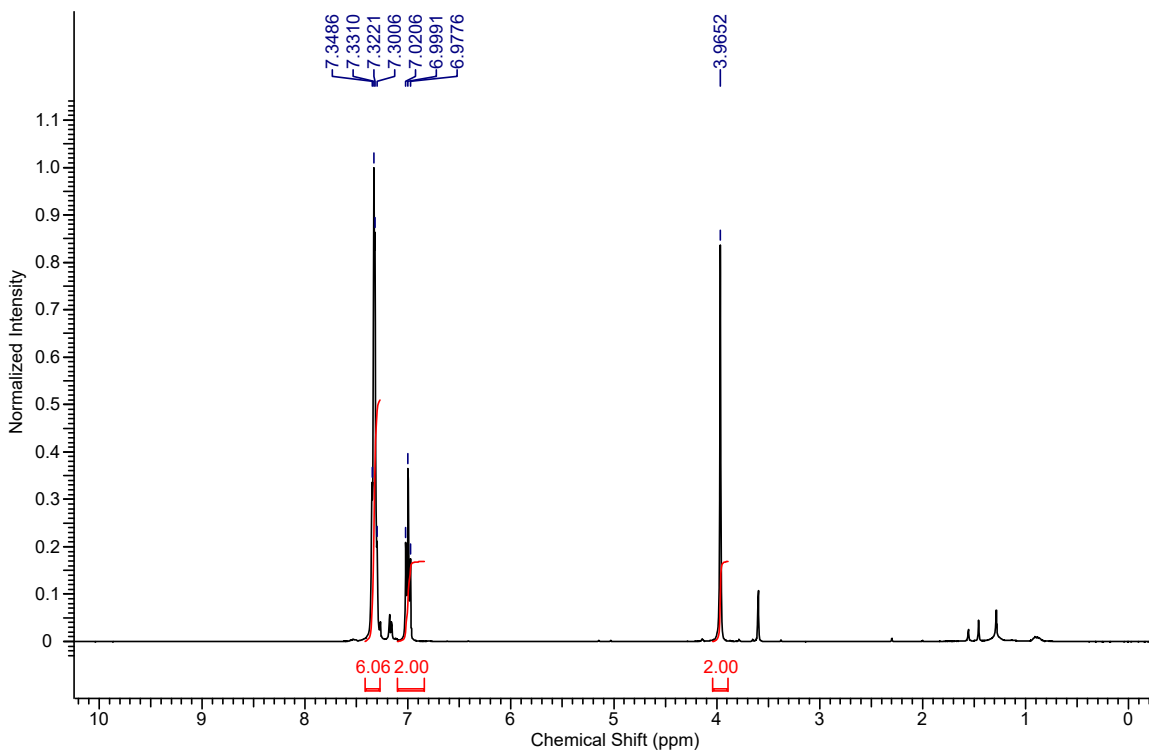
**(4-Chlorobenzyl)(phenylethynyl)sulfane (6.3c):**



**((4-Bromophenyl)ethynyl)(4-chlorobenzyl)sulfane (6.3d):**

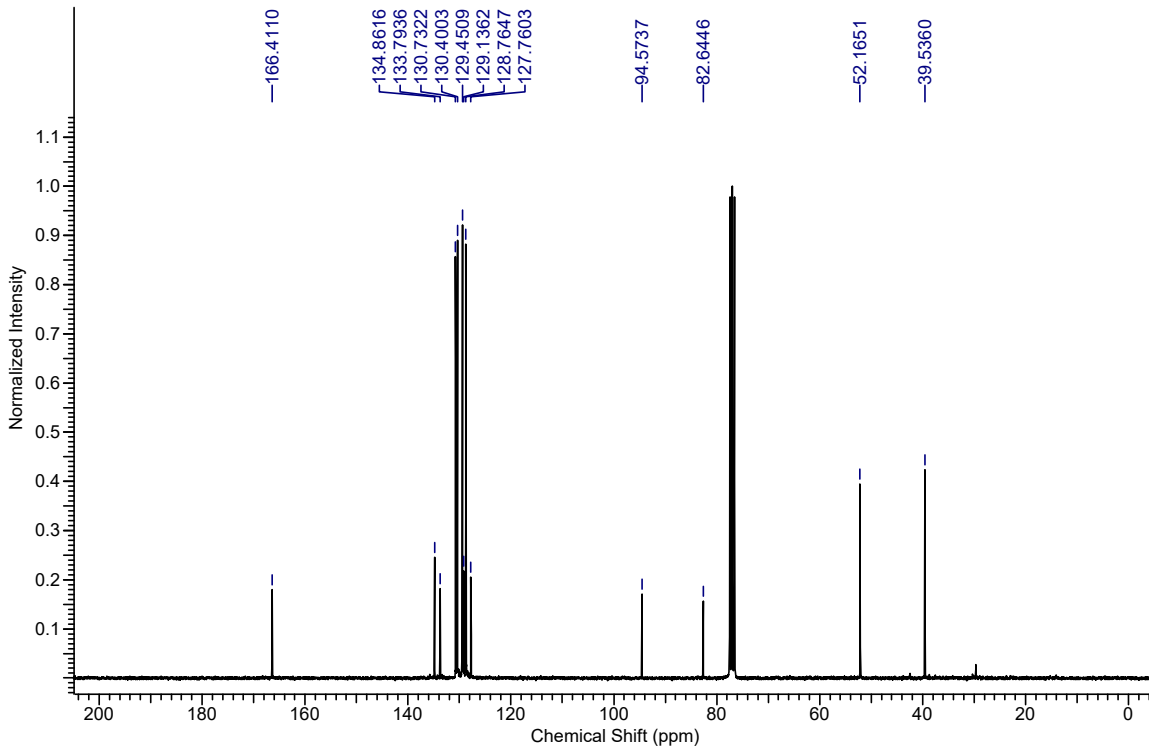
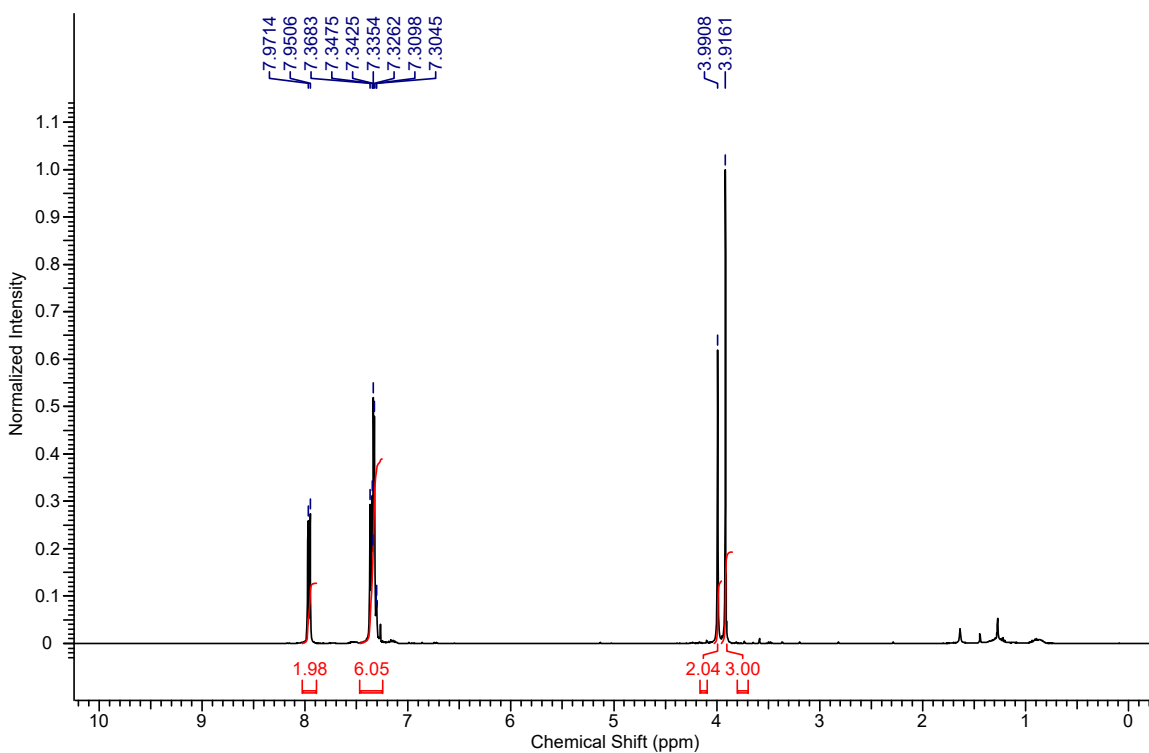


**(4-Chlorobenzyl)((4-fluorophenyl)ethynyl)sulfane (6.3e):**

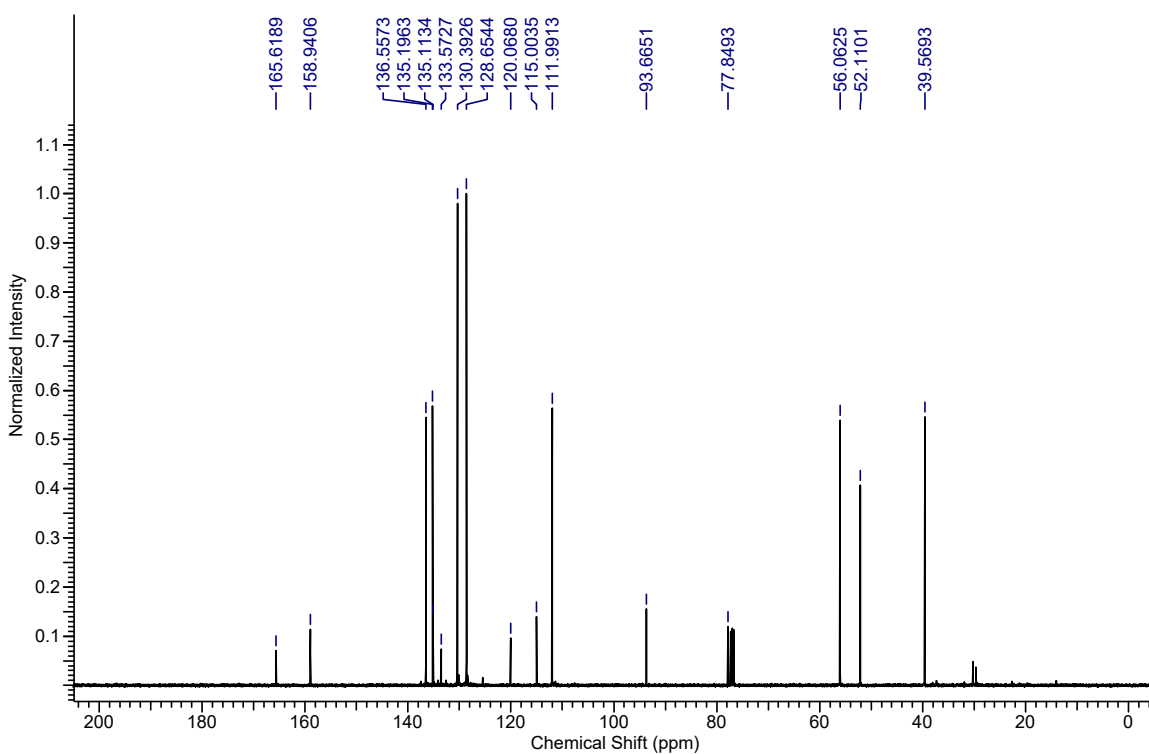
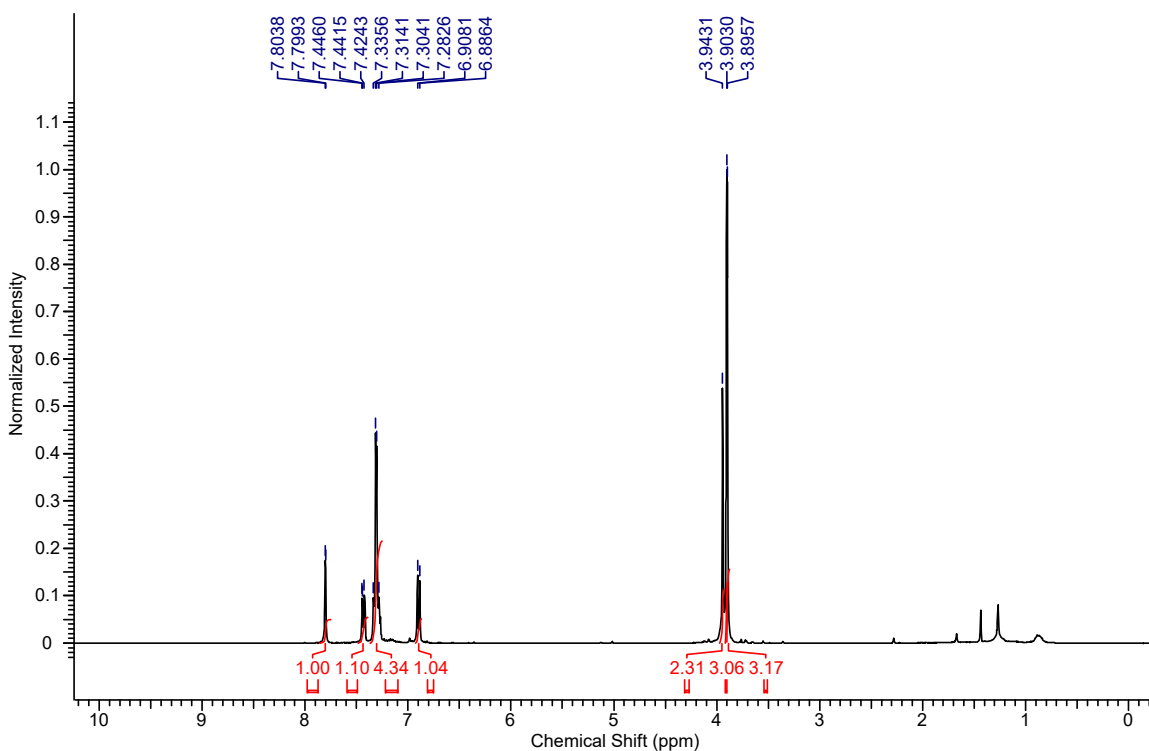




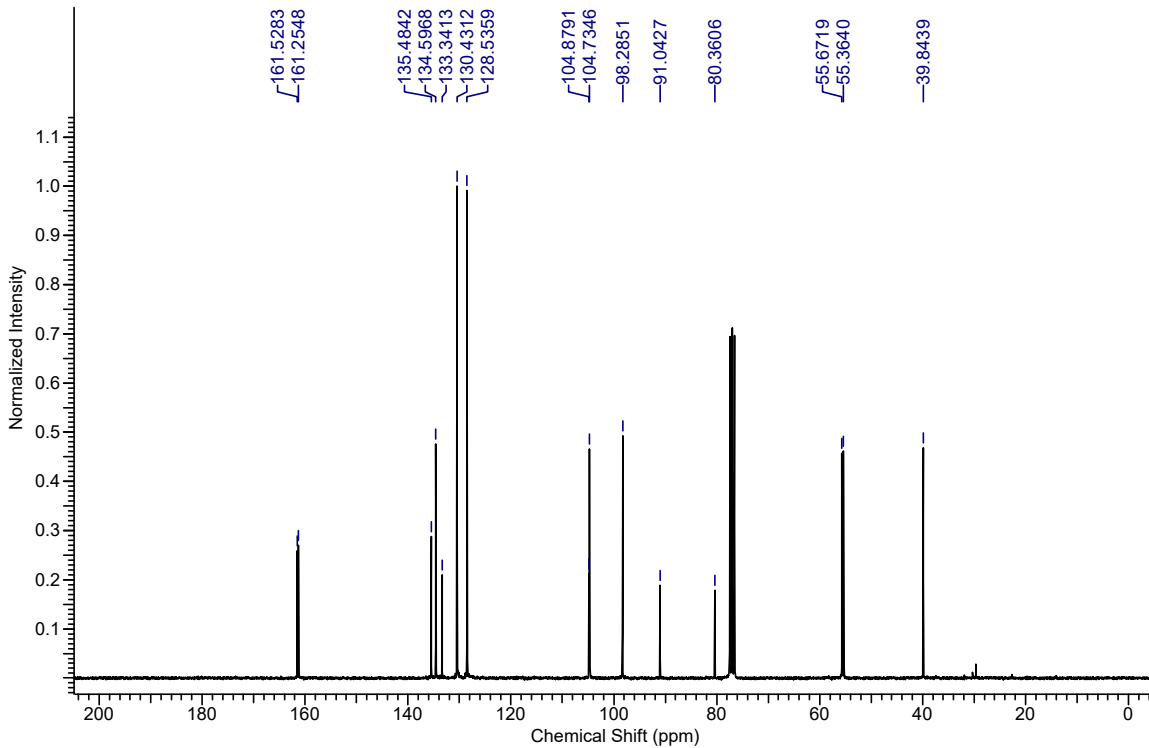
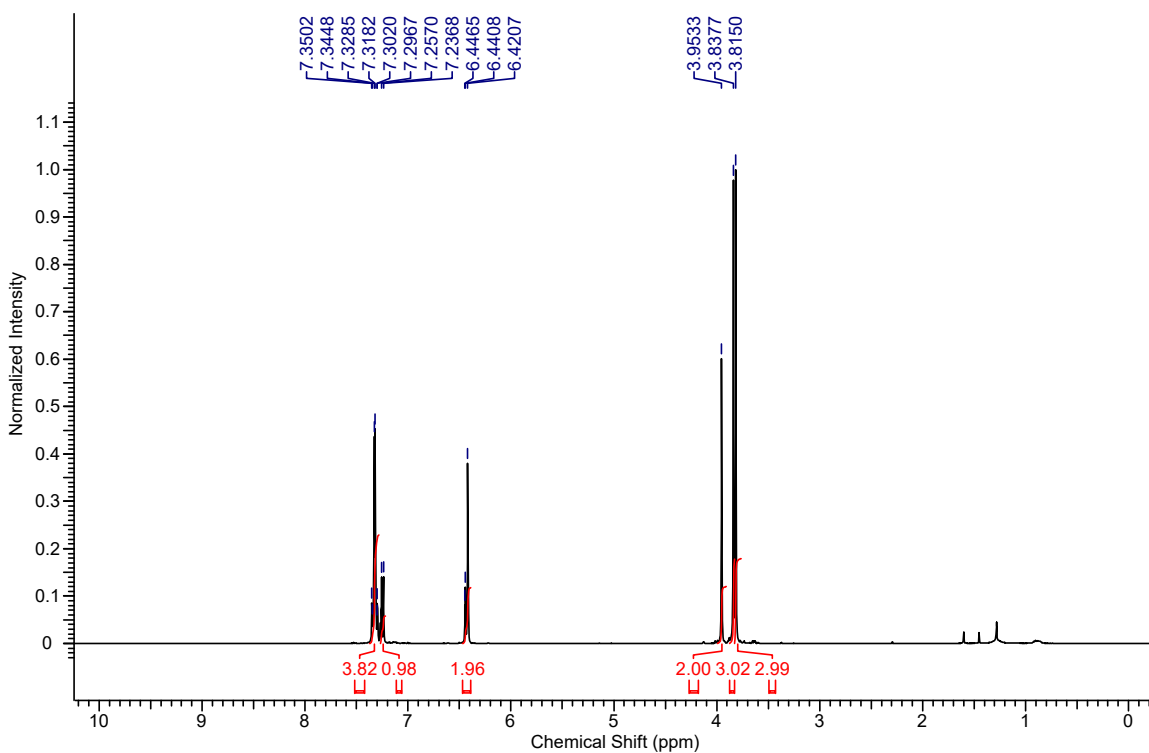
**Methyl 4-(((4-chlorobenzyl)thio)ethynyl)benzoate (6.3f):**



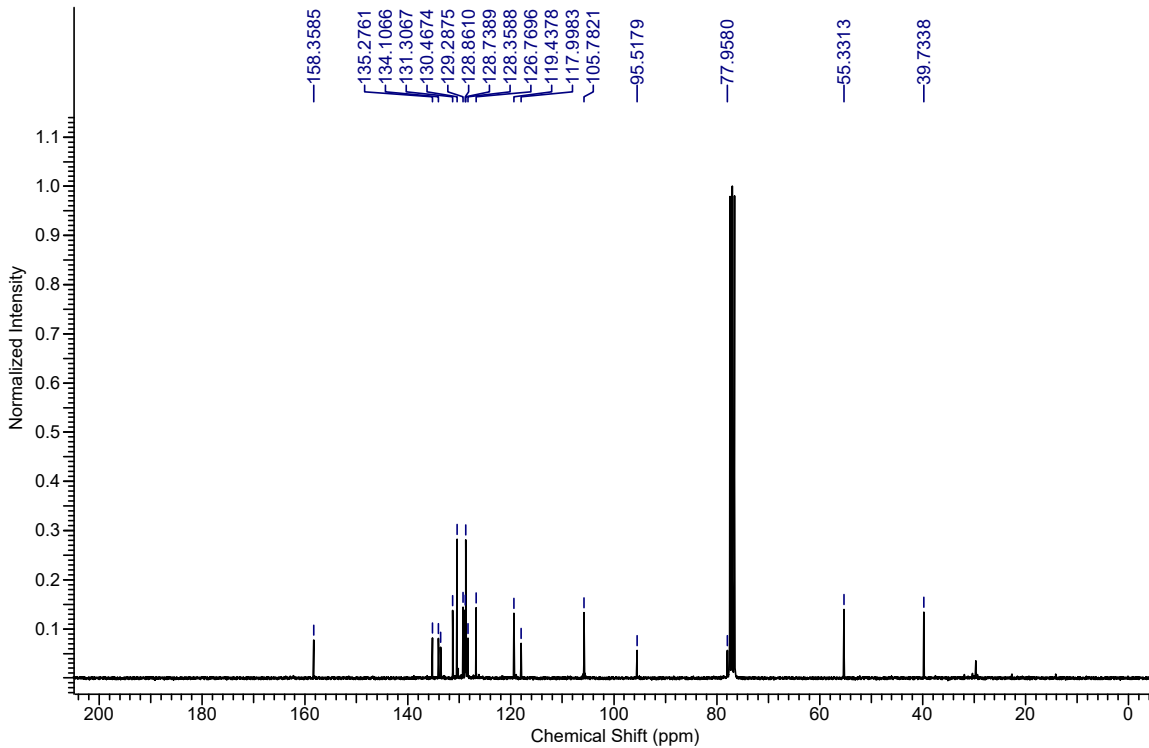
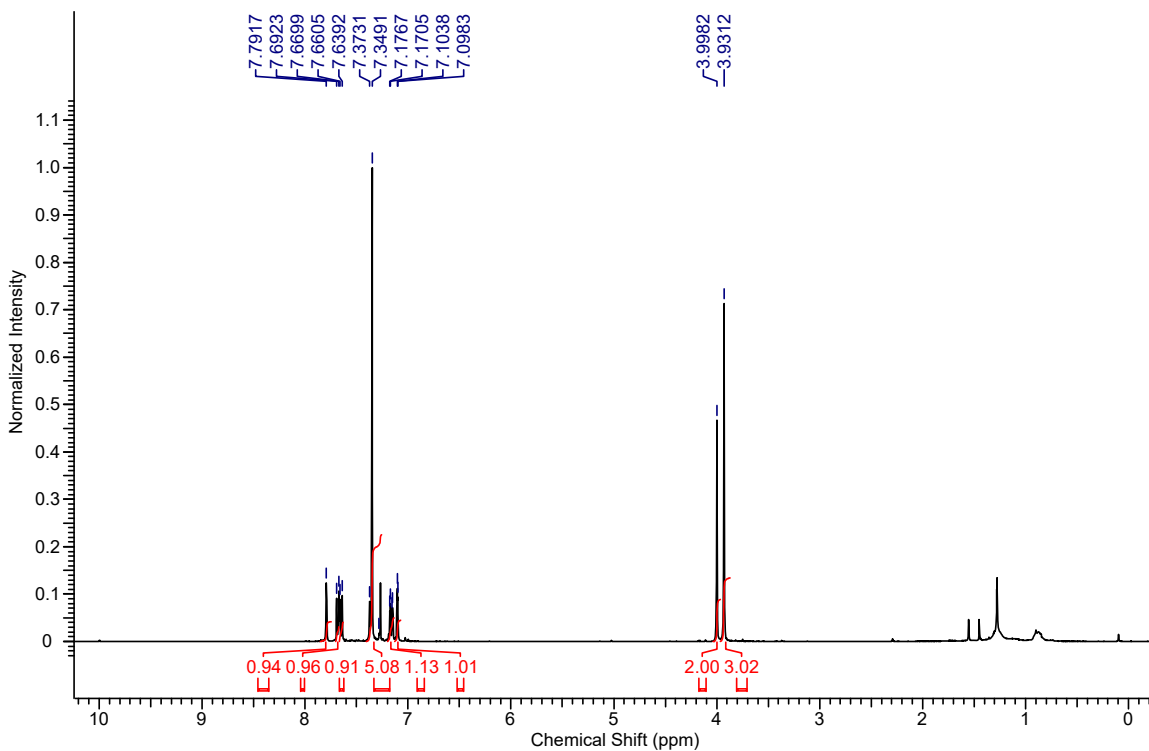
**Methyl 5-(((4-chlorobenzyl)thio)ethynyl)-2-methoxybenzoate (6.3g):**



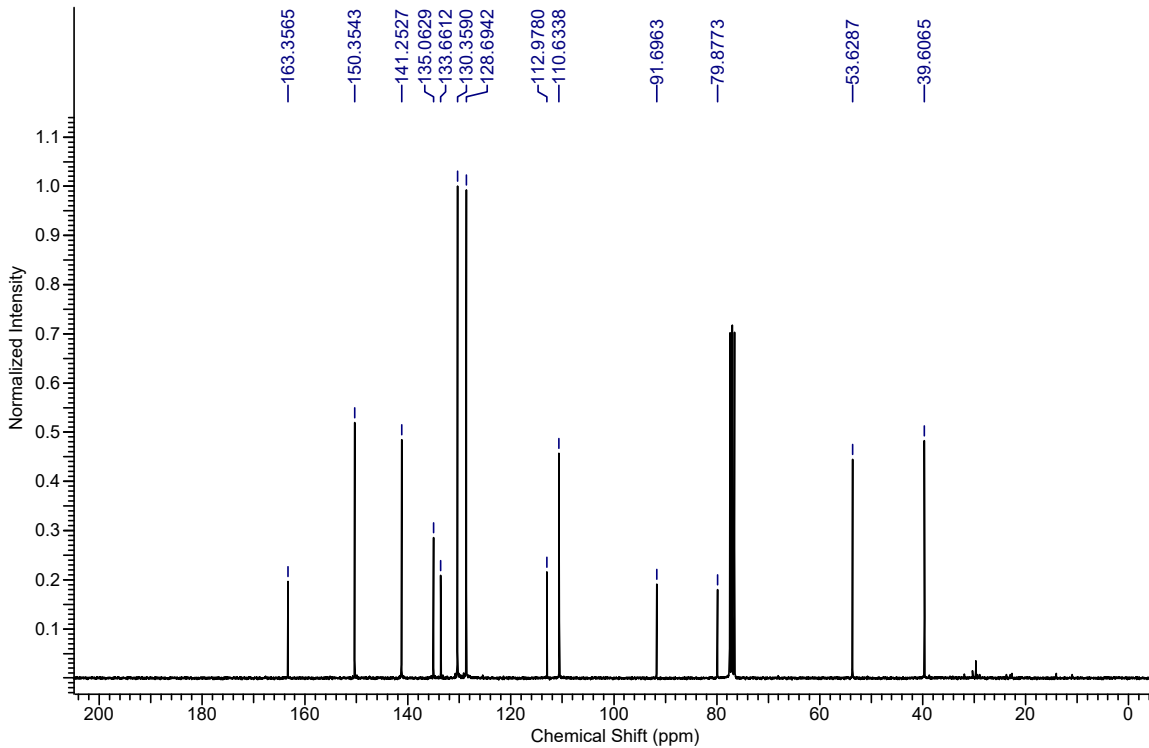
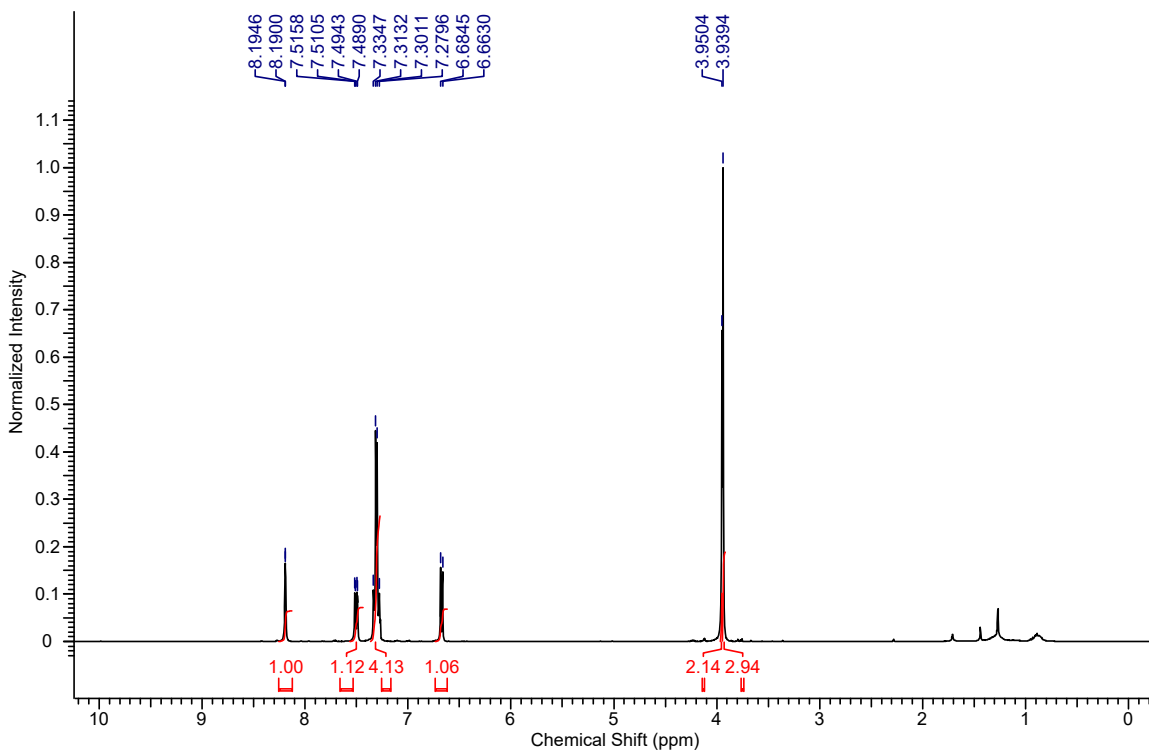
**(4-Chlorobenzyl)((2,4-dimethoxyphenyl)ethynyl)sulfane (6.3h):**



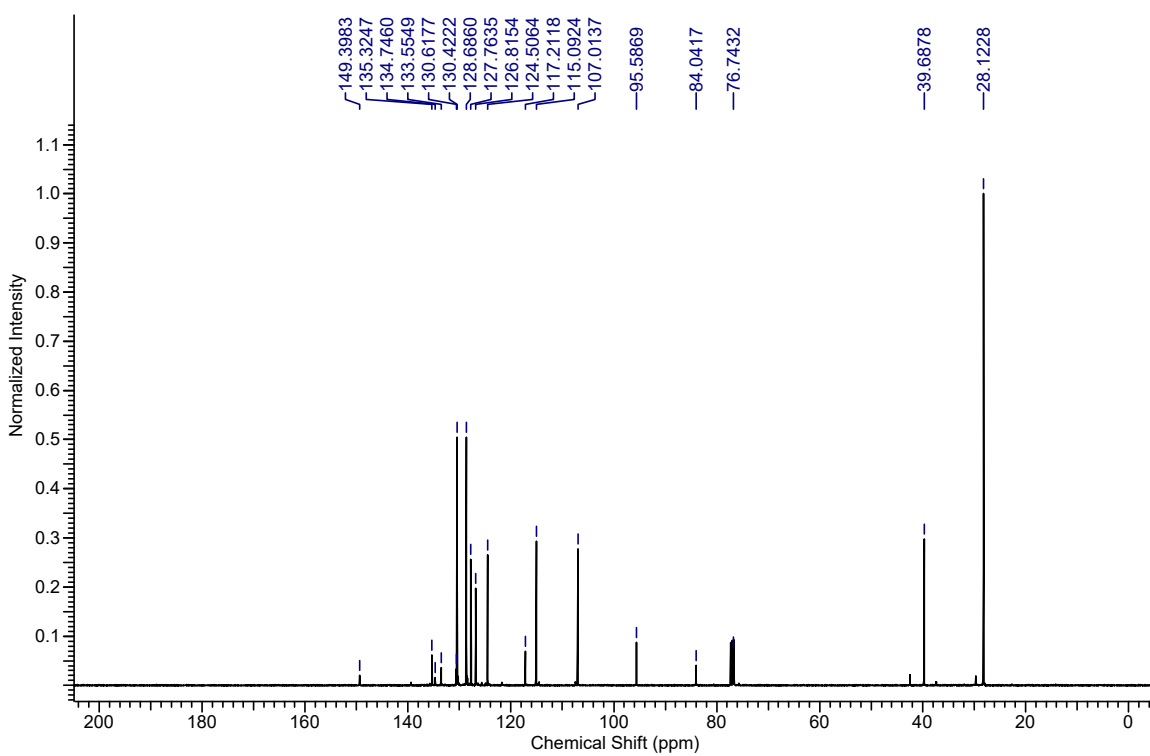
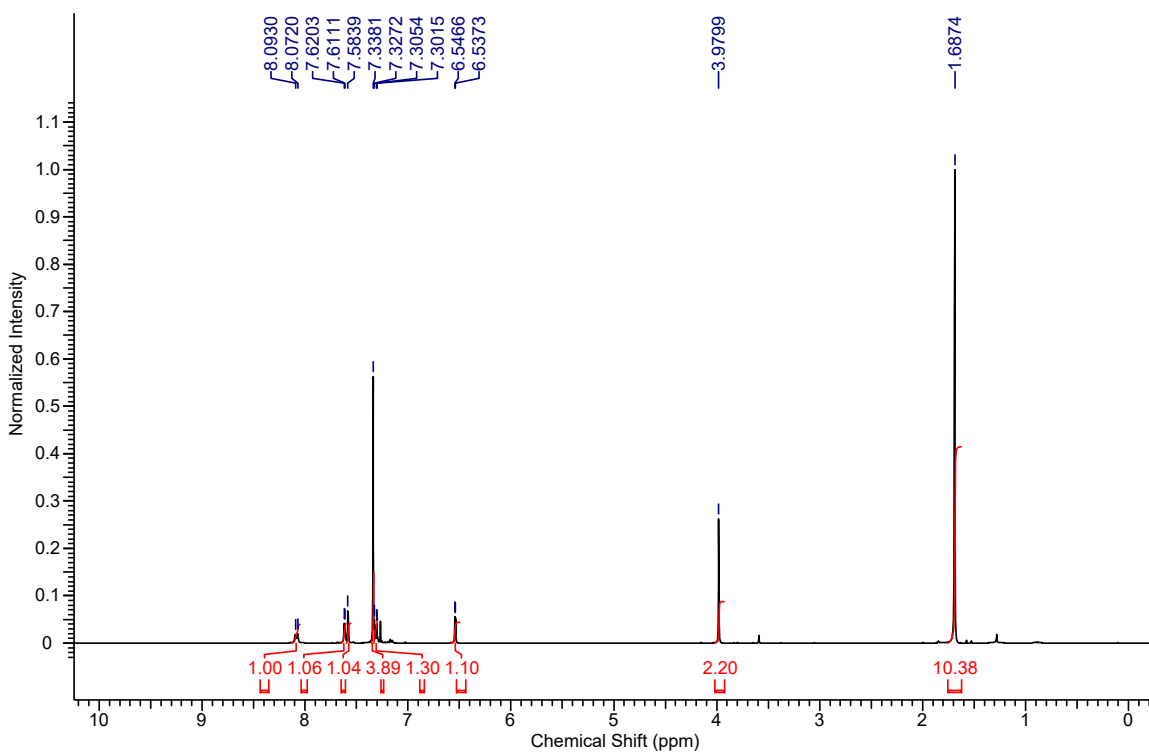
**(4-Chlorobenzyl)((6-methoxynaphthalen-2-yl)ethynyl)sulfane (6.3i):**



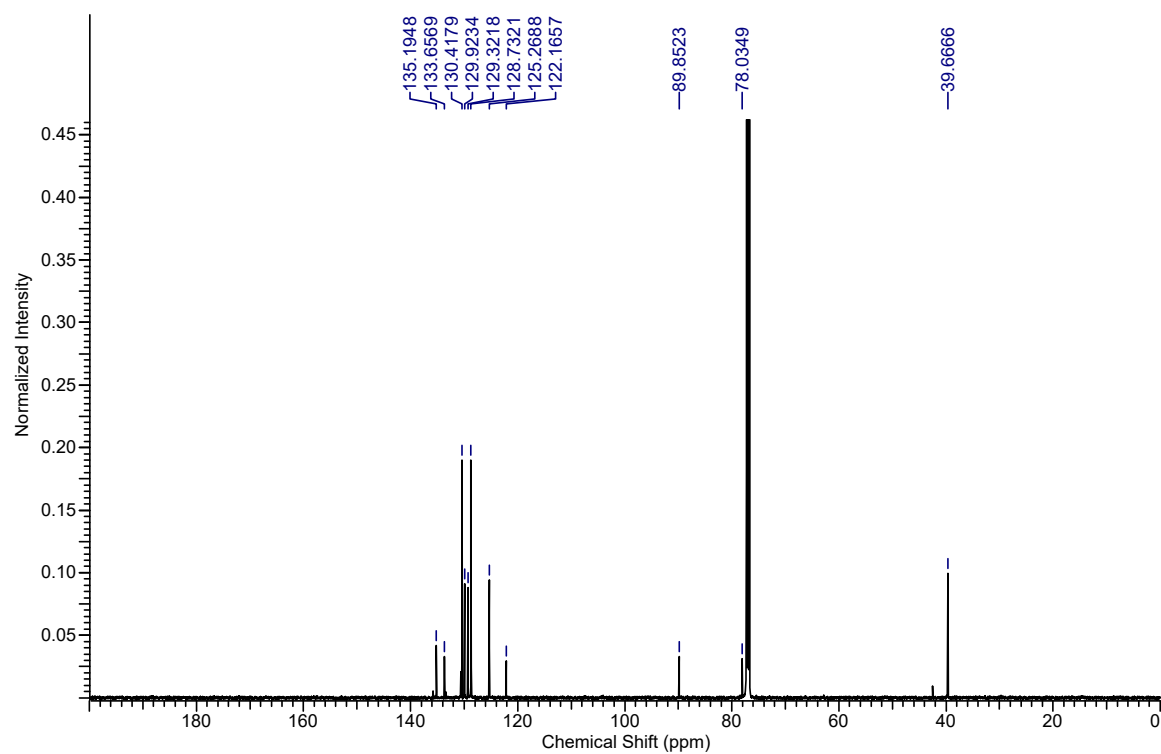
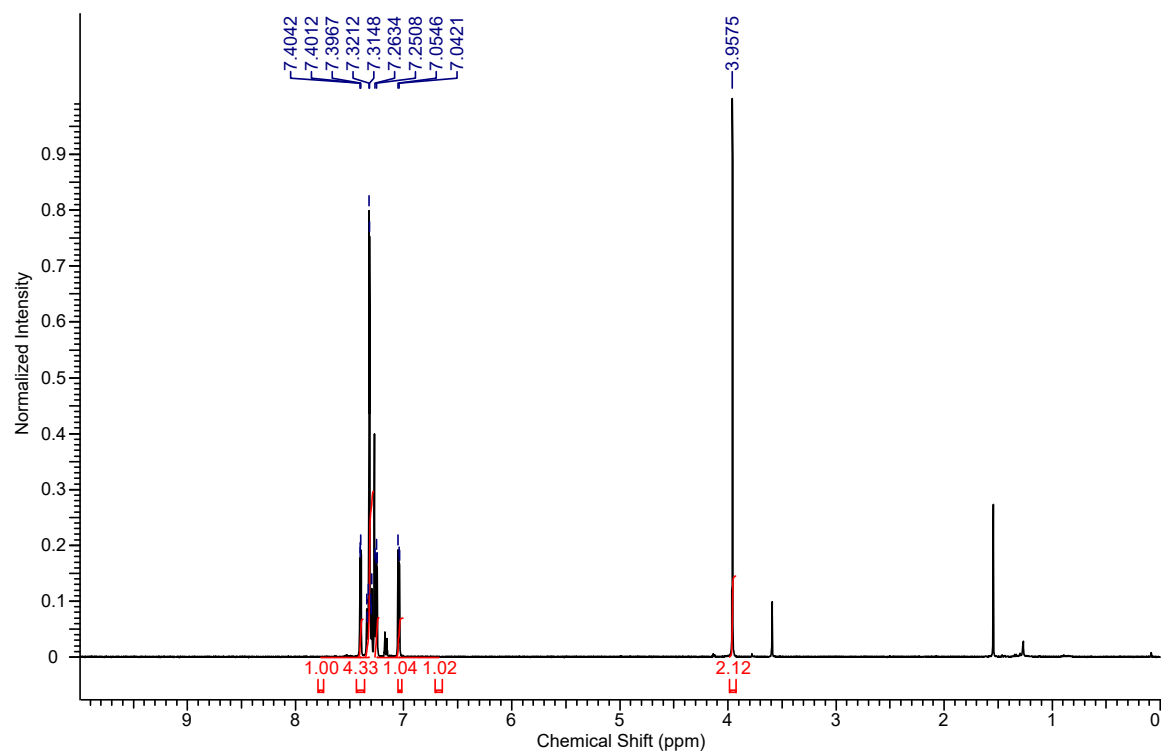
**5-(((4-Chlorobenzyl)thio)ethynyl)-2-methoxypyridine (6.3j):**



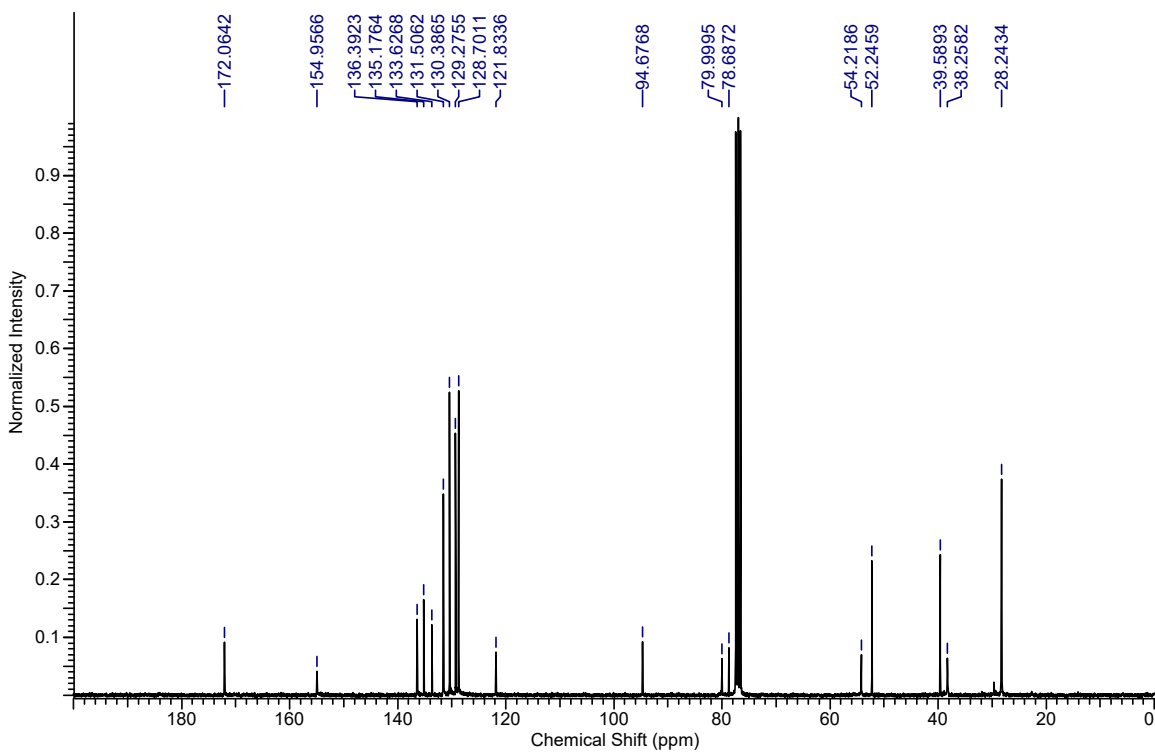
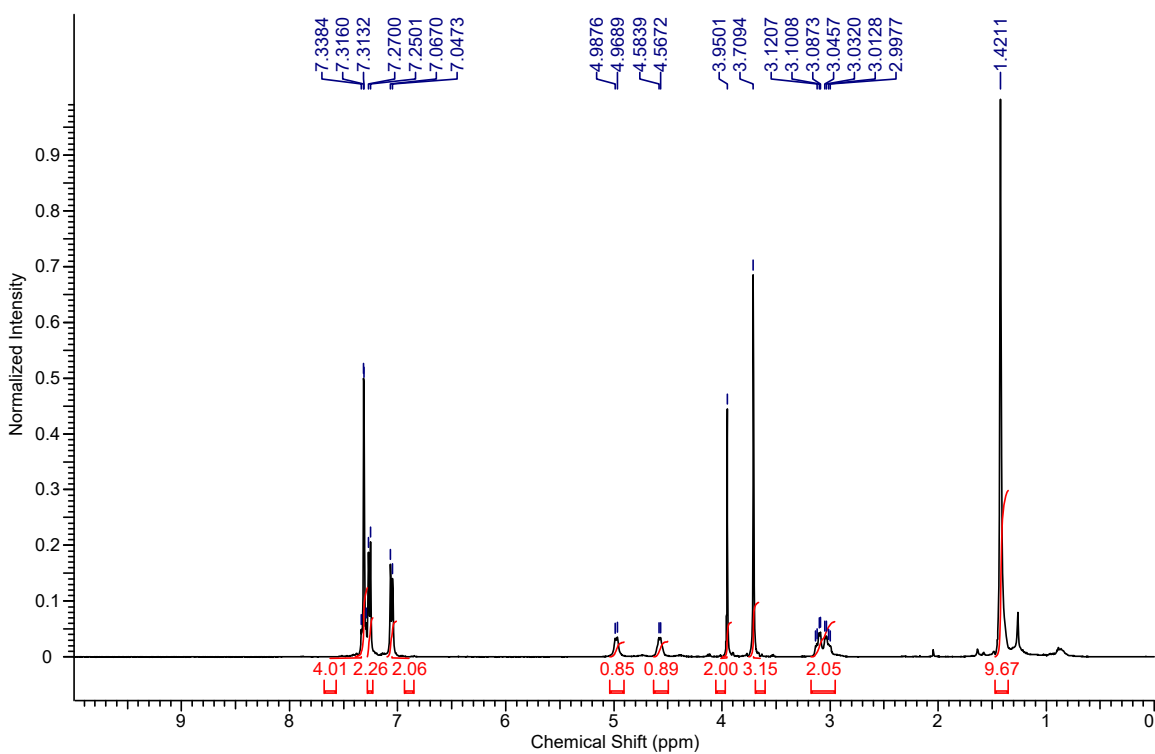
***tert*-Butyl 5-(((4-chlorobenzyl)thio)ethynyl)-1*H*-indole-1-carboxylate (6.3k):**



**3-(((4-Chlorobenzyl)thio)ethynyl)thiophene (6.3l):**

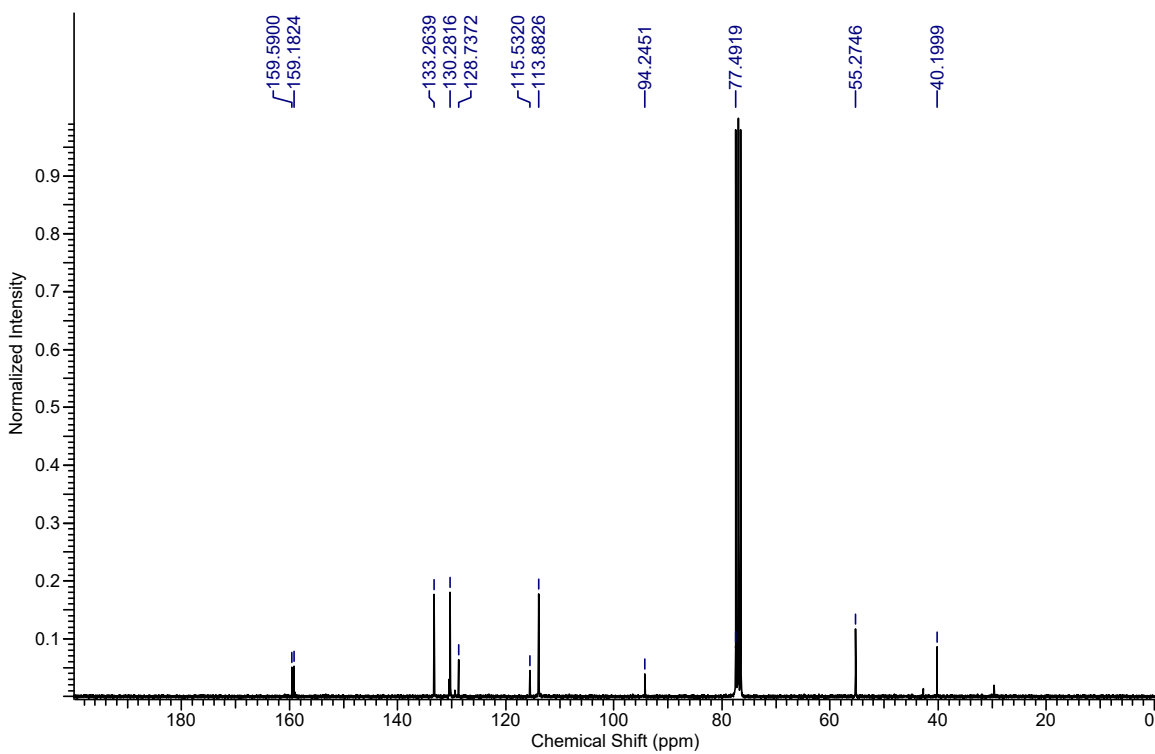
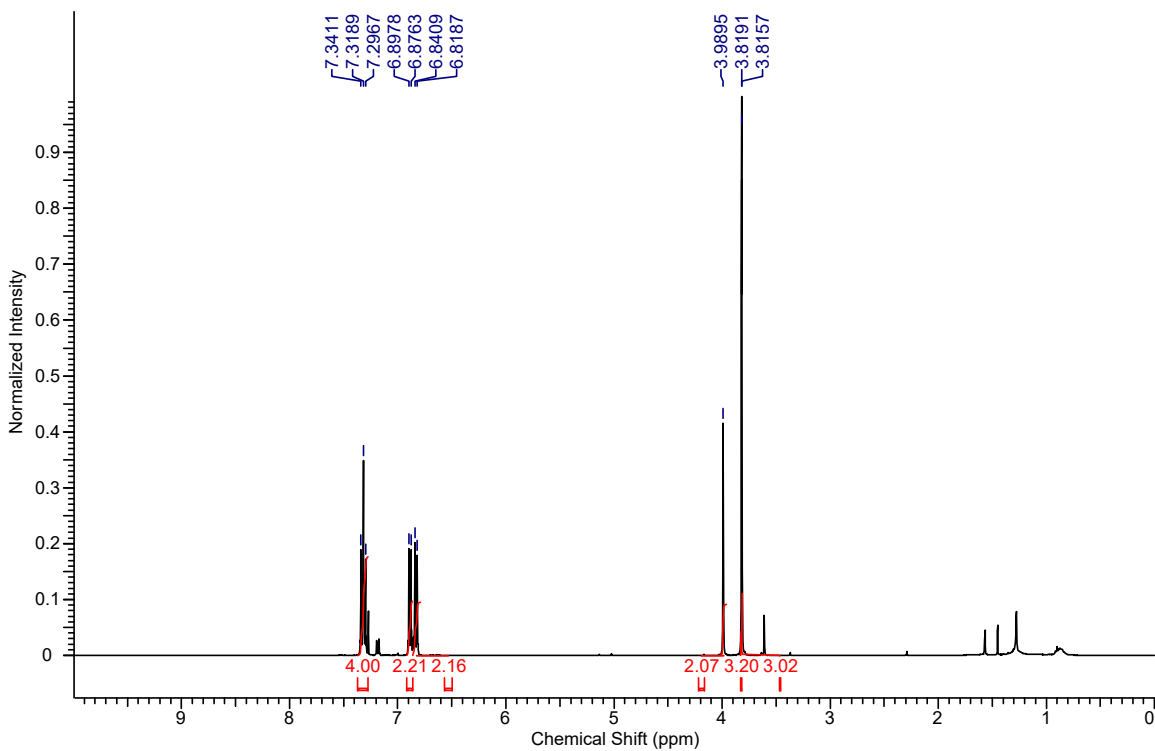


**Methyl (S)-2-((*tert*-butoxycarbonyl)amino)-3-(4-(((4-chlorobenzyl)thio)ethynyl)phenyl)propanoate (6.3m):**

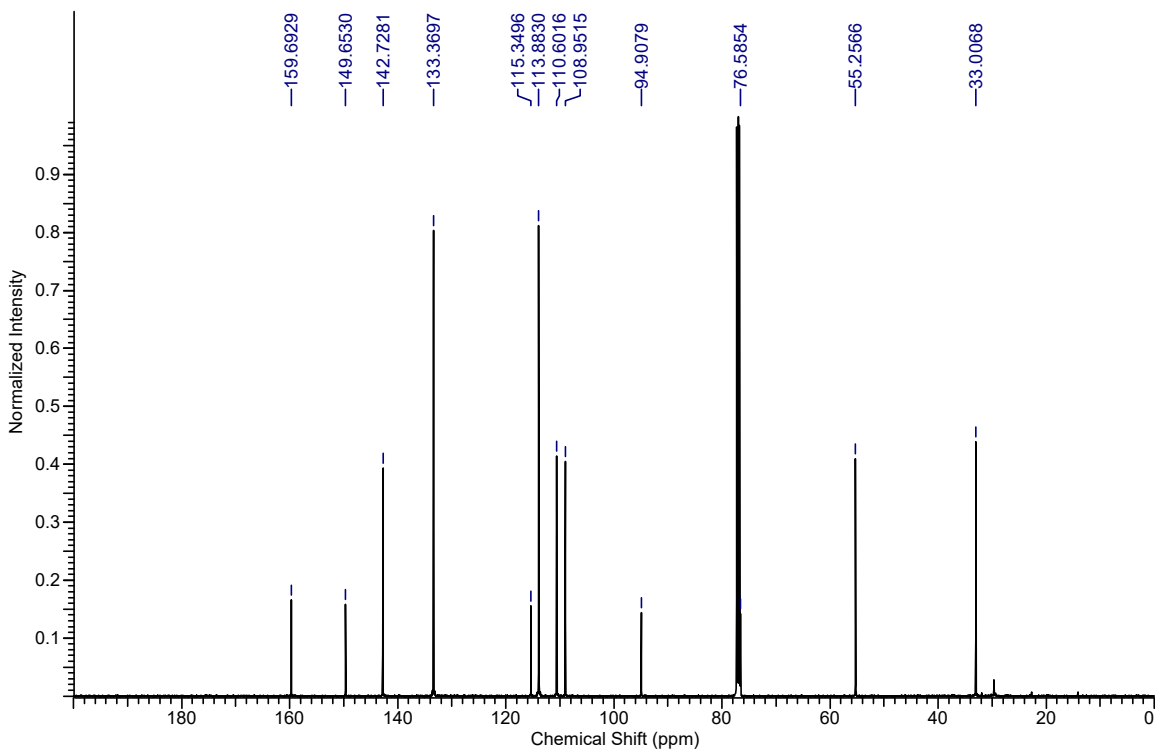
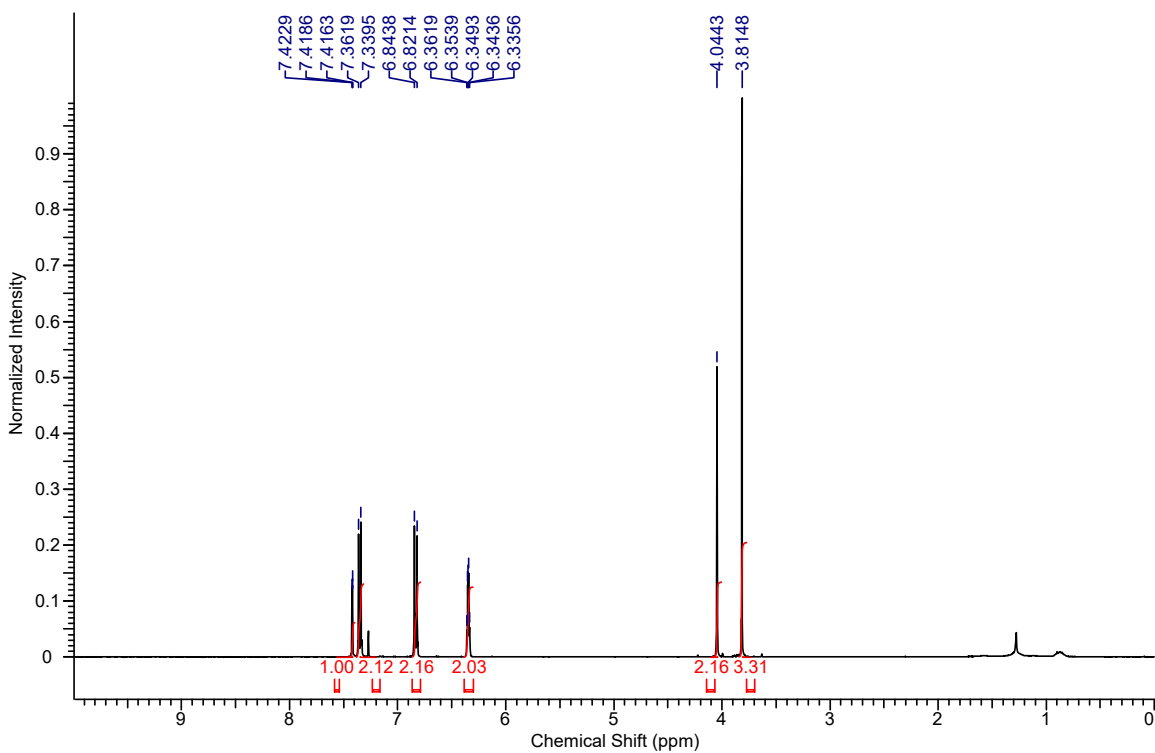




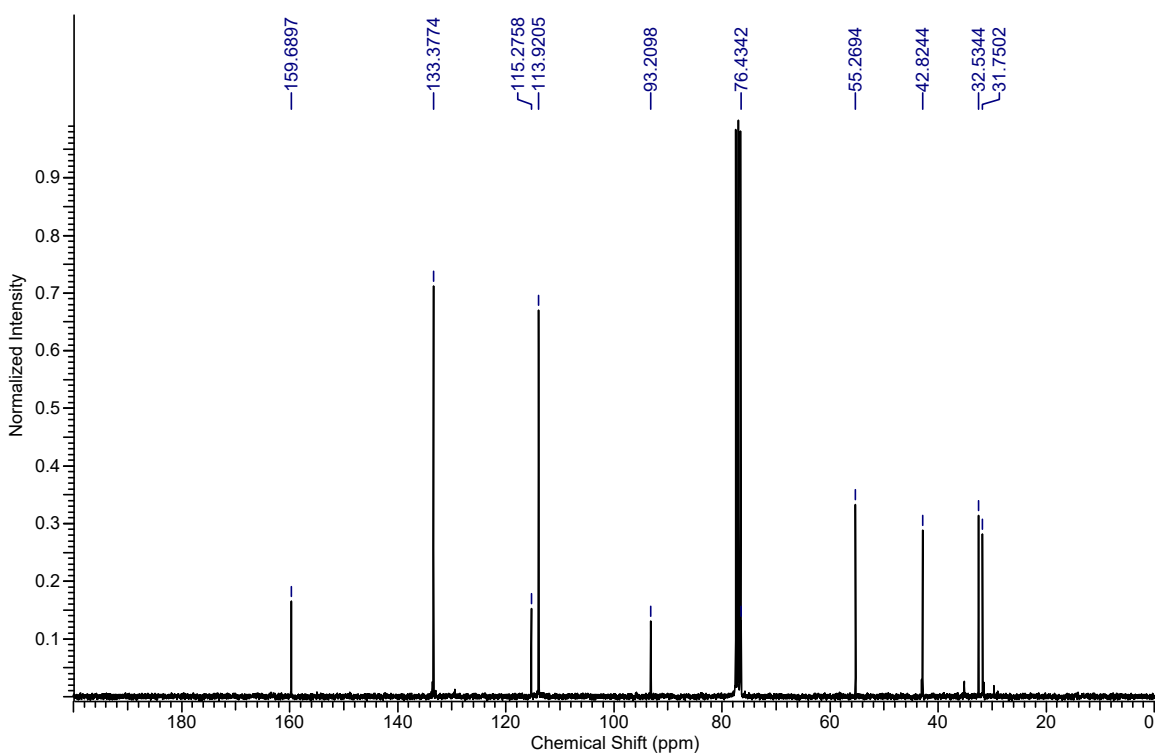
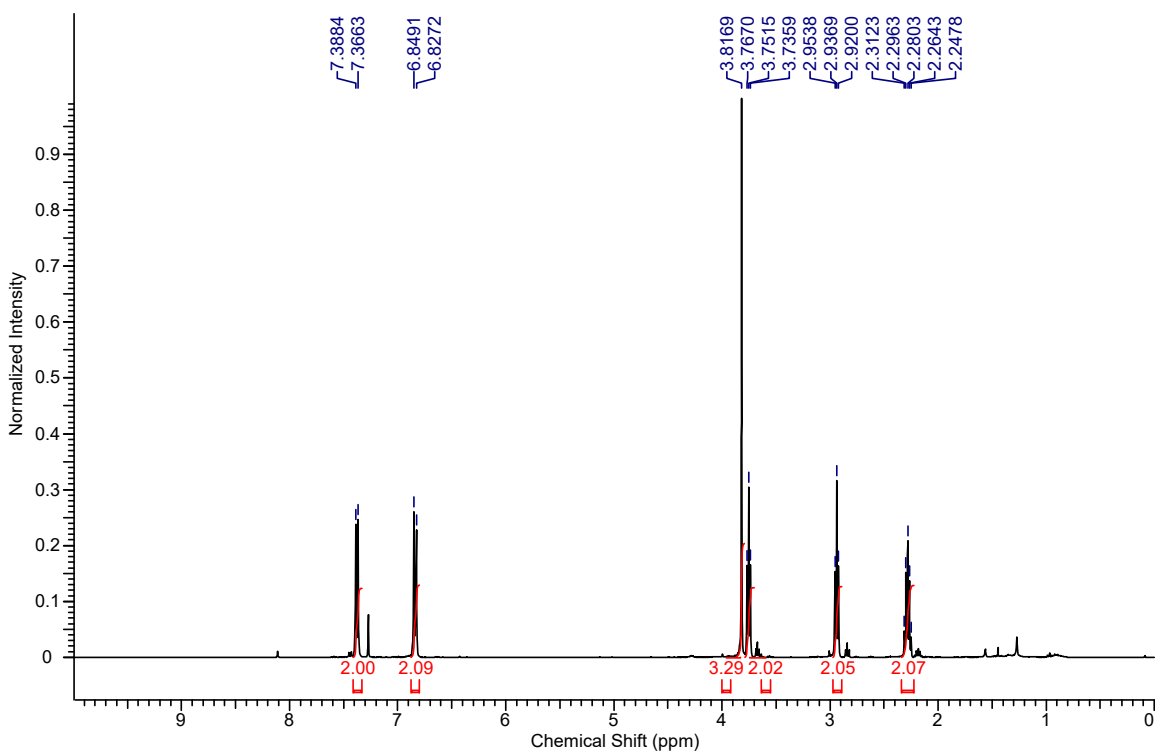
**(4-Methoxybenzyl)((4-methoxyphenyl)ethynyl)sulfane (6.3n):**



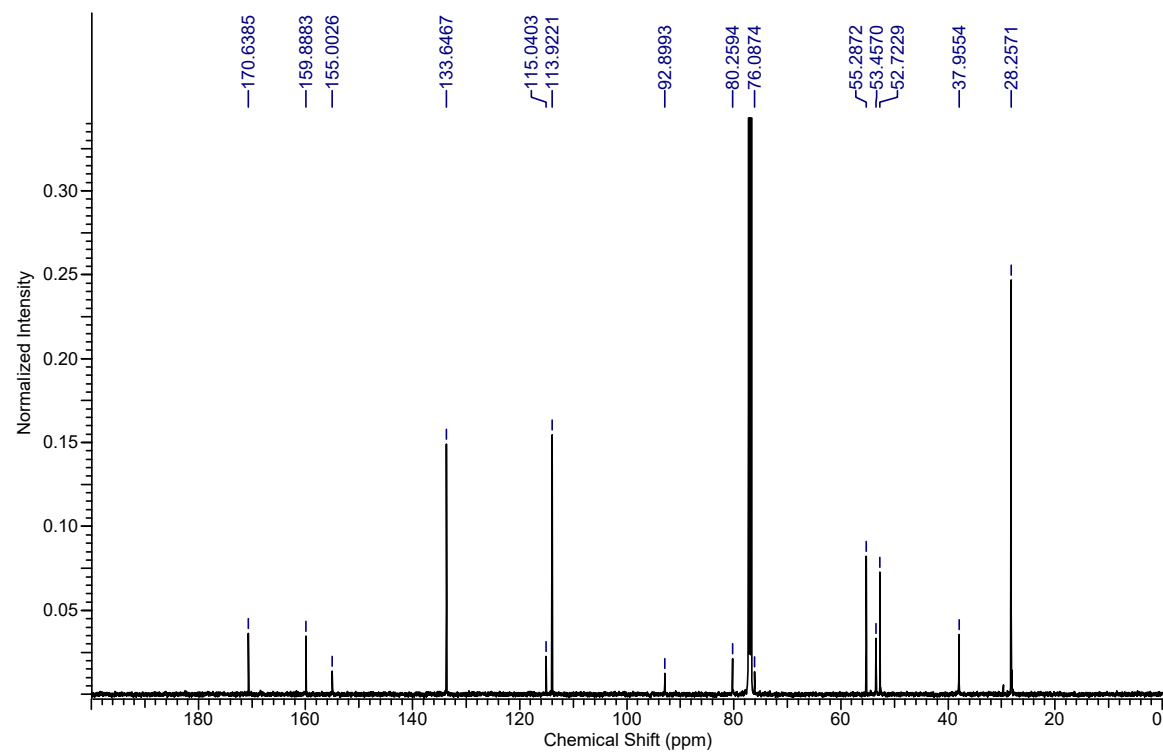
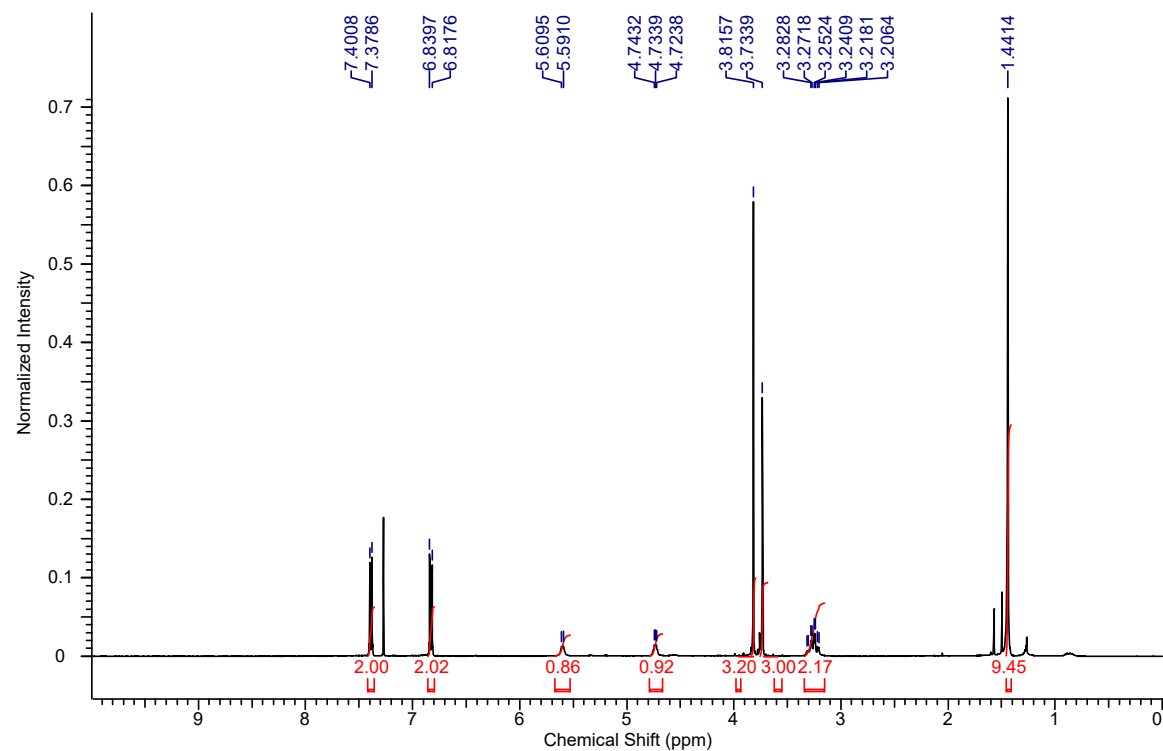
**2-(((4-Methoxyphenyl)ethynyl)thio)methyl)furan (6.3o):**



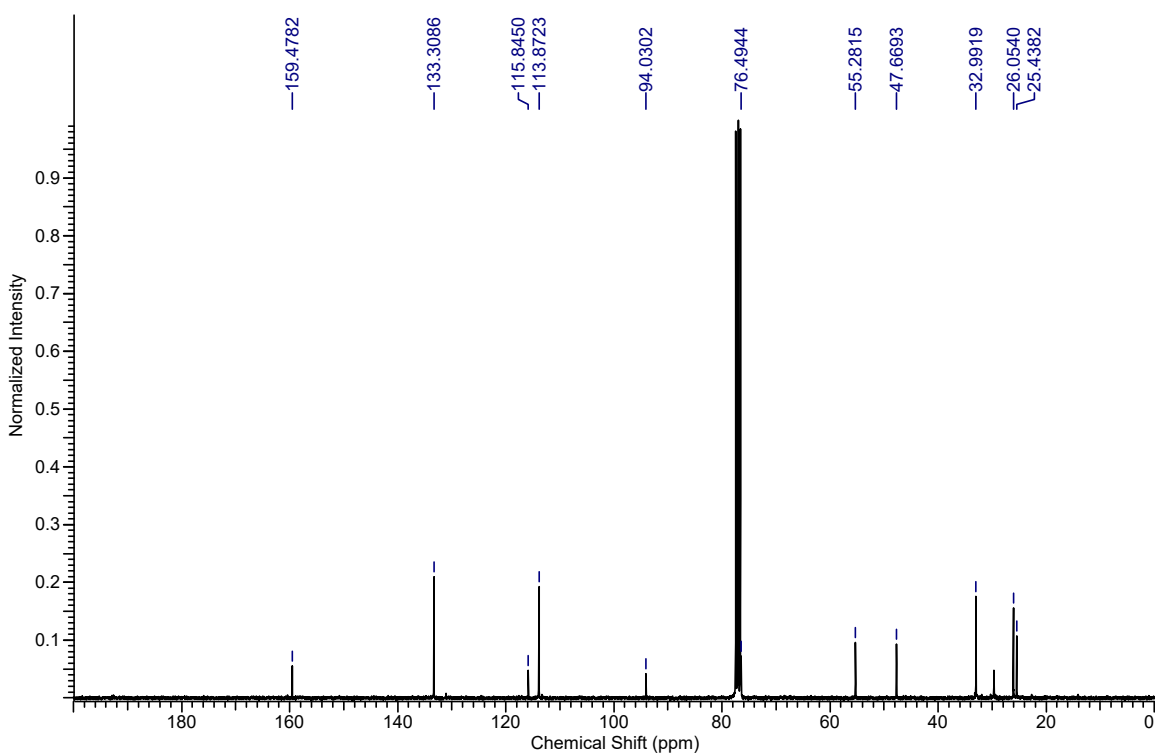
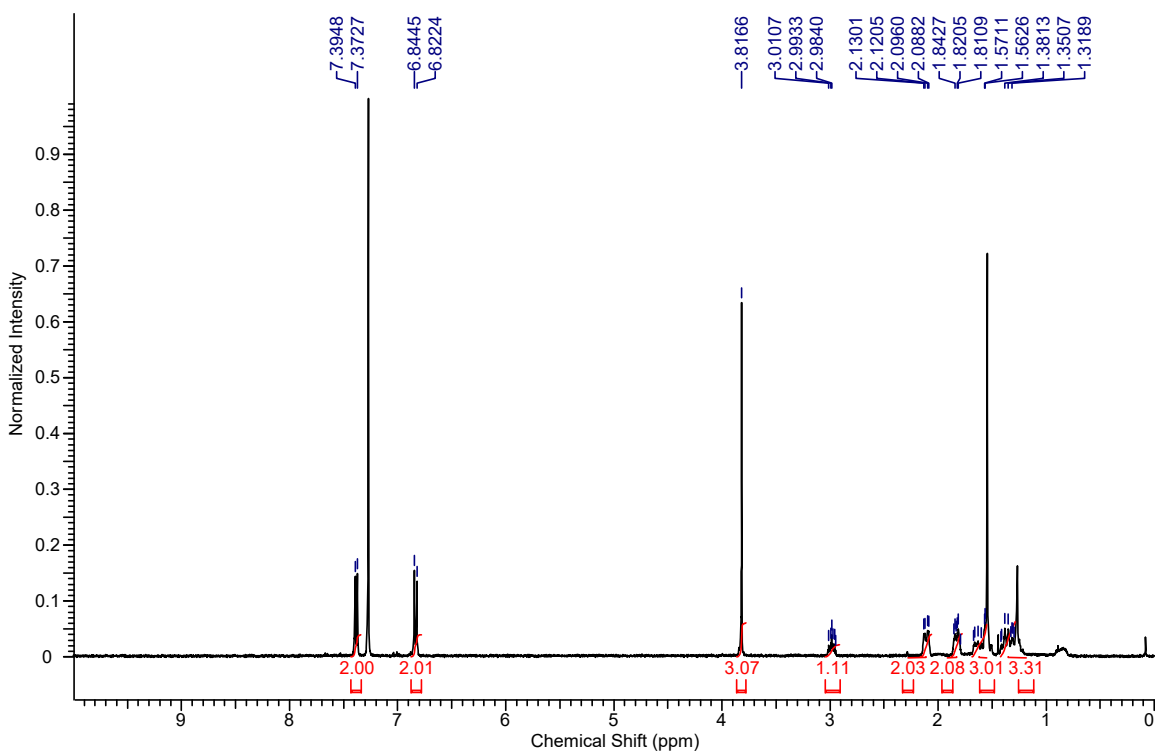
**(3-Chloropropyl)((4-methoxyphenyl)ethynyl)sulfane (6.3p):**



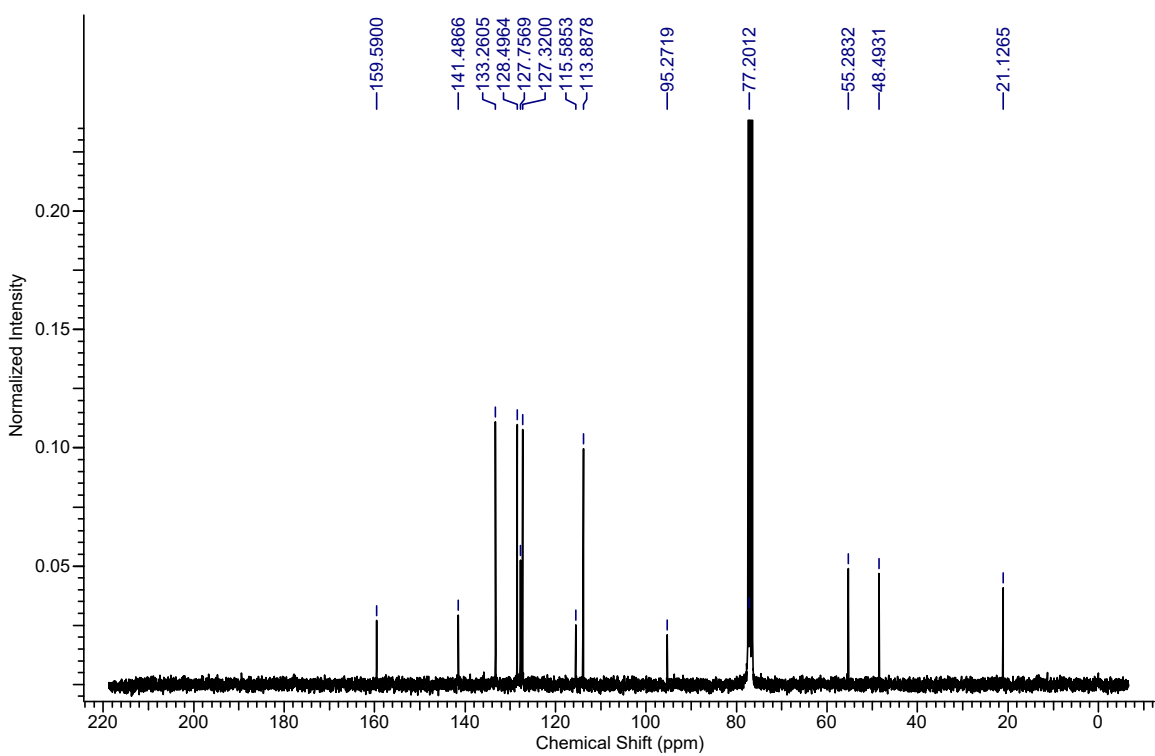
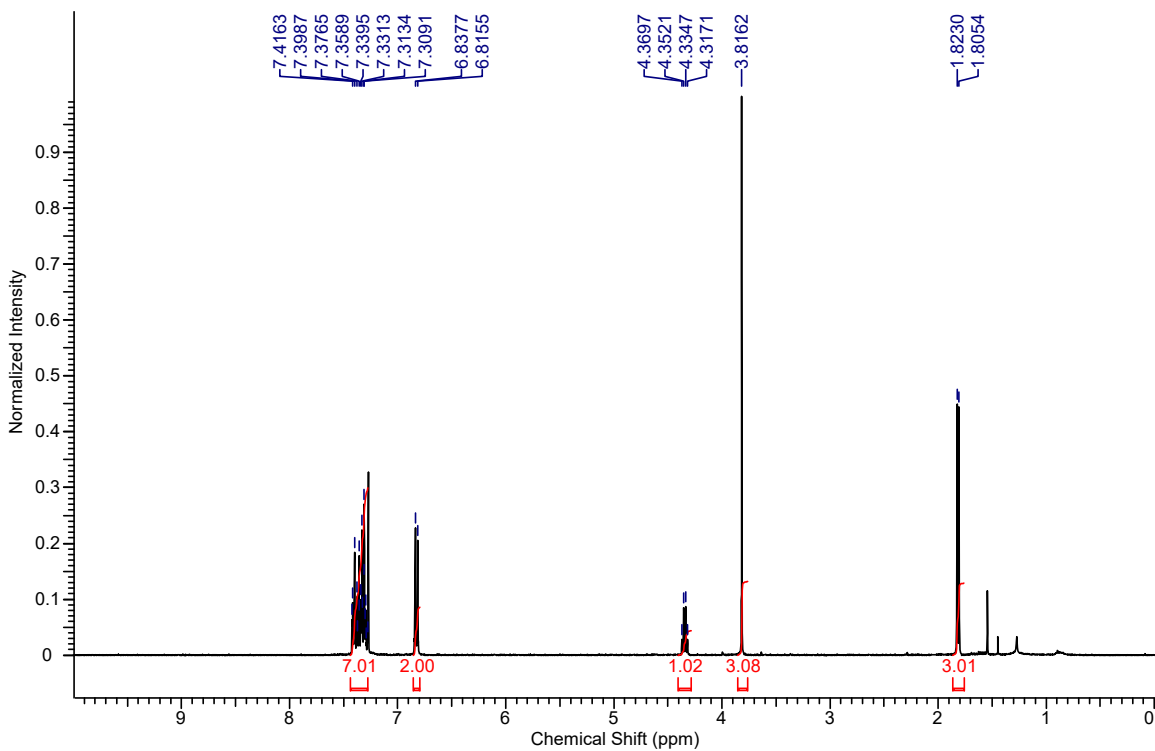
**Methyl *N*-(*tert*-butoxycarbonyl)-*S*-((4-methoxyphenyl)ethynyl)-*D*-cysteinate (6.3q):**



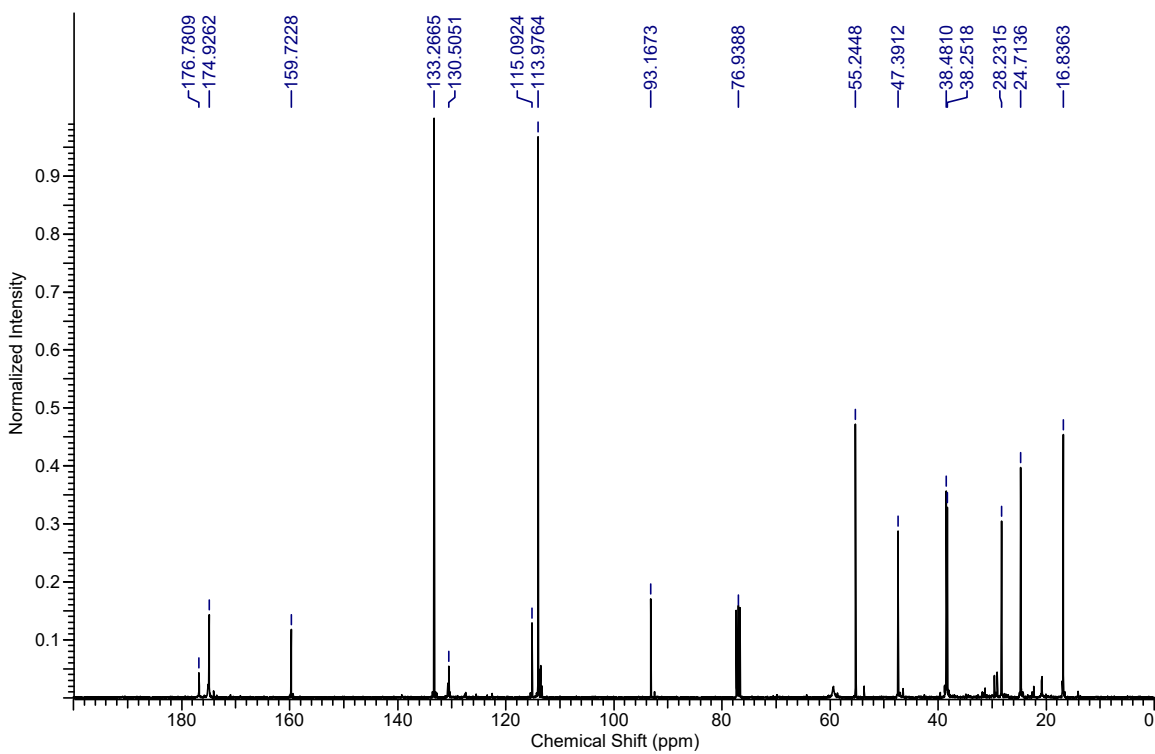
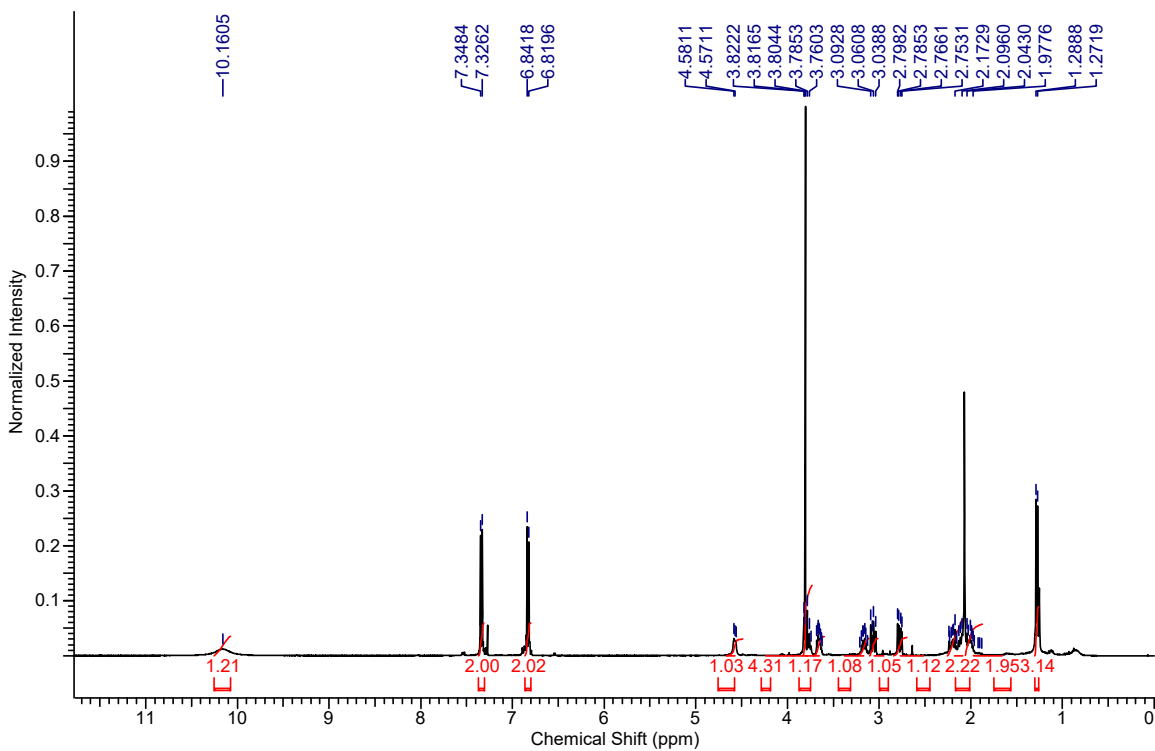
**Cyclohexyl((4-methoxyphenyl)ethynyl)sulfane (6.3r):**



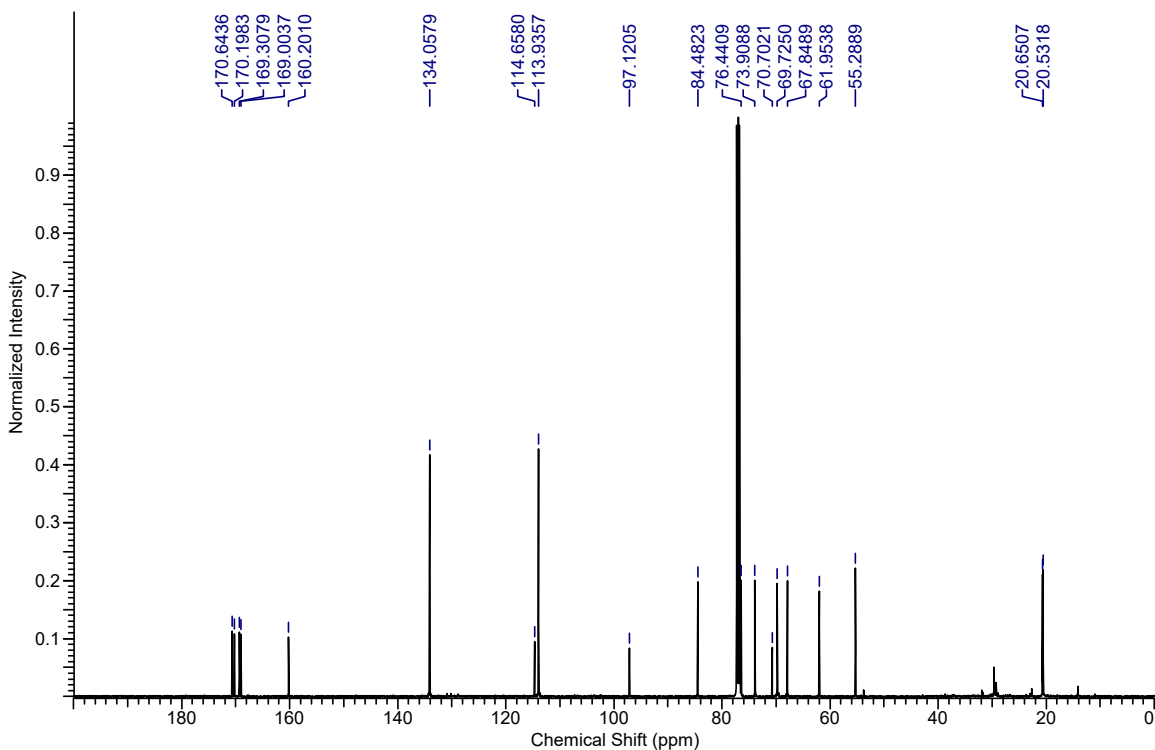
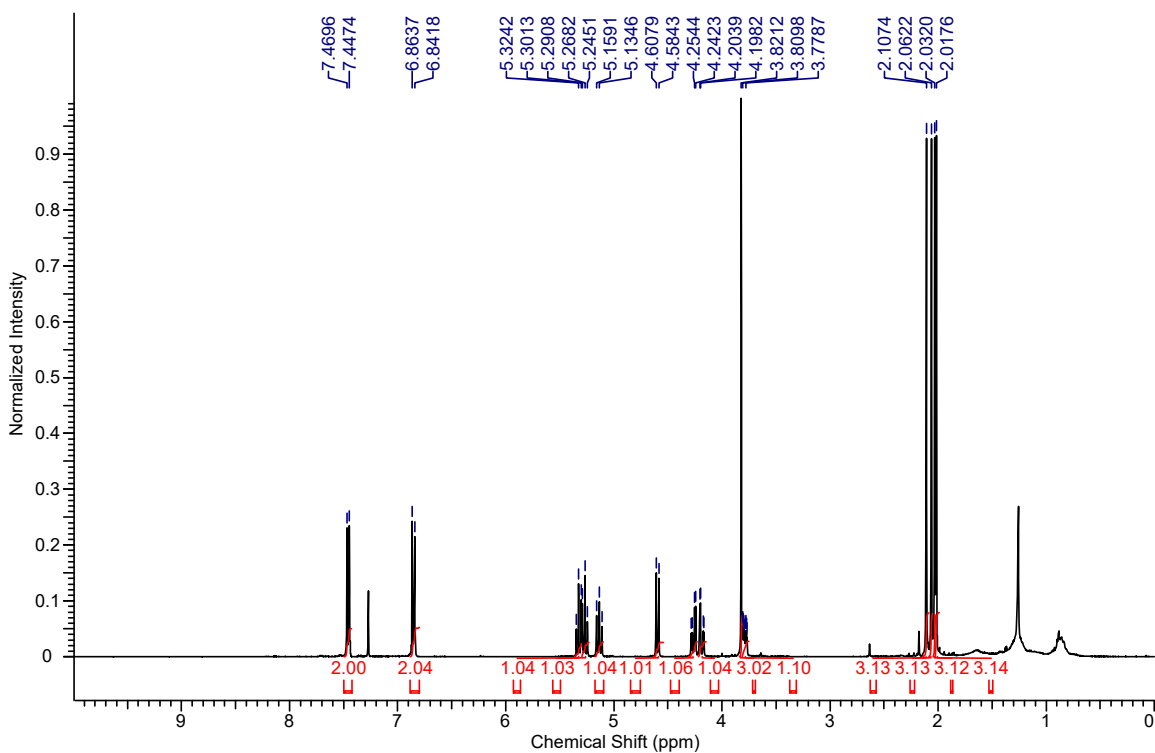
**(S)-((4-Methoxyphenyl)ethynyl)(1-phenylethyl)sulfane (6.3s):**



**((S)-3-(((4-Methoxyphenyl)ethynyl)thio)-2-methylpropanoyl)-L-proline (6.3t):**

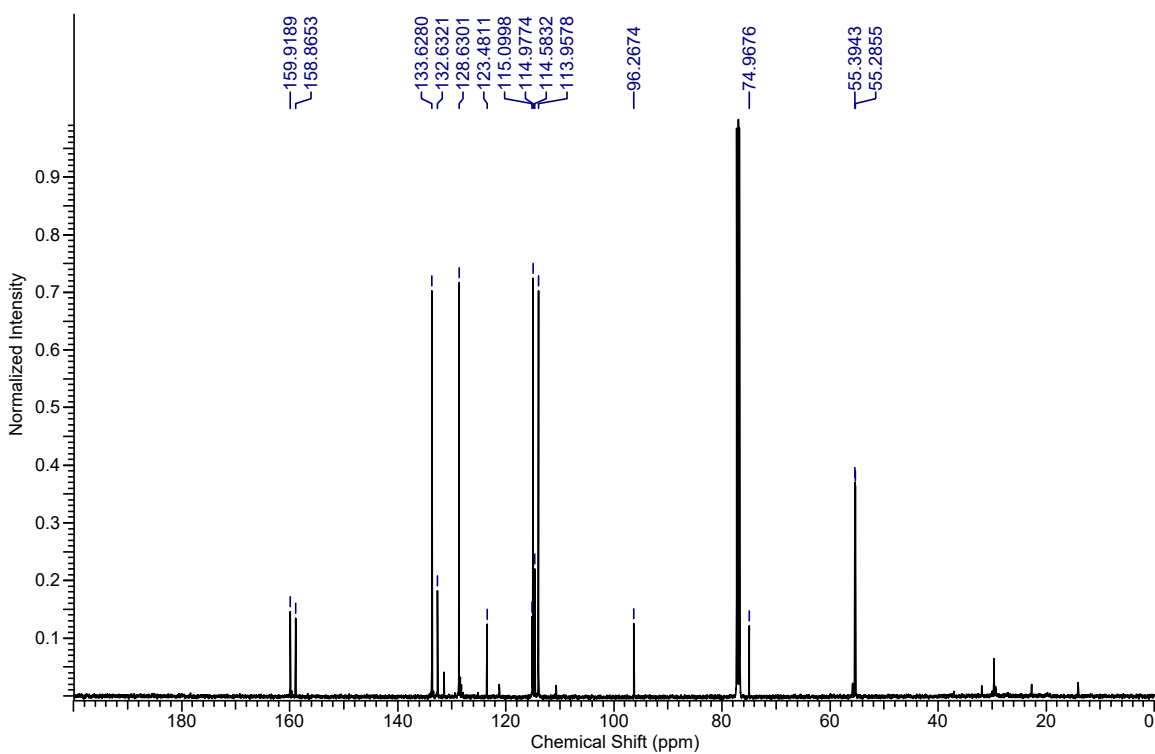
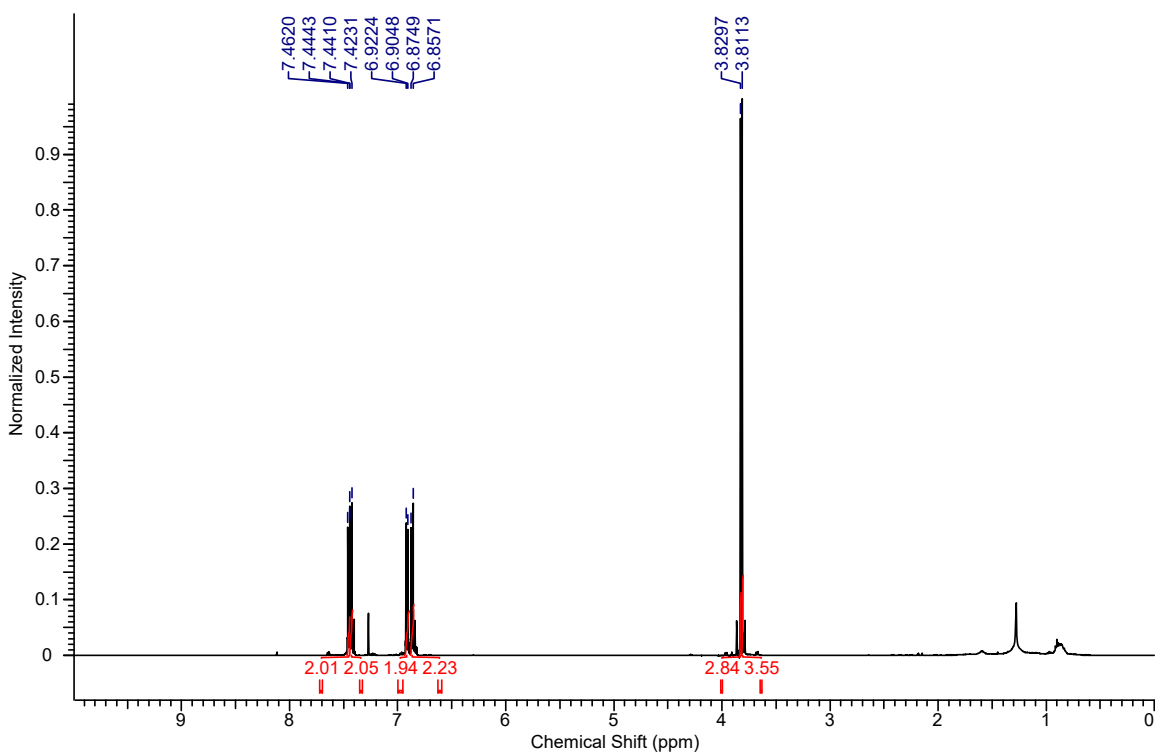


**(2*R*,3*R*,4*S*,5*R*,6*S*)-2-(Acetoxymethyl)-6-(((4-methoxyphenyl)ethynyl)thio)tetrahydro-2*H*-pyran-3,4,5-triyl triacetate (6.3u):**

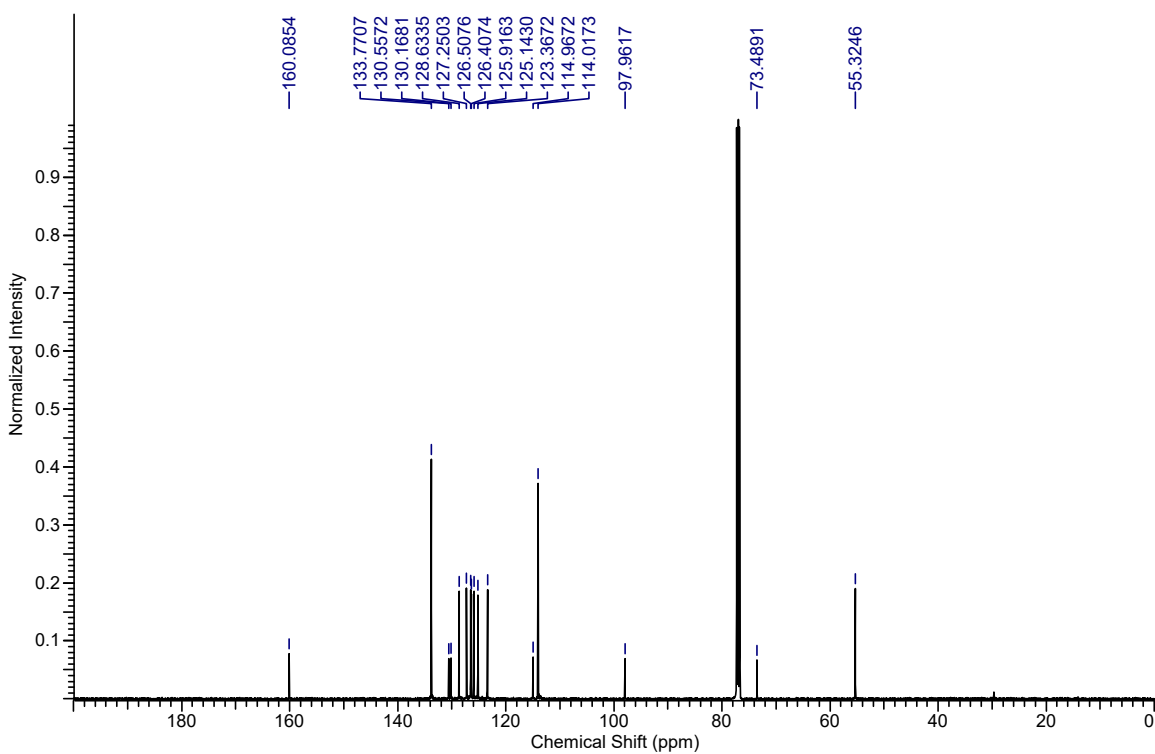
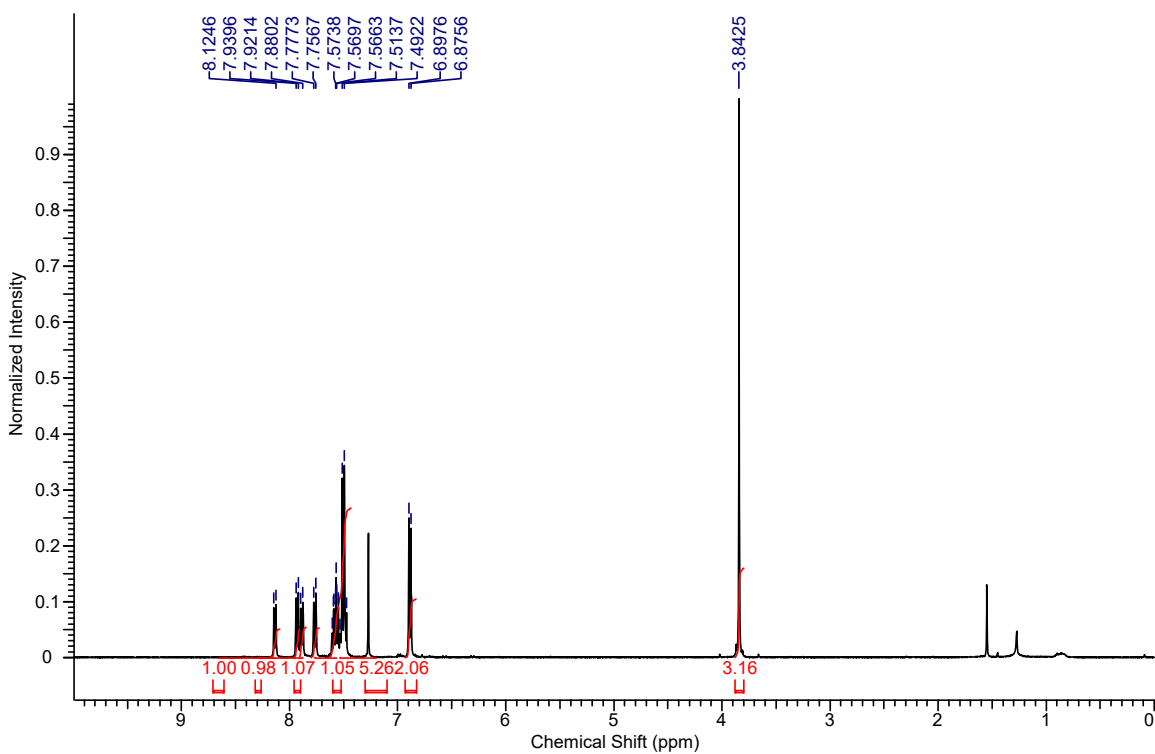




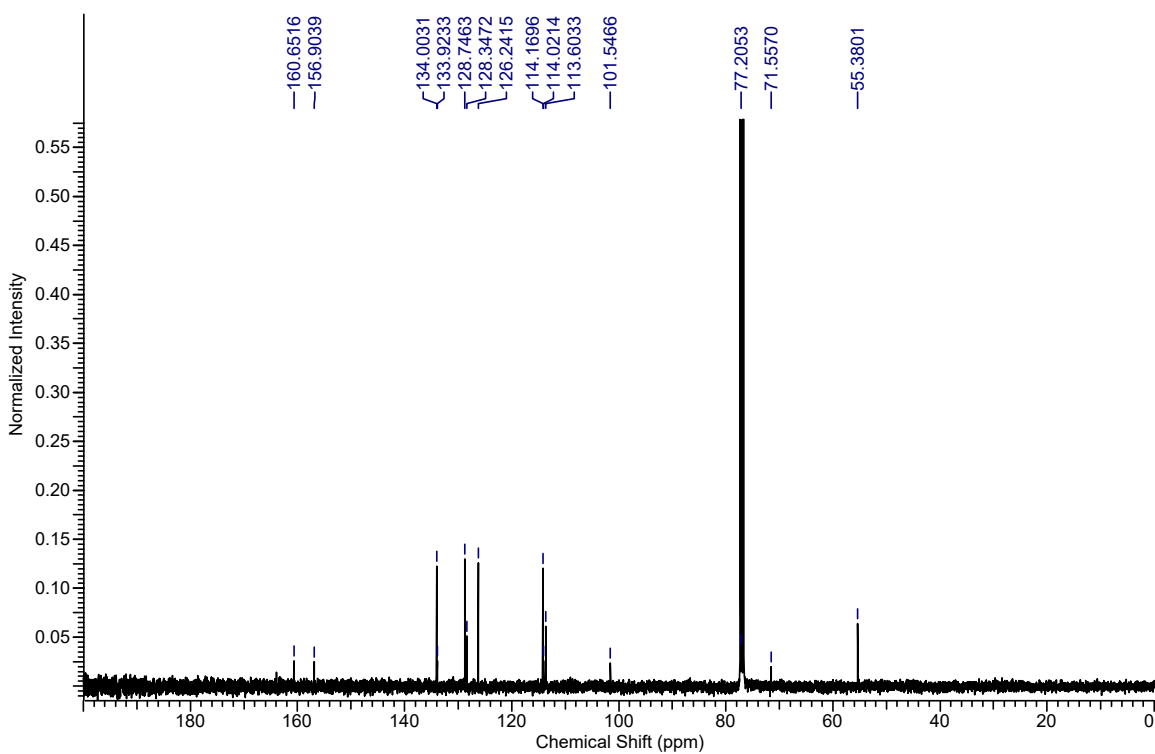
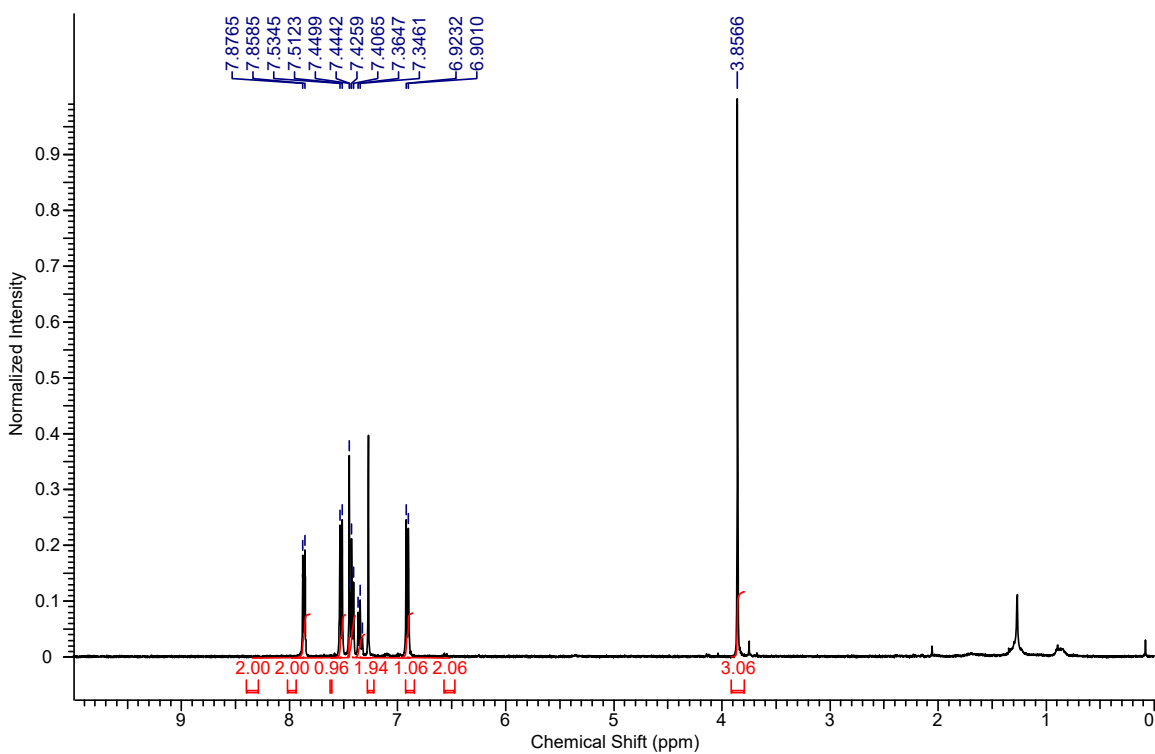
**(4-Methoxyphenyl)((4-methoxyphenyl)ethynyl)sulfane (6.3v):**



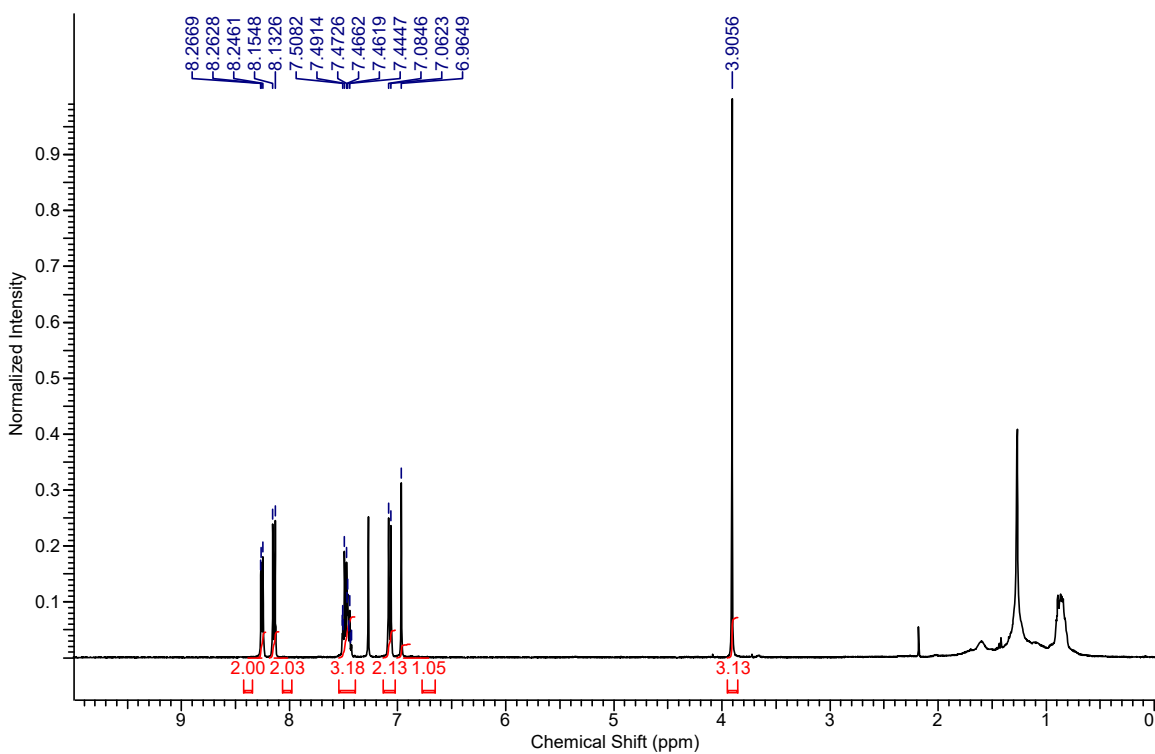
**((4-Methoxyphenyl)ethynyl)(naphthalen-1-yl)sulfane (6.3w):**



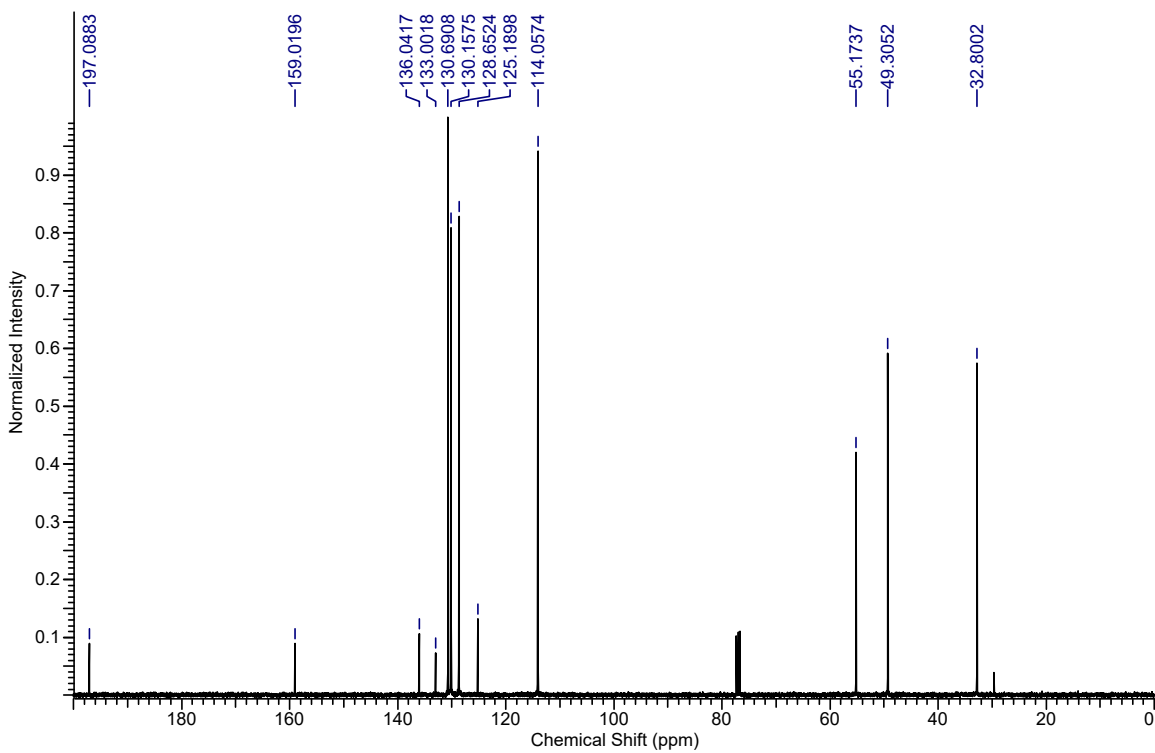
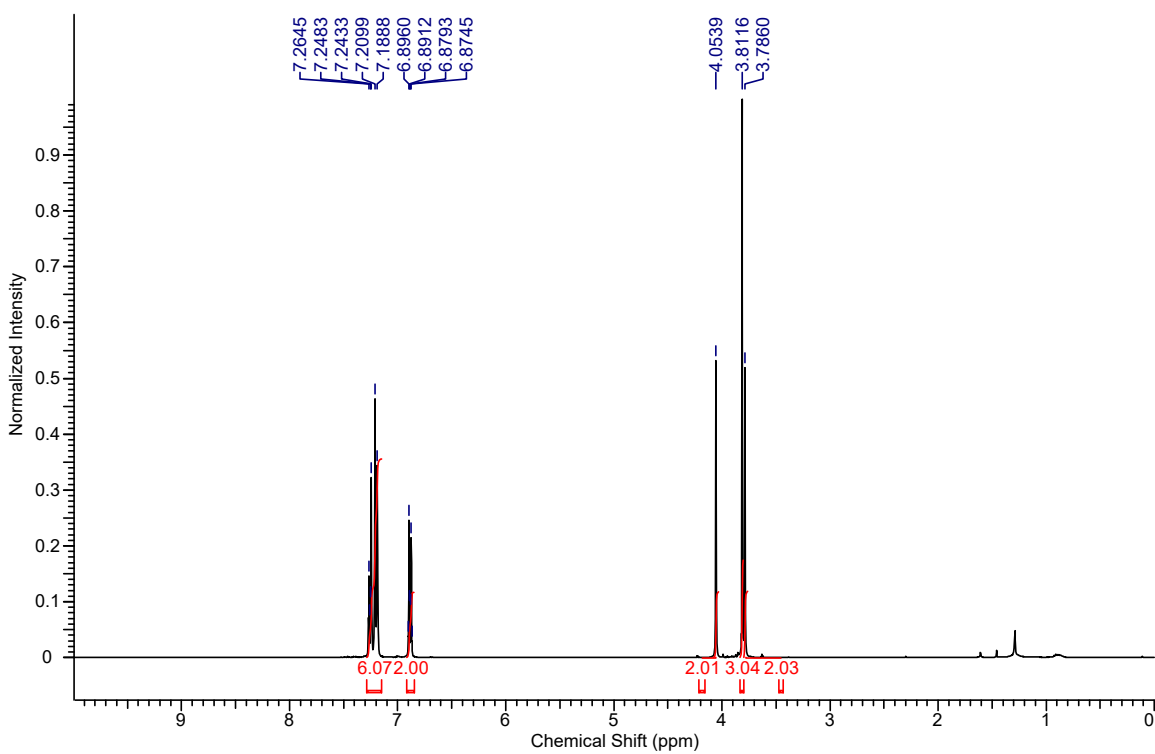
**2-(((4-Methoxyphenyl)ethynyl)thio)-4-phenylthiazole (6.3x):**



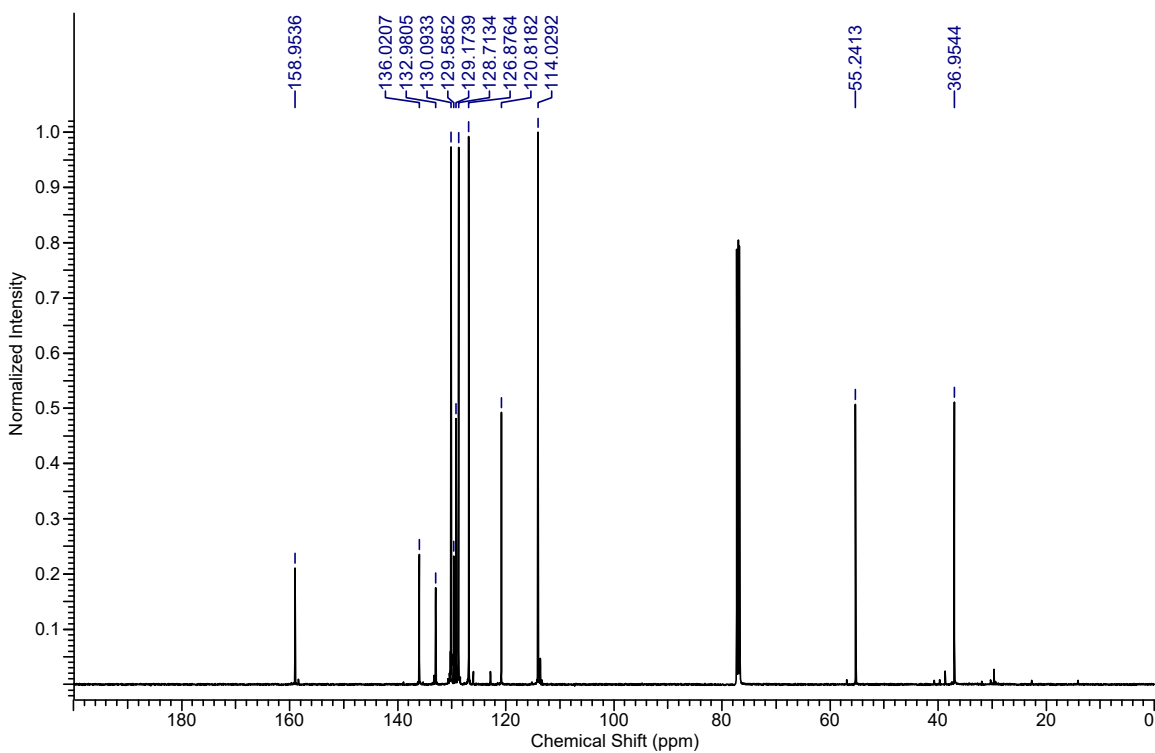
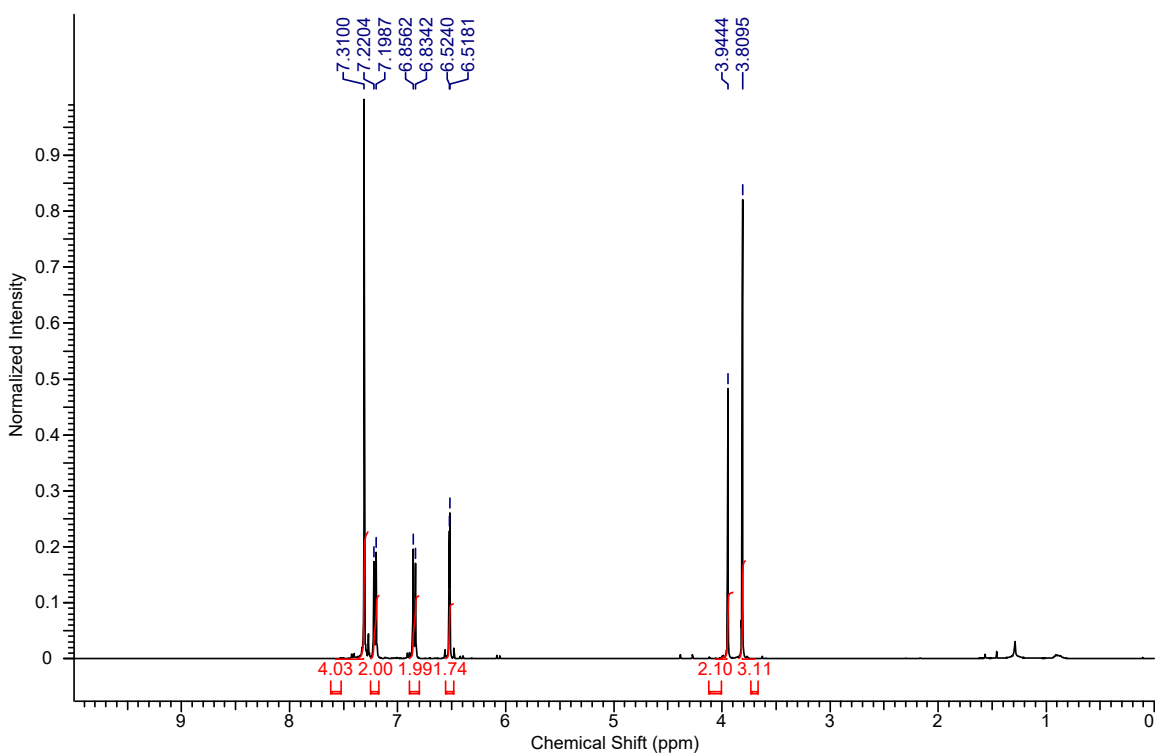
**3-(((4-Methoxyphenyl)ethynyl)thio)-5-phenyl-1*H*-1,2,4-triazole (6.3y):**



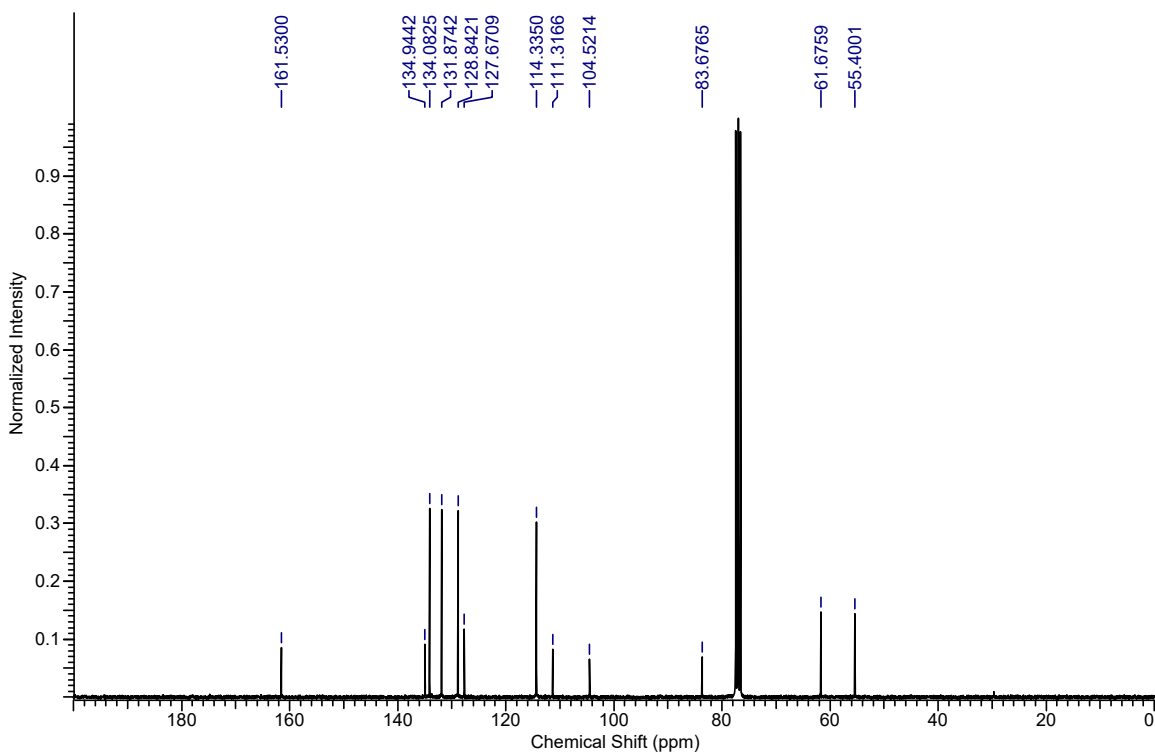
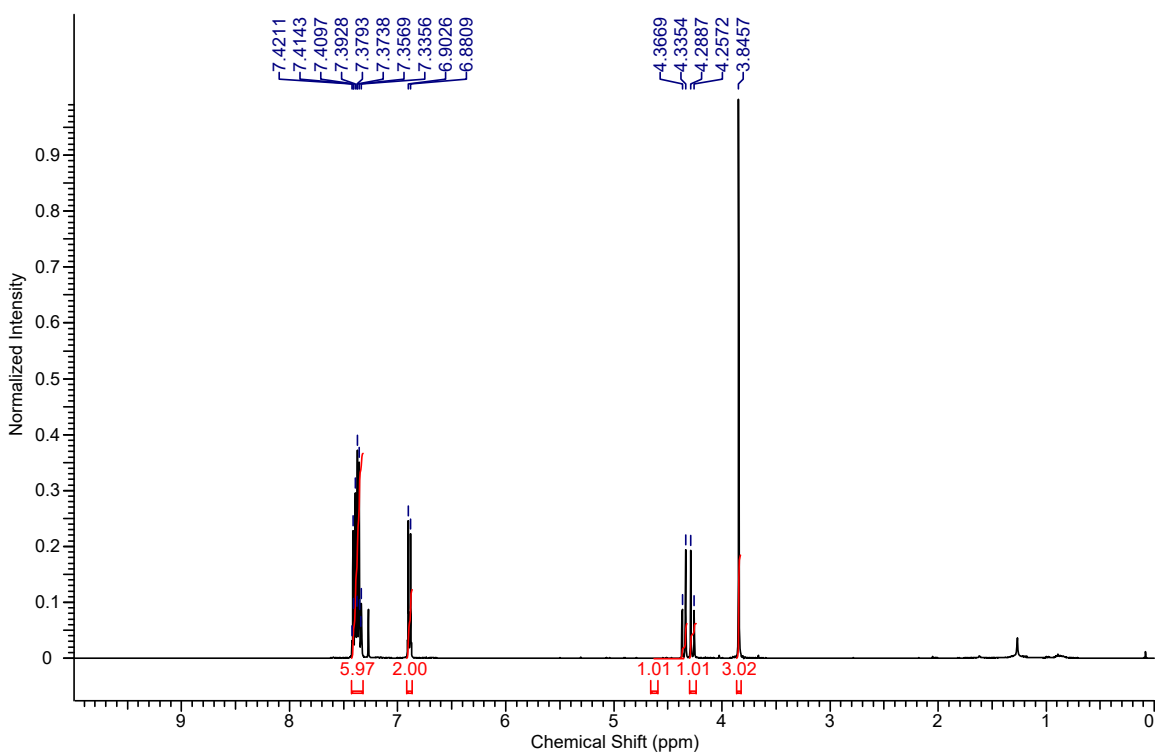
***S*-(4-Chlorobenzyl) 2-(4-methoxyphenyl)ethanethioate (6.4):**



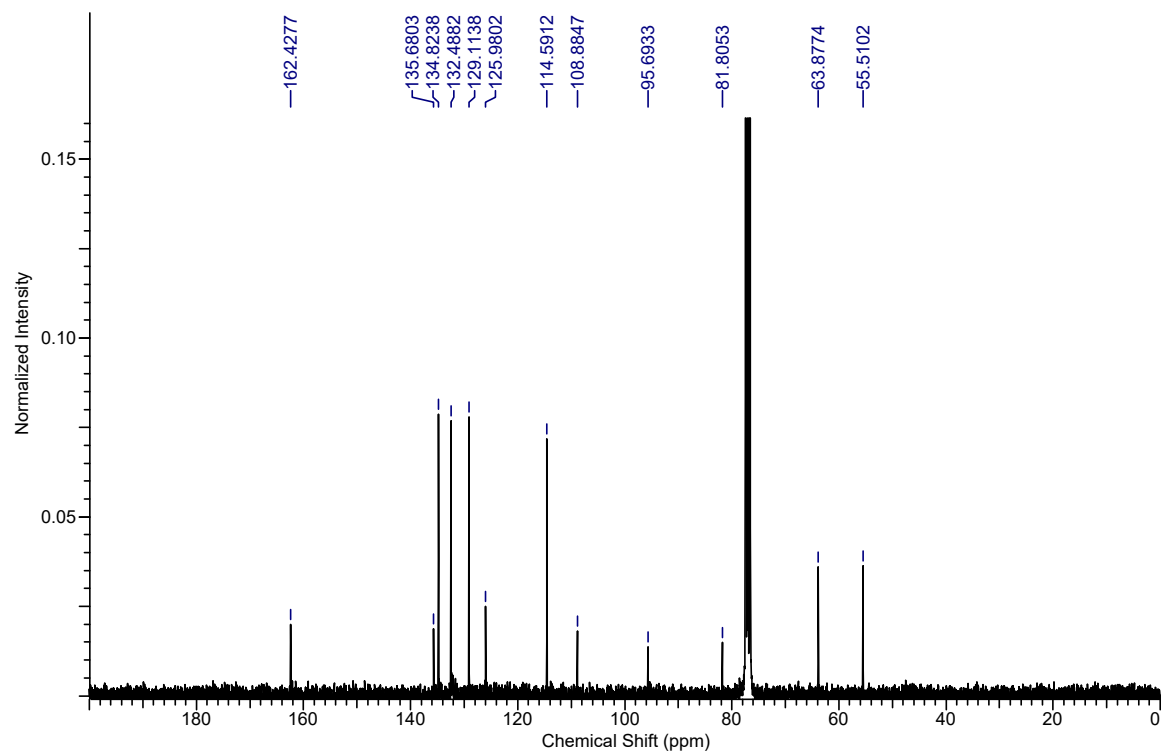
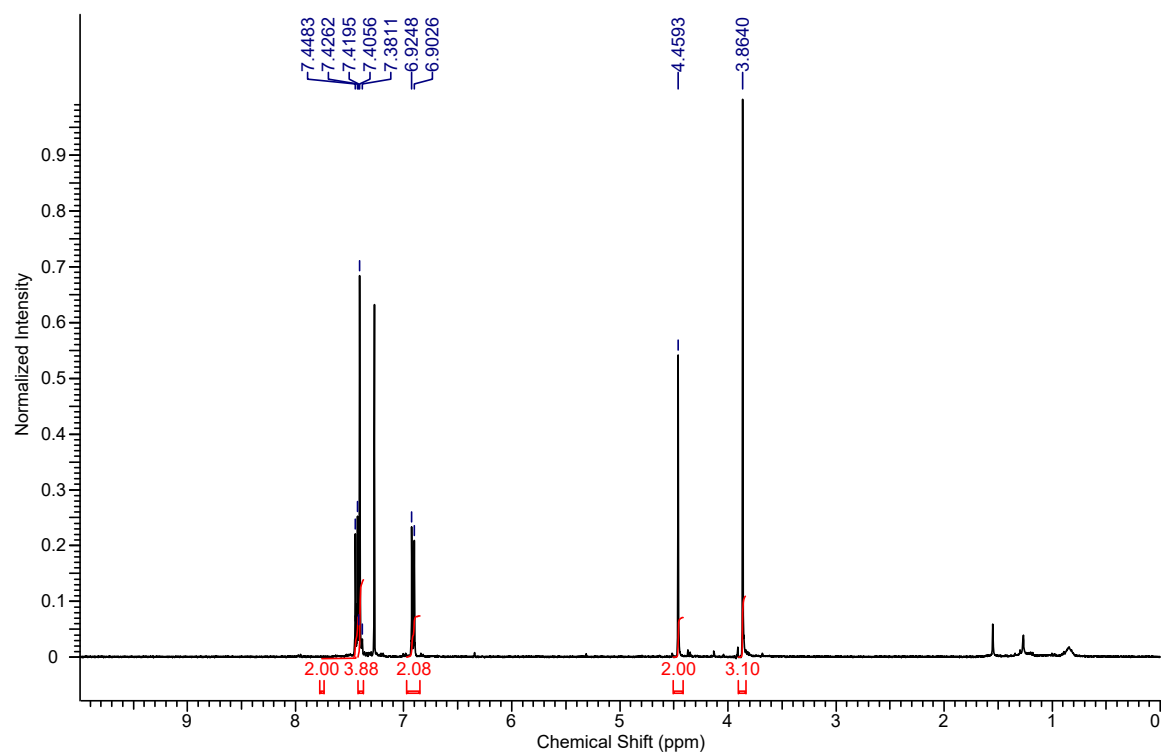
**(*E*)-(4-Chlorobenzyl)(4-methoxystyryl)sulfane (6.5):**



**1-Chloro-4-(((4-methoxyphenyl)ethynyl)sulfinyl)methyl)benzene (6.6):**

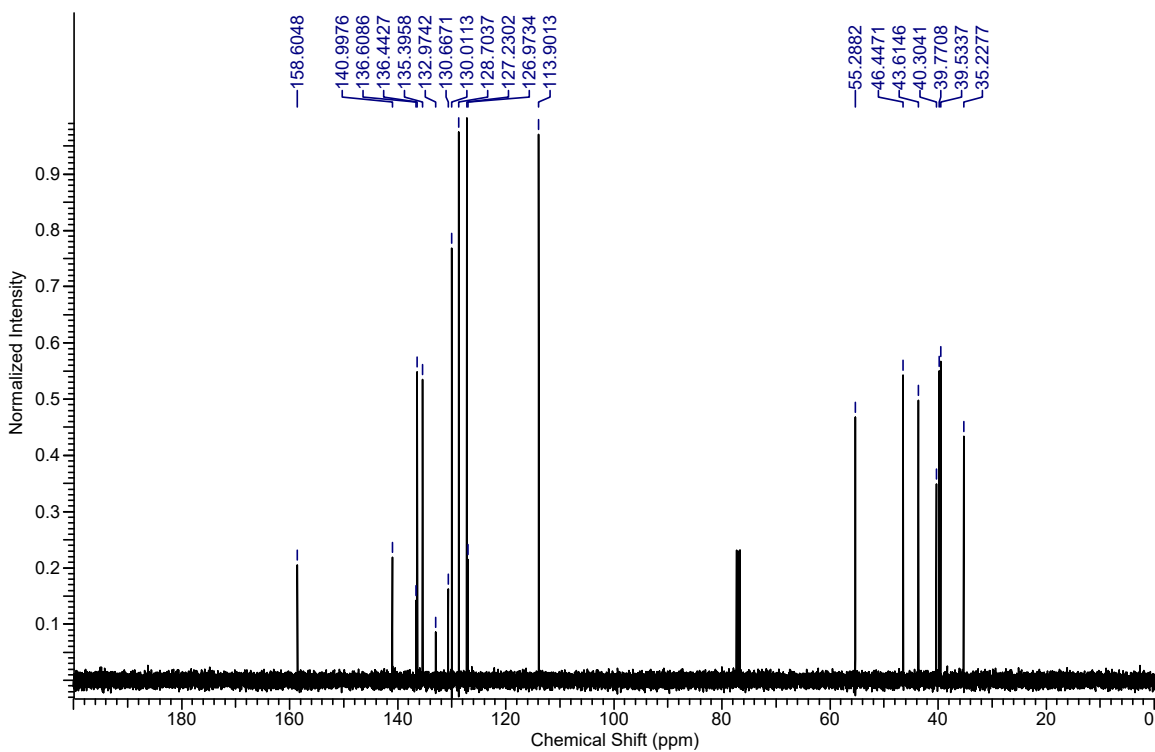
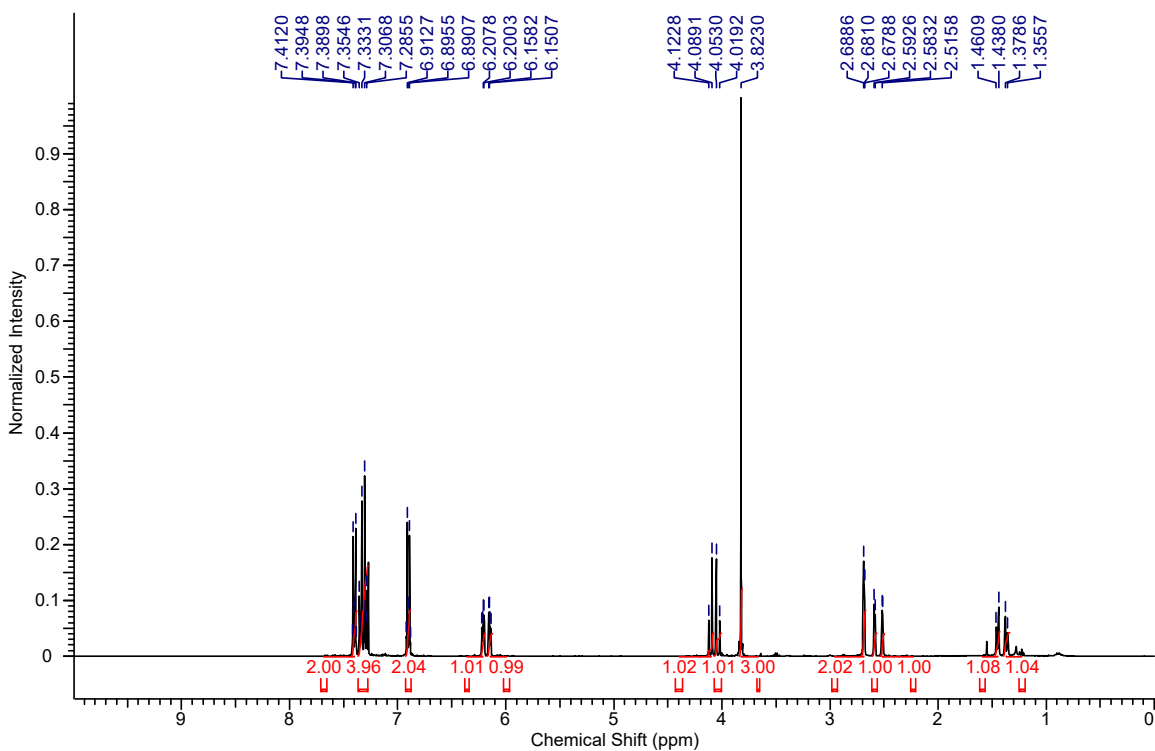


**1-Chloro-4-(((4-methoxyphenyl)ethynyl)sulfonyl)methyl)benzene (6.7):**

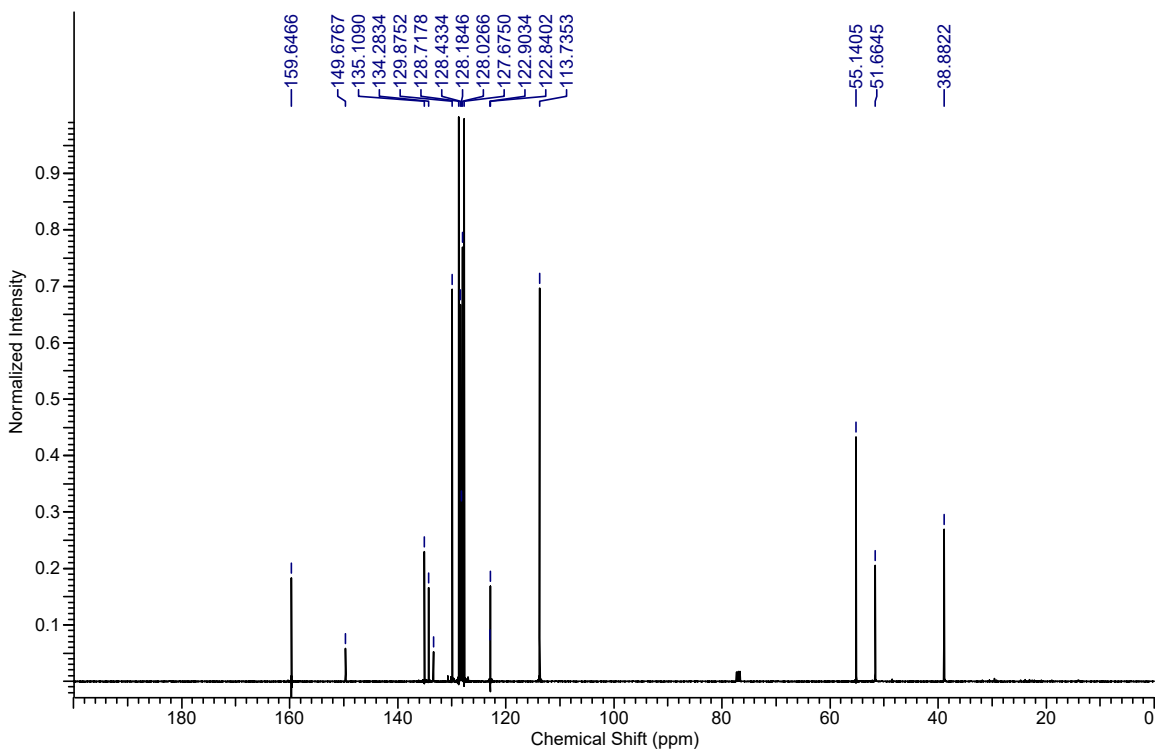
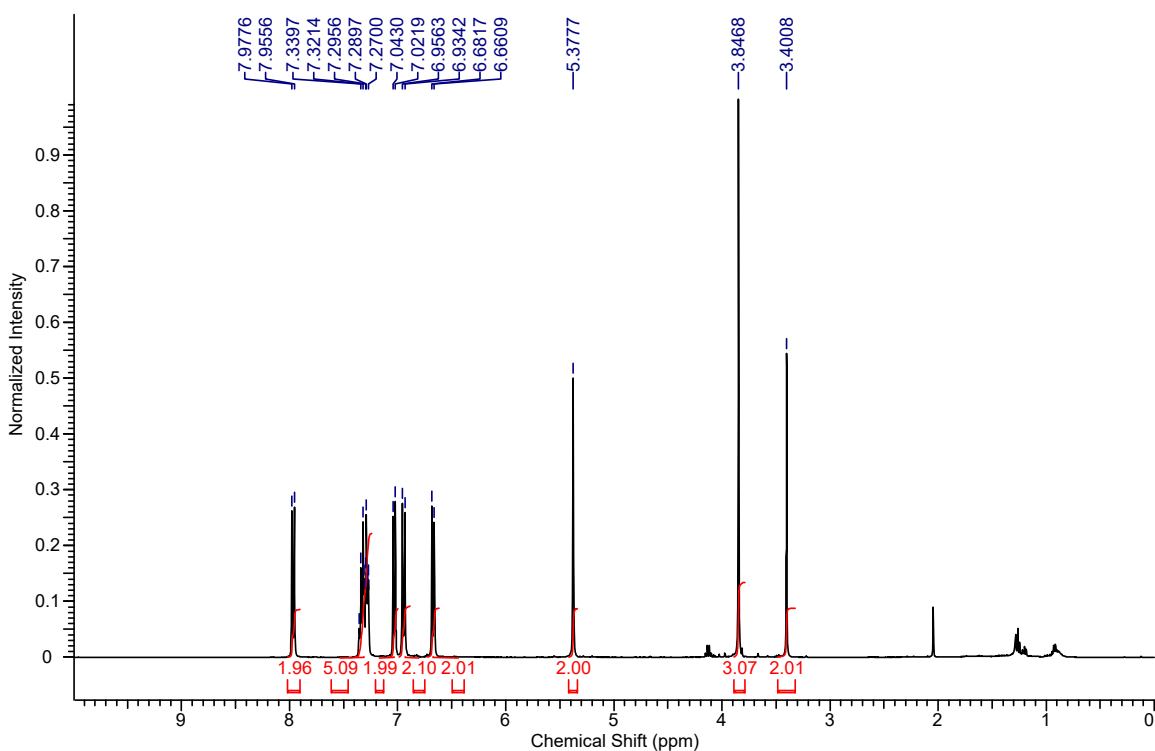




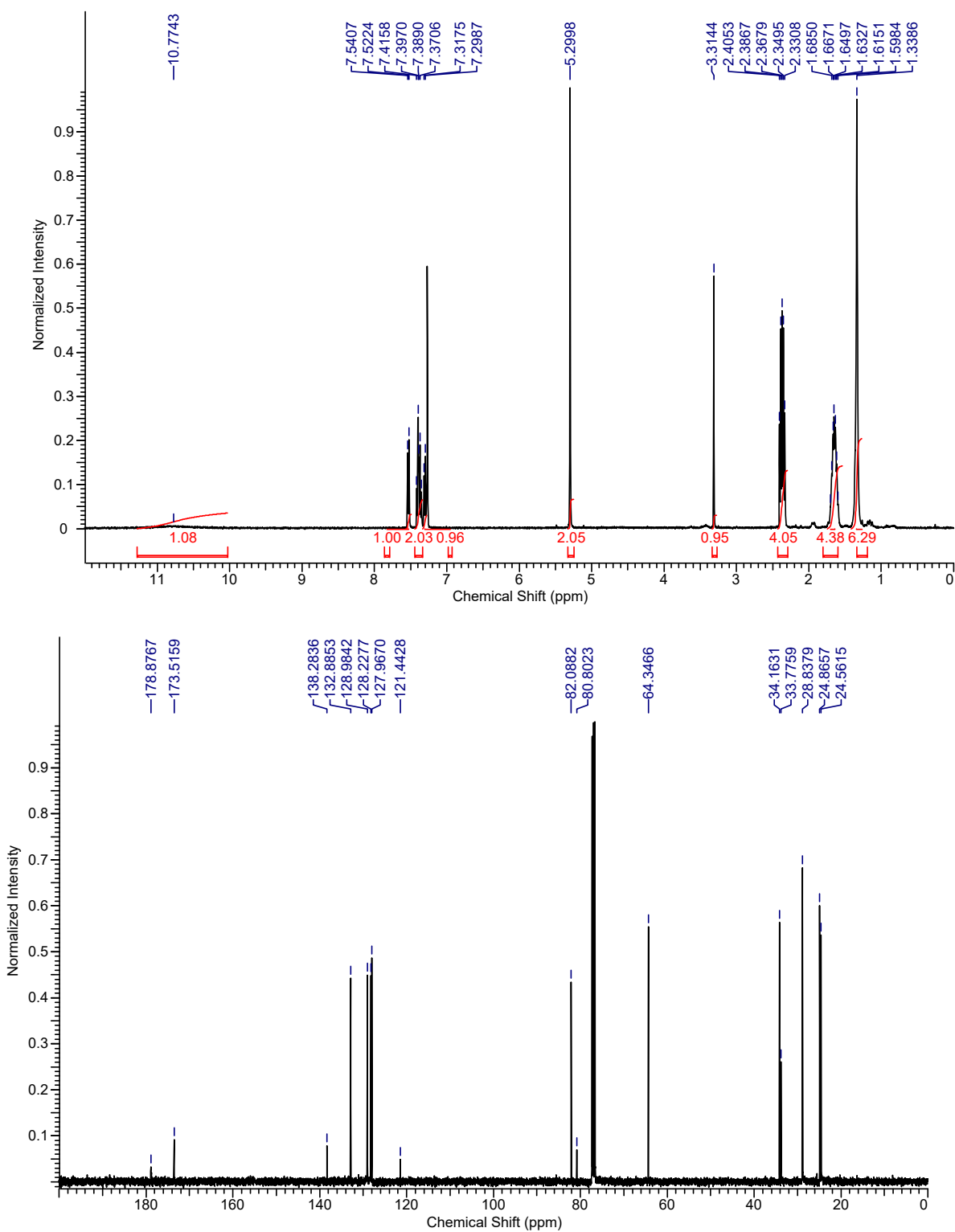
**(4-Chlorobenzyl)((1*S*,2*R*,5*S*,6*R*)-4-(4-methoxyphenyl)tricyclo[4.2.1.0<sup>2,5</sup>]nona-3,7-dien-3-yl)sulfane (6.8):**



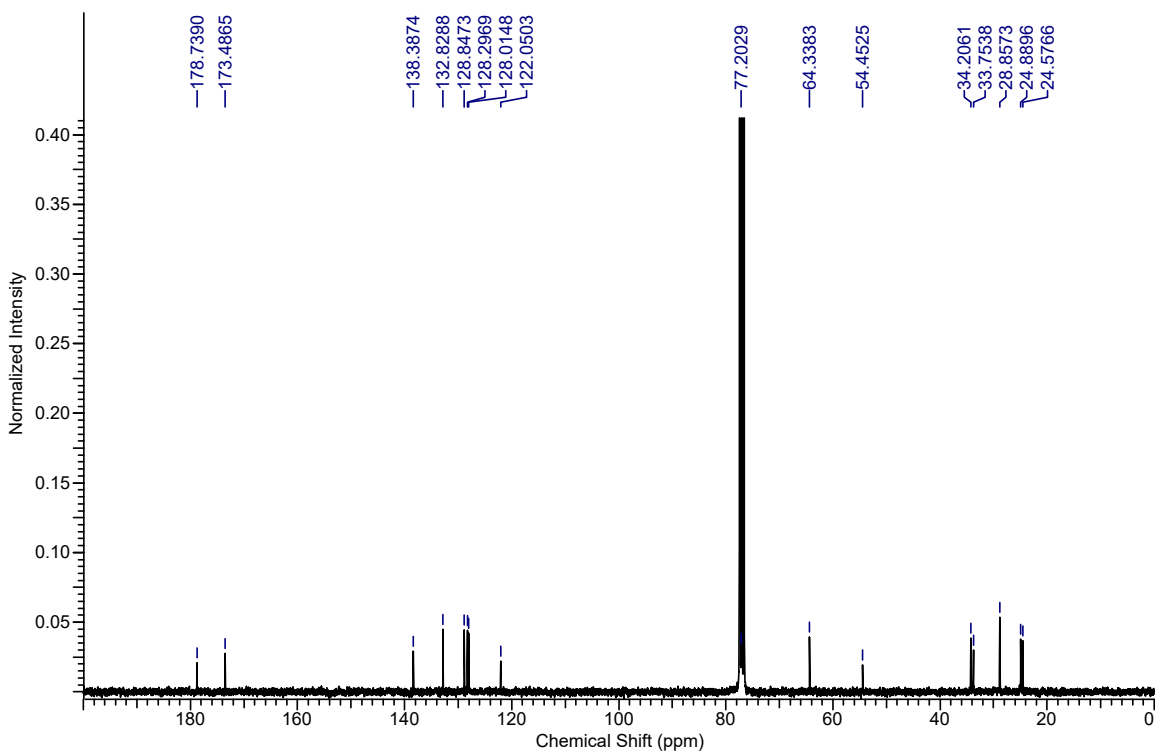
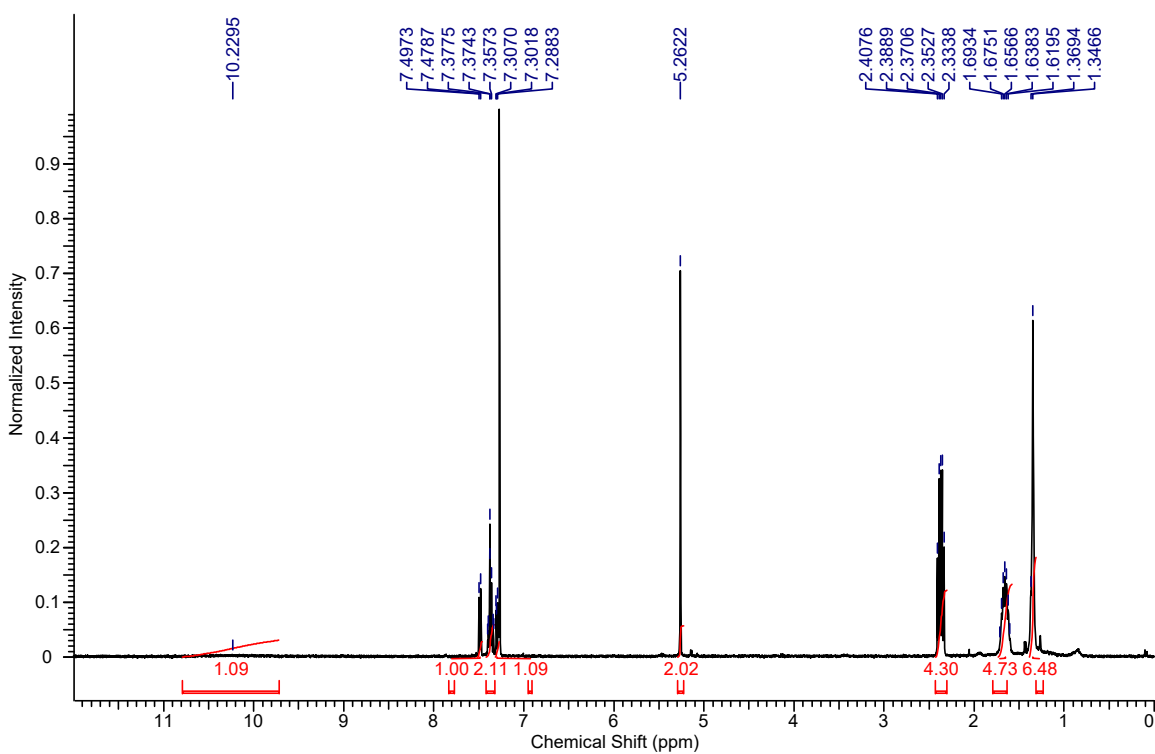
**1-Benzyl-5-((4-chlorobenzyl)thio)-4-(4-methoxyphenyl)-1*H*-1,2,3-triazole (6.9):**



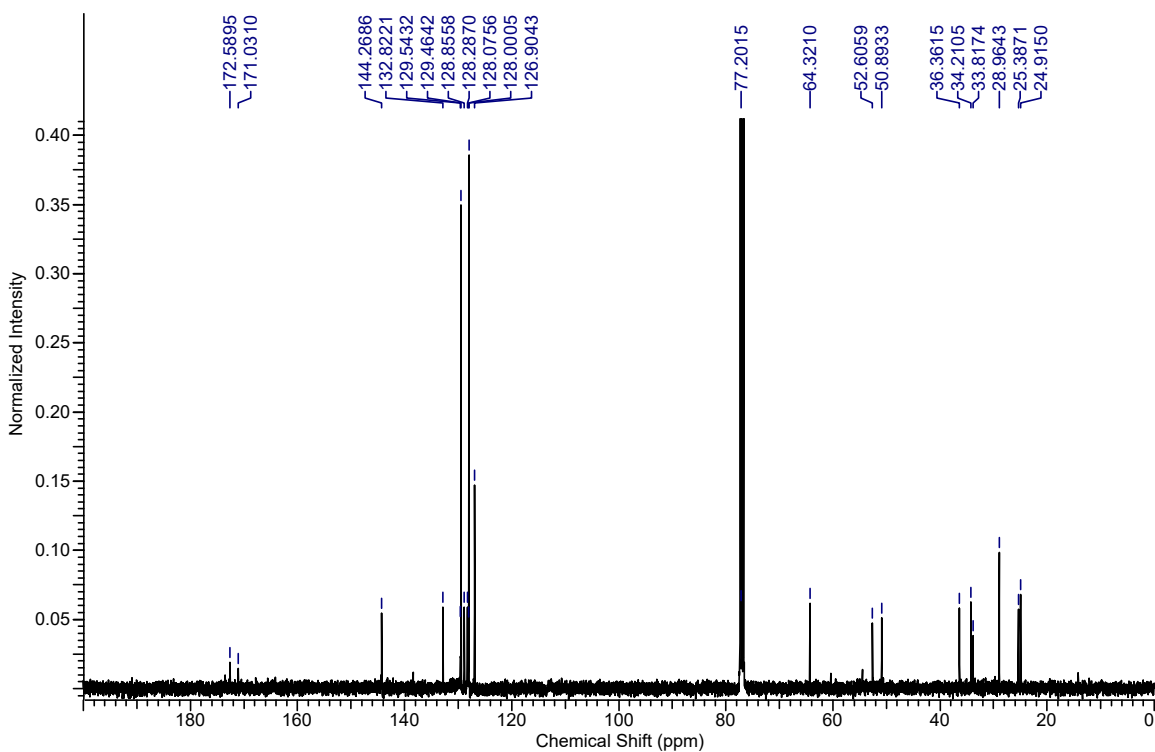
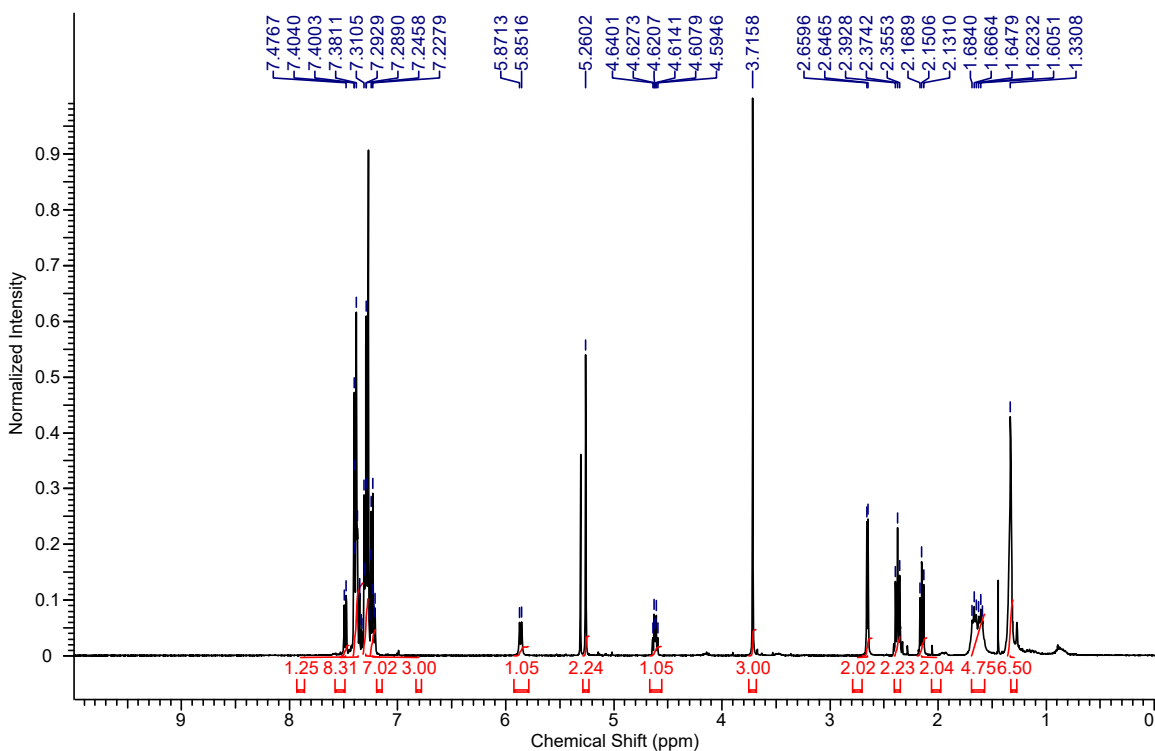
**9-((2-Ethynylbenzyl)oxy)-9-oxononanoic acid (10.13):**



**9-((2-(Bromoethynyl)benzyl)oxy)-9-oxononanoic acid (10.14):**

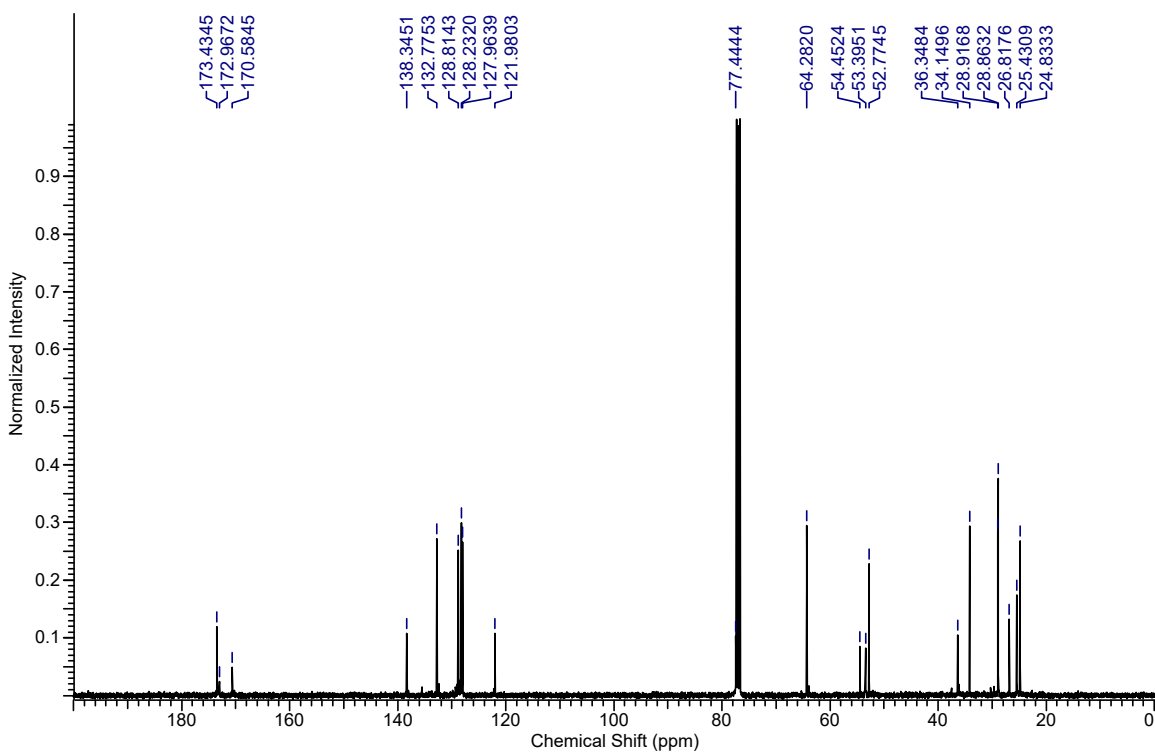
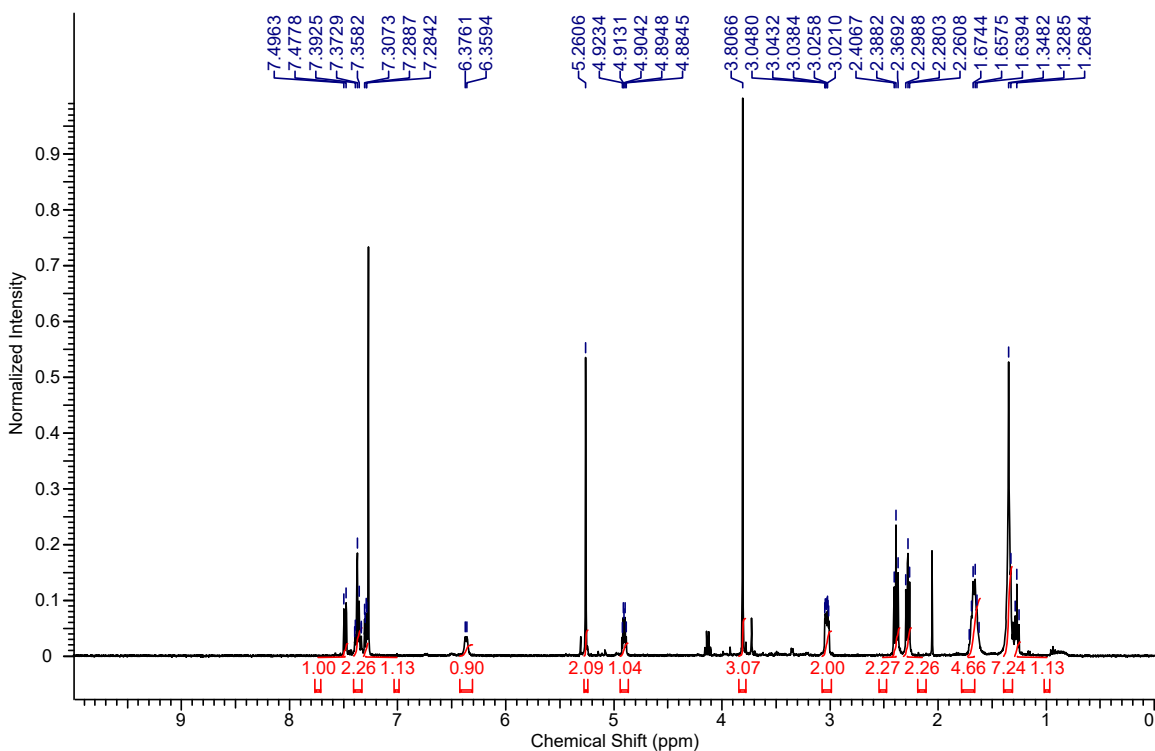


**2-(Bromoethynyl)benzyl (R)-9-((1-methoxy-1-oxo-3-(tritylthio)propan-2-yl)amino)-9-oxononanoate (10.15):**

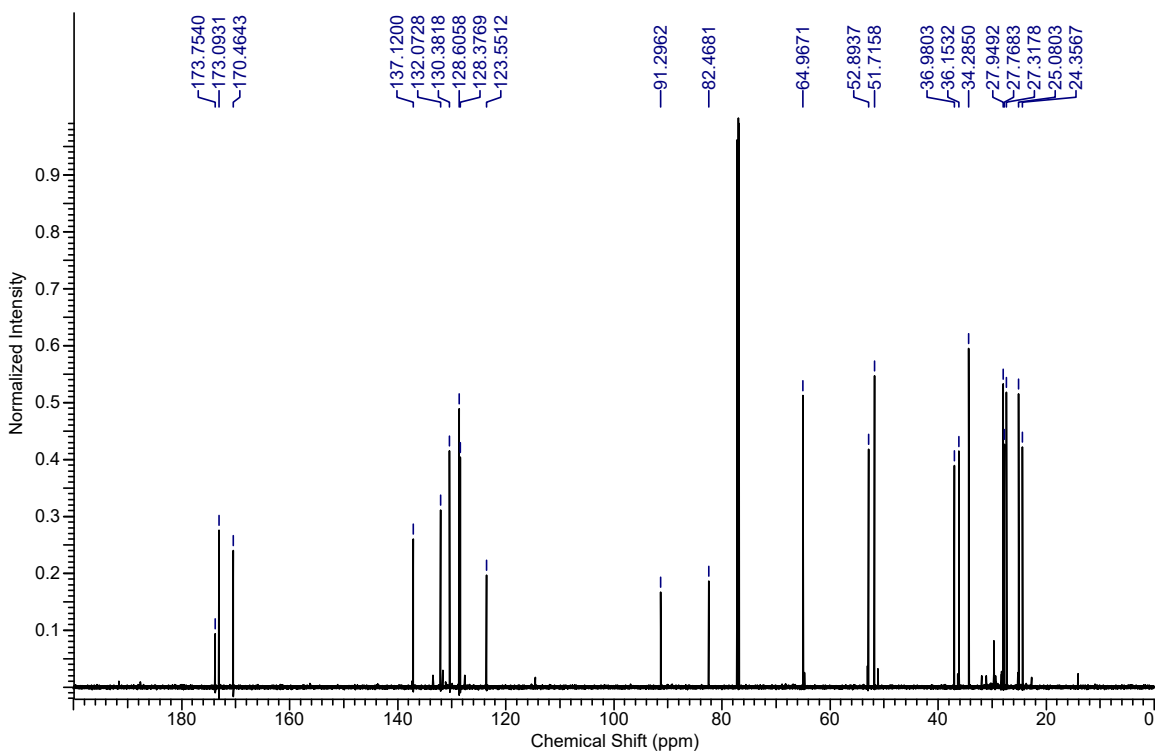
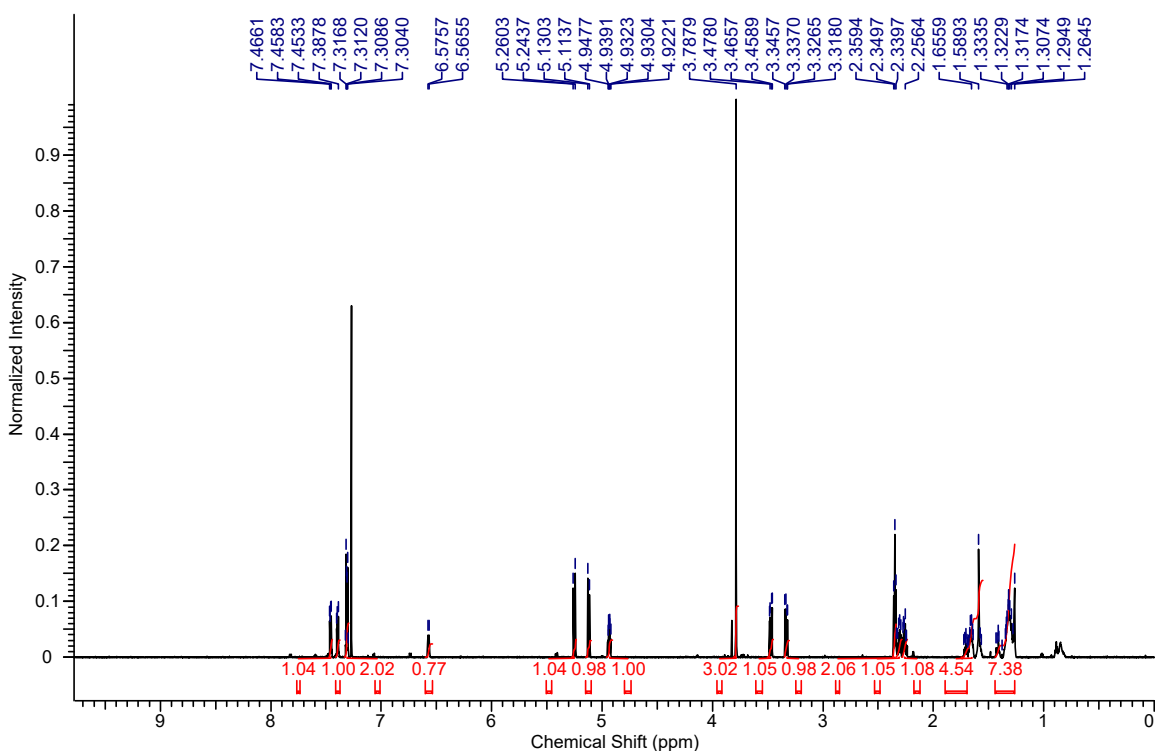


**2-(Bromoethynyl)benzyl  
oxononanoate (6.10):**

**(*R*)-9-((3-mercapto-1-methoxy-1-oxopropan-2-yl)amino)-9-**



# **Macrocycle (6.11):**



## 11. Supporting Information of Chapter 7

### 11.1 General

Reactions carried out under anhydrous conditions were performed under an inert argon or nitrogen atmosphere in glassware that had previously been dried overnight at 120 °C or flame dried and cooled under a stream of argon or nitrogen.<sup>29</sup> All chemical products were obtained from Sigma-Aldrich Chemical Company or Alfa Aesar, and were reagent quality. The following products were prepared according to their respective literature procedures: 1-ethynyl-2-nitrobenzene<sup>30</sup>, *tert*-butyl 4-ethynylisoindoline-2-carboxylate<sup>31</sup>, 1-(bromoethynyl)-4-methoxybenzene<sup>32</sup>, prop-2-yn-1-yl 4-methoxybenzoate<sup>33</sup>, (bromoethynyl)triisopropylsilane<sup>34</sup>, hex-5-yn-1-yl acetate<sup>35</sup>, ((hex-5-yn-1-yloxy)methyl)benzene<sup>36</sup>, hex-5-yn-1-yl 4-methylbenzenesulfonate<sup>37</sup> and hept-6-yne nitrile<sup>38</sup>. Technical solvents were obtained from VWR International Co. Anhydrous solvents (CH<sub>2</sub>Cl<sub>2</sub>, Et<sub>2</sub>O, THF, DMF, toluene, and *n*-hexane) were dried and deoxygenated using a GlassContour system (Irvine, CA). Isolated yields reflect the mass obtained following flash column silica gel chromatography. Organic compounds were purified using the method reported by W. C. Still<sup>39</sup> on silica gel obtained from Silicycle Chemical division (40-63 nm; 230-240 mesh). Analytical thin-layer chromatography (TLC) was performed on glass-backed silica gel 60 plates coated with a fluorescence indicator (Silicycle Chemical division, 0.25 mm, F<sub>254</sub>). Visualization of TLC plates was performed by UV (254 nm), KMnO<sub>4</sub> or *p*-anisaldehyde stains. All mixed solvent eluents are reported as v/v solutions. Concentration refers to removal of volatiles at low pressure on a rotary evaporator. All reported compounds were homogeneous by thin layer chromatography (TLC) and by <sup>1</sup>H NMR

---

<sup>29</sup> Shriver, D. F.; Drezdon, M. A. in *The Manipulation of Air-Sensitive Compounds*; Wiley-VCH: New York, 1986.

<sup>30</sup> Coffman, K. C.; Palazzo, T. A.; Hartley, T. P.; Fetting, J. C.; Tantillo, D. J.; Kurth, M. J. *Org. Lett.* **2013**, *15*, 2062-2065.

<sup>31</sup> Godin, É.; Bédard, A.-C.; Raymond, M.; Collins, S. K. *J. Org. Chem.* **2017**, *82*, 7576-7582.

<sup>32</sup> Santandrea, J.; Minozzi, C.; Cruché, C.; Collins, S. K. *Angew. Chem. Int. Ed.* **2017**, *56*, 12255-12259.

<sup>33</sup> Wu, X.-F.; Darcel, C. *Eur. J. Org. Chem.* **2009**, 1144-1147.

<sup>34</sup> Muriel, B.; Orce, U.; Waser, J. *Org. Lett.* **2017**, *19*, 3548-3551.

<sup>35</sup> Jameson, V. J. A.; Cochmé, H. M.; Logan, A.; Hanton, L. R.; Smith, R. A. J.; Murphy, M. P. *Tetrahedron* **2015**, *71* 8444-8453.

<sup>36</sup> Thiel, N. O.; Kemper, S.; Teichert, J. F. *Tetrahedron* **2017**, *73*, 5023-5028.

<sup>37</sup> Qian, Y.; Schürmann, M.; Janning, P.; Hedberg, C.; Waldmann, H. *Angew. Chem. Int. Ed.* **2016**, *55*, 7766-7771.

<sup>38</sup> Davison, E. C.; Fox, M. E.; Holmes, A. B.; Roughley, S. D.; Smith, C. J.; Williams, G. M.; Davies, J. E.; Rainthby, P. R.; Adams, J. P.; Forbes, I. T.; Press, N. J.; Thompson, M. J. *Eur. J. Org. Chem.* **2015**, 2498-2502.

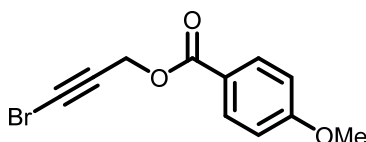
<sup>39</sup> Still, W. C.; Kahn, M.; Mitra, A. *J. Chem. Soc., Perkin Trans. 1* **2002**, 1494-1514.



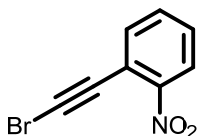
spectroscopy. NMR spectra were taken in deuterated  $\text{CDCl}_3$  using Bruker AV-300, AV-400 and AV-500 instruments unless otherwise noted. Signals of solvent served as internal standard ( $\text{CHCl}_3$ :  $\delta$  7.27 for  $^1\text{H}$ ,  $\delta$  77.0 for  $^{13}\text{C}$ ). The  $^1\text{H}$  NMR chemical shifts and coupling constants were determined assuming first-order behavior. Multiplicity is indicated by one or more of the following: s (singlet), d (doublet), t (triplet), q (quartet), m (multiplet), br (broad); the list of couplings constants ( $J$ ) corresponds to the order of the multiplicity assignment. High resolution mass spectrometry (HRMS) was done by the Centre régional de spectrométrie de masse at the Département de Chimie, Université de Montréal on an Agilent LC-MSD TOF system using ESI mode of ionization unless otherwise noted.

## 11.2 Synthesis of Precursors

**Procedure for Alkyne Bromination (A):** To a stirred solution of the aryl alkyne (1 equiv.) in acetone (0.2 M), *N*-bromosuccinimide (NBS, 1.2 equiv.) and AgNO<sub>3</sub> (20 mol%) were added at room temperature. The reaction mixture was stirred at room temperature for 15-60 minutes. Upon complete conversion of the starting material, the crude reaction mixture was concentrated under vacuum to provide a residue which was purified by column chromatography on silica-gel to afford the desired product.

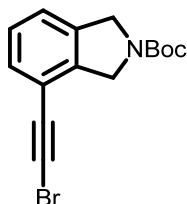


**3-Bromoprop-2-yn-1-yl 4-methoxybenzoate (7.2):** Following Procedure A, prop-2-yn-1-yl 4-methoxybenzoate (1.78 g, 9.36 mmol, 1.0 equiv.), NBS (2.00 g, 11.2 mmol, 1.2 equiv.) and AgNO<sub>3</sub> (0.318 g, 1.87 mmol, 20 mol%) were dissolved in acetone (47 mL) in a round bottom flask equipped with a stir bar. After purification by column chromatography on silica-gel (100 % hexanes → 5 % diethyl ether in hexanes), bromide **7.2** was obtained as a white solid (2.10 g, 83 % yield). <sup>1</sup>H NMR (400 MHz, CDCl<sub>3</sub>) δ = 8.03 (d, *J* = 9.0, 2H), 6.94 (d, *J* = 9.0 Hz, 2H), 4.92 (s, 2H), 3.88 (s, 3H); <sup>13</sup>C NMR (75 MHz, CDCl<sub>3</sub>) δ = 165.4, 163.7, 131.9, 121.7, 113.7, 74.4, 55.4, 53.0, 47.0; HRMS (ESI) *m/z* calculated for C<sub>11</sub>H<sub>9</sub>BrO<sub>3</sub> [M+H]<sup>+</sup> 268.9808; found 268.9806.

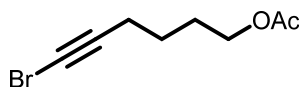


**1-(Bromoethynyl)-2-nitrobenzene (11.1):** Following Procedure A, 1-ethynyl-2-nitrobenzene (0.50 g, 3.40 mmol, 1.0 equiv.), NBS (0.726 g, 4.08 mmol, 1.2 equiv.) and AgNO<sub>3</sub> (0.116 g, 0.68 mmol, 20 mol%) were dissolved in acetone (17 mL) in a round bottom flask equipped with

a stir bar. After purification by column chromatography on silica-gel (100 % hexanes  $\rightarrow$  2.5 % diethyl ether in hexanes), bromide **11.1** was obtained as a yellow solid (0.548 g, 71 % yield). NMR data was in accordance with what was previously reported.<sup>40</sup>



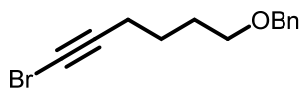
**tert-Butyl 4-(bromoethynyl)isoindoline-2-carboxylate (11.2):** Following Procedure A, *tert*-butyl 4-ethynylisoindoline-2-carboxylate (0.243 g, 1.00 mmol, 1.0 equiv.), NBS (0.214 g, 1.20 mmol, 1.2 equiv.) and AgNO<sub>3</sub> (0.034 g, 0.200 mmol, 20 mol%) were dissolved in acetone (10 mL) in a round bottom flask equipped with a stir bar. After purification by column chromatography on silica-gel (100 % hexanes  $\rightarrow$  10 % diethyl ether in hexanes), bromide **11.2** was obtained as a white solid (46 mg, 88 % yield). *Note that rotamers are formed and can result in complex splitting patterns in the <sup>1</sup>H NMR, or can cause doubling of some peaks in the <sup>13</sup>C NMR spectrum. For clarity, all peaks are reported.* <sup>1</sup>H NMR (400 MHz, CDCl<sub>3</sub>)  $\delta$  = 7.33-7.31 (m, 1H), 7.23-7.21 (m, 2H), 4.74-4.67 (m, 4H), 1.54-1.52 (m, 9H); <sup>13</sup>C NMR (75 MHz, CDCl<sub>3</sub>)  $\delta$  = 154.4, 154.3, 140.31, 140.27, 137.5, 137.2, 130.8, 130.4, 127.5, 123.1, 122.8, 117.8, 117.5, 79.9, 79.8, 54.0, 53.7, 52.6, 52.4, 52.0, 28.52, 28.47; HRMS (ESI) *m/z* calculated for C<sub>10</sub>H<sub>8</sub>BrN [M–Boc+H]<sup>+</sup> 223.9893; found 223.9884.



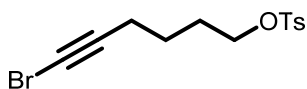
**6-Bromohex-5-yn-1-yl acetate (11.3):** Following Procedure A, hex-5-yn-1-yl acetate (0.701 g, 5.00 mmol, 1.0 equiv.), NBS (1.07 g, 6.00 mmol, 1.2 equiv.) and AgNO<sub>3</sub> (0.170 g, 1.00 mmol, 20 mol%) were dissolved in acetone (25 mL) in a round bottom flask equipped with a stir bar. After purification by column chromatography on silica-gel (100 % hexanes  $\rightarrow$  10 % diethyl

<sup>40</sup> Moodapelly, S. K.; Sharma, G. V. M.; Doddi, V. R. *Adv. Synth. Catal.* **2017**, 359, 1535-1540.

ether in hexanes), bromide **11.3** was obtained as a colorless liquid (0.728 g, 66 % yield).  $^1\text{H}$  NMR (400 MHz,  $\text{CDCl}_3$ )  $\delta$  = 4.08 (t,  $J$  = 6.4 Hz, 2H), 2.26 (t, 2H,  $J$  = 7.0 Hz, 2H), 2.05 (s, 3H), 1.78-1.71 (m, 2H), 1.63-1.56 (m, 2H);  $^{13}\text{C}$  NMR (75 MHz,  $\text{CDCl}_3$ )  $\delta$  = 171.1, 79.6, 63.8, 38.3, 27.7, 24.7, 20.9, 19.3; HRMS (APCI)  $m/z$  calculated for  $\text{C}_8\text{H}_{11}\text{BrO}_2$   $[\text{M}+\text{H}]^+$  219.0015; found 219.0013.

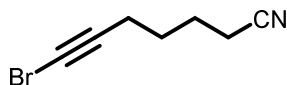


**(((6-Bromohex-5-yn-1-yl)oxy)methyl)benzene (11.4):** Following Procedure A, ((hex-5-yn-1-yl)oxy)methylbenzene (0.941 g, 5.00 mmol, 1.0 equiv.), NBS (1.07 g, 6.00 mmol, 1.2 equiv.) and  $\text{AgNO}_3$  (0.170 g, 1.00 mmol, 20 mol%) were dissolved in acetone (12 mL) in a round bottom flask equipped with a stir bar. After purification by column chromatography on silica-gel (100 % hexanes  $\rightarrow$  10 % diethyl ether in hexanes), bromide **11.4** was obtained as a colorless liquid (1.26 g, 94 % yield).  $^1\text{H}$  NMR (400 MHz,  $\text{CDCl}_3$ )  $\delta$  = 7.38-7.28 (m, 5H), 4.51 (s, 2H), 3.50 (t,  $J$  = 6.2 Hz, 2H), 2.25 (t,  $J$  = 7.0 Hz, 2H), 1.77-1.70 (m, 2H), 1.67-1.60 (m, 2H);  $^{13}\text{C}$  NMR (75 MHz,  $\text{CDCl}_3$ )  $\delta$  = 138.5, 128.3, 127.6, 127.5, 80.1, 72.9, 69.7, 37.9, 28.8, 25.0, 19.5; HRMS (ESI)  $m/z$  calculated for  $\text{C}_{13}\text{H}_{15}\text{BrO}$   $[\text{M}+\text{H}]^+$  267.0379; found 267.0387.

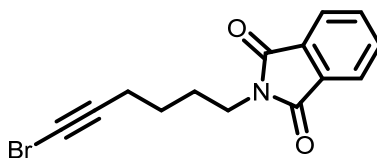


**6-Bromohex-5-yn-1-yl 4-methylbenzenesulfonate (11.5):** Following Procedure A, hex-5-yn-1-yl 4-methylbenzenesulfonate (1.26 mL, 5.00 mmol, 1.0 equiv.), NBS (1.07 g, 6.00 mmol, 1.2 equiv.) and  $\text{AgNO}_3$  (0.170 g, 1.00 mmol, 20 mol%) were dissolved in acetone (12 mL) in a round bottom flask equipped with a stir bar. After purification by column chromatography on silica-gel (100 % hexanes  $\rightarrow$  20 % diethyl ether in hexanes), bromide **11.5** was obtained as a white solid (1.56 g, 94 % yield).  $^1\text{H}$  NMR (400 MHz,  $\text{CDCl}_3$ )  $\delta$  = 7.80 (d,  $J$  = 8.3 Hz, 2H), 7.36 (d,  $J$  = 8.0 Hz, 2H), 4.06 (t,  $J$  = 6.2 Hz, 2H), 2.46 (s, 3H), 2.19 (t,  $J$  = 6.7 Hz, 2H), 1.79-1.73 (m, 2H), 1.59-1.52 (m, 2H);  $^{13}\text{C}$  NMR (75 MHz,  $\text{CDCl}_3$ )  $\delta$  = 144.7, 132.9, 129.8, 127.7, 79.1, 69.8,

38.5, 27.7, 24.0, 21.5, 18.9; HRMS (ESI)  $m/z$  calculated for  $C_{13}H_{15}BrO_3S [M+Na]^+$  352.9818; found 352.9821.

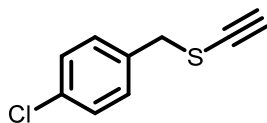


**7-Bromohept-6-ynenitrile (11.6):** Following Procedure A, hept-6-ynenitrile (0.165 g, 1.54 mmol, 1.0 equiv.), NBS (0.329 g, 1.85 mmol, 1.2 equiv.) and  $AgNO_3$  (0.052 g, 0.308 mmol, 20 mol%) were dissolved in acetone (8 mL) in a round bottom flask equipped with a stir bar. After purification by column chromatography on silica-gel (100 % hexanes  $\rightarrow$  15 % diethyl ether in hexanes), bromide **11.6** was obtained as a white solid (0.238 g, 83 % yield). NMR data was in accordance with what was previously reported.<sup>41</sup>

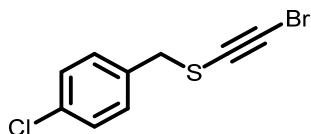


**2-(6-Bromohex-5-yn-1-yl)isoindoline-1,3-dione (11.7):** Following Procedure A, *N*-(5-hexynyl)phthalimide (1.14 g, 5.00 mmol, 1.0 equiv.), NBS (1.07 g, 6.00 mmol, 1.2 equiv.) and  $AgNO_3$  (0.170 g, 1.00 mmol, 20 mol%) were dissolved in acetone (25 mL) in a round bottom flask equipped with a stir bar. After purification by column chromatography on silica-gel (100 % hexanes  $\rightarrow$  20 % diethyl ether in hexanes), bromide **11.7** was obtained as a white solid (1.42 g, 93 % yield).  $^1H$  NMR (400 MHz,  $CDCl_3$ )  $\delta$  = 7.86-7.84 (m, 2H), 7.73-7.71 (m, 2H), 3.72 (t,  $J$  = 7.0 Hz, 2H), 2.28 (t,  $J$  = 7.0 Hz, 2H), 1.84-1.76 (m, 2H), 1.61-1.54 (m, 2H);  $^{13}C$  NMR (75 MHz,  $CDCl_3$ )  $\delta$  = 168.3, 133.9, 132.0, 123.2, 79.5, 38.3, 37.3, 27.6, 25.4, 19.2; HRMS (ESI)  $m/z$  calculated for  $C_{14}H_{12}BrNO_2 [M+H]^+$  306.0124; found 306.0126.

<sup>41</sup> Wang, Y.; Chen, C.; Zhang, S.; Lou, Z.; Su, X.; Wen, L.; Li, M. *Org. Lett.* **2013**, *15*, 4794-4797.



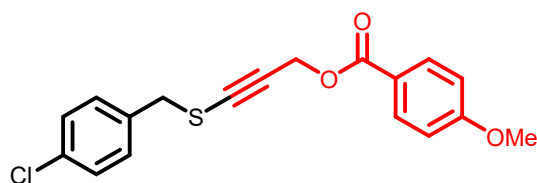
**(4-Chlorobenzyl)(ethynyl)sulfane (7.29):** (((4-chlorobenzyl)thio)ethynyl)triisopropyl-silane (0.076 g, 0.203 mmol, 1.0 equiv.) was solubilized in anhydrous tetrahydrofuran (2 mL) in a round bottom flask equipped with a stir bar, and the solution was cooled to 0 °C. A tetrabutylammonium fluoride (TBAF) solution (0.20 mL, 0.203 mmol, 1.0 equiv.) was then added dropwise to the reaction mixture under nitrogen. The reaction mixture was stirred at 0 °C for five minutes. After purification by column chromatography on silica-gel (100 % hexanes), alkyne **7.29** was obtained as a white solid (54 mg, 92 % yield). <sup>1</sup>H NMR (400 MHz, CDCl<sub>3</sub>) δ = 7.34-7.27 (m, 4H), 3.91 (s, 2H), 2.83 (s, 1H); <sup>13</sup>C NMR (75 MHz, CDCl<sub>3</sub>) δ = 135.0, 133.7, 130.3, 128.8, 83.8, 73.7, 38.9; HRMS (ESI) m/z calculated for C<sub>9</sub>H<sub>8</sub>ClS [M+H]<sup>+</sup> 183.0030; found 183.0033.



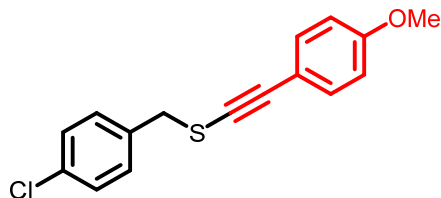
**(Bromoethynyl)(4-chlorobenzyl)sulfane (7.30):** Following Procedure A, (4-chlorobenzyl)(ethynyl)sulfane (0.043 mL, 0.236 mmol, 1.0 equiv.), NBS (0.051 g, 0.284 mmol, 1.2 equiv.) and AgNO<sub>3</sub> (0.008 g, 0.047 mmol, 20 mol%) were dissolved in acetone (1.2 mL) in a round bottom flask equipped with a stir bar. After purification by column chromatography on silica-gel (100 % hexanes), bromide **7.30** was obtained as a white solid (0.038 g, 61 % yield). <sup>1</sup>H NMR (400 MHz, CDCl<sub>3</sub>) δ = 7.35-7.24 (m, 4H), 3.91 (s, 2H); <sup>13</sup>C NMR (100 MHz, CDCl<sub>3</sub>) δ = 134.9, 133.8, 130.3, 128.8, 68.3, 52.4, 38.8; HRMS (ESI) m/z calculated for C<sub>9</sub>H<sub>6</sub>BrClS [M+H]<sup>+</sup> 260.9135; found 260.9128.

## 11.3 Synthesis of Alkynyl Sulfides

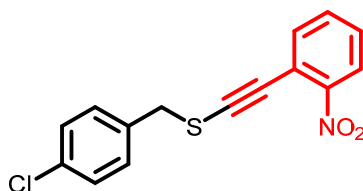
**Representative Procedure for the Cu-Catalyzed C(sp)-S Coupling:** A 118.5 mM solution of Cu(MeCN)<sub>4</sub>PF<sub>6</sub> (0.088 g, 0.237 mmol) in acetonitrile (2 mL) was prepared under nitrogen. The solution was sonicated under nitrogen until complete homogeneity. The bromoalkyne (0.237 mmol, 1.0 equiv.), the thiol (0.261 mmol, 1.1 equiv.), dtbbpy (0.013 g, 0.0474 mmol, 20 mol%) and 2,6-lutidine (0.055 mL, 0.474 mmol, 2.0 equiv.) were added to an 8 mL screw cap vial equipped with a stir bar. A septum was used to seal the vial and it was secured with parafilm. The vial was then purged with nitrogen for 2 minutes under vacuum. Afterwards, degassed acetonitrile (4.6 mL) was added to the vial under nitrogen. Once the vial was positioned onto a stir plate, the Cu(MeCN)<sub>4</sub>PF<sub>6</sub> solution (0.2 mL, 0.0237 mol, 10 mol%) was added in one portion. The reaction mixture was stirred for 10 minutes. Upon completion of the reaction (TLC), the reaction mixture was concentrated under vacuum to provide a residue which was purified by column chromatography on silica-gel.



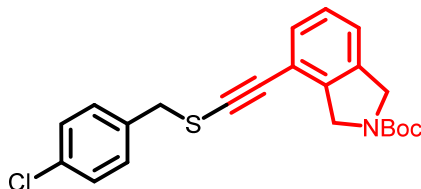
**3-((4-Chlorobenzyl)thio)prop-2-yn-1-yl 4-methoxybenzoate (7.3):** Following the representative procedure described above, the residue was purified by column chromatography on silica-gel (100 % hexanes → 10 % diethyl ether in hexanes) to afford alkynyl sulfide **7.3** as a colorless oil (74 mg, 90 % yield). <sup>1</sup>H NMR (400 MHz, CDCl<sub>3</sub>) δ = 8.02 (d, *J* = 9.0 Hz, 2H), 7.30-7.26 (m, 4H), 6.95 (d, *J* = 9.0 Hz, 2H), 4.97 (s, 2H), 3.89 (s, 2H), 3.88 (s, 3H); <sup>13</sup>C NMR (75 MHz, CDCl<sub>3</sub>) δ = 165.6, 163.6, 135.0, 133.7, 131.8, 130.4, 128.7, 121.9, 113.7, 90.7, 77.2, 55.4, 53.1, 39.2; HRMS (ESI) *m/z* calculated for C<sub>18</sub>H<sub>16</sub>ClO<sub>3</sub>S [M+H]<sup>+</sup> 347.0503; found 347.0512.



**(4-Chlorobenzyl)((4-methoxyphenyl)ethynyl)sulfane (7.6):** Following the representative procedure described above, the residue was purified by column chromatography on silica-gel (100 % hexanes  $\rightarrow$  2.5 % diethyl ether in hexanes) to afford alkynyl sulfide **7.6** as a white solid (72 mg, 96 % yield). NMR data was in accordance with what was previously reported.<sup>32</sup>



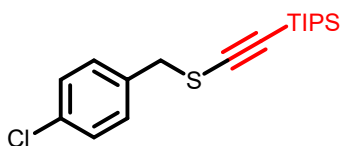
**(4-Chlorobenzyl)((2-nitrophenyl)ethynyl)sulfane (7.20):** Following the representative procedure described above, the residue was purified by column chromatography on silica-gel (100 % hexanes  $\rightarrow$  5 % diethyl ether in hexanes) to afford alkynyl sulfide **7.20** as an orange oil (71 mg, 98 % yield).  $^1\text{H}$  NMR (400 MHz,  $\text{CDCl}_3$ )  $\delta$  = 8.07 (d, 1H,  $J$  = 8.3 Hz), 7.55-7.51 (m, 1H), 7.45-7.32 (m, 6H), 4.06 (s, 2H);  $^{13}\text{C}$  NMR (75 MHz,  $\text{CDCl}_3$ )  $\delta$  = 148.1, 135.0, 133.8, 133.4, 132.9, 130.4, 128.8, 127.6, 124.7, 119.0, 91.9, 89.7, 39.8; HRMS (ESI)  $m/z$  calculated for  $\text{C}_{15}\text{H}_{11}\text{ClNO}_2\text{S}$   $[\text{M}+\text{H}]^+$  304.0194; found 304.0203.



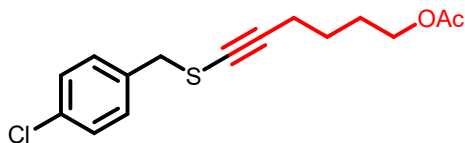
**tert-Butyl 4-(((4-chlorobenzyl)thio)ethynyl)isoindoline-2-carboxylate (7.21):** Following the representative procedure described above, the residue was purified by column chromatography on silica-gel (100 % hexanes  $\rightarrow$  10 % diethyl ether in hexanes) to afford alkynyl sulfide **7.21** as a white solid (93 mg, 98 % yield). *Note that rotamers are formed and can result in complex*



splitting patterns in the  $^1\text{H}$  NMR, or can cause doubling of some peaks in the  $^{13}\text{C}$  NMR spectrum. For clarity, all peaks are reported.  $^1\text{H}$  NMR (400 MHz,  $\text{CDCl}_3$ )  $\delta$  = 7.36-7.30 (m, 4H), 7.22-7.11 (m, 3H), 4.69-4.58 (m, 4H), 3.96 (s, 2H), 1.56-1.54 (m, 9H);  $^{13}\text{C}$  NMR (75 MHz,  $\text{CDCl}_3$ )  $\delta$  = 154.34, 154.27, 139.3, 139.1, 137.3, 137.0, 135.0, 134.9, 133.7, 130.3, 130.3, 130.0, 129.5, 128.8, 128.7, 127.43, 127.40, 122.5, 122.1, 118.2, 118.0, 92.1, 91.8, 83.2, 82.7, 79.8, 79.7, 52.6, 52.4, 52.2, 52.1, 39.7, 39.6, 28.5, 28.4; HRMS (ESI)  $m/z$  calculated for  $\text{C}_{22}\text{H}_{22}\text{ClINO}_2\text{SNa}$   $[\text{M}+\text{Na}]^+$  422.0952; found 422.0950.

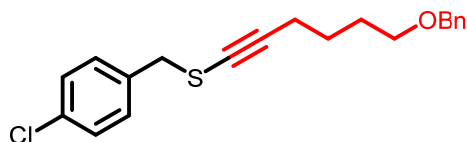


**(((4-Chlorobenzyl)thio)ethynyl)triisopropylsilane (7.23):** Following the representative procedure described above, the residue was purified by column chromatography on silica-gel (100 % hexanes) to afford alkynyl sulfide **7.23** as a colorless oil (74 mg, 93 % yield). NMR data was in accordance with what was previously reported.<sup>42</sup>

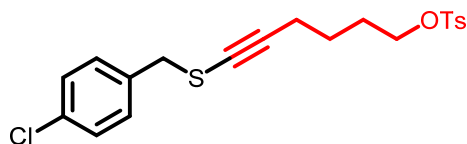


**6-((4-Chlorobenzyl)thio)hex-5-yn-1-yl acetate (7.24):** Following the representative procedure described above, the residue was purified by column chromatography on silica-gel (100 % hexanes  $\rightarrow$  10 % diethyl ether in hexanes) to afford alkynyl sulfide **7.24** as a colorless oil (49 mg, 70 % yield).  $^1\text{H}$  NMR (400 MHz,  $\text{CDCl}_3$ )  $\delta$  = 7.32-7.25 (m, 4H), 4.05 (t,  $J$  = 6.5 Hz, 2H), 3.84 (s, 2H), 2.31 (t,  $J$  = 6.9 Hz, 2H), 2.07 (s, 3H), 1.69-1.61 (m, 2H), 1.56-1.49 (m, 2H);  $^{13}\text{C}$  NMR (75 MHz,  $\text{CDCl}_3$ )  $\delta$  = 171.1, 135.5, 133.4, 130.3, 128.6, 95.5, 68.2, 63.8; 39.2, 27.6, 25.0, 21.0, 19.7; HRMS (ESI)  $m/z$  calculated for  $\text{C}_{15}\text{H}_{18}\text{ClO}_2\text{S}$   $[\text{M}+\text{H}]^+$  297.0711; found 297.0700.

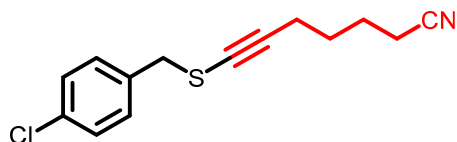
<sup>42</sup> Frei, R.; Waser, J. *J. Am. Chem. Soc.* **2013**, *135*, 9620-9623.



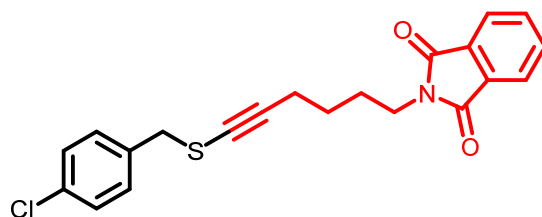
**(6-(Benzyloxy)hex-1-yn-1-yl)(4-chlorobenzyl)sulfane (7.25):** Following the representative procedure described above, the residue was purified by column chromatography on silica-gel (100 % hexanes  $\rightarrow$  10 % diethyl ether in hexanes) to afford alkynyl sulfide **7.25** as a colorless oil (56 mg, 68 % yield).  $^1\text{H}$  NMR (400 MHz,  $\text{CDCl}_3$ )  $\delta$  = 7.39-7.25 (m, 9H), 4.52 (s, 2H), 3.83 (s, 2H), 3.48 (t,  $J$  = 6.0 Hz, 2H), 2.31 (t,  $J$  = 7.0 Hz, 2H), 1.70-1.54 (m, 4H);  $^{13}\text{C}$  NMR (75 MHz,  $\text{CDCl}_3$ )  $\delta$  = 138.5, 135.6, 133.4, 130.3, 128.6, 128.3, 127.6, 127.5, 96.1, 72.9, 69.7, 67.8, 39.2, 28.8, 25.4, 19.9; HRMS (ESI)  $m/z$  calculated for  $\text{C}_{20}\text{H}_{22}\text{ClOS}$   $[\text{M}+\text{H}]^+$  345.1074; found 345.1077.



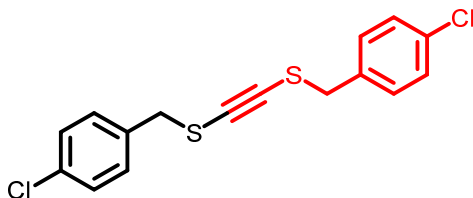
**6-((4-Chlorobenzyl)thio)hex-5-yn-1-yl 4-methylbenzenesulfonate (7.26):** Following the representative procedure described above, the residue was purified by column chromatography on silica-gel (100 % hexanes  $\rightarrow$  20 % diethyl ether in hexanes) to afford alkynyl sulfide **7.26** as a colorless oil (70 mg, 72 % yield).  $^1\text{H}$  NMR (400 MHz,  $\text{CDCl}_3$ )  $\delta$  = 7.79 (d,  $J$  = 8.3 Hz, 2H), 7.35 (d,  $J$  = 8.2 Hz, 2H), 7.29-7.22 (m, 4H), 4.01 (t,  $J$  = 6.2 Hz, 2H), 3.81 (s, 2H), 2.45 (s, 3H), 2.24 (t,  $J$  = 6.9 Hz, 2H), 1.69-1.61 (m, 2H), 1.52-1.43 (m, 2H);  $^{13}\text{C}$  NMR (75 MHz,  $\text{CDCl}_3$ )  $\delta$  = 144.7, 135.5, 133.4, 133.0, 130.3, 129.8, 128.6, 127.8, 95.1, 69.9, 68.5, 39.1, 27.7, 24.4, 21.6, 19.3; HRMS (ESI)  $m/z$  calculated for  $\text{C}_{20}\text{H}_{22}\text{ClO}_3\text{S}_2$   $[\text{M}+\text{H}]^+$  409.0693; found 409.0703.



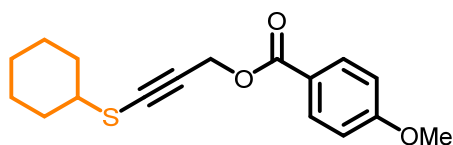
**7-((4-Chlorobenzyl)thio)hept-6-ynenitrile (7.27):** Following the representative procedure described above, the residue was purified by column chromatography on silica-gel (100 % hexanes → 20 % diethyl ether in hexanes) to afford alkynyl sulfide **7.27** as a colorless oil (50 mg, 79 % yield).  $^1\text{H}$  NMR (400 MHz,  $\text{CDCl}_3$ )  $\delta$  = 7.33-7.25 (m, 4H), 3.84 (s, 2H), 2.34-2.31 (m, 4H), 1.69-1.56 (m, 4H);  $^{13}\text{C}$  NMR (75 MHz,  $\text{CDCl}_3$ )  $\delta$  = 135.4, 133.4, 130.3, 128.6, 119.3, 94.6, 68.9, 39.1, 27.2, 24.2, 19.3, 16.7; HRMS (ESI)  $m/z$  calculated for  $\text{C}_{14}\text{H}_{15}\text{ClNS}$   $[\text{M}+\text{H}]^+$  264.0608; found 264.0605.



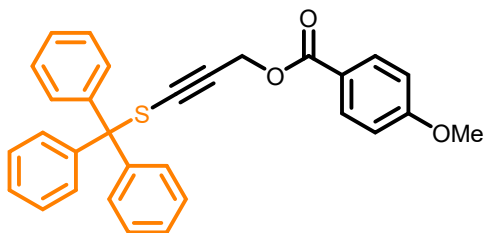
**2-((6-((4-Chlorobenzyl)thio)hex-5-yn-1-yl)isoindoline-1,3-dione (7.28):** Following the representative procedure described above, the residue was purified by column chromatography on silica-gel (100 % hexanes → 20 % diethyl ether in hexanes) to afford alkynyl sulfide **7.28** as a colorless oil (50 mg, 55 % yield).  $^1\text{H}$  NMR (400 MHz,  $\text{CDCl}_3$ )  $\delta$  = 7.86-7.82 (m, 2H), 7.73-7.70 (m, 2H), 7.29-7.23 (m, 2H), 3.82 (s, 2H), 3.70-3.66 (m, 2H), 2.32 (t,  $J$  = 7.0 Hz, 2H), 1.76-1.69 (m, 2H), 1.54-1.47 (m, 2H);  $^{13}\text{C}$  NMR (75 MHz,  $\text{CDCl}_3$ )  $\delta$  = 168.3, 135.9, 133.9, 133.3, 132.0, 130.3, 128.6, 123.1, 95.4, 68.3, 39.2, 37.3, 27.6, 25.8, 19.6; HRMS (ESI)  $m/z$  calculated for  $\text{C}_{21}\text{H}_{19}\text{ClNO}_2\text{S}$   $[\text{M}+\text{H}]^+$  384.0820; found 384.0818.



**1,2-Bis((4-chlorobenzyl)thio)ethyne (7.31):** Following the representative procedure described above, the residue was purified by column chromatography on silica-gel (100 % hexanes → 1 % diethyl ether in hexanes) to afford alkynyl sulfide **7.31** as a white solid (33 mg, 92 % yield).  $^1\text{H}$  NMR (400 MHz,  $\text{CDCl}_3$ )  $\delta$  = 7.30 (d,  $J$  = 8.4 Hz, 4H), 7.17 (d,  $J$  = 8.4 Hz, 4H), 3.78 (s, 4H);  $^{13}\text{C}$  NMR (100 MHz,  $\text{CDCl}_3$ )  $\delta$  = 135.0, 130.6, 130.4, 128.7, 87.9, 40.5; HRMS (ESI)  $m/z$  calculated for  $\text{C}_{16}\text{H}_{13}\text{Cl}_2\text{S}_2$   $[\text{M}+\text{H}]^+$  338.9830; found 338.9818.



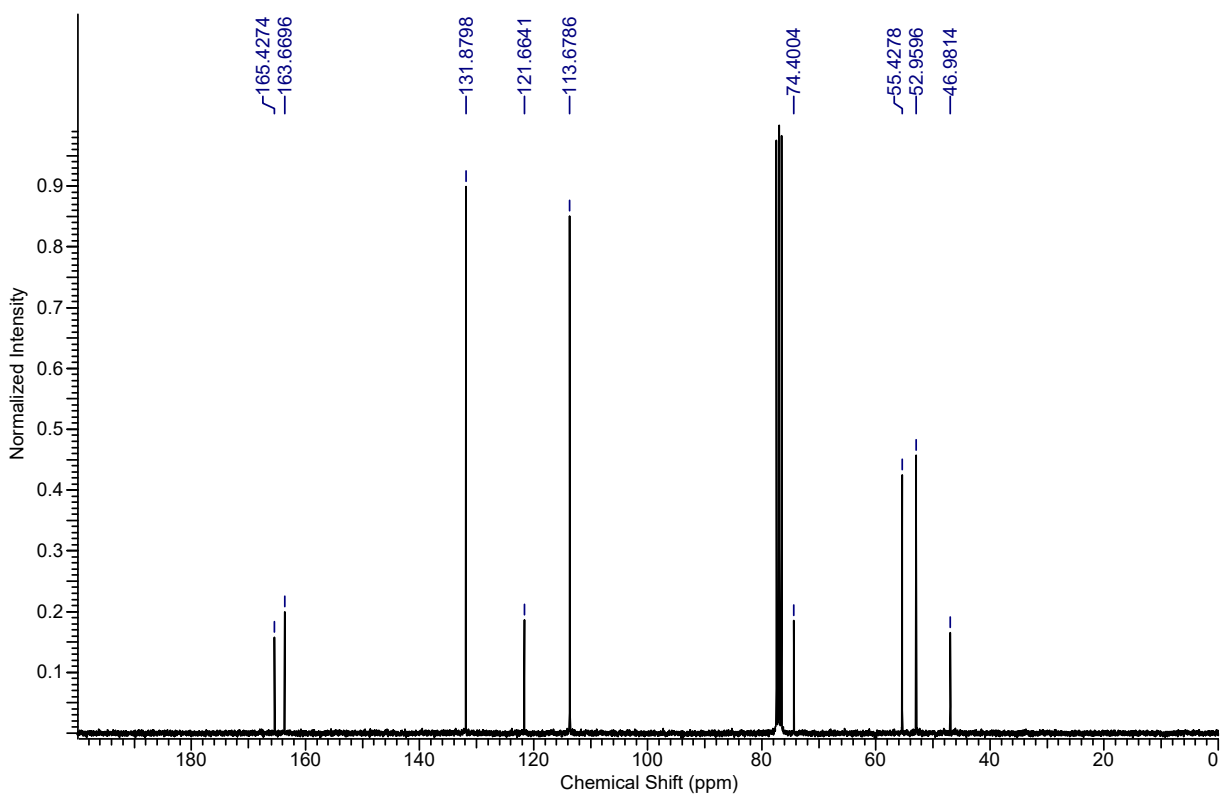
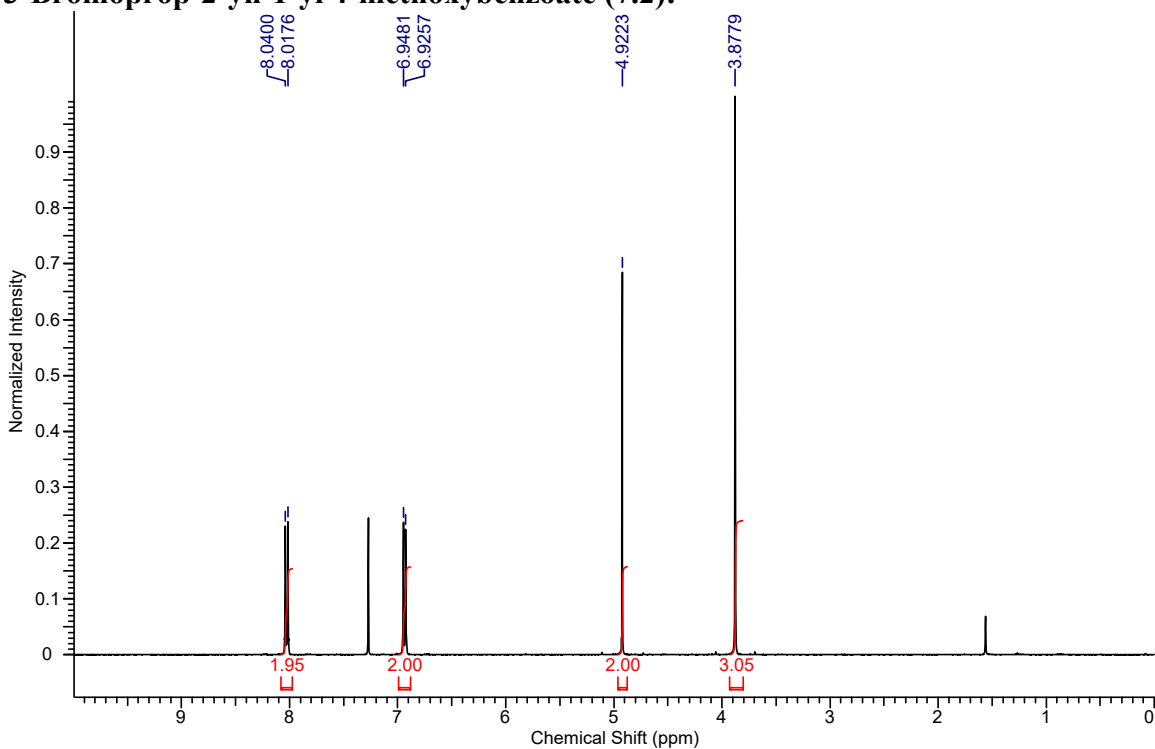
**3-(Cyclohexylthio)prop-2-yn-1-yl 4-methoxybenzoate (7.32):** Following the representative procedure described above, the residue was purified by column chromatography on silica-gel (100 % hexanes → 10 % diethyl ether in hexanes) to afford alkynyl sulfide **7.32** as a colorless oil (59 mg, 82 % yield).  $^1\text{H}$  NMR (400 MHz,  $\text{CDCl}_3$ )  $\delta$  = 8.02 (d,  $J$  = 9.0 Hz, 2H), 6.92 (d,  $J$  = 8.9 Hz, 2H), 5.03 (s, 2H), 3.86 (s, 3H), 2.97-2.90 (m, 1H), 2.07-2.03 (m, 2H), 1.82-1.78 (m, 2H), 1.64-1.60 (m, 1H), 1.54-1.26 (m, 5H);  $^{13}\text{C}$  NMR (75 MHz,  $\text{CDCl}_3$ )  $\delta$  = 165.6, 163.6, 131.9, 131.8, 122.1, 113.7, 113.6, 89.8, 77.2, 55.4, 53.5, 47.3, 32.9, 26.0, 25.4; HRMS (ESI)  $m/z$  calculated for  $\text{C}_{17}\text{H}_{21}\text{O}_3\text{S}$   $[\text{M}+\text{H}]^+$  305.1206; found 305.1219.



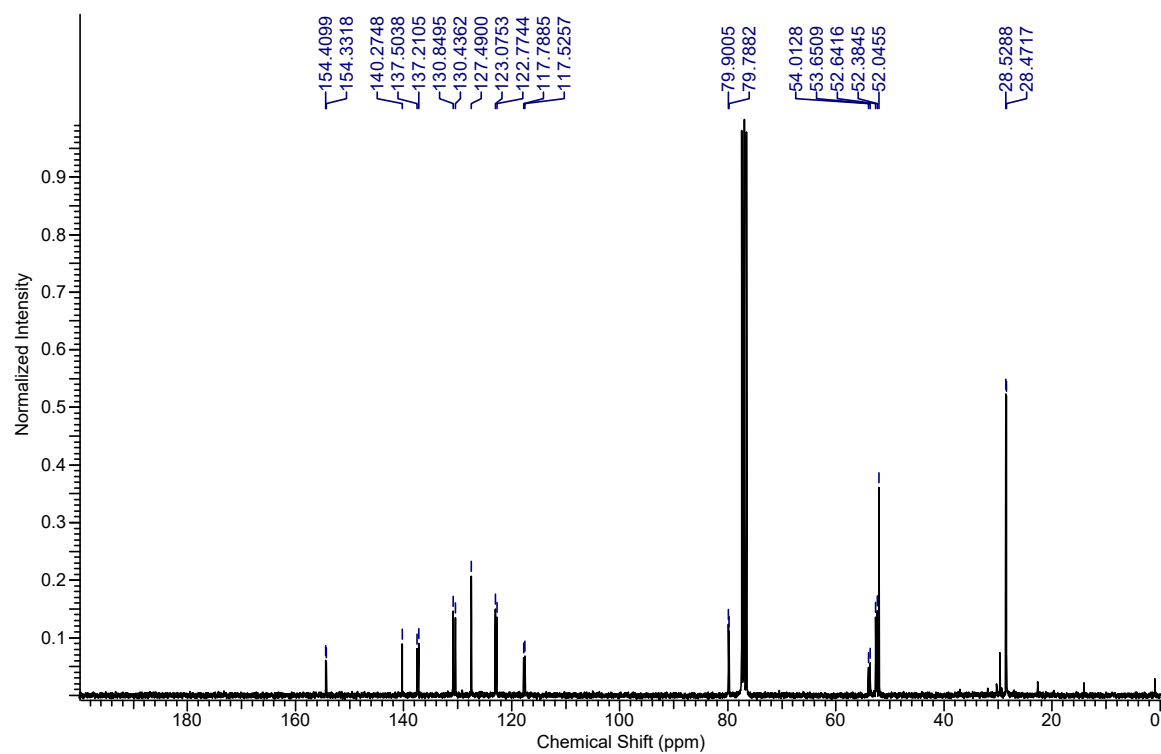
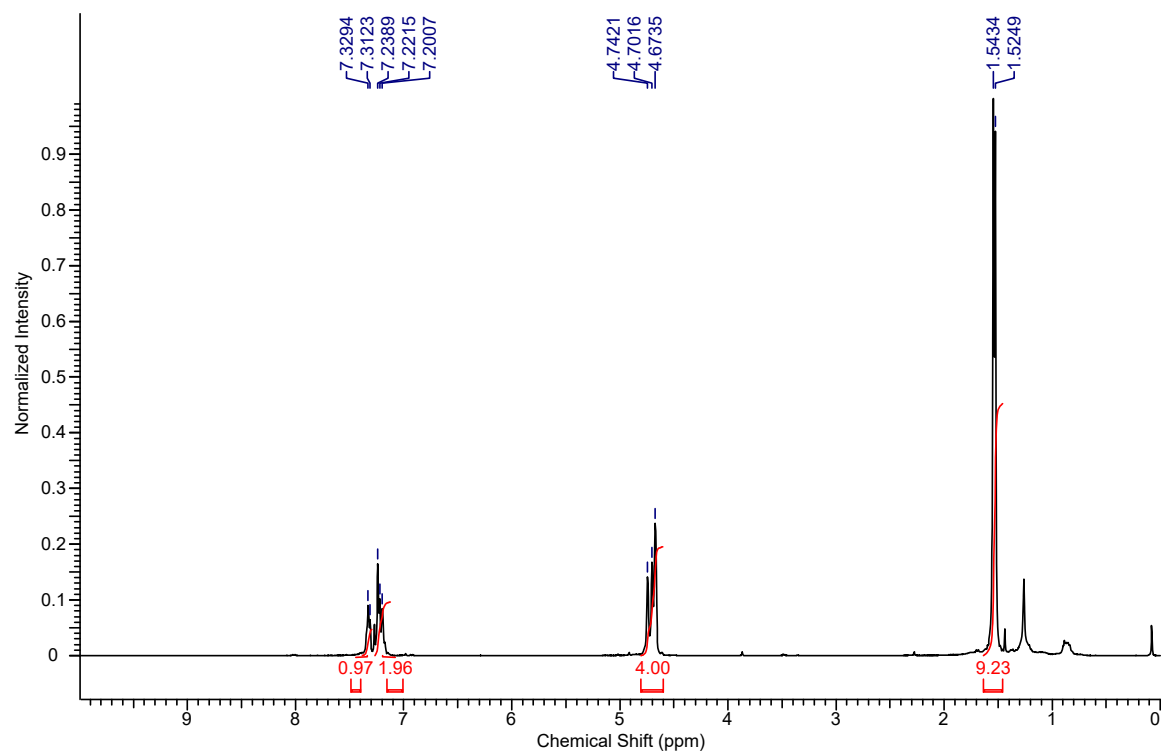
**3-(Tritylthio)prop-2-yn-1-yl 4-methoxybenzoate (7.33):** Following the representative procedure described above, the residue was purified by column chromatography on silica-gel (100 % hexanes  $\rightarrow$  10 % diethyl ether in hexanes) to afford alkynyl sulfide **7.33** as a white solid (89 mg, 80 % yield).  $^1\text{H}$  NMR (400 MHz,  $\text{CDCl}_3$ )  $\delta$  = 7.96 (d,  $J$  = 8.8 Hz, 2H), 7.35-7.25 (m, 15H), 6.95 (d,  $J$  = 8.8 Hz, 2H), 4.77 (s, 2H), 3.89 (s, 3H);  $^{13}\text{C}$  NMR (75 MHz,  $\text{CDCl}_3$ )  $\delta$  = 165.4, 163.5, 143.7, 131.8, 129.8, 127.89, 127.85, 127.3, 122.0, 113.6, 93.5, 79.3, 71.6, 55.4, 53.2; HRMS (ESI)  $m/z$  calculated for  $\text{C}_{30}\text{H}_{25}\text{O}_3\text{S}$   $[\text{M}+\text{H}]^+$  465.1519; found 465.1513.

## 11.4 NMR Data for all New Compounds

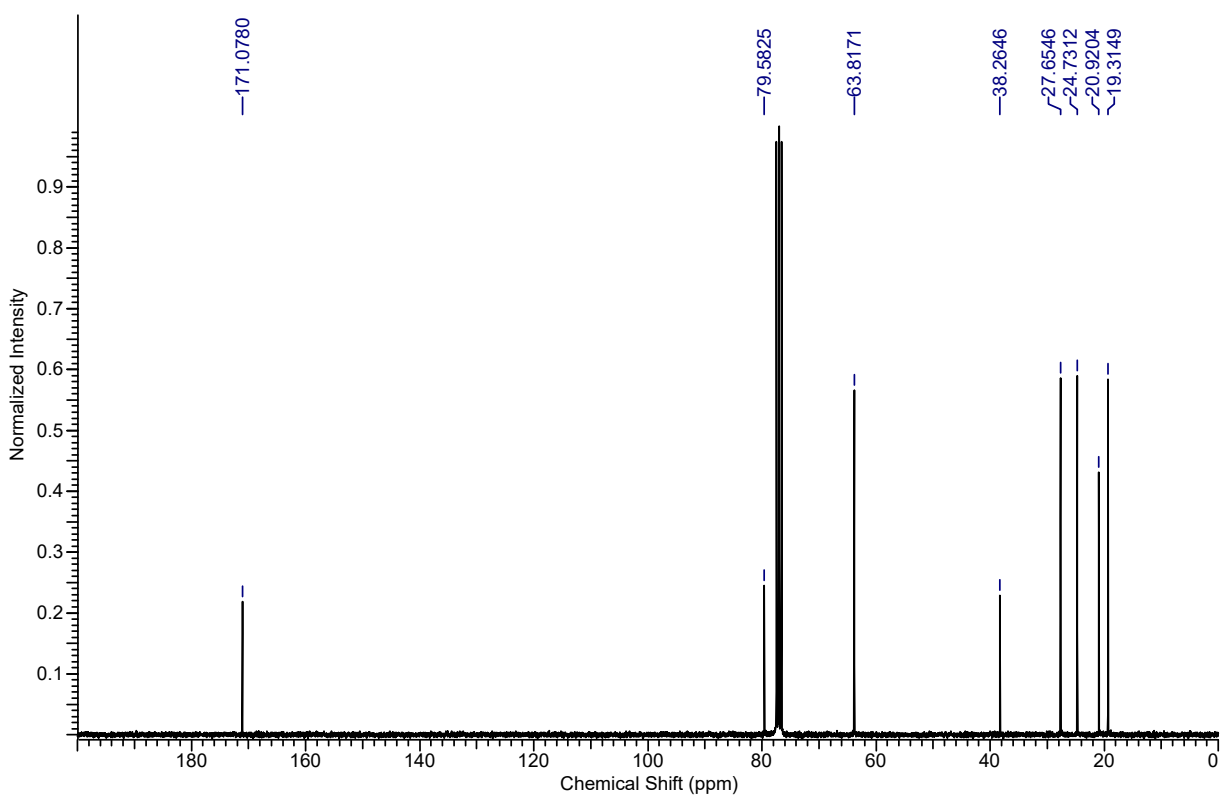
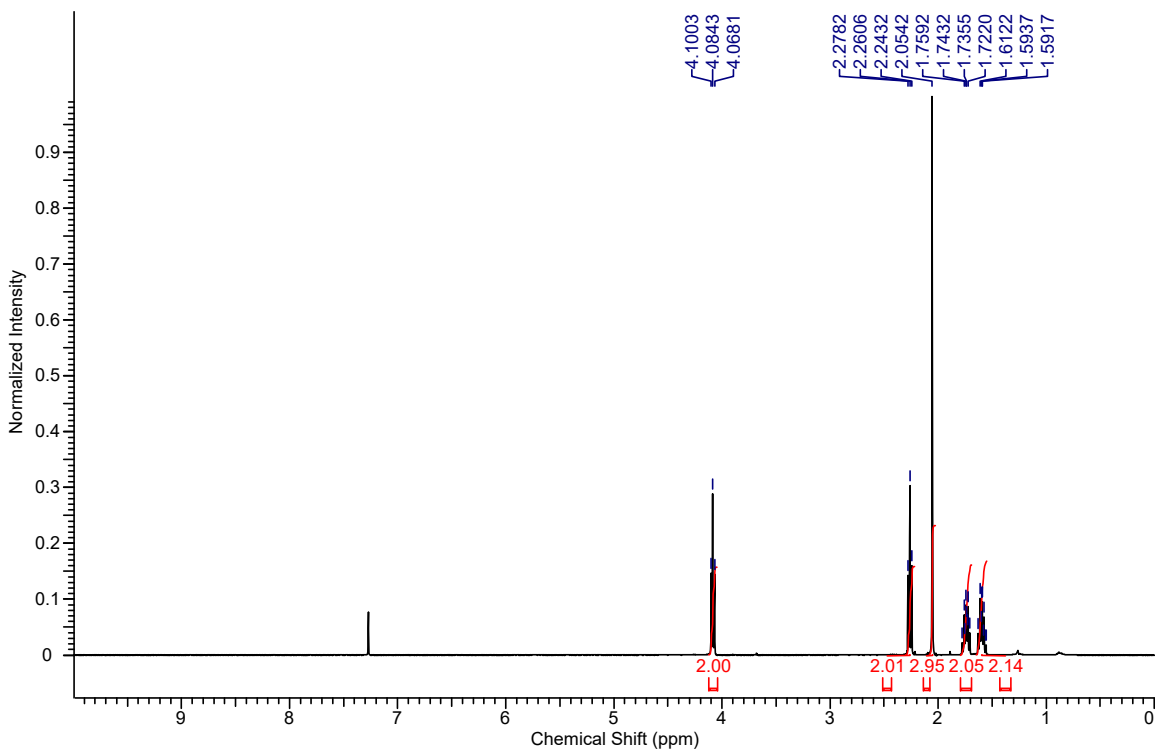
### 3-Bromoprop-2-yn-1-yl 4-methoxybenzoate (7.2):



***tert*-Butyl 4-(bromoethynyl)isoindoline-2-carboxylate (11.2):**

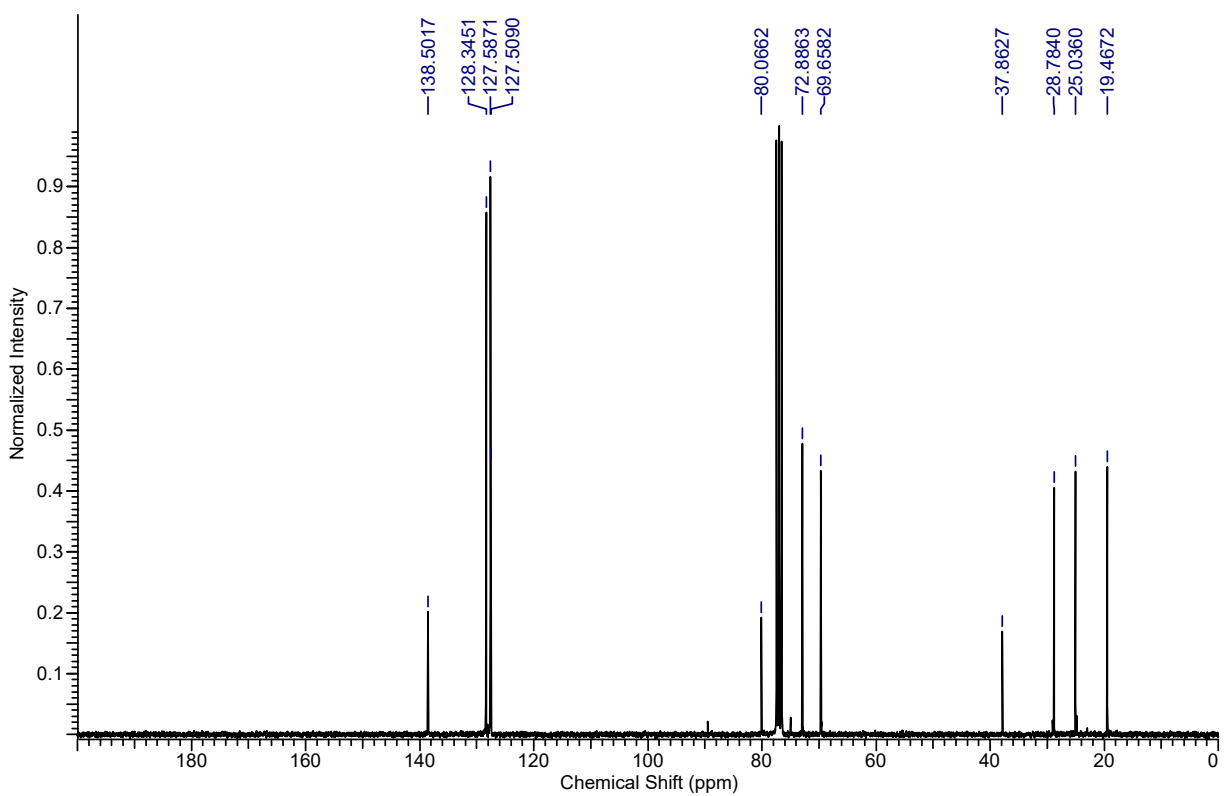
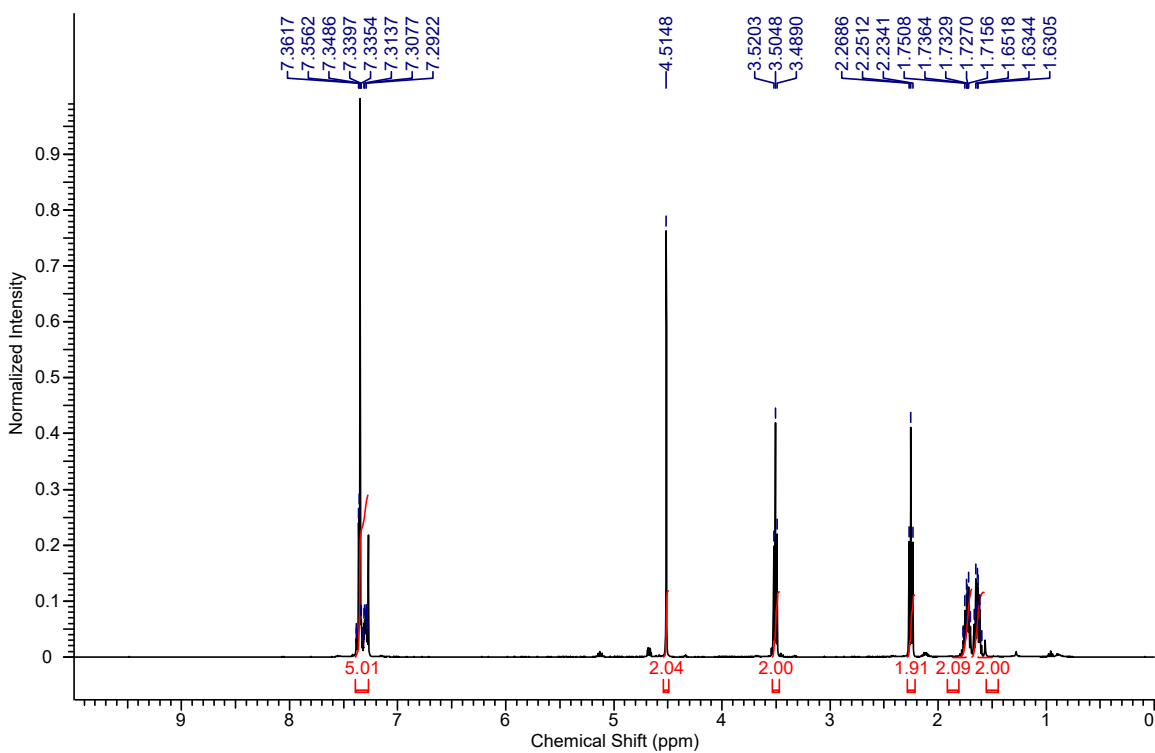


**6-Bromohex-5-yn-1-yl acetate (11.3):**

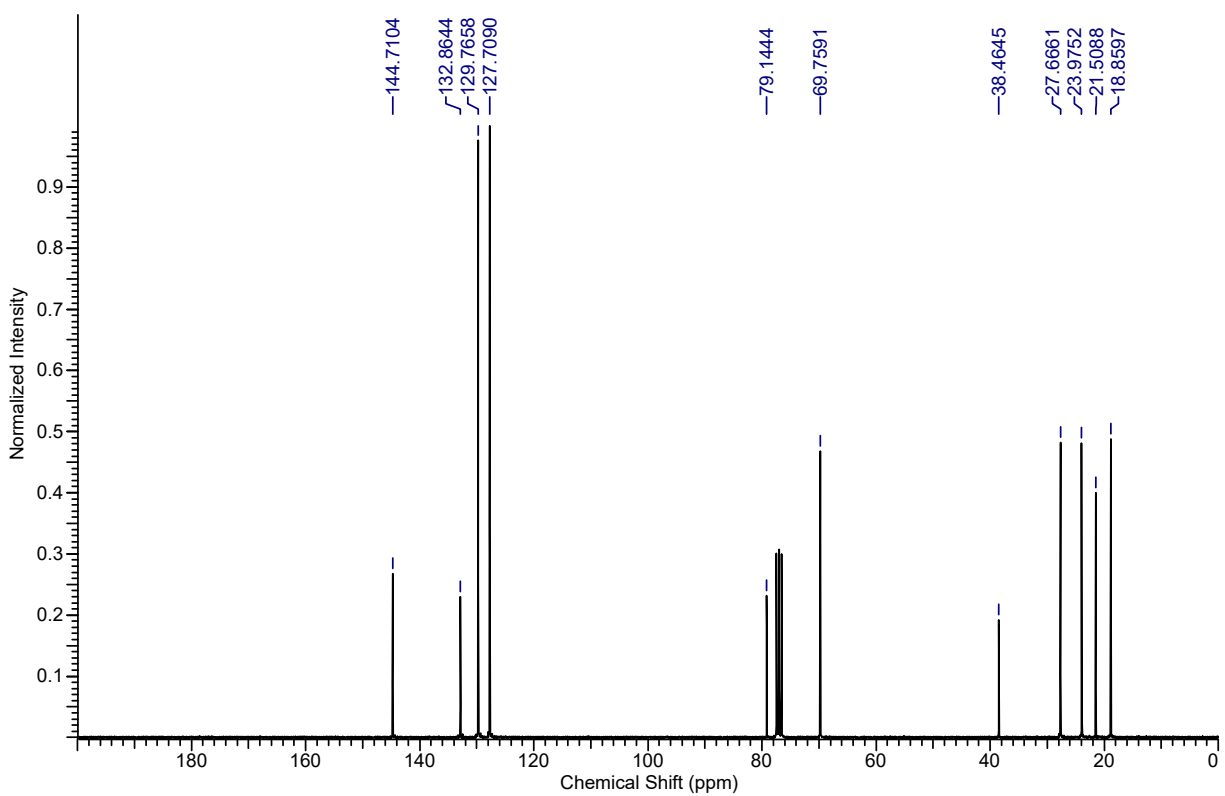
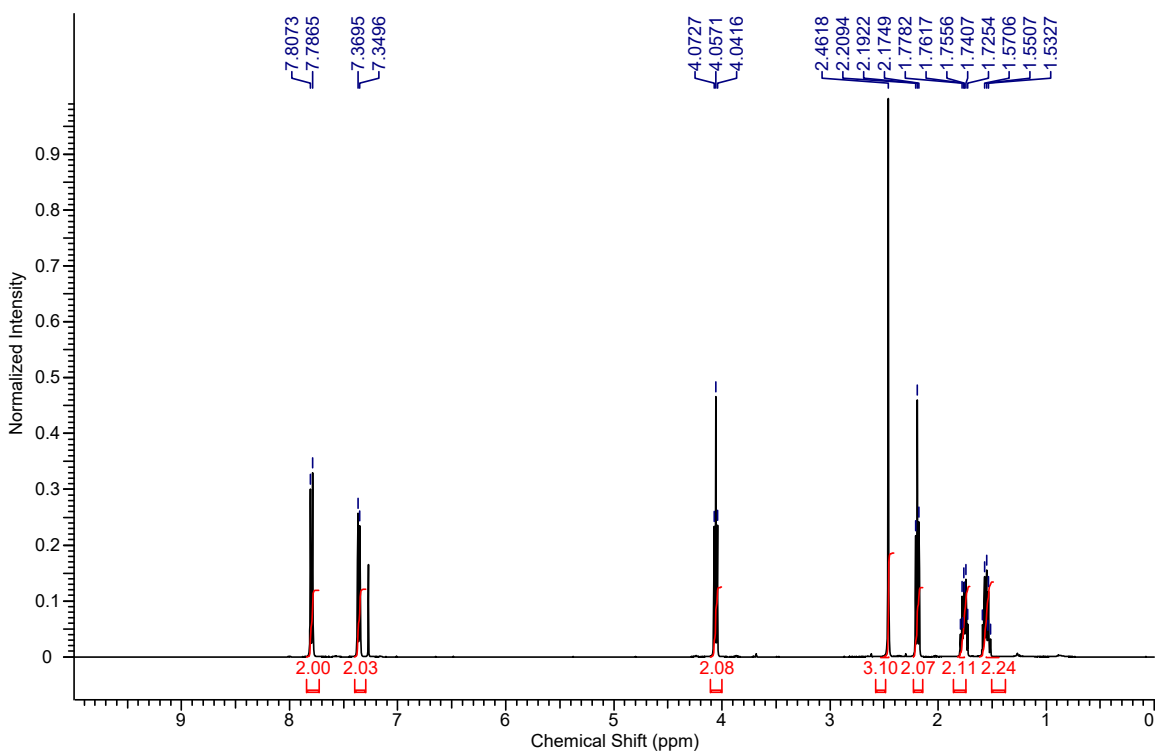




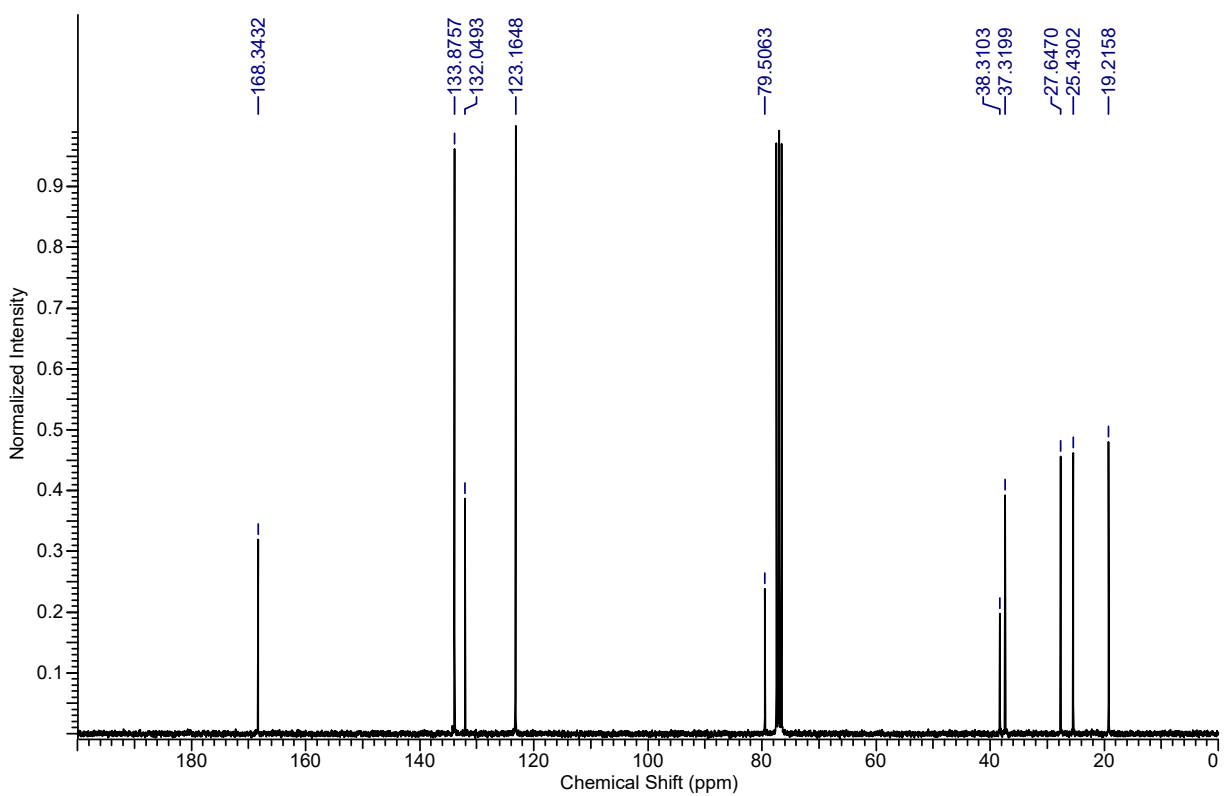
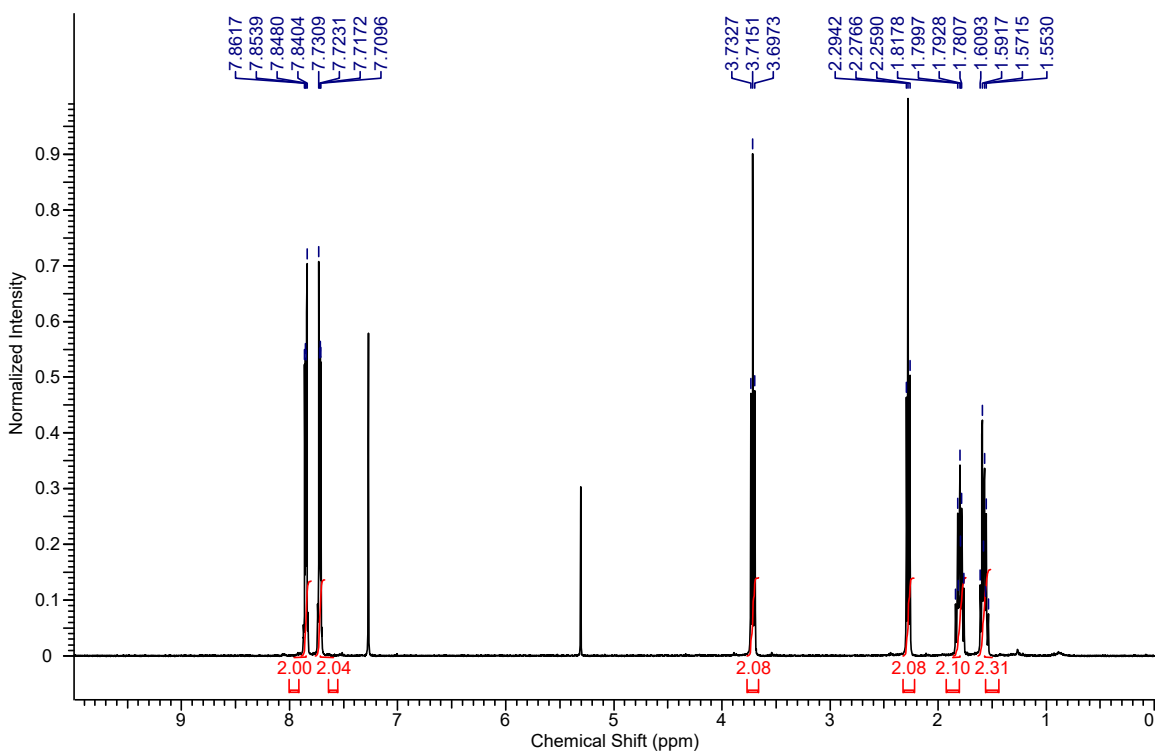
**(((6-Bromohex-5-yn-1-yl)oxy)methyl)benzene (11.4):**



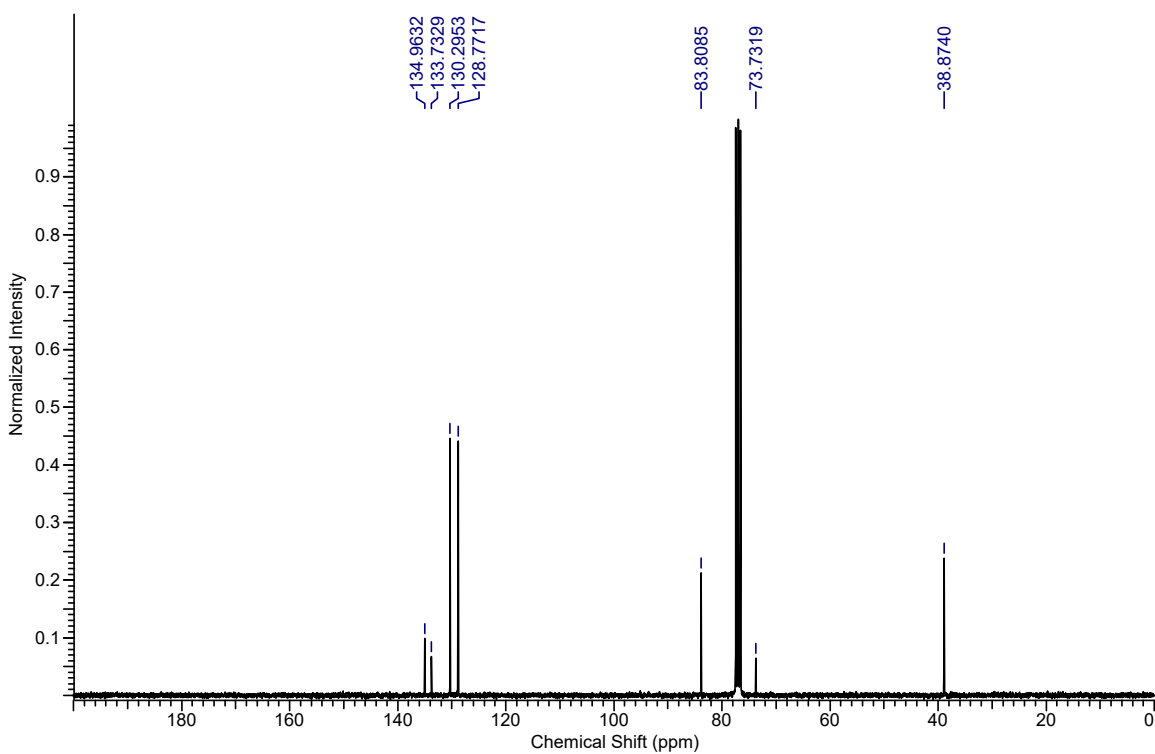
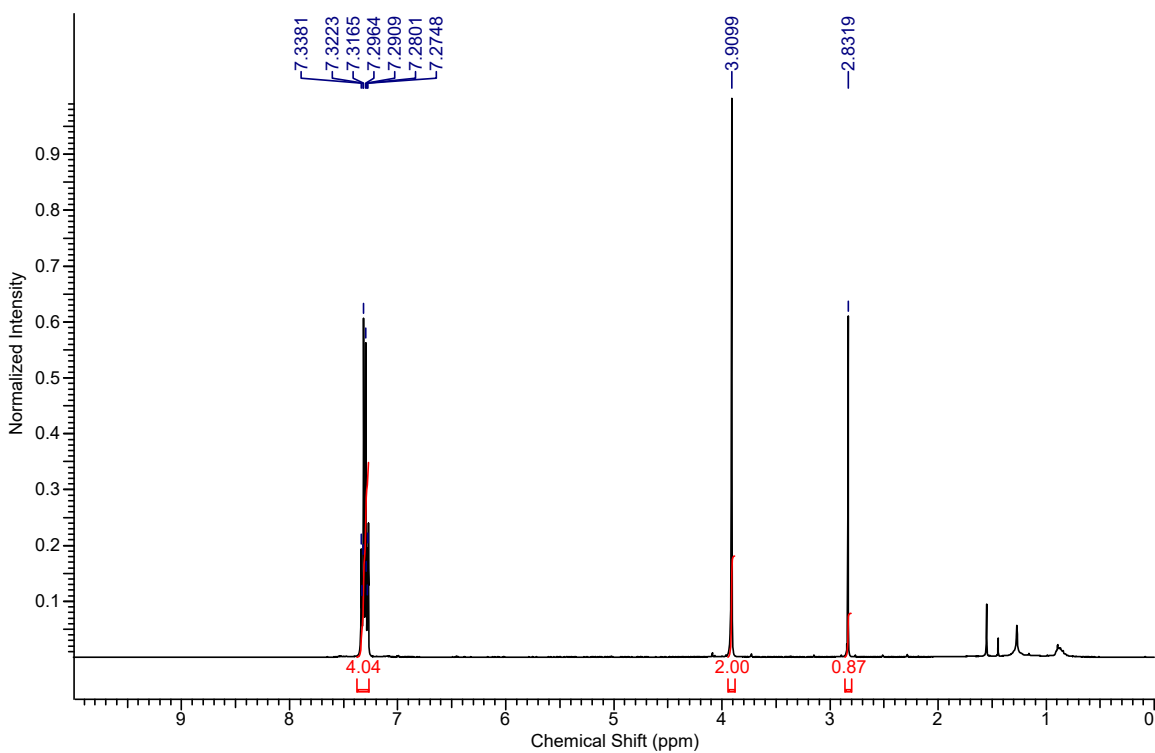
**6-Bromohex-5-yn-1-yl 4-methylbenzenesulfonate (11.5):**



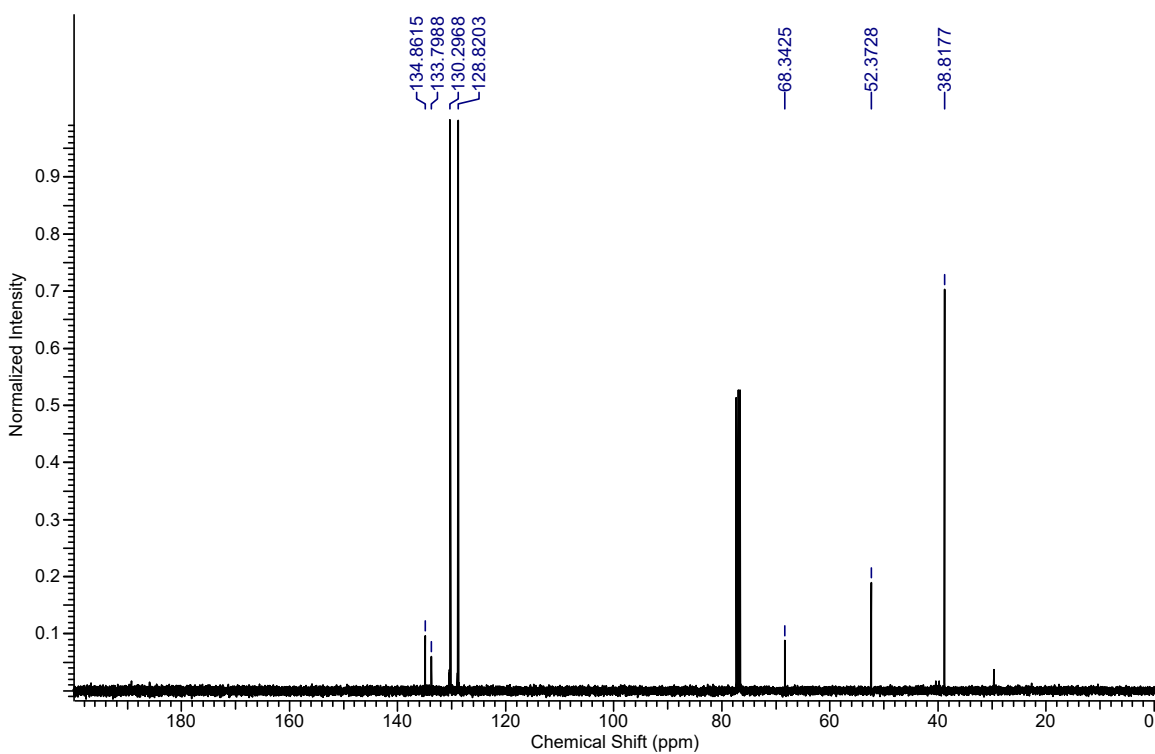
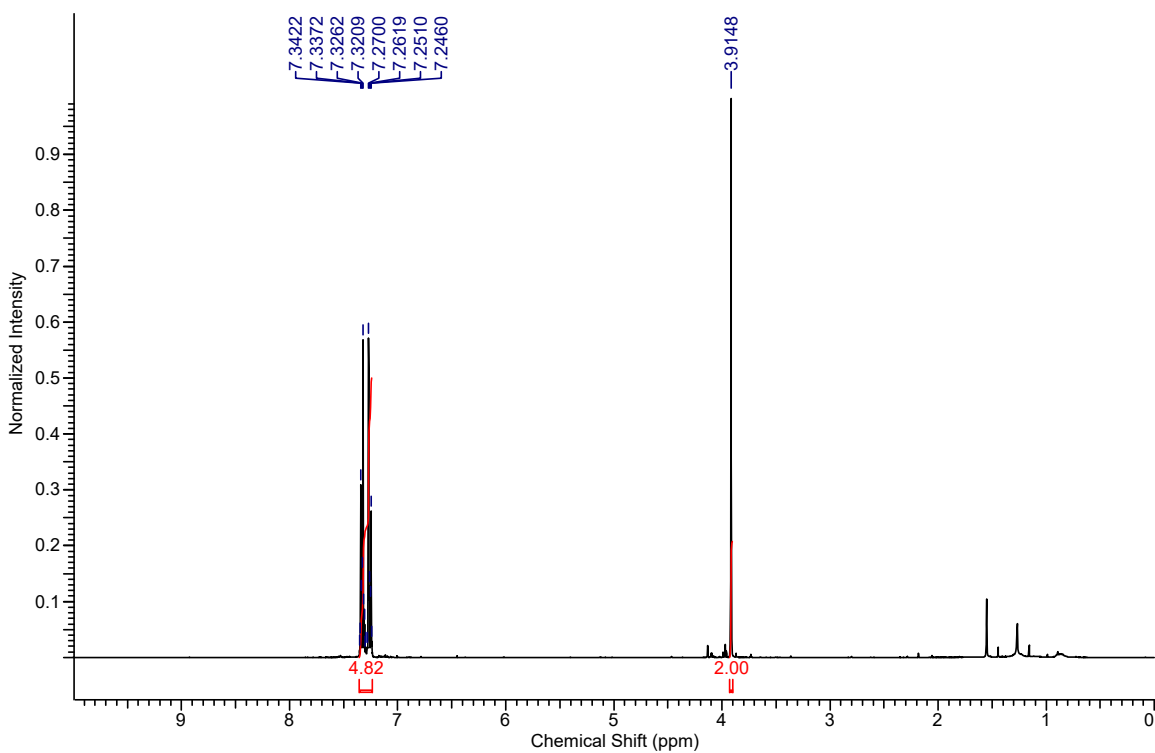
**2-(6-Bromohex-5-yn-1-yl)isoindoline-1,3-dione (11.7):**



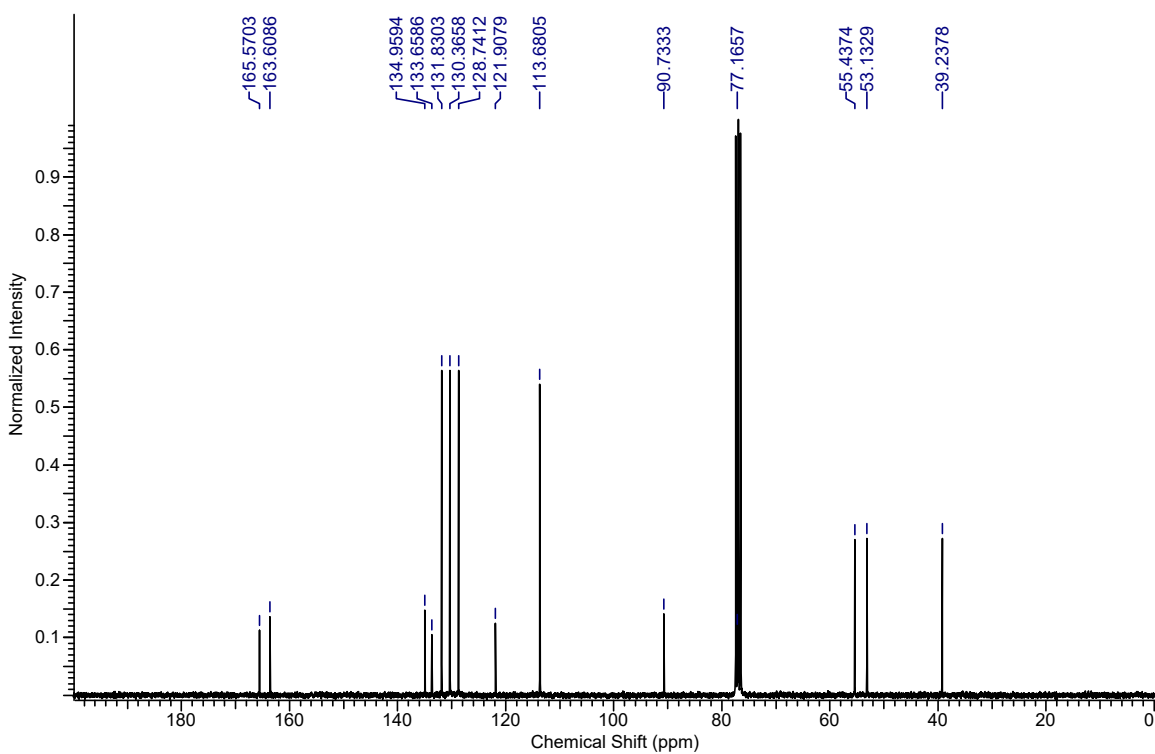
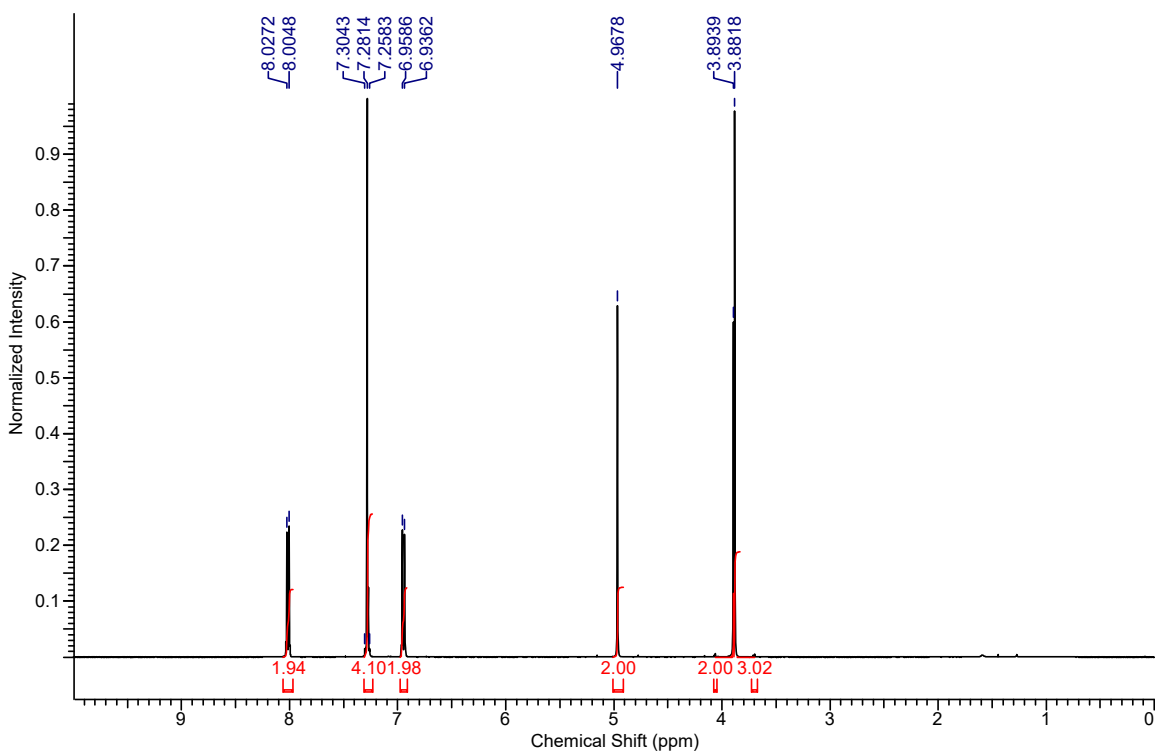
**(4-Chlorobenzyl)(ethynyl)sulfane (7.29):**



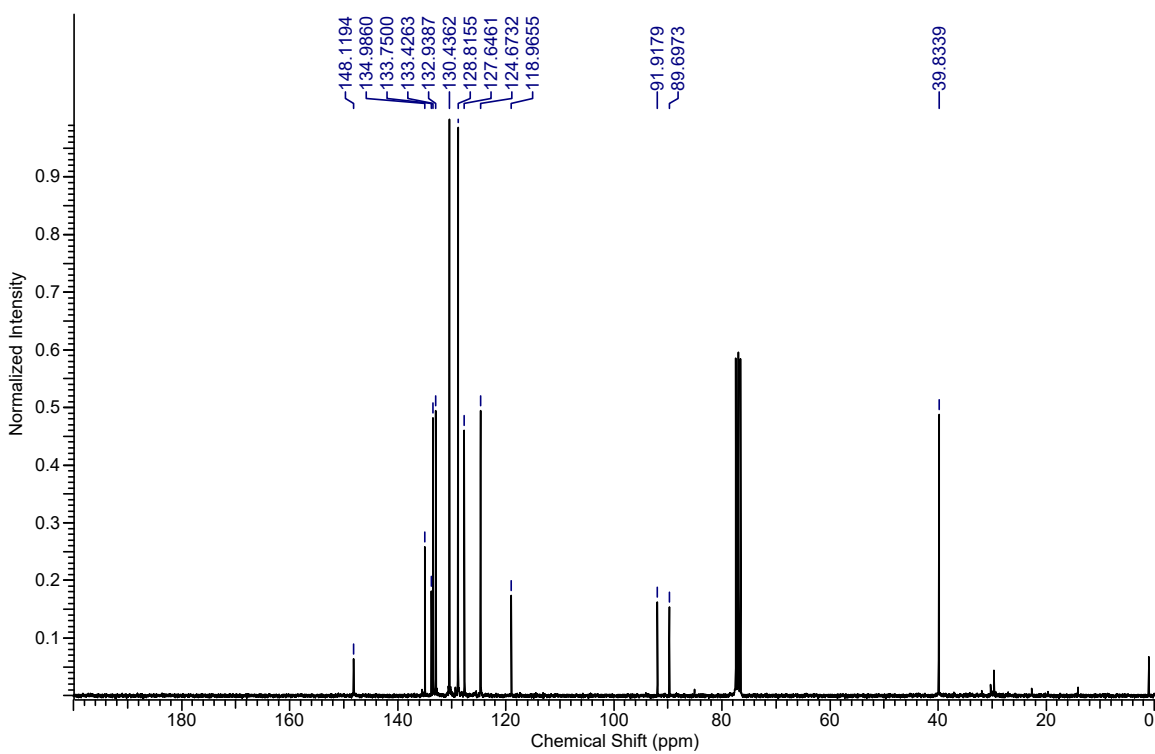
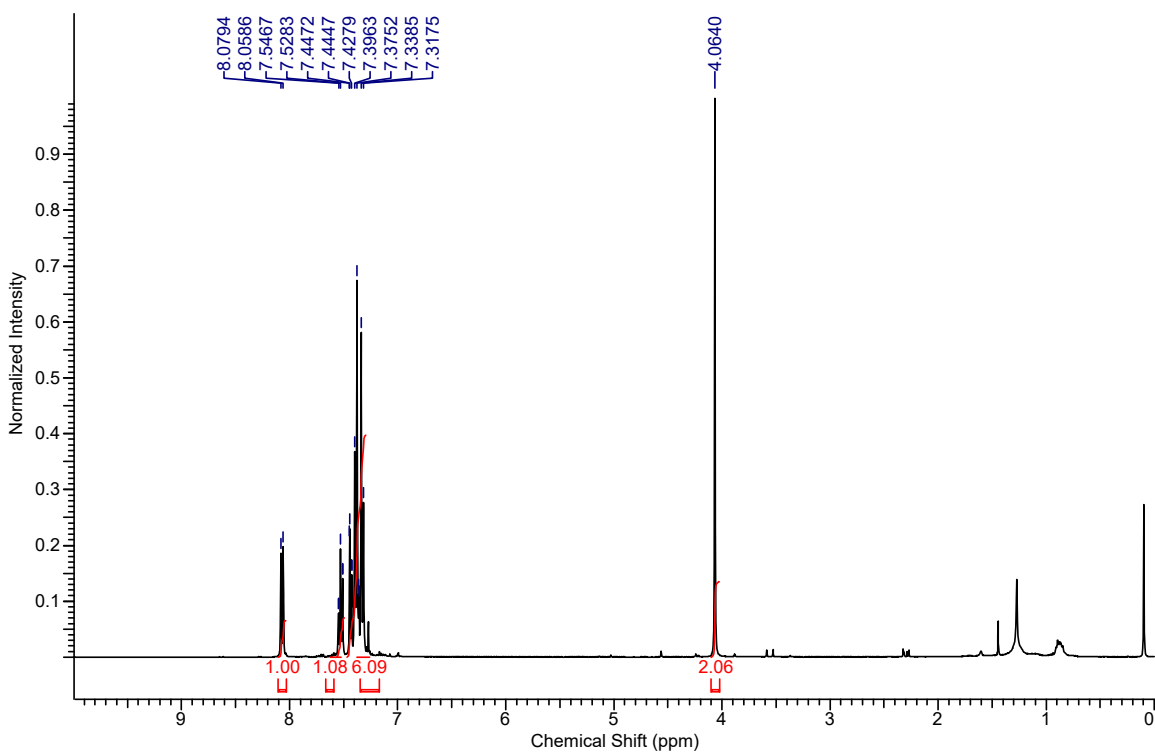
**(Bromoethynyl)(4-chlorobenzyl)sulfane (7.30):**



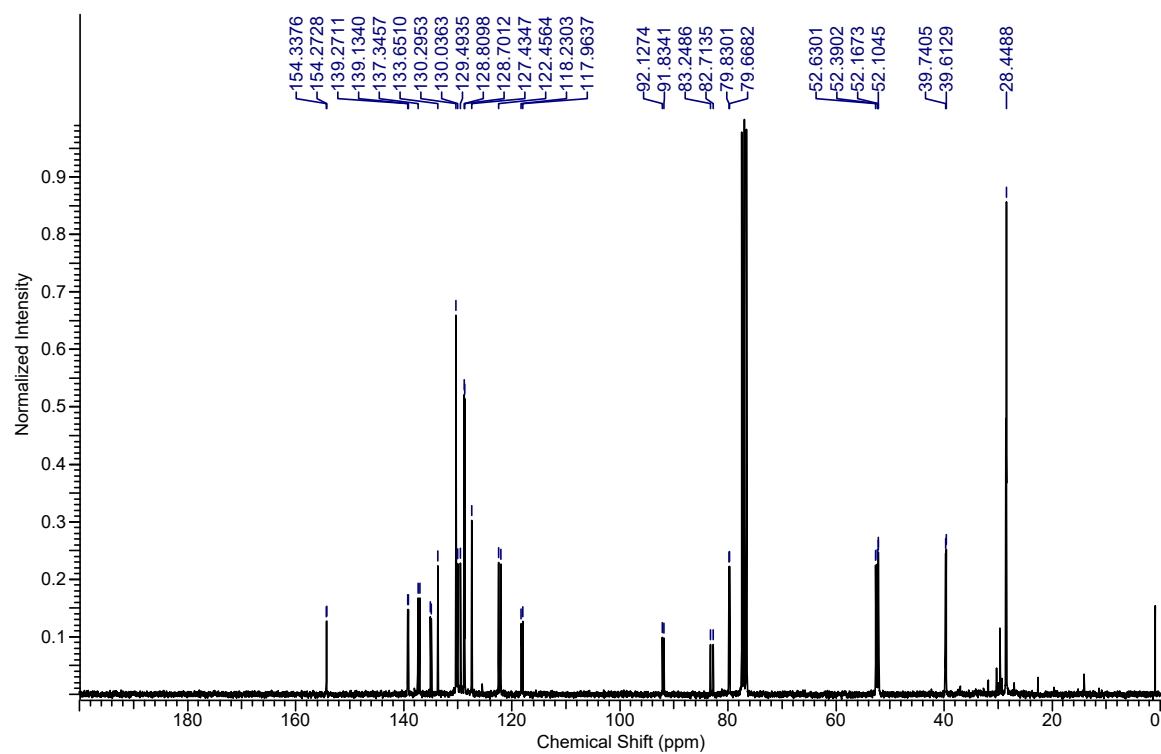
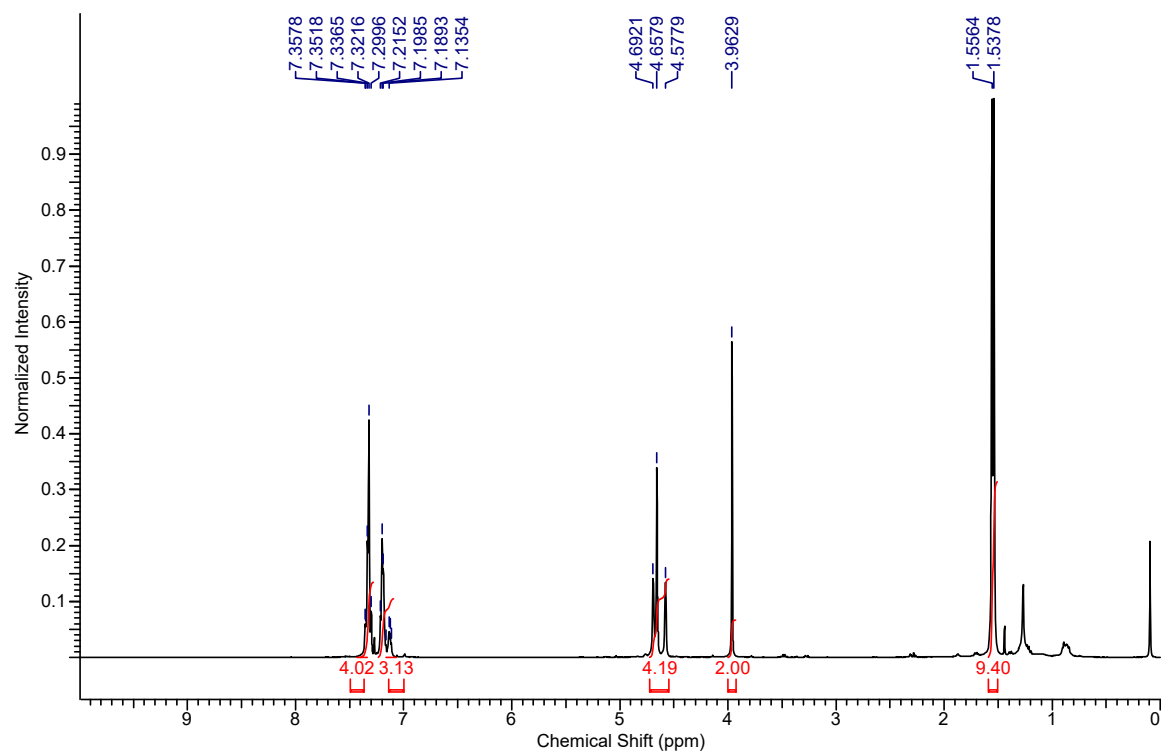
**3-((4-Chlorobenzyl)thio)prop-2-yn-1-yl 4-methoxybenzoate (7.3):**



**(4-Chlorobenzyl)((2-nitrophenyl)ethynyl)sulfane (7.20):**

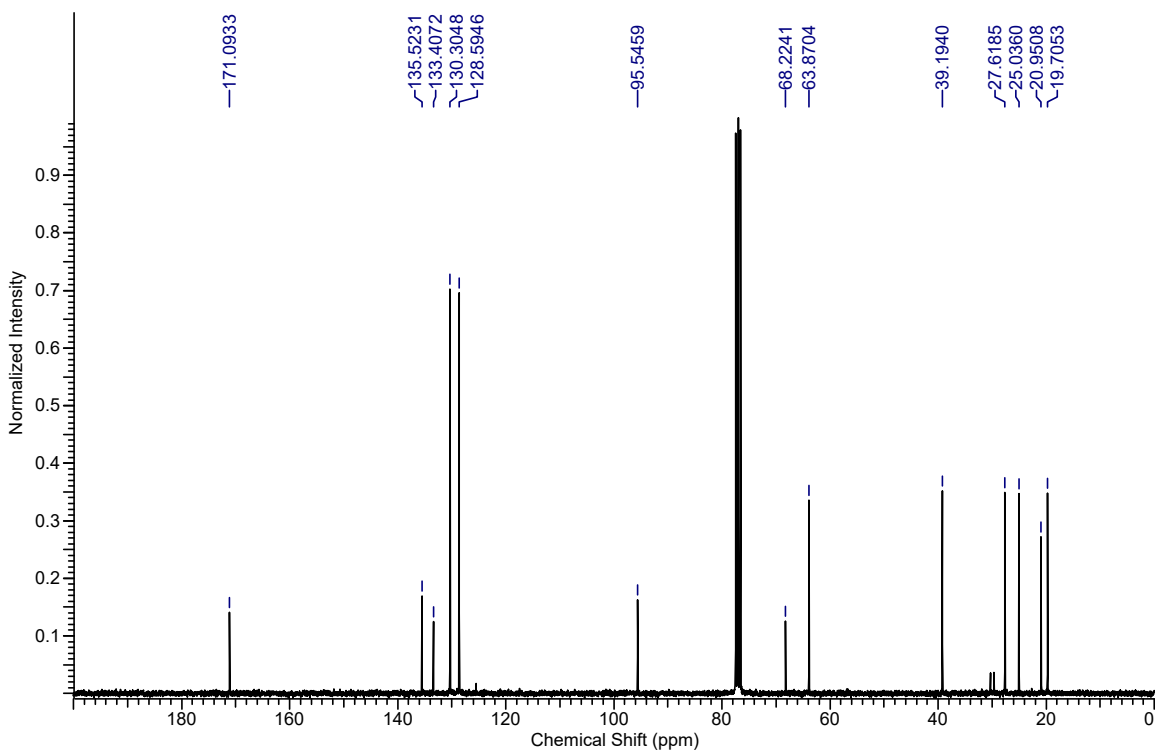
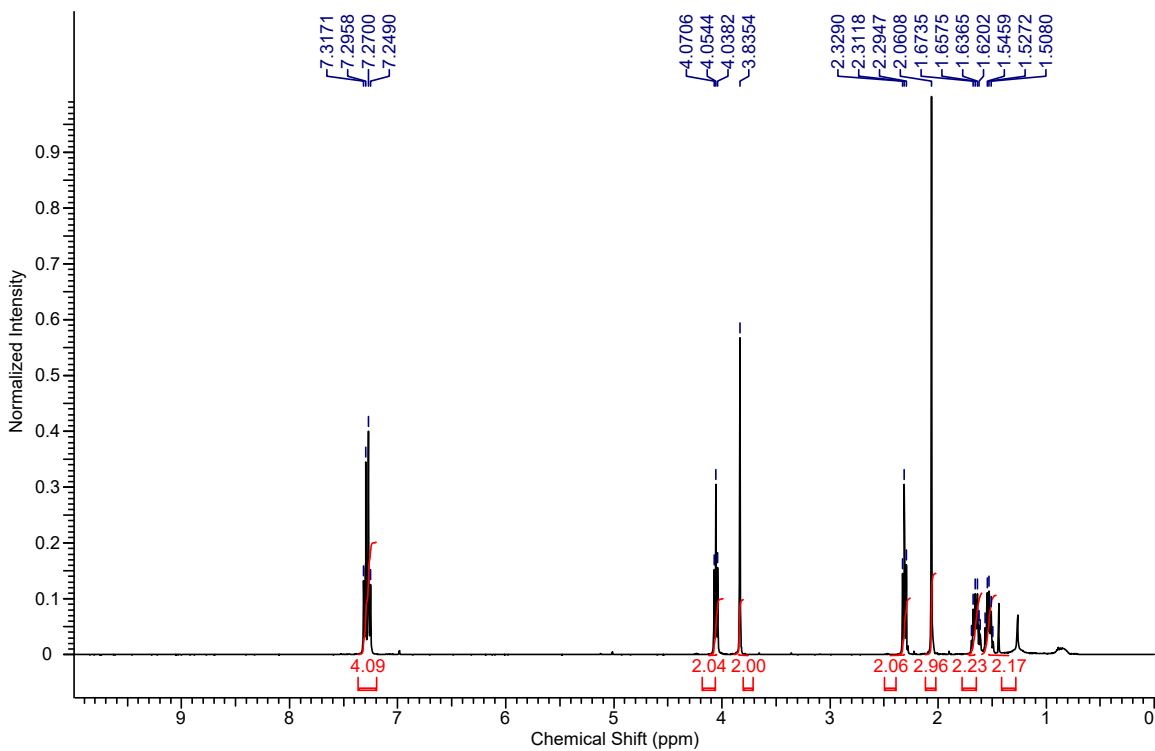


***tert*-Butyl 4-(((4-chlorobenzyl)thio)ethynyl)isoindoline-2-carboxylate (7.21):**

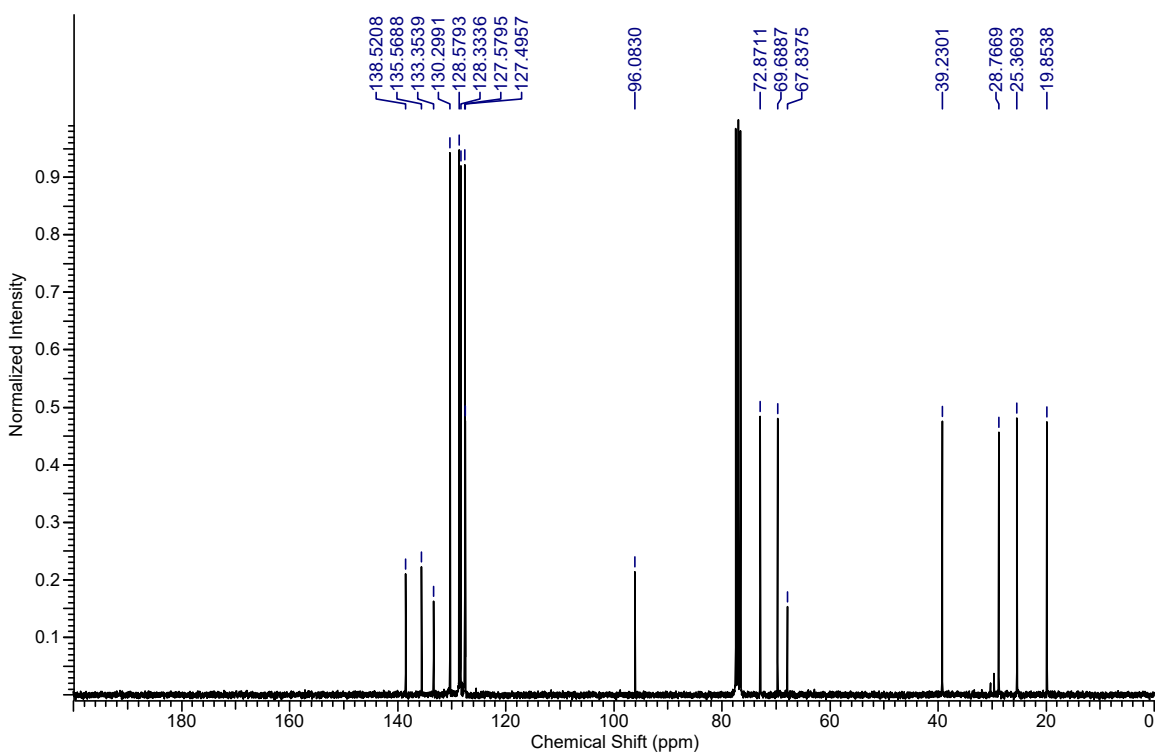
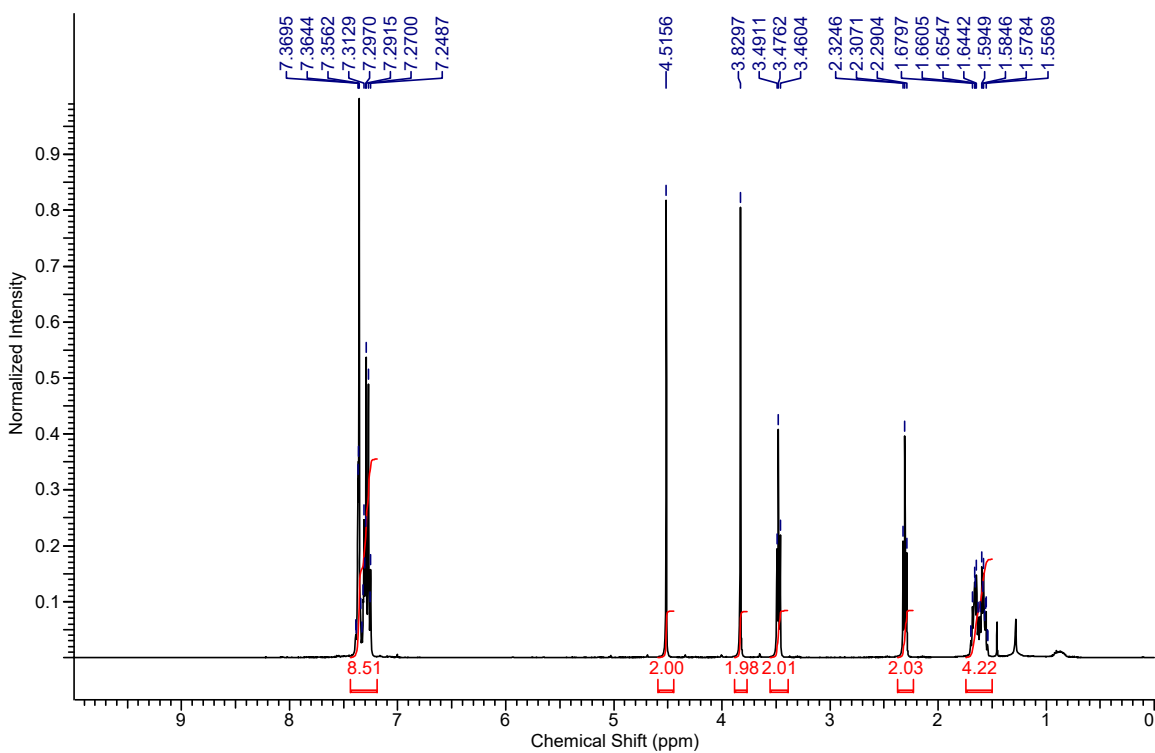




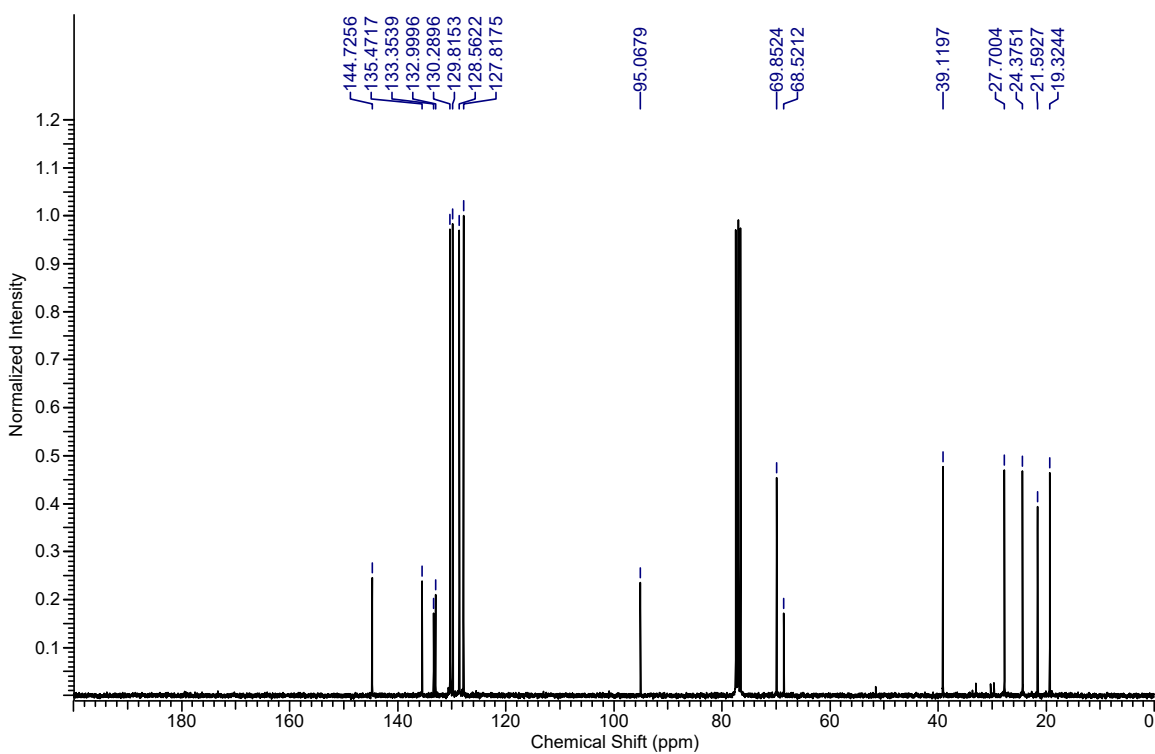
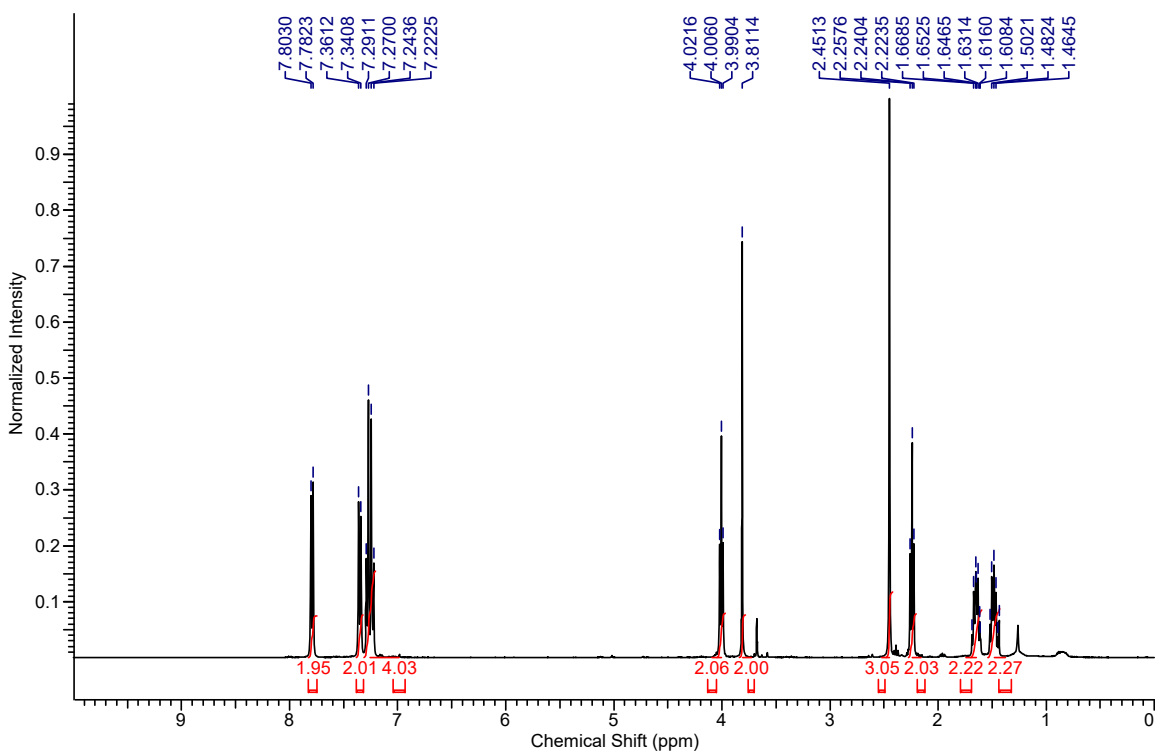
**6-((4-Chlorobenzyl)thio)hex-5-yn-1-yl acetate (7.24):**



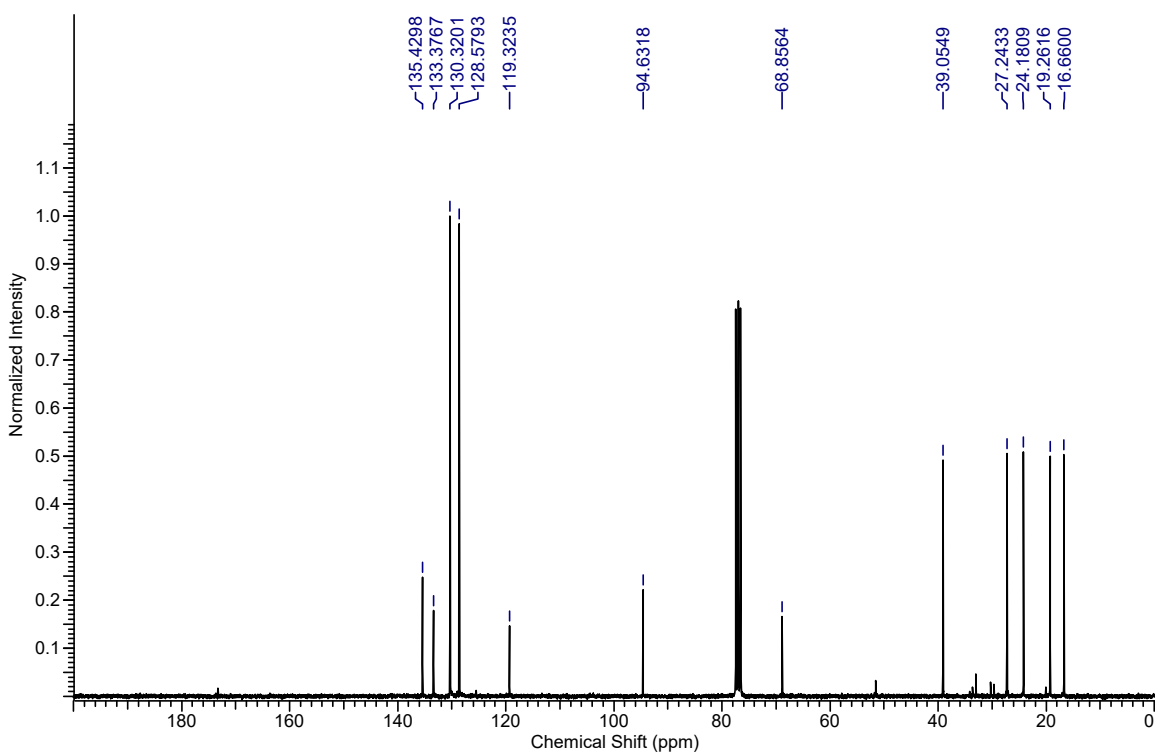
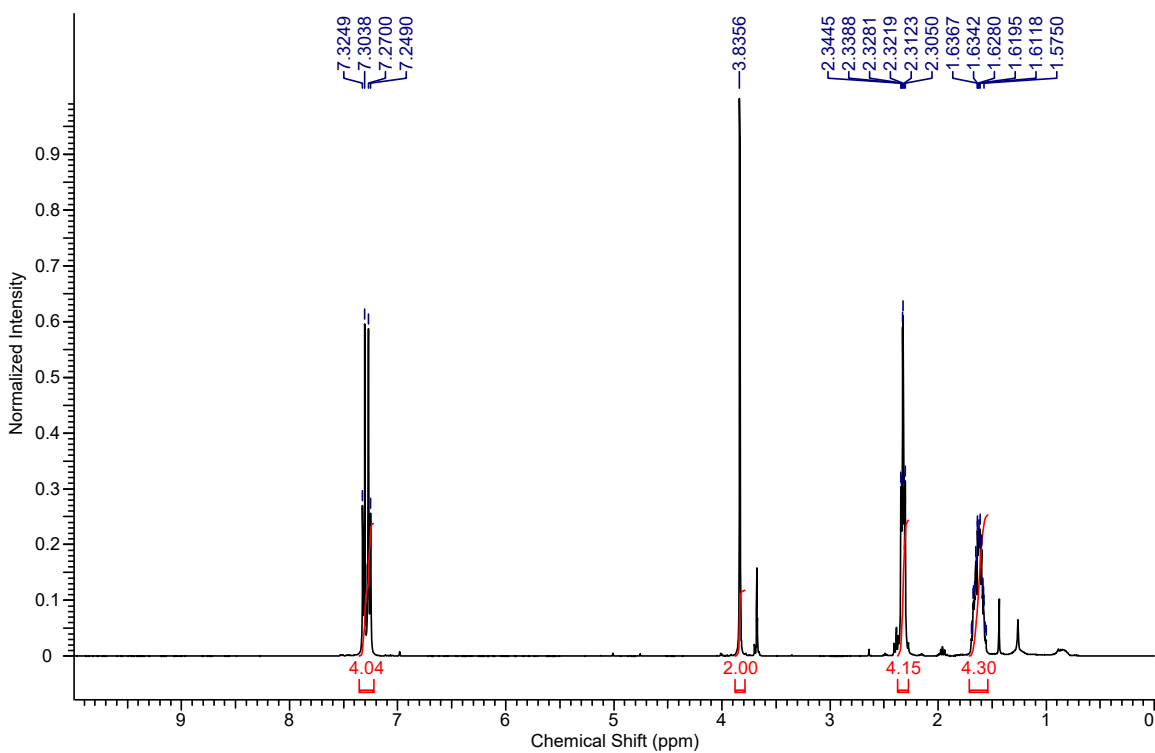
**(6-(Benzyloxy)hex-1-yn-1-yl)(4-chlorobenzyl)sulfane (7.25):**



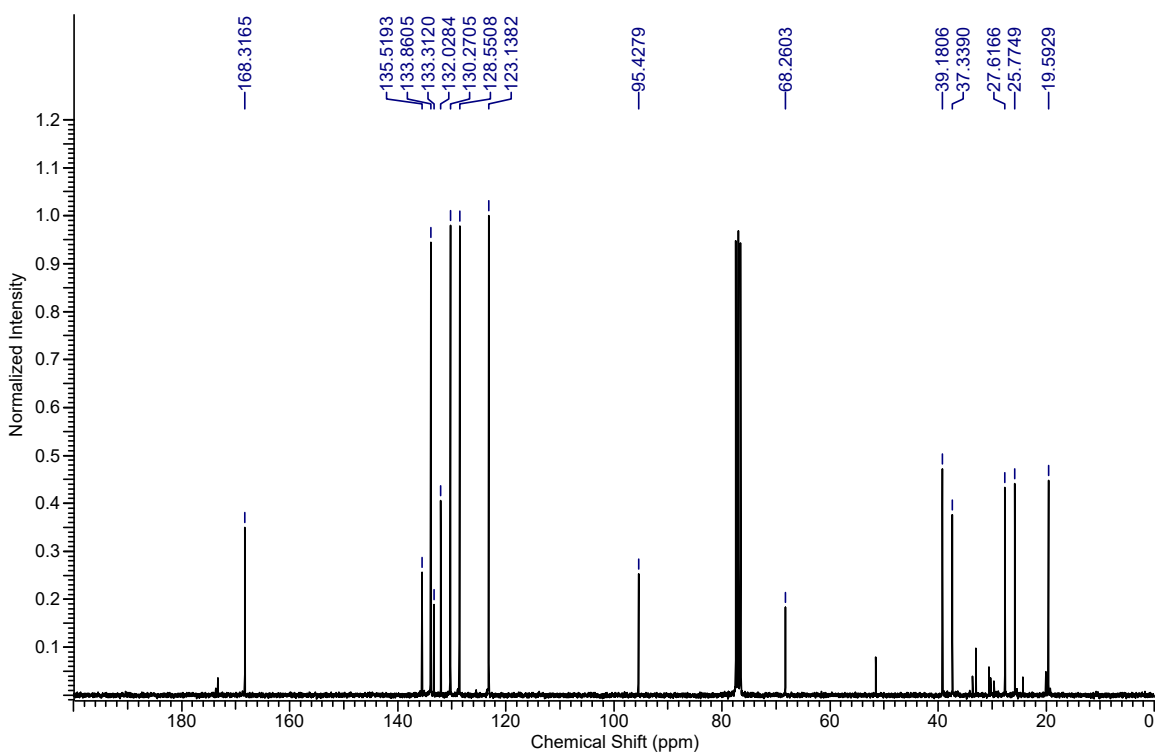
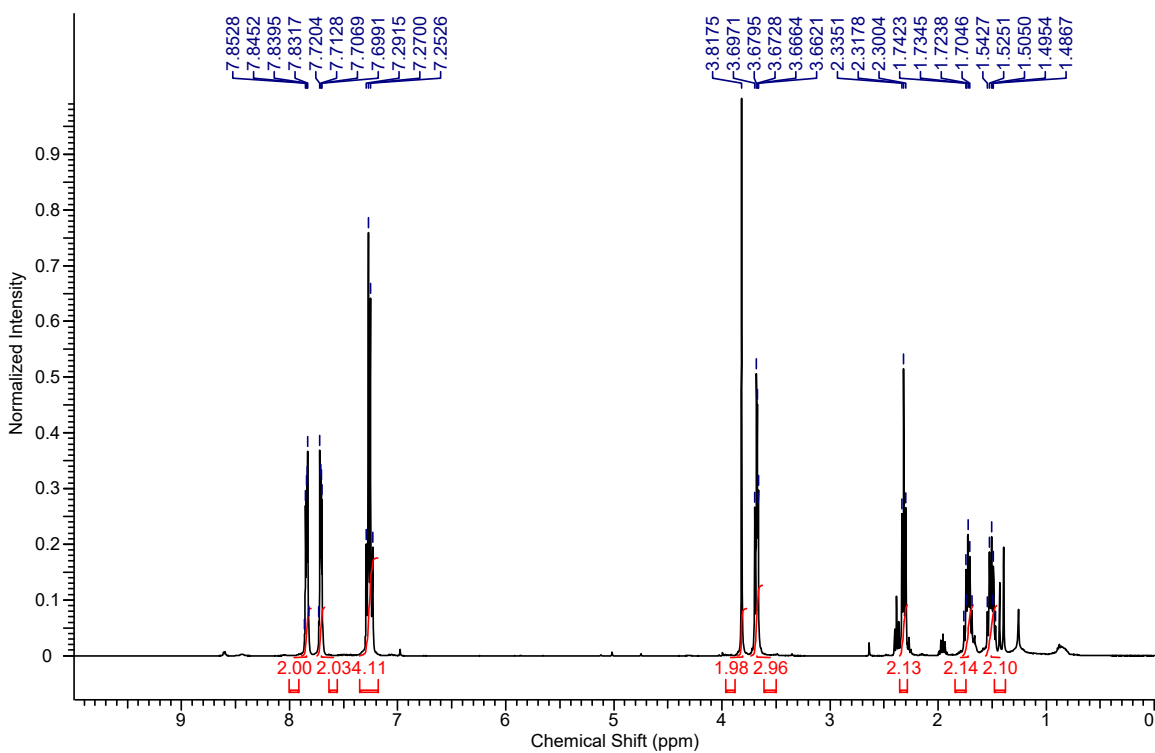
**6-((4-Chlorobenzyl)thio)hex-5-yn-1-yl 4-methylbenzenesulfonate (7.26):**



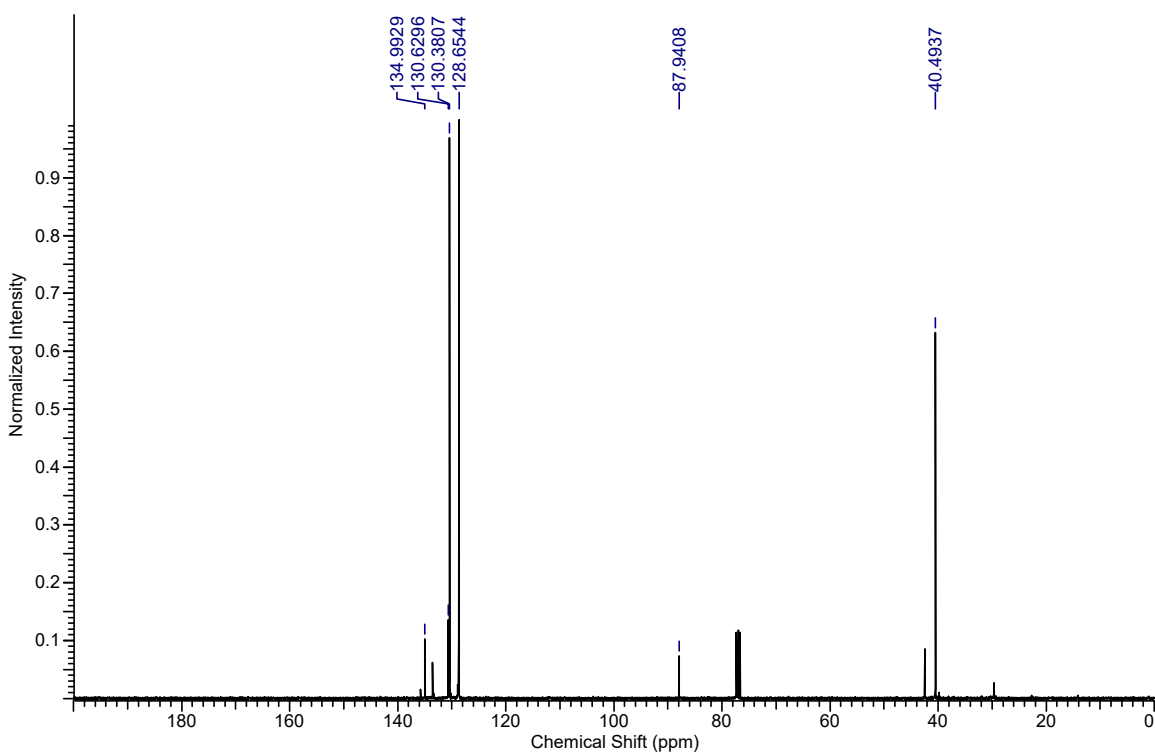
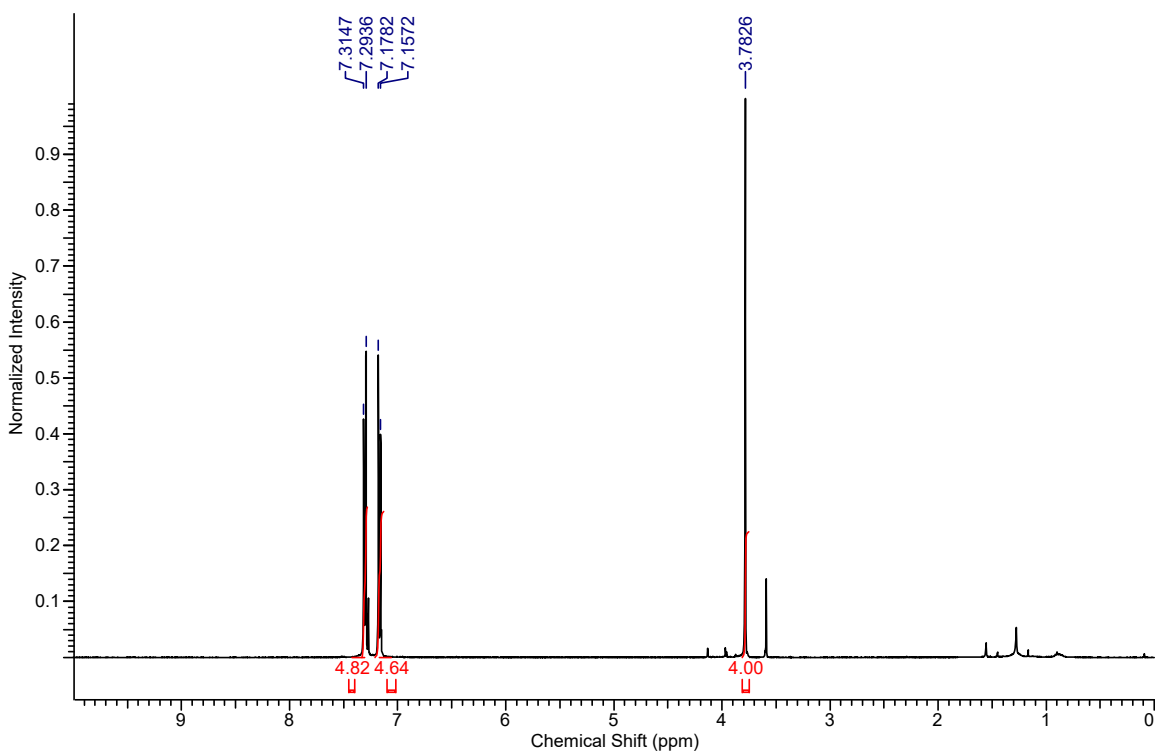
**7-((4-Chlorobenzyl)thio)hept-6-yne nitrile (7.27):**



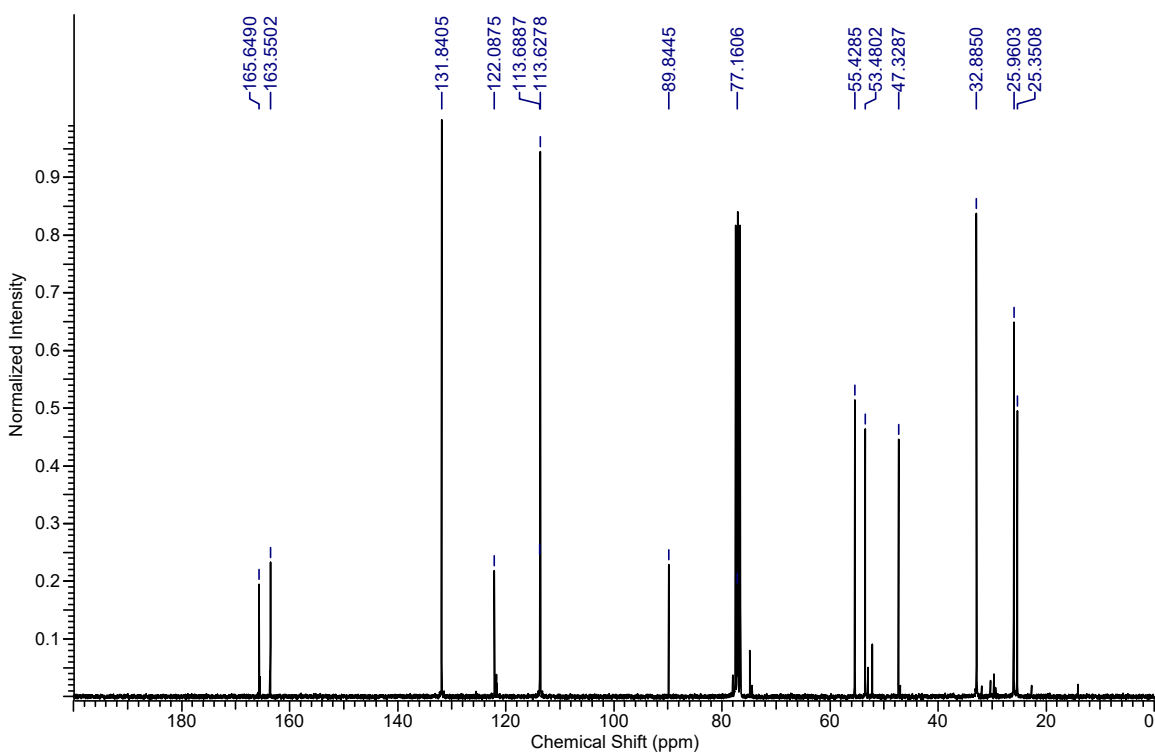
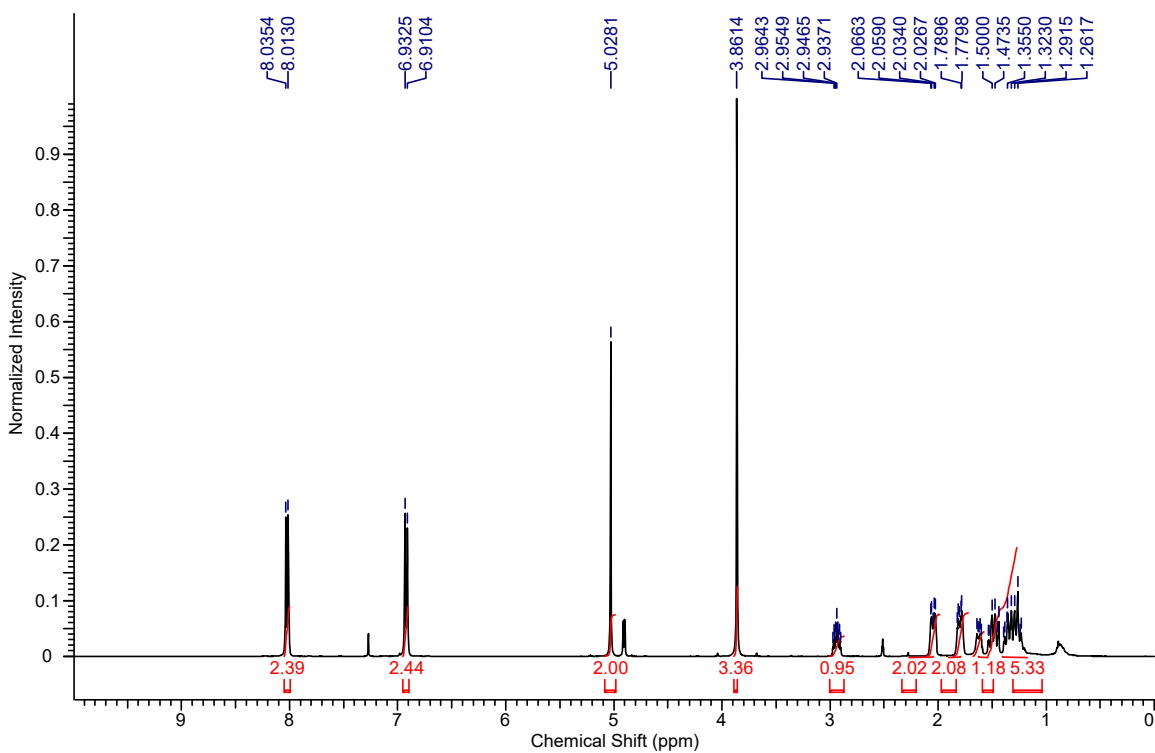
**2-(6-((4-Chlorobenzyl)thio)hex-5-yn-1-yl)isoindoline-1,3-dione (7.28):**



**1,2-Bis((4-chlorobenzyl)thio)ethyne (7.31):**



**3-(Cyclohexylthio)prop-2-yn-1-yl 4-methoxybenzoate (7.32):**



**3-(Tritylthio)prop-2-yn-1-yl 4-methoxybenzoate (7.33):**

